EMPIRICAL EVALUATION OF ARTIFICIAL INTELLIGENCE BASED CUSTOMISED WEATHER FORECASTING AND MONITORING MODEL FOR THE AGRICULTURE SECTOR

Edge Hill University

Pradeep Ruwan Padmasiri Galbokka Hewage

Department of Computer Science

Faculty of Arts and Sciences

A THESIS SUBMITTED IN PARTIAL FULFILLMENT OF THE REQUIREMENTS OF EDGE HILL UNIVERSITY FOR THE DEGREE OF DOCTOR OF PHILOSOPHY

November 2019

DECLARATION

This thesis is the result of my own work and includes nothing, which is the outcome of work done in collaboration except where specifically indicated in the text. It has not been previously submitted, in part or whole, to any university or institution for any degree, diploma, or other qualification.

Signed: _____

Date: _____

Pradeep Ruwan Padmasiri Galbokka Hewage MSc, MBCS, FHEA, PGDIP(IT), PGCertHE
Edge Hill University
Department of Computer Science

PUBLICATIONS

Peer-reviewed conference papers:

1. Hewage, P., Behera, A., Trovati, M. and Pereira, E., 2019, May. Long-Short Term Memory for an Effective Short-Term Weather Forecasting Model Using Surface Weather Data. In *IFIP International Conference on Artificial Intelligence Applications and Innovations* (pp. 382-390). Springer, Cham.
2. Hewage, P., Anderson, M. and Fang, H., 2017, October. An Agile Farm Management Information System Framework for Precision Agriculture. In *Proceedings of the 9th International Conference on Information Management and Engineering* (pp. 75-80). ACM.

Peer-reviewed journal articles

1. Hewage, P., Trovati, M., Pereira, E. and Behera, A., 2020. Deep learning-based effective fine-grained weather forecasting model. Pattern Analysis and Applications, pp.1-24.
2. Hewage, P., Behera, A., Trovati, M., Pereira, E., Ghahremani, M., Palmieri, F. and Liu, Y., 2020. Temporal convolutional neural (TCN) network for an effective weather forecasting using time-series data from the local weather station. Soft Computing, pp.1-30.

ABSTRACT

As a result of the evolution of agriculture from 1.0 to 4.0, modern-day agriculture is driven by smart systems and smart devices. The evaluation of the Internet of Things (IoT) and specific approaches in edge computing contributed towards understanding and predicting the weather conditions with a demonstrated impact on precision farming. Non-predictive or inaccurate weather forecasting can severely impact the community of users such as farmers. Farmers depend on the weather forecast so that various farming activities can be undertaken such as ploughing, cultivation, harvesting, and others. An inaccurate forecast directly impacts the farmer's ability to engage in these activities, negatively influencing their capability of managing the resources related to these operations. In addition, there are significant risks to life and property loss due to unexpected weather conditions. Numerical Weather Prediction (NWP) models run in major weather forecasting centres with several supercomputers to solve simultaneous complex non-linear mathematical equations. This requires considerable computing power to obtain a forecast based on current weather conditions. Such models provide the medium-range weather forecasts, i.e. every 6 hours up to 18 hours with a grid length of 10-20 km. However, a community of users often depend on more detailed short-to-medium-range forecasts with higher resolution regional or local forecasting models. Moreover, the regional or local weather forecasting may not be accurate based on the geographical appearance of location, such as the top of a mountain, land covered by several mountains, the slope of the land, etc. The first part of this research is to determine the competence of using neural networks for weather forecasting. The weather forecasting model is developed by exploring the set of models, namely Multi-Input and Multi-Output (MIMO) and Multi-Input and Single-Output (MISO). The proposed MIMO and MISO models are experimented with the state-of-the-art deep neural network approaches such as Long Short-Term Memory (LSTM) and Temporal Convolutional Networks (TCN), which are based on Artificial Neural Networks (ANN). The accuracy of the proposed model is compared to classic machine learning approaches as well as the well-established Weather Research and Forecasting (WRF) NWP model. The proposed model is also experimented using different deep learning configurations and controls for effective weather forecasting. The second part of this research is to apply similar neural network techniques aimed at developing and evaluating a lightweight, fine-grained and novel weather forecasting model, which consists of one or more local weather stations. The proposed model can be used as an efficient localised weather forecasting tool for the community of users, and it could be run on a standalone personal computer.

Keywords:

Long Short-Term Memory, Temporal Convolutional Networks, Weather Prediction, Weather Research and Forecasting model, Time-series Data Analysis, Neural Networks, Precision farming

ACKNOWLEDGEMENTS

Firstly, I would like to express my sincere gratitude to my Director of Studies, Dr Ardhendu Behera for the continuous support of my PhD study and related research and for his exceptional guidance, motivation and knowledge. This thesis would not have been possible without his professional guidelines and persistent help. Along with my Director of Studies, I would like to convey my special thanks to the rest of my supervisory panel: Dr Marcello Trovati and Prof. Ella Pereira, for their insightful comments, guidance, and encouragement. I am also grateful to Dr Alan Gadian (NCAS, University of Leeds) for his valuable support at the initial stage of this research.

My sincere thanks also go to Prof. Mark Anderson for his exceptional guidance during the first year of my PhD research. He initially identified my skills and suggested the most suitable project to build my expertise by arranging a real-world industry to work with. In addition, I would also like to convey my special thanks to the proprietor and the management team of 'Precision Decisions Ltd.' for giving me a great opportunity to conduct my research within the company and for giving me access to existing data and systems. A special thanks must go to Mr Rich Kavanagh, the Head of IT of the company, whose exceptional help allowed me to analyse the system and provided necessary guidelines and resources to implement the proposed weather model successfully.

In addition, I would also like to thank Prof Nik Bessis and the computing department academic staff for their immense support and valuable input towards my PhD. The help and support given by the university administration and the supporting staff are also highly valued.

I must take this opportunity to thank my parents and my family; they are always behind me and helped me in a numerous way to complete this project and thesis successfully.

Finally, I would like to thank my friends, who support each other through discussing their findings and problems and, especially for spending the time with me when I was struggling.

Once again, thank you very much indeed, everyone!

Table of Contents

LIST OF TABLES

LIST OF FIGURES

LIST OF ABBREVIATIONS AND ACRONYMS

ADSS	Agricultural Decision Support System
AI	Artificial Intelligence
ANFIS	Adaptive Neuro-Fuzzy Inference System
ANN	Artificial Neural Networks
API	Application Program Interface
ARPS	Advanced Regional Prediction System
ARW	Advanced Research WRF
CNN	Convolutional Neural Networks
CPU	Central Processing Unit
CRF	Conditional Random Fields
CSV	Comma-Separated Values
CTF	Control Traffic Farming
DNN	Deep Neural Network
EV	Explained Variance
GFS	Global Forecast System
GPS	Global Positioning System
GPU	Graphical Processing Unit
GRIB	General Regularly distributed Information in Binary
GSM	Global System for Mobile
IoT	Internet of Things
IT	Information Technology
LR	Learning Rate
LSTM	Long Short-Term Memory
MAE	Mean Absolute Error
MIMO	Multi-Input Multi-Output
MIN	Minimum
MISO	Multi-Input Single-Output
ML	Machine Learning
MLP	Multi-Layered Perceptron
MOS	Model Output Statistics
MSE	Mean Squared Error
NC	Now-casting
NCAR	National Centre for Atmospheric Research
NCAS	National Centre for Atmospheric Science
NCDC	National Climatic Data Centre

NCEP	National Centres for Environmental Prediction
NetCDF	Network Common Data Form
NLP	Natural Language Processing
NWP	Numerical Weather Prediction
Q2	2-meter specific humidity
RAM	Random Access Memory
RBF	Radial Basis Function
RBFN	Radial Basis Function Network
ReLU	Rectified Linear Unit
RMSE	Root Mean Squared Error
RNN	Recurrent Neural Networks
RTK	Real-Time Kinematic
SISO	Single-Input Single-Output
SR	Standard Regression
SRF	Short Range Forecast
SVM	Support Vector Machines
SVR	Support Vector Regression
TCN	Temporal Convolutional Neural
TSK	Skin Temperature
TSLB	Soil temperature
U10	X component of wind at 10m
UCAR	University Corporation for Atmospheric Research
UK	United Kingdom
UM	Unified Modelling
UPN	Unsupervised Pretrained Network
US	United States
V10	Y component of wind at 10m
VSRF	Very Short-Range Forecast
WI-FI	Wireless Fidelity
WMSE	Weighted Mean Squared Error
WPS	WRF Pre-processing System
WRF	Weather Research and Forecasting model
WRF-ARW	Advanced Research WRF model
XLAT	Reference Latitude
XLONG	Reference Longitude

1 Introduction

The evolution of the Internet of Things (IoT) has significantly contributed towards the understanding and prediction of weather conditions with a demonstrated impact on precision farming (Wolfert et al., 2017). Furthermore, specific approaches in edge computing were applied so that vital environmental data get collected to understand the weather conditions and their impact on agricultural practice (Shi and Dustdar, 2016). The concepts of IoT have evolved agriculture 4.0 so that precision farming can be done and better yield of agricultural output can be achieved by addressing the weather issues (Ozdogan et al., 2017). The smart greenhouse concepts are implemented using the modern technology so that farming can be done to manage data analysis at each stage of agriculture including ploughing, cultivation, harvesting, and final stages of crop extraction in farming (Seo et al., 2018). The accurate and more reliable weather forecasting is a vital aspect of agriculture 4.0 (Ozdogan et al., 2017; Wolfert et al., 2017).

The weather prediction process is enabled through integrating concepts of data by which predictive models are developed; therefore, accurate data sharing facilitates strong decision-making processes. The weather data is used in many industries and facilitates many purposes including agriculture. In general, agriculture 4.0 uses satellite and radar data and sensor data to ensure accurate weather prediction on a regional basis (Bendre et al., 2015). Agriculture 4.0 is considered as the fourth evolution expecting to bring revolution to the farming technology.

As a result of the evolution of agriculture from 1.0 to 4.0, modern-day agriculture is driven by smart systems and smart devices. The advanced technologies are used to develop low-cost sensors so that perfect weather forecasting can be done in an effective way (Tekinerdogan, 2018). Figure 1.1 depicts the evaluation of agriculture-related promoting factors (i.e. technologies) and their key features. The meteorological information are collected to do precise weather forecast to manage the dynamics of agriculture 4.0 (De Wit and Crookes, 2013).

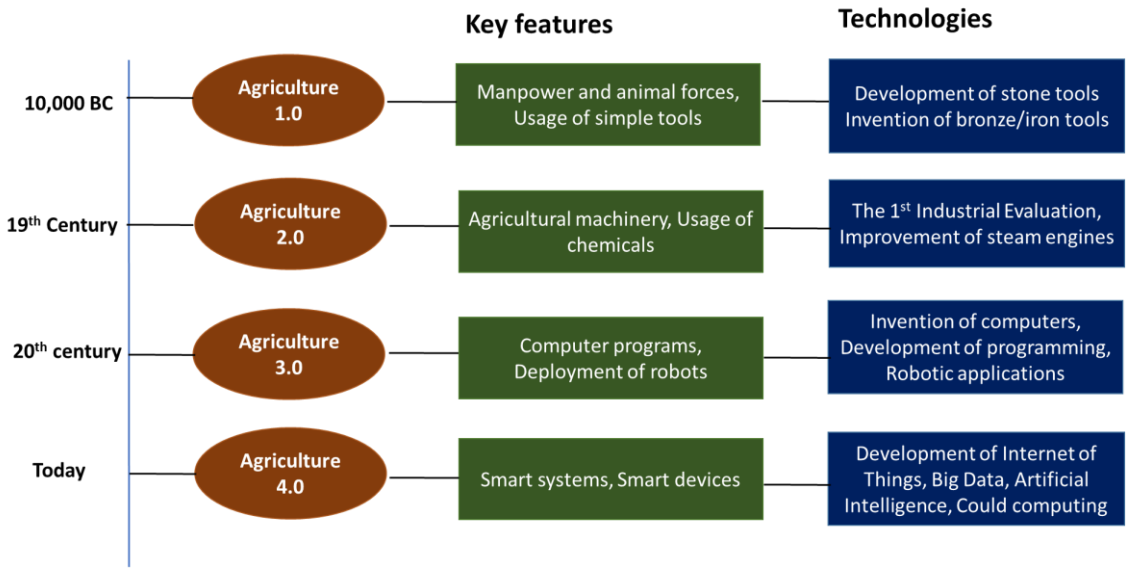

Figure 1.1 Evolution of agriculture.

The recent examples of the advancement in agriculture 4.0 include the development of an Agricultural Decision Support System (ADSS) which enables integration of regional weather forecast and agricultural practices using the human-computer system (Thorp et al., 2008). The classic example is the Watson Decision Platform provided by IBM which integrates the agricultural needs with regional weather forecasting using a cloud computing-based system (Czimber and Gálos, 2016). There are Unmanned Aerial Vehicles (UAVs) deployed to collect and track data related to weather so that they can be further analysed using a big data approach of edge computing (Valavanis and Vachtsevanos, 2015).

The AgriSupport II system is another example of edge computing that assists with supporting agriculture through performing an in-depth study of the factors that can impact agricultural output including regional weather condition (De Wit and Crookes, 2013). More specifically, edge computing enables the Adaptive Neuro-Fuzzy Inference System (ANFIS) model for the wire-Electrical Discharge Machining (wire-EDM) prediction model through which elements like meteorological data get collected and are reviewed in context with soil measurement and crop characteristics (Tan et al., 2014).

Non-predictive or inaccurate weather forecasting can severely impact the community of users. For example, farmers depend on the weather forecast for various farming activities such as ploughing, cultivation, harvesting, and other agricultural activities. An inaccurate forecast directly impacts the farmer's ability to perform these activities influencing their ability to manage the resources related to such operations (Ho et al., 2012). Besides, there

are significant risks to life and property loss due to the unexpected weather conditions (Fente and Singh, 2018). As described above, the ADSSs are still relying on the regional weather forecasting for precision farming (Czimber and Gálos, 2016; Thorp et al., 2008). Moreover, the regional weather forecast may not be accurate based on the geographical appearance of the location such as but not limited to, the top of a mountain, land covered by several mountains, and the slope of the land (Mass and Kuo, 1998). Therefore, an accurate, area-specific, and fine-grained weather prediction system would be valuable to the community of users as global/regional forecasting could be inaccurate for local use.

Weather forecasting refers to the scientific process of predicting the state of the atmosphere based on specific timeframes and locations (Hayati and Mohebi, 2007). It has three main stages namely, understanding the current weather conditions, calculating how this would change in the future and refining the details through meteorological expertise (Met Office, 2019). Numerical Weather Prediction (NWP) models utilise computer algorithms to provide a forecast based on current weather conditions. These algorithms are based on a large system of non-linear mathematical equations. More specifically, these models define a coordinate system which divides the earth into 3-dimensional grids. The weather parameters such as but not limited to winds, solar radiation, the phase change of water, heat transfer, relative humidity, and surface hydrology are measured within each grid and their interaction with neighbouring grids to predict atmospheric properties for the future (Lynch, 2006; NCEI, 2019). These NWP models run in major weather forecasting centres with large grids of supercomputers specifically for addressing the global/regional forecast (Met Office, 2019).

Many NWP models were developed recently such as Weather Research and Forecasting (WRF) model for which increasing high-performance computing power has facilitated the enhancement and introduction of regional or limited area models (Oana and Spataru, 2016). As a consequence, the WRF model has become the world's most widely-used atmospheric NWP model due to its higher resolution rate, accuracy, open-source nature, community support, and a wide range of usability within different domains (NCAR/UCAR, 2019; Powers et al., 2017). There are several challenges in NWP models such as the massive computational power required, limited model accuracy for specific geographical area predictions due to the chaotic nature of the atmosphere, the geographical appearance of the location, and reliability issues impacted by the time difference between the current time and forecasting time. Besides, the complexity of such

models poses significant difficulties in their implementation as well (Baboo and Shereef, 2010a; Hayati and Mohebi, 2007; Powers et al., 2017).

There are freely available datasets which can be utilised with the NWP models such as Global Forecast System (GFS) data ("Earth Science" 2018). In particular, the GFS 0.25 degrees dataset which is a freely available highest resolution data is often used by the atmospheric researchers and forecasters. This dataset allows forecasting the weather at a horizontal resolution of about 27 km (Commerce, 2015; Noaa, 2017). This implies that the NWP model can forecast data resolution up to 27 km. The lesser resolution prediction data are calculated by the model based on the results obtained for the maximum resolution. As a consequence, these models are viable for long-range forecast and not only for selected fine-grained geographical locations such as a farm, school, places of interest, and outdoor sports centre etc. (Powers et al., 2017; Routray et al., 2016; Skamarock et al., 2008).

To reduce the computational power of the NWP systems, data-driven computer modelling systems can be utilised (Hayati and Mohebi, 2007). In particular, Artificial Neural Networks (ANN) can capture nonlinear or complex underlying characteristics of a physical process with a high degree of accuracy (Fente and Singh, 2018). Recently, multivariate time-series forecasting deep models such as Recurrent Neural Networks (RNN), Long Short-Term Memory (LSTM), and Temporal Convolutional Networks (TCN) have gained considerable attention due to their superior performance (Jozefowicz et al., 2015; Kim and Reiter, 2017). Weather information are captured by time-series data and thus, the machine learning (ML) regression modelling techniques can be utilised to develop and evaluate Artificial Intelligence (AI) based neural network models for accurate weather predictions (Choi et al., 2011).

1.1 Motivations

This research project is sponsored by an award-winning precision farming service provider based in Yorkshire, North of England, called Precision Decisions ("Precision Decisions | Driving Farming Forwards", 2019). This company provides comprehensive precision services to a community of farmers based on agronomic and practical experiences (Blacker, 2019). The company utilises high-technology systems such as Real-Time Kinematic (RTK) for two-centimetre accuracy Global Positioning System (GPS) data, auto-steer using satellite signals to avoid machinery overlap, Control Traffic

Farming (CTF) to reduce the area of the field carrying traffic to improve soil health, and inter-machine information sharing systems. These technologies are used to provide services to farmers such as soil sampling, yield monitoring, protein monitoring, conductivity scanning, data management, and consultancy. The MIFarm application software provides an interface for the farmers combining those hi-tech services and hardware (Blacker, 2019). Recently, the company has implemented an intuitive tool to assess the variability of a crop/farm using satellite images ("Measure in-field variability from satellite", 2019). Moreover, they have completed the 'hands-free hectare' project successfully; a farm which grows and harvests a crop type entirely using autonomous machines or robots ("Hands-Free Hectare", 2018).

Even with such technologies available for the farmers, they still have to rely on the regional weather forecast for their daily activities. The regional weather forecast might not be accurate depending on the geographical location of the farm (such as the top of a mountain, the slope of the land, a land covered by several mountains, land closer to a sea), or the resolution of the forecast.

As a solution, this research endeavours to develop an accurate, fine-grained, and location-specific weather forecasting model for the farmers. Moreover, a wider set of users who rely on favourable weather conditions could get the advantage of the model, such as places of interest, schools, outdoor sports centres, and larger construction sites. While the NWP models are viable for long-range forecast and not only for a fine-grained geographical area, the proposed model could make a reliable and accurate prediction. This research is a part of the company's on-going development plan to introduce accurate weather forecasting to its MIFarm application (Symcox, 2017).

1.2 Rationale

The accurate weather forecast remains as a key factor of agriculture 4.0 as it helps to address the weather aberrations related aspects. The weather forecasting is integrated around aspects of accuracy, timeliness, usefulness, and the ability to meet the broadcasting needs. The temperature, humidity, wind speed, wind direction, rainfall, and other wealth aspects are part of weather forecasting in agriculture 4.0 (Ozdogan et al., 2017). Therefore, this project investigates how to obtain an accurate, fine-grained, and location-specific weather forecast for a community of users in a specific geographical

area. Concerning the agricultural sector, the farmer becomes the user and the farm is the geographical location. The following data are utilised throughout this study:

- Historical data linked to previous weather systems for pattern identification.
- Local weather station data collected from in-farm sensors such as current temperature, wind speed, wind direction, and soil moisture, etc.
- Predictive data from a well-established NWP model to evaluate the proposed fine-grained weather forecasting model.

Consequently, this work investigates the predictive data, historical data, and weather station data to create a novel forecasting model for the agricultural industry to get an intelligent and reactive output. As many different NWP models for the global and regional forecasts are based on non-linear mathematical equations, the study will seek to experiment with the data-driven approach and develop an area-specific weather forecasting model using cutting-edge deep neural network models. The proposed weather model could overcome the challenges of the existing NWP models.

In this study, the LSTM and TCN deep learning architectures are investigated over RNN since there is an inherent issue of the vanishing gradient problem of the RNN (Jozefowicz et al., 2015). The LSTM and TCN can overcome this vanishing gradient issue but it can easily use up the high capacity of memory (Lea et al., 2017; Shi et al., 2015). The TCN architecture has not been explored in the past for weather forecasting. Also, both the proposed approaches (i.e. LSTM and TCN) have not explored in terms of weather forecasting for as many as ten parameters on a local scale within several hours. Moreover, there is no previous attempt taken to compare the neural network-based weather prediction with an existing, well-established weather forecasting model such as WRF. Therefore, this is an entirely novel concept and very much worthy to study as this could make a considerable contribution to the computing industry, to a community of users, and especially for the agricultural sector.

Historical weather data extracted from the WRF model using GFS data are utilised to evaluate the proposed weather model at the first instant (i.e. using historical weather data or WRF data). Subsequently, the study seeks to use local weather station data to evaluate an area-specific fine-grained local weather forecasting model (i.e. using local weather station data).

1.3 Research Hypotheses

The overall goal of this work is to develop a fine-grained weather forecasting model for a community of users in a specific geographical area using artificial neural networks. This work assesses the extent of optimal performance for weather forecasting among different neural networks using historical weather data and local weather stations data. In achieving this overall goal, the following hypotheses have been formed.

H1: The proposed model is capable of making an accurate short-term and long-term weather prediction compared to an existing and well-established NWF model.

H2: Compared to the existing NWP model, the proposed model has less computational complexity.

H3: The proposed model can be applied for a real-life scenario, that is a fine-grained weather forecasting model for a community of users in a specific geographical area, such as a farm.

1.4 Phases of the research

In addressing the research goal, this study aims to develop and evaluate a lightweight, fine-grained, and novel weather forecasting model for the community of users. This is achieved by separating this study into two phases.

Phase 1:

This phase aims to test the research hypothesis H1 and H2 using the following steps.

- The proposed model is tested for the optimal performances for short-term weather forecasting among different neural network approaches using historical weather station data.
- The short-term prediction accuracy of the proposed model is compared to the prediction accuracy of an existing and well-recognised NWP model, such as WRF.
- The proposed model is tested in context to the ability of long-term weather prediction including the timeframe (i.e. how many hours) this model can make an accurate forecast compared to the existing NWP model.
- The computational complexity of the proposed model is then compared to the existing NWP model.

The main task of this phase was to determine the competence of using neural networks for weather forecasting. Moreover, if the neural network is capable of predicting the weather accurately, the proposed model will be tested to validate its persistency (i.e. the number of hours forward) to accurately predict the weather forecast. This is achieved by developing and evaluating a novel weather forecasting model using modern neural networks. Figure 1.2 depicts a general overview of phase one.

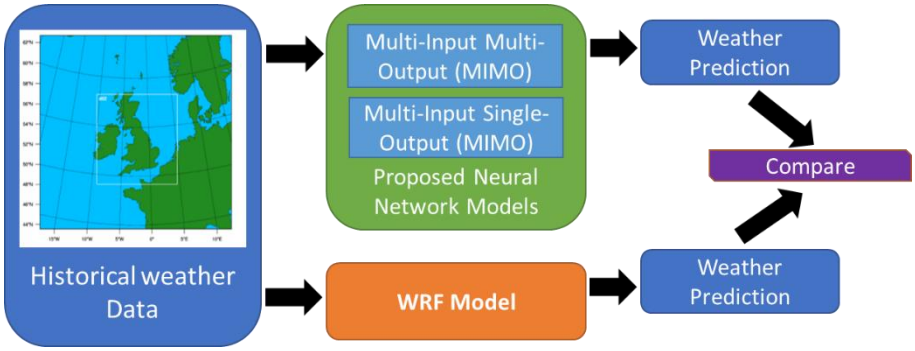

Figure 1.2 Overview of phase 1of the research.

As indicated in Figure 1.2, the WRF model is used to extract historical weather data from the GFS data. These data are integrated with the proposed ML models (MIMO and MISO) to get a weather prediction. The accuracy of the prediction is compared with the state-of-art WRF model prediction.

More specifically, a suitable ML model is proposed by exploring temporal modelling approaches of LSTM and TCN, then comparing its performance with the classic ML approaches such as Standard Regression (SR) and Support Vector Regression (SVR). Secondly, the proposed model is used for a short-term weather prediction and compares its accuracy with the well-established WRF model. Finally, the proposed model is reformed for long-term weather forecasting and is analysed for model accuracy compared with the performance of the state-of-art WRF model. Moreover, this process is used to determine the extent of the proposed neural network model's capabilities in producing weather forecasts accurately.

Phase 1 experiments are successful, meaning that the neural networks can be employed for weather forecasting. In these experiments, the historical weather data extracted from the GFS data running the WRF model are used as inputs for the proposed model. In addition to the NWP drawbacks discussed earlier, a minimum of three hours is required to access GFS data after taking the atmospheric measurements. This includes the time taken to upload data to the website and time taken for the data corrections (National

Centres for Environmental Information, 2019; NCAR/UCAR, 2019). The WRF model also takes time to extract the GFS data and is dependent on the computer system. Hence, the input data used in the proposed model are not the current atmospheric measurement data (i.e. older than 3 hours). Therefore, the study is focused on using the on-time local weather station data for weather forecasting.

Phase 2:

This phase aims to test the research hypothesis H3 by applying the knowledge generated from phase 1 to a real-life scenario with the following steps:

- The applicability of the outcome of phase 1 to local weather station data for short-term weather forecasting to be used by a community of users in a specific geographical area is tested and verified.
- The proposed model is tested for its applicability of long-term weather forecasting with the local weather station data.

The main task in this phase is to develop and evaluate a lightweight, fine-grained, area-specific, and novel weather forecasting system for the community of users utilising modern neural network technologies. The prediction is entirely based on input local weather station data. Figure 1.3 depicts the general overview of phase two.

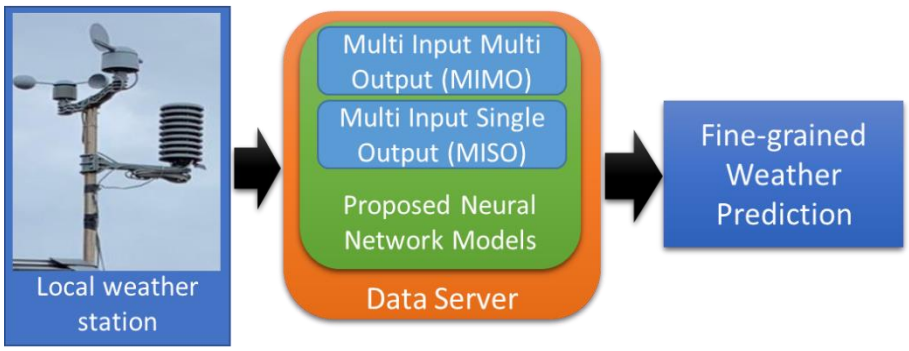

Figure 1.3 Overview of Phase 2 of the research.

As indicated in Figure 1.3, local weather stations are assembled and placed. This transfers time-series weather data to the servers using a Global System for Mobile (GSM) module. The server runs the proposed ML models and these models provide accurate and reliable fine-grained forecasting to the farmers.

Similar to Phase 1, the first part of phase 2 is to compare the performance of the proposed deep model approaches with the classic ML approaches. Then, the proposed model is

used with both short-term and long-term weather forecasting and the predicted results are evaluated concerning the ground truth.

1.5 Original contribution to the knowledge

Timely and accurate weather prediction helps to address the issues related to erratic weather and is a prominent aspect of agriculture 4.0. The main contribution is defining a model by exploring set of models for integrating weather prediction parameters into the software used in designated industry sectors such as agricultural industries for area-specific local weather forecasting for finer temporal and spatial resolution. This model is explored through the combination of parameters from global weather forecasting as well as local weather stations using an Artificial Neural Network to identify weather patterns and outputs are aligned with domain software recommendations. In addition to the main contribution, there are other contributions to the knowledge, such as;

- A complete neural network-based weather forecasting model up to 10 input/output weather parameters.
- Comparative study of a neural network-based weather prediction with a well-established and existing NWP model.
- Comparative study of classic machine learning approaches with cutting-edge deep neural network approach for weather forecasting
- Understanding the impact of using more than four interrelated weather prediction input parameters for a neural network-based weather forecasting model.
- Applying the TCN deep learning approach for weather forecasting.
- Exploration of deep learning and their usefulness in weather prediction.

1.6 Thesis outline

The rest of this thesis is organised as follows. Chapter 2 focuses on the background and literature review. It consists of an in-depth literature review of the WRF model, sensor technology to measure weather parameters, and neural network technology for weather forecasting while identifying the gaps in the knowledge. Besides, this chapter defines the methodology used to address the aim of this research in detail. Chapter 3 focuses on the research approach and methodology. This chapter consists of different approaches and strategies that have been followed and the methodology to address the research goal and research hypotheses. The approach to validate the research hypothesis is also discussed

here. Furthermore, this chapter discusses the data collection strategies, preparation for the study, and a detailed explanation of how to collect and prepare historical weather data and local weather station data.

Chapter 4 discusses the proposed model to answer the research goal and hypotheses. Chapter 5 focuses on the presentation of evidence and analysis of the findings by evaluating the hypothesis using the data-driven approach. This chapter presents all the evidence of the success or failure and answers the research goal and hypotheses. The final results are analysed in this section and further improvements are suggested. Chapter 6 discusses the conclusion and recommendations along with a summary of the overall research and determines whether the study has exactly answered the research question. The recommendations are grounded in the findings of the research study. The references and the appendices are attached to the document at the end of the thesis.

2 Background and Literature Review

2.1 Introduction

There has been a wide range of research performed in the field of weather forecasting to understand the ways of managing weather by using an appropriate form of forecasting since the technology started to evolve with time. The literature review focuses on using a source of published materials to critically review the research done in the field of weather forecasting; therefore, it can provide necessary direction to further study in the given subject.

There are hydrology-based models of regional and global weather forecasting which use simultaneous non-linear mathematical equations to predict the weather such as WRF. To reduce the computational power of NWP systems, data-driven computer modelling systems can be utilised. In particular, ML and deep learning have the capability of capturing nonlinear or complex underlying characteristics of a physical process with a great accuracy (Fente and Singh, 2018). Therefore, the study sought to consider developing a fine-grained area-specific weather forecasting model based on the latest deep neural network approaches.

A detailed discussion about weather forecasting, numerical weather forecasting models, physics parameters and sensor technology for weather forecasting, surface weather parameters, the weather forecast for a community of users, technology in the agriculture industry, and data-driven weather forecasting with artificial neural networks are presented here.

2.2 Weather forecasting and agriculture

The term weather forecasting refers to the scientific process of predicting the state of the atmosphere based on specific time frames and locations (Hayati and Mohebi, 2007).

Numerical Weather Prediction (NWP) utilises computer algorithms to provide a forecast based on current weather conditions by solving a large system of non-linear mathematical equations which are based on specific mathematical models. As described in Section 1, these models define a coordinate system, which divides the earth into a 3-dimensional grid. The weather parameters such as winds, solar radiation, the phase change of water, heat transfer, relative humidity, and surface hydrology are measured within each grid and their interaction with neighbouring grids to predict atmospheric properties for the future (Lynch, 2006). Therefore, the NWP technique was developed to address weather prediction issues by using a collaborative approach with neighbouring grids; however, it required a complex set of mathematical calculations.

Current technologies help to forecast are, (1) Now-casting (NC) - provides details about current variables of the weather and make the necessary forecast within 0-2 hours. The weather variables like the temperature of the air, surrounding humidity, the speed of the wind, and cloud study are also completed as a part of this. (2) Very Short-Range Forecast (VSRF) - The weather forecast is provided up to 12 hours and provides a detailed variable study for the weather elements which should get covered as a part of the NC. (3) Short Range Forecast (SRF) - provides weather forecast up to 72 hours and provides a comprehensive report about the movement of rain pattern, clouds, and the strong windfall effectively. These weather technologies are further used by weather channels and government agencies to provide correct information to the communities (Venäläinen et al., 2005).

The growth of agriculture as a core sector across the globe further emphasised the need to develop robust weather forecasting techniques to achieve better yield (Bendre et al., 2015). Calanca and Semenov (2013) argued that weather forecasting is an effective tool that can be applied across the industry. Cai Ximing et al. (2011) stated that agriculture can be the key segment which would obtain significant benefits through adopting weather models such as the WRF model. The agriculture-specific weather forecasting details are acquired through weather models that provide details about rainfall, dew point temperature, snowfall details, humidity specific information, wind speed, and other factors so that precautionary measures can be well adopted (Kenkel and Norris, 1995). Most agricultural activities are carried out in outdoors and are highly dependent on the fluctuation of the weather condition. Therefore, NWP provides weather-related inputs which are analysed from a physical parameter standpoint to do effective weather forecasting (Bauer et al., 2015; Schwoegler, 2003).

The issues faced by the agricultural sector due to irregular weather patterns during the early 19th century triggers numerous researches in the field of weather forecasting techniques. Warner (2010) stated that during the early period of the 19th century, the weather forecasting process was subjective and applied empirical rules. The weather forecasting methods employed were based on diagnostic methods which dated back to 1920s and those weather forecasts were primarily used for tracking the tropical cyclones. This, however, can be done only for the limited regional area. Most of the calculations were done manually whilst the first weather forecasting using computers was performed in the 1950s. The 1970s and 80s have been marked with weather forecasting for atmospheric dynamics based on MOS (Model Output Statistics) (Glahn and Lowry, 1972; Woodcock, 1984). The NWP models were enabled with the use of supercomputers which helped to improve the forecasting skills. Effective predictive metrics were developed over time so that accurate and timely weather forecasting was possible to achieve (Baboo and Shereef, 2010b).

2.3 Numerical Weather Prediction (NWP) models

The early stages of weather forecasting faced accuracy issues. Therefore, a quantitative approach was adopted to develop an effective forecasting approach. Since meteorology adopted a more quantitative approach with the advancement of technology and computer science, the forecast models became more accessible to researchers, forecasters, and other stakeholders. The Numerical Weather Prediction (NWP) concept was proposed by Lewis Fry Richardson in 1922 and its practical use began in 1955 after the development of programmable computers (Hayati and Mohebi, 2007). Many NWP systems have been developed in recently such as the Weather Research and Forecasting (WRF) model. Increasing high-performance computing power has facilitated their enhancement and the introduction of regional or limited area models (Oana and Spataru, 2016).

The Global Spectral Model was developed in 1980 as the first medium-range weather forecasting model by the National Meteorological Centre (Gordon and Stern, 1982). Further, the 3D-Var data assimilation scheme was developed to do advanced weather forecasting along with the AVN (Aviation Model) used by the Environmental Modelling Centre (Xue et al., 2003). All these global weather forecasting models further developed technology specific to other areas previously. Accordingly, climate-based models, air equality models, tropical cyclone models, and ocean models were developed to track output statistics related to weather forecasting effectively (Warner, 2010).

The research scholars have evaluated various weather forecasting models in their studies to get a broader view of the available technology. One such model was of the UM (Unified Model) which was initially developed by the UK Met office for weather forecasting and is effectively applied for accessing weather and climate patterns based on an applied numerical model (Met Office, 2019). The grid point base is used and the time scale and spatial scales were able to be utilised to do high-resolution weather modelling (Lynch, 2006). The WRF model became the world's most-used atmospheric NWP model due to its higher resolution rate, accuracy, open-source nature, community support, and high usability of large diversity within different domains (NCAR/UCAR, 2019; Powers et al., 2017).

2.3.1 Weather Research and Forecasting (WRF) model

WRF Model is one of the widely used weather models due to its applicability in various research and industries just beyond agriculture. The scholars have evaluated this technology from the perceptive of usage and benefits. The WRF model was developed by Norwegian physicist Vilhelm Bjerknes in the latter part of the 1990s as a part of a collaborative partnership with many environmental and meteorology organisations. The model involves solving various thermodynamic equations to build numerical weather-based predictions mainly through different vertical levels (NCAR/UCAR, 2019; Stensrud, 2007). The primary role of the WRF is to carry out analysis focusing on climate time scale via linking physical data between the land, atmosphere, and ocean (Knievel et al., 2007). The WRF model is currently the world's most-used atmospheric model (i.e. over 40,000 registered users in around 158 countries across the globe) since its initial public release in 2000. It is primarily based on simulations and provides high-resolution configuration through nesting options (Knievel et al., 2007; NCAR/UCAR, 2019; Powers et al., 2017).

Michalakes et al., (2005) shared comprehensive details about WRF as an effective weather forecasting model. They describe that the overall model of WRF works as "Rapid Refresh Model" and was intended to serve the purpose of both research and operations. This model's key features include being non-hydrostatic, enables vertical coordination to track atmospheric pressure, and has a higher resolution rate than other weather forecasting models (Michalakes et al., 2005). The model can establish two-way communication through both nesting and parent domain. It is one of the innovative software architectures that provide effective weather forecasting at the global level or regional level (Gochis , et al., 2013).

Michalakes et al., (2005) have further stated that the WRF model can be run in two different modes: 1) Ideal cases - use artificial initial conditions generated from the analytical procedures; 2) Real cases - use initial conditions created by assimilating observed data. This research is based on actual weather data; therefore, the ideal case is not considered. To investigate the model for real cases, it is necessary to install and configure WPS (WRF Pre-processing System), WRF ARW (Advanced Research WRF model), and the Post Processing software. The WRF post-processing is not described in this thesis because the main objective is to collect historical weather data for prediction and analyses. Interested researchers can refer to (UCAR, 2019) for further details. The WRF ARW and the WPS share common routines such as WRF I/O API. Therefore, the successful compilation of the WPS depends upon the successful compilation of the WRF ARW model (NCAR/UCAR, 2019).

GRIdded Binary or General Regularly-distributed Information in Binary is often used as GRIB data which is a concise data format commonly used in meteorology to store historical and forecast weather data (Noaa, 2017; Skamarock et al., 2008). According to (Commerce, 2015), Global Forecast System (GFS) GRIB data provides 0.25 degrees resolution and is freely available to download for every three hours. Therefore, the GFS three-hourly data are selected for this project with a horizontal resolution set to 10 km.

The researchers like Baboo and Shereef, (2010) and Hayati and Mohebi, (2007) endeavour that one of the primary challenges in the WRF is its requirement for massive computational power to solve the equations which describe the atmosphere. Furthermore, atmospheric processes are associated with highly chaotic dynamical systems which limit a model's accuracy. As a consequence, the model's forecast capabilities are less reliable as the difference between the current time and the forecast time increases (Hayati and Mohebi, 2007). Besides, the WRF is a large and complex model with different versions and applications leading to a need for greater understanding of the model, its implementation, and the different options associated with its execution (Powers et al., 2017). The GFS 0.25 degrees dataset is the freely available highest resolution dataset for the WRF model. This allows the user to forecast weather data at a horizontal resolution of about 27 km (Commerce, 2015; Noaa, 2017). This implies that the user can predict data with increased accuracy up to 27 km. The model calculates the fewer resolution data based on the results obtained. Thus, the model obtains better results for long-range forecast and not only for a selected geographical region, such as a farm, school, places of interest. (Powers et al., 2017; Routray et al., 2016; Skamarock et al., 2008).

2.4 Physics parameters and sensor technology for weather forecasting

The researchers have emphasised that atmospheric physics plays an important role in weather forecasting approach, therefore, relevant information were collected in the given field. The weather forecasting model based on atmospheric physics was initially proposed by Lewis Fry Richardson, an English scientist who used the numerical process to make weather predictions in 1922 (Richardson et al., 1993). The physics parameters are used to perform "Probabilistic weather prediction" which includes the study of both weather quantities and events. The NWP model uses the physics-based parameters by taking inputs in the form of physical parameters, lateral boundary conditions, and doing forecasting based on the initial conditions (Michalakes et al., 2005). These physics parameters set the necessary equations based on thermodynamics and fluid dynamics to analyse weather-related data and to evaluate the necessary rate of change in weather effectively. The physics parameters help define the time-stepping procedure, therefore, desired weather forecasting is done on time by using the computational grids and linking it with other weather-based physics elements (Sawyer, 1962).

The sensor-based technology is used to collect critical physics-based parameters from a weather satellite, radiosondes, and through other observation systems such as local weather stations (Sawyer, 1962; Sellers et al., 1995). These physics parameters also incorporate the equations of motion by creating a system-based simulation to do effective weather forecasting (Ho et al., 2012). The term "Parameterization" is also used as a part of physics parameters to deploy various weather-based variables on a single scale such as using grid box and climate model to develop equations of fluid motion for predictive weather forecast operations (Baigorria et al., 2007).

The parameters of weather forecasting play an important role. Therefore, researches like Pielke (2013), Yáñez-Morroni et al. (2018) and Sawyer (1962) have shared a comprehensive understanding of the critical parameters which are part of the weather forecasting model. The physics-based parameters that impact the weather such as atmospheric pressure, temperature, wind direction, wind speed, dew point, snow, rain perception, water droplets, humidity, and other factors are analysed from a physical parameter standpoint to do effective weather forecasting (Pielke, 2013). Ecology-based physical parameters are also obtained through evaluation of the distribution of sunlight, analysis of atmospheric elements like gases, water vapour, and oxygen to facilitate

weather forecasting (Yáñez-Morroni et al., 2018). The meteorological parameters around pressure, temperature, humidity, and precipitation are used to develop physics parameters and are further linked to the simulation for performing necessary weather forecasting and interpretation. The physics parameters are influenced by the earth location, the horizon, albedo, and precipitation. These parameters are set for short wave and long wave spectral range as it facilitates necessary meteorological measurement and climatology related findings to link with the weather forecasting (Sawyer, 1962).

A weather satellite can provide physical data from large weather systems and is capable of receiving weather data on a worldwide scale. The satellite can provide physics-based data related with the formation of clouds, track hurricane formation, humidity formation, ocean movement, and other key details (Surussavadee and Aonchart, 2013). Doppler radar is another key sensor that gathers physics parameters through measurement of sound waves. Radar antennae are used to broadcast the sound waves and collect physics data from dust particles, air-based humidity or through ice crystals. Reflection of the sound waves provides a picture of the precipitation for tracking wind progression for weather forecasting (Heilig, 2009). GPS (Global Positioning System) enabled weather balloons are also used to measure the condition of the weather by placing them at high altitude to collect vital physics-based parameters such as temperature, atmospheric pressure, and humidity (Dethloff et al., 2001).

2.4.1 Physics parameters and WRF model

Mitchell et al., (2014) argued that the weather forecast tool WRF provides realistic and seamless weather predictions and acts as a multimodal prediction capability. Different schemes should be designed to conceptualise the necessary parameters and perform uniform predictions. There are multiple physical configurations required for the weather predictions. Credible information are provided by incorporating various modules and using terrestrial information (Mitchell et al., 2014). The "*namelist.wps*" and "*namelist.input*" files need to be configured before running the WRF model for real cases to set up parameters and other initial model conditions (Skamarock et al., 2008). The concepts around plug-compatible physics optimise the WRF model to provide better output (Pielke, 2013). The correlation and coefficient are performed for real values in the model so it can depict the right magnitude difference and compute the values regarding weather forecasting (Surussavadee and Aonchart, 2013).

2.4.2 Surface weather Parameters

The researchers have classified the meteorological data into two main types, namely surface weather data and the upper air data. The surface weather data contains physical parameters that are measured directly by instrumentation at the earth's surface (i.e. somewhere between ground level and 10 meters) (US EPA, 2016). Therefore, the surface weather data can be considered as tangible data and includes air pressure, wind speed, wind direction, rain, rain rate, soil moisture, soil temperature, dew point, snow, heat index, and temperature. (Faroux et al., 2007; Thornton et al., 2014; US EPA, 2016). In contrast, upper air data contains physical parameters that are measured in different vertical layers of the atmosphere (US EPA, 2016). For example, GFS data considered 36 different pressure layers when collecting upper-air data (Hamill et al., 2011; NCAR/UCAR, 2019).

Surface weather data can be observed simply from local weather stations. These are the fundamental data used for weather forecasting and warning messages relevant to the issues being addressed (Gounaris et al., 2010; Mittal et al., 2015). The upper air data can be measured using radars and satellites (Haimberger et al., 2008). Global weather forecasting models combine both surface weather data and upper air data to create weather maps targeting global weather prediction (Met Office, 2019; Surussavadee and Aonchart, 2013). Lahoz et al. (2010) argued that low-resolution weather prediction could be made using only the surface weather parameters. Klein and Glahn (1974), and Gneiting and Raftery (2005) developed a successful local weather prediction model using surface weather data. Therefore, the surface weather parameters can be used for local weather forecasting.

As per the report by Met Office, (2019), agriculture remains heavily dependent on weather-related attributes. The agriculture-specific weather forecasting requires details about rainfall, dew point temperature, snowfall details, humidity specific information, wind speed, and other related factors to adopt the precautionary measures effectively (Cai Ximing et al., 2011).

2.5 Weather forecast for a community of users

The researchers have identified that weather forecasting is a chaotic and data-intense process, therefore, it is required to simplify the process of the weather forecast (Baboo and Shereef, 2010b; Hayati and Mohebi, 2007; Powers et al., 2017). The accuracy of the

climate and weather is important for the community since their daily lives are influenced by the weather greatly. Therefore, analysing weather in the right way to have a high degree of accuracy can be significantly useful to the end community of users. Effective weather forecasting can help the community in various ways such as, but not limited to, helping farmers to be productive based on the predicted weather conditions such as rain-related weather information to start the harvest, to provide right care to the crops, and human lives could be saved from natural disasters like hurricane, droughts, lightning, heavy rains, and airlines. The shipping industry also needs weather information about wind conditions, cyclones, and water movement to facilitate safe commutation (Baboo and Shereef, 2010b; Calanca and Semenov, 2013).

Weather forecasting incorporates the urban meteorology principles to provide benefits to a wide range of community. The turbine mills need weather forecasts specific to wind energy to manage electricity manufacturing. The government also sources it as a community need input for the global movement of greenhouse gases, hail, snow, and wind to adopt necessary environmental actions. The fishermen need forecasting about offshore weather before going out to the sea. Therefore, it is considered that weather forecasting is a requirement of the entire global community and is capable of effectively helping every human being directly or indirectly (Ho et al., 2012). Therefore, the common theme identified through a review of relevant research highlights that weather forecasting allows numerous significant benefits to the community beyond just agricultural usage.

2.6 Technology in Agriculture

Real-Time Kinematic (RTK) is one of the cutting-edge technologies used in the agricultural industry for two-centimetre accuracy. The Global Positioning System (GPS) data for farming machinery are used for activities such as fertilising and ploughing. Some other cutting-edge technologies utilised by the agricultural sector are an auto-steer system which uses satellite signals to avoid machinery overlap, Control Traffic Farming (CTF) to reduce the area of the field carrying traffic to improve the soil health, and inter-machinery information sharing systems for sharing specific information related to the current job. Real-time Nitrogen status of the crops can be measured by the latest equipment Yara N-Sensor. Topcon receivers are utilised to the RTK guidance system. 'Hand-Free Hectare' and 'Satellite Catapult' are on-going researches in the agriculture industry experimenting in farming a field autonomously without human contribution and enabling the use of satellite observations to detect variability in the field respectively

(Blacker, 2019). Even though such cutting-edge technologies are available to the farmers, they still rely on the regional weather forecast for their day-to-day farming activities.

2.6.1 Weather modelling in the Agriculture

The researchers like Venäläinen et al., (2005) and Baboo and Shereef, (2010) have focused on providing an understanding on the hydrology-based approach of the weather forecasting model. WRF uses the hydrology-based model to perform atmospheric research on the climate and help the agricultural industry with strategic decision making. Therefore, farmers can use effective cultivation, dairy farming can use the right method for cattle breeding, farming products can be well protected from rainfall, the wind, haze, and related adverse weather conditions (Venäläinen et al., 2005). Weather forecasting technology is also upgraded regularly to integrate it with other agricultural practices (Baboo and Shereef, 2010b). The WRF also deploys the satellite radiance analysis to collect both global and regional level weather data. Therefore, effective forecasting can be done for related agricultural industries such as dairy farming, farm product manufacturers, and agricultural packaging to be able to manage daily operations based on the conditions (Cai Ximing et al., 2011).

Visualisation techniques like weather reports, wind and rainfall movement details are currently used in various regional NWP models to help agricultural sector to understand weather-related elements (Baigorria et al., 2007). Table 2.1 shows a summary of the state-of-the-art weather forecasting models which can be used in the agricultural sector with their pros and cons.

Table 2.1 Comparison of various weather forecasting models.

Weather forecasting model	**Pros**	**Cons**
Computer algorithms based early weather forecasting models (Innocenti et al., 2017; Reddy and Babu, 2017).	Uses computer devices for calculations Hydrostatic Ideal for limited area forecasting Available the open-source code Ideal for area-specific weather forecasting with a limited number of parameters	Uses complex statistical-based and non-linear mathematical equations High use of computer power Need a detailed understanding of algorithms Requires long processing time Requires constant adjustment to manage a perfect weather forecast

Weather Research and Forecasting (WRF) model (Powers et al., 2017; Skamarock et al., 2008).	Uses computer devices to calculations Non-hydrostatic Enables vertical coordination to track atmospheric pressure higher resolution rate Open-source Update regularly Ability to establish two-way communication through nesting Provide effective weather forecasting at the global level or regional level Not requires a sophisticated understanding of algorithms	Uses complex non-linear mathematical equations Requires high computation requirement Less reliable as the difference between the current time and the forecast time increases Needs a greater understanding of the model, its implementation and the different options associated
Global Spectral Model (Díaz et al., 2016; Tenzer, 2017).	Uses computer devices to calculations Hydrostatic/ non-hydrostatic High-resolution medium-range weather forecasting Open-source	Uses complex non-linear mathematical equations Requires high computation requirement Needs a greater understanding of the model Requires long processing time
UM (Unified Model) (Cullen, 1993; Kelly et al., 2019).	Uses computer devices to calculations Non-hydrostatic Enables vertical coordination Higher-resolution rate Two-way communication through nesting Can use for both global and regional level Not requires a detailed understanding of algorithms Update regularly	Requires high computation requirement to complex non-linear mathematical equations Requires long processing time Less reliable as the difference between the current time and the forecast time increases Needs a greater understanding of the model for installation Not open source
Aviation Model (AVN) (Xue et al., 2003).	Uses computer devices Hydrostatic High accuracy for a limited number of parameters such as wind turbulence data Open-source Update regularly	Limited information about the weather about aviation-related factors Uses complex non-linear mathematical equations and high computer power Requires long processing time Needs a greater understanding of the model

High-Resolution Limited Area Model (HIRLAM) (Cats and Wolters, 1996; Korsholm et al., 2008).	Uses computer devices Hydrostatic/ non-hydrostatic High-resolution regional weather forecast Open-source	Large systems of mathematical equations and requires high computer power Not suitable for large-area forecasting Requires long processing time An essential requirement to a detailed understanding of the model
Regional Atmospheric Modelling System (RAMS) (Cotton et al., 2003; Gómez et al., 2016).	Calculations are carried through high-performance computer devices Nonhydrostatic Can use for both global and regional level Higher-resolution rate Not requires a detailed understanding of algorithms	Requires massive computational power to solve mathematical equations Requires long processing time Not open source Less reliable as the difference between the current time and the forecast time increases
European Centre for Medium-Range Weather Forecasts (ECMWF) (Benedetti et al., 2009; Rémy et al., 2019).	Ideal for global weather forecasting Can be used for regional forecasting Uses computers to solve complex mathematical equations Nonhydrostatic It is not essential to have a detailed understanding of algorithms Update regularly	Less resolution for regional forecasting Requires massive computer power to solve nonlinear mathematical equations. Not open source Less reliable as the difference between the current time and the forecast time increases

According to Section 2.1.1 and Table 2.1, there are several challenges identified in the NWP models. The common challenges are that they use high computing power to execute a large number of non-linear simultaneous equations, and it requires a long time for processing. Besides, most of the models discussed in Table 2.1 are suitable for global or regional weather forecasting. As described in Section 2.1, the data-driven computer modelling systems can be utilised to reduce the computational power of NWP systems (Hayati and Mohebi, 2007). In particular, ML and deep learning have the capability of capturing nonlinear or complex underlying characteristics of a physical process with a high degree of accuracy (Fente and Singh, 2018).

2.7 Machine learning and Deep learning

The ML is also a prominent subject of discussion by the researchers when it comes to reviewing weather forecasting models. ML uses a different approach for computing compared with the traditional or conventional programming paradigms. The traditional method follows step by step instructions to solve a problem while the ML enables a system to automatically learn and progress from experience without being explicitly programmed (Harrington, 2012). Therefore, understanding the structure of the data and fit those data into human-understandable models are considered as the main goal of ML (Michie et al., 1994). This goal is achieved by classifying tasks into broad categories and explaining how learning is achieved for each category (Harrington, 2012). ML is a subfield or an application of Artificial Intelligence (AI) (Bifet et al., 2018; Michie et al., 1994).

Supervised learning and unsupervised learning are the most commonly used ML methods (Caruana and Niculescu-Mizil, 2006). The process of learning algorithms from the training dataset is simply called supervised learning. This is achieved by creating/updating an algorithm to map (i.e. algorithm to learn mapping function) the input variable to output variable (Jain, 2018). The corresponding output variable can be predicted when there is new input data with the approximate mapping function process (Brownlee, 2016).

In contrast, unsupervised learning provides more knowledge about data by either modelling the underlying or hidden structure or by distribution of the data. Therefore, this method only uses the input data and not the corresponding output variables in the training dataset (Brownlee, 2016; Jain, 2018). There are common applications of unsupervised ML such as 1) Clustering - dataset is automatically split according to the similarity 2) Anomaly detection - unusual data points are discovered in the dataset automatically 3) Association mining - sets of items frequently appear in the dataset are identified 4) Latent variable models - the number of features is reduced in the dataset or decomposing the dataset into multiple components (Libbrecht and Noble, 2015; Sadoddin and Ghorbani, 2007; Zander et al., 2005).

In supervised learning, the learning algorithm is iteratively making predictions using the input variables. Corrections are made based on the output variables until the algorithm achieves desirable accuracy or acceptable level of performance (Caruana and Niculescu-Mizil, 2006; Goodrich and Arel, 2014). However, the computational complexity is high

in supervised learning as it yields accurate and reliable results/predictions compared to unsupervised learning (Brownlee, 2016; Jain, 2018).

Moreover, there are two main categories in supervised ML, namely regression ML algorithms and classification ML algorithms (Bernardo et al., 1998; Brownlee, 2017). The output variable is the main difference between these two categories where the output variable in classification is categorical (i.e. discrete or categorical) while that for regression is numerical (Brownlee, 2017). Therefore, classification algorithms are utilised to predict the class of given data points such as classification of spam emails and non-spam emails, positive and negative sentiment, types of soils, and types of crops. The regression algorithms are utilised to predict the continuous values such as predicting fuel prices, house prices, weather, and the demand of customers (Bernardo et al., 1998; Brownlee, 2017; LeBlanc and Tibshirani, 1996).

The accuracy is the most significant factor in weather forecasting. Moreover, it is feasible to create a training dataset with historical weather data which consists of both input and output data (i.e. labels). Therefore, the supervised learning method is selected for the proposed fine-grained area-specific weather forecasting model. Besides, weather forecasting is a predictive analysis targeting on predicting continuous values. Therefore, regression ML algorithms are selected for this research. Artificial Neural Network (ANN) or neural network is a type of ML model commonly used in supervised learning (Simpson, 2018).

2.7.1 Machine learning and neural networks

The scholars like Bifet et al., (2018) and Educba, (2018) have explained that ML could be defined as a set of algorithms that analyses the input data, learns from the analysed data, and use that knowledge to discover the pattern for future predictions (i.e. intelligent decisions). The neural network is one set of algorithms used in ML for modelling the data using interconnected neurons (Educba, 2018). The typical examples of ML include Google maps, Netflix, Google search, and Amazon Alexa (Bifet et al., 2018). The examples of neural networks include image recognition, speech recognition, search engines, and image compression (Educba, 2018). In 1950, the idea of the neural network was born with perceptron algorithm which is a simplified model of a human neuron that can accept an input and performs a computational task on that input (Simpson, 2018).

The neural networks process information similar to the human brain (Xin Yao, 1999; Zhang et al., 1998). There are a large number of interconnected processing elements

commonly known as neurons or nodes acting as the basic building blocks for information processing. These neurons work in parallel to solve a specific problem (Abuaqel et al., 2017; Goves et al., 2016). These networks can find a way to solve the problem itself and the operation may be unpredictable (Omidvar and Elliott, 1997). Neural networks allow the creation of computational models to achieve the state-of-the-art performance in many different domains (Zhang et al., 1998). These networks allow modelling based on algorithms and are applied to recognise the patterns while analysing the data (Basheer and Hajmeer, 2000).

2.7.2 Deep learning

Deep learning is a subset of ML (or class of ML algorithms) which uses its hidden layer architecture (i.e. multiple layers) to progressively extract higher-level features from the raw input data (Lecun et al., 2015; Mahapatra, 2019). For example, in natural language processing, lower layers categories letter comes first, second little higher-level categories words and, then higher-level category sentences (Mahapatra, 2019). Gulli and Pal (2017) have stated that deep learning allows stacked neural networks and includes several layers known as nodes as a part of an overall composition. The computation takes place at the node since it allows the combination of data input through sets of coefficients. The activation function gets established based on the input-weight products while signal progresses take place in the network (Shi et al., 2015). There are various layers of nodes that includes neuron-like switches to facilitate managing of the data feed (Walczak, 2019).

Krizhevsky et al. (2012) has argued that the key concepts of deep neural networks include layers of nodes that allow passing of data through multistep processes to enable the recognition of the correct pattern. The input and output layers allow deep learning to follow a composed data analysis approach while it helps with recombining the features from previous neural networks (Lecun et al., 2015). The feature hierarchy allows the handling of large complex data that includes high dimensions and billions of parameters(Goodfellow et al., 2016; Ngiam et al., 2011). Deep learning addresses the challenges of processing raw data and discerning similarities (Goodfellow et al., 2016). Ba and Frey (2013) have stated that neural networks through deep learning allow automatic feature extraction that can be done without the intervention of humans. Neural networks enabled through a deep learning model act as a powerful mechanism to execute multiple threads and allow parallel computations (Goodfellow et al., 2016). There is a

specialised debugger system that concerns the internal structure and facilitates further inference and training (Mahapatra, 2019; Ngiam et al., 2011).

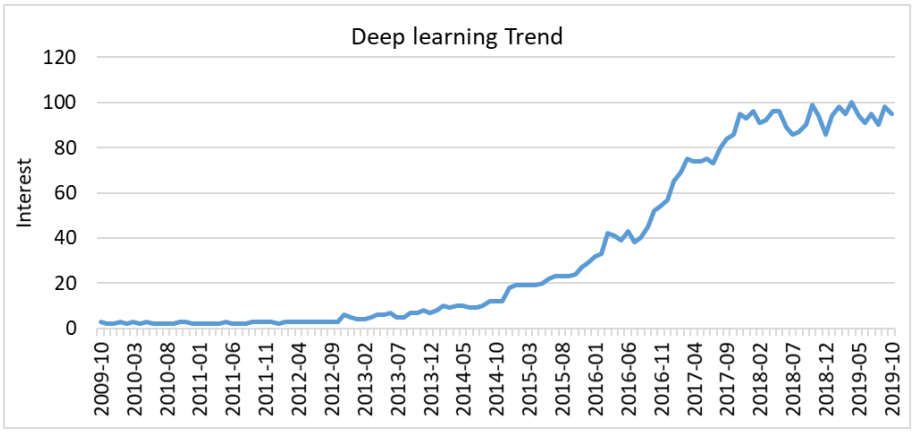

Figure 2.1 Trend of 'Deep Learning' on google (image Reference ("Google Trends," n.d.)).

Deep learning has gained significant popularity during the last decade due to its supremacy in terms of accuracy when training with larger datasets (Esteva et al., 2019). The Google Trends graphs in Figure 2.1 shows that the attention drawn by deep learning approach during the last ten years (From October 2009 to October 2019). The Y-axis represents the search interest relative to the highest in the chart (i.e. the value 100 is the peak popularity), and X-axis represents the Year.

As depicted in Figure 2.2, one of the principal advantages of deep learning is that the learning algorithms can learn high-level features from data in an incremental manner allowing elimination of the need of domain expert and hard-core feature extraction (Goodfellow et al., 2016). In contrast, a domain expert needs to identify most of the applied features of the traditional ML to reduce the complexity of the data and make patterns more visible for the learning algorithms (Kapoor, 2019; Mahapatra, 2019).

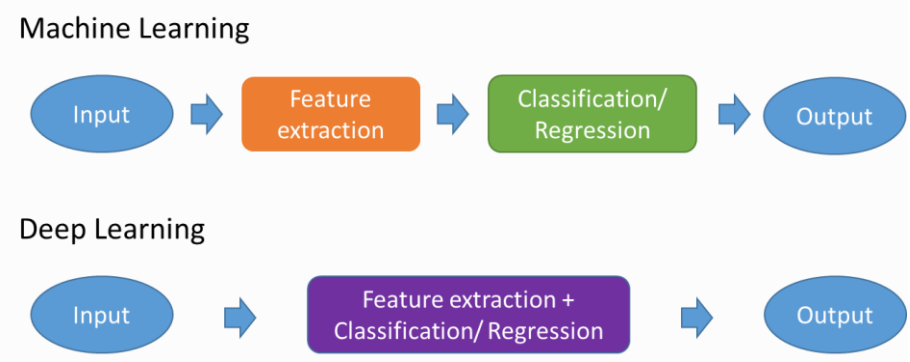

Figure 2.2 Feature extraction: Machine learning vs Deep learning.

Subsequently, deep learning works towards solving a problem end-to-end while ML will breakdown the problem statement into different parts, solve them individually, and combine the results at the end. For instance, deep learning takes the image as input and provides the location and name of the object at the output in the object detection problem. In ML, a bounding box object detection algorithm is required to identify a possible object as the input to recognise relevant objects (Moradi et al., 2019; Zhao et al., 2019).

Both traditional ML and deep learning revolve around data to deliver intelligence or accurate prediction (Moradi et al., 2019). One of the key differences between those two architectures is performance. In general, deep learning is not performing well for a small dataset whilst ML yields comparatively better results as it has to learn through pre-programmed defined criteria (Moradi et al., 2019; Zhang et al., 2019). Moreover, the training process takes long-time by deep learning algorithms due to larger datasets and a higher number of parameters. In contrast, the training process takes less time by the ML algorithms, usually a few seconds to a few hours (Kapoor, 2019; Mahapatra, 2019). In the testing phase, a deep learning algorithm takes less time to run when compared with the ML algorithms (Moradi et al., 2019).

The deep learning models are performing well for larger datasets targeting higher accuracy (Goodfellow et al., 2016). Besides, it is feasible to present larger dataset with weather information for the training purpose. Moreover, accuracy is the most significant factor in weather forecasting. Besides, a deep learning approach is capable of solving a problem end to end, able to learn high-level features from data in an incremental manner, eliminate the need of domain expertise, hard-core feature extraction, and takes less forecasting time compared to the traditional machine approaches even though the training time is high. Besides, it is practicable to produce larger labelled training datasets with historical weather data. The deep learning approach is selected for this research due to the benefits and adaptive nature,

2.7.3 Common deep learning models

There are three main deep learning architectures, namely Unsupervised Pretrained Networks (UPNs), Convolutional Neural Networks (CNNs), and Recurrent Neural Networks (Goodfellow et al., 2016; Ngiam et al., 2011). As described in Section 2.5, unsupervised learning is not considered in this research. Therefore, the UPNs are not discussed here and the interesting researchers could refer to (Goodrich and Arel, 2014; Liu et al., 2015). The CNN accepts fixed-size inputs, generates fixed size outputs, and

originally designed with recognised images/video (i.e. related to the computer vision discipline although this can be applied in other areas) (Kalchbrenner et al., 2014; Kim, 2014). Moreover, a two-dimensional squared sliding window is used in the CNNs along an axis and convolute to identify patterns (i.e. convolute with the original two-dimensional image to identify patterns) (Britz, 2015). Therefore, CNNs are ideal for images and classification problems in ML (Britz, 2015; Kalchbrenner et al., 2014; Sermanet et al., 2012). As described in Section 2.5, the classification category is not ideal for weather forecasting. Therefore, CNNs are not discussed further and interesting researchers could refer to (Britz, 2015; Le, 2015; Sermanet et al., 2012).

Although, researchers like Zaremba et al., (2014) have identified a prominent theme that deep learning models hold a complex set of sequences, RNNs are capable of handling arbitrary input/output lengths and use their internal memory to process an arbitrary sequence of inputs (Zaremba et al., 2014). These algorithms are originally designed to recognise sequences (or designed to work with sequence prediction) such as natural language processing and can be used for both classification and regression problems (Chung et al., 2014; Mandic and Chambers, 2001). The internal memory units allow learning and generalising across sequences of inputs rather than individual patterns (Chung et al., 2014). In RNN, each neuron may pass its signal latterly in a given layer, forward to the next layer, and the output may feedback as an input to the network with the next input vector (Mandic and Chambers, 2001). Therefore, RNNs can learn broader abstractions from the input sequences by adding state or memory to the network (Jozefowicz et al., 2015; Le, 2015).

A series of data which are indexed in time order is called as the time-series data. Furthermore, data that represents a state in time can be called as the temporal data. RNNs are ideal for time-series information (Jozefowicz et al., 2015). Regression technique is often employed to develop and evaluate neural network models for accurate weather prediction as the weather information is captured by time-series data consisting real numbers (Choi et al., 2011). Therefore, the RNN is selected for this predictive analysis research.

There are two major issues to address the typical RNNs, namely 1) train the network with backpropagation and 2) gradient vanishing or exploding during the training process (Jozefowicz et al., 2015; Venkatachalam, 2019). In deep neural networks, propagation refers to the forward transfer of the signal of the input data through its parameters to make a decision. Backpropagation refers to altering the parameters in reverse through the

network to minimise information about the error (Yosinski et al., 2014). Therefore, the deep network first guesses about data using its parameters, then the network measure performance with a loss function, and finally the error adjusts the wrong-headed parameters with backpropagation. The recurrent or loop connections are breaking down the backpropagation process in RNNs creating a major issue (Jozefowicz et al., 2015; Yosinski et al., 2014).

The gradient is calculated in RNNs to update the weights of the network (Mikolov et al., 2010). This gradient tends to get much smaller on moving backwards into the network (i.e. in the backpropagation process) resulting in the neurons of the earlier layers learn very slowly as compared with the neurons of the layers appear in the later part of the hierarchy. This is called the gradient vanishing or exploding during the training process and results in taking much longer time by the network training process and decrease in the prediction accuracy of the model (Hochreiter, 1998; Pascanu et al., 2012). The earlier layers in a deep neural network work as basic building blocks as they are responsible for learning and detecting simple patterns. The next layers and the complete network do not work towards in producing accurate results if the earlier layers give improper and inaccurate results. (Hochreiter, 1998; Jozefowicz et al., 2015; Pascanu et al., 2012).

As a solution for the issues related with training the network with backpropagation and the vanishing gradient problem in RNNs, German researchers Sepp Hochreiter and Juergen Schmidhuber have introduced a variation of RNN called LSTM in 1997 (Hochreiter and Schmidhuber, 2006, 1997). The LSTM allows recurrent nets to continue learning over many steps by maintaining a more constant error.

Gated cells are used in LSTM to contain information outside the normal flow of the RNN where information can be stored, written to, or read from a cell much similar to the data in the computer memory (Akram and El, 2016; Breuel, 2015). Therefore, these gated memory blocks that are connected into the layers work as neurons. Compared to the classic neuron, each block has three gates that make it smarter, such as 1) Forget gate - decides what information to discard 2) Input gate - decides which values from the input to update 3) Output gate - decides what to output based on the input and the memory. Therefore, each gated cell is working as a mini-state machine in LSTM networks where gates of the units have weights that have been learnt during the training process (Hochreiter and Schmidhuber, 2006).

The RNN iterative process of making guesses, backpropagation error, and adjusting weights via gradient descent allows the cells to learn when to allow data to enter, leave or be deleted (Akram and El, 2016; Venkatachalam, 2019). Consequently, the LSTM allows creating a large stacked recurrent network to address the complex problems in ML and achieve state-of-the-art-results (Venkatachalam, 2019). Therefore, the LSTM networks are used in many complex real-life applications such as text generation, handwriting recognition, music generation, language translation, and image captioning (Moawad, 2019). Weather forecasting is a complex process due to the chaotic nature of the atmosphere (Fente and Singh, 2018). Moreover, the LSTM is capable of overcoming major issues with the RNNs. Therefore, the deep learning with LSTM approach is proposed for the fine-grained weather forecasting model in this research.

In addition to the LSTM deep neural approaches, the Bi-directional LSTM has taken considerable attraction since its initial induction in 2001 for time series data (Asif Khan et al., 2018). Data are preserved from inputs that have already passed through the LSTM networks using its hidden state (i.e. the LSTM only preserves the information of the past). In contrast, the Bi-LSTM networks will run inputs in two ways, namely from the past to the future and from the future to the past. That is, the Bi-LSTM can run the inputs backwards to preserve information from the future when compared with the LSTM networks (Althelaya et al., 2018; Graves and Schmidhuber, 2005; Salehinejad et al., 2017). Therefore, the Bi-LSTM can preserve information from both past and future using the combined two hidden states. This process is helped by Bi-LSTM for a better understanding of the context. Thus, it targets a more accurate forecast compared to the LSTM networks in sequence-to-sequence applications (i.e. it knows the full inputs at prediction time) (Graves et al., 2013).

The RNN becomes the default choice for sequence modelling due to their superior ability to capture temporal dependencies in sequential data. Specifically, the LSTM has taken considerable attraction due to its great ability to capture long term dependencies (Hewage et al., 2019). In 2017, a variation of deep learning for the sequential modelling named Temporal Convolutional Networks (TCN) was introduced with distinguishing characteristics. The main two characteristics are, the architecture can take a sequence of any length and map it to an output sequence similar to the RNNs, and the convolutions in the architecture are causal meaning that there is no information “leakage” from future to the past (Bai et al., 2018; Roy, 2019).

The TCN has exhibited longer memory architecture than LSTM with the same capacity and constantly performs better than LSTM architectures on a vast range of sequential modelling tasks. Besides, the TCN architecture allows flexible receptive field size, parallelism, variable lengths inputs, stable gradient, capturing local information along with temporal information stable gradient, and low memory requirement for training (Rémy, 2019; Roy, 2019). The TCN architecture is more effective across diverse sequence modelling tasks than recurrent architectures such as LSTM and is regarded as a natural starting point and a powerful toolkit for sequence modelling (Bai et al., 2018). In addition to the proposed LSTM approach, the TCN deep learning approach is also proposed for the fine-grained weather forecasting model due to its distinguishing characteristics and benefits.

2.8 Neural networks and weather forecasting

The closely related neural networks and weather forecasting literature have been discussed by many prominent journals and researchers since they play a vital role in providing direction to the weather forecasting. Neural Networks-based weather forecasting has evolved significantly during the last three decades and has been documented by various scholars accordingly. Before 2000, the Model Output Statistics (MOS) was the most widely used approach to improve the ability of the numerical models to forecast by relating model outputs to observational data (Glahn and Lowry, 1972; US Department of Commerce, n.d.; Woodcock, 1984). A mixed statistical or dynamic technique for weather forecasting was introduced by Kruizinga and Murphy in 1983. The work by Abdel-Aal and Elhadidy (1995) added a new perception to dynamic modelling in 1991. These approaches have limitations and challenges such as massive computational requirements, lack of design methodologies for selecting the model architecture and parameters, and are time-consuming to predict weather forecasts resulting less reliability as the difference between the current time and the forecast time increases (Abdel-Aal and Elhadidy, 1995; Glahn and Lowry, 1972; Skamarock et al., 2008).

An Artificial Neural Network-based minimum temperature prediction system was introduced in 1991 using the backpropagation algorithms (Rumelhart and McClelland, 1987; Schizas et al., 1991). This concept considerably reduced the computational requirements of MOS directing in an effective forecast (Abdel-Aal and Elhadidy, 1995). A snowfall and rainfall forecasting model was introduced in 1995 from weather radar images with ANN (Ochiai et al., 1995). The results have shown that the ANN is more

effective than the traditional cross-correlation method and the persistence prediction method produces a substantial reduction in prediction error. In 1998, Oishi et al. developed a severe rainfall prediction method using AI (Oishi et al., 1998). The development method was unique as it introduced inference (i.e. Knowledge-based) rather than using numerical simulations. A Multi-Polynomial High Order Neural Network (M-PHONN) based rainfall prediction model was developed in 2001 (Qi and Zhang, 2001). This new model has features such as increasing the speed, accuracy, and robustness of the rainfall estimate. Therefore, this model could be used to complement the already established Auto-Estimator algorithms.

A multilayer perceptron network was trained with the backpropagation algorithm with momentum for temperature forecasting in 2002 (Jaruszewicz and Mandziuk, 2002). The results were very encouraging and demonstrated the potential for future weather forecasting applications. In the same year, a comparative study was carried out analysing different neural network models for daily maximum and minimum temperature and the wind speed (Maqsood et al., 2002). The results have shown that the Radial Basis Function Network (RBFN) produced the most accurate forecast when compared with the Elman Recurrent Neural Network (ELNN) and Multi-Layered Perceptron (MLP) networks. In 2005, a rough set of the fuzzy neural network was introduced to forecast weather parameters; dew temperature, wind speed, temperature, and visibility (Li and Liu, 2005). This model has several fuzzy rules and their initial weights were estimated with a deeper network for weather forecasting. Moreover, Hayati and Mohebi proposed a successful model for temperature forecasting based on MLP (Hayati and Mohebi, 2007).

A feature-based neural network model was introduced in 2008 to predict maximum temperature, minimum temperature, and relative humidity (Mathur et al., 2008). Neural Network features are extracted over different periods as well as from the time-series weather parameter itself. In particular, feedforward ANN is utilised in this approach with backpropagation for supervised learning. The prediction results have a high degree of accuracy and this modelling is recommended as an alternative to traditional meteorological approaches (Abhishek et al., 2012a; Reddy et al., 2012; Shrivastava et al., 2012). In 2012, a Backpropagations Neural Network (BPN) was implemented for temperature forecasting (Abhishek et al., 2012b; Nayak et al., 2012). This network has successfully identified the non-linear structural relationship between various input weather parameters. Furthermore, a new hybrid model was introduced in 2014 to forecast temperature which was based on an Ensemble of Neural Networks (ENN) (Ahmadi et al.,

2014). The results suggested that including image data would improve the prediction results. In the same year, a deep neural network-based feature representation for weather prediction model was developed for the temperature and dew point prediction (Liu et al., 2014).

In 2015, eight different novel regression tree structures were applied to short-term wind speed prediction (Troncoso et al., 2015). The author also compared the best regression tree approach against other AI approaches such as Support Vector Regression (SVR), MLP, extreme learning machines, and multi-linear regression approach. The best regression tree yields the best results for wind speed prediction. In the same year, a deep neural network was introduced for ultra-short-term wind forecasting successfully (Dalto et al., 2015). Deep learning with LSTM layers has been introduced to precipitation nowcasting by Shi et al. (Shi et al., 2015). The experimental results show that the LSTM network can capture spatiotemporal correlations and can be used for precipitation nowcasting. In the same year, a model was developed to predict the temperate in Nevada using a deep neural network with stacked denoising auto-encoders with higher accuracy of 97.97% compared with traditional neural networks which had an accuracy rate as 94.92% (Hossain et al., 2015). In 2016, the multi-stacked deep learning LSTM approach was utilised for forecasting weather parameters of temperature, humidity, and wind speed (Akram and El, 2016). The author suggested that the model could be used to predict other weather parameters based on the effectiveness and accuracy of the results.

There was further research done through evaluating traditional ML methods which analysed radiation forecasting in 2017 (Voyant et al., 2017). The author concluded that the SVR, regression trees, and forests have produced a promising outcome for radiation forecasting. In 2018, the Backpropagation Neural (BPN) network's performance was compared with linear regression and regression tree for temperature forecasting (Sharaff and Roy, 2018). As a result, a significantly better temperature prediction was yielded by the BPN. In 2018, short-term local rain and temperature forecasting model was developed using deep neural networks (Yonekura et al., 2018a). The author concluded that the deep neural networks yield the highest accuracy for rain prediction among several ML methods. In the same year, the neural network approach was utilised to create models to predict sea surface temperature and soil moisture (Patil and Deo, 2018; Rodríguez-Fernández et al., 2018).

The above existing weather forecasting models can predict up to a maximum of four weather parameters. Besides, weather forecasting is an entirely non-linear process and

each parameter often depends upon one more other parameters (Elsner and Tsonis, 1992; Glahn and Lowry, 1972; Taylor and Buizza, 2002). For instance, the temperature could be dependent on pressure, humidity, wind, dew point, etc. These larger numbers of interrelated parameters work together aiming towards an accurate weather forecast in a more reliable NWP such as Met Office and WRF models (Met Office, 2019; NCAR/UCAR, 2019). The existing ML and deep learning weather forecasting models have considered only one or up to five parameters for the weather forecasting, mainly on the regional scale often over a long term of days. The selected state-of-the-art ML and deep learning-based systems for weather forecasting and their pros and cons are discussed in Table 2.2.

Table 2.2 Pros and cons of existing machine learning and deep learning weather forecasting approaches.

ML and deep learning-based weather forecast techniques	**Pros**	**Cons**	**Input/output parameters**
Modelling and forecasting the daily maximum temperature using abductive machine learning (Abdel-Aal and Elhadidy, 1995) (Machine learning)	considerably reduced the computational requirements compared to NWP Faster and highly automated model synthesis improved prediction accuracies compared to statistical forecasting models Suitable for long-term prediction	Can use to predict single output parameter Not suitable for area-specific weather forecasting Needs a greater understanding of the model before use	Input: temperature, wind speed, wind direction, pressure, humidity Output: Daily maximum temperature
Snowfall and rainfall forecasting from weather radar images with artificial neural networks (Ochiai et al., 1995) (Machine learning)	Accurate compared to traditional cross-correlation methods 10% less computational training time compared to tradition ANN methods Can be used to area-specific or regional forecasting	Limited to predict a single parameter at a time Complex model Limited to short-term forecasting (up to 3 hours)	Inputs: Snowfall and rainfall Outputs: Snowfall and rainfall
Rainfall estimation using M-PHONN	Increased speed and accuracy compared to traditional ANN	Not suitable for area-specific weather forecasting	Input: Cloud top temperature, cloud

model (Qi and Zhang, 2001) (Machine learning)	Ideal for very short time rainfall forecasting (up to 1-hour) Can be used for short-term forecasting with limited accuracy (up to 6 hours)	Requires satellite data to process Complex model	growth, and rainfall Output: Rainfall
Intelligent weather monitoring systems using connectionist models (Maqsood et al., 2002) (Machine learning)	Accurate forecasting compared to ELNN and MLP Suitable for very long-term forecasting (up to 30 days) Able to predict all three parameters at once using the same model	Not suitable for area-specific weather forecasting High model complexity The accuracy decreases exponentially if the number of days increases	Input: Daily Maximum, daily minimum temperature, and wind speed Output: Daily Maximum, daily minimum temperature, and wind speed
An efficient weather forecasting system using artificial neural network (Baboo and Shereef, 2010b) (Machine learning)	Able to use both short-term and long-term forecasting Reliable short-term forecasting (up to 3 hours) Less model complexity	Limited to single parameter prediction Less reliable as the difference between the current time and the forecast time increases Time-consuming to execution	Input: Pressure, temperature, humidity, wind speed, and wind direction Output: Temperature
A rough set-based fuzzy neural network algorithm for weather prediction (Li and Liu, 2005) (Machine learning)	Can use a single model to predict four parameters Accurate short-term or medium-term forecasting Suitable for area-specific weather forecasting	Complex learning algorithm Not suitable for long-term forecasting Needs a greater understanding of the model before use Need specific equipment to measure the input due temperature	Input: Dew temperature, wind speed, Output: Dew temperature, wind speed, temperature, visibility
Deep neural networks for ultra-short-term wind forecasting (Dalto et al., 2015) (Deep learning)	Results show that careful selection of deep neural networks outperforms shallow ones Can be used for regional or localised wind forecasting	Limited to very short-term forecasting (less than an hour). Complex model Can use to predict single output parameter	Input: Wind Output: Wind
Weather forecasting using deep learning techniques (Salman et al., 2015)	Accurate RNN based forecasting results compared to Conditional Restricted Boltzmann Machine (CRBM), and	Limited to short-term forecasting (up to 3 hours) Vanishing gradient issue	Input: Rainfall Output: Rainfall

(Deep learning)	Convolutional Network (CN) models Faster execution time	Use to predict a single output parameter	
Short-term local weather forecast using dense weather station by a deep neural network (Yonekura et al., 2018a) (Deep learning)	Yield the highest accuracy for rain prediction compared to Support Vector Regression (SVR) and Random Forest (RF). Able to predict data accurately up to an hour Use local weather stations to gather input data	Limited to very short-term forecasting (less than 1-hour) Limited to predict single weather parameter at a time (either rain or temperature) High model complexity	Input: Temperature, humidity, pressure, Wind, and Rain Output: rain or temperature
Convolutional LSTM Network: A Machine Learning Approach for Precipitation Nowcasting (Shi et al., 2015) (Deep learning)	Able to produce a state-of-the-art performance for up to 6 hours Suitable for area-specific forecasting Outperformed the fully connected LSTM approach No vanishing gradient issue	Limited to single output prediction Not suitable for regional forecasting	Input: precipitation Output: precipitation
Forecasting the weather of Nevada: A deep learning approach (Hossain et al., 2015) (Deep learning)	Stacked denoising auto-encoder deep model able to predicts accurate long-term temperature Able to use for area-specific temperature forecasting	Limited to single output parameters Not applicable for very short-term temperature forecasting	Input: Pressure, humidity, temperature, and wind speed Output: Temperature
Sequence to Sequence Weather Forecasting with Long Short-Term Memory Recurrent Neural Networks (Akram and El, 2016) (Deep learning)	Forecast general weather variables with reasonable accuracy up to 24 hours compared to the ground truth Suitable for regional forecasting	Limited to predict a single output parameter at a time Complex model Not suitable for area-specific weather forecasting	Input: Temperature, humidity, and wind speed Output: Temperature, humidity, and wind speed
A Deep Learning Methodology Based on Bidirectional Gated Recurrent Unit for Wind Power Prediction (Deng et al., 2019)	Able to predict the wind power up to 6 hours Suitable for both area-specific and regional wind power forecasting	The output contains a single parameter Considerable time consuming to train the network compared to LSTM	Input: Wind speed and wind direction Output: Wind power

As per information from Table 2.2, the surface weather parameters are considered for weather parameter forecasting instead of upper-air parameters, except Qi and Zhang, (2001) and Li and Liu, (2005). This includes pressure, temperature, wind speed, wind direction, wind speed, dew point, rainfall, snow, and humidity. Besides, there is no identified attempt to predict agriculture-related weather parameters such as soil moisture and soil temperature. Moreover, (Deng et al., 2019) have used the bidirectional recurrent network with weather-related input parameters successfully to predict the wind power up to 6 hours. Therefore, bidirectional LSTM experiments in long-term forecasting are compared with the proposed model.

Based on the information from Table 2.2 and other related work, it is evident that further research in the field of weather forecasting is done in context with the following key aspects:

- There has been no attempt to compare an AI-based weather prediction with a well-established and existing weather forecasting model such as WRF.
- There has been little or no attempt to compare traditional machine learning approaches with cutting-edge deep neural network approach for weather forecasting.
- Most of the existing approaches use five or less interrelated input parameters for the neural network-based weather forecasting model.
- A complete AI-based weather forecasting model with up to 10 input/output weather parameters is yet to be explored.
- There has been no attempt taken to utilise modern deep learning approaches of TCN for weather forecasting.

2.9 Summary

The literature summary highlighted the viewpoint of various research scholars in the field of weather forecasting, and it highlights that agriculture dependency on weather has resulted in the rise of various prominent technologies for weather forecasting approaches. The research argued that farmers remain highly dependent on receiving the right forecast to perform various farming activities. Even farmers using modern cutting-edge technologies for their day-to-day activities still rely on the regional weather forecast for their farming activities. As a solution, this research is focused on developing a weather forecasting model for a selected geographical area, such as a farm. Data-driven computer modelling systems can be utilised to reduce the computational power of NWPs. Deep

models for multivariate time-series forecasting often use RNN, LSTM, and TCN. Such models have attracted considerable attention due to their superior performance.

Based on the related work and critical review of literature, it is evident that there has been no attempt to compare an AI-based weather prediction with a well-established and existing weather forecasting model such as WRF. Also, there has been very little or no attempt taken to compare traditional ML approaches with cutting-edge deep neural networks for weather forecasting. Most of the existing approaches use less than or equal five interrelated input parameters for the neural network-based weather forecasting model. A complete AI-based weather forecasting model with up to 10 input/output weather parameters is yet to be explored and there has been no attempt taken to utilise modern deep learning approaches of TCN for weather forecasting.

3 Methodology and Data collection

3.1 Introduction

The research approach goes through relevant information collection to prove or disqualify the hypothesis by following a systematic process and to manage the sharing of logical findings. This is an empirical-based study and is focused on analysing quantitative temporal weather data. As described in Section 1.4, there are two main phases in this research. The first phase aims to determine the competency of using neural networks for weather forecasting. If this phase becomes successful, the research focus is moved to Phase 2 which is to develop and evaluate a lightweight, fine-grained, and novel weather forecasting model for the community of users using neural networks.

The data collection and preparation are discussed in the second part of this chapter. The first phase of this research experiments with the historical weather data or WRF data and phase two experiments with the local weather station data. Besides, this section also discusses creating, training, testing, and validation of both the datasets for ML purposes.

3.2 Research approach and methodology

As described in Section 1.4, there are two main phases in this research. The first phase aims to determine the competence of using neural networks for weather forecasting. This phase tests the research hypothesis H1 and H2. If this phase is successful, the research focus is moved to Phase 2, which is to develop and evaluate a lightweight, fine-grained, and novel weather forecasting model. This phase tests the research hypothesis H3. In both Phases as described in Section 1.4 and Section 2.7.3, a suitable ML model is proposed by exploring the temporal modelling approach of LSTM and TCN and compared its performance with classic ML (i.e. baseline approaches).

To determine the competency of using ML for weather forecasting (i.e. Phase 1), the dataset should have the training analysis, predicted the weather, and ground truth to

compare the prediction. For instance, the dataset should have seven days of data to analyse and predict the next 3-hour forecast and actual weather data after 3 hours (i.e. ground truth) to compare the predicted results. If the present weather data utilise for these experiments, there will be a waiting time to receive the ground truth to compare. Therefore, the historical weather data are recommended (or WRF data) for Phase 1 of this research.

NWP models can forecast data resolution up to 27 km, and the lesser resolution prediction data is calculated by the model based on results obtained (Commerce, 2015; Noaa, 2017). Therefore, the Local weather stations data are recommended to develop and evaluate a lightweight and fine-grained weather forecasting model (i.e. Phase 2) as it uses area-specific data. As described in Section 2.2.2, Surface weather parameters are utilised for both historical weather data and local weather station data.

3.2.1 Surface weather parameters

As discussed in Section 2.8, researchers use surface weather parameters for weather forecasting using ML and deep learning approaches. As presented in Table 2.2, these surface weather parameters include pressure, temperature, wind speed, wind direction, wind speed, dew point, rainfall, snow, and humidity. In literature, there is no identified attempt to predict agriculture-related weather parameters such as soil moisture and soil temperature. As discussed in Section 1.4.2, the main advantage of the surface weather parameters is the ability to measure them directly by instrumentation at the earth's surface.

Therefore, the above weather parameters are selected to be used as the historical weather data for this study. Table 3.1 presents the surface weather parameters for the historical weather data. These ten weather parameters are identified by considering the information from Table 2.2, their usefulness in precision farming, and their ability to extract from GRIB data using the WRF model (Hewage et al., 2019). The surface parameters of wind direction and wind speed can be calculated from the WRF surface variables U_{10} and V_{10} (NCAR/UCAR, 2019). The *XLAT*- Reference Latitude and *XLONG*- Reference Longitude parameters are used with each data point for location identification.

Table 3.1 Surface weather parameters for historical weather data.

Parameter	Description	Measuring Unit
TSK	Skin temperature or surface temperature	^{o}K
PSFC	Surface pressure	Pa
U10	X component of wind at 10m	m/s
V10	Y component of wind at 10m	m/s
Q2	2- meter specific humidity	Kg/Kg
Rainc	Convective rain (Accumulated precipitation)	mm
Rainnc	Non-convective rain	mm
Snow	Snow water equivalent	Kg/m^2
TSLB	Soil temperature	^{o}K
SMOIS	Soil Moisture	m^3/m^3

Similar to the historical weather data, ten surface weather parameters are selected for local weather station data based on the ability to measure them using local weather station sensors and their usefulness in precision farming (Hewage et al., 2020). Table 3.2 shows the weather parameters which are utilised within the research for local weather station data.

Table 3.2 Surface weather parameters for local weather station data.

Parameter	**Description**	**Units**
BM	Barometer	Hectopascals
Pres	Air Pressure	Hectopascals
Temp	Temperature	Celsius
Humid	Relative Humidity	Percentage
WS	Wind Speed	Meters/ second
WD	Wind Direction	Degrees (0-360)
RR	Rain Rate- the intensity of rainfall	Millimetres/hour
Rain	Rain	Millimetre
DP	Dew point	Fahrenheit
HI	Heat Index- The temperature feels like	Celsius

As described in Section 2.7.3, both historical weather data and local weather station data are time-series sequential data. Therefore, sequential data modelling techniques can be applied for these data to create and evaluate a fine-grained weather forecasting model.

3.2.2 Sequence modelling and prediction

The modelling task is to define a network structure which involves time-series surface weather data sequence $x_0, \dots, x_T$ and wishes to predict some corresponding outputs $y_0, \dots, y_T$ at each time. For instance, there are ten different weather parameters in data at a given time $t, x_t = [p_1, \dots, p_{10}]$. The aim is to predict the value y_t at time t, which is constrained to only previously observed inputs: $x_0, \dots, x_t$. Therefore, the sequence modelling network can be defined as a function $\mathcal{F} : \mathcal{X}^{\mathrm{T}+1} \rightarrow \mathcal{Y}^{T+1}$ that produces the mapping $\hat{y}_0, \dots, \hat{y}_T = \mathcal{F}(x_0, \dots, x_T)$, if it satisfies the causal constraints, i.e. y_t only depends on $x_0, \dots, x_t$ and not on any future inputs $x_{t+1}, \dots, x_T$. The main idea of learning in the sequence modelling is to find a network $\mathcal{F}$ which minimizes the loss (ℓ) between the actual outputs and the predictions, $\ell(y_0, \dots, y_T, \mathcal{F}(x_0, \dots, x_T))$ in which the sequences and predictions are drawn according to some distribution.

The WRF model with GFS- GRIB data can produce a large amount of historical weather data. Recurrent Neural Networks (RNN), LSTM, and TCN are extremely expressive models which are appropriate in such a scenario (Gulli and Pal, 2017; Hewage et al., 2019; Jozefowicz et al., 2015; Lea et al., 2017). These networks have attracted considerable attention due to their superior performance based on their ability to learn highly complex vector-to-vector mapping (Elman, 1990; Graves, 2012). The LSTM/TCN is a specialised form of RNN that is designed for sequence modelling (Chung et al., 2014; Elman, 1990). Highly dimensional hidden states $\boldsymbol{H}$ are the basic building blocks of RNN which are updated with non-linear activation function $\mathcal{F}$. At a given time t, the hidden state $\boldsymbol{H}_t$ is updated by $\boldsymbol{H}_t = \mathcal{F}(\boldsymbol{H}_{t-1}, x_t)$. The structure of $\boldsymbol{H}$ works as the memory of the network.

The state of the hidden layer at a given time is conditioned on its previous state. The RNN is extremely deep as they maintain a vector activation through time at each timestep. This will result in a highly time-consuming training phase due to the exploding and the vanishing gradient problems (Jozefowicz et al., 2015). The development of LSTM and TCN architectures have addressed the gradient vanishing issue (Hochreiter and Schmidhuber, 1997). Therefore, the state-of-art LSTM and TCN architectures are considered within this research to minimize the loss $\ell(y_0, \dots, y_T, \mathcal{F}(x_0, \dots, x_T))$ for effective modelling and prediction of time-series weather data.

3.2.3 Neural Network model training

The process of finding the patterns in the training dataset that map the input data attributes to the target (i.e. the answer to predict or label) is called as model training (McDaniel et al., 2016). In supervised learning, model training helps to determine the optimal values for all the 'weights' and the 'bias' form labelled input data (Graves, 2012). There are different controls configured during this process, such as learning rate, optimiser, cost function, epoch, batch-size, and other deep network-related parameters.

3.2.3.1 ***Learning Rate (LR)***

The LR is the most crucial hyperparameter followed by network configuration (Greff et al., 2017). The 'how much to change the model' factor is controlled by the LR in response to the estimated error obtained each time the model weights are updated. If LR is too small, then the model requires a lengthy training process, and if it is too large, the results lead towards an unstable training process (Brownlee, 2019; Gers et al., 1999). Therefore, it is quite challenging to arrange the learning rate in an ML model. To overcome this challenge, the LR scheduler is introduced to adjust the LR during training by reducing it according to a pre-defined schedule (Lau, 2017; Zeiler, 2012). There are three types of LR schedulers, namely, time-based decay, step-decay, and exponential-decay. In time-based decay, the LR is updated by a decreasing factor in each epoch, and in step-decay, the LR drops by a factor for every few epochs. In exponential-decay, the LR is dropped exponentially for every epoch (Chin et al., 2015).

3.2.3.2 ***Optimiser***

Optimisers are generally used in ML networks to minimise a given cost function by updating the model parameters such as weights and bias values (Gulli and Pal, 2017). In simple terms, the model is shaped to its most accurate possible form by 'futzing' with the weights and the optimisers (Pienaar and Malekian, 2019). Stochastic optimisers such as Adam (Patacchiola and Cangelosi, 2017; Zambaldi et al., 2018) and SGD (Li et al., 2017) are widely used to solve the cost function in deep models (Gulli and Pal, 2017; Keras, 2019; Kuo et al., 2018).

3.2.3.3 ***Epoch***

The term of an epoch can be defined as one complete presentation of the dataset to be learned during the model training process (Shoeb and Guttag, 2010). Many epochs are used in learning machines such as feedforward neural networks that use iterative algorisms during the learning phase (Hochreiter and Schmidhuber, 2006). Therefore, the

epoch is a measure which determines the number of times the training dataset is used once it is got to update the weights (McDaniel et al., 2016).

3.2.3.4 *Number of samples and Batch size*

It is well known that the sample is a single row of data in a dataset. Therefore, several samples can be defined as the total number of samples (i.e. total number of rows) in a dataset. In general, the training dataset comprised of many samples. The training dataset can be divided into one or more batches and the batch-size can be defined as the number of samples to propagate through before updating the internal model parameters. The popular batch sizes include 32, 64, 128, and 256. If the sample size is a lower figure, the training process uses less memory and is efficient.

3.2.3.5 *Cost function*

A measure of how good a neural network concerning its given training sample and the expected output can be called as the cost function (Jozefowicz et al., 2015). This is not a vector (i.e. a single value that rates how good the neural network did as a whole) and also depend on variables such as weights and biases. There are two main requirements which satisfy a cost function; namely, it must be able to write the average as it is needed to compute the gradient concerning the weights and biases for a single training data and it must not be dependent on any activation values of a neural network besides output variable (Alexandre and de Sá, 2006; Wen et al., 2015).

There are several cost functions which can be used to calculate the loss in a neural network with LSTM layers such as but not limited to Mean Squared Error (MSE), Mean Absolute Error (MAE), Root Mean Squared Error (RMSE), Quadratic cost, Cross-entry cost, Exponential cost, Hellinger distance, Kullback-Leibler divergence (Joho et al., 2001; Jozefowicz et al., 2015; Mandic and Chambers, 2000). Most of these cost functions are suited for classification of the ML algorithms. The standard cost functions for regression of the ML algorithm are MSE, MAE, and RMSE (Duan et al., 2016; Zhao et al., 2017).

The proposed deep regression models are mainly evaluated using the most common metrics of MSE which is calculated as in Equation 3.1. The MAE and RMSE metrics are used occasionally throughout this study and are calculated as Equation 3.2, and Equation 3.3, respectively.

$$\boldsymbol{MSE = \frac{1}{n} \sum_{i=1}^{n} (y_a - y_b)^2} \quad \textbf{(3.1)}$$

$$\boldsymbol{MAE = \frac{1}{n} \sum_{i=1}^{n} | y_a - y_b |} \quad \textbf{(3.2)}$$

$$\boldsymbol{RMSE = \sqrt{\frac{1}{n} \sum_{i=1}^{n} (y_a - y_b)^2}} \quad \textbf{(3.3)}$$

Where y_a is the actual expected output, y_b is the model's prediction, and n is the number of samples for Equations 3.1, 3.2, and 3.3.

3.2.3.6 *Deep network-related parameters*

The model configuration is one of the key parameters related to the deep networks. This parameter defines the number of layers in the deep network and the different number of nodes in each layer (Jozefowicz et al., 2015).

3.2.4 Neural Network model testing and validation

The testing dataset is used to test the model performance in terms of accuracy. The model performance is the way to evaluate the solution to a problem (Balci, 1994). That is, the trained model is used to predict parameters and compare the results with the labels to calculate the model accuracy. The model accuracy could be calculated as a numerical figure in regression models and the common evaluation metrics are MSE, MAE, and RMSE (Jozefowicz et al., 2015). Each model performance is analysed and is compared to determine the optimal model for weather forecasting as there are different ML models trained with different configurations and controls.

The validation dataset is used to analyse the performance of the optimal model concerning the ground truth. In this research, the validation dataset is also used to compare the performance of the proposed model with the well-established WRF model. The efficiency of the training, testing, and validation process highly depends upon the computer hardware.

3.2.4.1 *Hardware used*

In this study, each experiment is carried out using general-purpose computers with Intel core i7 Central Processing Unit (CPU) having 3.4 GHz clock speed processor which has four cores, eight logical processors, and 32 GB physical Random-Access Memory (RAM). In addition to other basic configurations, these machines are comprised of 8 GB Graphical Processing Unit (GPU) memory.

3.2.5 Neural Network based proposed forecasting model

As described in Section 1.2.2 and Section 2.7.3, the state-of-art LSTM and TCN architectures are suggested for the proposed forecasting model as there are two phases in this study. Therefore, there are four main sections to cover in both Phase1 (steps (a) and (b)) and Phase 2 (steps (c) and (d)). The steps (c) and (d) are investigated only if steps (a) and (b) are successful;

a) Proposed short-term forecasting model for WRF data (Hypothesis H1 and H2)
b) Utilised the proposed model for long term forecasting for WRF data (Hypothesis H1 and H2).
c) Performance of the proposed short-term forecasting model for weather station data (Hypothesis H3).
d) Proposed model for long-term forecasting for Weather station data (Hypothesis H3).

The overall goal of this research can be achieved by following the above steps. These steps also help to test the research hypothesis by following the hypothesis steps, which are described in Section 1.3. In WRF data, short-term refers to 3 hours and long-term refers to 6, 9, 12, 24, and 48 hours. In weather station data, short-term refers to 1 hour and long-term refers to 2, 3, 6, 9, 12, 18, and 24 hours.

3.2.5.1 *Proposed short-term forecasting models for WRF data*

In phase 1 of this research, the proposed deep learning models are trained with different configurations and controls. The results are subsequently evaluated via the Mean Squared Error (MSE). These models are evaluated using WRF test dataset to select the optimal model or a model with the least MSE which can be used as a tool for future forecasting. The selected optimal model is used to forecast the weather parameters for the WRF validation data (Model Prediction) and the model predicted values are evaluated concerning the ground truth. Similarly, the WRF model has been run in forecast mode using the same format GRIB data for July 2018 (WRF Prediction). These WRF predicted values are evaluated to the ground truth. Then, the model prediction is compared with the WRF prediction to determine the possibility to use the proposed model for short-term weather forecasting. The deep learning LSTM and TCN approaches are proposed for the fine-grained forecasting model.

3.2.5.1.1 LSTM

As shown in Table 3.3, six different network configurations are considered for LSTM models. Each network configuration has a different number of layers and each layer consists of a different number of nodes. These configurations have experimented with different controls mainly learning rate and optimiser. These controls can be treated as approximately independent (Greff et al., 2017). The batch-size (=128) and the activation function (='tanh') are kept constant during these experiments as these controls are not significantly affected by the outcome of a regression modelling (Breuel, 2015; Chniti et al., 2017; Greff et al., 2017). The other obvious hyperparameter is data_dim=10 (i.e. the number of parameters in each timeslot), timesteps=56 (i.e. eight timeslots per day and training for seven days), the shape of the training dataset (675,924, 56, 10) where 675,924 is the number of samples in the WRF training dataset followed by data_dim and timesteps.

Table 3.3 Different LSTM layer configurations.

Configuration	**Layer 1**	**Layer 2**	**Layer 3**	**Layer 4**	**Layer 5**
Config1	128	512	512	256	
Config2	256	2048	2048	1024	256
Config3	256	512	1024	512	256
Config4	256	1024	1024	512	
Config5	64	256	512	128	
Config6	128	512	256		

The proposed LSTM models experiment with both fixed learning rate (default LR=0.01) and adaptive LR using the LR scheduler (initial LR=0.01 and is reduced to half of the current LR in every 20 epochs). The both SGD and Adam optimiser experiment with the proposed LSTM deep models. The MSE cost function is selected to find the loss for the LSTM based experiments as this study is based on regression modelling.

3.2.5.1.2 TCN

The proposed deep models using the TCN approach have investigated with different configurations and controls. There are four basic network configurations considered in these experiments such as stack TCN layers of 1, 2, 3, and 4. According to Bai et al., (2018); Lea et al., (2017); Pelletier et al., (2019), the following controls are kept constant within these experiments as they do not impact on the final results significantly in the

regression model for time-series data; kernel size: 2, dilations: 7, dilation values are: 1, 2, 4, 8, 16, 32, 64, batch size-64, and dropout rate-0, learning rate- 0.01.

In TCN, the convolution filter slides over the dataset and it will extract the highest level of feature (Bai et al., 2018; Deshpande, 2019; Sahoo, 2018). There are some specific features related to smaller filter sizes such as a smaller receptive field, the capture of smaller and more sophisticated features, and the ability to extract a vast amount of information, better computationally efficient, better weight sharing, and requirement of significantly more memory. On the other hand, the larger filter sizes have specific features such as larger respective field, the capture of quite generic features, a higher number of internal weights and computationally expensive, easy to learn simple non-linear features, and a need for comparatively smaller memory (Sahoo, 2018). Therefore, both smaller filter sizes and larger filter sizes are investigated with proposed TCN models such as 32, 64, 128, 256, and 512.

It is a convention to apply a nonlinear activation layer immediately after each convolutional layer to introduce nonlinearity to a system that has been computing linear operations in the convolutional layers. The linear and the tanh activation functions work better for the regression problems and Rectified Linear Unit (ReLU) works better for the classification problems (Bai et al., 2018; Deshpande, 2019; Pelletier et al., 2019). Therefore, both linear and tanh activation functions are investigated with proposed TCN models.

3.2.5.2 *Proposed long-term forecasting model for WRF data*

The short-term optimal model is re-tuned for long-term weather forecasts, such as 6, 9, 12, 24, and 48 hours. The long-term weather forecasting model for the WRF data is proposed based on the optimal model which is found in short-term weather forecasting. If this is an LSTM model, then the optimal model is re-tuned for the long-term forecasting timeslots. This is taken as the LSTM-WL (i.e. without loading the optimal model weights-using only the optimal configurations and controls). These models are evaluated with the WRF-testing dataset and calculate the MSE values concerning the ground truth. Similarly, the optimal model is loaded with its optimal model weights and are re-tuned for the long-term forecasting timeslots. This is taken as the LSTM-LW (i.e. loading the optimal model weights and using the optimal configurations and controls). These LSTM-LW models are also evaluated with the WRF-testing dataset.

As described in Section 2.7.3, in contrast to the LSTM, the Bi-LSTM has used two layers; one layer performs the operations following the forward direction (time-series data) of the data sequence, and the other layer applies its operations on in the reverse direction of the data sequence (Althelaya et al., 2018). Therefore, the long-term forecasting is investigated with the Bi-LSTM assuming that Bi-LSTM provides better prediction compared to the LSTM-WL and LSTM-LW. These Bi-LSTM models are evaluated with the WRF testing dataset. The evaluation results of LSTM-WL, LSTM-LW, and Bi-LSTM will be compared to each other and the final model for long-term weather forecasting can be proposed.

On the other hand, if the short-term optimal model is based on TCN then the optimal model configuration and controls are re-tuned for the long-term forecasting timeslots. This is taken as the TCN-WL (i.e. using only the optimal configurations without loading the optimal model weight). Moreover, the optimal model is investigated with loading optimal weights in addition to the optimal configurations and controls. This is taken as the TCN-LW (i.e. TCN model with load optimal weights). These TCN-WL and TCN-LW models are also evaluated using the WRF testing dataset. Finally, a comparison is made between TCN-WL and TCN-LW and a final model for long-term forecasting can be proposed.

Similar to short-term forecasting, the proposed final long-term forecasting model is used to predict weather parameters for the WRF validation dataset for each timeslot. The predicted values are evaluated to the ground truth. Subsequently, the WRF model is run in the forecasting model for the same validation dataset and get the prediction (WRF prediction). This WRF prediction is evaluated to the ground truth. Finally, the model prediction is compared with the WRF predictions to determine the capability of neural networks for a long-term weather prediction for each time slot. This result also helps to determine up to what extent the proposed model can be used for weather prediction if neural networks are capable of doing long-term forecasting.

3.2.5.3 *Proposed short-term forecasting model for weather station data*

This is the starting section of Phase 2 of the overall research and is conducted only if Phase 1 is successful. Moreover, if Phase 1 is successful means that the proposed approach can be utilised for weather forecasting. Similar to the WRF data, a short-term weather forecasting model is proposed using the cutting-edge LSTM and TCN deep learning approaches. Besides, the similar neural network architectures, which are

described in Section 3.2.5.1, are employed with the weather station data. These training and evaluations are carried using the weather station training dataset and the weather station testing dataset. The evaluation results are analysed, and the optimal model is selected as the proposed short-term weather forecasting model. The performance of the optimal model is compared with the ground truth using the weather station validation dataset.

3.2.5.4 *Proposed long-term forecasting model for weather station data*

Similar to Section 3.2.5.2, if the proposed short-term optimal model is based on LSTM, then the performance of different long-term models of LSTM-WL, LSTM-WL, and Bi-LSTM for all timeslots are compared. If the proposed short-term model is based on TCN, then the performance of long-term models of TCN-WL and TCN-WL are. These models are trained/re-tuned using the weather station training dataset and are evaluated using the weather station testing dataset. Based on the evaluation of the results, the optimal model is selected as the proposed model for long-term forecasting. Subsequently, the selected optimal model is used for weather prediction for the weather station validation dataset for each long-term forecasting timeslots and results are compared with the ground truth.

In this research, a suitable ML model is proposed for weather forecasting by exploring temporal deep modelling approaches of LSTM and TCN and comparing its performance with baseline approaches.

3.2.6 Baseline approaches

The proposed LSTM and TCN architectures have been compared with the classic ML approaches such as SR (Bishop, 2006) and SVR (Chang and Lin, 2011). These approaches do not consider the temporal information, instead count as another dimension in multivariate weather data (Lin et al., 2007).

3.2.6.1 *Standard Regression (SR)*

The focus of the SR is to examine the linear relationship between input parameters. There are two different SR modes; simple linear regression- for two parameters, and multiple linear regression- for multiple parameters (Purwanto et al., 2010). In standard regression, the best fit straight-line terminology is employed to establish the relationship between a dependent variable and one or more independent variables. In multiple linear regression, the best fit line is accomplished by reducing the least square error (Kavitha et al., 2016; Ray, 2015). Equation 3.4 represents the simple linear relationship between variables y

and p. As represented in Equation 3.5, the Multiple linear regression equation is quite similar to the simple regression but has more variables (Kavitha et al., 2016; Ray, 2015).

$$\boldsymbol{y = mp + b} \quad \textbf{(3.4)}$$

$$\boldsymbol{y = b_0 + b_1p_1 + b_2p_2 + b_3p_3 \ldots . + b_{10}p_{10}} \quad \textbf{(3.5)}$$

Where y is the dependent variable and $p_1,\ p_2,\ p_3 \ldots\ p_{10}$ are the independent weather parameters, m is the slope of the regression line and $b_0,\ b_1,\ b_2 \ldots\ b_{10}$ are constants. In the SR, there must be a linear relationship between independent and dependent variables and its sensitivity to outliers can significantly affect the regression line and eventually, the forecast values (Ray, 2015).

3.2.6.2 *Support Vector Regression (SVR)*

In contrast to standard regression, the Support Vector Regression (SVR) endeavours to fit the error within a certain threshold. This can be achieved by attracting a maximum number of points towards the boundary of the best fit line or hyperplane. Equations 3.6 and Equation 3.7 demonstrate this process in detail (Bhattacharyya, 2018; Kavitha et al., 2016). Different kernels can be utilised with the SVR, namely, '*linear'*, 'radial basis function (*rbf)'* and *'polynomial'*. These kernels map the original non-linear data into a higher dimensional space intending to make it linear. In general, the '*rbf'* has higher accuracy and higher time consumption compared to linear and polynomial (Drucker et al., 1997). The Cost and gamma parameters are needed to tune in SVR for better training and prediction (Bakharia, 2016).

$$\boldsymbol{y = ax + b} \quad \textbf{(3.6)}$$

$$\boldsymbol{-e \ \leq y - ax + b \leq e} \quad \textbf{(3.7)}$$

Assuming that e is the distance between the boundary line and the hyperplane, equation 3.6 shows the general equation of the hyperplane. Where a is the slope and b is a constant. Therefore, the hyperplane must satisfy Equation 3.7. The SVR has minimised this e value to get the boundary lines as close as possible to the hyperplane. Besides, the SVR only takes points within the boundary lines with the least error rate and gives a better fitting model (Bakharia, 2016).

For SVR, the *'linear'* and *'rbf'* kernels are used in these experiments. The parameter C in the linear kernel is selected among the range [0.01 - 10000] in multiples of 10. The parameters C in *'rbf'* is selected as above but γ is selected among the range [0.0001, 0.001, 0.01, 0.1, 0.2, 0.5, 0.6, 0.9]. The grid search algorithm technique is utilised to

optimise both C and γ parameters and they are used with the relevant kernels to train and test the SVR models. The best baseline performance is compared with the proposed LSTM and TCN networks. The proposed approaches and the baseline approaches experiment with historical weather data and local weather station data.

3.3 Data collection and preparation

As described in Section 1.1, there are two types of data utilised within this research.

1) Historical weather data or WRF data.
2) Local weather station data.

3.3.1 Historical weather data (WRF data)

The WRF model is used to extract historical weather data from the GRIB formatted GFS data. As described in Section 2.1.1, the WRF model is an NWP model. This model can be installed and run in two different ways, namely ideal cases (i.e. use artificial initial conditions generated from the analytical procedure) and real cases (i.e. use initial conditions created by assimilating observed data). Ideal cases are not considered as the actual data is observed and utilised in the study.

3.3.1.1 *WRF components*

To investigate the model for real cases, it is necessary to install and configure WPS (WRF Pre-processing System), WRF-ARW (Advanced Research WRF model), and Post Processing software (NCAR/UCAR, 2019). The WRF post-processing is not described in this thesis as the main objective is to collect historical weather data for prediction and analysis. Interested researchers could refer to (UCAR, 2019) for further details.

The WRF-ARW and the WPS share the common routines such as WRF I/O API (WRF Input/ Output Application Program Interface). Therefore, the successful compilation of the WPS depends upon the successful compilation of the WRF-ARW model (NCAR/UCAR, 2019). Figure 3.1 depicts the main components of the WRF model. Data, WRF executable files, and post-processing software are shown in orange colour rectangles, blue colour rounded rectangles, and the green colour terminator, respectively.

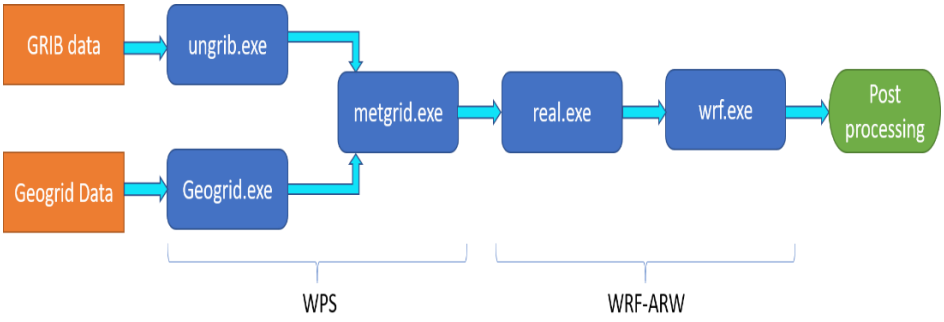

Figure 3.1 WRF block diagram.

Table 3.4 Sample GRIB data sources and their resolutions.

Name	**Resolution**	**Availability**	**Website**
NCEP/NCAR Reanalysis (R1/NNRP)	209 Km 6-hourly	Jan 1948 - Present	http://rda.ucar.edu/datasets/ds090.0
NCEP/DOE Reanalysis (R2)	209Km 6-hourly	Jan 1979 - Present	http://rda.ucar.edu/datasets/ds091.0
ERA-Interim Data	1.125^0–0.703^0 6-hourly	Jan 1979 - Present	http://rda.ucar.edu/datasets/ds627.0
ECMWF's Operational Model Analysis	Varying	Jan 2011 - Present	http://rda.ucar.edu/datasets/ds113.0
NCEP GDAS/FNL Reanalysis	0.25^0 6-hourly	July 2015 - Present	http://rda.ucar.edu/datasets/ds083.3
NCEP GFS/FNL Reanalysis	1^0 6-hourly	Aug 1999 - Present	http://rda.ucar.edu/datasets/ds083.2
GFS Gridded Model Data	0.5^0 24-hourly	Dec 2002- Present	http://rda.ucar.edu/datasets/ds335.0
GFS Gridded Model Data	0.25^0 3-hourly & 12-hourly	Jan 2015 - Present	http://rda.ucar.edu/datasets/ds084.1

The geogrid static data are freely available to download from the National Centre for Atmospheric Research (NCAR) website. These define the simulation domain and interpolate terrestrial data sets to the model grids such as computing latitude and longitude for each grid point, soil categories, land and sea category, terrain height, vegetation fraction, slope category and so on. The simulation domain is defined using the information specified by the user (Fernández-Quiruelas et al., 2015; Mandel et al., 2011). As per section 2.1.1, the GRIB data is used to run a WRF simulation or a forecast. Table 3.4 shows types of these GRIB data available and their resolution.

All the data sources presented in Table 3.4 have global coverage. As per this table, the GRIB formatted GFS data provides 0.25 degrees resolution and is available to freely download once in every three hours. Therefore, the GFS three-hourly data are selected for this study. These GRIB data are converted to an intermediate metgrid file using the geogrid.exe and ungrib.exe in the WPS. The output of this process is taken as the input of the WRF-ARW model which will be able to produce the simulation output or weather prediction. Both metgrid files and WRF outs are in the NetCDF (Network Common Data Form) format. Therefore, special tools or WRF post-processing system are required to read the output(Li et al., 2003; Rew and Davis, 1990).

The namelist.wps file helps to configure the WPS and operates with different weather parameters and boundary conditions based on user demands. The default namelist.wps file produces 257 output weather parameters for a given GFS data. Please Refer Appendix 1 for a sample list of weather parameters. Besides, the WRF model can also be run as a 2-way nested domain. The main benefit of running a 2-way nested domain is that the outer-domain can focus on low-resolution data prediction while the inter-domain can perform higher resolution forecasting. The 2-way nested domain method can improve system efficiency by reducing the usage of computer power for low-resolution data in non-crucial areas (Moeng et al., 2007). As this research only considers higher resolution data, the 2-way nested domain method is ignored.

3.3.1.2 *Collection of historical weather data*

The historical weather data are gathered by running the WRF model for a single domain and using the default namelist.wps file. There are 257 parameters in the WRF output in the format of netCDF. A Python program with the ncdump tool is utilised to extract data from the NetCDF output files. Figure 3.2 shows the sample parameters and sample dataset for the parameter XLAT. These extracted data are then written to a Comma-Separated Values (CSV) file and stored.

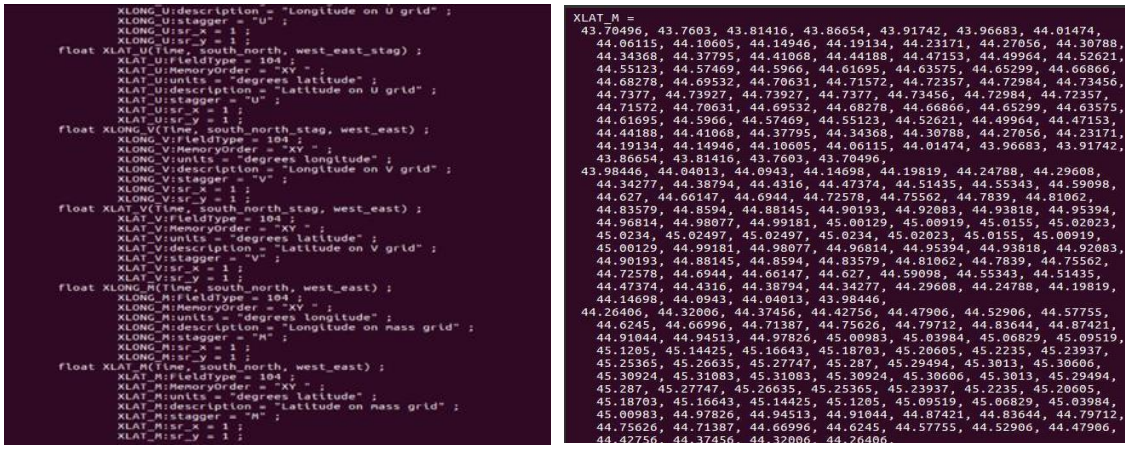

Figure 3.2 Sample output parameters and XLAT data.

Figure 3.3 shows a sample description of a parameter. The selected parameter is the 'accumulated melted snow' and it has a three-dimensional shape of (1, 69, 74). The first, second, and third dimensions are represented by time, latitude, and longitude respectively. The measuring unit of the parameter is kgm^{-2} and this file is saved in the NetCDF format and. This example has a single timeslot dimension but NetCDF files can work with several timeslot dimensions (Rew and Davis, 1990). As described in Section 3.2.1, there are 12 parameters extracted (i.e. ten surface weather parameters and two data reference parameters).

ACSNOM
<type 'netCDF4._netCDF4.Variable'>
float32 ACSNOM(Time, south_north, west_east)
FieldType: 104
MemoryOrder: XY
description: ACCUMULATED MELTED SNOW
units: kg m-2
stagger:
coordinates: XLONG XLAT XTIME
unlimited dimensions: Time
current shape = (1, 69, 74)

Figure 3.3 Sample description of a parameter in a WRF output.

3.3.1.3 *Different dataset for historical weather data*

A total of 12 weather parameters are extracted from January 2018 to May 2018. This is used as the training dataset to train the proposed models. Similarly, the parameters in the June 2018 data are used to test the models. This is done to test different trained neural network models to identify the best model for forecasting. The extracted parameters in July 2018 are considered as the validation dataset which is used as the ground truth to compare perdition from the optimal model. The WRF model is run in forecast mode using the same format GRIB data for July 2018 (i.e. WRF prediction dataset) to evaluate the

overall prediction performance of the WRF model. Each of these datasets has 5451 rows (i.e. 5451 different latitude and longitudes) which covers the whole United Kingdom in 10 Kilometre horizontal resolution.

3.3.1.4 *Data preparation for Historical Weather Data*

The gathered historical weather data are prerequisites to prepare before they can be used in neural network models (Graves, 2012). This dataset should follow the below four steps;

a) Clean data and interpolate to remove NULL values.
b) Normalise data the value in between -1 and 1.
c) Apply the sliding window.
d) Remove rows with NaN values.

It is practically observed that the historical weather data extracted from the WRF model are always clean and contained no NULL values. In this context, 'clean' means that there is no irrelevant data nor any labels, text, characters or symbols in the data. Therefore, the step (a) is optional for the historical dataset. If there are any NULL values, these NULL values must be removed and data must be cleaned before they can be used with the ML models (Graves et al., 2006; Jozefowicz et al., 2015). Therefore, these NULL values are removed and replaced with the arithmetic mean of the two adjacent vertical data items of the dataset (i.e. interpolating the dataset). This is called linear interpolation and it can be achieved by using simple Python code.

After the dataset has been linearly interpolated to include the missing values, each weather parameter is normalized using min and max operation for the training dataset to keep the value in between -1 and 1 using Equation 3.8. It is not mandatory to normalise the independent data for the neural networks in theory. But, relevant studies show that neural network training is often more efficient with normalised data and leads to a better prediction (Rafiq et al., 2001). More specifically, the magnitude of two predictors are far apart if the numerical data are not normalised, and change in neural networks weight has a more relative influence on larger input magnitudes (McCaffrey, 2014).

$$\widehat{\boldsymbol{p_i}} = \mathbf{2}\,\{(\boldsymbol{p_i} - \mathbf{min}(\boldsymbol{p_i}))/(\mathbf{max}\,(\boldsymbol{p_i}) - \mathbf{min}(\boldsymbol{p_i}))\} - \mathbf{1} \qquad \textbf{(3.8)}$$

Where $i = 1, \ldots, 10$ (weather parameters described in Section).

The training data set of both historical weather data and local weather station data have been normalised to keep each value between -1 and 1, and the same maximum and

minimum parameter values are used to normalise the testing and the validation datasets. The predicted values are generated from the neural networks in the normalised format (i.e. input data are already in the normalised form). These data will be de-normalised and converted into the human-understandable format using Equation 3.9. These de-normalised data are used to compare the predicted results with the ground truth.

$$\hat{p}_i = \left(\left(\frac{\hat{p}_i+1}{2}\right) * (\max(p_i) - \min(p_i)) + \min(p_i)\right) \tag{3.9}$$

Where $i = 1, \ldots, 10$ (weather parameters described in Section 3.2.1).

A temporal sliding window is used to prepare the weather data which is in the normalised form. This is a fixed length of data that slide through the data stream to create a new dataset (Frank et al., 2001; Szegedy et al., 2013). Overview of the sliding window process is depicted in Figure 3.4 with window size=6.

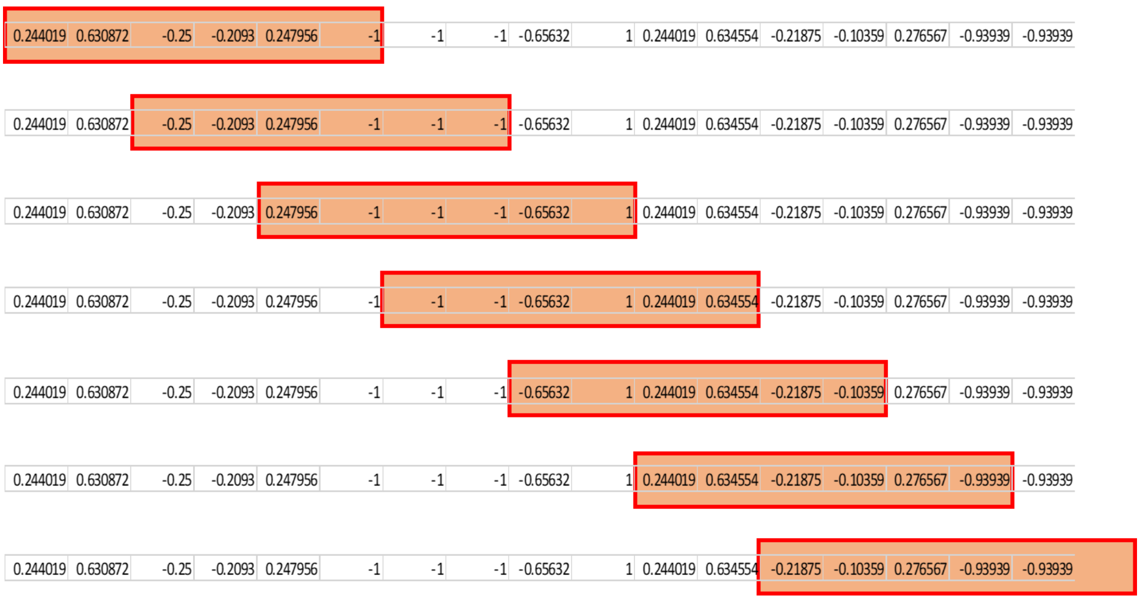

Figure 3.4 Explaining the Sliding window process with window size=6.

Figure 3.3 shows how the sliding window approach works for a single row. In here, the gap between two consecutive windows is two. Therefore, the window is hopped every two cells and creates a record (i.e. new row) for the new dataset. This process is repeated for all the records in the dataset. In this example, the sliding window creates seven rows of data which can directly be used as the input for the neural networks. Subsequently, there are not enough data to create a complete row in the last row (i.e. it needs six fields, but the last record only has five in Figure 3.4 example). This will generate a NaN value to fill the missing figure. Therefore, this new table could contain several NaN values repressing many rows. These rows should be removed before use with neural networks.

Seven days' temporal resolution on each dataset is used as the input to the ML models for historical weather data and the next 48 hours data as a label (i.e. model output or prediction). The gap between two consecutive sliding windows is three hours. Therefore, it will generate new datasets using the sliding window method;

- The historical weather training dataset is ~6.5GB with a sample size of 675,924 (each sample consists of 730 columns of data) – use as WRF training dataset.
- Historical weather testing dataset is ~1.19GB with a sample size of 114,450- use as WRF testing dataset.
- The historical weather validation dataset is ~1.002GB with a sample size of 125373- use as WRF validation dataset.

Furthermore, the WRF model runs in the forecasting model with the WRF validation dataset to get weather predictions. The predicted dataset has 5451 rows with 2480 columns (i.e. ten parameters, eight times per data prediction, for a total of 31 days; 10x8x31=2480). The same WRF validation dataset will be used to get predictions from the neural networks models and compare the output with the WRF model predictions to evaluate the model.

3.3.2 Local weather station data

Local weather stations are placed in farms to measure actual weather parameters. These data will be utilised to experiment with the proposed model for an accurate and fine-grained weather forecasting for a community of users in a specific geographical area. The necessary required components are brought from different vendors and are assembled to construct local weather stations.

3.3.2.1 *Local weather stations*

These are standalone systems directly communicate with the server to send fine-grained temporal resolution (e.g. every15 minutes) of weather data. There are key features of these weather stations such as full computer-controlled kit, weather underground support, use of standard grove connectors, a real-time clock, and fully open-source code which can be edited according to the purpose (Hewage et al., 2020; SwitchDoc Labs, 2016).

The main components of the local weather stations include:

- Weatherboard to attach different weather sensors and data logging to the Raspberry Pi device.
- Raspberry Pi device for computation, data preparation, and logging activities.

- Different sensors such as and not limited to wind vane, anemometer, barometer, thermometer, photodetector, lightning detector, hygrometer, pyranometer, and rain gauge to measure the environmental values.
- Solar panel to power up and operate the entire weather station.
- GSM (Global System for Mobile) module to communicate with the server. The Weatherboard comes with a WI-FI module for wireless high-speed connection to the Internet to send data to the server. The GSM module is useful in locations where WI-FI signals are not available.

Several weather sensors can be attached to the weatherboard to measure over 20 different environmental values such as but not limited to, wind speed, wind direction, rain, outside temperature, outside humidity, lighting detection, barometric pressure, atmospheric pressure, altitude, in-box temperature, in-box humidity, wind gust, rain rate, soil temperature, soil moisture, ultraviolet density, dust count, and light colour (sensing air pollution) (Hewage et al., 2020; SwitchDoc Labs, 2016). Figure 3.5 depicts the block diagram of the main components of a weather station.

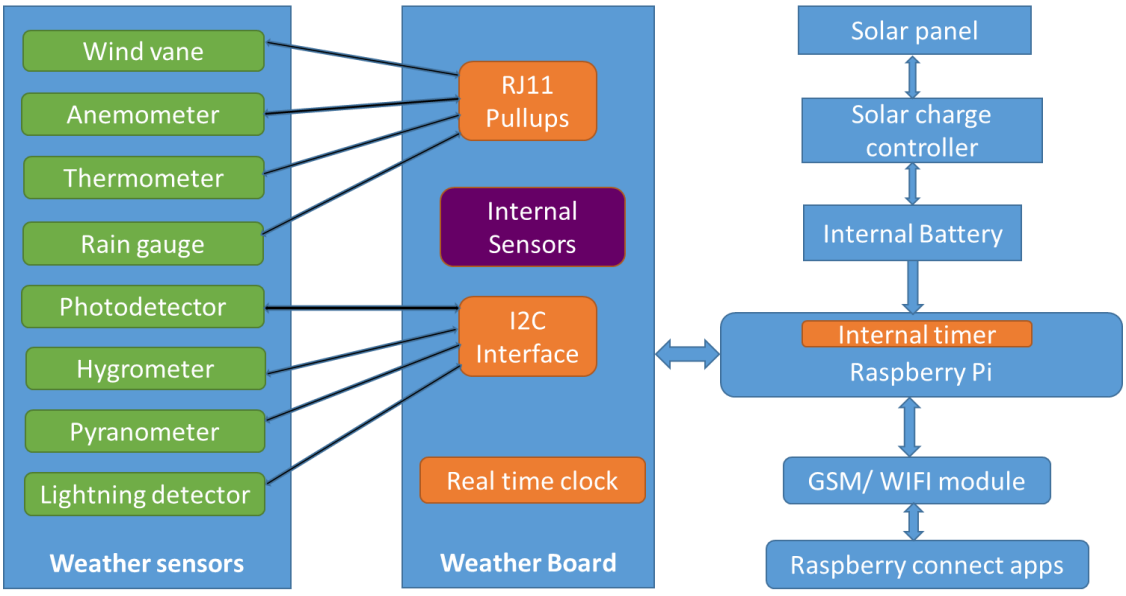

Figure 3.5 Main components of a local weather station.

As depicted in Figure 3.5, the solar panel charges the internal battery. This battery power is used by the Raspberry Pi to control all the components of the weather station. The purple colour internal sensors are applied to measure inbox parameters such as inbox temperature and inbox humidity. The green colour sensors are attached externally to the box to measure outside box environmental values.

The captured time-series weather parameters utilising different sensors are sent to the data server using the GSM module which is attached to the Raspberry Pi. The GSM module uses standard mobile phone signals to transmit data. This process is continued at 15 minutes intervals to record different environmental values within the data server. The Raspberry Pi app can be used as an interface to control the data collection and transmit procedures. In this research, these data are used in the server to develop and evaluate the forecasting models.

As described in Section 3.2.1, there are 10 surface weather parameters utilised within the local weather experiments. That is some weather parameters are ignored among the approximately 20 environmental values. The reason is that the preliminary experiments show that the ignored parameters have minimal impact on the weather forecasting results. These include inbox-temperature, inbox-humidity, wind gust, and altimeter. Moreover, the underground weather is also not measured in these experiments.

There are six local weather stations placed for data logging to the server. The reason for using many weather stations is to train different models for different locations as the forecasting can vary depending on the geographical appearance of the location/farm. Besides, these weather stations are placed to cover various parts of the United Kingdom (UK) such as Yorkshire, Newcastle, Wigan, Liverpool, Coventry, and Sutton.

3.3.2.2 *Different dataset for local weather station data*

The weather data is collected at every 15-minute interval for the period of 20/01/2018 to 22/08/2018 to train the proposed models. Similarly, data have been collected for the period of 23/08/2018 to 11/09/2018 to test and data from 12/09/2018 to 30/09/2018 to validate the proposed model. The neural network optimal model is used with the validation of the dataset to get the weather prediction and then to analyse the results.

3.3.2.3 *Data Preparation for Local Weather Station data*

Similar to Section 3.3.1.3, the gathered local weather stations data are prerequisites to prepare before they can be used in the ML models. Each dataset should follow the same four steps as the above section; a) clean data and interpolate to remove NULL values, b) normalise the data, c) apply sliding window, and d) remove rows with NaN values.

It is mandatory to remove NULL values for the local weather station data as there are some unexpected figures/labels and some NULL values in the data. The reason for these NULL values is that the relevant sensor is unable to measure the environmental value at

that time due to a technical difficulty or error occurred during the transmission data from the weather station to the server (Pearson and Raxworthy, 2009; SwitchDoc Labs, 2016). These NULL values are removed and replaced with the arithmetic mean of the two adjacent vertical data items in the dataset (i.e. linearly interpolating the dataset).

Similar to Section 3.3.1.3, after linearly interpolated, each weather parameter is normalized using min and max operation for the training, testing, and validation datasets to keep the value in between -1 and 1. Subsequently, the temporal sliding window is applied to prepare data and to remove rows of NaN values. Similar to the historical weather data, seven days temporal resolution on each dataset is used as the input to the ML models and the next 48 hours data as a label. The gap between two consecutive sliding windows is taken as 1 hour for local weather station data. As a result, the following datasets are generated.

- Local weather station training dataset is ~665MB with a sample size of 5726 (each sample consists of 6800 columns of data)- use as Weather station training dataset.
- Local weather station testing dataset is ~36 MB with a sample size of 288- use as Weather station testing dataset.
- Local weather station validation dataset is ~36 MB with a sample size of 288- use as Weather station validation dataset.

3.4 Summary

In Phase 1 of this research, the different classic ML and the proposed approach are trained with different configurations and controls. These models are evaluated, and the optimal model has been selected which can be used as a tool for future forecasting. The selected optimal model is used to forecast the weather parameters for the WRF validation dataset, and a comparison is made between model prediction and WRF prediction to determine the possibility of using the proposed model for short-term weather forecasting. Then, the optimal model is re-tuned for long-term weather forecasts and the model predictions are compared to the WRF predictions to determine up to what extent the proposed model can be used for weather forecasting. If Phase 1 is successful, then the research focus will move to use local weather station data as the input for weather prediction as there are several challenges in forecasting with global weather data. Similar steps to the above are followed

with the local weather station data to determine short-term and long-term weather forecasting models for a selected geographical area.

There are two types of data gathered and prepared, namely historical weather data and the local weather station data. The WRF model is used to extract the historical weather data using the GRIB formatted 3-hour GFS data. Local weather stations are built, calibrated, and placed to capture environmental values. These weather stations transmit data to the server. After preparation, these datasets will be used to train, test, and validate the proposed neural network models for the weather forecasting. The local weather stations have the ability to read underground weather such as soil moisture, soil temperature, etc. This requires buying and connecting relevant sensors to the weatherboard. It is recommended to collect the underground weather and get the forecast for these parameters as well. The results will be beneficial to the farmers for decision making. This area will be investigated in future studies.

4 Towards deep learning weather forecasting models

4.1 Introduction

This chapter presents the proposed weather forecasting models utilising the LSTM and TCN deep learning approaches to be used with historical weather data and local weather station data. As described in Section 2.8, Bi-LSTM deep learning approach is also considered to use with the proposed models due to its extensive ability to understand the problem context and thus target a more accurate forecast compared to the LSTM in sequence-to-sequence applications.

The new model is proposed by analysing the existing deep learning-based weather forecasting techniques. Therefore, the two main sections of this chapter are analysing the existing deep learning models for weather forecasting and proposing a weather forecasting model to accomplish the overall research goal and test research hypothesises. Besides, the second part of this chapter discusses the architecture of the proposed models and how it can be used with the proposed deep learning approaches of LSTM and TCN.

4.2 Analysis of existing deep learning weather forecasting models

The existing deep learning weather forecasting models with their differences and contributions are discussed in Table 4.1. Pros and cons of the existing state-of-the-art ML and deep learning approaches are discussed in Table 2.2 in Section 2.8. As discussed in Section 2.7, only deep learning models are considered in this study for the fine-grained weather forecasting model targeting a community of users in a specific geographical area. Based on the performances of these deep models, a model is proposed to solve the regression problem involving fine-grained weather forecasting model for a community of users in a specific geographical area.

Table 4.1 Existing deep learning weather forecasting models, their contributions and drawbacks.

Model	Model description, contribution, and analysis	Drawbacks
Ultra-short-term wind forecasting model (Dalto et al., 2015).	Contributed to a deep neural network for weather forecasting which outperformed the shallow ones compared to the MSE values. High accuracy wind forecast compared to shallow networks. Regional or area-specific forecast.	Single input and a single output parameter. Able to predict the wind parameter for less than 1-hour. Higher computational complexity compared to shallow neural networks. Not considered interrelated parameters during the forecasting process.
Deep neural network rainfall prediction model (Hernández et al., 2016).	Contributed to an architecture based on Deep Learning rainfall prediction model which outperformed the multi-layer perception ML models. Higher accuracy rainfall forecast based on MSE. Area-specific forecast up to 24 hours.	Single input and a single output. Not applicable for regional weather forecasting. Results may not be accurate as the observations of the interrelated parameters are not considered in the forecasting process.
RNN short-term forecasting model (Salman et al., 2015).	Contributed to deep learning RNN for weather forecasting which outperformed CRBM and CN networks. High accuracy rainfall forecast compared to CRBM and CN based on MSE values. Area-specific short-term forecast.	Uses only single input and predicts a single output. High memory consumption compared to the CRBM and CN based models. Applicable only for 6-hour forecast. Not considered the interrelated parameters for forecasting process.
Deep neural network short-term forecasting model (Yonekura et al., 2018b).	Contributed to a deep model which outperformed the SVR and RF compared to MSE values. Higher accuracy rain and temperature forecasting compared to SVR and RF. Predict one parameter at a given time. Area-specific forecasting. Five inputs and single-output (Multi-input Single-output).	Predict only a single output parameter at a time. Able to predict forecast for less than 1-hour. Not applicable for regional forecasting. High computational complexity compared to SVR and RF. Vanishing gradient issue during the training process.
LSTM multi-layered weather forecasting model	Contributed a comparison study of single-layer and multi-layer LSTM models for weather forecasting. The results show that the multi-layer	Applicable only for 6-hour weather forecast. Able to predict a single output parameter at a time.

(Salman et al., 2018).	LSTM yields accurate prediction compared to the single-layer ones. Accurate humidity, dew point, temperature, and pressure forecast compared to the ground truth and based on MSE. Regional or area-specific forecasting. Four inputs and single output at a time (Multi-input single-output)	High computer complexity in multi-layer LSTM models compared to the single-layer models. Requires specific hardware such as GPU memory units for a productive output. Uses up much memory in storing partial results for their multiple cell gates in the case of the long input sequence.
Precipitation nowcasting model (Shi and Dustdar, 2016).	Contributed a convolutional LSTM Network and outperformed the fully connected LSTM approach for precipitation nowcasting. Accurate precipitation forecasting comparatively to the ground truth based on MSE values. Area-specific very short-term forecast.	Able to predict less than 1-hour forecast. Single input and a single output. Prediction might not accurate as interrelated parameters are not considered. Requires GPU memory units for a productive output. Not suitable for regional forecasting.
DNN based feature representation model (Liu et al., 2014).	Contributed a DNN model which represents the features of the raw weather data layer by layer which outperformed the classical SVR. Highly accurate temperature, dew point, pressure and wind speed forecasting compared to SVR. Regional long-term forecast up to 24 hours. Four inputs and single output at a time (multi-input Single-output).	Not suitable for an area-specific weather forecast. Able to predict only a single output at a time. For a productive output, this model requires specific hardware such as GPU memory units. High computational complexity compared to SVR. Uses a large number of components whose purpose is not immediately apparent.
A deep neural network model for temperature forecasting (Hossain et al., 2015).	Contributed a stacked auto-encoder deep learning model for weather forecasting. 97.97% accurate temperature forecast compared to the ground truth. Area-specific long-term forecast up to a month. Four inputs and single-output (Multi-input single-output).	Able to predict a single output parameter at a time. Not suitable for regional forecasting. Uses up a lot of memory in storing partial results. Training process is not efferent and time-consuming.
Sequence to sequence weather forecasting model (Akram and El, 2016).	Contributed multi-stacked LSTMs to map sequences of weather values of the same length. Reasonably accurate temperature, humidity, and wind speed	Not suitable for area-specific weather forecasting. Uses multiple cell gates due to the long input sequence and uses a lot of memory.

	forecasting compared to the ground truth based on MSE values. Regional forecast up to 24 hours. Three inputs and three outputs (Multi-input multi-outputs).	It is recommended to use GPU memory units for faster output.
Bi-LSTM wind power forecasting model (Deng et al., 2019).	Contributed the bidirectional gated recurrent network for weather power forecasting. The model established an accurate relationship between the power and wind speed, wind direction compared to the ground truth based on the MSE values. Local or regional forecast. Two inputs and a single-output (Multi-input Single-output).	Able to predict parameters for up to 6 hours. Uses only a single observational weather parameter and not considered the interrelated parameters for an accurate prediction. Recommended to use specific hardware such as GPU memory units for productive output.

Many of the researches discussed in Table 4.1 use MSE as their evaluation matrix. It is much easier to analyse the results if they present it as a percentage of the accuracy. For example, Hossain et al., (2015) described the prediction accuracy as 97.97% compared to the ground truth. However, this is not viable to some weather parameters. The reason is that the prediction accuracy is calculated as $\left(\frac{predicted\ value - actual\ value}{actual\ value}\right) * 100\%$. There are some instances where the actual value is equal to zero. If this applies to the equation, then an error occurs when attempting to divide by zero (Charu, 2019). In practical situations, the actual value can be zero in many parameters such as rain, rain rate, snow, and temperature, etc.

The information from Table 4.1 show that the deep learning approach can be used for both regional and area-specific weather forecasting with their own drawbacks. In particular, Salman et al., (2015), Yonekura et al., (2018) and Liu et al., (2014) outperformed the classic ML approaches with deep learning models. Besides, Akram and El, (2016), Dalto et al., (2015), Salman et al., (2015) and Salman et al., (2018) concluded their research that the deep neural networks outperformed the shallow ones in weather forecasting. Therefore, a deep neural network is prepared for this study rather than shallow networks. Besides, the all state-of-the-art deep models discussed in Table 4.1 use less than five interrelated input parameters. One of the contributions of this research is developing a complete weather forecasting model with ten inputs and output parameters.

When analysing the information in Table 4.1, there are three types of regressions, namely multi-input multi-output (MIMO), multi-input single-output (MISO), and single-input

single-output (SISO). All of these regressions can show state-of-the-art performances with deep learning approaches. Two facts determine the prediction accuracy of a selected parameter, namely its previous observations and previous observations of the interrelated parameters (Jincai et al., 1996). Besides, more interrelated parameters with previous observations will target to a more accurate prediction compared to less interrelated parameters (Di et al., 2015). Therefore, SISO regression is not mainly considered within this study as the main goal is to get an accurate forecast. As a consequence, both MIMO and MISO models are proposed to solve the regression problem involving weather forecasting.

4.3 MIMO and MISO deep learning weather forecasting models

As discussed in Section 4.2, both MIMO and MISO regression models are proposed for this research. That is the proposed weather forecasting model is developed by exploring the set of models, namely MIMO and MISO. In the MIMO, all the weather parameters (i.e. ten surface weather parameters in this study) are fed into the network, which is expected to predict the same number of parameters (i.e. ten parameters in this study) as the output. Therefore, only one model is required for short-term weather forecasting. Figure 4.1 depicts the necessary arrangement of the MIMO;

Figure 4.1 Proposed MIMO deep learning model architecture.

In the MISO approach, all of the weather parameters (i.e. ten surface weather parameters in this study) are fed into the network which is expected to predict a single parameter. In this approach, ten different models are required for short-term weather forecasting as each of them is trained to predict a particular weather parameter. Figure 4.2 depicts the necessary arrangement of the MISO;

Figure 4.2 Proposed MISO deep learning model architecture.

As described in Section 1.2.2, Section 2.7.3, and Section 3.2.2, the LSTM and TCN deep neural approaches are proposed for the weather forecasting models. Therefore, the proposed model variances are MIMO-LSTM, MISO-LSTM, MIMO-TCN, and MISO-TCN.

4.3.1 MIMO-LSTM model variance

Deep Neural Network (DNN) with LSTM layers, a specialised form of the RNN allows stacked neural networks and includes several layers as part of overall composition known as nodes. These nodes use the combination of data and input through a set of coefficients allowing it to carry out computational tasks (Jozefowicz et al., 2015). The proposed DNN with stacked LSTM layers for the MIMO model variance is presented in Figure 4.3 as a).

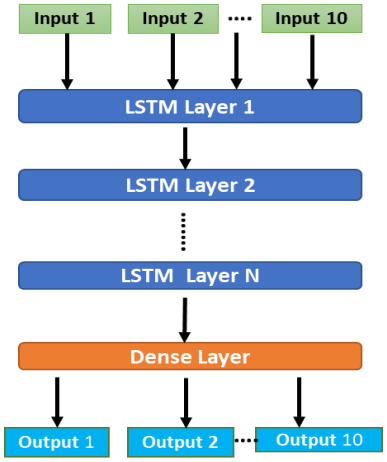

a) Proposed MIMO-LSTM model variance.

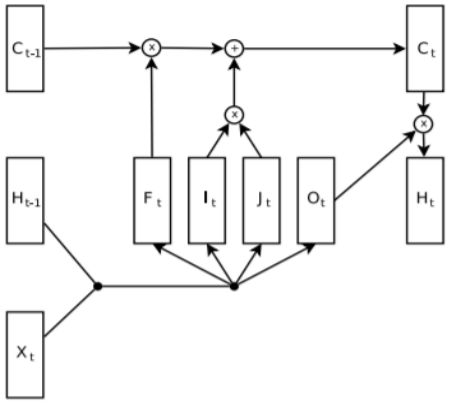

b) LSTM memory cell.

Figure 4.3 a) Proposed layered MIMO-LSTM model variance and b) LSTM memory cell used for this research (image reference (Jozefowicz et al., 2015)).

The number of layers and the number of memory cells in each layer is decided experimentally for the best performance. These models can learn long-term dependencies by incorporating memory units. These memory units allow the network to learn, forget previously hidden states, and update the hidden states. Figure 4.3 b) depicts the general

arrangement of an LSTM memory cell. Larger datasets are used to train the LSTM models and this process often requires multiple days even with the Graphical Processing Unit (Behera et al., 2018).

The proposed MIMO-LSTM model variance is a lightweight model that consists of LSTM layers and Dense layer in addition to input and output layers. As discussed in Section 3.2.1, ten surface weather parameters are used as the inputs for this model variance. This model variance provides outputs which are the predicted weather parameters. As Donahue et al. (2014) stated, the LSTM can learn long-term dependencies by incorporating memory units. It is these memory units that allow the network to learn, forget previously hidden states, and update hidden states.

Figure 4.3 b) shows the LSTM general memory architecture which is used in this research. According to (Jozefowicz et al., 2015), the LSTM model takes input $x_t = [p_1, p_2, p_3 \ldots. \ p_{10}]$ at a given timestamp t, where $p_1, p_2, p_3 \ldots. \ p_{10}$ are input weather parameters (i.e. 10 surface weather parameters). In the given time t, the model updates the memory cells for long-term c_{t-1} and short-term h_{t-1} reminiscence of the previous timestep $t-1$ via:

$$\boldsymbol{i_t} = \mathbf{tanh}(\boldsymbol{w_{xi}x_t} + \boldsymbol{w_{hi}h_{t-1}} + \boldsymbol{b_i})$$

$$\boldsymbol{j_t} = \mathbf{sigm}\big(\boldsymbol{w_{xj}x_t} + \boldsymbol{w_{hi}h_{t-1}} + \boldsymbol{b_j}\big)$$

$$\boldsymbol{f_t} = \mathbf{sigm}\big(\boldsymbol{w_{xf}x_t} + \boldsymbol{w_{hf}h_{t-1}} + \boldsymbol{b_f}\big)$$

$$\boldsymbol{o_t} = \mathbf{tanh}(\boldsymbol{w_{xo}x_t} + \boldsymbol{w_{ho}h_{t-1}} + \boldsymbol{b_o})$$

$$\boldsymbol{c_t} = \boldsymbol{c_{t-1}} \odot \ \boldsymbol{f_t} + \boldsymbol{i_t} \odot \ \boldsymbol{j_t}$$

$$\boldsymbol{h_t} = \mathbf{tanh}(\boldsymbol{c_t}) \odot \boldsymbol{o_t} \qquad \textbf{(4.1)}$$

The notations of Equation 4.1 are w_*-weight matrices, b_*- biases, $\odot$- element-wise vector product, i_t- input gate, j_t- input moderation gate contributing to memory, f_t- forgot gate, and o_t-output gate as a multiplier between memory gates. According to Behera et al., (2018); Jozefowicz et al.,(2015), there are two kinds of hidden states to allow the LSTM to make complex decisions over a short period namely c_t and h_t. The LSTM has the ability to selectively consider its current inputs or forget its previous memory by switching the gates i_t and f_t. Similarly, the output gate o_t learns how much memory cell c_t is needed to be transferred to the hidden state h_t. Compared to the RNN, these

additional memory cells give the ability to learn enormously complex and long-term temporal dynamics with the LSTM.

There are quite a few model libraries that are used to enable neural networks and deep learning models in a computer system such as TensorFlow, BVLC, Theano, and Pfnetand (Reimers and Gurevych, 2017). These model libraries are used as the backend of popular neural network models and each model library has its advantages and limitations while the most used is the TensorFlow backend (Abadi et al., 2016; "TensorFlow," 2018). TensorFlow has a vast repository of data, however, it is complicated and not easy to use. Keras is a high-level Application Program Interface (API) and is more user-friendly. It allows rapid prototyping with a TensorFlow backend. Keras allows the building and testing of neural networks by reducing the lines of codes and has powerful APIs while its guiding principles are based on modularity (Keras, 2019). There are aspects like a sample, epoch, and batches are set so that data can be processed independently and distinctive phrases are identified (Keras, 2019; Krizhevsky et al., 2012). Therefore, the Keras API is selected for this research as an LSTM tool.

4.3.2 MISO-LSTM model variance

MISO-LSTM model variance uses the similar MIMO-LSTM architectural elements with a different output layer. Figure 4.4 depicts the proposed DNN with stacked LSTM layers for the MISO model variance. Similar to Section 4.3.1, the weather parameters (i.e. ten input surface parameters) are fed into the network and is expected to predict a single parameter as the output in MISO-LSTM variance.

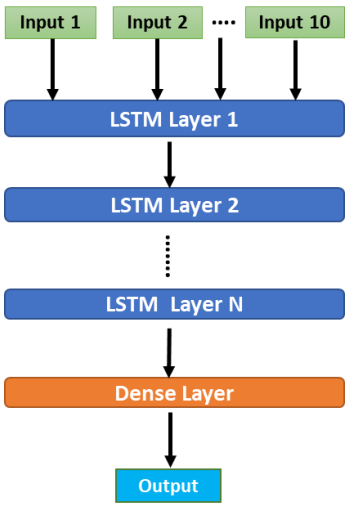

Figure 4.4 Proposed MISO-LSTM model variance.

A typical criticism of the LSTM architecture is that it has a large number of components whose purpose is not immediately apparent (Jozefowicz et al., 2015). Moreover, LSTMs can easily use up a lot of memory in storing partial results for their multiple cell gates in the case of the long input sequence. This is the case for the time-series weather data. Therefore, the TCN architecture has been explored for modelling and predicting fine-grained weather data.

4.3.3 MIMO- TCN model variance

The TCN approach was initially developed to examine long-range patterns using a hierarchy of temporal convolutional filters (Lea et al., 2017). The key characteristics of TCNs are: 1) it involves convolutions which are causal and 2) like in RNN, the network can take a sequence of any length and map it to an output sequence of the same length. Figure 4.7. a) presented the proposed fine-grained weather forecasting DNN model with stacked TCN layers for the MIMO variance. The proposed architecture is informed by recent generic convolutional architectures for sequential data (Bai et al., 2018; Lea et al., 2017). The architecture is simple (e.g. no skip connections across layers, conditioning, and context stacking or gated activations), uses autoregressive prediction, and has a very long memory. Moreover, it allows both very deep networks and very long effective history and is achieved through dilated convolutions that enable an exponentially large receptive field (Yu and Koltun, 2015). For example, for a 1-D sequence of a given weather parameter p^1, i.e. $p = (p_0^1, \dots, p_t^1)$ and a filter $f : \{0, \dots, k-1\}$, the dilation convolution operation F on element $s = p_{\hat{t}}^1$ (where $\hat{t} = 0, \dots, t$) of the sequence is defined as the Equation 4.2 given below.

$$\boldsymbol{F(s) = (p *_d f)(s) = \sum_{i=0}^{k-1} f(i) \cdot p_{s-d.i}} \quad \textbf{(4.2)}$$

Where d is the dilation factor, k refers to the filter size, and $s - d.i$ accounts for the direction of the past. Stacked units of one-dimensional convolution with activation functions are used to build the TCN (Kim and Reiter, 2017). Figure 4.4 b) depicts the architectural elements in a TCN with configurations dilation factors $d = 1, 2, \ and \ 4$. The dilation introduces a fixed step between every adjacent filter taps. Larger dilations and larger filter sizes k enable effectively expanding the receptive field (Bai et al., 2018; Lea et al., 2017). In these convolutions, the increment of d exponentially increases the depth of the network. This guarantees that there is some filter hits each input within the effective history (Bai et al., 2018).

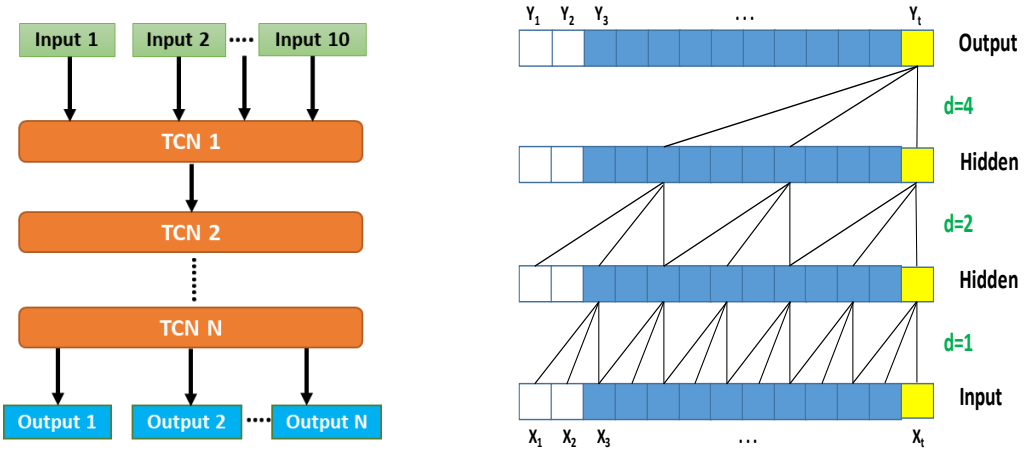

a) Proposed MIMO-TCN model variance. b) A typical TCN layer architecture.

Figure 4.5 a) Proposed layered MIMO-TCN model variance and b) Architectural elements in a TCN with causal convolution and different dilation factors.

As per Figure 4.7, the input to the TCN is $\boldsymbol{x_t}$ and output $\boldsymbol{y_t}$. The $\boldsymbol{x_t}$ contains the 10-dimensional weather parameters. As per section 2.6, it is evident that there has been no attempt to experiment TCN for weather forecasting in the literature. Similar to Section 4.3.1, the TCN approach is implemented using the Keras open-source neural-network tool using a Python environment (Gulli and Pal, 2017; Keras, 2019; Krizhevsky et al., 2012).

4.3.4 MISO-TCN model variance

Similar to Section 4.3.2, the same MIMO-TCN architecture is used for the MISO-TCN. Both these networks accept ten input weather parameters as the input. The MISO-TCN model is designed to predict a single parameter as the output rather than ten as in MIMO-TCN. The proposed DNN with stacked LSTM layers for the MISO model variance is presented in Figure 4.8.

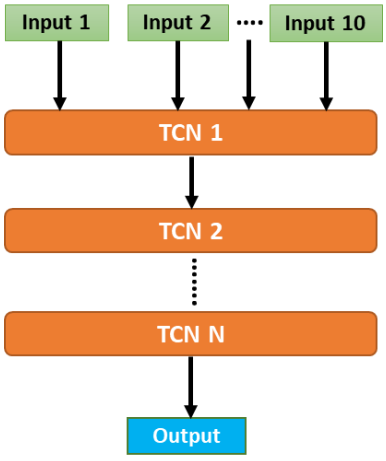

Figure 4.6 Proposed MISO-TCN model variance.

In addition to the LSTM and the TCN deep neural approaches, the Bi-directional LSTM has taken considerable attraction from its initial introduction in 2001 for time series data (Asif Khan et al., 2018).

4.3.5 Deep learning with Bi-directional LSTM (Bi-LSTM)

Similar to the LSTM and TCN, the Bi-LSTM can be used with both MIMO and MISO models. In LSTM, data are preserved from inputs that have already passed through its hidden state (i.e. the LSTM only preserves the information of the past). In contrast, as described in Section 2.7.3, the Bi-LSTM networks will run inputs in two ways, namely from the past to the future and from the future to the past. That is, the Bi-LSTM can run the inputs backwards to preserve information from the future compared to the LSTM networks (Althelaya et al., 2018; Graves and Schmidhuber, 2005; Salehinejad et al., 2017). Therefore, the Bi-LSTM can preserve information from both past and future using the two hidden states combined. This process is helped by Bi-LSTM to better understand the context and thus targets a more accurate forecast compared to the LSTM networks in sequence-to-sequence applications (i.e. it knows the full inputs at prediction time) (Graves et al., 2013). Figure 4.9 depicts the basic structure of a Bi-LSTM.

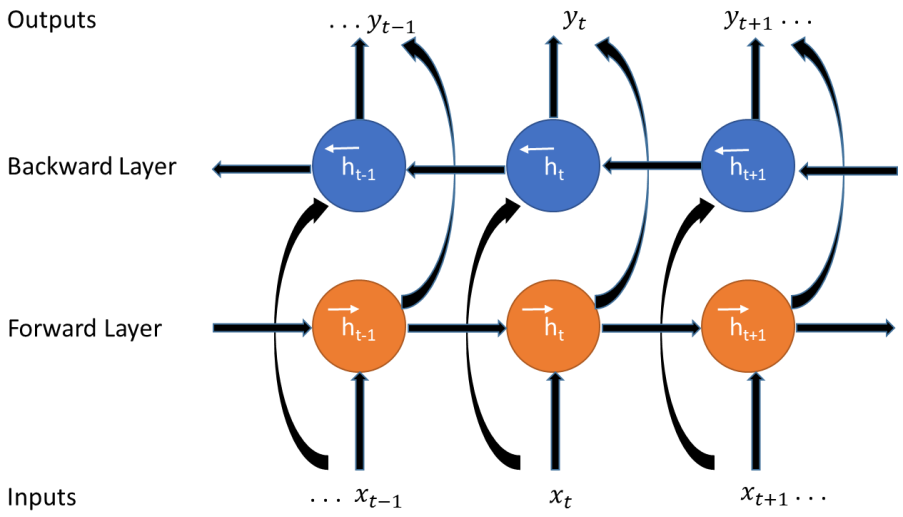

Figure 4.7 Structure of a bidirectional network.

As presented in Figure 4.5, Bi-LSTM processes data in both directions with two separate hidden layers. The processed results are sent to the output layer. Equation 4.3 and Equation 4.4 represent the calculation of hidden vector sequence $h = (h_1, h_2, \ldots, h_t)$ and output vector sequence $y = (y_1, y_2, \ldots, y_T)$ based on input sequence $x = (x_1, x_2, \ldots, x_T)$ in conventional RNN (Schuster and Paliwal, 1997).

$$\boldsymbol{h_t = \mathcal{H}(W_{xh}x_t + W_{hh}h_{t-1} + b_n} \quad \textbf{(4.3)}$$

$$\boldsymbol{y_t = W_{hy}h_t + b_y} \quad \textbf{(4.4)}$$

Notations of the Equation 4.3 and 4.4 are: W- weight matrices (for an example W_{xh} is the input-hidden weight matrix); b- bias vector; $\mathcal{H}$- hidden layer function. The $\mathcal{H}$ can be calculated by recalling Equation 4.1. In Bi-LSTM, forward hidden sequence $\underset{h}{\rightarrow}$ and backward hidden sequence $\underset{h}{\leftarrow}$ are computed as Equation 4.7 with the output sequence y by iterating the backward layer from $t = T$ to 1, the forward layer from $t = 1$ to T and then updating the output layer as in Equation 4.7 (Graves et al., 2013).

$$\underset{\boldsymbol{h_t}}{\rightarrow} = \boldsymbol{\mathcal{H}}\left(\boldsymbol{W}_{\underset{xh}{\rightarrow}}\boldsymbol{x_t} + \boldsymbol{W}_{\underset{h}{\rightarrow}\underset{h}{\rightarrow}}\underset{\boldsymbol{h_{t-1}}}{\rightarrow} + \boldsymbol{b}_{\underset{h}{\rightarrow}}\right) \quad \textbf{(4.5)}$$

$$\underset{\boldsymbol{ht}}{\leftarrow} = \boldsymbol{\mathcal{H}}\left(\boldsymbol{W}_{\underset{xh}{\leftarrow}}\boldsymbol{x_t} + \boldsymbol{W}_{\underset{h}{\leftarrow}\underset{h}{\leftarrow}}\underset{\boldsymbol{h_{t+1}}}{\leftarrow} + \boldsymbol{b}_{\underset{h}{\leftarrow}}\right) \quad \textbf{(4.6)}$$

$$\boldsymbol{y_t = W}_{\underset{h}{\rightarrow}\underset{y}{\rightarrow}}\underset{\boldsymbol{h_t}}{\rightarrow} + \boldsymbol{W}_{\underset{hy}{\leftarrow}}\underset{\boldsymbol{h_t}}{\leftarrow} + \boldsymbol{b_y} \quad \textbf{(4.7)}$$

Deep Bi-LSTM networks refer to stacking multiple Bi-LSTM hidden layers on top of each other to establish a network. This iterative process can be represented by Equation 4.8, 4.9, and 4.10 which replace each hidden state h_n with forwarding and backwards hidden states $\underset{h^n}{\rightarrow}$ and $\underset{h^n}{\leftarrow}$ (Fan et al., 2014).

$$\underset{\boldsymbol{h_n^t}}{\rightarrow} = \boldsymbol{\mathcal{H}}\left(\boldsymbol{W}_{\underset{h^{n-1}}{\longrightarrow}\underset{h^n}{\rightarrow}}\underset{\boldsymbol{h_t^{n-1}}}{\longrightarrow} + \boldsymbol{W}_{\underset{h^n}{\rightarrow}\underset{h^n}{\rightarrow}}\underset{\boldsymbol{h_{t-1}^n}}{\longrightarrow} + \boldsymbol{b}^{\boldsymbol{n}}_{\underset{h}{\rightarrow}}\right) \quad \textbf{(4.8)}$$

$$\underset{\boldsymbol{h_t^n}}{\leftarrow} = \boldsymbol{\mathcal{H}}\left(\boldsymbol{W}_{\underset{h^{n-1}}{\longleftarrow}\underset{h^n}{\leftarrow}}\underset{\boldsymbol{h_t^{n-1}}}{\longleftarrow} + \boldsymbol{W}_{\underset{h^n}{\leftarrow}\underset{h^n}{\leftarrow}}\underset{\boldsymbol{h_{t-1}^n}}{\longleftarrow} + \boldsymbol{b}^{\boldsymbol{n}}_{\underset{h}{\leftarrow}}\right) \quad \textbf{(4.9)}$$

$$\boldsymbol{y_t = W}_{\underset{h^N}{\longrightarrow}\underset{y}{\rightarrow}}\underset{\boldsymbol{h_t^N}}{\rightarrow} + \boldsymbol{W}_{\underset{h^N}{\longleftarrow}\underset{y}{\leftarrow}}\underset{\boldsymbol{h_t^N}}{\leftarrow} + \boldsymbol{b_y} \quad \textbf{(4.10)}$$

Bi-LSTM can produce a better prediction for the time series data compared with the LSTM due to two-way data preservation (Fan et al., 2014; Graves, 2012; Yulita et al., 2017). The only drawback of these networks is that they are less efficient for training, testing, and predicting data compared to the LSTM (i.e. Bi-LSTM has taken time to train models and testing) (Salehinejad et al., 2017). As per section 2.6, it is evident that there has been no attempt taken to experiment Bi-LSTM for weather forecasting in the literature. Similar to the LSTM and TCN networks, the Keras open-source library is used to implement the Bi-LSTM models.

4.4 Summary

There are two deep models proposed to solve the regression problem involving weather forecasting, namely MIMO and MISO. That is the proposed weather forecasting model is developed by exploring the set of models, namely MIMO and MISO. As LSTM and TCN deep neural approaches are proposed for the weather forecasting models, the proposed model variances in this study are MIMO-LSTM, MISO-LSTM, MIMO-TCN, and MISO-TCN. In MISO model, all of the input weather parameters (i.e. ten surface weather parameters in this study) are fed into the network and is expected to predict a single parameter. Whereas, in the MISO, ten different models are required as each of them is trained to predict a particular weather parameter.

In addition to the LSTM and the TCN deep neural approaches, the Bi-LSTM deep approach is also considered for this study. Recently, the Bi-LSTM has taken considerable attraction due to its performances. There are quite a few model libraries that are used to enable neural networks and deep learning models in a computer system such as TensorFlow, BVLC, Theano, and Pfnetand. The most common model library, TensorFlow, has a vast repository of data; however, it is complicated and not easy to use. Keras is a high-level API more user-friendly and allows rapid prototyping with a TensorFlow backend. Therefore, the Keras API is selected as a tool to develop the proposed deep learning models for this study.

5 Evaluation, Results and Discussions

5.1 Introduction

This chapter is organised in order to assess the research hypothesis. In the first instance, the WRF historical data is used to determine that the proposed deep learning model is suitable for short-term weather forecasting compared to the well-recognised WRF model. Then the study is focused on applying the proposed model for long term weather forecasting. The long-term prediction results are compared with the WRF model to identify up to what extent (i.e. the number of hours ahead) the proposed model can be used for weather forecasting. Additionally, the above experiments are successful means that the neural network technology can be utilised to weather forecasting.

As described in Section 2.1.1, there are several challenges in NWP models and accessing real-time global data. Therefore, the study is focused on using the local weather station data for both short-term and long-term weather forecasting. Therefore, there are mainly two types of results, namely; 1) Phase 1 results- using historical weather data 2) Phase 2 results- using local weather stations data. The following steps are followed for each type of experiment; i) compare the performances of proposed neural network weather forecasting model with the existing approaches ii) determine the accuracy of the proposed model for short-term forecasting iii) identify the capability to use the proposed model for long-term forecasting and determine the accuracy of such a process.

5.2 Using Historical Weather Data

As described in Section 2.1.1, the WRF model is used to extract the historical GRIB format GFS weather data and separate the surface weather parameters. These data are used to train (with WRF training dataset), test (with WRF testing dataset), and validate (with WRF validation dataset) the proposed model. Moreover, the WRF model is run in the forecasting mode with the WRF validation dataset and get the prediction (WRF

prediction dataset) to compare the performance of the proposed model and the WRF model.

5.2.1 Comparison of machine learning techniques for weather forecasting

As described in Section 3.2.6, the performances of classic ML approaches (i.e. SR and SVR) are compared with the proposed deep learning approaches (i.e. LSTM and TCN). As described in sections 4.3, these models are evaluated using two different regression types, namely MIMO and MISO.

5.2.1.1 *MIMO Machine learning models*

The SVR approach is not compatible with the MIMO (Santamaría-Bonfil et al., 2016; Smola and Schölkopf, 2004). Therefore, the SR is used as the baseline approach for MIMO to compare with proposed LSTM, and TCN approaches. The represented model variances for each approach are MIMO-SR, MIMO-LSTM, and MIMO-TCN, respectively.

5.2.1.1.1 Baseline MIMO approaches

5.2.1.1.1.1 Standard Regression

As described in Section 3.2.6, the SR model is trained with the WRF training dataset. The WRF testing dataset is used to get a prediction using the trained model. The prediction results are compared with the ground truth. The error figures are calculated for each parameter, and the evaluation report is presented in Table 5.1. These calculations are carried out for the normalised data (i.e. prediction data and the ground truth are in the normalised form).

Table 5.1 Evaluation of the baseline baseline-SR model variance for MIMO model.

Parameter	MSE	MAE	RMSE	EV
TSK	0.003701561	0.037689863	0.060840454	0.853775978
PSFC	0.005361072	0.007335346	0.007320398	0.998259068
U10	0.008420962	0.047147669	0.1117658	0.85456109
V10	0.015627757	0.066887967	0.117337031	0.125011028
Q2	0.009980163	0.064986551	0.099900768	0.831790566
Rainc	0.006125415	0.034882298	0.078265031	0.008365691
Rainnc	0.021599896	0.060246922	0.146969035	0.463460743
Snow	0.000016626	0.008734304	0.00406839	0
TSLB	0.004349349	0.022340292	0.065949594	0.99417007
SMOIS	0.000979215	0.005438701	0.009894565	0.999852359

5.2.1.1.2 Proposed MIMO approaches

5.2.1.1.2.1 LSTM

As described in Section 3.2.5.1.1, the deep learning with LSTM approach is used with various configurations and controls for these experiments. Please refer Appendix 2 for a sample evaluation report. The summary of the MIMO-LSTM evaluation is presented in Table 5.2. In this section, there are 24 experiments to discover the optimal MIMO-LSTM model variance.

Table 5.2 Evaluation of MIMO-LSTM model variance- Summary Report.

Configuration	Optimiser	Best MSE
1	Adam	0.00660156752937796
	SGD	0.00607736654637046
	Adaptive Adam	0.571018543304204
	Adaptive SGD	0.00493256751552592
2	Adam	0.112312899733773
	SGD	0.00821901463346447
	Adaptive Adam	0.571018543304204
	Adaptive SGD	0.00830940222839769
3	Adam	0.00719272525270204
	SGD	0.00832014021725155
	Adaptive Adam	0.525576052478436
	Adaptive SGD	0.0079421664562867
4	Adam	0.00897196207715143
	SGD	0.00501471974482657
	Adaptive Adam	0.591042582535899
	Adaptive SGD	0.0053223055228665
5	Adam	0.00520147593407018
	SGD	0.00624769625825993
	Adaptive Adam	0.47283546624289
	Adaptive SGD	0.00927240672088578
6	Adam	0.00467935662817302
	SGD	0.00369984356548565
	Adaptive Adam	0.47283546624289
	Adaptive SGD	0.00373632111990271

The model weights for each experiment are saved in every ten epochs. Then these weights are used to create the appropriate models and to get a prediction for the WRF testing dataset. The results are subsequently evaluated with respect to the ground truth and discover the least MSE for the optimal model. As shown in Table 5.2, the optimal model for MIMO-LSTM model variance is found in configuration 6 (i.e. model has three LSTM

layers, and each layer has 128, 512, and 256 nodes respectively) with the SGD optimiser, 128 batch size and fixed learning rate of 0.01. MSE is used as the loss function for these models, which is calculated as Equation 3.1. The least MSE is found in the 230 epochs, and this model weights are saved as the optimal model weights for MIMO-LSTM model variance. Figure 5.1 shows the evaluation results for the Config6 with SGD optimiser and fixed learning rate of 0.01.

As per Figure 5.1, the least MSE for the overall MIMO-LSTM model variance is equal to 0.00369984356548565. Subsequently, Table 5.1 shows the MSE values for each parameter relevant to its epoch. Therefore, the highlighted MSE values for each parameter are recorded as its optimal MSE values for MIMO-LSTM.

Epoch	Loss	Total MSE	Total MAE	Total RMSE	SkinTemp	SufPres	U10	V10	Humidity	Rainc	Rainnc	Snow	SoilTemp	SoilMoist
10	0.018276248	0.018276248	0.097509523	0.13518967	0.006969704	0.026743824	0.019782048	0.024171676	0.06948714	0.00442288	0.00369892	0.001489522	0.025276568	0.000720207
20	0.010491723	0.010491723	0.07367275	0.10242911	0.003016563	0.017683031	0.016468085	0.014004315	0.026875837	0.003955931	0.002790341	0.000800964	0.018683763	0.000638397
30	0.007523045	0.007523045	0.061365407	0.08673548	0.002516259	0.009656541	0.012383327	0.012098094	0.014679401	0.00391121	0.00303135	0.000535528	0.015856147	0.000562598
40	0.006522759	0.006522759	0.055906084	0.0807636	0.002501436	0.005692685	0.011518328	0.010999072	0.012009272	0.003830122	0.003196626	0.000397381	0.014567475	0.000515194
50	0.005952916	0.005952916	0.052568104	0.07715514	0.002491464	0.004200898	0.010698189	0.010086523	0.010824773	0.003720171	0.003202032	0.000288901	0.013505651	0.000510554
60	0.005502095	0.005502095	0.050302197	0.07417612	0.002493842	0.003399132	0.010006282	0.00934145	0.01026063	0.003608489	0.003223685	0.000217228	0.011954516	0.000515698
70	0.005198917	0.005198917	0.048420096	0.07210351	0.002447826	0.002897133	0.009454106	0.008534861	0.009890192	0.003515361	0.003151641	0.000157288	0.01141835	0.00052241
80	0.004930477	0.004930477	0.047142384	0.070217356	0.002428205	0.002494656	0.009529544	0.008143179	0.009282479	0.00343884	0.003150833	0.000117734	0.010209189	0.000510106
90	0.0047486	0.0047486	0.045854159	0.068910375	0.002404724	0.00229572	0.009298923	0.007470253	0.009175058	0.003374076	0.003054555	8.73E-05	0.0098244	0.000501394
100	0.004560462	0.004560462	0.044633655	0.06753119	0.002431744	0.002158779	0.009102077	0.006859458	0.009048901	0.003310385	0.003057649	6.53E-05	0.009091093	0.000479187
110	0.004453985	0.004453985	0.043926356	0.06673818	0.002420098	0.002146414	0.008998319	0.006655634	0.00881492	0.003272729	0.002980084	4.87E-05	0.008735539	0.00046744
120	0.004355957	0.004355957	0.043357451	0.06599967	0.002534212	0.002182413	0.008570047	0.006454783	0.00912948	0.00323225	0.0030163	3.70E-05	0.007952559	0.000450506
130	0.004116224	0.004116224	0.04188745	0.06415781	0.002478839	0.002191433	0.006959129	0.006509389	0.008898494	0.003178422	0.003018756	2.80E-05	0.007458258	0.000441562
140	0.004153562	0.004153562	0.041957674	0.06444813	0.00259901	0.002093182	0.007394831	0.006686883	0.008982712	0.00314815	0.002951023	2.05E-05	0.007216162	0.000443171
150	0.004177298	0.004177298	0.042055531	0.06463202	0.002789594	0.002019832	0.007554862	0.006774078	0.009240215	0.003113639	0.0030215	1.53E-05	0.006796531	0.00044743
160	0.004201576	0.004201576	0.042109783	0.06481956	0.002856683	0.002138621	0.007472065	0.007279143	0.009165541	0.003059278	0.002941815	1.14E-05	0.006627113	0.000464072
170	0.004133309	0.004133309	0.04139621	0.064290814	0.002775918	0.002202021	0.007054817	0.007569754	0.009055813	0.003012055	0.002859891	8.68E-06	0.006326685	0.000467455
180	0.004200863	0.004200863	0.041605329	0.06481406	0.002906216	0.002147288	0.007198409	0.007529963	0.009703296	0.002991537	0.003012214	6.85E-06	0.006029691	0.000483169
190	0.00416025	0.00416025	0.041214385	0.064500004	0.003182824	0.002058711	0.008289297	0.006892907	0.009314587	0.002962265	0.002879161	5.20E-06	0.005505256	0.000512291
200	0.003944039	0.003944039	0.039649268	0.062801585	0.003082931	0.002042752	0.006270979	0.006971994	0.009410158	0.002934188	0.002997862	4.16E-06	0.005179504	0.000545865
210	0.003935014	0.003935014	0.039518267	0.06272969	0.003195882	0.002144509	0.006549131	0.007374453	0.009164603	0.002912455	0.003100918	3.50E-06	0.004341848	0.00056284
220	0.003844938	0.003844938	0.038622109	0.06200757	0.003307656	0.002010803	0.006408483	0.006311056	0.009872749	0.002897357	0.002992446	2.84E-06	0.004040619	0.000605371
230	0.003699844	0.003699844	0.037537898	0.06082634	0.003271054	0.002112675	0.005394089	0.006311009	0.009881492	0.002878811	0.003070845	2.39E-06	0.003427306	0.000648767
240	0.003880733	0.003880733	0.038505509	0.062295526	0.003460772	0.002177067	0.006689046	0.0053539	0.010723675	0.002871775	0.004023603	2.22E-06	0.00284235	0.000662919
250	0.003972302	0.003972302	0.038337381	0.063026205	0.003516005	0.002096369	0.005313642	0.004716563	0.01118155	0.002896062	0.006496077	2.29E-06	0.002806731	0.000697734
260	0.004139672	0.004139672	0.039369135	0.064340286	0.003877571	0.00225446	0.006052786	0.004741847	0.011367044	0.002885173	0.00643688	1.89E-06	0.002993184	0.000785878
270	0.004190736	0.004190736	0.039129027	0.0647359	0.004579625	0.002133449	0.005444672	0.0042303	0.01055951	0.002900269	0.008351362	1.71E-06	0.002965335	0.000741111

Figure 5.1 Evaluation results for LSTM configuration 6-SGD. The row with the best MSE is highlighted.

5.2.1.1.2.2 TCN

As described in Section 3.2.5.1.2, there are different configurations and controls which can be used with the TCN approach for MIMO variance. According to (Bai et al., 2018; Lea et al., 2017; Pelletier et al., 2019) the following controls are kept constant within this study as these do not impact final results significantly in the regression model for time-series data; kernel_size-2, dilations-7 where dilation values are- 1, 2, 4, 8, 16, 32, 64, batch size-64, and dropout rate-0, learning rate- 0.0.

In contrast to the LSTM, the 'save the best model' approach is used while training the MIMO-TCN model variance rather saving weights for every ten epochs. In this case, the system checks the loss function value for each epoch with the saved model. Only if the new loss value was smaller than the saved model loss, the system saved the new model as the best model (Chen, 2018; Keras, 2019). The saved best model is used to get the prediction for the testing dataset and evaluate the results with respect to the ground truth. Table 5.3 presents the summary of MSE for each configuration and control in MIMO-TCN model variance. In this section, there are 40 experiments to discover the optimal MIMO-TCN model variance.

Table 5.3 Analysis of the MIMO-TCN model variance. The evaluation metric is MSE, and least MSE is the best.

No of Filters	TCN layers	Activation: Linear	Activation: tanh
32	1	0.007129386	0.006315798
	2	0.006625198	0.007042421
	3	0.007125658	0.007325659
	4	0.007736131	0.007509462
64	1	0.005380642	0.005977792
	2	0.006608716	0.007616931
	3	0.006860351	0.007467944
	4	0.009262335	0.007076726
128	1	0.006594512	0.005759116
	2	0.007439891	0.007218564
	3	0.007524525	0.007549621
	4	0.007697892	0.007603901
256	1	0.007088403	0.006348704
	2	0.00736649	0.006707881
	3	0.007209218	0.007031739
	4	0.009162578	0.008156796
512	1	0.006231652	0.005767795
	2	0.007068991	0.007073388
	3	0.007610388	0.008974239
	4	0.009454301	0.112069921

As per table 5.3, the MIMO-TCN model variance yields the best results (optimal model) with configurations and controls of 64 filters, one TCN layers, and linear activation function. Please refer Appendix 3 for a sample TCN results. The prediction of the above optimal model is compared with the ground truth and evaluated and is presented in Table 5.4.

Table 5.4 Evaluation results for the TCN optimal model for the MIMO model variance.

Parameter	MSE	MAE	RMAE	EV
TSK	0.003578392	0.046120698	0.059819662	0.77990222
PSFC	0.000279068	0.012727534	0.016705336	0.993016541
U10	0.00632667	0.074595386	0.079540367	0.762839854
V10	0.010195208	0.056267205	0.100971319	0.772671759
Q2	0.006578324	0.05967569	0.081106864	0.822500765
Rainc	0.004785024	0.019457236	0.069173865	-0.14229846
Rainnc	0.021204848	0.033308357	0.145618841	0.476569176
Snow	0.000001602	0.002786925	0.004000977	0
TSLB	0.000485899	0.010468689	0.022043126	0.993455768
SMOIS	0.000356974	0.007902617	0.018893763	0.999439895

5.2.1.1.3 Compare baseline approaches and proposed approaches for optimal MIMO model

Table 5.5 and Figure 5.2 shows the comparison results of baseline-SR, MIMO-LSTM, and MIMO-TCN model variances. These results are subsequently evaluated via the MSE for normalised data. These results are used to assess the optimal MIMO model (i.e. least MSE) after comparing the performance of all models.

Table 5.5 Comparison of machine learning approaches for MIMO model. Lower MSE is better and is shown highlighted.

Parameter	Baseline SR	Model variance	
		MIMO-LSTM	MIMO-TCN
TSK	0.003701561	0.003271054	0.003578392
PSFC	0.005358824	0.002112675	0.000279068
U10	0.008420962	0.005394089	0.006326671
V10	0.015627757	0.006311009	0.010195208
Q2	0.009980163	0.009881492	0.006578324
Rainc	0.006125415	0.002878811	0.004785024
Rainnc	0.021599896	0.003070845	0.015204848
Snow	0.000016552	0.000002394	0.000001602
TSLB	0.004349349	0.003427306	0.000485899
SMOIS	0.000979024	0.000648767	0.000756974

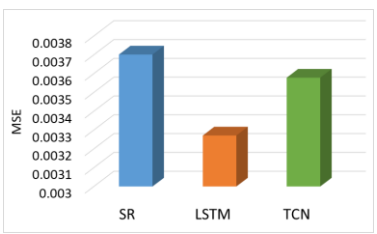

a) TSK

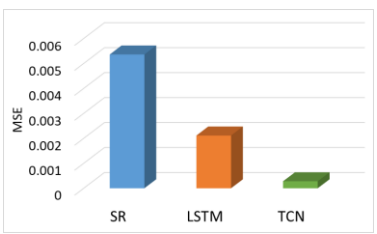

b) PSFC

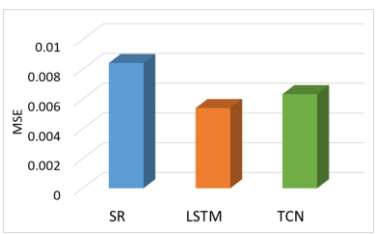

c) U10

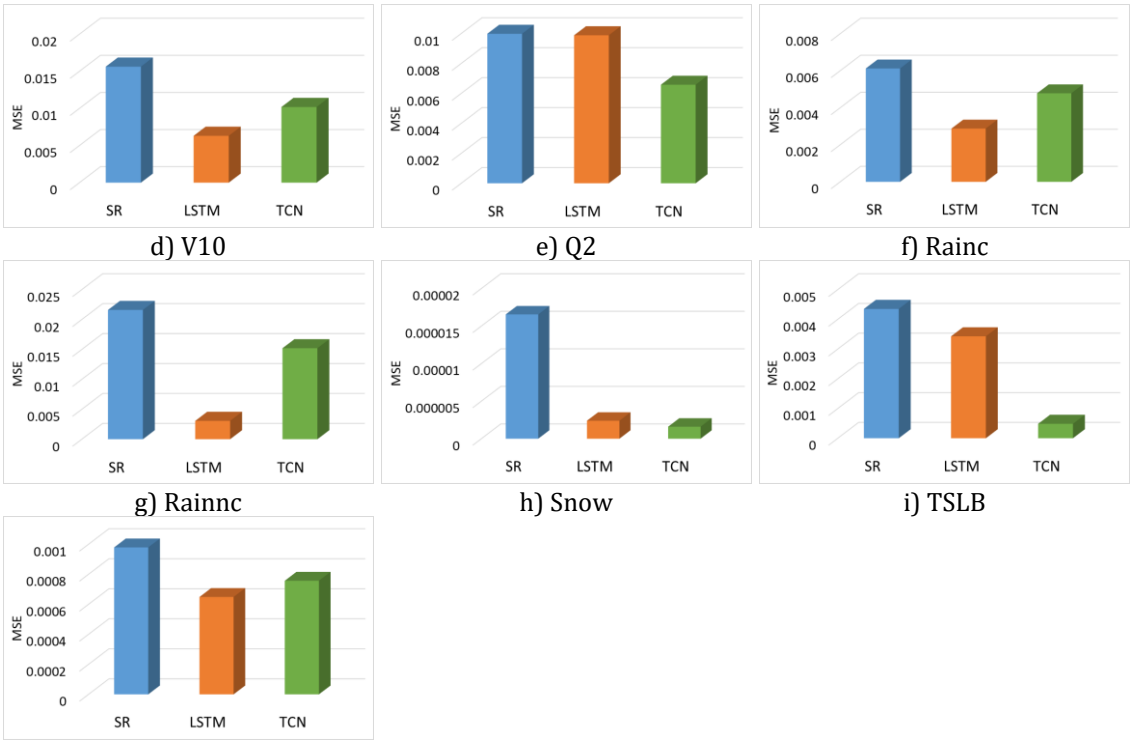

Figure 5.2 MIMO analysis of different approaches to predicting different weather parameters (SR- Standard Regression, LSTM- Long Short-Term Memory, TCN- Temporal Convolutional Network).

As per Table 5.5 and Figure 5.2, the deep learning with LSTM approach provides high accuracy output with least MSE for six parameters out of 10. Therefore, the MIMO-LSTM model variance has been selected as the proposed optimal in MIMO.

5.2.1.2 *MISO Machine learning model*

Similar to Section 5.2.1.1, the baseline approaches are compared with the proposed approaches to determine the optimal MISO model with least MSE. The SR, SVR, LSTM, and TCN neural network approaches are considered in this section and baseline-SR, baseline-SVR, MISO-LSTM, and MISO-TCN are the represented model variances for MISO.

5.2.1.2.1 Baseline approaches

5.2.1.2.1.1 SR

The system executes one code for each parameter to analyse the SR model. Each code predicted the weather for the appropriate parameter. The combined predicted results (i.e. combination of 10 predictions for ten surface weather parameters) are compared with the

ground truth, and the evaluation results are shown in Table 5.6. In this section, there are10 different codes are executed for each parameter.

Table 5.6 Evaluation of MIMO model with the SR approach.

Parameter	MSE	MAE	RMSE	EV
TSK	0.002401549	0.033694546	0.049005605	0.853776125
PSFC	0.00009359	0.006235455	0.00967419	0.998259326
U10	0.005820971	0.052148235	0.076295285	0.85456125
V10	0.009827752	0.065888867	0.09913502	0.858607021
Q2	0.00698015	0.059986458	0.083547292	0.831791012
Rainc	0.004125379	0.024884457	0.06422911	0.00836579
Rainnc	0.021597916	0.060223346	0.146962295	0.463462021
Snow	0.0000016555	0.008735346	0.001286649	0
TSLB	0.000934762	0.02234301	0.030573881	0.994170143
SMOIS	0.000359895	0.007139561	0.018970906	0.999852125

5.2.1.2.1.2 SVR

As described in Section 3.2.6.2, parameters are optimised for both linear and Radial Basis Function (*rbf*) kernels. Table 5.7 presents the cost values for 'linear' kernel, and Table 5.8 presents the cost and gamma values for the '*rbf*' kernel. As this process is massively time-consuming (Chin-Chia Hsu et al., 2006; Wu et al., 2009), one-fifth of the training dataset is used. That is every fifth record in the WRF training dataset used for parameter optimisation in SVR for both kernels. In parameter optimisation, there are 20 different codes executed (i.e. 10 for linear kernel and 10 for *rbf* kernel).

Table 5.7 SVR linear parameter tuning.

Parameter	C
TSK	10
PSFC	0.1
U10	10
V10	10
Q2	0.1
Rainc	0.001
Rainnc	0.01
Snow	1
TSLB	0.1
SMOIS	0.1

Table 5.8 SVR- *rbf* parameter tuning.

Parameter	C	Gamma
TSK	1	0.9
PSFC	10	0.9
U10	1	0.9
V10	1	0.9
Q2	1	0.9
Rainc	10000	0.001
Rainnc	10000	0.001
Snow	1	0.9
TSLB	1	0.9
SMOIS	1	0.9

Table 5.7 and Table 5.8 cost and gamma values are utilised with the SVR model code with the relevant parameter and trained the models using the WRF training dataset. The model predictions are evaluated and are presented in Table 5.9. In this section, there are 20 different programs executed.

Table 5.9 Evaluation results of SVR linear and *rbf* kernels.

Parameter	SVR Kernal='linear'	SVR Kernal='rbf'
TSK	0.002254852	0.002398545
PSFC	0.000092565	0.000089001
U10	0.005712145	0.005620015
V10	0.009235801	0.008465238
Q2	0.006901244	0.00689121
Rainc	0.003956207	0.003997512
Rainnc	0.019257844	0.021254879
Snow	0.0000009875	0.0000052144
TSLB	0.000846326	0.000847989
SMOIS	0.000285655	0.00029541

As indicated in Table 5.9, some parameters yield high accuracy outcome in the *rbf* kernel, while others in the linear kernel. Therefore, the combined models have been selected as the optimal model for MIMO with SVR (i.e. for the TSK parameter: linear kernel, PSFC parameter: RGF kernel, etc.). For Table 5.9, the evaluation metric is MSE and the lower MSE values are better and highlighted.

5.2.1.2.2 Proposed MISO approaches

5.2.1.2.2.1 LSTM

Similar to the MIMO-LSTM model variance, various configurations and controls are utilised for training and testing LSTM networks. Each parameter is trained and tested

with each configuration and control, but many of the parameters shown their lease MSE in configuration 1 and configuration 5. Appendix 4 presented a sample evaluation report for the MISO-LSTM model variance. Table 5.10 presents a summary of the least MSE found in various configurations and controls for each parameter. In this section, there are 120 experiments needed to carry out for selected configurations and controls.

Table 5.10 Best MSE found to each parameter in various configurations and controls for MISO-LSTM model variance.

Parameter	Best MSE for various configurations and controls			
	Config 1-adam	**Config 1- sgd**	**Config 6_adam**	**Config 6_sgd**
TSK	0.005949996	0.002066529	0.004696077	0.002041361
PSFC	0.000081591	0.000439629	0.000176554	0.000277838
U10	0.003008846	0.003090299	0.007356794	0.002748407
V10	0.004476656	0.003732091	0.003921446	0.003821692
Q2	0.010912588	0.007412029	0.010566528	0.006379222
Rainc	0.003167429	0.002826046	0.003167429	0.002799961
Rainnc	0.000519068	0.000502061	0.000519068	0.000523782
Snow	0.00000000	0.000000445	0.000000000	0.000000174
TSLB	0.004325722	0.000909574	0.003494298	0.000724035
SMOIS	0.000871767	0.000645901	0.00024636	0.00049283

5.2.1.2.2.2 TCN

Similar to MIMO-TCN model variance, the ‘save the best model’ method is utilised with different configurations and controls while training the models. Each trained model is evaluated with the testing dataset to determine the optimal MISO-TCN model variance. Please refer to Appendix 5 for a sample evaluation report. Table 5.11 presents the summary of the optimal MSE found in each parameter with model configuration and controls. In this section, there are 120 experiments to carry out for selected configuration and control.

As presented in Table 5.11, the least MSE values are found in different controls and configurations in each parameter. The above configurations are combined for the complete MISO-TCN model variance. Similar to the MIMO-TCN model variance, the following controls are retained constant within these experiments; kernel_size-2, dilations-7 where dilation values are- 1, 2, 4, 8, 16, 32, 64, batch size-64, and dropout rate-0, learning rate- 0.01.

Table 5.11 Summary of configurations and controls for MISO-TCN model variance for each parameter with least MSE.

Parameter	Optimal MSE	Configuration and controls
TSK	0.001738656	No of filters:256, no of TCN layers: 1, activation: tanh
PSFC	0.0000874041	No of filters:64, no of TCN layers: 1, activation: tanh
U10	0.004384032	No of filters:256, no of TCN layers: 3, activation: linear
V10	0.007427616	No of filters: 256, no of TCN layers: 3, activation: tanh
Q2	0.006752483	No of filters: 32, no of TCN layers: 2, activation: linear
Rainc	0.003260107	No of filters: 128, no of TCN layers:2, activation: tanh
Rainnc	0.001895714	No of filters: 64, no of TCN layers: 3, activation: linear
Snow	0.000000134	No of filters: 32, no of TCN layers: 3, activation: linear
TSLB	0.000376134	No of filters: 64, no of TCN layers: 1, activation: tanh
SMOIS	0.000099891	No of filters: 64, no of TCN layers: 1, activation: tanh

5.2.1.2.3 Compare baseline approaches and proposed approaches for Optimal MISO

Similar to Section 5.2.1.1.3, the proposed deep model variants are compared with classic ML approaches for MISO. The comparison results are shown in Table 5.12 and Figure 5.3. These results are subsequently evaluated via MSE for the normalised data. This is used to assess the optimal models for each parameter.

Table 5.12 MISO model comparison with different machine learning approaches. Lower MSE is better and is shown highlighted.

Parameter	SR	SVR	LSTM	TCN
TSK	0.002401549	0.002254852	0.002041361	0.001738656
PSFC	0.00009359	0.0000890012	0.0000816	0.0000874041
U10	0.005820971	0.005620015	0.002748407	0.004384032
V10	0.009827752	0.008465238	0.003732091	0.007427616
Q2	0.00698015	0.006901244	0.006379222	0.006752483
Rainc	0.004125379	0.003956207	0.002799961	0.003260107
Rainnc	0.021597916	0.019257844	0.000502061	0.001895714
Snow	0.0000016555	0.000000987	0.000000174	0.000000134
TSLB	0.000934762	0.000847989	0.000724035	0.000376134
SMOIS	0.000359895	0.000285655	0.00024636	0.000099891

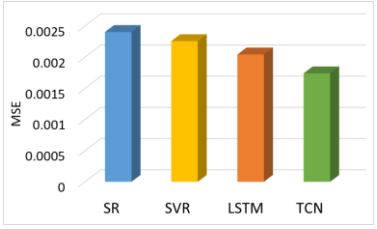

a) TSK

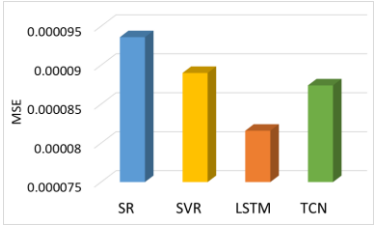

b) PSFC

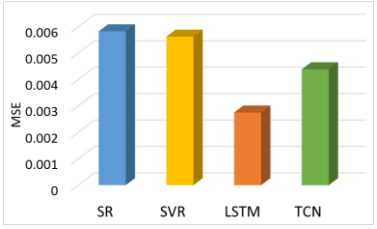

c) U10

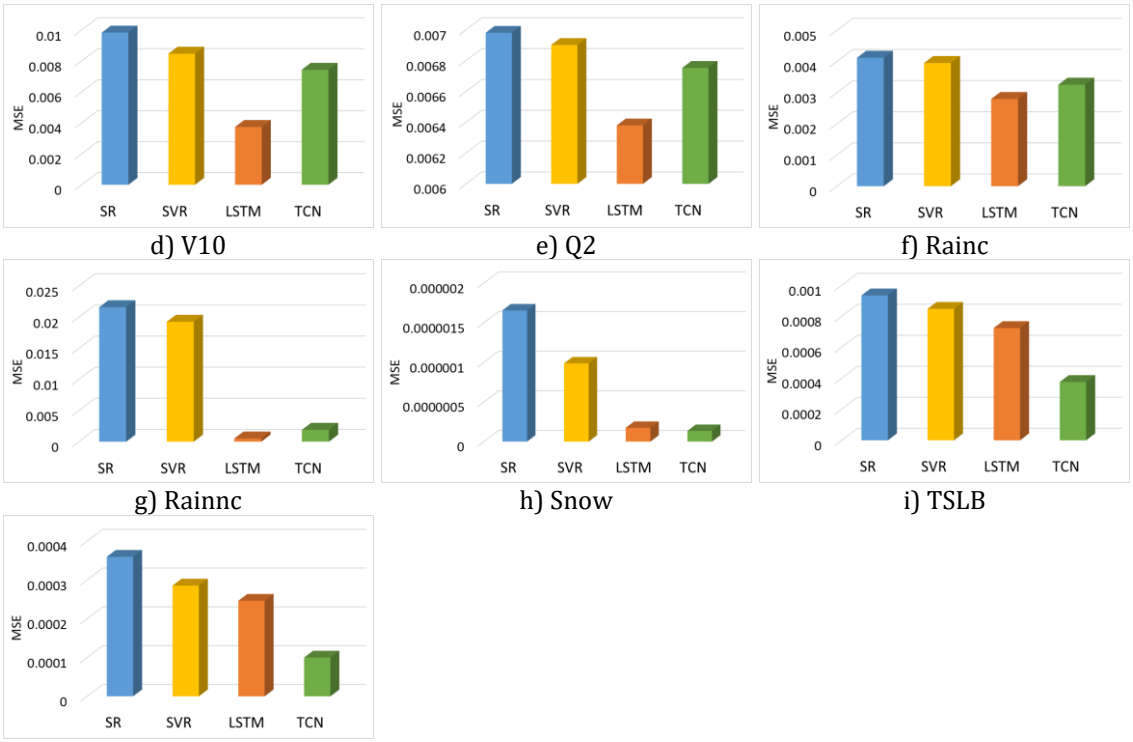

Figure 5.3 MISO model analysis of different approaches to predicting different weather parameters.

As per Table 5.12 and Figure 5.3, the MISO-LSTM model variance provides better performance with the least MSE for six parameters out of ten. Thus, the MISO-LSTM model variance (i.e. combined model with ten parameters) has been selected as the proposed optimal model for MISO.

This proves that the proposed approaches produce high performance with minimal errors compared to the baseline approaches in both MIMO and MISO models, as presented in Figure 5.2 and Figure 5.3. The reason is that the selected parameters do not follow a linear path within selected sequential timeslots (Bishop, 2006; McCREA et al., 2005) and there is a non-linear interrelationship among parameters (Graves, 2012; Jozefowicz et al., 2015; Kavitha et al., 2016). Besides, the sequential information is not encoded by the SR and SVR. The LSTM and TCN encode both multivariate and sequential information by taking them into another dimension in the input data (Bai et al., 2018; Basak et al., 2007; Jozefowicz et al., 2015).

As shown in Figure 5.2 and Figure 5.3, the LSTM yields better results for the U10 and V10 parameters compared to the other neural network techniques. The wind direction and the wind speed change intensely with the time due to the chaotic nature of the atmosphere (Dalto et al., 2015; Wang et al., 2011). The memory associated with the LSTM model is

able to preserve sequence information over time, and it could be obtained reliable results such an intensive change parameter (Hochreiter and Schmidhuber, 1997; Tai et al., 2015).

5.2.2 Comparison of MIMO and MISO optimal models

As described in Section 5.2.1, deep learning with LSTM is proposed for both MIMO and MISO optimal models. The following topics are mainly considered within this section;

- Proposing a short-term forecasting model
- Compare the proposed model prediction with the WRF model prediction

5.2.2.1 *Proposing a model for short-term forecasting*

According to Section 5.2.1.1.3 and Section 5.2.1.2.3, the MIMO-LSTM and MISO-LSTM model variances are proposed for the weather forecasting using the WRF historical weather data. In this section, these two models have compared determine the optimal model for short-term forecasting. Table 5.13 and Figure 5.4 present the evaluation results for MIMO-LSTM and MISO-LSTM model variances.

Table 5.13 Comparison of MSE for optimal MIMO and optimal MISO models.

Parameter	Model variance	
	MIMO	**MISO**
TSK	0.0032710542	0.002041361
PSFC	0.0021126748	0.000081591
U10	0.0053940886	0.002748407
V10	0.0063110087	0.003732091
Q2	0.009881492	0.006379222
Rainc	0.0028788105	0.002799961
Rainnc	0.0030708453	0.000502061
Snow	0.00000239	0.000000174
TSLB	0.0034273062	0.000724035
SMOIS	0.0006487666	0.00024636

Table 5.13 and Figure 5.4 present the comparison of MSE in each variable for both MIMO-LSTM and MISO-LSTM model variances. As shown, slightly better results are produced by the MISO-LSTM model variance compared to the MIMO-LSTM model variance in all the parameters. The reason for is that the MIMO-LSTM is concerned with the overall MSE, while MISO is concerned with MSE of the selected individual parameter. In MISO-LSTM model variance, the model is trained to get to the optimal result for the selected output parameter (CHANG et al., 2007; Hewage et al., 2019).

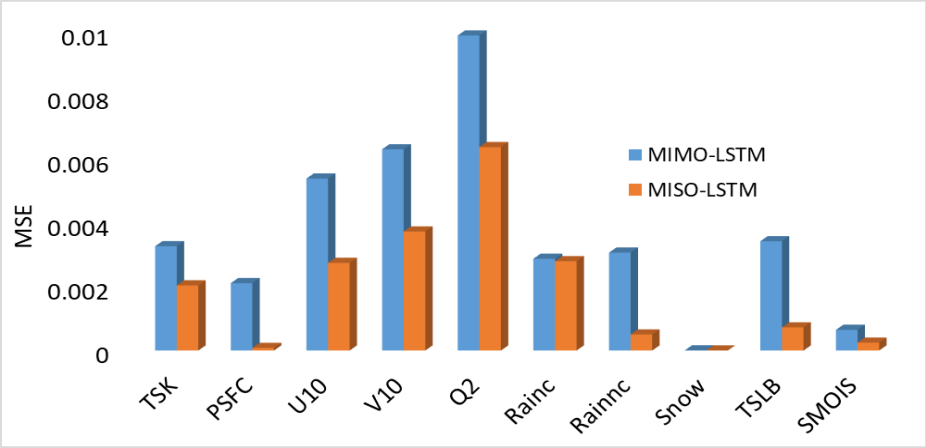

Figure 5.4 Comparison of MIMO and MISO optimal models.

According to these results, there is no significant gap between MSE values for each variable when compared MIMO-LSTM and MISO-LSTM model variances. These differences are less than 0.04 for each variable. These error figures are significantly smaller. Moreover, the MISO-LSTM model variance requires ten different models for the prediction of 10 different weather parameters. Therefore, the MIMO-LSTM model variance is considered to be the ultimate proposed model for short term weather forecasting since it is much more efficient (only one model to run) rather than running ten different models in MISO.

5.2.2.2 *Compare the proposed model prediction with the WRF model prediction*

As described in Section 3.2.5.1, the WRF validation dataset is utilised to get weather predictions using the proposed model (i.e. MIMO-LSTM model variance). Similarly, the WRF model is run in forecast mode using the WRF validation dataset to get weather forecasting results. Both WRF and proposed model predicted values are compared with respect to the ground truth. Table 5.14 and Figure 5.5 present the MSE comparison values for each parameter. Before comparison, the model prediction is de-normalised and converted to the human-understandable format. The reason for this is that the WRF prediction is often in real/actual values (i.e. not normalised nor in any other format) and is easy to understand (NCAR/UCAR, 2019).

Table 5.14 Comparison of the proposed deep model with the WRF forecasting model for 3-hour prediction. Lower MSE is better and is shown highlighted.

Parameter	MSE	
	WRF Model	**Proposed Deep Model**
TSK	4.0209727	2.7882845
PSFC	227869.02	123881.22
U10	10.540705	5.327054
V10	12.0824	4.6248293
Q2	0.000001112	0.000000771
Rainc	15.942339	0.11341145
Rainnc	18.627722	0.83847433
Snow	0.0	0.016857434
TSLB	8.140333	2.6088953
SMOIS	0.00008523	0.000024246839
Overall	22793.84	12389.753

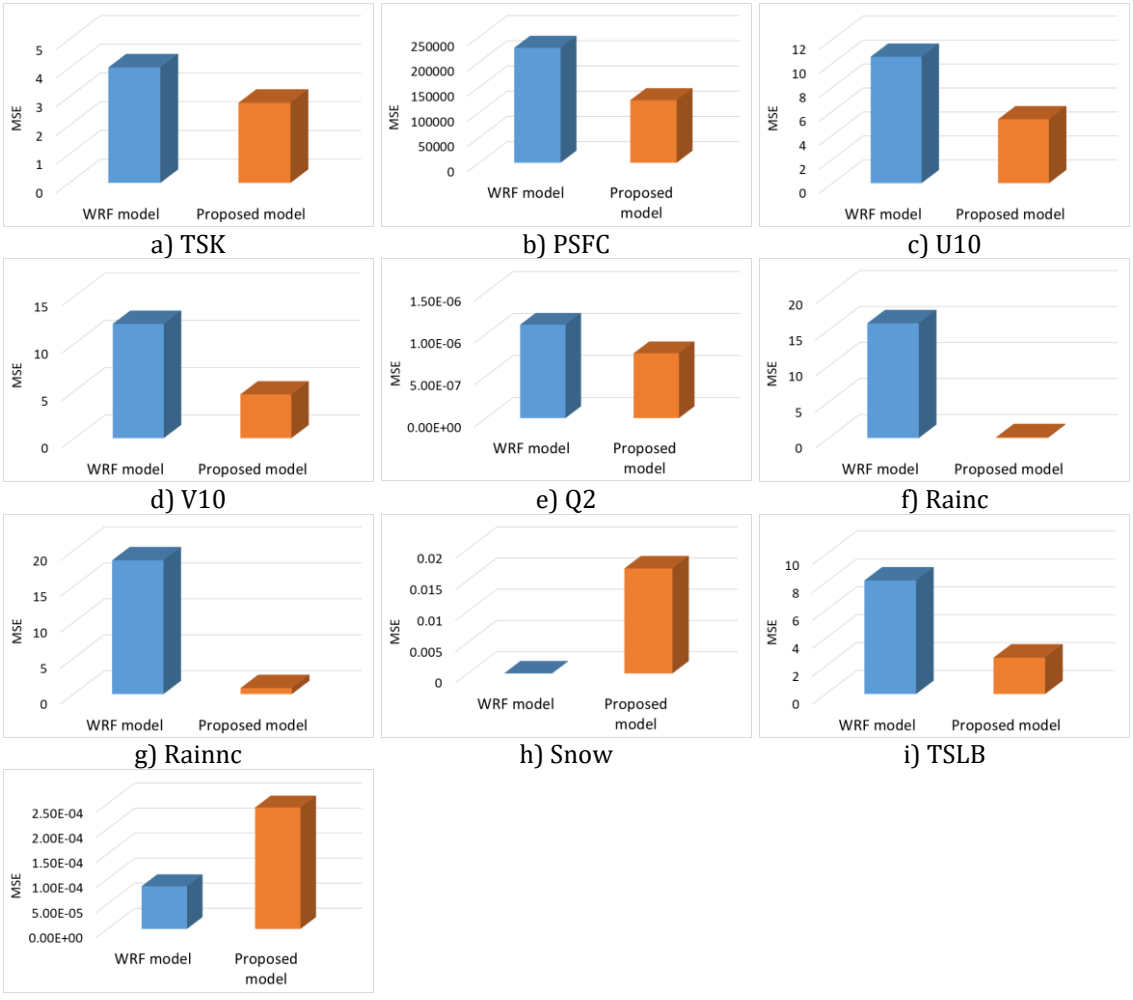

a) TSK b) PSFC c) U10

d) V10 e) Q2 f) Rainc

g) Rainnc h) Snow i) TSLB

j) SMOIS

Figure 5.5 Analysis of weather prediction of the WRF model and proposed deep learning model.

When comparing Table 5.14 and Figure 5.5, the proposed deep model provides comparatively better results (highlighted in the table) on eight occasions out of ten. The WRF model provides the best results for the Snow and Soil Moisture (SMOIS) variables. On both occasions, these error figures are quite small. For example, MSE for the variable snow is 0.0168574 kg/m2. This is quite a small and therefore, negligible. Similarly, the SMOIS has a minimal and negligible error value. The overall error comparison of WRF model prediction and the proposed deep learning model prediction is presented in Figure 5.6.

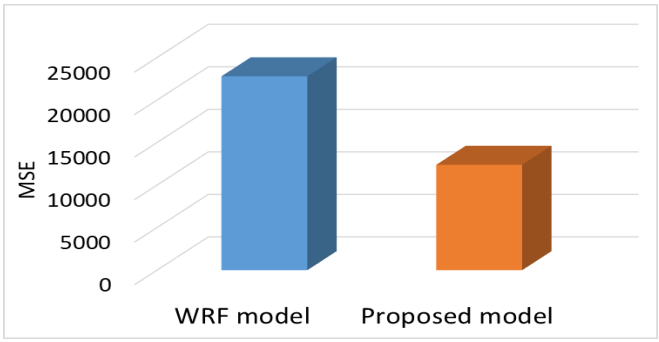

Figure 5.6 Overall MSE comparison of WRF model and proposed model predictions.

According to Figure 5.6, the proposed model yields much more accurate weather predictions compared to the state-of-the-art WRF model. As there are 125,373 samples in the July 2018 validation data, the proposed deep model and the WRF models will produce a similar number of outputs as the predicted data. It is difficult to visualise all of these predictions because of the large sample size and therefore, a random sample of the 100 samples has been taken from the test set to compare with the respective ground truth. Figure 5.7 shows a comparison of the proposed deep model verses WRF predictions. For each graph, the ground truth, WRF prediction, and the proposed deep model's predictions are represented by each line with blue, green, and red colours, respectively.

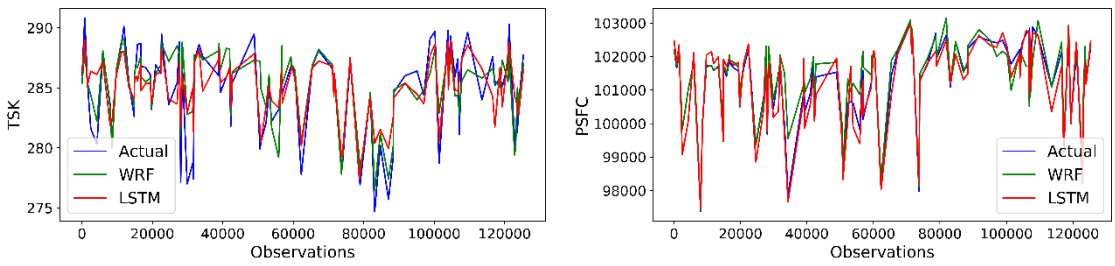

a) TSK b) PSFC

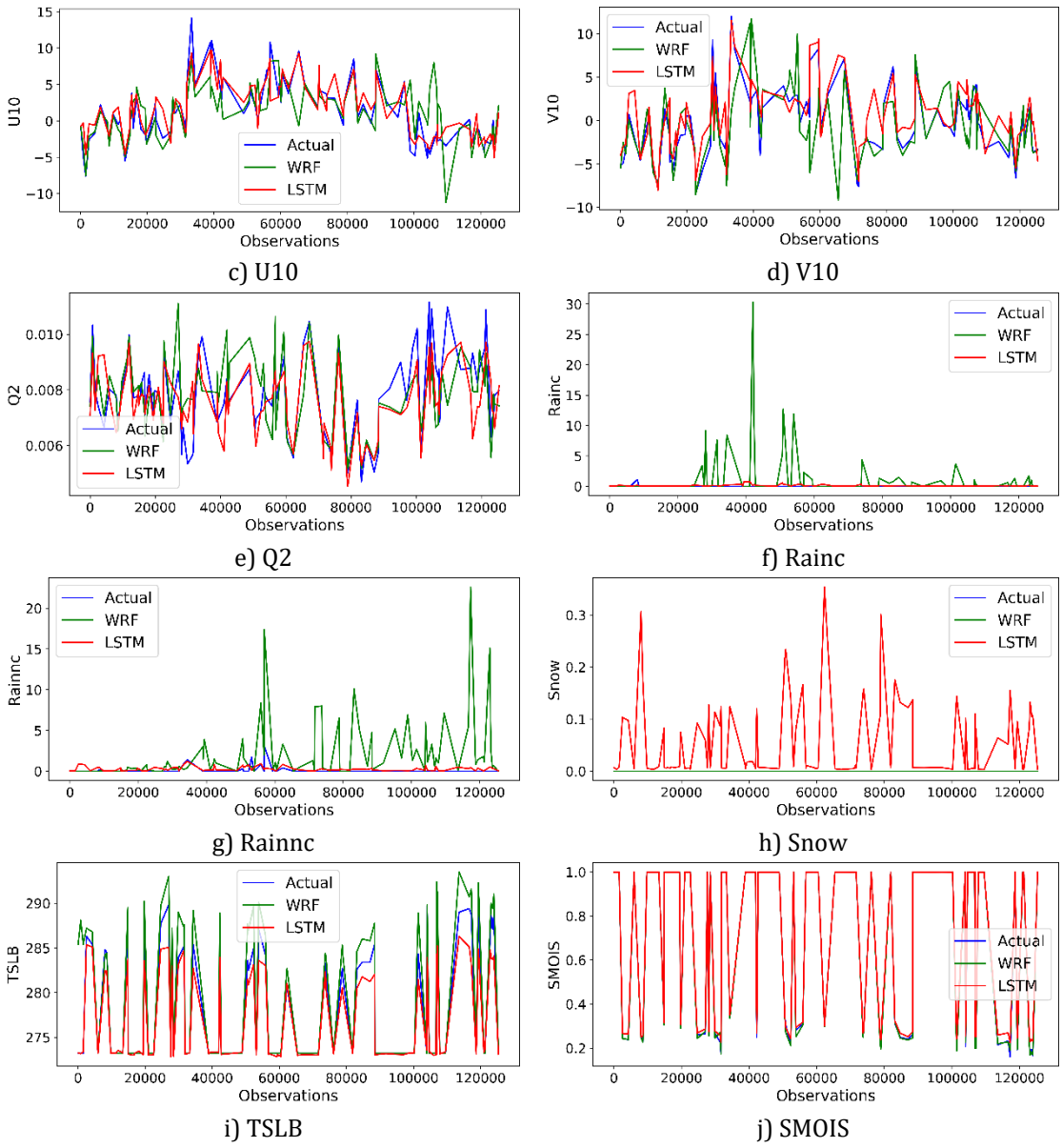

Figure 5.7 Comparison of WRF prediction vs the proposed deep learning model prediction for 100 random data samples with respect to the ground truth.

As per Figure5.7, the red line-chart (proposed model prediction) follows closely to the blue line-chart (ground truth) compared to the green-chart (WRF prediction). The WRF prediction is widely diverted in the parameters Rainc and Rainnc compared to the actual values. The deep model prediction is diverted in the parameter snow compared to the actual values. According to Figure 5.7 (h), the highest snow prediction is 0.34 kg/m2. This is quite a small figure and can be considered negligible. Overall, the proposed deep learning model provides a better short-term (i.e. up to 3 hours) prediction compared to the WRF model. In general, these results prove that the proposed deep learning model can be used for short-term weather forecasting. Overall, the proposed model is more accurate than the state-of-art WRF model.

The proposed model is evaluated mainly using the MSE metric. While evaluating the results, there are some other matrices also employed such as MAE, RMSE, and in some cases EV. All of these evaluation matrices work in a similar manner to calculate the error (Willmott and Matsuura, 2005). Therefore, the classification evaluation method is employed as a different type of evaluation metric or a different measurement to verify that the above results are accurate.

5.2.2.3 *Classification evaluation*

Code is written to calculate what percentage of the predicted results are diverted from its ground truth. In this context, the feasible range is calculated first based on the output prediction (y_p), defined rate (r), and ground truth (y_a). This analysis uses ten different rates, such as 1, 2, 3, 4, 5, 10, 15, 20, 30, and 50 in percentages. Therefore, the experiment is a success for the rate r, if the predicted value is within the range of

$$\boldsymbol{y_a - \left(y_a * \frac{r}{100}\right) < y_p \leq y_a + \left(y_a * \frac{r}{100}\right)} \quad \textbf{(5.1)}$$

Equation 5.1 is applied to each predicted data in the dataset and finally, the success rate is calculated based on Equation 5.2.

$$\boldsymbol{success\ rate = \left(\frac{No\ of\ samples\ within\ Eq(1)}{Total\ No\ of\ samples}\right) * 100\%} \quad \textbf{(5.2)}$$

Thus, Equation 5.2 provides the percentage of samples within the rate (r) relative to the ground truth (y_a). For example, if the ground truth is ten and the rate is 1%, then the predicted values must be within the range $9.9 < y_p \leq 10.1$. The code is used to check this condition for all samples and to finally calculate the success rate.

The only practical issue in the analysis is that if the ground truth is equal to zero, then the left-hand side and the right-hand side of Equation 5.2 become zero (i.e. from equation 5.1, $\left(y_a * \frac{r}{100}\right)$ is equal to $\left(\frac{0}{100}\right)$ if y_a is equal to 0, thus check the condition $0 < y_p \leq 0$). This means the condition is only checked $y_p = 0$ or not or any r value. This contradicts the basic requirement to calculate what percentage of the predicted results are diverted from its ground truth. Subsequently, if the ground truth is equal to zero, there is negligible predicted value in many times resulting unsatisfied the Equation 5.1.

In a practical situation, the values of some weather parameters can be zero. Some examples are rain, snow, rain rate, even temperature. This is one of the main reasons the regression modelling prefers to use averages to calculate the errors, such as MSE, MAE,

and RMSE. As shown in Figure 5.8 (a), there are several zero values in the ground truth file, mainly in the fields of Rainc, Rainnc, and Snow. As shown in Figure 5.8 (b), the Rainc, Rainnc, and snow proposed predicted values are relatively minimal and therefore, negligible. Therefore, the following conditions are applied to the predicted dataset to overcome this issue.

$$if\ Rainc < 0.1\ mm\ then\ Rainc = 0$$
$$if\ Rainnc < 0.1\ mm\ then\ Rainnc = 0$$
$$If\ snow < 0.1\ kg/m^2\ then\ snow = 0$$

By default, the WRF model often ignores negligible values when processing the weather prediction to present a viable prediction to users (Gallus and Segal, 2004; Mirocha et al., 2010; NCAR/UCAR, 2019). A sample of corresponding WRF prediction dataset is presented in Figure 5.8 (c). Figure 5.8 (d) presented the predicted dataset after correction. Figure 5.9 presented the results of the classification evaluation with and without corrections and its comparison to the WRF prediction.

1	2	3	4	5	6	7	8	9	10
287.9	101544	-3.4	-3.3	0.00998	0	0	0	273.2	1
287.9	101557	-3.3	-3.6	0.00996	0	0	0	273.2	1
288	101571	-3.4	-3.8	0.00996	0	0	0	273.2	1
288.1	101586	-3.6	-3.9	0.00997	0	0	0	273.2	1
288.2	101601	-3.8	-4	0.00998	0	0	0	273.2	1
288.2	101615	-4	-4	0.00997	0	0	0	273.2	1
288.2	101630	-4.1	-4	0.00997	0	0	0	273.2	1
288.2	101646	-4.2	-3.8	0.00997	0	0	0	273.2	1
288.2	101661	-4.3	-3.7	0.00994	0	0	0	273.2	1
288.2	101675	-4.4	-3.6	0.00985	0	0	0	273.2	1

a) Sample of a ground truth

1	2	3	4	5	6	7	8	9	10
287.4111	101828.3	-3.86655	-1.31475	0.008726	0.022951	0.069619	0.004865	273.213	0.998572
287.4612	101842.4	-3.826	-1.37788	0.008733	0.022272	0.06789	0.004853	273.2278	0.998562
287.5467	101855.2	-3.6871	-1.44265	0.008766	0.021982	0.066982	0.004815	273.2485	0.998557
287.5987	101865.6	-3.5186	-1.48809	0.00881	0.021813	0.066941	0.004773	273.2714	0.99855
287.6418	101878.1	-3.33817	-1.55869	0.008847	0.021683	0.066272	0.004728	273.2915	0.998546
287.6676	101886.7	-3.2102	-1.53739	0.008869	0.021411	0.065771	0.00468	273.3012	0.998544
287.693	101893.1	-3.1172	-1.44794	0.008889	0.021017	0.065022	0.004624	273.3089	0.998542
287.7097	101901.9	-3.02884	-1.42049	0.008891	0.020551	0.063785	0.004573	273.3135	0.99854
287.7108	101908.3	-2.95564	-1.34724	0.008885	0.020215	0.063043	0.004535	273.3116	0.99854
287.7468	101919.9	-2.90862	-1.32361	0.008862	0.019911	0.061638	0.004505	273.3056	0.998544

b) Corresponding proposed model prediction

1	2	3	4	5	6	7	8	9	10
287.9	101546	-3.5	-3.5	0.00991	0	0	0	287.9	1
288	101560	-3.4	-3.8	0.00988	0	0	0	288	1
288	101574	-3.4	-4	0.00988	0	0	0	288	1
288.1	101588	-3.6	-4.2	0.00989	0	0	0	288.1	1
288.2	101603	-3.7	-4.3	0.00989	0	0	0	288.2	1
288.2	101618	-3.8	-4.3	0.00988	0	0	0	288.2	1
288.1	101633	-3.9	-4.3	0.00989	0	0	0	288.1	1
288.1	101648	-4.1	-4.2	0.00989	0	0	0	288.1	1
288	101663	-4.2	-4	0.00986	0	0	0	288	1
287.9	101677	-4.2	-3.9	0.00976	0	0	0	287.9	1

c) Corresponding WRF prediction

1	2	3	4	5	6	7	8	9	10
287.4111	101828.3	-3.86655	-1.31475	0.008726	0	0	0	273.213	0.998572
287.4612	101842.4	-3.826	-1.37788	0.008733	0	0	0	273.2278	0.998562
287.5467	101855.2	-3.6871	-1.44265	0.008766	0	0	0	273.2485	0.998557
287.5987	101865.6	-3.5186	-1.48809	0.00881	0	0	0	273.2714	0.99855
287.6418	101878.1	-3.33817	-1.55869	0.008847	0	0	0	273.2915	0.998546
287.6676	101886.7	-3.2102	-1.53739	0.008869	0	0	0	273.3012	0.998544
287.693	101893.1	-3.1172	-1.44794	0.008889	0	0	0	273.3089	0.998542
287.7097	101901.9	-3.02884	-1.42049	0.008891	0	0	0	273.3135	0.99854
287.7108	101908.3	-2.95564	-1.34724	0.008885	0	0	0	273.3116	0.99854
287.7468	101919.9	-2.90862	-1.32361	0.008862	0	0	0	273.3056	0.998544

d) Proposed model prediction with corrections

Figure 5.8 Ground truth and the predicted data with and without corrections in normalised form (order of the data TSK, PSFC, U10, V10, Q2, Rainc, Rainnc, Snow, TSLB, and SMOIS).

As shown in Figure 5.9, the proposed model with the correction yields much better performance compared to the WRF model. The WRF model provides better performance for the parameters SMOIS and U10 for almost all rates. The parameters V10 and Q2 also provide much better results in the WRF model up to 10% rate. However, the gap between the WRF model and the proposed model is quite small and can be considered negligible. The overall performances are analysed, and the results are shown in Table 5.15 and Figure 5.10.

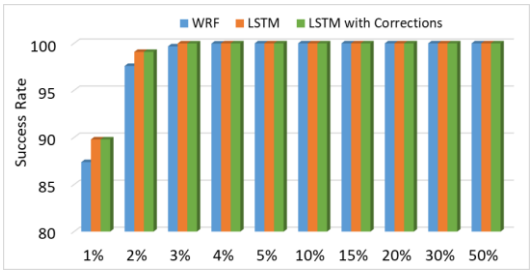

a) TSK

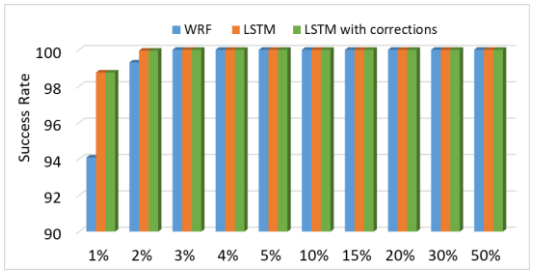

b) PSFC

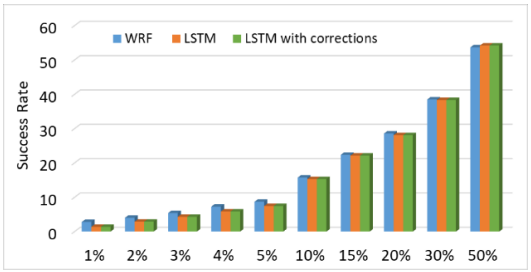

c) U10

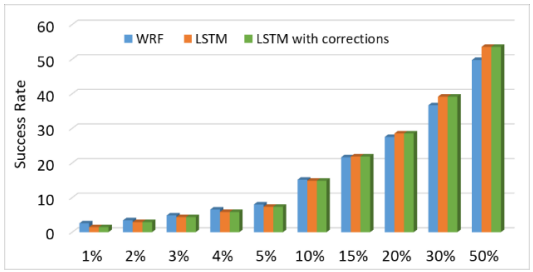

d) V10

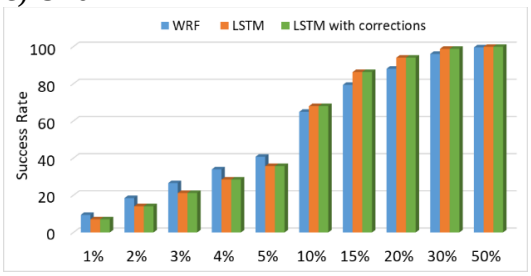

e) Q2

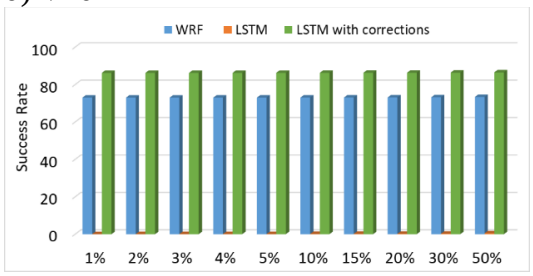

f) Rainc

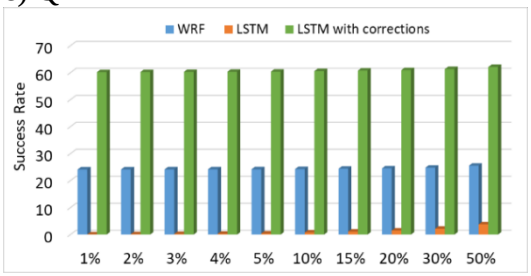

g) Rainnc

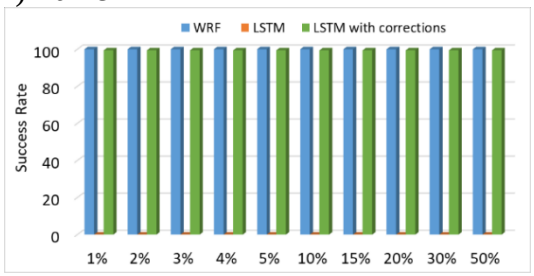

h) Snow

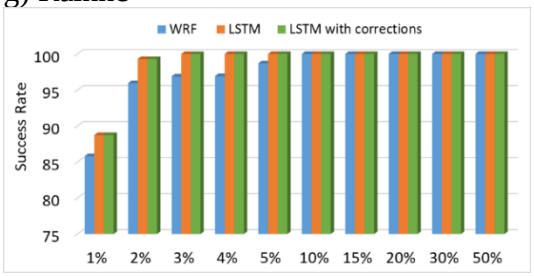

i) TSLB

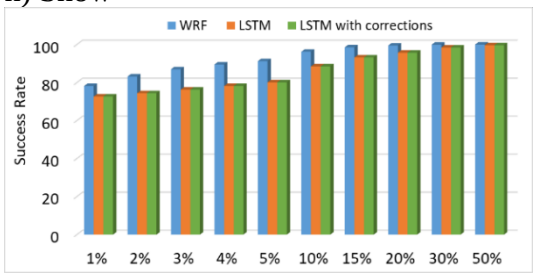

j) SMOIS

Figure 5.9 Classification evaluation of the prediction of the WRF model and the proposed model with and without corrections.

From the results presented in Table 5.15, it is apparent that the proposed model with corrections produces accurate results compared to the WRF model at all the selected rate. For example, the proposed model is 4.83% more accurate than the WRF model for the rate of 1%. Furthermore, as shown in Figure 5.10, much better overall performance is provided by the proposed model with a small correction compared to the WRF model for every rate with a higher success rate. Therefore, this proved the suggestion from Section 5.2.2.2, the proposed model can be used for weather forecasting, and it provides much better performance compared to the WRF model up to 3 hours prediction.

Table 5.15 Classification evaluation of the model variance MIMO-LSTM. The high success rate is better and is highlighted.

Rate	Success rate as a percentage			Accuracy gain: MIMO-LSTM vs WRF
	WRF	Proposed model	Proposed model With Corrections	
1%	55.73999186	35.99746357	60.57109585	4.831103986%
2%	59.91074633	39.28030756	63.84987198	3.939125649%
3%	61.7505364	40.64383879	65.20981392	3.459277516%
4%	63.13137597	41.86842462	66.42985332	3.298477344%
5%	64.46045002	43.10321999	67.6610594	3.200609382%
10%	68.92815838	48.74981057	73.28826781	4.360109433%
15%	71.94754852	52.47796575	76.99999202	5.052443509%
20%	74.13159133	54.80015633	79.30343854	5.171847208%
30%	76.91121693	57.71442017	82.18412258	5.27290565%
50%	80.19366211	61.15678814	85.5290214	5.335359288%

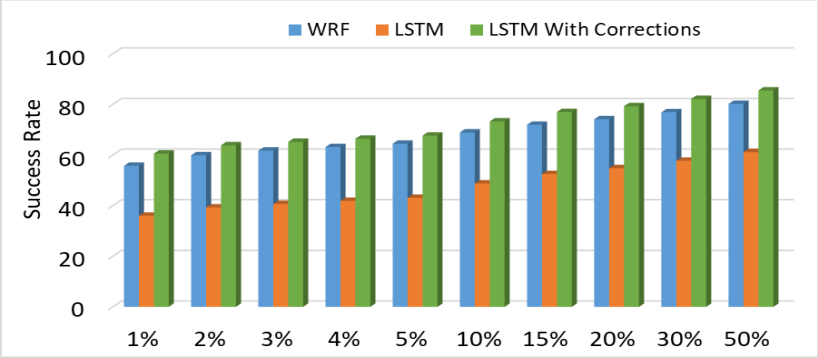

Figure 5.10 Overall classification evaluation the proposed MIMO-LSTM model variance.

5.2.3 Neural Network based Long-term Weather Prediction

As described in Section 5.2.2, ML technology can be utilised for short-term weather forecasting for up to three hours. This section is focused on long-term weather forecasting using the same historical weather data with ten surface parameters. As described in Section 3.2.5.2, there are three main subdivisions in this section.

- Select an appropriate approach to propose a long-term weather forecasting model.
- Use the proposed model for weather forecasting for 6 hours, 9 hours, 12 hours, 24 hours and 48 hours.
- Compare the predictions for each timeslot with the WRF model predictions.

5.2.3.1 *Select an appropriate approach to propose a long-term weather forecasting model*

As described in Section 5.2.2, the MIMO-LSTM model variance has been selected for short-term weather forecasting. Therefore, the same deep learning model with LSTM layers explores the long-term forecasting with the following variations. All these three variants use the same configuration and controls comparable to the MIMO-LSTM short-term forecasting optimal model.

a) Load the LSTM optimal model weights (3-hour) and re-train models for the long-term forecasting (shortened form: LSTM LW)
b) Train models for each time frame without loading the optimal model weights (shortened form: LSTM WL)
c) Use Bi-directional LSTM (shortened form: Bi-LSTM)

Therefore, the long-term weather forecasting model variances can be taken as LSTM LW, LSTM WL, and Bi-LSTM. A sample evaluation report is attached in Appendix 6 for each of the variations above. Table 5.16 and Figure 5.11 present the summarised comparison of these three variations for each long-term timeslot.

Table 5.16 Comparison of model variances LSTM LW, LSTM WL, and Bi-LSTM.

Parameter	**LSTM LW**	**LSTM WL**	**Bi-LSTM**
TSK	N/A	0.003271054	0.002371392
PSFC	N/A	0.002112675	0.001007641
U10	N/A	0.005394089	0.008889356
V10	N/A	0.006311009	0.010825
Q2	N/A	0.009881492	0.00885295
Rainc	N/A	0.002878811	0.004197211
Rainnc	N/A	0.003070845	0.025307791
Snow	N/A	0.00000239	0.00000106
TSLB	N/A	0.003427306	0.001056143
SMOIS	N/A	0.000648767	0.000677912

a) 3 Hour

Parameter	**LSTM LW**	**LSTM WL**	**Bi-LSTM**
TSK	0.003105633	0.004730743	0.003375287
PSFC	0.001950991	0.004029587	0.002242924
U10	0.013234701	0.013253746	0.014492277
V10	0.013633886	0.021873929	0.021943057
Q2	0.012803255	0.013993448	0.011232816
Rainc	0.005710668	0.005831303	0.005537389
Rainnc	0.06383751	0.06560797	0.05560357
Snow	0.0000001207	0.000002179	0.00000229

TSLB	0.002277339	0.002344848	0.001502663
SMOIS	0.000859006	0.000971699	0.000840205

b) 6 Hour

Parameter	LSTM LW	LSTM WL	Bi-LSTM
TSK	0.004679656	0.003785324	0.002954833
PSFC	0.00337704	0.005435103	0.002543765
U10	0.016287696	0.01789222	0.015199178
V10	0.022693845	0.032980144	0.026619522
Q2	0.016228491	0.017330563	0.014454748
Rainc	0.007961646	0.007261488	0.006792006
Rainnc	0.08320849	0.087723635	0.0691833
Snow	0.0000021387	0.000013947	0.00000186
TSLB	0.002113115	0.002125454	0.002216928
SMOIS	0.001027248	0.001156121	0.00075886

c) 9 Hour

Parameter	LSTM LW	LSTM WL	Bi-LSTM
TSK	0.005215215	0.005734219	0.004921308
PSFC	0.00554942	0.007137636	0.002907219
U10	0.017265592	0.01956549	0.017388191
V10	0.026892692	0.031699125	0.030242065
Q2	0.021506328	0.023158018	0.019144539
Rainc	0.011005162	0.009307778	0.008792502
Rainnc	0.09170363	0.100893565	0.07564226
Snow	0.000002031	0.000036374	0.000000454
TSLB	0.001918304	0.001969762	0.001659219
SMOIS	0.00062474	0.000726021	0.000572403

d) 12 Hour

Parameter	LSTM LW	LSTM WL	Bi-LSTM
TSK	0.003225559	0.003989982	0.003520491
PSFC	0.012482793	0.010315491	0.007714262
U10	0.026440082	0.026202237	0.024926782
V10	0.03660787	0.042136274	0.036013693
Q2	0.026067492	0.030222168	0.02755576
Rainc	0.08263268	0.07865509	0.078575564
Rainnc	0.15932418	0.16492906	0.158401
Snow	0.0000004652	0.000137658	0.000442552
TSLB	0.004401047	0.004503616	0.005910429
SMOIS	0.001600785	0.001434334	0.001202147

e) 24 Hour

Parameter	LSTM LW	LSTM WL	Bi-LSTM
TSK	0.004480547	0.005869389	0.003708232
PSFC	0.018504778	0.013365718	0.016115312

U10	0.045134	0.037737582	0.03475978
V10	0.04253545	0.04715329	0.042574175
Q2	0.050479617	0.04151997	0.038551033
Rainc	0.061815947	0.068089165	0.059418406
Rainnc	0.16204703	0.16313162	0.15197921
Snow	0.000003723	0.000231712	0.0000640
TSLB	0.007845704	0.012153346	0.005880864
SMOIS	0.00158867	0.001342647	0.001104945

j) 48 Hour

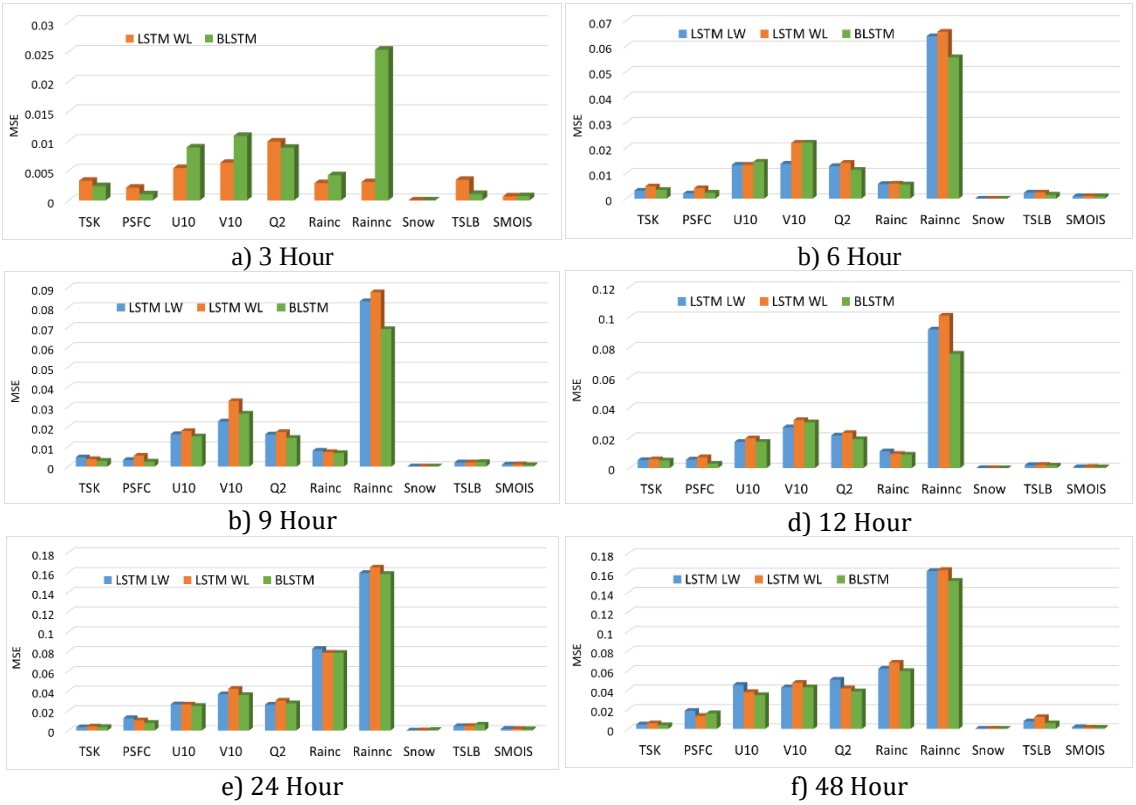

a) 3 Hour

b) 6 Hour

b) 9 Hour

d) 12 Hour

e) 24 Hour

f) 48 Hour

Figure 5.11 Comparison of model variances LSTM LW, LSTM WL, and Bi-LSTM (The notation of Bi-LSTM is visualised as BLSTM).

As implied by table 5.16 and Figure 5.11, the Bi-LSTM provides slightly better results compared to the LSTM LW except for the timeslot 3-hour. The reason for this is that the LSTM LW only preserves the information of the past as the only inputs it has seen are from the past. There are two layers used by the Bi-LSTM, one layer performs the operations following the same direction of the data sequence, and the other layer applies its operations in the reverse direction of the data sequence (Althelaya et al., 2018). This two-layer arrangement is facilitated an accurate weather prediction compared to the LSTM LW. The LSTM WL produces weaker results compared to both LSTM LW and Bi-LSTM. The reason for this is that the LSTM LW used its optimal weight, which is

already configured to re-train and yield a prediction (Hochreiter and Schmidhuber, 1997). The Bi-LSTM model is also trained at the beginning, similar to the LSTM WL. However, the Bi-LSTM provides more accurate results due to the ability to preserve the past and future values (Althelaya et al., 2018).

The overall MSE comparison for each timeslot is shown in Table 5.17 and Figure 5.12. The LSTM WL data has been removed from this table and graph as these models do not perform to the expected level. As per the overall results, it is evident that the Bi-LSTM yields better results compared to the LSTM for weather forecasting.

Table 5.17 Compare LSTM and Bi-LSTM model variances based on overall MSE values for each timeslot.

Timeslots	LSTM	Bi-LSTM
3 Hour	0.003699844	0.006318646
6 Hour	0.011741312	0.011677248
9 Hour	0.015757935	0.014072499
12 Hour	0.018168312	0.016127016
24 Hour	0.035278295	0.034456268
48 Hour	0.039443548	0.03541559

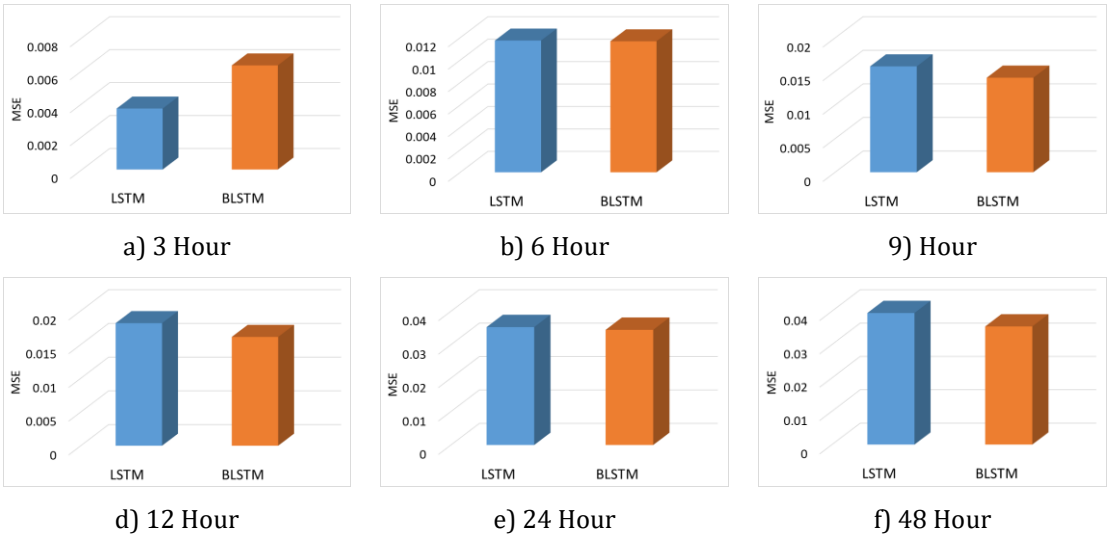

Figure 5.12 Comparison of LSTM and BLSTL for long-term weather forecasting.

The only drawback of the Bi-LSTM is the time taken for training, testing, and predicting data (Salehinejad et al., 2017). This is less efficient compared to the LSTM LW. Moreover, according to Table 5.17, there is a slight gap in the overall figures of MSE in both LSTM LW and Bi-LSTM. Therefore, the LSTM LW model variance has been

selected as the proposed model for long-term forecasting for an effective and efficient outcome.

5.2.3.2 *Use the proposed model for long-term weather forecasting*

The proposed model consists of three LSTM layers with other controls. As described in Section 5.2.3.1, the LSTM with loading the optimal weight method is used for the long-term weather prediction. Therefore, the optimal model is re-tuned (i.e. load optimal model weight and re-train models) for long-term timeslots. While retuning, the optimal models are found in different epochs such as 80, 10, 10, 10, and 10 for timeslots 6, 9, 12, 24, and 48 hours, respectively as shown in Figure 5.13. These optimal models are used as weather prediction models (i.e. proposed MIMO-LSTM) for the relevant timeslot. The prediction results will be compared with the well-known WRF results to determine the accuracy and suitability of these new models.

Epoch	Loss	Total MSE	Total MAE	Total RMSE	SkinTemp	SufPres	U10	V10	Humidity	Rainc	Rainnc	Snow	SoilTemp	SoilMoist
10	0.011880832	0.011880832	0.047026494	0.108999215	0.003731211	0.002185203	0.012854352	0.013167098	0.014048727	0.006119361	0.063629046	2.48146E-06	0.002096815	0.000974029
20	0.011889752	0.011889752	0.051545577	0.109040126	0.005614922	0.002947571	0.011071177	0.013335191	0.01677148	0.007184937	0.059253287	1.99601E-06	0.00180137	0.000915595
30	0.011946544	0.011946544	0.046494962	0.10930026	0.003721001	0.0022465	0.012735943	0.01419268	0.013358736	0.006295456	0.064201206	7.43781E-07	0.001755331	0.000957846
40	0.012283988	0.012283988	0.048452309	0.11083315	0.003946102	0.002666186	0.015601515	0.013403405	0.013299466	0.005994819	0.065014794	3.90059E-07	0.002092412	0.000820788
50	0.011968353	0.011968353	0.047357106	0.109399974	0.003802319	0.002693907	0.012771716	0.014566889	0.013339048	0.006059669	0.06385493	3.63632E-07	0.001811673	0.000783019
60	0.01184735	0.01184735	0.047151309	0.108845524	0.003671956	0.002680889	0.013538075	0.013685755	0.013493523	0.005832097	0.06298571	2.25716E-07	0.001729121	0.000856148
70	0.011799956	0.011799956	0.046568167	0.10862758	0.003252286	0.002202216	0.011237701	0.01622022	0.015044644	0.005824219	0.06160926	1.83367E-07	0.00192054	0.000688296
80	0.011741312	0.011741312	0.045655386	0.108357325	0.003105633	0.001950991	0.013234701	0.013633886	0.012803255	0.005710668	0.06383751	1.20664E-07	0.002277339	0.000859006
90	0.012112958	0.012112958	0.04740905	0.11005889	0.003269029	0.001732615	0.013996867	0.01698269	0.013135998	0.005770418	0.06306092	1.51211E-07	0.002452568	0.000728323
100	0.012187444	0.012187444	0.048374469	0.11039675	0.003405049	0.001708889	0.013968434	0.018579261	0.013793162	0.005720335	0.061504878	1.69814E-07	0.00249288	0.000701383
110	0.012657643	0.012657643	0.05070106	0.11250619	0.004262536	0.002003955	0.015268126	0.02327254	0.012695582	0.005686414	0.06064813	1.62963E-07	0.001822816	0.000916167
120	0.012829151	0.012829151	0.049755243	0.113265835	0.003915706	0.002255355	0.01458518	0.02340477	0.012871401	0.00566747	0.062535815	1.67224E-07	0.00239053	0.000665109
130	0.013627052	0.013627052	0.053838368	0.11673497	0.004222805	0.002664993	0.016297309	0.03063119	0.013408243	0.00567446	0.060534995	1.33536E-07	0.001795727	0.001040662
140	0.013653389	0.013653389	0.053063726	0.116847716	0.004031833	0.002775423	0.014514714	0.02910935	0.014565311	0.005629259	0.06255872	1.12849E-07	0.002342	0.001007178
150	0.013472496	0.013472496	0.051782125	0.116071075	0.003526571	0.002482961	0.013233547	0.030468164	0.013498244	0.005674074	0.06269933	1.26655E-07	0.002138502	0.001003449
160	0.013516137	0.013516137	0.052800921	0.116258934	0.003454343	0.002500062	0.016590854	0.028890422	0.013912486	0.005647554	0.061493102	9.34166E-08	0.001607068	0.001065381
170	0.013407045	0.013407045	0.05258392	0.11578879	0.003472979	0.00250838	0.014671385	0.028681722	0.014318332	0.005668049	0.06124811	7.21905E-08	0.002071	0.001430414
180	0.013301829	0.013301829	0.051897612	0.11533356	0.003659899	0.002420059	0.012969964	0.027121764	0.015814813	0.005646311	0.061921947	7.28623E-08	0.002188269	0.001275198
190	0.013242478	0.013242478	0.052232255	0.11507596	0.003871053	0.002349507	0.013302174	0.026180876	0.015240627	0.005633408	0.06210364	5.08693E-08	0.002199922	0.001543519
200	0.013652145	0.013652145	0.052859727	0.116842404	0.003343507	0.002428929	0.012679976	0.03132901	0.015193537	0.00563848	0.062400546	3.82936E-08	0.002390753	0.001116677

a) 6-Hour

Epoch	Loss	Total MSE	Total MAE	Total RMSE	SkinTemp	SufPres	U10	V10	Humidity	Rainc	Rainnc	Snow	SoilTemp	SoilMoist
10	0.015757935	0.015757935	0.055693333	0.12553059	0.004679656	0.00337704	0.016287696	0.022693845	0.016228491	0.007961646	0.08320849	2.13871E-06	0.002113115	0.001027248
20	0.016377352	0.016377352	0.05758737	0.12797405	0.004780752	0.004161583	0.015768358	0.024669867	0.017805502	0.007928615	0.08485703	3.94859E-07	0.002780593	0.001020818
30	0.016225789	0.016225789	0.056997567	0.12738049	0.004396642	0.00394337	0.016345497	0.024135446	0.018725771	0.007424103	0.08399795	1.33924E-07	0.002588698	0.000700276
40	0.016889573	0.016889573	0.058274614	0.12995991	0.004091627	0.003541212	0.023068156	0.025812227	0.017774226	0.007382475	0.08432323	5.61554E-08	0.00227121	0.000631322
50	0.015881893	0.015881893	0.055916136	0.12602338	0.003115935	0.003512865	0.017332496	0.025864141	0.017602265	0.007014104	0.081535935	7.06454E-08	0.00186925	0.000971862
60	0.016796989	0.016796989	0.058133409	0.12960319	0.003795971	0.003075606	0.021199834	0.026161082	0.021123258	0.006922953	0.08180809	8.13968E-08	0.002633235	0.001249783
70	0.017635695	0.017635695	0.06026591	0.13279945	0.003228196	0.003066612	0.023100615	0.027171036	0.025604945	0.006963012	0.08208669	7.74571E-08	0.003423439	0.001712335
80	0.017547182	0.017547182	0.060411342	0.13246578	0.002949332	0.003273398	0.022983102	0.029731503	0.02371691	0.006989821	0.080700785	9.1216E-08	0.0037328	0.001394077
90	0.017949101	0.017949101	0.060925115	0.13397425	0.002661645	0.003416948	0.02212525	0.032491915	0.025065918	0.006881265	0.08195113	9.07774E-08	0.003301371	0.001595485
100	0.018190717	0.018190717	0.062394377	0.13487296	0.002803703	0.003402452	0.024458399	0.034984346	0.026161322	0.006845449	0.07862746	1.1193E-07	0.003748103	0.000875838
110	0.017026861	0.017026861	0.060662873	0.13048702	0.002764516	0.00336351	0.024438854	0.030594964	0.022807699	0.006948222	0.074446276	1.25099E-07	0.003371792	0.00153265
120	0.01747755	0.01747755	0.06080798	0.13220268	0.002764753	0.003259942	0.023535227	0.031763922	0.024674775	0.007017958	0.07808133	1.944E-07	0.002698125	0.000979277
130	0.017094668	0.017094668	0.060410833	0.13074657	0.002576924	0.003335403	0.023330005	0.030339586	0.025773872	0.00703206	0.074659914	1.96977E-07	0.002670562	0.001228146
140	0.018113356	0.018113356	0.064531514	0.13458587	0.00334275	0.003557617	0.024213657	0.031598367	0.024424609	0.007457991	0.082915045	3.71141E-07	0.002859531	0.000763623
150	0.018422959	0.018422959	0.06482559	0.1357312	0.002699622	0.003552596	0.02457906	0.031169334	0.024581714	0.007370967	0.0866783	3.60684E-07	0.002456277	0.001141363
160	0.017858673	0.017858673	0.063119786	0.13363636	0.002892328	0.003501765	0.020936118	0.032180637	0.025767589	0.007646391	0.08192321	5.47187E-07	0.002749522	0.000988633
170	0.017876867	0.017876867	0.062951145	0.13370441	0.003300311	0.003563964	0.020314913	0.032290924	0.027064811	0.007804983	0.08029603	5.54635E-07	0.002957341	0.001174839
180	0.017933326	0.017933326	0.062476464	0.13391536	0.003237417	0.003455933	0.021472199	0.032769695	0.025042387	0.007832415	0.08121826	6.219E-07	0.003055916	0.001248424
190	0.017714157	0.017714157	0.061627537	0.13309455	0.003638247	0.003581857	0.019355508	0.032510065	0.023253022	0.007725931	0.08291529	5.32091E-07	0.00310764	0.001053481
200	0.018595811	0.018595811	0.063346221	0.13636644	0.004599463	0.003611667	0.02131773	0.033541203	0.02467186	0.007319229	0.08648799	5.27329E-07	0.003480847	0.000927581

b) 9-Hour

Epoch	Loss	Total MSE	Total MAE	Total RMSE	SkinTemp	SufPres	U10	V10	Humidity	Rainc	Rainnc	Snow	SoilTemp	SoilMoist
10	0.018168312	0.018168312	0.063213759	0.13478991	0.005215215	0.00554942	0.017265592	0.026892692	0.021506328	0.011005162	0.09170363	2.03197E-06	0.001918304	0.00062474
20	0.018508941	0.018508941	0.062819209	0.13604759	0.00577887	0.005310341	0.016907116	0.027853396	0.021553569	0.010309829	0.09405656	9.32677E-08	0.002475688	0.000843951
30	0.01881445	0.01881445	0.062807294	0.13716576	0.005732369	0.004024884	0.017273948	0.02721256	0.026104566	0.00973269	0.09392474	1.79693E-08	0.002298528	0.0018402
40	0.018732654	0.018732654	0.063061912	0.13686728	0.006817689	0.002891949	0.022314554	0.02761125	0.021102173	0.009103359	0.092818625	1.26624E-08	0.003022199	0.001644727
50	0.019155814	0.019155814	0.063730995	0.13840455	0.004793331	0.003231146	0.026248788	0.028889831	0.02459779	0.009090507	0.09141317	2.07434E-08	0.00240194	0.00089161
60	0.019534009	0.019534009	0.064953147	0.13976413	0.00549422	0.003385383	0.029479	0.029457167	0.02482446	0.008990956	0.090143636	2.70911E-08	0.002714725	0.00085051
70	0.019925085	0.019925085	0.067691709	0.14115624	0.006466243	0.003789936	0.030867876	0.031851623	0.023245657	0.009020241	0.088062584	2.46055E-08	0.004559531	0.001387129
80	0.02039999	0.02039999	0.07019725	0.14282854	0.006846574	0.003929815	0.034896195	0.033238024	0.024830071	0.009081832	0.08516334	2.39362E-08	0.00456646	0.001447573
90	0.020479311	0.020479311	0.070280744	0.14310594	0.005561492	0.004183779	0.032013264	0.03360095	0.028006002	0.00917886	0.087113604	2.39714E-08	0.004130787	0.001004341
100	0.020603129	0.020603129	0.072553816	0.14353791	0.006559047	0.004386804	0.028914856	0.03481124	0.026264356	0.0097702	0.08967066	2.471E-08	0.004340007	0.001314096
110	0.020208527	0.020208527	0.068170527	0.14215672	0.005426755	0.004303248	0.026014872	0.03164566	0.022644183	0.009985281	0.09680126	2.5219E-08	0.004412526	0.000851467
120	0.020712192	0.020712192	0.068695856	0.14391729	0.005347285	0.004477984	0.02849259	0.033286467	0.02119362	0.01037	0.09859387	1.82773E-08	0.004358369	0.001001719
130	0.020497048	0.020497048	0.067991013	0.1431679	0.005170254	0.004658661	0.027230944	0.03288422	0.021944176	0.010436207	0.0982031	2.14096E-08	0.003426644	0.001016253
140	0.022201666	0.022201666	0.071454163	0.14900224	0.005441561	0.005012208	0.025829012	0.034125216	0.024831053	0.012658997	0.10928951	2.49729E-08	0.003819484	0.001009597
150	0.035390579	0.035390579	0.10206884	0.18812384	0.015071535	0.012291354	0.037173413	0.046244223	0.025679681	0.009132251	0.1995135	2.09872E-09	0.007725423	0.001074392
160	0.021682148	0.021682148	0.07031585	0.1472486	0.005265066	0.005495853	0.02517384	0.036284804	0.022308592	0.01113453	0.10694081	1.69008E-08	0.003273835	0.000944134
170	0.022999838	0.022999838	0.073690015	0.15165699	0.005675666	0.006105296	0.028019242	0.035426605	0.02515365	0.010038584	0.11430279	1.62984E-08	0.003916081	0.001360467
180	0.022167217	0.022167217	0.071161168	0.14888659	0.005787159	0.005903522	0.025867606	0.036394164	0.022941379	0.010809409	0.1096971 85	1.93009E-08	0.003310693	0.000961037
190	0.021263284	0.021263284	0.068970337	0.14581934	0.005502604	0.005881147	0.025363903	0.035533357	0.022658037	0.009996519	0.10294915	1.8799E-08	0.003583193	0.001164913
200	0.022493377	0.022493377	0.071593823	0.14997794	0.005527182	0.006324725	0.027104	0.036824547	0.022385085	0.011801347	0.110730484	1.93184E-08	0.003187064	0.001049322

c) 12-Hour

Epoch	Loss	Total MSE	Total MAE	Total RMSE	SkinTemp	SufPres	U10	V10	Humidity	Rainc	Rainnc	Snow	SoilTemp	SoilMoist
10	0.035278295	0.035278295	0.084798039	0.18782514	0.003225559	0.012482793	0.026440082	0.03660787	0.026067492	0.08263268	0.15932418	4.65178E-07	0.004401047	0.001600785
20	0.038526183	0.038526183	0.094821279	0.19628087	0.007801083	0.009863263	0.029195528	0.055139005	0.045684904	0.07770445	0.15050963	6.96557E-09	0.006083079	0.003280893
30	0.042508376	0.042508376	0.101289001	0.20617558	0.009394499	0.010084411	0.03930838	0.08359845	0.035668395	0.07718168	0.15418398	1.79992E-09	0.012594576	0.003069381
40	0.045238581	0.045238581	0.100059619	0.21269362	0.009053104	0.009487113	0.04058452	0.060868595	0.037865322	0.07864509	0.20404524	1.06445E-09	0.009241772	0.002595051
50	0.054377599	0.054377599	0.105520305	0.23319007	0.009864598	0.012005068	0.04484045	0.04004732	0.03956266	0.07957821	0.30422497	6.69296E-10	0.009840525	0.003812197
60	0.04919757	0.04919757	0.097970994	0.22180521	0.010007803	0.01365881	0.03710723	0.04508776	0.035365295	0.07936354	0.26306534	7.41822E-10	0.006222983	0.002096949
70	0.050991201	0.050991201	0.101289488	0.2258123	0.010218216	0.011574603	0.03703297	0.046678953	0.0470371	0.07951516	0.26834944	7.03968E-10	0.006907712	0.00259782
80	0.047091502	0.047091502	0.098425509	0.21700577	0.011361425	0.01044426	0.033679176	0.049000453	0.054099843	0.0798721	0.2238894	8.56535E-10	0.006443065	0.002125299
90	0.048896684	0.048896684	0.098396479	0.22112598	0.011231925	0.010486415	0.036623493	0.048496626	0.049189944	0.080369145	0.2449911	4.34007E-10	0.005673097	0.001905083
100	0.04768123	0.04768123	0.098292005	0.21836033	0.011160671	0.011275074	0.032614965	0.04881925	0.05063022	0.082412496	0.23173787	6.76899E-10	0.006393679	0.001768075
110	0.050832711	0.050832711	0.102366767	0.22546114	0.012417804	0.012072334	0.034504138	0.052208826	0.05384289	0.080886975	0.25362018	7.08069E-10	0.007232836	0.001541128
120	0.052808578	0.052808578	0.104876316	0.22980118	0.012684858	0.01224992	0.03429458	0.052305315	0.0627469	0.081723414	0.26173085	5.38239E-10	0.008356131	0.001993794
130	0.052786363	0.052786363	0.104996646	0.22975282	0.012458004	0.012107072	0.036881108	0.053248703	0.063766345	0.08048129	0.25932655	8.46556E-10	0.007952649	0.001641898
140	0.056903973	0.056903973	0.109957169	0.23854554	0.014271903	0.011812016	0.039059155	0.0537714	0.06472012	0.0811419	0.29314673	6.2965E-10	0.008712303	0.002404193
150	0.051209426	0.051209426	0.102883986	0.226295	0.010422079	0.011420611	0.039816942	0.05305741	0.059796773	0.08006839	0.24818857	4.02581E-10	0.007822258	0.001501247
160	0.054407555	0.054407555	0.107164499	0.23325428	0.012308086	0.011514108	0.03818642	0.05476732	0.06914177	0.08078609	0.2670897	5.09291E-10	0.008878582	0.001403457
170	0.053810722	0.053810722	0.105568876	0.23197138	0.012048912	0.011561659	0.038795292	0.05286536	0.06509044	0.08179374	0.26572466	3.39706E-10	0.008823274	0.001403897
180	0.052988258	0.052988258	0.102958477	0.23019177	0.010306744	0.011484533	0.03863995	0.05366018	0.05838738	0.08014045	0.26851523	5.07206E-10	0.007443136	0.001304965
190	0.055379674	0.055379674	0.108269359	0.23532887	0.013458454	0.0126105	0.04037479	0.05116131	0.06793118	0.08121871	0.27681202	5.41363E-10	0.008690842	0.001538952
200	0.051780626	0.051780626	0.101589085	0.22755352	0.010444876	0.011364442	0.03630859	0.050317705	0.06338877	0.08100908	0.25530696	4.15137E-10	0.008185733	0.001480075

d) 24-Hour

Epoch	Loss	Total MSE	Total MAE	Total RMSE	SkinTemp	SufPres	U10	V10	Humidity	Rainc	Rainnc	Snow	SoilTemp	SoilMoist
10	0.039443548	0.039443548	0.104953038	0.19860399	0.004480547	0.018504778	0.045134	0.04253545	0.050479617	0.061815947	0.16204703	3.72323E-06	0.007845704	0.00158867
20	0.050524607	0.050524607	0.133930303	0.22477679	0.010866623	0.040970627	0.064053625	0.05533227	0.067824066	0.06539377	0.17919685	2.05741E-06	0.02009033	0.001515825
30	0.052402805	0.052402805	0.1348322	0.22891657	0.015541649	0.058866363	0.047961455	0.07329825	0.056366853	0.072956555	0.17619486	5.94387E-07	0.020514319	0.002327148
40	0.051256524	0.051256524	0.12096036	0.22639905	0.010983861	0.023254588	0.049383994	0.07441978	0.070140794	0.082910486	0.18060051	3.00314E-07	0.019207379	0.00166354
50	0.051267052	0.051267052	0.11994868	0.22642228	0.009666085	0.016976401	0.0572509	0.06261647	0.08337076	0.07359093	0.18676947	4.98233E-07	0.019855833	0.002573184
60	0.049496081	0.049496081	0.11386743	0.22247717	0.011778341	0.019321507	0.05004405	0.061706565	0.072427385	0.07189906	0.18587373	8.04124E-07	0.020058883	0.001850511
70	0.048560495	0.048560495	0.112098717	0.22036447	0.012362056	0.021895798	0.05497312	0.05139867	0.0679441	0.06550986	0.19189109	9.12338E-07	0.017525863	0.002103506
80	0.048983753	0.048983753	0.111347737	0.22132273	0.009686956	0.021653697	0.054013036	0.054473672	0.0683569	0.0647887	0.19698375	7.85495E-07	0.017810628	0.002069383
90	0.05108366	0.05108366	0.115232204	0.22601694	0.008507939	0.02290317	0.05941409	0.054790188	0.0672797	0.0753799	0.20089215	1.04119E-06	0.019084297	0.002584158
100	0.049484016	0.049484016	0.11077446	0.22245002	0.008547222	0.021124588	0.051336087	0.055467412	0.06887612	0.07565808	0.19537593	1.03455E-06	0.016417656	0.002036024
110	0.05054124	0.05054124	0.112859597	0.2248138	0.008532953	0.02735787	0.052848577	0.056025293	0.05893893	0.07725379	0.20753527	6.50297E-07	0.014649896	0.002269133
120	0.049887057	0.049887057	0.11134138	0.22335409	0.00889026	0.0230664	0.05232882	0.05481144	0.06947364	0.07185504	0.19915302	9.2668E-07	0.016689576	0.00260148
130	0.05227106	0.05227106	0.114624717	0.22862867	0.009102572	0.022088705	0.05594286	0.055981126	0.07545797	0.07807255	0.20496728	7.19629E-07	0.018393109	0.002703738
140	0.049085165	0.049085165	0.109927742	0.22155172	0.008590626	0.02364545	0.052092195	0.0536312	0.06400545	0.07092992	0.1991491	6.39672E-07	0.016179232	0.002627839
150	0.050831696	0.050831696	0.111734662	0.22545888	0.009157714	0.02112529	0.05354362	0.05538808	0.06958353	0.084630236	0.1959997	5.63357E-07	0.016719183	0.002169046
160	0.052010723	0.052010723	0.11320649	0.22805862	0.009589119	0.02217054	0.057535175	0.05482255	0.06859484	0.074872866	0.2124232	4.7422E-07	0.017298764	0.002799693
170	0.051436705	0.051436705	0.112424355	0.22679664	0.009342629	0.020731773	0.053644046	0.05638351	0.07153681	0.07736952	0.20584235	5.34336E-07	0.017016387	0.002499485
180	0.05122375	0.05122375	0.111993094	0.22632663	0.009092827	0.021802187	0.052157465	0.057126038	0.06865697	0.07233395	0.21173841	4.90415E-07	0.016773527	0.002555619
190	0.055251136	0.055251136	0.117734482	0.23505564	0.009587382	0.019760707	0.068171956	0.055953916	0.073888734	0.10670089	0.1984176	4.20704E-07	0.016638845	0.003390926
200	0.053046262	0.053046262	0.114054637	0.23031777	0.009882971	0.021564616	0.05648321	0.05913056	0.072209984	0.0753728	0.21711051	3.46599E-07	0.016259646	0.002447967

e) 48-Hour

Figure 5.13 Comparison of MSE for each timeslot to identify the optimal models. The lease MSE is the best and is highlighted in each timeslot.

5.2.3.3 *Compare proposed model predictions with the WRF model predictions for each timeslot*

Similar to the short-term weather forecasting, the optimal model for each timeslot is used to forecast the weather parameters for the WRF validation dataset (model prediction), and the model predicted values are evaluated with respect to the ground truth. The WRF

model has been run in forecast mode using the same format GRIB data for July 2018 (WRF prediction) based on the same conditions as model prediction (i.e. input seven days data and predict weather parameters for timeslot 6, 9, 12, 24 and 48). The WRF predicted values are evaluated with respect to the ground truth. Finally, the model prediction and WRF prediction are compared to determine to what extent the deep learning model can be used for weather forecasting. Please refer to Appendix 7 for sample analysis of comparing the model prediction and WRF prediction with respect to the ground truth for each timeslot. Figure 5.14 shows a comparison of MSE values related to the proposed model and the WRF model for each time slot.

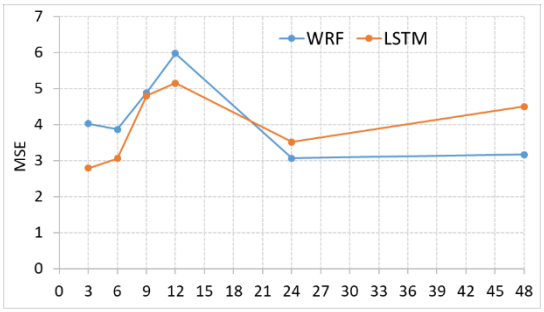

a) TSK

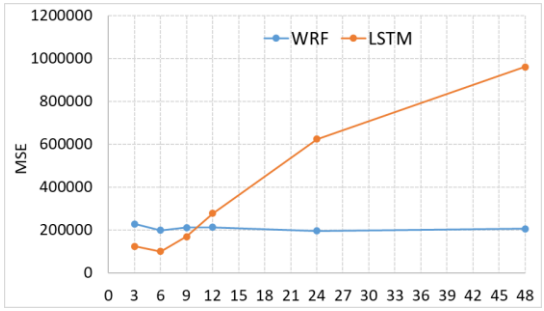

b) PSFC

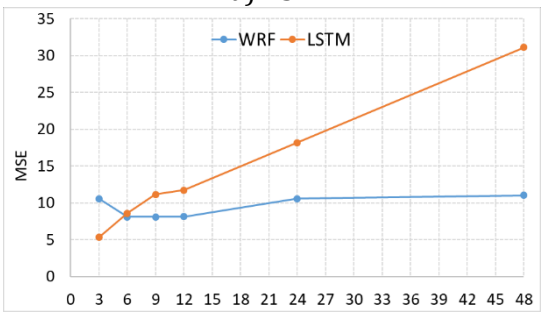

c) U10

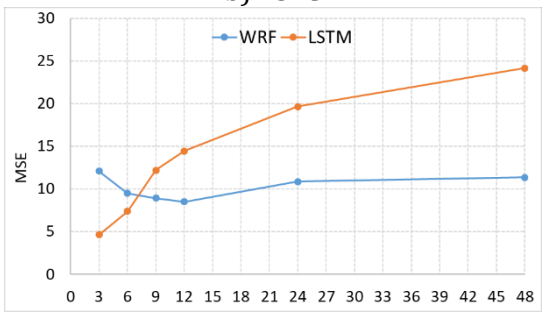

d) V10

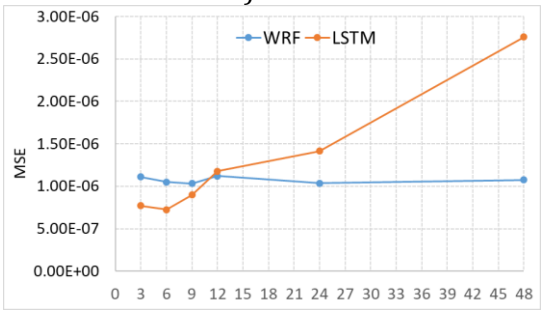

e) Q2

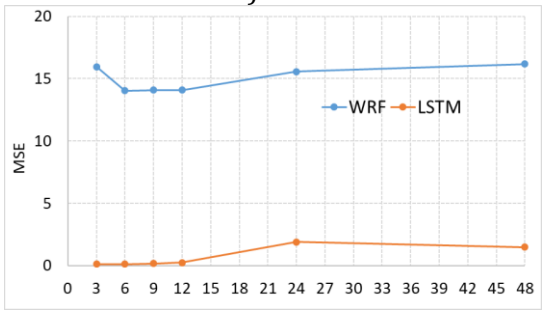

f) Rainc

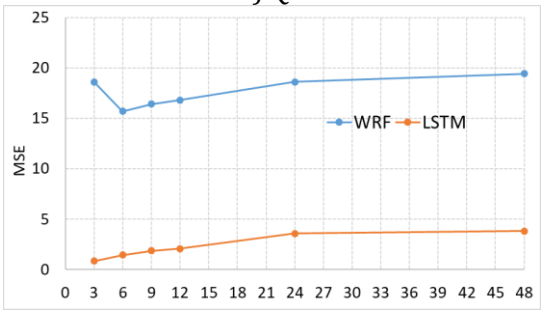

g) Rainnc

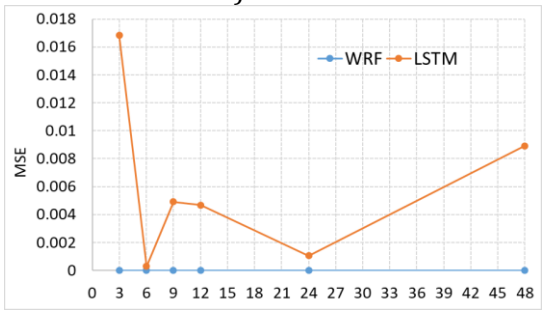

h) Snow

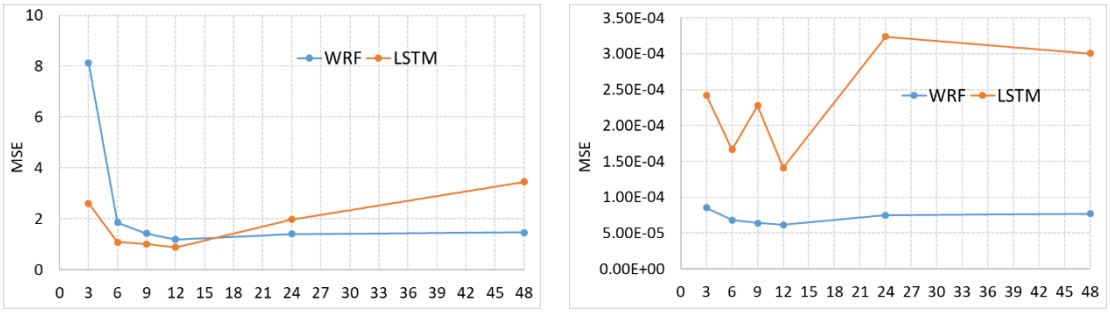

i) TSLB j) SMOIS

Figure 5.14 Comparison of proposed model prediction with WEF prediction for long-term forecasting.

As per information from Figure 5.14, it is evident that the WRF model produces better forecasting results for the very long-term compared to the deep learning model. The reason for this is that the WRF model is combined with many other climate models (Hernández-Ceballos et al., 2014; Liu et al., 2012; NCAR/UCAR, 2019) and data comes into the system globally (Commerce, 2015; NCAR/UCAR, 2019). The MIMO-LSTM model has predicted these outputs based on five months of training data. Increasing the sample size of the training dataset could result in an increase in the accuracy of predictions in neural network models (Gulli and Pal, 2017). The Rainc and Rainnc parameters show much better results in the deep learning model compared to the WRF model for long-term forecasting. The experiments of (Yonekura et al., 2018a) already proved that the deep neural network models yield the highest accuracy for rain prediction.

Contrarily, the SMOIS and snow parameters show weak results in deep learning compared to the WRF model at all timeslots. Simply, these error patterns are rather low (maximum error: Snow-0.016kg/m2, SMOIS-0.00035 m3/m3) and can be considered negligible. The reason for diverting these figures is that we trained and tested the model using the winter and spring weather data (Jan-June) and attempted to predict the summer (July 2018) forecast. This could be resolved by increasing the size of the sample data, such as training with two years of complete training data. In all other cases, the deep learning model provides, to some extent, a more accurate prediction than the WRF model. Table 5.18 and Figure 5.15 shows the comparison of overall error values of the WRF model and proposed deep learning model.

Table 5.18 Comparison of overall error values of the WRF model and proposed MIMO-LSTM model for each timeslot. Lower MSE is better and is highlighted.

Timeslot	Overall MSE	
	WRF	**Proposed deep model**
3 Hours	22793.84	12389.753
6 Hours	19929.73	9969.903
9 Hours	21141.912	16931.824
12 Hours	27810.596	27809.496
24 Hours	19621.064	62337.93
48 Hours	30509.21	95995.89

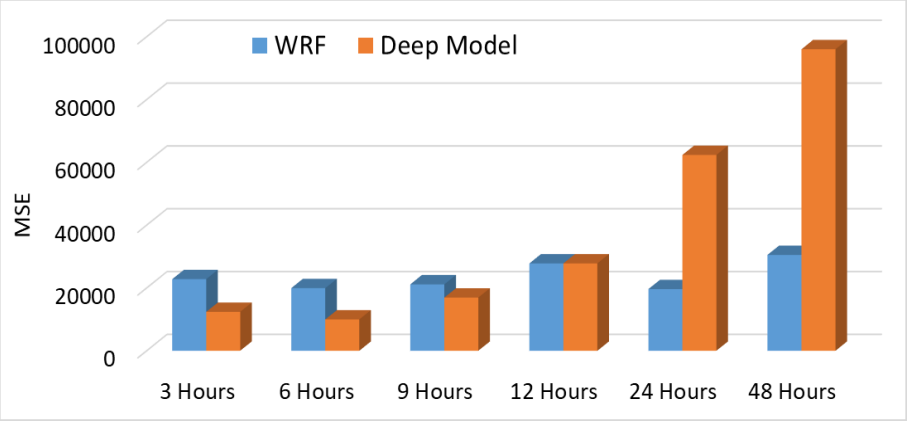

Figure 5.15 Comparison of overall MSE values of the WRF model and proposed deep learning model for each timeslot.

As indicated in Figure 5.15, the proposed MIMO-LSTM model produces better predictions compared to the WRF model for predictions up to 12 hours overall. Therefore, we can use deep learning with MIMO-LSTM model for up to 12 hours of weather forecasting with higher accuracy compared to the well-established WRF model. The comparison of WRF prediction vs the MIMO-LSTM model prediction for 50 random data samples concerning the ground truth is shown in Figure 5.16. Please refer Appendix 8 for a comparison of 100 random data samples for historical weather data. For each graph, the ground truth, WRF prediction, and the proposed deep model's predictions are represented by each line with blue, green, and red colours, respectively.

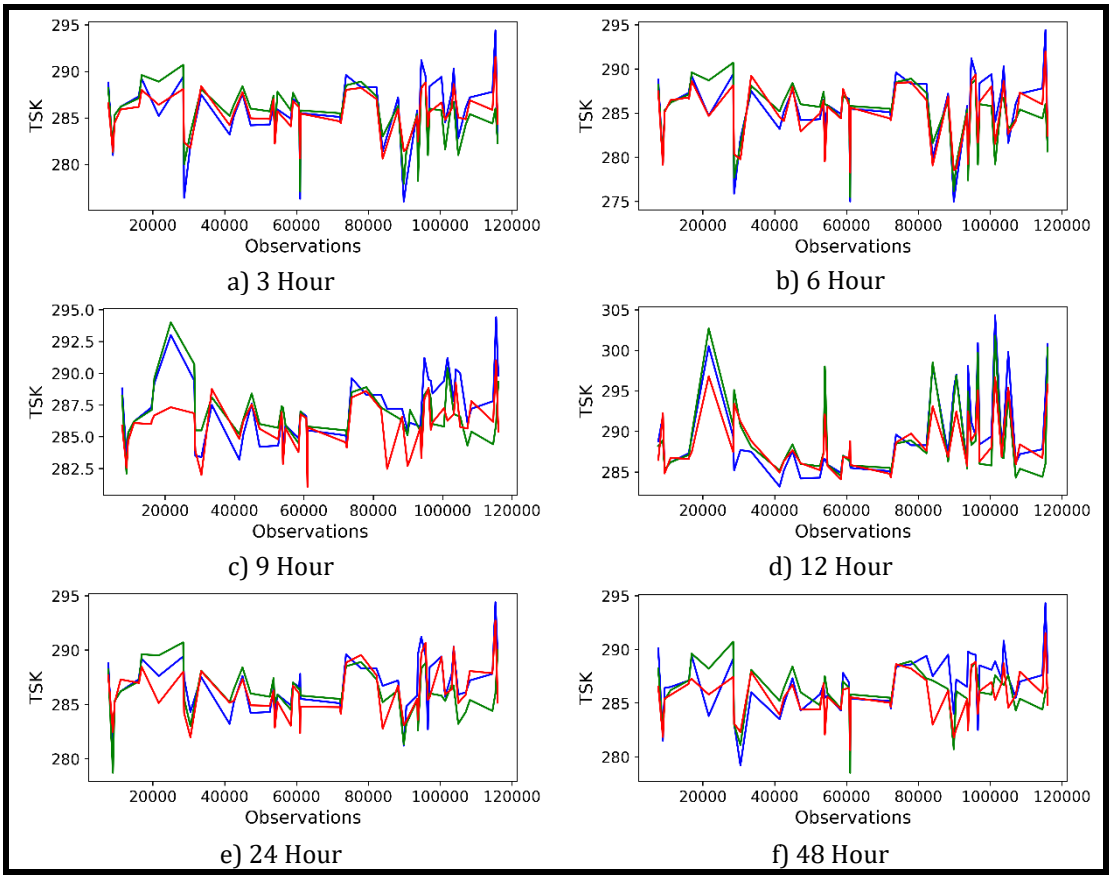
TSK
Observations
a) 3 Hour
b) 6 Hour
c) 9 Hour
d) 12 Hour
e) 24 Hour
f) 48 Hour
Actual
MIMO-LSTM
WRF

i) TSK

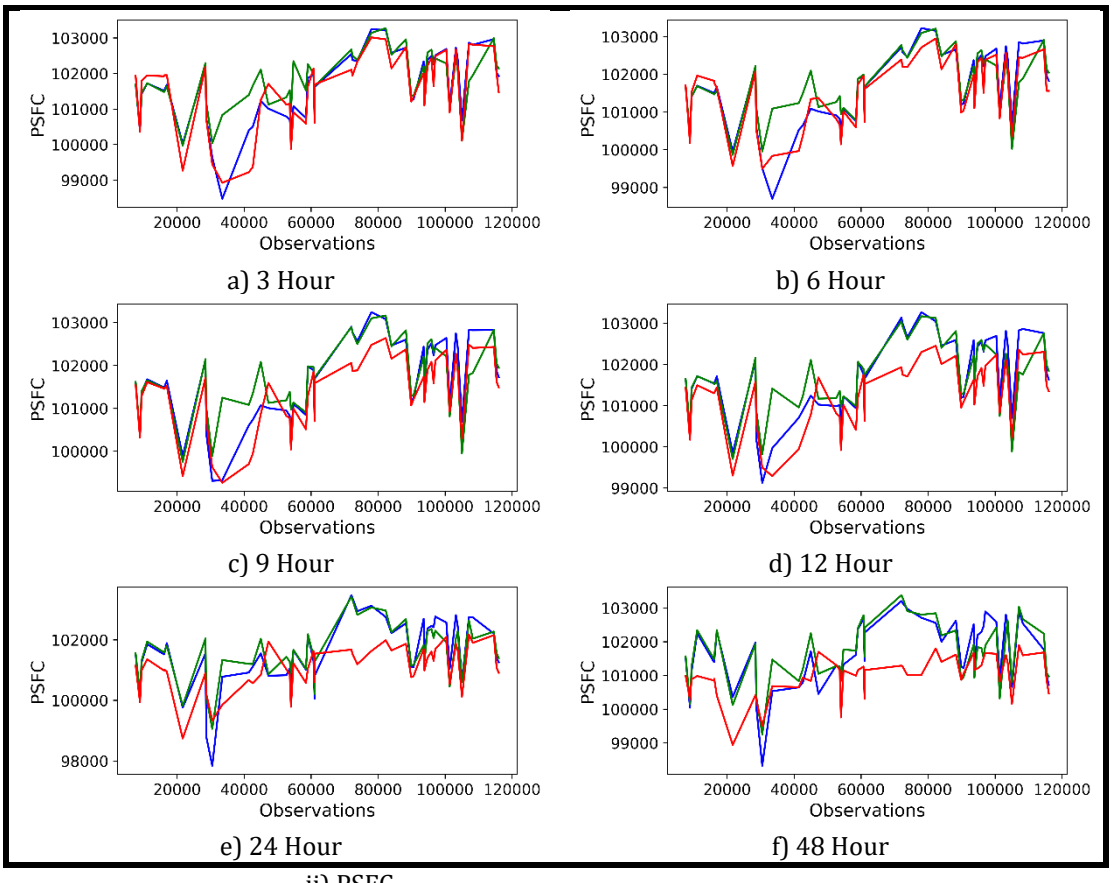
PSFC
Observations
a) 3 Hour
b) 6 Hour
c) 9 Hour
d) 12 Hour
e) 24 Hour
f) 48 Hour
Actual
MIMO-LSTM
WRF

ii) PSFC

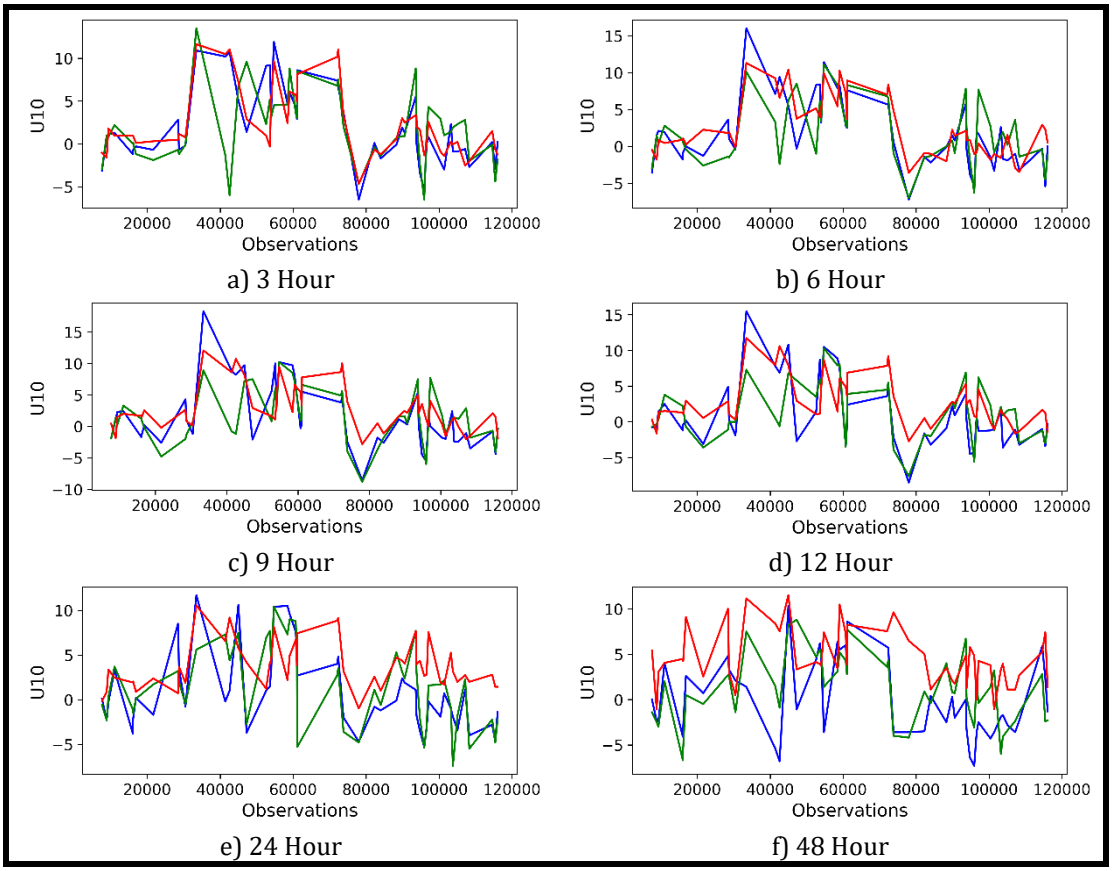

a) 3 Hour b) 6 Hour

c) 9 Hour d) 12 Hour

e) 24 Hour f) 48 Hour

iii) U10

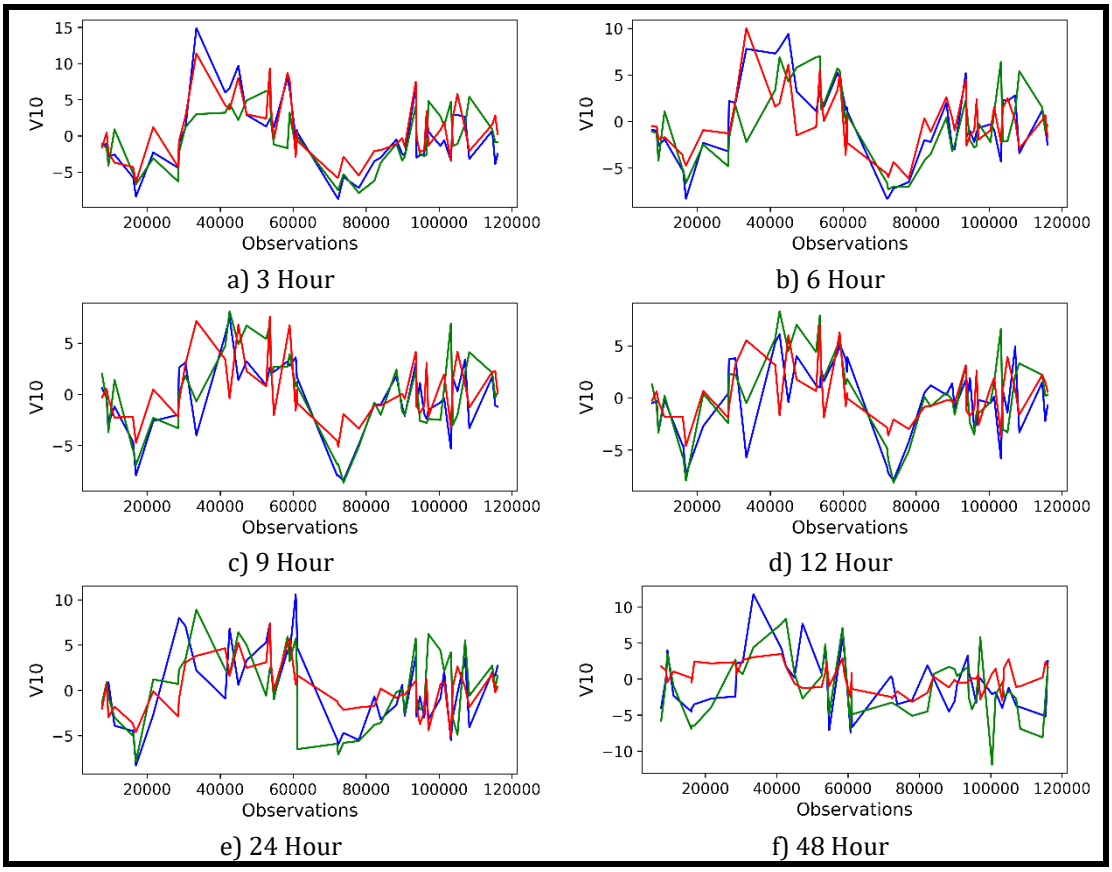

a) 3 Hour b) 6 Hour

c) 9 Hour d) 12 Hour

e) 24 Hour f) 48 Hour

iv) V10

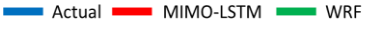

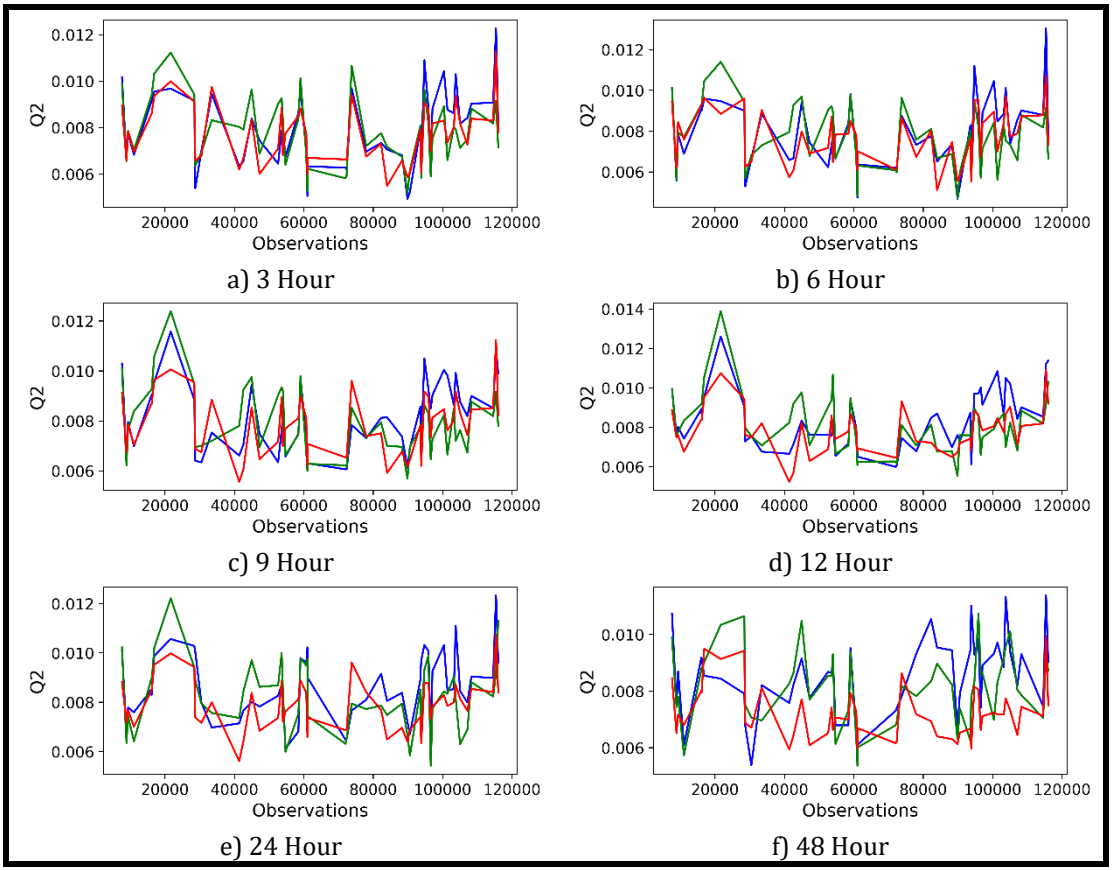
Q2
Observations
a) 3 Hour
b) 6 Hour
c) 9 Hour
d) 12 Hour
e) 24 Hour
f) 48 Hour
Actual
MIMO-LSTM
WRF

v) Q2

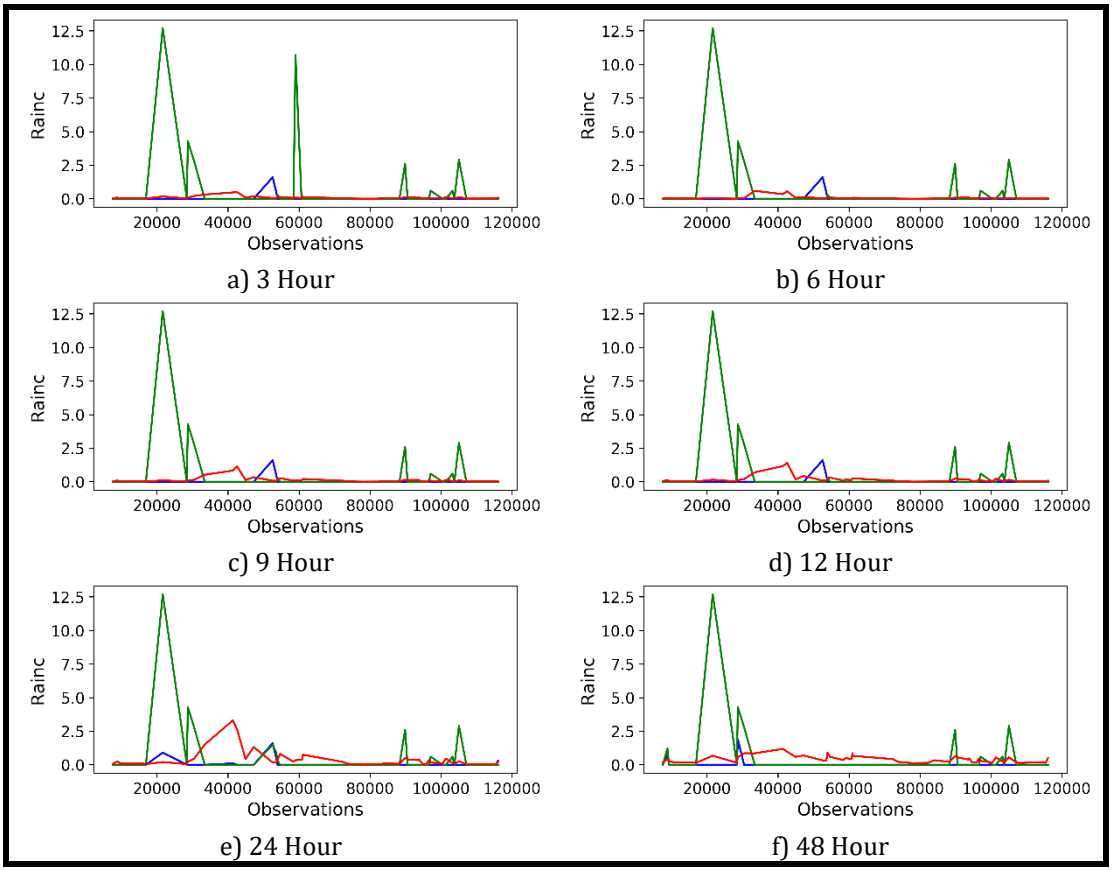
Rainc
Observations
a) 3 Hour
b) 6 Hour
c) 9 Hour
d) 12 Hour
e) 24 Hour
f) 48 Hour
Actual
MIMO-LSTM
WRF

vi) Rainc

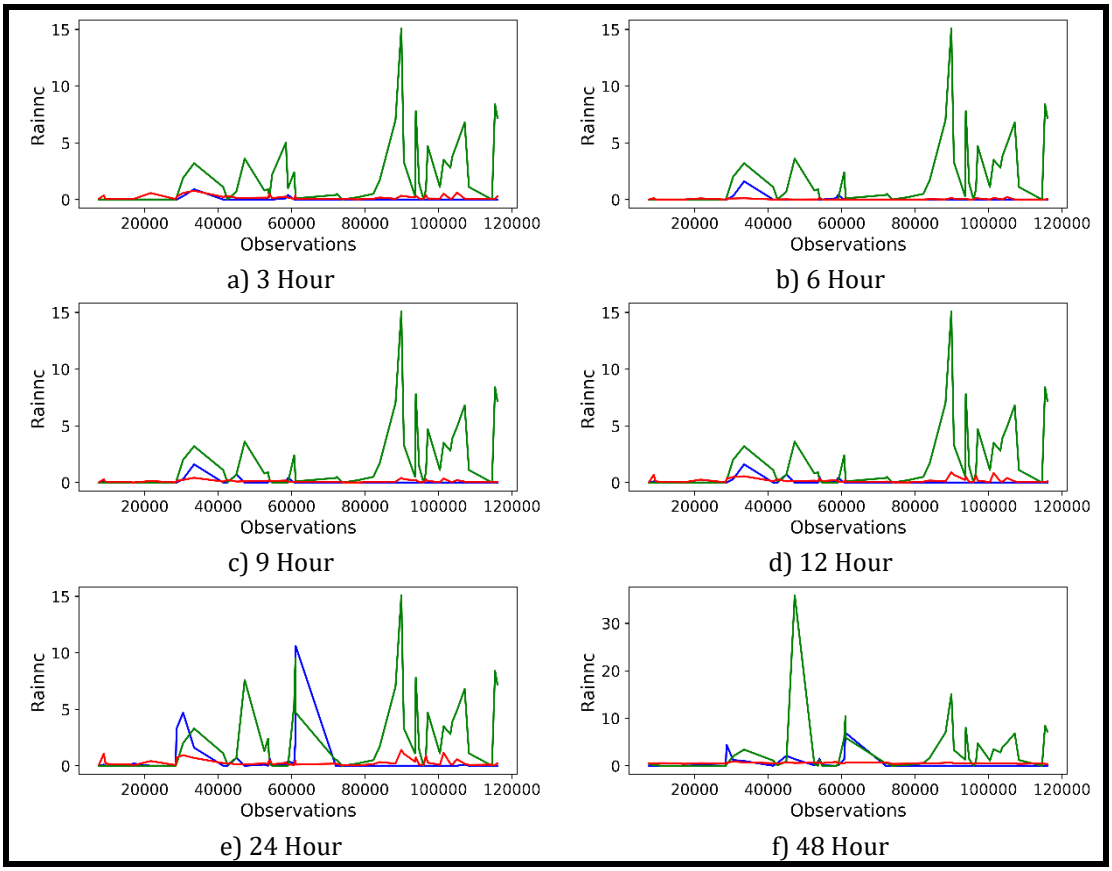

vii) Rainnc

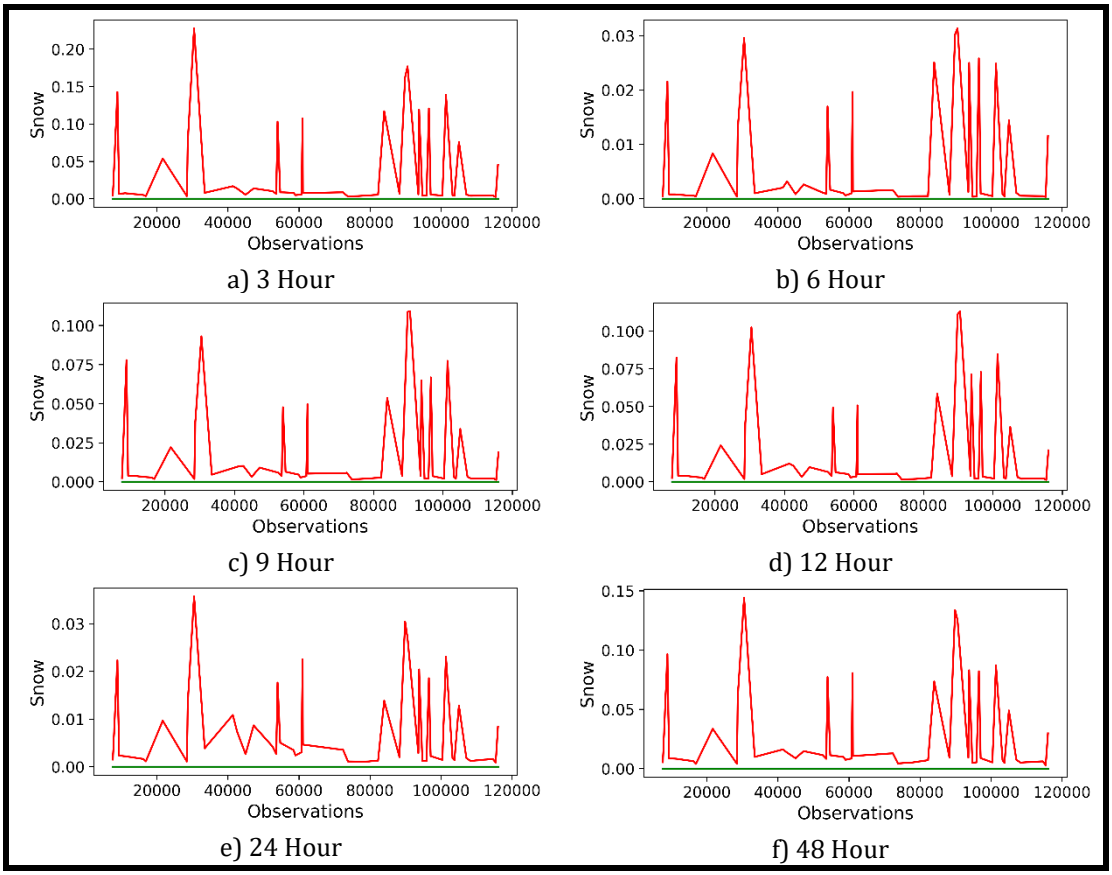

viii) Snow

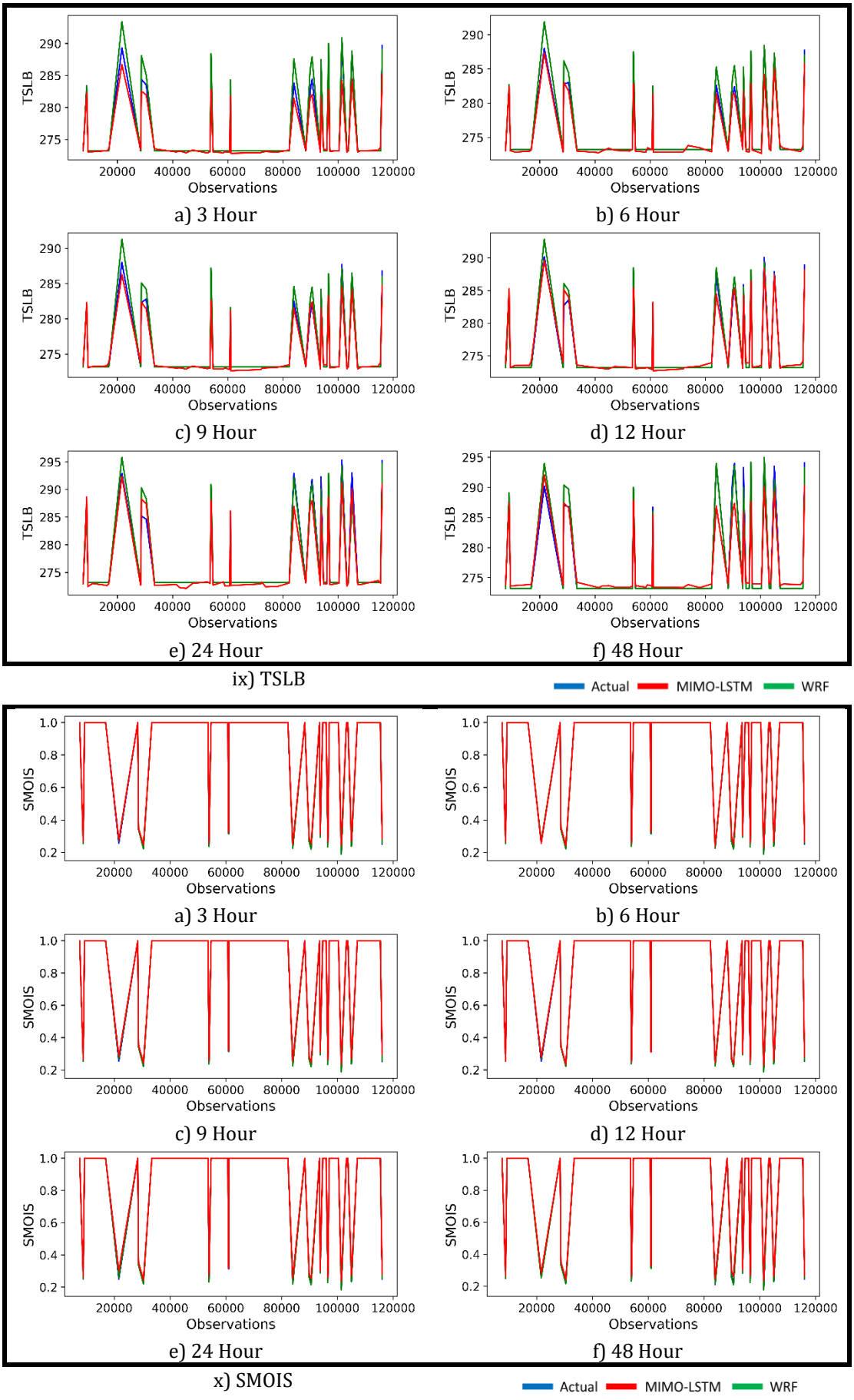

Figure 5.16 Comparison of WRF prediction vs the proposed model prediction for 50 random data samples with respect to the ground truth.

As per Figure 5.16, the red line-chart (deep model prediction) followed closely to the blue line-chart (ground truth) to some extent and diverted with time increases in many parameters. The green line-chart (WRF model prediction) also diverted from the blue line-chart when time increased, but this diversion is relatively small compared with the red line-chart. As shown in Figure 5.16 (vi), and Figure 5.16 (vii), the rainc and rainnc values are accurate in the deep learning model compared to the WRF model for up to 48 hours. As discussed earlier, the WRF model produces a better prediction for the Snow and SMOIS parameters. As shown in Figure 5.16 (x), the difference is negligible for the parameter SMOIS. As shown in Figure 5.16 (viii), the maximum snow values are shown in the 3 hours line-chart. This value is equal to 0.24 kg/m^{2,} and this is a relatively negligible figure. Overall, the deep learning model delivers a better forecasting prediction compared to the WRF model for up to 12 hours.

5.2.4 Computational complexity

As discussed in Section 2.3, NWP models, such as WRF, utilises computer algorithms to provide a forecast based by solving a large system of non-linear mathematical equations. These NWP models run in major weather forecasting centres with large grids of supercomputers, specifically addressing global/regional forecast (Met Office, 2019). As described in Section 2.1, the data-driven computer modelling systems, such as ML and deep learning models, can be utilised to reduce the computational power of NWP systems (Hayati and Mohebi, 2007). The proposed model could run on a standalone computer, and it could easily be deployed.

Time is taken to predict the next 48-hour weather forecast for the both WRF model and the proposed model shown below. These figures are based on running each model with a conventional computer with the hardware specified in Section 3.2.4.1. Seven days weather data covering the whole of the UK with 10 km resolution is the input to both models.

- WRF model: 9 hours and 24 minutes
- Proposed model: 2 minute and 12 second

The WRF model needs more time and more computational power to solve a large number of mathematical equations compared to the proposed model. Therefore, the above figures apparent that the proposed model is less computation complex and lightweight compared to the WRF model. Besides, the complexity of the NWP models (such as WRF) poses

significant difficulties in their implementation (Hayati and Mohebi, 2007; Powers et al., 2017).

Moreover, the WRF model needs a larger number of weather parameters to get a prediction. For instance, the GFS data consists of over 257 local and global weather parameters. Each of these parameters is involved in the calculation of the weather forecast (NCAR/UCAR, 2019; NCEI, 2019). This increased number of parameters increases the computational complexity of the NWP model. The proposed model uses only ten input parameters for a medium-range accurate forecast by reducing the computational complexity of the model.

As described in Section 1.2, the proposed model can be used for weather prediction. Even, this model generates more accurate predictions compared to the well-recognised WRF model for up to 12 hours. The historical weather data is used to evaluate and validate these models. The only issue is the proposed model still use the WRF model to extract GRIB data to use as input for the new model (i.e. GFS GRIB data). On the other hand, it requires a minimum of three hours of access GFS data after taking the atmospheric measurements. This includes the time taken to upload data to the website (NCAR/UCAR, 2019; NCEI, 2019). Besides, the WRF model also taken the time to extract the GFS data depend on the computer system. Hence, the input data which are used in the new model are not the current atmospheric measurement data (i.e. older more than 3 hours). Therefore, it is not practicable to use WRF data with the new model, and it will be highly beneficial to consider the use of local weather station data for weather forecasting.

5.3 Using Weather Station Data

Section 5.1 evidenced that the Neural Network approaches can be used for weather forecasting. Furthermore, the neural network predictions have higher accuracy compared to the state-of-art WRF model for up to 12 hours. The focus of this section is to get a weather forecast using highly accessible data instead of waiting for the GRIB-GFS data and extract them from the WRF model. Therefore, the goal of this section is to validate the proposed deep neural networks approach for a fine-grained and area-specific weather forecast using local weather station data for precision agriculture and other interesting industries. There are three steps to achieve this goal, similar to Section 5.1.

- Compare the performances of proposed neural network weather forecasting model variances (i.e. MIMO-LSTM, MISO-LSTM, MIMO-TCN, and MISO-TCN) with the existing approaches using local weather station data.
- Use the proposed model for short-term forecasting.
- Evaluate the proposed model for long-term forecasting with necessary changes.

5.3.1 Comparing neural network approaches for fine-grained and area-specific weather forecasting

Similar to Section 5.2.1, this section aims to propose an efficient Neural Network-based short-term (up to 1-hour) weather forecasting model by exploring temporal modelling approaches of LSTM and TCN and compare its performance with the existing classic ML approaches, such as SR and SVR. Similar to the section mentioned above, all these ML approaches are evaluated in MIMO and MISO proposed models.

5.3.1.1 *Machine learning approaches with MIMO*

As described Section 5.2.1.1, the classic ML approaches such as SR and SVR are compared to proposed cutting-edge deep learning approaches to propose an optimal weather forecasting model for the weather station data.

5.3.1.1.1 Baseline approaches for MIMO

5.3.1.1.1.1 SR

The Weather station training dataset is used to train a model using the SR approach. The trained model is evaluated using the weather station validation dataset. The testing dataset is used to select the best model with the optimal MSE among a number of different models (i.e. model with different configurations and controls). Therefore, the testing dataset is not used in this experiment. The evaluation results are shown in Table 5.19. This evaluation is carried out using the actual values and not the normalised data (i.e. the normalised predictions are converted to the human-understandable form and compared with the actual ground truth values).

Table 5.19 Evaluation results for baseline-SR for MIMO model.

Parameter	MSE	MAE	RMSE
Barometer	0.0091116011	0.063254585	0.095454707
Pressure	0.0091145042	0.064218744	0.095469913
Temperature	7.372159474	1.452545265	2.715172089
Humidity	80.62451233	12.23548757	8.979115342
Wind speed	4.669748612	1.215484565	2.160960113
Wind direction	23525.56626	142.2325212	153.3804624
Rain rate	0.009573162	0.064521265	0.097842537
Rain	0.008228854	0.054254858	0.090713031
Dew point	41.17251214	2.986525632	6.416581032
Heat index	23.99016002	2.012515263	4.897975094

5.3.1.1.2 Proposed approaches for MIMO

5.3.1.1.2.1 LSTM

Similar to Section 5.2.1.1.2.1, the proposed MIMO-LSTM model variance is evaluated with several configurations and controls to find an optimal model with least MSE. Please refer to Appendix 9 for a sample evaluation report. Table 5.20 presents a summary report of the MIMO-LSTM evaluation using the weather station testing dataset. Similar to the above section, the 'save model weight at every ten epochs' technique is used in this evaluation. In this section, there are 24 experiments to carry out for selected configurations and controls.

As shown in Table 5.20, the optimal model with the least MSE found is in configuration 6 with the 'Adam' optimiser, a fixed learning rate of 0.01, a batch size=128, and the location of 30 Epochs. The evaluation report for this model configuration is shown in Figure 5.17.

Table 5.20 Evaluation of LSTM-MIMO model variance for weather station data-Summary report.

Configuration	Optimiser	Best MSE
1	Adam	0.030383936
	SDG	0.67523283
	Adaptive- Adam	0.518730355
	Adaptive- SGD	0.059738597
2	Adam	0.038549076
	SDG	0.052075434
	Adaptive- Adam	1.035494329
	Adaptive- SGD	0.044312811
3	Adam	0.042534545
	SDG	0.070035556
	Adaptive- Adam	0.827577624
	Adaptive- SGD	0.052600262
4	Adam	0.034480336
	SDG	0.055260465
	Adaptive- Adam	0.518730355
	Adaptive- SGD	0.045125196
5	Adam	0.032913437
	SDG	0.077247863
	Adaptive- Adam	0.577940676
	Adaptive- SGD	0.06037214
6	Adam	0.029460589
	SDG	0.045601065
	Adaptive- Adam	0.518730355
	Adaptive- SGD	0.04796627

Epoch	Loss	Total MSE	Total MAE	Total RMSE	Barometer	Pressure	Temp	Humid	Wspeed	Wdirec	Rrate	Rain	Dpoint	Hindex
10	0.034107108	0.034107108	0.108349894	0.1846811	0.17848282	0.18107975	0.14125057	0.16029635	0.23980094	0.36036104	0.07103596	0.07001514	0.12154793	0.13671787
20	0.02954915	0.02954915	0.097619433	0.17131594	0.16997503	0.16721344	0.13647832	0.13470235	0.2125997	0.33656883	0.07093121	0.0698651	0.115691334	0.13451591
30	0.029460589	0.029460589	0.095639069	0.17164089	0.15634187	0.1594056	0.12645416	0.16868205	0.20931469	0.33754754	0.071298026	0.07196441	0.12755524	0.12659027
40	0.030160072	0.030160072	0.09788207	0.17366655	0.15201497	0.15237398	0.1378458	0.15247755	0.20528299	0.35807562	0.07142904	0.07427224	0.11790431	0.13470083
50	0.032135243	0.032135243	0.099036958	0.17926306	0.16875654	0.16392176	0.13587645	0.11894302	0.21526924	0.37893334	0.07111206	0.0701585	0.11964756	0.13844675
60	0.038044778	0.038044778	0.11161159	0.1950507	0.16662605	0.16699667	0.1454079	0.15499462	0.2383657	0.4177307	0.07439997	0.078708135	0.12452205	0.14517458
70	0.039055985	0.039055985	0.107296426	0.19762588	0.18262134	0.1796787	0.13673967	0.12177737	0.22226693	0.44563994	0.071576044	0.069509156	0.124484405	0.13397318
80	0.044833328	0.044833328	0.118214644	0.21173882	0.18815541	0.1820349	0.15417701	0.1496161	0.24355401	0.4707324	0.072379164	0.07080586	0.12935188	0.16045855
90	0.040022497	0.040022497	0.113011271	0.20005623	0.18270423	0.18232739	0.15432486	0.14645982	0.2503674	0.4190989	0.07284177	0.07008582	0.13145055	0.15003093
100	0.045218137	0.045218137	0.120721634	0.21264558	0.18412966	0.17953487	0.18040077	0.14546712	0.26546285	0.44700104	0.07271414	0.071082756	0.14310227	0.17675103
110	0.046394557	0.046394557	0.121942778	0.21539396	0.19036418	0.1857993	0.17857532	0.14336088	0.27830118	0.44919214	0.073923476	0.071478084	0.14544901	0.17259736
120	0.048002944	0.048002944	0.124086369	0.21909575	0.19139914	0.1842405	0.1859243	0.15823784	0.2959289	0.4462908	0.07420694	0.08735957	0.14099282	0.17342857
130	0.047685333	0.047685333	0.125922622	0.21836972	0.19384316	0.18824933	0.18458267	0.15603597	0.27557465	0.45250854	0.073737495	0.092991866	0.13892367	0.17700996
140	0.047595783	0.047595783	0.125146105	0.21816458	0.19053522	0.18541873	0.19088753	0.15684561	0.29177764	0.43867308	0.07587726	0.095004305	0.14030628	0.17943843
150	0.045261775	0.045261775	0.120342686	0.21274814	0.19280158	0.18801314	0.17313565	0.15217066	0.28699765	0.43123025	0.073492914	0.072714984	0.13785344	0.17013247
160	0.046797429	0.046797429	0.122366483	0.21632713	0.19975215	0.19213739	0.16777572	0.15523334	0.28630477	0.44539577	0.07301922	0.07860657	0.13787413	0.16745928
170	0.048473592	0.048473592	0.124051467	0.22016719	0.20002052	0.19621941	0.17041166	0.15043288	0.2797298	0.46162733	0.077726126	0.09459083	0.14035355	0.16887574
180	0.048263887	0.048263887	0.123495635	0.21969044	0.20017447	0.19685675	0.16918896	0.15128258	0.27796334	0.46302003	0.07536712	0.092687644	0.13888918	0.1645982
190	0.047679961	0.047679961	0.12282161	0.21835741	0.1989219	0.19419295	0.17229421	0.15354139	0.2800251	0.45702145	0.073205546	0.07558068	0.14127095	0.1671732
200	0.048023633	0.048023633	0.122941637	0.21914296	0.20049107	0.19827947	0.16691057	0.15124169	0.28853533	0.45592445	0.07356082	0.08516188	0.13837239	0.16450329
210	0.047824495	0.047824495	0.123047522	0.21868812	0.2007572	0.19678745	0.16960733	0.1502698	0.2828759	0.45781574	0.07403213	0.08011133	0.1396351	0.16388403
220	0.047216472	0.047216472	0.12116488	0.21729352	0.2015698	0.19706765	0.16812363	0.14918657	0.276571	0.45742002	0.07373597	0.07449703	0.13752253	0.1629497
230	0.047376308	0.047376308	0.121260543	0.21766101	0.2024815	0.1973666	0.17303269	0.1514307	0.2779177	0.45369834	0.07366395	0.07384433	0.13779685	0.16730632
240	0.047027571	0.047027571	0.121376976	0.21685842	0.20414717	0.19883585	0.1710688	0.15571696	0.27939624	0.44714317	0.074346974	0.075946026	0.13778639	0.16514239
250	0.047071637	0.047071637	0.121640037	0.21696	0.20229027	0.19741403	0.17249963	0.15272047	0.27612433	0.44951466	0.07429774	0.075691275	0.14039566	0.16874458
260	0.04714559	0.04714559	0.120692955	0.21713036	0.20230621	0.19904761	0.1715802	0.15218052	0.27694577	0.45147413	0.0741802	0.075611226	0.13767344	0.16615622
270	0.046221766	0.046221766	0.120168619	0.21499248	0.20673907	0.20272839	0.17280608	0.14970605	0.27405187	0.43883154	0.07373566	0.07531339	0.13909832	0.16723944
280	0.045425514	0.045425514	0.119348868	0.21313262	0.20136423	0.19800417	0.1457536	0.15358251	0.28586546	0.44248626	0.07214218	0.073825374	0.1397484	0.14823216
290	0.038534756	0.038534756	0.1114821	0.19630271	0.20765847	0.20219725	0.14186999	0.13914128	0.2575763	0.38489333	0.073577344	0.07197847	0.12700595	0.14366959
300	0.041885993	0.041885993	0.114932265	0.20466068	0.20940587	0.20403273	0.14692605	0.14193578	0.2782224	0.40514287	0.0748064	0.082206436	0.12622294	0.14768933

Figure 5.17 Evaluation results for MIMO-LSTM model variance for Configuration 6 with 'Adam' optimiser. The row with the best MSE is highlighted.

According to Figure 5.17, the least MSE is equal to 0.029460589, and this value is recorded with the normalised data. The validation dataset is used with the above optimal MIMO-LSTM model variance to get a weather prediction. The results are de-normalised and evaluated with the ground truth, as shown in Table 5.21.

Table 5.21 Evaluation of MIMO-LSTM model variance.

Parameter	MSE	MAE	RMSE
Barometer	0.007569974	0.056349196	0.08700559
Pressure	0.007083774	0.054011453	0.084165156
Temperature	2.9798136	0.9351834	1.7262137
Humidity	29.029621	3.5467129	5.387914
Wind speed	2.0961268	1.003048	1.4478006
Wind direction	3783.2769	43.839752	61.508347
Rain rate	0.00114398	0.01208018	0.0338228
Rain	0.0000109	0.00111625	0.003296755
Dew point	19.998379	1.6345986	4.471955
Heat index	11.032139	1.8201575	3.3214664

5.3.1.1.2.2 TCN

Similar to Section 5.2.1.1.2.2, there are different configurations and controls utilised to discover the optimal MIMO-TCN. The similar controls are kept constant during these experiments and utilise the ‘save best model’ approach. Table 5.22 shows the summary of the evaluation report. Please refer to Appendix 10 for a sample evaluation report. In this section, there are 40 experiments to carry out for selected configurations and controls.

As per table 5.22, the optimal model for the MIMO-TCN variance is found in the configuration and controls of 256 filters, one TCN layer, and ‘tanh’ activation function. The weather station validation dataset is used to evaluate this optimal model. First, the predicted output for the above configuration is de-normalised and then compared with the ground truth, and the MSE for each parameter is calculated. The results of this process are shown in Table 5.23.

Table 5.22 MIMO-TCN analysis. The optimal model with least MSE is highlighted.

No of Filters	TCN layers	Activation: Linear	Activation: tanh
32	1	0.0442102	0.035241569
	2	0.042216352	0.037659987
	3	0.03612543	0.039659869
	4	0.048012452	0.041983233
64	1	0.03373083	0.033271397
	2	0.033534372	0.036429466
	3	0.043976752	0.039012146
	4	0.044710453	0.039457896
128	1	0.040125466	0.026724573
	2	0.041897433	0.027292923
	3	0.043650215	0.03156479
	4	0.046015479	0.033998653
256	1	0.032124572	0.026642543
	2	0.03923651	0.027989856
	3	0.041012148	0.02995659
	4	0.04779821	0.033021454
512	1	0.045956742	0.027268749
	2	0.049774588	0.031444546
	3	0.051217459	0.035659836
	4	0.056728855	0.041142636

Table 5.23 Evaluation results for optimal MIMO-TCN model variance.

Parameter	MSE	MAE	RMAE
Barometer	0.003305803	0.037975818	0.057496108
Pressure	0.003601799	0.039164443	0.060014986
Temperature	2.8303354	0.91098636	1.68236
Humidity	24.027027	3.205585	4.901737
Wind speed	1.9519161	1.0310366	1.3971099
Wind direction	4106.5347	43.897945	64.08225
Rain rate	0.001456705	0.021238849	0.038166806
Rain	0.0000167	0.002216114	0.004086915
Dew point	24.394356	2.250649	4.939064
Heat index	9.148514	1.6465291	3.024651

5.3.1.1.3 Comparison of baseline approaches and proposed approaches for MIMO model

Table 5.24 and Figure 5.18 present the evaluation results after comparing baseline-SR, MIMO-LSTM, and MIMO-TCN model variances. These results are evaluated using the

MSE matric. This is used to assess the best model after comparing the performance of all the models of MIMO.

Table 5.24 MIMO model analysis of SR, LSTM, and TCN in predicting different weather parameters. The lower MSE is better and shown in highlighted.

Parameter	Model variances		
	Baseline-SR	**MIMO-LSTM**	**MIMO-TCN**
Barometer	0.0091116	0.007569974	0.003305803
Pressure	0.009114504	0.007083774	0.003601799
Temperature	7.372159	2.9798136	2.8303354
Humidity	80.62451	29.029621	24.027027
Wind Speed	4.669748	2.0961268	1.9519161
Wind Direction	23525.566	3783.2769	4106.5347
Rain Rate	0.009573162	0.001143982	0.001456705
Rain	0.008228854	1.09E-05	1.67E-05
Dew point	41.172512	19.998379	24.394356
Heat Index	23.99016	11.032139	9.148514

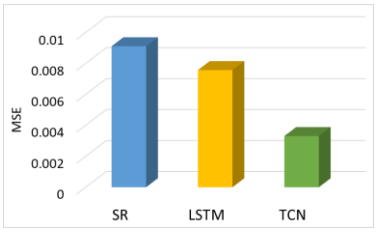

a) Barometer

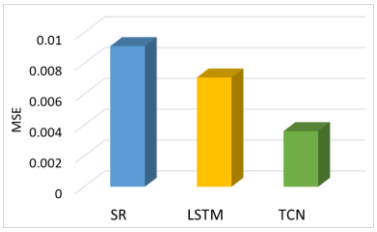

b) Pressure

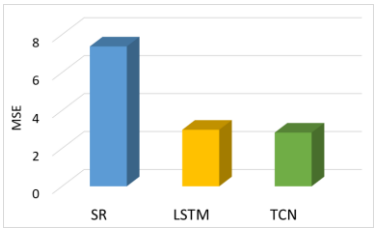

c) Temperature

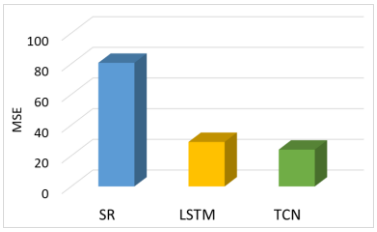

d) Humidity

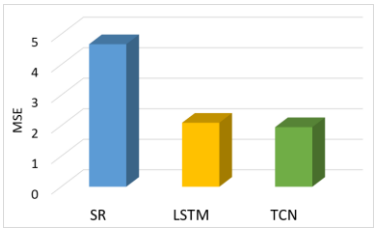

e) Wind speed

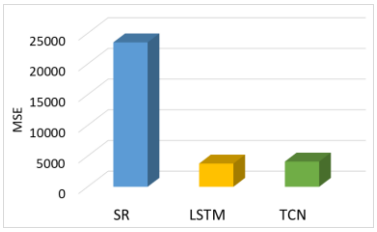

f) Wind direction

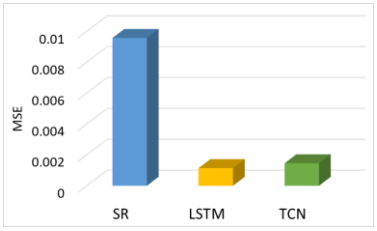

g) Rain rate

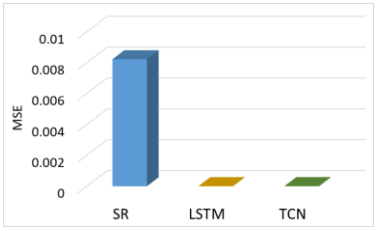

h) Rain

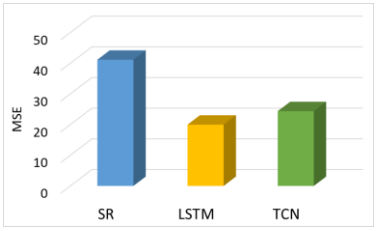

i) Dew point

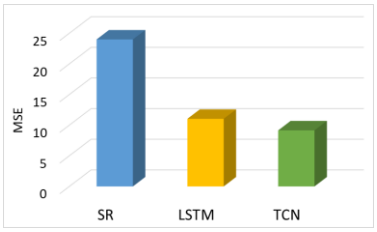

j) Heat index

Figure 5.18 MIMO analysis of different techniques in predicting different weather parameters.

According to Table 5.24 and Figure 5.18, the MIMO-TCN model variance provides better results in six out of ten parameters. Therefore, the MIMO-TCN model variance has been selected as the proposed model in MIMO.

5.3.1.2 *MISO neural networks*

Similar to Section 5.2.1.2, the MISO models are created with classic ML approaches such as SR and SVR and proposed deep learning approaches such as LSTM and TCN (i.e. model variances of MISO-LSTM and MISO-TCN). These models are evaluated to determine an optimal model for MISO.

5.3.1.2.1 Baseline approaches for MISO

5.3.1.2.1.1 SR

Ten different SR models are developed to represent each parameter in multi-input SR. These models are trained with the training dataset and finally evaluated with the validation dataset. Table 5.25 presents the evaluation results after comparing the predicted values with the ground truth. Similar to Section 5.2.1.2.1.1, the SR prediction is de-normalised before comparing to the ground truth. In this section, there are ten different models to train and test representing each parameter.

Table 5.25 Evaluation of baseline-SR for MISO model.

Parameter	MSE	MAE	RMSE
Barometer	0.006052928	0.069625005	0.077800564
Pressure	0.006040654	0.069636285	0.07772165
Temperature	7.4294343	2.082642	2.725699
Humidity	80.41223	6.8781376	8.967287
Wind speed	4.660474	1.701152	2.158813
Wind direction	23529.016	122.22709	153.39171
Rain rate	0.006573259	0.07476329	0.08107564
Rain	0.005008375	0.07051124	0.070769876
Dew point	44.836395	4.6009636	6.6959987
Heat index	23.886951	3.73143	4.887428

5.3.1.2.1.2 SVR

As described in Section 5.2.1.2.1.2, the parameters are optimised with 'linear' and '*rbf*' kernels. Table 5.26 presents the cost values for each parameter linear kernel, and table 5.27 presents the cost and gamma values for the *rbf* kernel. In parameter optimisation, there are 20 different codes to experiment within. The C and gamma values provided by Table 5.26 and Table 5.27 are used to create models for each parameter. Altogether 20 programs are executed where one set of 10 parameters for the linear kernel with optimised cost values, and the other is set of 10 parameters in the '*rbf*' kernel with optimised cost and gamma values. All the results are de-normalised and compared with the ground truth. The results of this process are presented in Table 5.28. In this section, there are 20 different models to train and test to represent each kernel.

Table 5.26 Cost values for SVR for linear kernel.

Parameter	Best cost value
Barometer	0.001
Pressure	0.001
Temperature	0.1
Humidity	0.1
Wind speed	0.1
Wind direction	1
Rain rate	0.1
Rain	0.1
Dew point	0.1
Heat index	0.1

Table 5.27 Cost and gamma values for SVR for *rbf* kernel.

Parameter	Best cost value	Best gamma value
Barometer	1	0.1
Pressure	1	0.1
Temperature	1	0.2
Humidity	10	0.2
Wind speed	10	0.5
Wind direction	1000	0.0001
Rain rate	100	0.0001
Rain	1000	0.0001
Dew point	1	0.5
Heat index	1	0.2

Table 5.28 Evaluation results of SVR linear and *rbf* kernels. The evaluation metric is MSE. The least MSE is the best and is highlighted.

Parameter	SVR Kernel=' rbf'	SVR Kernel='linear'
Barometer	0.015126812	0.010888682
Pressure	0.014858767	0.010738483
Temperature	13.373324	6.6375537
Humidity	55.036636	53.577785
Wind Speed	2.9299066	2.6081274
Wind Direction	6177.982	16527.996
Rain Rate	0.002406244	0.001692935
Rain	0.0000251	0.0000297
Dewpoint	78.94774	84.072655
Heat Index	42.923523	21.148586

There are some parameters that provide better performance for the linear kernel while others are better for the *rbf* kernel. Therefore, the combined model is selected as the optimal model for the SVR (i.e. Barometer with linear kernel, wind direction with *rbf* kernel, etc.).

5.3.1.2.2 Proposed approaches for MISO

5.3.1.2.2.1 LSTM

As described Section 5.2.1.2.2.1, the similar configurations and controls are utilised for the LSTM-MISO model variance. In this case, the six configurations are utilised to create models with two optimisers (i.e. Adam and SGD) and only for the fixed learning rate of 0.01. The adaptive learning rate method is not used here to reduce the complexity of

experiments. Please refer to Appendix 11 for a sample evaluation report. Configuration 1, configuration five and configuration six yield higher performances compared to the other configurations. Table 5.29 presents a summary report for the above configurations. In this section, 120 experiments are carried out with selected configurations and controls.

Table 5.29 Best MSE found for each parameter in LSTM-MIMO model variance. The least MSE is better and is highlighted.

Parameter	Optimal MSE					
	Config1 - Adam	Config1 – SGD	Config5 - Adam	Config5 – SGD	Config6 - Adam	Config6 - SGD
Barometer	0.014348842	0.03524592	0.014640401	0.040140964	0.015224963	0.032323095
Pressure	0.013591958	0.03443334	0.013718473	0.041699743	0.013981406	0.032317061
Temperature	0.011345458	0.099812315	0.012140766	0.033917827	0.011213889	0.019738242
Humidity	0.009414103	0.022676787	0.010070267	0.027716481	0.010408232	0.01985851
Wind speed	0.129971616	0.058718044	0.043135769	0.061063361	0.038659616	0.051772386
Wind direction	0.117587778	0.120334177	0.112957981	0.122671151	0.113660647	0.114253978
Rain rate	0.005517046	0.005050923	0.005517046	0.005110873	0.005517046	0.00514825
Rain	0.004974048	0.004767614	0.004974048	0.004757281	0.004974048	0.004773101
Dew point	0.011537577	0.817569852	0.011311761	0.014811731	0.011347561	0.014364105
Heat index	0.011079868	0.022556223	0.011915847	0.030602	0.012069368	0.021105004

As shown in Table 5.29, the optimal MSE values are found in various configurations and controls in different parameters. The combination of each parameter with its optimal MSE is taken as the optimal model for LSTM-MISO model variance. The weather station validation dataset is used with this model to get a forecast to compare its accuracy with the ground truth after converting the normalise data into the human-understandable format. The evaluation results are shown in Table 5.30.

Table 5.30 Evaluation results for LTSM-MISO model variance.

Parameter	MSE	MAE	RMSE
Barometer	0.003995666	0.035073567	0.06321128
Pressure	0.003750399	0.03348094	0.0612405
Temperature	2.5194325	0.7456182	1.587272
Humidity	18.087887	2.6218567	4.2529855
Wind speed	1.6269077	0.9049273	1.2755029
Wind direction	3974.5454	45.148834	63.043995
Rain rate	0.001146236	0.015885605	0.033856105
Rain	0.0000106	0.001200271	0.003258569
Dew point	18.107563	1.2307862	4.255298
Heat index	7.449141	1.2544837	2.7293115

5.3.1.2.2.2 Exploring LSTM Single-Input Single-Output (SISO)

While MIMO and MISO deep learning models have experimented for weather forecasting, the research focus has brought attention to the deep learning SISO models. The applicability of this SISO model experiments with the LSTM approach. The general architecture of the SISO-LSTM model is depicted in Figure 5.19.

Figure 5.19 The proposed MISO deep model architecture for weather forecasting.

The same MISO-LSTM optimal model variance configurations and controls are utilised within this SISO- LSTM model variance analysis, such as; barometer: config1-Adam, temperature: config5-Adam, wind direction: config5-SGD, etc. Please refer to Appendix 12 for a sample evaluation report. Table 5.31 presents a summary of SISO- LSTM model variance valuation report. In this section, there are ten models to experiment which represent each parameter.

Table 5.31 Evaluation results of SISO-LSTM model variance.

Parameter	MSE	MAE	RMSE
Barometer	0.182388832	0.225255307	0.427070055
Pressure	0.182223182	0.225588988	0.426876073
Temperature	0.231083682	0.269661163	0.480711641
Humidity	0.227312026	0.263423089	0.47677251
Wind speed	0.237174219	0.338607592	0.487005358
Wind direction	0.371560259	0.487503175	0.609557429
Rain rate	0.095169354	0.122731833	0.308495307
Rain	0.094797344	0.115317102	0.307891773
Dew point	0.150715861	0.171364284	0.388221407
Heat index	0.251057567	0.251057567	0.501056451

The SISO-LSTM model variance performance is compared with the MIMO-LSTM and MISO-LSTM model variances to find its applicability. This comparison report is presented in Table 5.32 and Figure 5.20. All these MSE values are calculated in the normalised format (i.e. predicted normalised data compared with the normalised ground truth for the weather station testing dataset).

Table 5.32 Comparison of optimal MSE in each parameter for MIMO-LSTM, MISO-LSTM, and SISO-LSTM model variances.

Parameter	Model variances		
	SISO-LSTM	MIMO-LSTM	MISO-LSTM
Barometer	0.182388832	0.15634187	0.014348842
Pressure	0.182223182	0.1594056	0.013591957
Temperature	0.231083682	0.12645416	0.012140766
Humidity	0.227312026	0.16868205	0.009414103
Wind Speed	0.237174219	0.20931469	0.038659617
Wind direction	0.371560259	0.33754754	0.12267116
Rain Rate	0.095169354	0.071298026	0.005050922
Rain	0.094797344	0.07196441	0.004757281
Dew Point	0.150715861	0.12755524	0.01131176
Heat Index	0.251057567	0.12659027	0.011079869

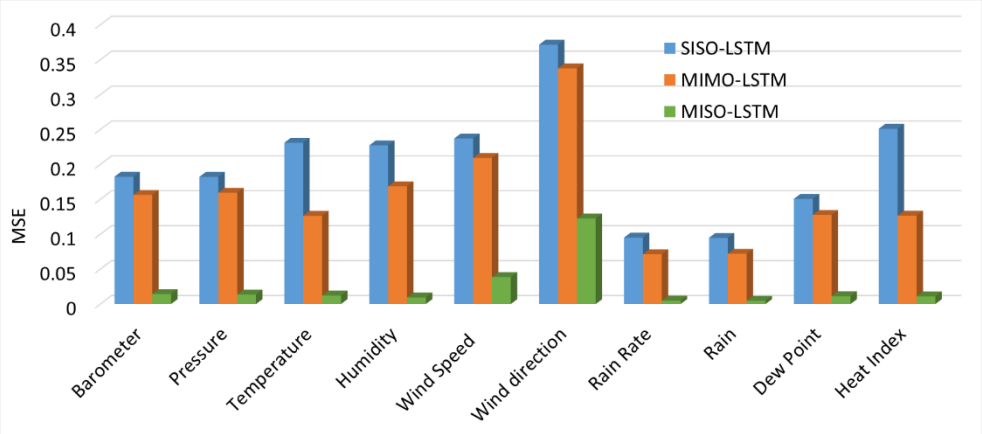

Figure 5.20 Comparison of model variances LSTM-MIMO, LSTM-MISO, and LSTM-SISO.

As indicated in Figure 5.20, the SISO-LSTM model variance yields higher MSE for all parameters. As the experiment uses only one parameter as an input for each training/testing model, this experiment proves that each weather parameter depends upon or is interrelated to other weather parameters rather than dependent upon itself. The prediction accuracy of a selected weather parameter depends upon its previous observations and the observations of the interrelated parameters (Di et al., 2015; Jincai et al., 1996). This is the reason the MIMO-LSTM and MISO-LSTM model variances provide better prediction performances compared to the SISO-LSTM model variance. Moreover, these results prove that the SISO deep modelling concept is not successful for

weather modelling. Therefore, the SISO concept is not practised with other ML approaches such as SR, SVR, and TCN.

5.3.1.2.2.3 TCN

Similar to Section 5.2.1.2.2.2, different configurations and controls are utilised to discover the optimal model for MISO-TCN model variance. The same controls described in the above section are kept constant during these experiments and use the 'save the best model approach'. Optimal MSE for each parameter is found in different configuration and different controls. Please refer Appendix 13 to a sample evaluation report. Table 5.33 presents a summary of this evaluation, where the optimal MSE is found for each parameter. In this section, 100 different experiments are carried out to represent the selected configurations and controls.

Table 5.33 Summary of configurations and controls for each parameter with least MSE.

Parameter	Optimal MSE	Configuration and controls
Barometer	0.001521964	No of filters: 256, no of TCN layers: 1, activation: tanh
Pressure	0.002024501	No of filters: 256, no of TCN layers: 1, activation: linear
Temperature	0.009870145	No of filters: 256, no of TCN layers: 1, activation: linear
Humidity	0.01006111	No of filters: 64, no of TCN layers: 2, activation: linear
Wind Speed	0.044360427	No of filters: 256, no of TCN layers: 2, activation: tanh
Wind direction	0.115209464	No of filters: 256, no of TCN layers: 1, activation: tanh
Rain rate	0.005125052	No of filters: 64, no of TCN layers: 4, activation: linear
Rain	0.004834251	No of filters: 256, no of TCN layers: 4, activation: tanh
Dew point	0.01126207	No of filters: 64, no of TCN layers: 1, activation: linear
Heat index	0.010076128	No of filters: 256, no of TCN layers: 1, activation: tanh

Table 5.34 Evaluation results for MISO-TCN model variance.

Parameter	MSE	MAE	RMSE
Barometer	0.000423817	0.014543533	0.020586805
Pressure	0.000558613	0.016262714	0.023634989
Temperature	2.048237	0.69914323	1.4311663
Humidity	19.33102	2.736332	4.3967056
Wind speed	1.8668145	0.9522951	1.3663142
Wind direction	3732.787	40.07244	61.09654
Rain rate	0.001163059	0.009628055	0.034103647
Rain	0.0000108	0.001413302	0.003284824
Dew point	18.028023	1.4789369	4.245942
Heat index	6.774312	1.2190325	2.6027508

Each of the individual models with the optimal MSE for each parameter (i.e. Table 5.33 models) are combined together to make the optimal model of MISO-TCN model variance. This new model is evaluated using the weather station validation dataset. The prediction results are de-normalised and compared with the ground truth values. Table 5.34 presents the evaluation results.

5.3.1.2.3 Comparison of baseline and proposed approaches for MISO model

The proposed MISO-TCN and MISO-LSTM model variances are compared with the classic ML MISO models of SR and SVR. The comparison results are shown in Table 5.35 and Figure 5.21. These results are subsequently evaluated via the MSE, and these MSE figures are calculated for the actual prediction and ground for the weather station validation dataset.

Table 5.35 MIMO analysis of SR, LSTM, and TCN in predicting different weather parameters. The least MSE is better and shown in highlighted.

Parameter	Model variances			
	Baseline-SR	**Baseline-SVR**	**MISO-LSTM**	**MISO-TCN**
Barometer	0.006052928	0.010888682	0.003995666	0.000423817
Pressure	0.006040654	0.010738483	0.003750399	0.000558613
Temperature	7.4294343	6.6375537	2.5194325	2.048237
Humidity	80.41223	53.577785	18.087887	19.33102
Wind Speed	4.660474	2.6081274	1.6269077	1.8668145
Wind Direction	23529.016	6177.982	3974.5454	3732.787
Rain Rate	0.006573259	0.001692935	0.001146236	0.001163059
Rain	0.005008375	0.000025097	0.0000106183	0.0000108
Dewpoint	44.836395	78.94774	18.107563	18.028023
Heat Index	23.886951	21.148586	7.449141	6.774312

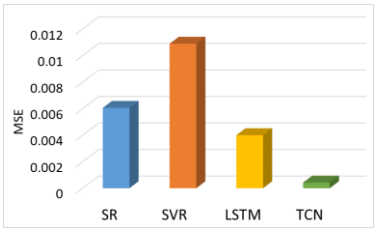

a) Barometer

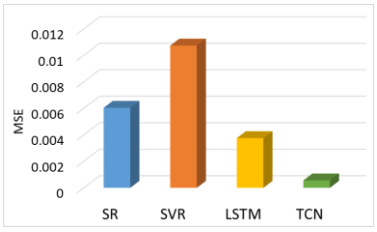

b) Pressure

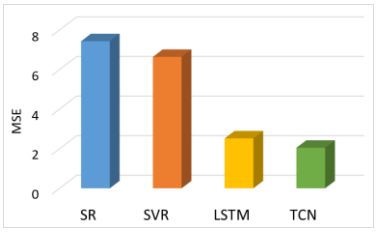

c) Temperature

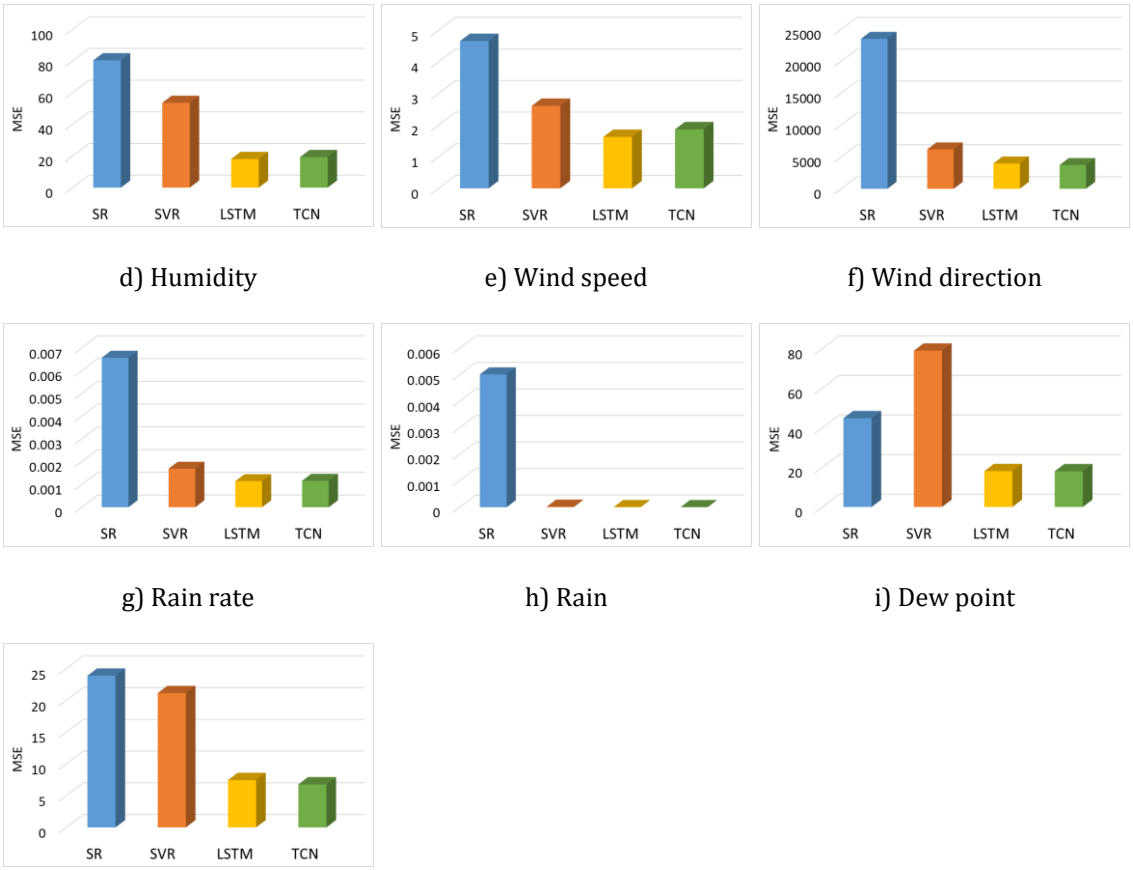

d) Humidity e) Wind speed f) Wind direction

g) Rain rate h) Rain i) Dew point

j) Heat index

Figure 5.21 MISO model analysis of different variances in predicting different weather parameters.

As Figure 5.21 and Table 5.35 indicated, the TCN provides better prediction results for the MISO model compared to other models. The deep learning model with LSTM layers also provides significant prediction results, but out of ten, six parameters provided better results in TCN approach with MISO model. Thus, the TCN combined model with ten parameters has been selected as the MISO model. All of these ten models have ten different TCN configurations with a different number of TCN layers, activation function, and a number of filters.

In Figure 5.18 and Figure 5.21, both LSTM and TCN deep learning models produce comparatively smaller errors compared to the standard regression and SVR. This implies that there is a non-linear interrelationship among parameters (Graves, 2012; Jozefowicz et al., 2015; Kavitha et al., 2016) and the selected parameter does not follow a linear path within selected sequential timeslots (Bishop, 2006; McCREA et al., 2005). Moreover, the standard regression and the SVR does not encode sequential information while LSTM

and TCN encode both multivariate and sequential information by taking them into another dimension in the input data (Bai et al., 2018; Basak et al., 2007; Jozefowicz et al., 2015).

As seen in Fig. 5.18 and Fig. 5.21, there are some parameters that have quite large errors. For instance, the humidity error is higher compared to seven other parameters. The reason for this is that the actual humidity figures are within a higher range of 70 to 100. According to Eq. 3.1, part of the MSE calculation is the square value of the difference between actual and predicted ones. The predicted values should be a higher range figure. Therefore, the MSE can get higher values if the actual figures are higher and predicted values not much closer to the actual. The similar condition is applied to the wind direction, dew point, and heat index parameters.

According to Fig. 5.18 and Fig. 5.21, the LSTM approach provides better or very similar results compared to the TCN approach for the parameters of wind speed, wind direction, rain rate, and dew point. This could be due to a higher variance of actual data in these parameters (Schmidhuber, 2015). These data items divert enormously from mean compared to the other variables such as pressure, temperature, barometer, rain, and heat index. In addition, there is a difference between error values in rain and rain rate in Fig. 5.18 and Fig. 5.21. The rain rate is classified according to the rate of precipitation per hour (Sachidananda and Zrnić, 1987). Therefore, the rain rate value is calculated for the last hour and rain is measured based on the frequency of data logged to manually calculate the cumulative rain. This indicates that there could be a substantial difference between rain and rain rate values endorsing different error values.

5.3.2 Comparison of MIMO and MISO optimal models

As described in Section 5.2.1, the MIMO-TCN and MISO-TCN proposed model variances yield better performance for short-term weather prediction for local weather station data. Table 5.36 and Figure 5.22 show a comparison between MIMO-TCN and MISO-TCN model variances error values to identify an optimal model for short-term weather forecasting.

Table 5.36 Compare MIMO-TCN and MISO-TCN model variances. The evaluation matric is MSE, and lower MSE is best and is highlighted.

Parameter	MIMO	MISO
Barometer	0.003305803	0.000423817
Pressure	0.003601799	0.000558613
Temperature	2.8303354	2.048237
Humidity	24.027027	19.33102
Wind Speed	1.9519161	1.8668145
Wind Direction	4106.5347	3732.787
Rain Rate	0.001456705	0.001163059
Rain	0.0000167	0.0000108
Dewpoint	24.394356	18.028023
Heat Index	9.148514	6.774312

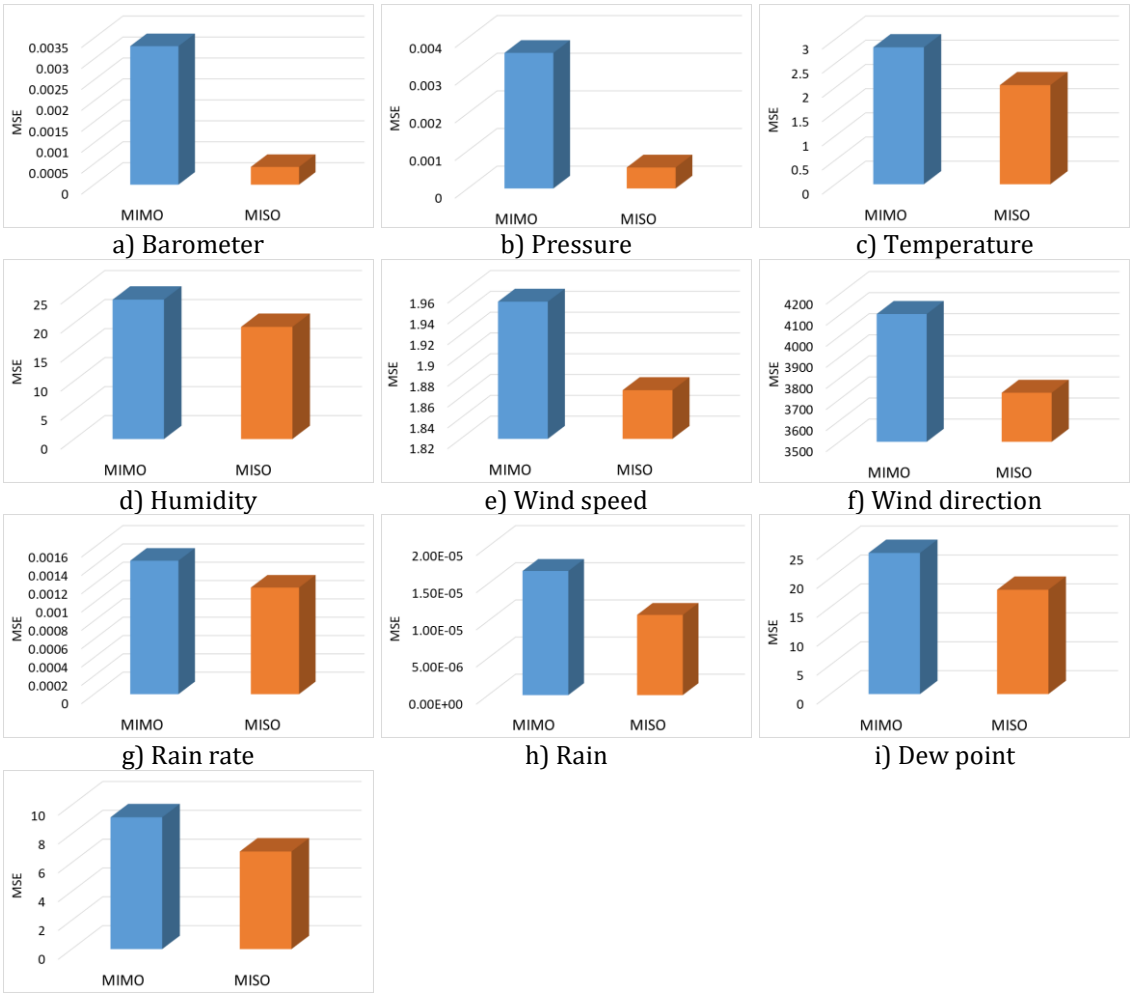

a) Barometer b) Pressure c) Temperature

d) Humidity e) Wind speed f) Wind direction

g) Rain rate h) Rain i) Dew point

j) Heat index

Figure 5.22 Evaluate MIMO-TCN and MISO-TCN model variances. The lower MSE is the best.

According to Table 5.36 and Figure 5.22, the proposed MISO model has lower error values compared to the proposed MIMO. This is probably because it took into account the interaction correlations between different weather parameters. Therefore, the MISO-TCN model has been selected as the tool to forecast the weather for a selected geographical area using local weather station parameters.

The proposed MISO-TCN model is used to predict data using the validation dataset. The predicted parameter values are compared with the actual ones. Fig. 5.23 compares a random 100 samples of predicted data and the ground truth from the validation dataset. For each graph, the ground truth, and the proposed MISO deep model's predictions are represented by each line with blue and red colours, respectively.

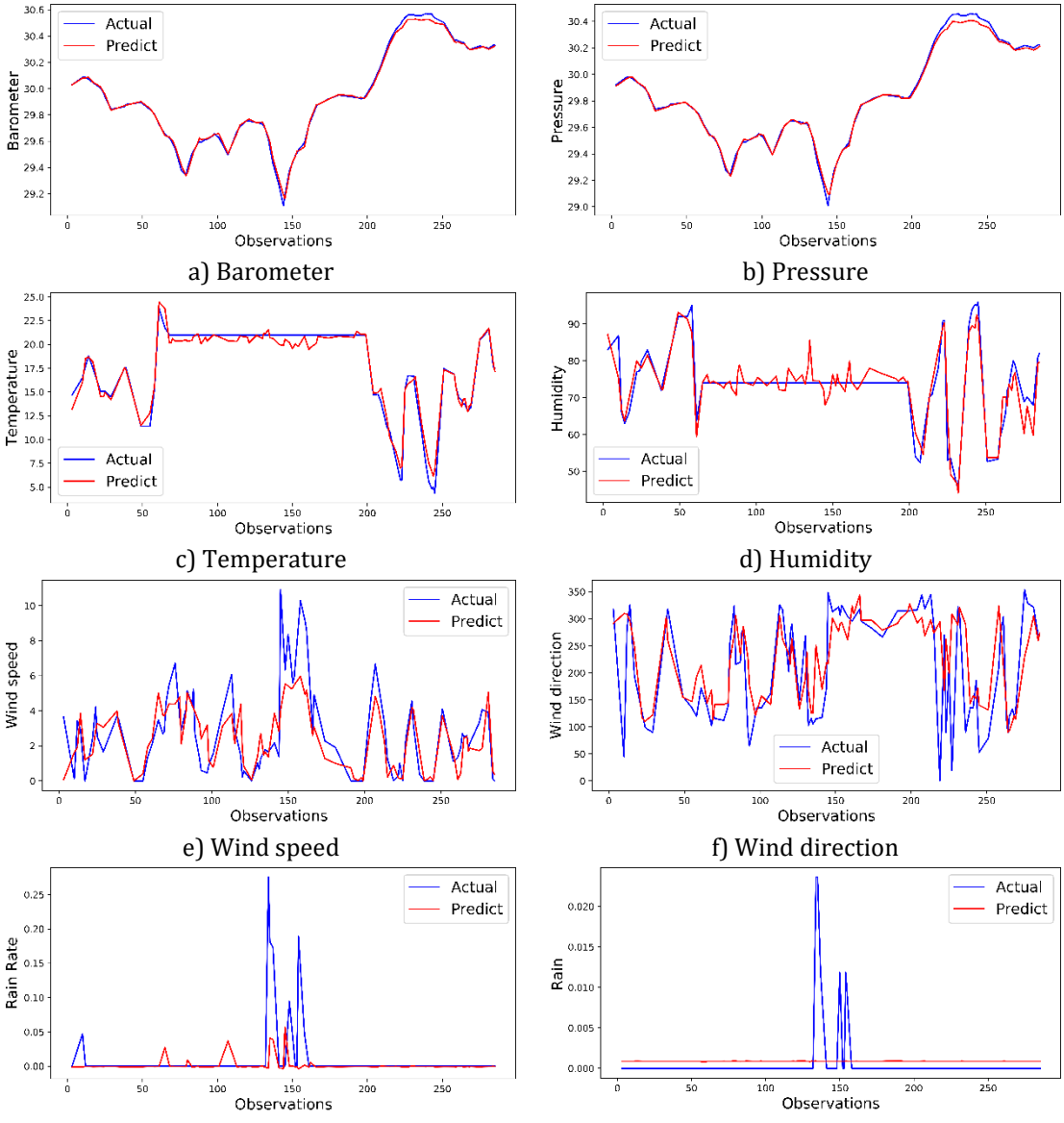

a) Barometer b) Pressure

c) Temperature d) Humidity

e) Wind speed f) Wind direction

g) Rain rate h) Rain

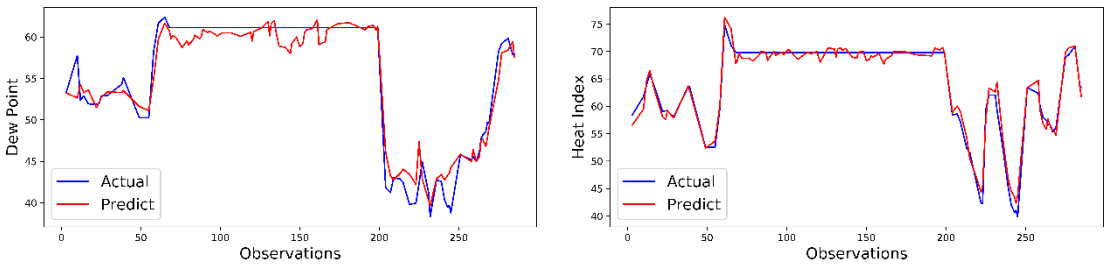

i) Dew point j) Heat index

Figure 5.23 Comparison of actual values and the proposed model prediction.

Figure 5.23. Figure 5.23 demonstrates that the red colour line chart (predicted values) closely follows the blue line chart (ground truth) in many parameters. The predicted values are diverted exceedingly in rain rate and rain parameters. According to Figure 8g and Figure 8h, the highest figures for rain and rain rates are 0.24mm and 0.25mm/hour respectively. These values are relatively quite small and can be considered negligible. Overall, the proposed MISO model is producing effective results which can be utilised to the short-term weather forecasting for a selected geographical area.

5.3.3 Proposed model for long-term weather prediction

As described in Section 5.3.2, the MISO-TCN generated higher accuracy short-term (1-hour) prediction for Local weather station data. The deep models of Bi-LSTM and SISO concepts are ignored at this stage as they are outperformed in previous sections. This section aims to retune the proposed MISO-TCN model for more extended periods of 2, 3, 6, 9, 12, 18, and 24 hours. The 'save the best model approach' is utilised while retuning the models. As described in Section 3.2.5.2, if the proposed short-term model is based on TCN, then the performance of long-term models of TCN-WL (without loading short-term optimal model weights) and TCN-LW (loaded with short-term optimal model weights) are compared. Therefore, the proposed model variances for the long-term forecasting are TCN-WL and TCN-LW. The weather station training dataset is used to train/retune these models, and the weather station testing dataset is used to evaluate those models. The optimal model is chosen based on the evaluation results for each timeslot.

In this case, there are ten individual modes for each method (i.e. TCN-WL and TCN-LW), which represent each parameter need to retune for each timeslot. There are seven different timeslots. Therefore, in this section, there are 140 individual models to re-train and evaluate (i.e. ten parameters for seven timeslots). Comparison of overall MSE for TCN-WL and TCN-LW for each timeslot is shown in Table 5.37 and Figure 5.24. Please refer to Appendix 14 for a sample evaluation report for each timeslot.

Table 5.37 Comparison of TCN-WL and TCN-LW model variances.

Time	Overall MSE	
	TCN WL	TCN LW
2	570.4730225	563.0042725
3	720.9248047	670.3707886
6	930.9603271	929.4086914
9	999.4702148	945.2125854
12	1052.606689	1052.396973
18	1510.699463	1049.252563
24	1299.575684	1211.212646

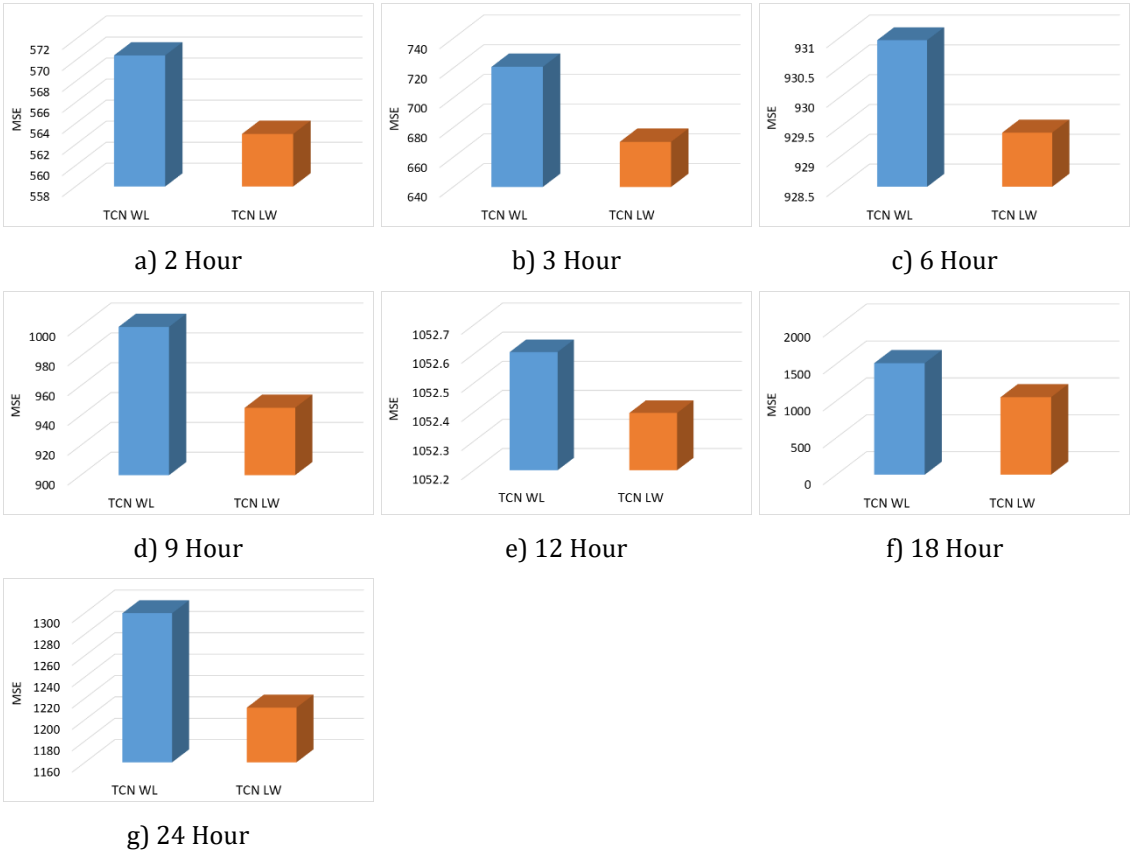

a) 2 Hour b) 3 Hour c) 6 Hour

d) 9 Hour e) 12 Hour f) 18 Hour

g) 24 Hour

Figure 5.24 Comparison of TCN-WL and TCN-WL model variances.

As per information from Figure 5.24 and Table 5.37, the TCN-LW yields better performance with minimum MSE for each timeslot compared to the TCN-WL. The reason is that the TCN-LW has used an already trained model for a specific domain issue (i.e. weather forecasting) and, then retune the model weights match to the new dataset. This process is highly efficient and directed to an accurate result (Hochreiter and Schmidhuber, 1997). Therefore, TCN-LW model variance is selected as the long-term weather forecasting models for the weather station data.

Table 5.38 and Figure 5.25 present the summary of evaluation results for the optimal models for each parameter at each timeslot. These are calculated on the data in the normalised form. Appendix 15 shows the comparison of predicted results to the ground truth for 100 sets of random data from the validation dataset for each timeslot (i.e. after de-normalising the predicted data to the human-understandable format and compared with the ground truth).

Table 5.38 MSE for saved the best models for each parameter: MISO-TCN long-term forecasting.

Parameter	1	2	3	6	9	12	18	24
Barometer	0.002076916	0.015901655	0.024086033	0.053096528	0.073861631	0.124978887	0.192134968	0.298616451
Pressure	0.001945692	0.011051216	0.013019966	0.047201681	0.099501107	0.120865501	0.212799633	0.269017231
Temperature	0.01216418	0.024454928	0.04524594	0.088169437	0.099630563	0.10016648	0.108323128	0.109965725
Humidity	0.010701872	0.027061418	0.04177346	0.078032536	0.103088642	0.118589158	0.120291006	0.12806465
Wind speed	0.044435158	0.075127839	0.092829066	0.120608897	0.125807085	0.139735703	0.140008575	0.149006794
Wind Direction	0.12296849	0.173362198	0.218211832	0.279203681	0.298094872	0.313163059	0.376084732	0.389930909
Rain rate	0.005708397	0.004038433	0.005178649	0.004847353	0.004399635	0.004283268	0.004718017	0.00419405
Rain	0.005812216	0.004707018	0.004419363	0.00735798	0.004468292	0.004719651	0.004471535	0.004368936
Dew point	0.011651516	0.007356989	0.009622774	0.022991496	0.028536608	0.034159852	0.040293042	0.043526875
Heat index	0.011076465	0.023467487	0.044937868	0.07848461	0.099149089	0.103952541	0.109156926	0.118862578

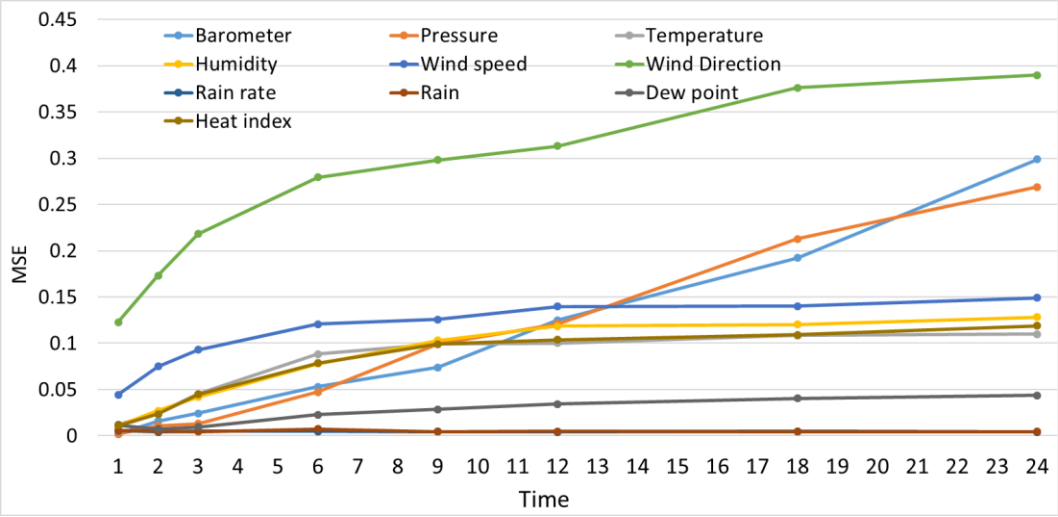

Figure 5.25 MSE for the best model in each timeslot: TCN-MISO long-term forecasting.

As shown in Figure 5.25, the MSE values are increasing (i.e. accuracy of the model decreasing) when the prediction time increases. This has already been observed with the WRF data and even in the well-recognised WEF model. Similar to the short-term forecasting, the wind direction parameter shows higher error values compared to all the parameters. This reason for this is that the variance of the wind direction data is quite high (Schmidhuber, 2015).

The barometer and pressure predictions provide minor error values until 9 to 12 hours and then increase rapidly. This is because of the areas of high atmospheric pressure moving to the low-pressure areas and vice-versa. Usually, these areas refer to many hundreds of miles (Anderberg, 2015). Therefore, it is quite hard to predict these parameters for quite a long time as the data is taken from a single location (i.e. location of the local weather station). Moreover, the temperature, humidity, dew point, and heat index parameters often change while the atmospheric pressure is changing (Anderberg, 2015; Ji et al., 2018; Society, 2011).

Figure 5.26 shows how these MSE values change with the time for each individual parameter. As per Figure 5.25 (g) and Figure 5.25 (h), the rain and rain rate MSE values are changed marginally throughout each timeslot, and these are quite small values. This means the prediction accuracy is quite high for these parameters. This also proved that the prediction results for the rain are quite accurate for the deep neural networks (Yonekura et al., 2018a).

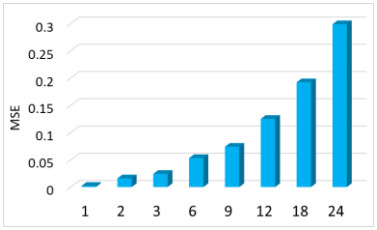

a) Barometer

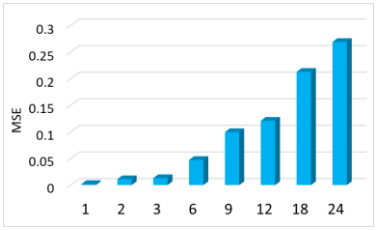

b) Pressure

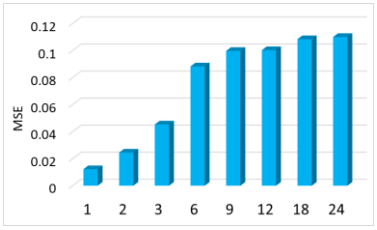

c) Temperature

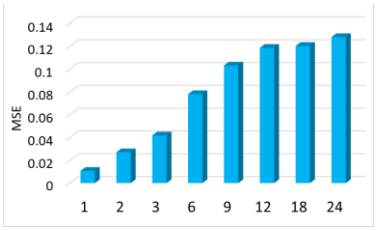

d) Humidity

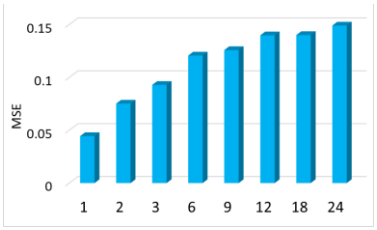

e) Wind speed

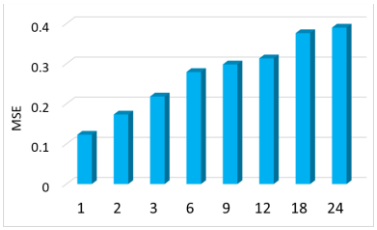

f) Wind direction

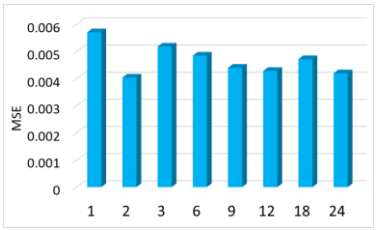

g) Rain rate

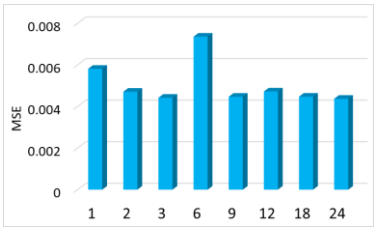

h) Rain

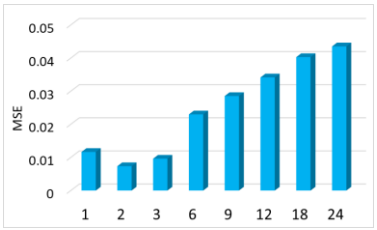

i) Dew point

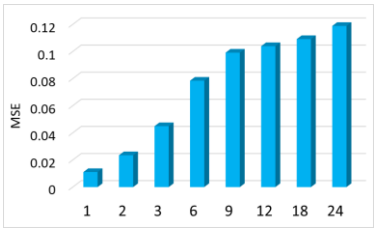

j) Heat index

Figure 5.26 MSE change with the time: TCN-MISO long-term forecasting.

As indicated in Figure 5.25, the proposed deep learning MISO model can be used for weather forecasting. There are some parameters able to produce slightly improved accuracy of forecasting results up to 24 hours (i.e. Rain and Rain rate) while others can produce slightly accurate forecasting up to 9 to 12 hours. The proposed MISO optimal model is used with the weather station validation dataset to get a prediction and compared with the ground truth and results shown in Figure 5.25. The predicted result is de-normalised and compared with the real ground truth. A random 50 data samples are selected to present as it is not practical to present the whole dataset. For each graph, the ground truth, and the proposed MISO deep model's predictions are represented by each line with blue and red colours, respectively.

Figure 5.26 (i) and Figure 5.26 (ii) show that the predicted results of the barometer and pressure values change rapidly after 9 to 12 hours. However, the proposed MISO model can produce a more accurate prediction for these two parameters for up to 12 hours. Even though the parameters rain and rain rates look diverted exceedingly in Figure 5.26 (vii) and Figure 5.26 (viii), the actual figures are quite small and can be considered negligible (i.e. highest rain- 0.25 mm and highest rain rate- 0.024 mm/hour). For all other parameters, the predicted values closely follow the ground truth up to 9 to 12 hours and then divert from the actual. Overall, the proposed MISO can be used for weather forecasting, and it has the ability to produce some accurate results up to 9 to 12 hours.

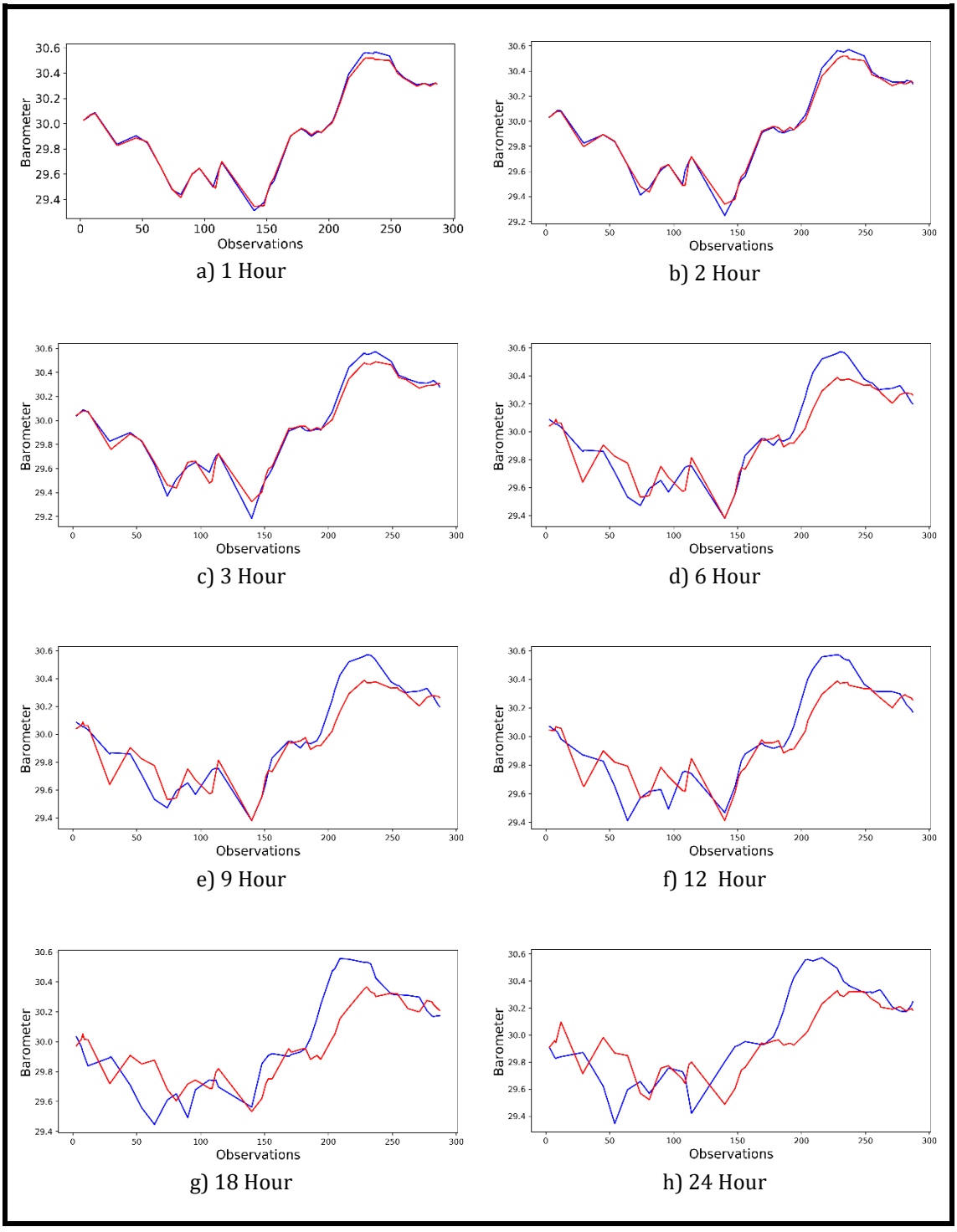
Barometer
Observations
a) 1 Hour
b) 2 Hour
c) 3 Hour
d) 6 Hour
e) 9 Hour
f) 12 Hour
g) 18 Hour
h) 24 Hour
i) Barometer
Ground truth
MISO-TCN model prediction

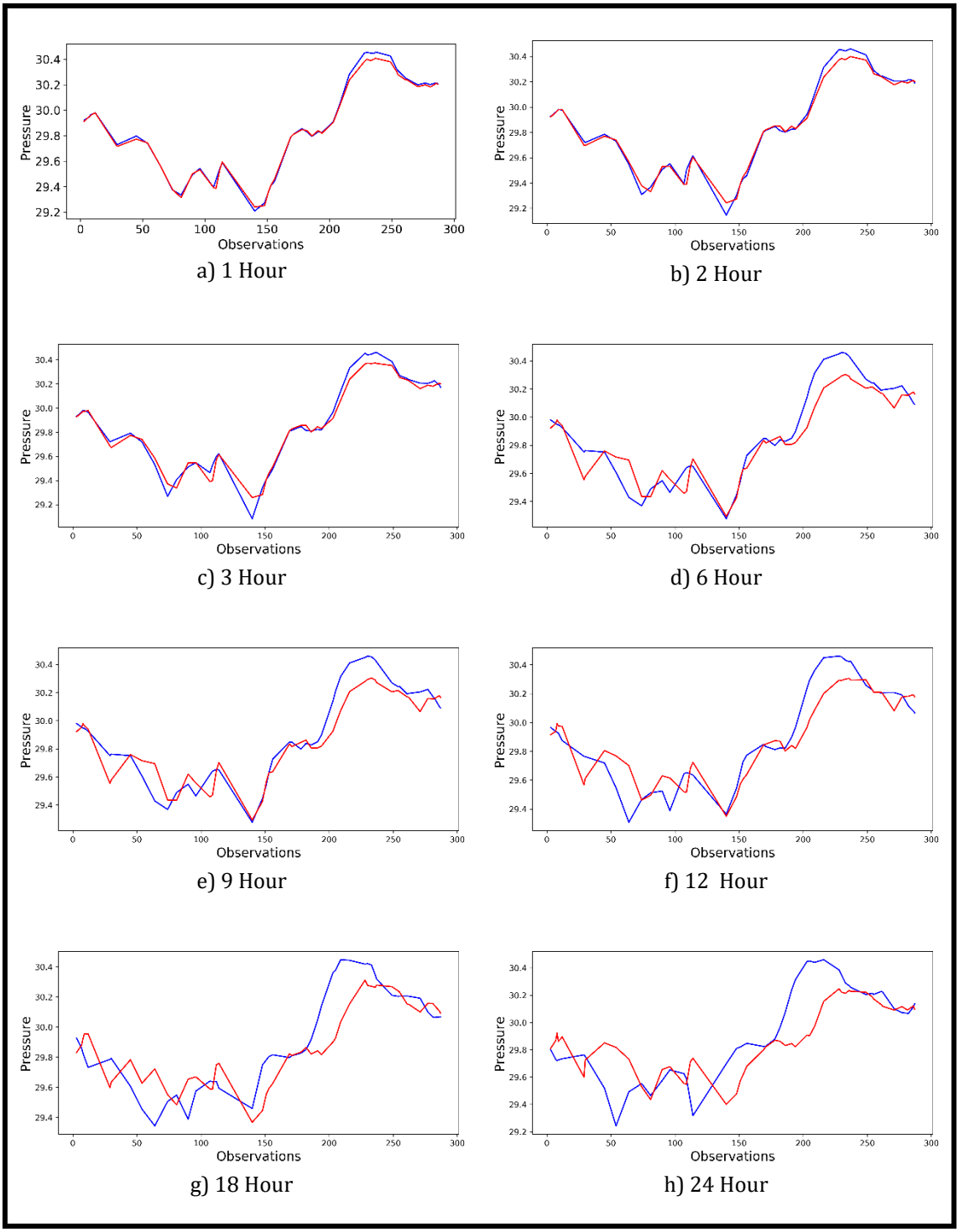
Pressure
Observations
a) 1 Hour
b) 2 Hour
c) 3 Hour
d) 6 Hour
e) 9 Hour
f) 12 Hour
g) 18 Hour
h) 24 Hour
Ground truth
MISO-TCN model prediction

ii) Pressure

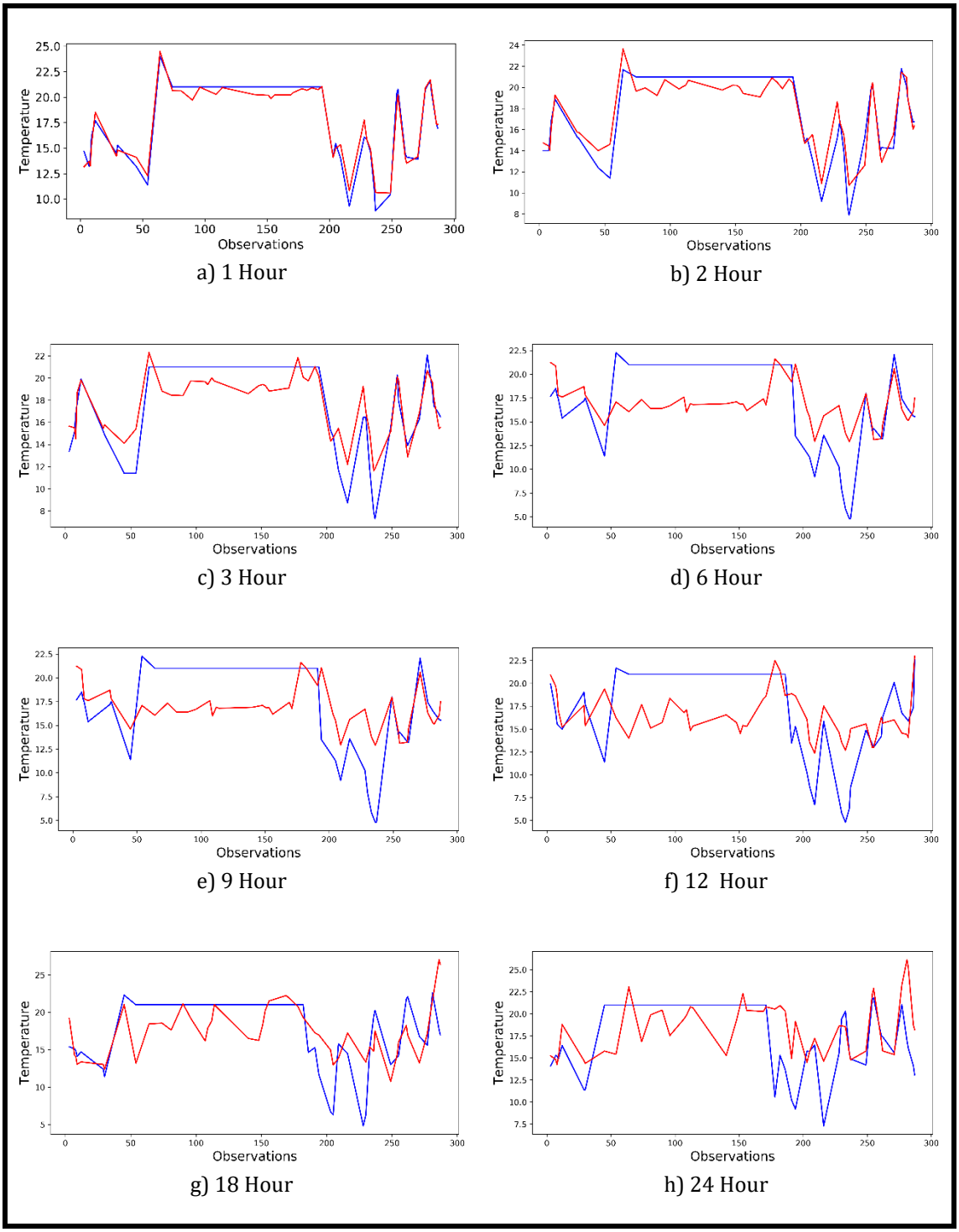

iii) Temperature

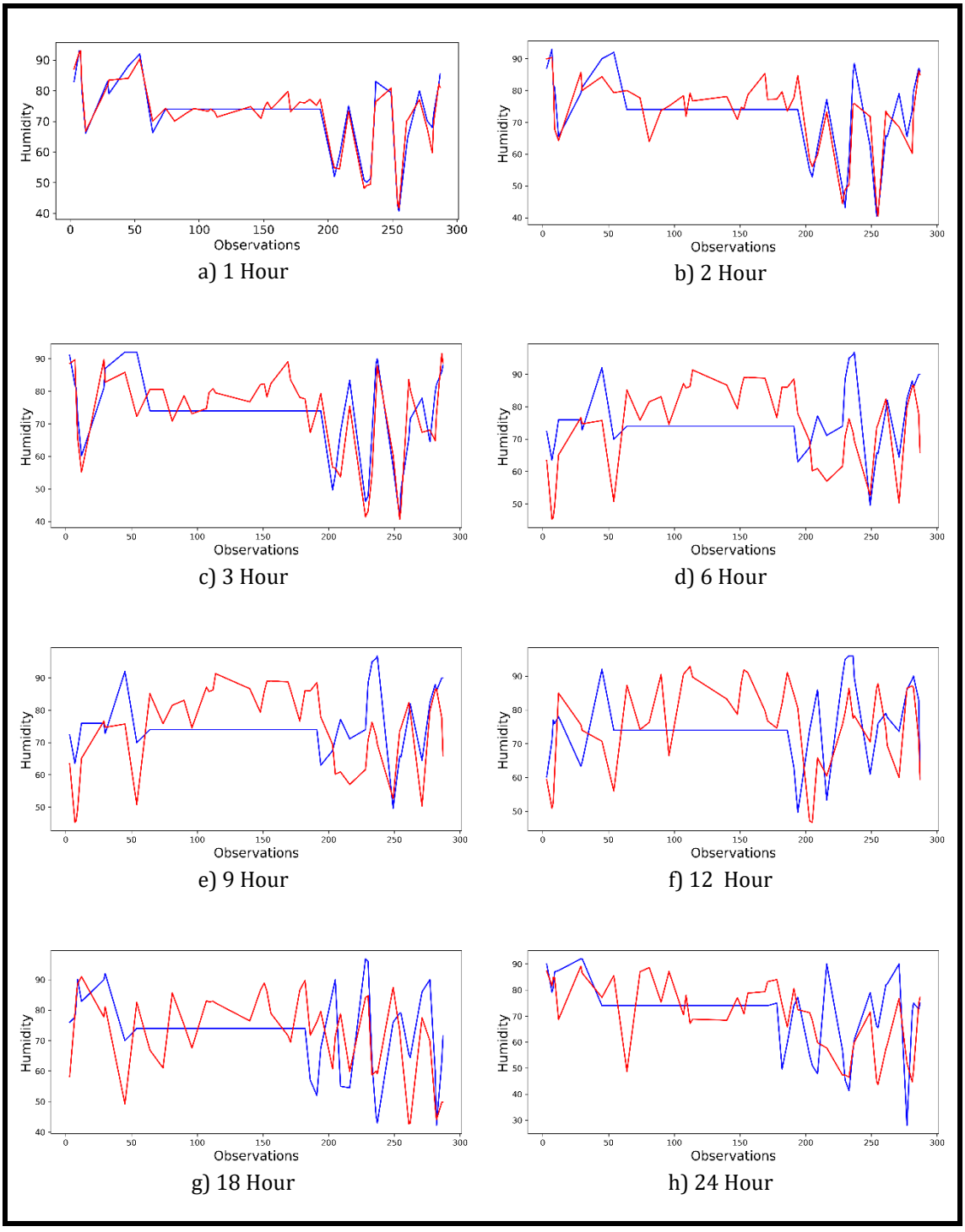
Humidity
Observations
a) 1 Hour
b) 2 Hour
c) 3 Hour
d) 6 Hour
e) 9 Hour
f) 12 Hour
g) 18 Hour
h) 24 Hour
Ground truth
MISO-TCN model prediction

iv) Humidity

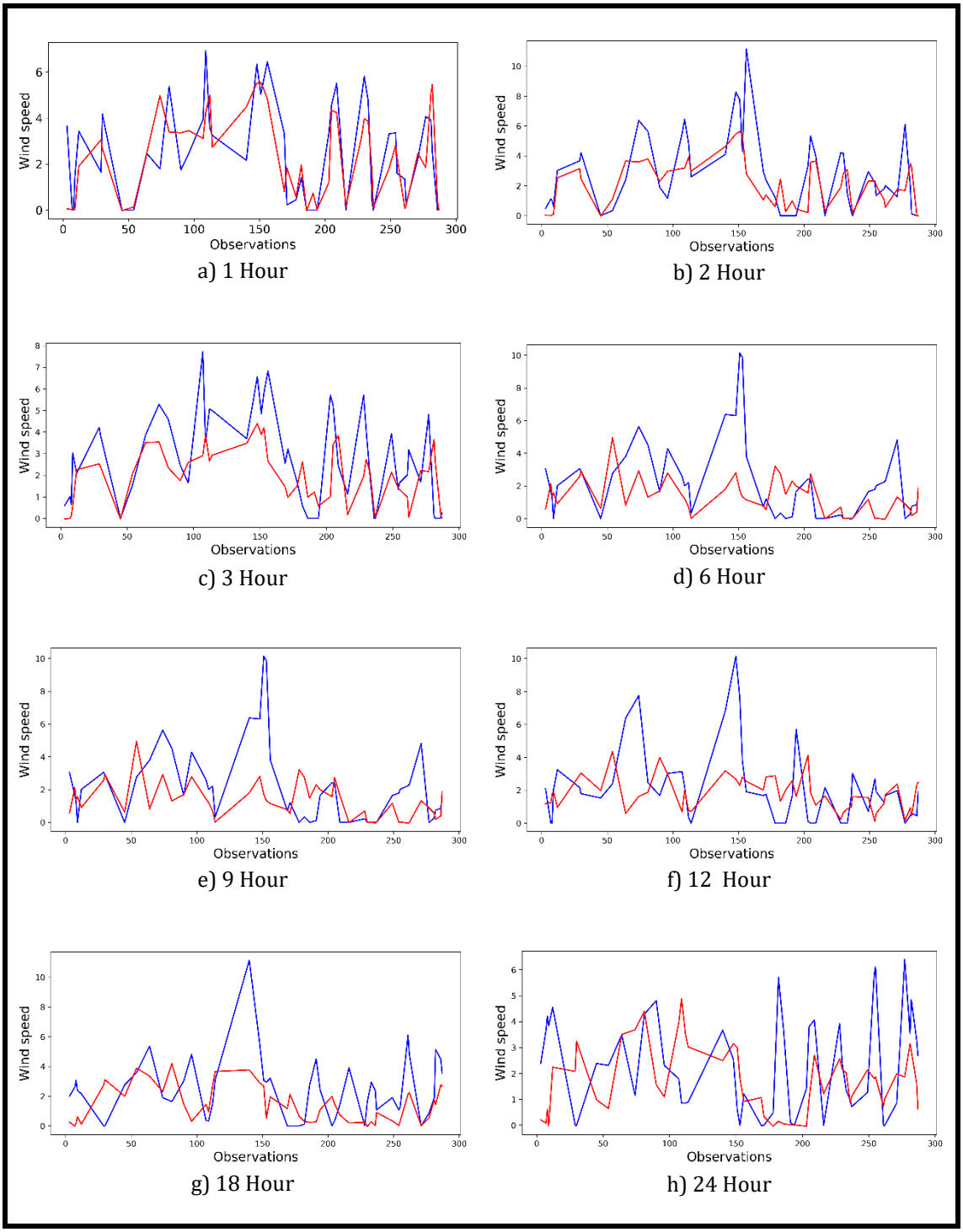

a) 1 Hour

b) 2 Hour

c) 3 Hour

d) 6 Hour

e) 9 Hour

f) 12 Hour

g) 18 Hour

h) 24 Hour

v) Wind speed

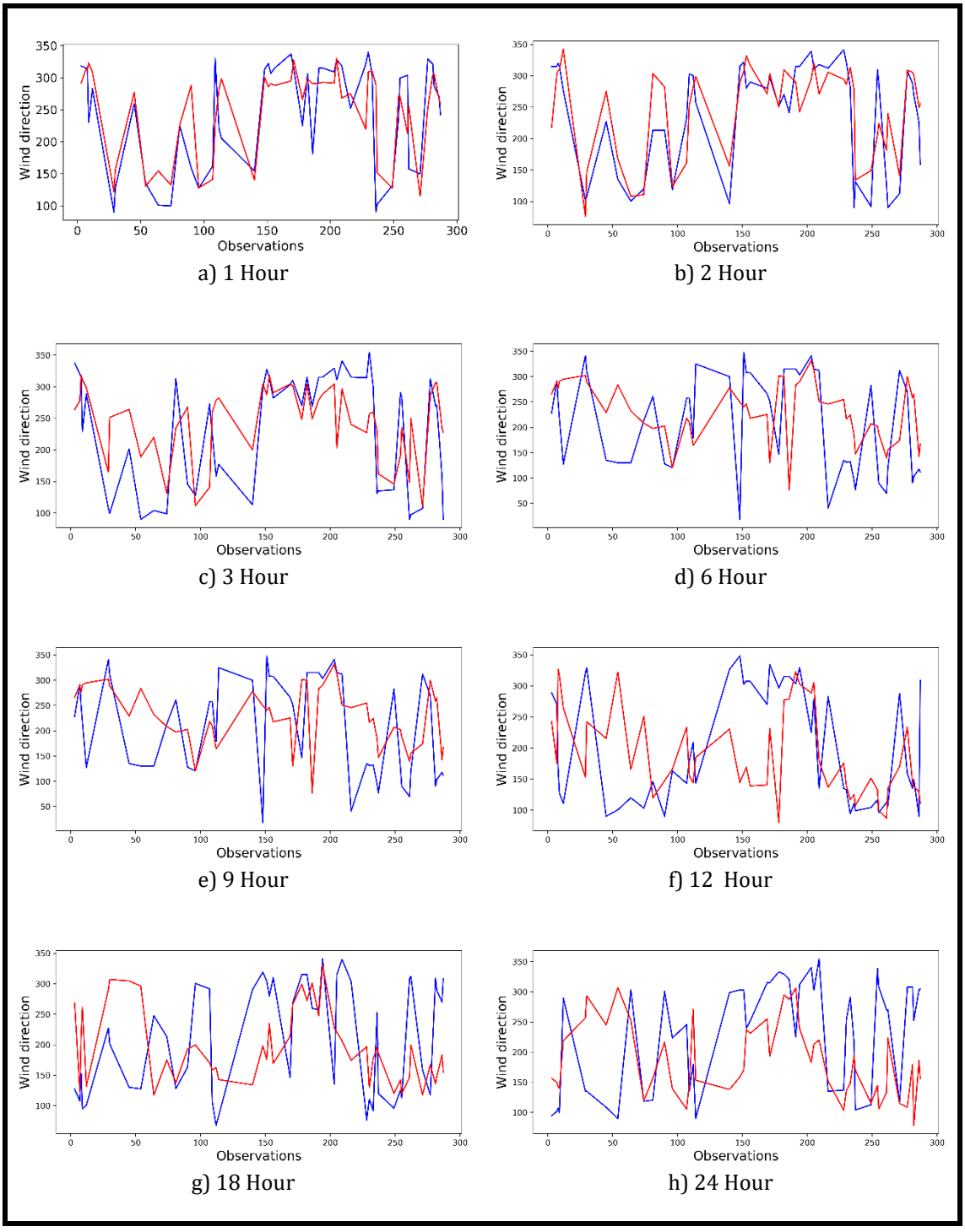

vi) Wind direction

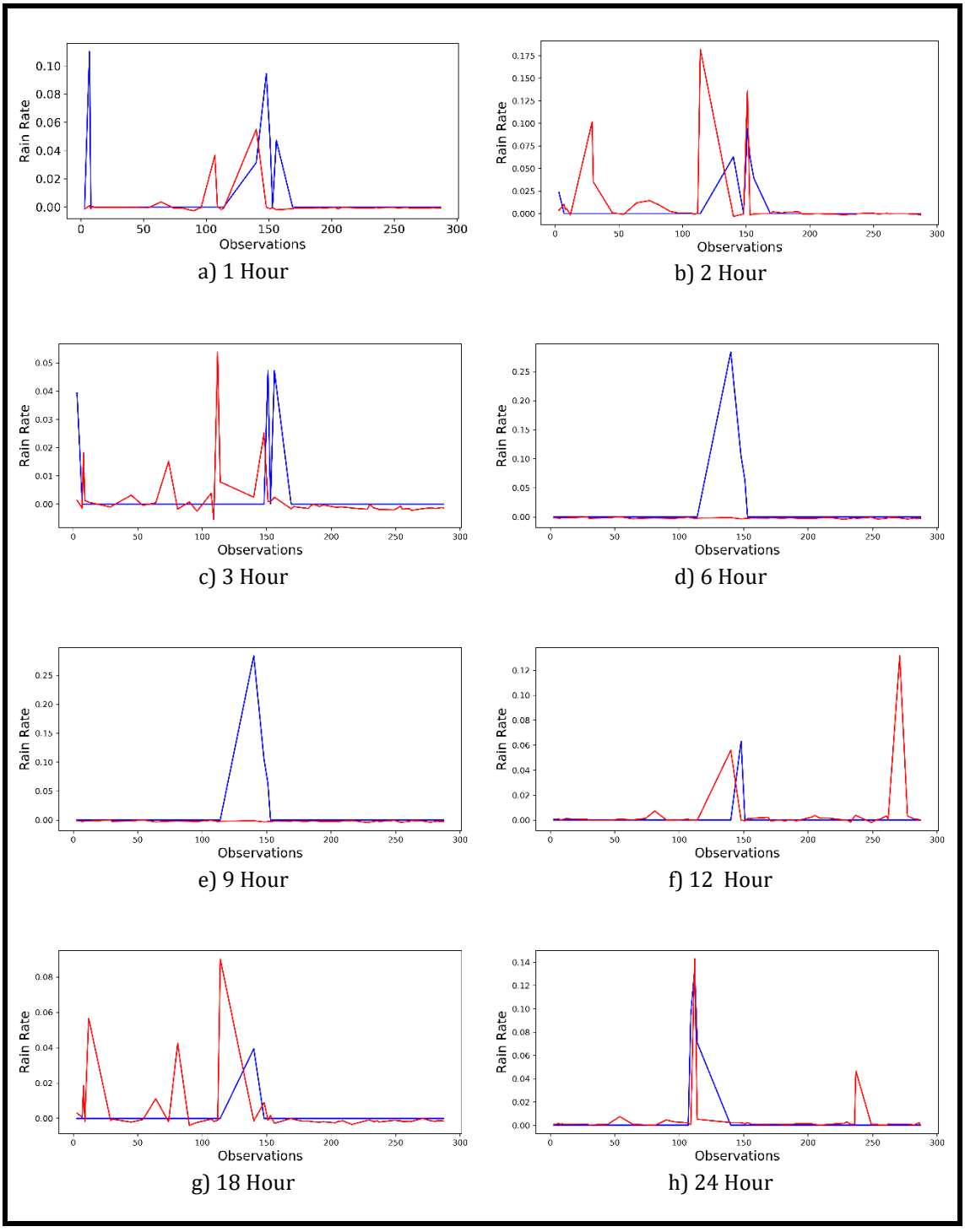

vii) Rain rate

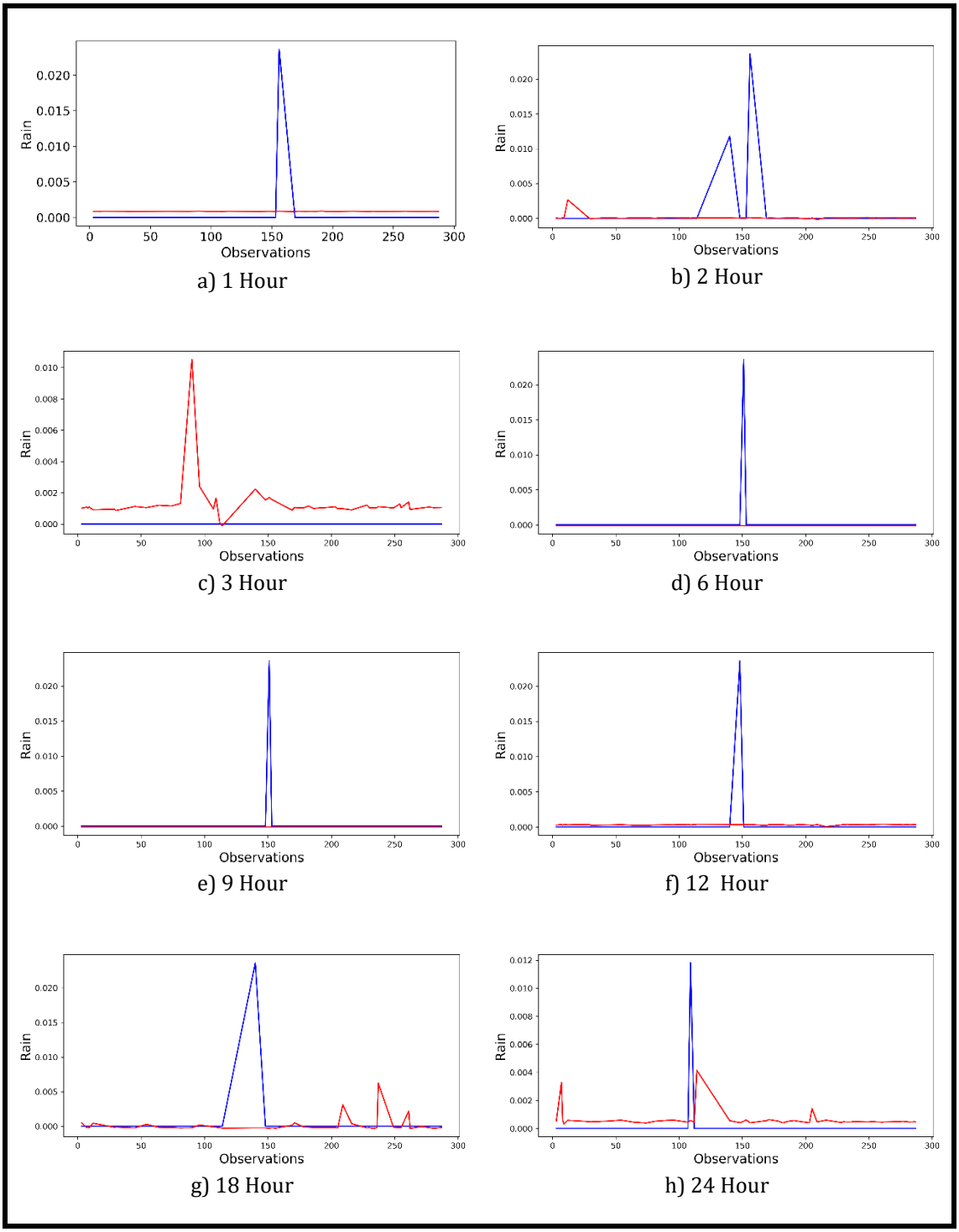
Rain
Observations
a) 1 Hour
b) 2 Hour
c) 3 Hour
d) 6 Hour
e) 9 Hour
f) 12 Hour
g) 18 Hour
h) 24 Hour
Ground truth
MISO-TCN model prediction

viii) Rain

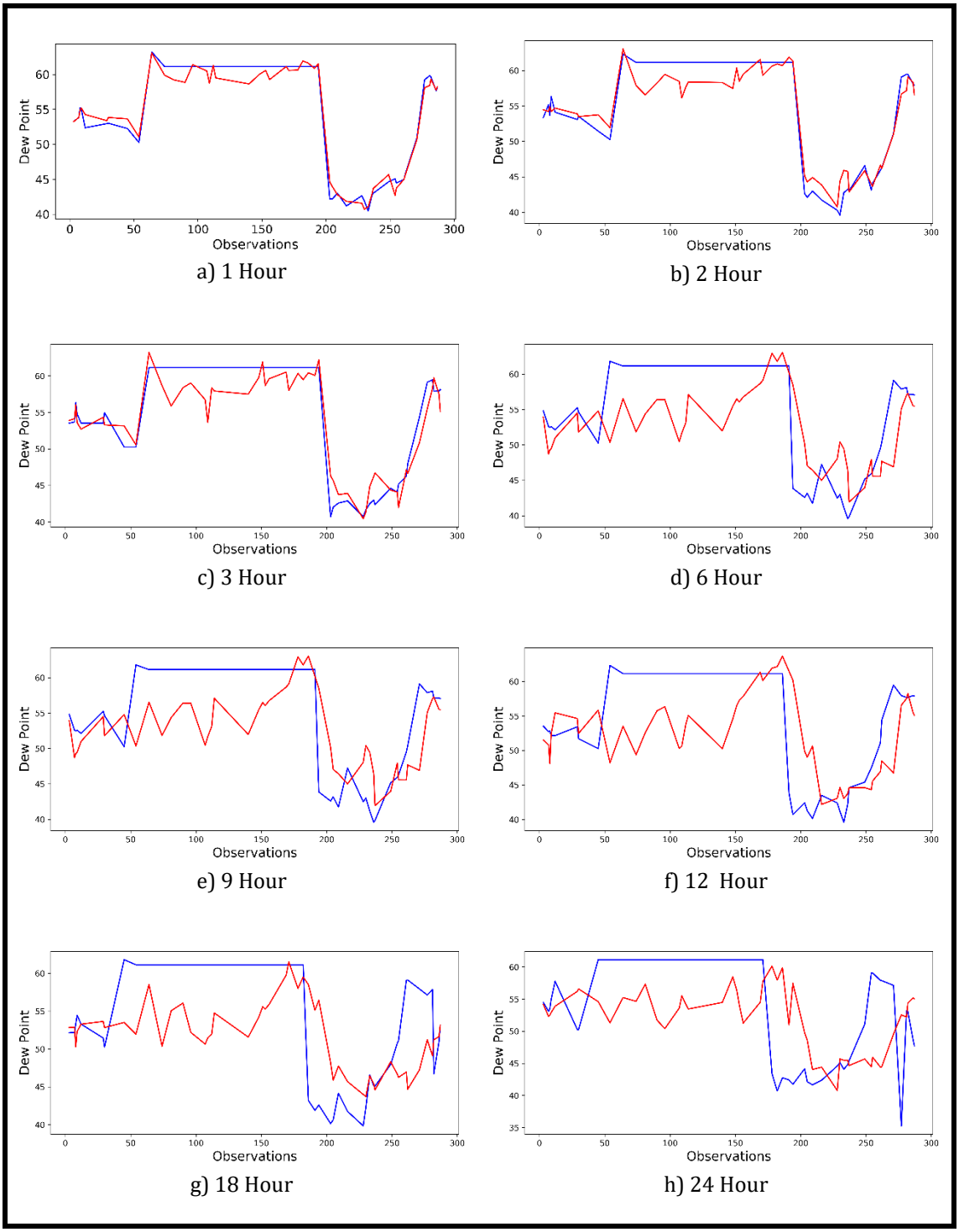
Dew Point
Observations
a) 1 Hour
b) 2 Hour
c) 3 Hour
d) 6 Hour
e) 9 Hour
f) 12 Hour
g) 18 Hour
h) 24 Hour
Ground truth
MISO-TCN model prediction

ix) Dew point

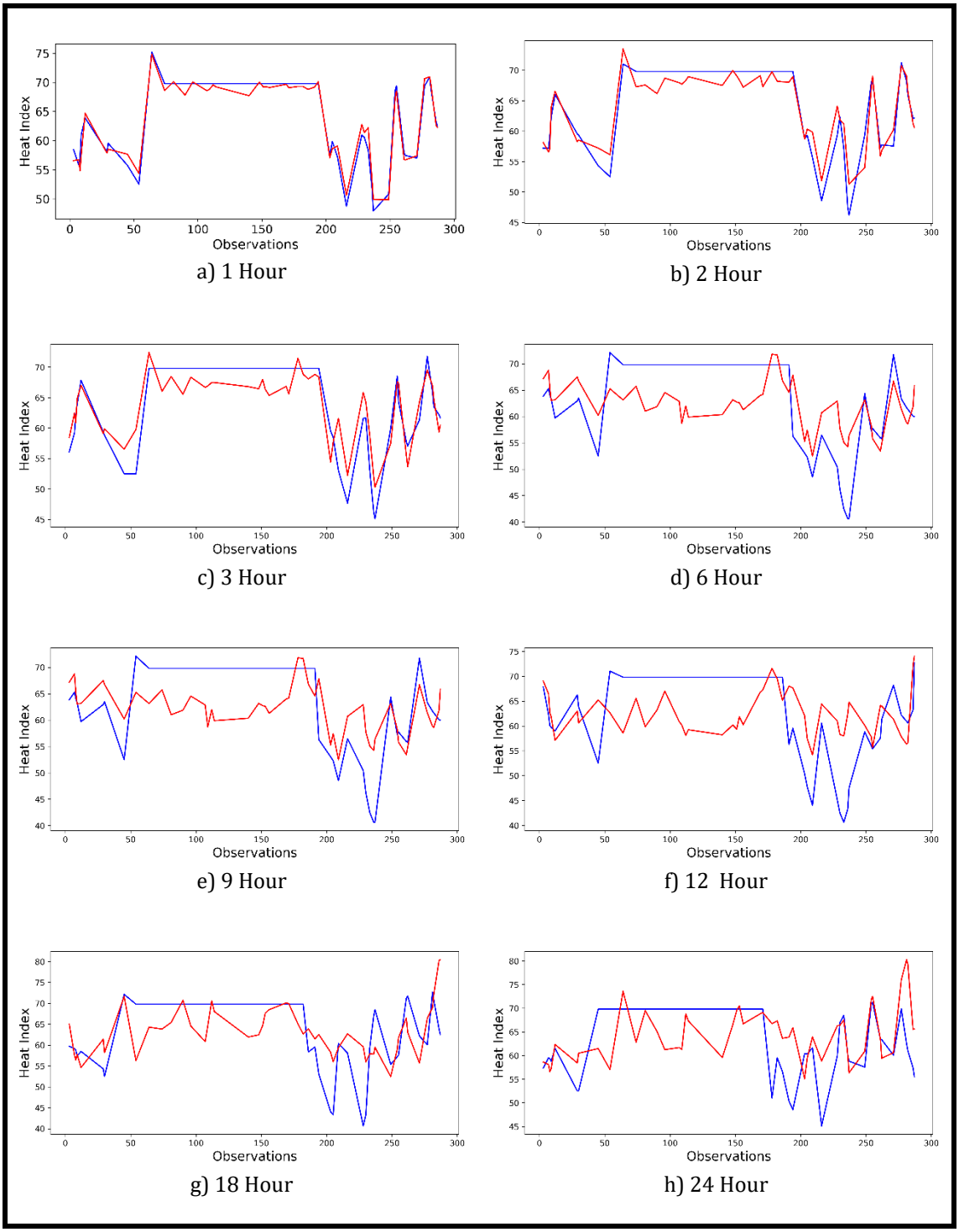

Figure 5.27 Comparison of proposed TCN-MISO prediction with the ground truth for each timeslot for random 50 datasets.

5.4 Discussion

As discussed in Section 2.8, there has been no previous attempt to compare an AI-based weather prediction with a well-established and existing NWP model. This study has significantly advanced the current knowledge by comparing the above two models. As shown in Figure 5.15, Phase 1 of this study apparent that the AI-based deep learning proposed model is able to produce more accurate medium-range weather forecast (i.e. up to 12 hours) compared to the well-established WRF NWP model. This is also proved that the deep learning models have the capability of capturing non-linear or complex underlying characteristics of a physical process with a high degree of accuracy. Besides, Section 2.6 demonstrates that there are several challenges in the NWP models including that use of high computing power to execute a large number of non-linear simultaneous equations, and it requires a long time for processing. As Section 5.2.4 discussed, the proposed model can overcome these computational complexity issues. This also validates the statement in Section 2.1 that the data-driven computer modelling systems can be utilised to reduce the computational power of NWP systems.

As described in Section 2.8, there is a knowledge gap which has been little or no attempt to compare classic ML approaches with cutting-edge deep neural network approach for weather forecasting. This study compared classic ML approaches such as SR and SVR with cutting-edge deep learning approaches of LSTM and TCN for both historical weather data and local weather station data with MIMO and MISO regression models. As shown in Figure 5.2, Figure 5.3, Figure 5.18, and Figure 5.21, it is evidenced that the modern deep learning approaches performed significantly better than the classic ML approaches in each occasion.

As discussed in Section 2.7, the TCN has exhibits more extended memory architecture than LSTM with the same capacity and constantly performs better than LSTM architectures on a vast range of sequential modelling tasks. Section 2.8 discussed that there had been no attempt to utilise the TCN for weather forecasting. The cutting-edge TCN deep learning approach is introduced in this study for weather forecasting by filling the knowledge gap. Besides, as per information from Table 1.24 and Table 1.35, the TCN approach with the proposed model is able to produce a more accurate weather forecast for local weather station data compared to classic ML approaches and LSTM.

As per information from Table 2.2 in Section 2.8, the existing AI-based weather forecasting models use only five or less interrelated input parameters. Besides, a complete

AI-based weather forecasting model has not been explored yet. This study significantly contributes to the current knowledge by exploring a complete AI-based weather forecasting model with ten input/output parameters. Even, phase 2 of this research demonstrates that the proposed model can be used for fine-grained area-specific weather forecasting for the community of users in a specific geographical area.

5.5 Summary

The first part of the research findings shows that the deep neural network approach can be utilised for weather forecasting for the historical weather data. Also, this model generates more accurate predictions compared to the well-established WRF model for up to 12 hours. The only issue is that the WRF model is still used with the proposed deep learning model to extract GRIB data to use as inputs. Besides, it requires a minimum of three hours of access GFS data after taking the atmospheric measurements, including the time taken to upload data to the website (National Centers for Environmental Information, 2019; NCAR/UCAR, 2019). In accession to the WRF drawbacks, this model also needed the time to pull out the GFS data dependent on the data processor system. Hence, the input data which are used in the new model are not the current atmospheric measurement data (i.e. older than 3 hours). Therefore, it is not practicable to use WRF data with the new model, and it will be highly beneficial to consider the use of local weather station data for weather forecasting.

The second part of the research findings shows that the deep neural network approach can be utilised for weather forecasting for a selected fine-grained geographical location. Further, this novel lightweight weather model can predict data more accurately up to 9 - 12 hours. Consequently, this new model could make a significant impact on a community of users who rely on the weather for their day-to-day activities. For example, the weather condition can be predicted and monitored within a few hours' time interval, by running the TCN code, without relying on the regional weather forecasting. The only requirement is to access the local weather station data, which could be achieved by setting up an economical weather station in specific locations or farms. Furthermore, a broader set of users who rely on favourable weather conditions could get the advantage of the model, such as places of interest, schools, outdoor sports centres, construction sites, etc.

6 Conclusion and Recommendation

The first phase of this research demonstrates that the proposed lightweight model for the historical weather data/WRF data can be utilised for weather forecasting up to 12 hours. The model has outperformed the state-of-the-art WRF model for up to 12 hours. The proposed model is able to run on a standalone computer and it can be easily deployed in a selected geographical region for fine-grained, short to medium-term weather prediction. For instance, the proposed lightweight model could be deployed using a low-cost and low-power device such as NVIDIA jetson nano developer kit (cost around $99 and power 5V/4A) (Aufranc, 2019). Besides, the proposed model is able to overcome several challenges of the WRF model such as the understanding of the model, its installation, and its execution and portability. In particular, the deep model is portable and can be easily installed in a Python environment for effective results (Gulli and Pal, 2017; Skamarock et al., 2008). This process is highly efficient compared to the WRF model.

The existing NWP models are limited to regional forecasting. Besides, the existing machine learning-based weather forecasting models are limited to predict a maximum of five weather parameters. The proposed new weather forecasting model can predict as many as ten parameters. The Phase 1 experiment results show that the neural network approach can be applied for weather prediction.

The regional weather forecasting may not be accurate based on the geographical appearance of the location (such as the top of a mountain, land covered by several mountains, and the slope of the land). As a solution, a short-term weather forecasting system is suggested in Phase 2 for the community of users utilising local weather station data and the same Phase 1 architecture.

In Phase 2, a novel lightweight weather model is introduced which can be utilised for accurate weather forecasting for a selected fine-grained geographical location up to 12 hours. Consequently, this new model could make a significant impact on a community of

users who rely on the weather for their day-to-day activities. For example, the weather condition can be predicted and monitored within a few hours' time interval by running the proposed model (i.e. TCN code) without relying on the regional weather forecasting such as WRF or Met office. The only requirement is accessing the local weather station data which could be achieved by setting up an economical weather station in specific locations or farms.

The proposed model has advantages over the regional and global forecasting models including lower computational power consumption, ease of installation, and greater portability. While the NWP models are viable for long-range forecast and not for a fine-grained geographical area, the proposed model could make a reliable and accurate prediction as this uses the data related to that specific location.

6.1 Assessing the research hypotheses

The overall goal of this study is to obtain an effective and fine-grained weather forecasting model for a community of users in a specific geographical area. This has been achieved in two phases throughout the research study. In phase 1, it is empirically demonstrated that machine learning approaches can be used for weather forecasting. Moreover, this technology is able to produce a more accurate forecast of up to 12 hours when compared with the state-of-art WRF model. In phase 2, it is empirically demonstrated that the lightweight TCN based deep learning model can be used for weather forecasting using local weather stations data for a selected geographical area. The weather forecasting model is developed by exploring the set of models, namely MIMO and MISO. Table 6.1 assess the research hypotheses created in Section 1.3.

Table 6.1 Answering research guiding questions.

Research Hypothesis	Outcomes
H1: The proposed model is capable of making an accurate short-term and long-term weather prediction compared to an existing and well-established NWF model.	The proposed model with LSTM and TCN layers is classified into two regressions, namely MIMO and MISO. These regression models are compared with classic machine learning approaches such as SR and SVR (Please refer to Section 5.2.1.1.3 and Section 5.2.1.2.3). As per Section 5.2.2.1, the proposed model with LSTM layers has produced optimal performances for weather forecasting using historical weather data/WRF data. Section 5.2.2.2 compares the proposed model prediction with the WRF model prediction for the WRF validation dataset. The result shows that the proposed model has provided better results on eight occasions out of 10 parameters. The error rates of the remaining two parameters are negligible. Overall, as per information in Figure 5.6, the proposed model predicts an accurate short-term (i.e. 3 hours) weather forecast compared to the existing well-recognised WRF model. Consequently, the proposed LSTM model is used for long-term weather forecasting. and the results are compared with the well-established WRF model for verification purposes. As per Section 5.2.3.3, the results show that the proposed model can be used for the long-term weather forecasting and is capable of producing better predictions up to 12 hours as a whole compared to the state-of-art WRF model. This concludes that the research hypothesis H1 is valid and successful.
H2: Compared to the existing NWP model, the proposed model has less computational complexity.	As discussed in Section 5.2.4, the data-driven computer modelling systems can be utilised to reduce the computational power of the NWP systems. The proposed model could run on a standalone computer while NWP models usually run in large grids of supercomputers. It is also observed that the WRF model takes 9 hours and 24 minutes to get 48-hour weather forecast covering the entire UK. The proposed model can produce a similar forecast within 2 minutes and 12 seconds. Moreover, the WRF model needs a larger number of local and global weather parameters to make a prediction and it causes an increase of the computational complexity in the NWP model. The proposed model further reduces the computational complexity by reducing the required ten parameters. This concludes that the research hypothesis H2 is valid and successful.
H3: The proposed model can be applied for a real-life scenario, that is a fine-	Similar to assessing the hypothesis H1, the proposed models are classified into two regressions. These regression models are compared with the classic machine learning approaches (please refer to Section 5.3.1.1.3 and Section 5.3.1.2.3). As per Section 5.3.2, the proposed model with TCN layers has produced the optimal performance for weather forecasting done using local weather station data. Besides, the proposed deep learning with TCN layer model predictions for the validation dataset is compared with the ground

grained weather forecasting model for a community of users in a specific geographical area, such as a farm.	truth. The results show that the proposed model is producing effective results and can be utilised for short-term weather forecasting for a selected geographical area. As per Section 5.3.3, the proposed weather forecasting model is used for long-term predictions using the validation dataset. Also, the results are compared with the ground truth. The results show that some parameters produce forecasting results with improved accuracy for up to 24 hours (Rain and Rainnc) while others can produce accurate forecasts up to 9 to 12 hours. Overall, it ensures that the proposed model can be used for long-term weather forecasting and it can produce slightly accurate results up to 12 hours. This concludes that the research hypothesis H3 is valid and successful.

6.2 Limitations and Recommendations

The first phase of this research is carried out using ten different surface weather parameters. An increased number of inputs would probably lead to enhanced results. For example, there are 36 different pressure levels defined in the WRF model (Skamarock et al., 2008). Only the value of pressure at two meters is considered within this research. It is possible to increase the accuracy of the results by introducing all 36 possible pressure levels to the proposed model. However, this will increase the model complexity requiring a large number of parameters to estimate. Furthermore, weather data from January to May are utilised for training the deep model. An increase in the size of the training dataset could help in improving the results of a deep learning network (Gulli and Pal, 2017; Jozefowicz et al., 2015).

Besides, the MIMO approach is utilised within the first phase of this research to predict the weather data. Table 5.13 and Figure 5.4 show that the MISO approach produces better MSE values compared to the MIMO. Therefore, there is a huge potential the MISO approach will increase the accuracy of the results; even though this method is less efficient compared to the MIMO. Moreover, the Bi-LSTM yields high accuracy, long-term prediction compared to the LSTM as presented in Table 5.16 and Figure 5.11. Therefore, more accurate results could be generated by the Bi-LSTM; even if this method is not efficient due to the high time-consumption.

In Phase 2 of the research, data of only 93 days are used to train the proposed model. Increasing the size of the training data sample could result in better prediction in ANN (Gulli and Pal, 2017; Jozefowicz et al., 2015). The created model can be fine-tuned with more data to get better performance. Furthermore, Raspberry Pi weather stations capable

of attaching many sensors to measure the atmospheric parameters are used in this research. There could be a possibility to improve the prediction by introducing some more weather parameters which support the Raspberry Pi weatherboard such as soil temperature, soil moisture, snow, solar radiation balance, and pressure at different levels.

In addition to the above recommendations, there are some limitations to this research as well. The training process of the deep model is complex as there are several configurations and controls to manage and the time consumption is increased for training depending on the size of the dataset. There are some controls kept constant during the training process in both TCN and LSTM. Besides, there are some control experiments with limited possibilities (For example, Adam and SGD are the only optimisers' experiments with deep learning LSTM models among many alternatives). There could be a possibility to improve the prediction results if the experiment uses constant controls as variables or controls with many different options. Again, each of these experiments consumes comparatively a long time for completion. As a solution, there could be a possibility to use high specification hardware resources to train the models (For instance, 24 GB GPU memory with 16 core CPU and 32 GB RAM). On the contrary, these training experiments are carried out at once and the trained model is used for prediction. The prediction process is not complex nor time-consuming. Therefore, it is fairly unsought to only spend excessively on high specific hardware for the training process.

The other main limitation is that the practical difficulties in selecting appropriate parameters for weather prediction. As there are many weather forecasting parameters (i.e. more than 257), it is not practically possible to classify in such a way as to identify a subset of parameters for the machine learning models. It is practically impossible to calculate the impact of removing or fixing a subset of input parameters on the generated model output. The other limitation is that the deep learning models prefer larger datasets to train models targeting accurate prediction (Dalto et al., 2015; Hochreiter and Schmidhuber, 1997). The training complexity is increased when increasing the size of the training dataset.

6.3 Reflection and future work

According to the results of this research, it is apparent that the proposed deep neural network is able to produce accurate and fine-grained medium-range weather forecasting results. This study has hugely contributed to the knowledge by accomplishing the main contribution and other contributions as described in Section 1.5. Furthermore, a wider set

of users who rely on favourable weather conditions could get the advantage of the model such as farms, places of interest, schools, outdoor sports centres, and larger construction sites.

This research initially targeted on developing a fine-grained weather forecasting model. However, there could be a different way to carry out this research to achieve both regional and fine-grained forecasting by connecting data from different weather stations in different geographical areas. The selected weather station data can be used for fine-grained forecast while a combination of different weather stations data could be used to regional forecast.

Besides, the WRF model produces better forecasting results on a very long-term basis compared to the deep learning model. The reason is that the WRF model is combined with many other climate models (Hernández-Ceballos et al., 2014; Liu et al., 2012; NCAR/UCAR, 2019) and data are globally entered as input into the system (Commerce, 2015; NCAR/UCAR, 2019). The proposed lightweight fine-grained weather forecasting model could be combined with existing climate model targeting a more accurate and long-term weather forecast (i.e. over 12 hours). In the meantime, it is praiseworthy to consider combining the local weather station data to regional weather data. This could increase the accuracy of the proposed model.

Therefore, the future studies of this research include; combining different local weather station data for a regional level forecast, combining the existing climate models to the proposed forecasting model, and combining local and regional weather forecast data for an accurate and fine-grained weather model.

7 References

Abadi, M., Barham, P., Chen, J., Chen, Z., Davis, A., Dean, J., Devin, M., Ghemawat, S., Irving, G., Isard, M., Kudlur, M., Levenberg, J., Monga, R., Moore, S., Murray, D.G., Steiner, B., Tucker, P., Vasudevan, V., Warden, P., Wicke, M., Yu, Y., Zheng, X., 2016. TensorFlow: A System for Large-Scale Machine Learning. Presented at the 12th {USENIX} Symposium on Operating Systems Design and Implementation ({OSDI} 16), pp. 265–283.

Abdel-Aal, R.E., Elhadidy, M.A., 1995. Modeling and Forecasting the Daily Maximum Temperature Using Abductive Machine Learning. Wea. Forecasting 10, 310–325. https://doi.org/10.1175/1520-0434(1995)010<0310:MAFTDM>2.0.CO;2

Abhishek, K., Singh, M.P., Ghosh, S., Anand, A., 2012a. Weather Forecasting Model using Artificial Neural Network. Procedia Technology, 2nd International Conference on Computer, Communication, Control and Information Technology(C3IT-2012) on February 25 - 26, 2012 4, 311–318. https://doi.org/10.1016/j.protcy.2012.05.047

Abhishek, K., Singh, M.P., Ghosh, S., Anand, A., 2012b. Weather Forecasting Model using Artificial Neural Network. Procedia Technology, 2nd International Conference on Computer, Communication, Control and Information Technology(C3IT-2012) on February 25 - 26, 2012 4, 311–318. https://doi.org/10.1016/j.protcy.2012.05.047

Abuaqel, I., Alsadoun, F., Almulhim, M., Aljallal, M.A., Alghuraibi, M., Alzahrani, M., Alharby, A., Olatunji, S.O., 2017. Prediction models aided postoperative decision making based on neural network and support vector machines. 2017 International Conference on Informatics, Health & Technology (ICIHT) 1–7. https://doi.org/10.1109/ICIHT.2017.7899137

Ahmadi, A., Zargaran, Z., Mohebi, A., Taghavi, F., 2014. Hybrid model for weather forecasting using ensemble of neural networks and mutual information, in: 2014 IEEE Geoscience and Remote Sensing Symposium. Presented at the 2014 IEEE Geoscience and Remote Sensing Symposium, pp. 3774–3777. https://doi.org/10.1109/IGARSS.2014.6947305

Akram, M., El, C., 2016. Sequence to Sequence Weather Forecasting with Long Short-Term Memory Recurrent Neural Networks. International Journal of Computer Applications 143, 7–11. https://doi.org/10.5120/ijca2016910497

Althelaya, K.A., El-Alfy, E.M., Mohammed, S., 2018. Evaluation of bidirectional LSTM for short-and long-term stock market prediction, in: 2018 9th International Conference on Information and Communication Systems (ICICS). Presented at the 2018 9th International Conference on Information and Communication Systems (ICICS), pp. 151–156. https://doi.org/10.1109/IACS.2018.8355458

Anderberg, J., 2015. How to Use a Barometer. The Art of Manliness. URL https://www.artofmanliness.com/articles/fair-or-foul-how-to-use-a-barometer/ (accessed 7.23.19).

Asif Khan, M., Naveed, T., Yagoub, E., Zhu, G., 2018. Bidirectional Long Short-Term Memory (BILSTM) with Conditional Random Fields (CRF) for Knowledge Named Entity Recognition in Online Judges (OJS). International Journal on Natural Language Computing 7, 01–08. https://doi.org/10.5121/ijnlc.2018.7401

Aufranc, J.-L., 2019. NVIDIA Introduces $99 Jetson Nano Developer Kit. CNX Software - Embedded Systems News. URL https://www.cnx-software.com/2019/03/19/nvidia-jetson-nano-developer-kit/ (accessed 10.19.19).

Ba, J., Frey, B., 2013. Adaptive dropout for training deep neural networks, in: Burges, C.J.C., Bottou, L., Welling, M., Ghahramani, Z., Weinberger, K.Q. (Eds.), Advances in Neural Information Processing Systems 26. Curran Associates, Inc., pp. 3084–3092.

Baboo, S.S., Shereef, I.K., 2010a. An Efficient Weather Forecasting System using Artificial Neural Network. International Journal of Environmental Science and Development 321–326. https://doi.org/10.7763/IJESD.2010.V1.63

Baboo, S.S., Shereef, I.K., 2010b. An Efficient Weather Forecasting System using Artificial Neural Network. International Journal of Environmental Science and Development 321–326. https://doi.org/10.7763/IJESD.2010.V1.63

Bai, S., Kolter, J.Z., Koltun, V., 2018. An Empirical Evaluation of Generic Convolutional and Recurrent Networks for Sequence Modeling. arXiv:1803.01271 [cs].

Baigorria, G.A., Jones, J.W., Shin, D.-W., Mishra, A., O'Brien, J.J., 2007. Assessing uncertainties in crop model simulations using daily bias-corrected Regional Circulation Model outputs. Climate Research 34, 211–222. https://doi.org/10.3354/cr00703

Bakharia, A., 2016. SVM Parameter Tuning in Scikit Learn using GridSearchCV. Medium. URL https://medium.com/@aneesha/svm-parameter-tuning-in-scikit-learn-using-gridsearchcv-2413c02125a0 (accessed 2.22.19).

Balci, O., 1994. Principles of simulation model validation, verification, and testing.

Basak, D., Pal, S., Patranabis, D., 2007. Support vector regression. Neural Information Processing-Letters and Reviews 11, 203–224.

Basheer, I.A., Hajmeer, M., 2000. Artificial neural networks: fundamentals, computing, design, and application. Journal of Microbiological Methods, Neural Computting in Micrbiology 43, 3–31. https://doi.org/10.1016/S0167-7012(00)00201-3

Bauer, P., Thorpe, A., Brunet, G., 2015. The quiet revolution of numerical weather prediction. Nature 525, 47–55. https://doi.org/10.1038/nature14956

Behera, A., Keidel, A., Debnath, B., 2018. Context-driven Multi-stream LSTM (M-LSTM) for Recognizing Fine-Grained Activity of Drivers. Pattern Recognition 16.

Bendre, M., Thool, R., Thool, V., 2015. Big data in precision agriculture: Weather forecasting for future farming. Presented at the 2015 1st International Conference on Next Generation Computing Technologies (NGCT), IEEE, pp. 744–750.

Benedetti, A., Morcrette, J., Boucher, O., Dethof, A., Engelen, R., Fisher, M., Flentje, H., Huneeus, N., Jones, L., Kaiser, J., 2009. Aerosol analysis and forecast in the European centre for medium-range weather forecasts integrated forecast system: 2. Data assimilation. Journal of Geophysical Research: Atmospheres 114.

Bernardo, J., Berger, J., Dawid, A., Smith, A., 1998. Regression and classification using Gaussian process priors. Bayesian statistics 6, 475.

Bhattacharyya, I., 2018. Support Vector Regression Or SVR. Coinmonks. URL https://medium.com/coinmonks/support-vector-regression-or-svr-8eb3acf6d0ff (accessed 2.22.19).
Bifet, A., Gavaldà, R., Holmes, G., Pfahringer, B., 2018. Machine learning for data streams: with practical examples in MOA. MIT Press.
Bishop, C.M., 2006. Pattern Recognition and Machine Learning. Springer.
Blacker, C., 2019. Precision Decisions | Driving Farming Forwards [WWW Document]. URL http://www.precisiondecisions.co.uk/ (accessed 7.25.19).
Breuel, T.M., 2015. Benchmarking of LSTM Networks. arXiv:1508.02774 [cs].
Britz, D., 2015. Understanding convolutional neural networks for NLP. URL: http://www. wildml. com/2015/11/understanding-convolutional-neuralnetworks-for-nlp/(visited on 11/07/2015).
Brownlee, J., 2019. Understand the Impact of Learning Rate on Neural Network Performance. Machine Learning Mastery. URL https://machinelearningmastery.com/understand-the-dynamics-of-learning-rate-on-deep-learning-neural-networks/ (accessed 7.31.19).
Brownlee, J., 2017. Difference Between Classification and Regression in Machine Learning. Machine Learning Mastery. URL https://machinelearningmastery.com/classification-versus-regression-in-machine-learning/ (accessed 10.28.19).
Brownlee, J., 2016. Supervised and Unsupervised Machine Learning Algorithms. Machine Learning Mastery. URL https://machinelearningmastery.com/supervised-and-unsupervised-machine-learning-algorithms/ (accessed 10.28.19).
Cai Ximing, Hejazi Mohamad I., Wang Dingbao, 2011. Value of Probabilistic Weather Forecasts: Assessment by Real-Time Optimization of Irrigation Scheduling. Journal of Water Resources Planning and Management 137, 391–403. https://doi.org/10.1061/(ASCE)WR.1943-5452.0000126
Calanca, P., Semenov, M.A., 2013. Local-scale climate scenarios for impact studies and risk assessments: integration of early 21st century ENSEMBLES projections into the ELPIS database. Theor Appl Climatol 113, 445–455. https://doi.org/10.1007/s00704-012-0799-3
Caruana, R., Niculescu-Mizil, A., 2006. An Empirical Comparison of Supervised Learning Algorithms, in: Proceedings of the 23rd International Conference on Machine Learning, ICML '06. ACM, New York, NY, USA, pp. 161–168. https://doi.org/10.1145/1143844.1143865
Cats, G., Wolters, L., 1996. The Hirlam project [meteorology]. IEEE Computational Science and Engineering 3, 4–7.
Chang, C.-C., Lin, C.-J., 2011. LIBSVM: A Library for Support Vector Machines. ACM Trans. Intell. Syst. Technol. 2, 27:1–27:27. https://doi.org/10.1145/1961189.1961199
CHANG, F.-J., CHIANG, Y.-M., CHANG, L.-C., 2007. Multi-step-ahead neural networks for flood forecasting. Hydrological Sciences Journal 52, 114–130. https://doi.org/10.1623/hysj.52.1.114
Charu, C., 2019. Neural Networks and Deep Learning: A Textbook.
Chen, P., 2018. Time Series Forecasting : Temporal Convolutional Networks vs. AutoML XGBoost Regression. [WWW Document]. Medium. URL https://medium.com/@peijin/time-series-forecasting-temporal-convolutional-networks-vs-automl-xgboost-regression-2e4b31eded6b (accessed 7.19.19).
Chin, W.-S., Zhuang, Y., Juan, Y.-C., Lin, C.-J., 2015. A Learning-Rate Schedule for Stochastic Gradient Methods to Matrix Factorization, in: Cao, T., Lim, E.-P.,

Zhou, Z.-H., Ho, T.-B., Cheung, D., Motoda, H. (Eds.), Advances in Knowledge Discovery and Data Mining, Lecture Notes in Computer Science. Springer International Publishing, pp. 442–455.
Chin-Chia Hsu, Chih-Hung Wu, Shih-Chien Chen, Kang-Lin Peng, 2006. Dynamically Optimizing Parameters in Support Vector Regression: An Application of Electricity Load Forecasting, in: Proceedings of the 39th Annual Hawaii International Conference on System Sciences (HICSS'06). Presented at the Proceedings of the 39th Annual Hawaii International Conference on System Sciences (HICSS'06), pp. 30c–30c. https://doi.org/10.1109/HICSS.2006.132
Chniti, G., Bakir, H., Zaher, H., 2017. E-commerce Time Series Forecasting Using LSTM Neural Network and Support Vector Regression, in: Proceedings of the International Conference on Big Data and Internet of Thing, BDIOT2017. ACM, New York, NY, USA, pp. 80–84. https://doi.org/10.1145/3175684.3175695
Choi, T., Hui, C., Yu, Y., 2011. Intelligent time series fast forecasting for fashion sales: A research agenda, in: 2011 International Conference on Machine Learning and Cybernetics. Presented at the 2011 International Conference on Machine Learning and Cybernetics, pp. 1010–1014. https://doi.org/10.1109/ICMLC.2011.6016870
Chung, J., Gulcehre, C., Cho, K., Bengio, Y., 2014. Empirical Evaluation of Gated Recurrent Neural Networks on Sequence Modeling. arXiv:1412.3555 [cs].
Commerce, N.C. for E.P.W.S.S.D. of, 2015. NCEP GFS 0.25 Degree Global Forecast Grids Historical Archive. https://doi.org/10.5065/D65D8PWK
Cotton, W.R., Pielke Sr, R., Walko, R., Liston, G., Tremback, C., Jiang, H., McAnelly, R., Harrington, J.Y., Nicholls, M., Carrio, G., 2003. RAMS 2001: Current status and future directions. Meteorology and Atmospheric Physics 82, 5–29.
Cullen, M., 1993. The unified forecast/climate model. Meteorological Magazine 122, 81–94.
Czimber, K., Gálos, B., 2016. A new decision support system to analyse the impacts of climate change on the Hungarian forestry and agricultural sectors. Scandinavian Journal of Forest Research 31, 664–673.
Dalto, M., Matuško, J., Vašak, M., 2015. Deep neural networks for ultra-short-term wind forecasting, in: 2015 IEEE International Conference on Industrial Technology (ICIT). Presented at the 2015 IEEE International Conference on Industrial Technology (ICIT), pp. 1657–1663. https://doi.org/10.1109/ICIT.2015.7125335
De Wit, M., Crookes, D.J., 2013. Improved decision-making on irrigation farming in arid zones using a system dynamics model. South African Journal of Science 109, 1–8.
Deng, Y., Jia, H., Li, P., Tong, X., Qiu, X., Li, F., 2019. A Deep Learning Methodology Based on Bidirectional Gated Recurrent Unit for Wind Power Prediction. Presented at the 2019 14th IEEE Conference on Industrial Electronics and Applications (ICIEA), IEEE, pp. 591–595.
Deshpande, A., 2019. A Beginner's Guide To Understanding Convolutional Neural Networks Part 2 [WWW Document]. URL https://adeshpande3.github.io/A-Beginner%27s-Guide-To-Understanding-Convolutional-Neural-Networks-Part-2/ (accessed 8.1.19).
Dethloff, K., Abegg, C., Rinke, A., Hebestadt, I., Romanov, V.F., 2001. Sensitivity of Arctic climate simulations to different boundary-layer parameterizations in a regional climate model. Tellus A 53, 1–26. https://doi.org/10.1034/j.1600-0870.2001.01073.x

Di, Z., Duan, Q., Gong, W., Wang, C., Gan, Y., Quan, J., Li, J., Miao, C., Ye, A., Tong, C., 2015. Assessing WRF model parameter sensitivity: A case study with 5 day summer precipitation forecasting in the Greater Beijing Area. Geophysical Research Letters 42, 579–587. https://doi.org/10.1002/2014GL061623

Díaz, S., Kattge, J., Cornelissen, J.H., Wright, I.J., Lavorel, S., Dray, S., Reu, B., Kleyer, M., Wirth, C., Prentice, I.C., 2016. The global spectrum of plant form and function. Nature 529, 167–171.

Donahue, J., Hendricks, L.A., Rohrbach, M., Venugopalan, S., Guadarrama, S., Saenko, K., Darrell, T., 2014. Long-term Recurrent Convolutional Networks for Visual Recognition and Description. arXiv:1411.4389 [cs].

Drucker, H., Burges, C.J.C., Kaufman, L., Smola, A., Vapnik, V., 1997. (PDF) Support vector regression machines [WWW Document]. ResearchGate. URL https://www.researchgate.net/publication/309185766_Support_vector_regression_machines (accessed 2.22.19).

Duan, Y., Lv, Y., Wang, F.-Y., 2016. Travel time prediction with LSTM neural network. Presented at the 2016 IEEE 19th International Conference on Intelligent Transportation Systems (ITSC), IEEE, pp. 1053–1058.

Earth Science [WWW Document], 2018. URL http://geometocea.res.in/home/online-links/online-data-links (accessed 2.21.19).

Educba, 2018. Machine Learning vs Neural Network | Best 5 Useful Comparison. EDUCBA. URL https://www.educba.com/machine-learning-vs-neural-network/ (accessed 10.11.19).

Elman, J.L., 1990. Finding Structure in Time. Cognitive Science 14, 179–211. https://doi.org/10.1207/s15516709cog1402_1

Elsner, J.B., Tsonis, A.A., 1992. Nonlinear Prediction, Chaos, and Noise. Bull. Amer. Meteor. Soc. 73, 49–60. https://doi.org/10.1175/1520-0477(1992)073<0049:NPCAN>2.0.CO;2

Esteva, A., Robicquet, A., Ramsundar, B., Kuleshov, V., DePristo, M., Chou, K., Cui, C., Corrado, G., Thrun, S., Dean, J., 2019. A guide to deep learning in healthcare. Nature medicine 25, 24–29.

Fan, Y., Qian, Y., Xie, F.-L., Soong, F.K., 2014. TTS synthesis with bidirectional LSTM based recurrent neural networks, in: INTERSPEECH.

Faroux, S., Masson, V., Roujean, J., 2007. ECOCLIMAP-II: a climatologic global data base of ecosystems and land surface parameters at 1 km based on the analysis of time series of VEGETATION data, in: 2007 IEEE International Geoscience and Remote Sensing Symposium. Presented at the 2007 IEEE International Geoscience and Remote Sensing Symposium, pp. 1008–1011. https://doi.org/10.1109/IGARSS.2007.4422971

Fente, D.N., Singh, D.K., 2018. Weather Forecasting Using Artificial Neural Network, in: 2018 Second International Conference on Inventive Communication and Computational Technologies (ICICCT). Presented at the 2018 Second International Conference on Inventive Communication and Computational Technologies (ICICCT), pp. 1757–1761. https://doi.org/10.1109/ICICCT.2018.8473167

Fernández-Quiruelas, V., Fernández, J., Cofiño, A.S., Blanco, C., García-Díez, M., Magariño, M., Fita, L., Gutiérrez, J.M., 2015. WRF4G: WRF experiment management made simple. Geoscientific Model Development Discussions 8, 6551–6582. https://doi.org/10.5194/gmdd-8-6551-2015

Frank, R.J., Davey, N., Hunt, S.P., 2001. Time Series Prediction and Neural Networks. Journal of Intelligent and Robotic Systems 31, 91–103. https://doi.org/10.1023/A:1012074215150

Gallus, W.A., Segal, M., 2004. Does Increased Predicted Warm-Season Rainfall Indicate Enhanced Likelihood of Rain Occurrence? Wea. Forecasting 19, 1127–1135. https://doi.org/10.1175/820.1
Gers, F.A., Schmidhuber, J., Cummins, F., 1999. Learning to forget: continual prediction with LSTM 850–855. https://doi.org/10.1049/cp:19991218
Glahn, H.R., Lowry, D.A., 1972. The Use of Model Output Statistics (MOS) in Objective Weather Forecasting. J. Appl. Meteor. 11, 1203–1211. https://doi.org/10.1175/1520-0450(1972)011<1203:TUOMOS>2.0.CO;2
Gneiting, T., Raftery, A.E., 2005. Weather Forecasting with Ensemble Methods. Science 310, 248–249. https://doi.org/10.1126/science.1115255
Gómez, I., Ronda, R.J., Caselles, V., Estrela, M.J., 2016. Implementation of non-local boundary layer schemes in the Regional Atmospheric Modeling System and its impact on simulated mesoscale circulations. Atmospheric Research 180, 24–41.
Goodfellow, I., Bengio, Y., Courville, A., 2016. Deep learning. MIT press.
Goodrich, B., Arel, I., 2014. Unsupervised neuron selection for mitigating catastrophic forgetting in neural networks, in: 2014 IEEE 57th International Midwest Symposium on Circuits and Systems (MWSCAS). Presented at the 2014 IEEE 57th International Midwest Symposium on Circuits and Systems (MWSCAS), pp. 997–1000. https://doi.org/10.1109/MWSCAS.2014.6908585
Google Trends [WWW Document], n.d. . Google Trends. URL https://trends.google.com/trends/explore?date=2009-09-11%202019-10-11&q=deep%20learning (accessed 10.11.19).
Gordon, C.T., Stern, W.F., 1982. A Description of the GFDL Global Spectral Model. Mon. Wea. Rev. 110, 625–644. https://doi.org/10.1175/1520-0493(1982)110<0625:ADOTGG>2.0.CO;2
Gounaris, G., Vlissidis, A., Michail, K., 2010. WEATHER STATIONS DISTRIBUTED MODEL FOR DATA PROCESS AND ON-LINE INTERNET PRESENTATION 8.
Goves, C., North, R., Johnston, R., Fletcher, G., 2016. Short Term Traffic Prediction on the UK Motorway Network Using Neural Networks. Transportation Research Procedia, Towards future innovative transport: visions, trends and methods 43rd European Transport Conference Selected Proceedings 13, 184–195. https://doi.org/10.1016/j.trpro.2016.05.019
Graves, A., 2012. Supervised Sequence Labelling, in: Graves, A. (Ed.), Supervised Sequence Labelling with Recurrent Neural Networks, Studies in Computational Intelligence. Springer Berlin Heidelberg, Berlin, Heidelberg, pp. 5–13. https://doi.org/10.1007/978-3-642-24797-2_2
Graves, A., Fernández, S., Gomez, F., Schmidhuber, J., 2006. Connectionist Temporal Classification: Labelling Unsegmented Sequence Data with Recurrent Neural Networks, in: Proceedings of the 23rd International Conference on Machine Learning, ICML '06. ACM, New York, NY, USA, pp. 369–376. https://doi.org/10.1145/1143844.1143891
Graves, A., Jaitly, N., Mohamed, A., 2013. Hybrid speech recognition with Deep Bidirectional LSTM, in: 2013 IEEE Workshop on Automatic Speech Recognition and Understanding. Presented at the 2013 IEEE Workshop on Automatic Speech Recognition and Understanding, pp. 273–278. https://doi.org/10.1109/ASRU.2013.6707742
Graves, A., Schmidhuber, J., 2005. Framewise phoneme classification with bidirectional LSTM and other neural network architectures. Neural Networks, IJCNN 2005 18, 602–610. https://doi.org/10.1016/j.neunet.2005.06.042

Greff, K., Srivastava, R.K., Koutník, J., Steunebrink, B.R., Schmidhuber, J., 2017. LSTM: A Search Space Odyssey. IEEE Transactions on Neural Networks and Learning Systems 28, 2222–2232. https://doi.org/10.1109/TNNLS.2016.2582924

Gulli, A., Pal, S., 2017. Deep Learning with Keras. Packt Publishing Ltd.

Haimberger, L., Tavolato, C., Sperka, S., 2008. Toward Elimination of the Warm Bias in Historic Radiosonde Temperature Records—Some New Results from a Comprehensive Intercomparison of Upper-Air Data. J. Climate 21, 4587–4606. https://doi.org/10.1175/2008JCLI1929.1

Hamill, T.M., Whitaker, J.S., Kleist, D.T., Fiorino, M., Benjamin, S.G., 2011. Predictions of 2010's Tropical Cyclones Using the GFS and Ensemble-Based Data Assimilation Methods. Mon. Wea. Rev. 139, 3243–3247. https://doi.org/10.1175/MWR-D-11-00079.1

Hands Free Hectare [WWW Document], 2018. URL http://www.precisiondecisions.co.uk/hands-free-hectare-brings-in-first-robot-wheat-harvest-farmers-weekly-24-08-18 (accessed 7.25.19).

Harrington, P., 2012. Machine learning in action. Manning Publications Co.

Hayati, M., Mohebi, Z., 2007. Application of Artificial Neural Networks for Temperature Forecasting. International Journal of Electrical and Computer Engineering 1, 5.

Heilig, A., 2009. The search for and location of inhomogeneities in seasonal snowpacks utilizing ground-penetrating radar technology.

Hernández, E., Sanchez-Anguix, V., Julian, V., Palanca, J., Duque, N., 2016. Rainfall prediction: A deep learning approach. Presented at the International Conference on Hybrid Artificial Intelligence Systems, Springer, pp. 151–162.

Hernández-Ceballos, M.A., Skjøth, C.A., García-Mozo, H., Bolívar, J.P., Galán, C., 2014. Improvement in the accuracy of back trajectories using WRF to identify pollen sources in southern Iberian Peninsula. Int J Biometeorol 58, 2031–2043. https://doi.org/10.1007/s00484-014-0804-x

Hewage, P., Behera, A., Trovati, M., Pereira, E., 2019. Long-Short Term Memory for an Effective Short-Term Weather Forecasting Model Using Surface Weather Data, in: MacIntyre, J., Maglogiannis, I., Iliadis, L., Pimenidis, E. (Eds.), Artificial Intelligence Applications and Innovations, IFIP Advances in Information and Communication Technology. Springer International Publishing, pp. 382–390.

Hewage, P., Behera, A., Trovati, M., Pereira, E., Ghahremani, M., Palmieri, F., Liu, Y., 2020. Temporal convolutional neural (TCN) network for an effective weather forecasting using time-series data from the local weather station. Soft Computing 1–30.

Ho, C.K., Stephenson, D.B., Collins, M., Ferro, C.A.T., Brown, S.J., 2012. Calibration Strategies: A Source of Additional Uncertainty in Climate Change Projections. Bulletin of the American Meteorological Society 93, 21–26. https://doi.org/10.1175/2011BAMS3110.1

Hochreiter, S., 1998. The vanishing gradient problem during learning recurrent neural nets and problem solutions. International Journal of Uncertainty, Fuzziness and Knowledge-Based Systems 6, 107–116.

Hochreiter, S., Schmidhuber, J., 2006. Long Short-Term Memory. https://doi.org/10.1162/neco.1997.9.8.1735

Hochreiter, S., Schmidhuber, J., 1997. Long Short-Term Memory. Neural Computation 9, 1735–1780. https://doi.org/10.1162/neco.1997.9.8.1735

Hossain, M., Rekabdar, B., Louis, S.J., Dascalu, S., 2015. Forecasting the weather of Nevada: A deep learning approach, in: 2015 International Joint Conference on Neural Networks (IJCNN). Presented at the 2015 International Joint Conference on Neural Networks (IJCNN), pp. 1–6. https://doi.org/10.1109/IJCNN.2015.7280812

Innocenti, M.E., Johnson, A., Markidis, S., Amaya, J., Deca, J., Olshevsky, V., Lapenta, G., 2017. Progress towards physics-based space weather forecasting with exascale computing. Advances in Engineering Software 111, 3–17.

Jain, P., 2018. Difference between Supervised and Unsupervised Learning. GeeksforGeeks. URL https://www.geeksforgeeks.org/difference-between-supervised-and-unsupervised-learning/ (accessed 10.11.19).

Jaruszewicz, M., Mandziuk, J., 2002. Application of PCA method to weather prediction task, in: Proceedings of the 9th International Conference on Neural Information Processing, 2002. ICONIP '02. Presented at the Proceedings of the 9th International Conference on Neural Information Processing, 2002. ICONIP '02., pp. 2359–2363 vol.5. https://doi.org/10.1109/ICONIP.2002.1201916

Ji, D., Dong, W., Hong, T., Dai, T., Zheng, Z., Yang, S., Zhu, X., 2018. Assessing Parameter Importance of the Weather Research and Forecasting Model Based On Global Sensitivity Analysis Methods. Journal of Geophysical Research: Atmospheres 123, 4443–4460. https://doi.org/10.1002/2017JD027348

Jincai, D., Jianhua, D., Yamin, C., Fuquan, H., Xinzhang, T., 1996. Helicity as a Method for Forecasting Severe Weather Events. Adv. Atmos. Sci. 13, 533–538. https://doi.org/10.1007/BF03342043

Joho, M., Lambert, R.H., Mathis, H., 2001. Elementary cost functions for blind separation of non-stationary source signals. Presented at the 2001 IEEE International Conference on Acoustics, Speech, and Signal Processing. Proceedings (Cat. No. 01CH37221), IEEE, pp. 2793–2796.

Jozefowicz, R., Zaremba, W., Sutskever, I., 2015. An Empirical Exploration of Recurrent Network Architectures. In International Conference on Machine Learning 2342–2350.

Kalchbrenner, N., Grefenstette, E., Blunsom, P., 2014. A convolutional neural network for modelling sentences. arXiv preprint arXiv:1404.2188.

Kapoor, A., 2019. Deep Learning vs. Machine Learning: A Simple Explanation - By Ajay Kapoor [WWW Document]. URL https://hackernoon.com/deep-learning-vs-machine-learning-a-simple-explanation-47405b3eef08 (accessed 10.28.19).

Kavitha, S., Varuna, S., Ramya, R., 2016. A comparative analysis on linear regression and support vector regression, in: 2016 Online International Conference on Green Engineering and Technologies (IC-GET). Presented at the 2016 Online International Conference on Green Engineering and Technologies (IC-GET), pp. 1–5. https://doi.org/10.1109/GET.2016.7916627

Kelly, B.T., Pruitt, S., Su, Y., 2019. Characteristics are covariances: A unified model of risk and return. Journal of Financial Economics 134, 501–524.

Kenkel, P.L., Norris, P.E., 1995. Agricultural Producers' Willingness to Pay for Real-Time Mesoscale Weather Information. Journal of Agricultural and Resource Economics 20, 356–372.

Keras, 2019. Home - Keras Documentation [WWW Document]. URL https://keras.io/ (accessed 1.28.19).

Kim, T.S., Reiter, A., 2017. Interpretable 3D Human Action Analysis with Temporal Convolutional Networks. arXiv:1704.04516 [cs].

Kim, Y., 2014. Convolutional neural networks for sentence classification. arXiv preprint arXiv:1408.5882.

Klein, W.H., Glahn, H.R., 1974. forecasting local weather by means of model output statistics. Bull. Amer. Meteor. Soc. 55, 1217–1227. https://doi.org/10.1175/1520-0477(1974)055<1217:FLWBMO>2.0.CO;2
Knievel, J.C., Bryan, G.H., Hacker, J.P., 2007. Explicit Numerical Diffusion in the WRF Model. Mon. Wea. Rev. 135, 3808–3824. https://doi.org/10.1175/2007MWR2100.1
Korsholm, U.S., Baklanov, A., Gross, A., Mahura, A., Sass, B.H., Kaas, E., 2008. Online coupled chemical weather forecasting based on HIRLAM–overview and prospective of Enviro-HIRLAM. HIRLAM newsletter 54, 151–168.
Krizhevsky, A., Sutskever, I., Hinton, G.E., 2012. ImageNet Classification with Deep Convolutional Neural Networks, in: Pereira, F., Burges, C.J.C., Bottou, L., Weinberger, K.Q. (Eds.), Advances in Neural Information Processing Systems 25. Curran Associates, Inc., pp. 1097–1105.
Kruizinga, S., Murphy, A.H., 1983. Use of an Analogue Procedure to Formulate Objective Probabilistic Temperature Forecasts in The Netherlands. Mon. Wea. Rev. 111, 2244–2254. https://doi.org/10.1175/1520-0493(1983)111<2244:UOAAPT>2.0.CO;2
Kuo, N.I.H., Harandi, M.T., Suominen, H., Fourrier, N., Walder, C., Ferraro, G., 2018. DecayNet: A Study on the Cell States of Long Short Term Memories.
Lahoz, W., Khattatov, B., Ménard, R., 2010. Data Assimilation and Information, in: Lahoz, W., Khattatov, B., Menard, R. (Eds.), Data Assimilation: Making Sense of Observations. Springer Berlin Heidelberg, Berlin, Heidelberg, pp. 3–12. https://doi.org/10.1007/978-3-540-74703-1_1
Lau, S., 2017. Learning Rate Schedules and Adaptive Learning Rate Methods for Deep Learning [WWW Document]. Towards Data Science. URL https://towardsdatascience.com/learning-rate-schedules-and-adaptive-learning-rate-methods-for-deep-learning-2c8f433990d1 (accessed 1.28.19).
Le, Q.V., 2015. A tutorial on deep learning part 2: Autoencoders, convolutional neural networks and recurrent neural networks. Google Brain 1–20.
Lea, C., Flynn, M.D., Vidal, R., Reiter, A., Hager, G.D., 2017. Temporal Convolutional Networks for Action Segmentation and Detection, in: 2017 IEEE Conference on Computer Vision and Pattern Recognition (CVPR). Presented at the 2017 IEEE Conference on Computer Vision and Pattern Recognition (CVPR), IEEE, Honolulu, HI, pp. 1003–1012. https://doi.org/10.1109/CVPR.2017.113
LeBlanc, M., Tibshirani, R., 1996. Combining estimates in regression and classification. Journal of the American Statistical Association 91, 1641–1650.
LeCun, Y., Bengio, Y., Hinton, G., 2015. Deep learning. nature 521, 436–444.
Li, J., Liao, W., Choudhary, A., Ross, R., Thakur, R., Gropp, W., Latham, R., 2003. Parallel netCDF: A Scientific High-Performance I/O Interface. arXiv:cs/0306048.
Li, K., Liu, Y.S., 2005. A rough set based fuzzy neural network algorithm for weather prediction, in: 2005 International Conference on Machine Learning and Cybernetics. Presented at the 2005 International Conference on Machine Learning and Cybernetics, pp. 1888-1892 Vol. 3. https://doi.org/10.1109/ICMLC.2005.1527253
Li, Z., Zhou, F., Chen, F., Li, H., 2017. Meta-SGD: Learning to learn quickly for few-shot learning. arXiv preprint arXiv:1707.09835.
Libbrecht, M.W., Noble, W.S., 2015. Machine learning applications in genetics and genomics. Nature Reviews Genetics 16, 321–332. https://doi.org/10.1038/nrg3920

Lin, K., Lin, Q., Zhou, C., Yao, J., 2007. Time Series Prediction Based on Linear Regression and SVR, in: Third International Conference on Natural Computation (ICNC 2007). Presented at the Third International Conference on Natural Computation (ICNC 2007), pp. 688–691. https://doi.org/10.1109/ICNC.2007.780

Liu, J.N.K., Hu, Y., You, J.J., Chan, P.W., 2014. Deep Neural Network Based Feature Representation for Weather Forecasting. Proceedings on the International Conference on Artificial Intelligence (ICAI) 7.

Liu, M., Li, S., Shan, S., Chen, X., 2015. AU-inspired Deep Networks for Facial Expression Feature Learning. Neurocomputing 159, 126–136. https://doi.org/10.1016/j.neucom.2015.02.011

Liu, Z., Liu, S., Hu, F., Li, J., Ma, Y., Liu, H., 2012. A comparison study of the simulation accuracy between WRF and MM5 in simulating local atmospheric circulations over Greater Beijing. Sci. China Earth Sci. 55, 418–427. https://doi.org/10.1007/s11430-011-4310-2

Lynch, P., 2006. The emergence of numerical weather prediction: Richardson's dream. Cambridge Univ. Press, Cambridge.

Mahapatra, S., 2019. Why Deep Learning over Traditional Machine Learning? [WWW Document]. Medium. URL https://towardsdatascience.com/why-deep-learning-is-needed-over-traditional-machine-learning-1b6a99177063 (accessed 10.11.19).

Mandel, J., Beezley, J.D., Kochanski, A.K., 2011. Coupled atmosphere-wildland fire modeling with WRF-Fire. Geosci. Model Dev. 4, 591–610. https://doi.org/10.5194/gmd-4-591-2011

Mandic, D.P., Chambers, J., 2001. Recurrent neural networks for prediction: learning algorithms, architectures and stability. John Wiley & Sons, Inc.

Mandic, D.P., Chambers, J.A., 2000. On the choice of parameters of the cost function in nested modular RNN's. IEEE Transactions on Neural Networks 11, 315–322.

Maqsood, I., Khan, M.R., Abraham, A., 2002. Intelligent Weather Monitoring Systems Using Connectionist Models 10, 21.

Mass, C.F., Kuo, Y.-H., 1998. Regional Real-Time Numerical Weather Prediction: Current Status and Future Potential. Bull. Amer. Meteor. Soc. 79, 253–264. https://doi.org/10.1175/1520-0477(1998)079<0253:RRTNWP>2.0.CO;2

Mathur, S., Kumar, A., Ch, M., 2008. International Journal of Computational Intelligence - A Feature Based Neural Network Model for Weather Forecasting.

McCaffrey, B.J., 2014. How To Standardize Data for Neural Networks - [WWW Document]. Visual Studio Magazine. URL https://visualstudiomagazine.com/articles/2014/01/01/how-to-standardize-data-for-neural-networks.aspx (accessed 7.29.19).

McCREA, M., Barr, W.B., Guskiewicz, K., Randolph, C., Marshall, S.W., Cantu, R., Onate, J.A., Kelly, J.P., 2005. Standard regression-based methods for measuring recovery after sport-related concussion. Journal of the International Neuropsychological Society 11, 58–69. https://doi.org/10.1017/S1355617705050083

McDaniel, P., Papernot, N., Celik, Z.B., 2016. Machine Learning in Adversarial Settings. IEEE Security Privacy 14, 68–72. https://doi.org/10.1109/MSP.2016.51

Measure in-field variability from satellite [WWW Document], 2019. URL http://www.precisiondecisions.co.uk/agriculture/misat (accessed 7.25.19).

Met Office, 2019. How weather forecasts are created [WWW Document]. Met Office. URL https://www.metoffice.gov.uk/weather/learn-about/how-forecasts-are-made/_index_ (accessed 2.21.19).

Michalakes, J., Dudhia, J., Gill, D., Henderson, T., Klemp, J., Skamarock, W., Wang, W., 2005. The weather research and forecast model: software architecture and performance, in: Use of High Performance Computing in Meteorology. WORLD SCIENTIFIC, pp. 156–168. https://doi.org/10.1142/9789812701831_0012

Michie, D., Spiegelhalter, D.J., Taylor, C., 1994. Machine learning. Neural and Statistical Classification 13.

Mikolov, T., Karafiát, M., Burget, L., Černocký, J., Khudanpur, S., 2010. Recurrent neural network based language model. Presented at the Eleventh annual conference of the international speech communication association.

Mirocha, J.D., Lundquist, J.K., Kosović, B., 2010. Implementation of a Nonlinear Subfilter Turbulence Stress Model for Large-Eddy Simulation in the Advanced Research WRF Model. Mon. Wea. Rev. 138, 4212–4228. https://doi.org/10.1175/2010MWR3286.1

Mitchell, T.D., Carter, T.R., Jones, P.D., Hulme, M., New, M., 2014. A comprehensive set of high-resolution grids of monthly climate for Europe and the globe: the observed record (1901-2000) and 16 scenarios (2001-2100). 31.

Mittal, Y., Mittal, A., Bhateja, D., Parmaar, K., Mittal, V.K., 2015. Correlation among environmental parameters using an online Smart Weather Station System, in: 2015 Annual IEEE India Conference (INDICON). Presented at the 2015 Annual IEEE India Conference (INDICON), pp. 1–6. https://doi.org/10.1109/INDICON.2015.7443621

MOAWAD, A., 2019. The magic of LSTM neural networks [WWW Document]. Medium. URL https://medium.com/datathings/the-magic-of-lstm-neural-networks-6775e8b540cd (accessed 11.5.19).

Moeng, C.-H., Dudhia, J., Klemp, J., Sullivan, P., 2007. Examining Two-Way Grid Nesting for Large Eddy Simulation of the PBL Using the WRF Model. Mon. Wea. Rev. 135, 2295–2311. https://doi.org/10.1175/MWR3406.1

Moradi, B., Aghapour, M., Shirbandi, A., 2019. Compare of Machine Learning And Deep Learning Approaches for Human Activity Recognition (No. 2516–2314). EasyChair.

National Centers for Environmental Information, 2019. Global Forecast System (GFS) [WWW Document]. URL https://www.ncdc.noaa.gov/data-access/model-data/model-datasets/global-forcast-system-gfs (accessed 7.19.19).

Nayak, R., Patheja, P.S., Waoo, A.A., 2012. An artificial neural network model for weather forecasting in Bhopal, in: IEEE-International Conference On Advances In Engineering, Science And Management (ICAESM -2012). Presented at the IEEE-International Conference On Advances In Engineering, Science And Management (ICAESM -2012), pp. 747–749.

NCAR/UCAR, 2019. WRF Model Users Site [WWW Document]. URL http://www2.mmm.ucar.edu/wrf/users/ (accessed 1.21.19).

NCEI, 2019. Numerical Weather Prediction | National Centers for Environmental Information (NCEI) formerly known as National Climatic Data Center (NCDC) [WWW Document]. National Centers for Environmental Information. URL https://www.ncdc.noaa.gov/data-access/model-data/model-datasets/numerical-weather-prediction (accessed 2.21.19).

Ngiam, J., Khosla, A., Kim, M., Nam, J., Lee, H., Ng, A.Y., 2011. Multimodal deep learning. Presented at the Proceedings of the 28th international conference on machine learning (ICML-11), pp. 689–696.

Noaa, 2017. Reading GRIB Files [WWW Document]. URL http://www.cpc.ncep.noaa.gov/products/wesley/reading_grib.html (accessed 1.23.19).

Oana, L., Spataru, A., 2016. Use of Genetic Algorithms in Numerical Weather Prediction, in: 2016 18th International Symposium on Symbolic and Numeric Algorithms for Scientific Computing (SYNASC). Presented at the 2016 18th International Symposium on Symbolic and Numeric Algorithms for Scientific Computing (SYNASC), IEEE, Timisoara, Romania, pp. 456–461. https://doi.org/10.1109/SYNASC.2016.075

Ochiai, K., Suzuki, H., Shinozawa, K., Fujii, M., Sonehara, N., 1995. Snowfall and rainfall forecasting from weather radar images with artificial neural networks, in: Proceedings of ICNN'95 - International Conference on Neural Networks. Presented at the Proceedings of ICNN'95 - International Conference on Neural Networks, pp. 1182–1187 vol.2. https://doi.org/10.1109/ICNN.1995.487781

Oishi, S., Ikebuchi, S., Kojiri, T., 1998. Severe rainfall prediction method using artificial intelligence, in: SMC'98 Conference Proceedings. 1998 IEEE International Conference on Systems, Man, and Cybernetics (Cat. No.98CH36218). Presented at the SMC'98 Conference Proceedings. 1998 IEEE International Conference on Systems, Man, and Cybernetics (Cat. No.98CH36218), pp. 4820–4825 vol.5. https://doi.org/10.1109/ICSMC.1998.727615

Omidvar, O., Elliott, D.L., 1997. Neural Systems for Control. Elsevier.

Ozdogan, B., Gacar, A., Aktas, H., 2017. Digital agriculture practices in the context of agriculture 4.0. Journal of Economics Finance and Accounting 4, 186–193.

Pascanu, R., Mikolov, T., Bengio, Y., 2012. Understanding the exploding gradient problem. ArXiv abs/1211.5063.

Patacchiola, M., Cangelosi, A., 2017. Head pose estimation in the wild using convolutional neural networks and adaptive gradient methods. Pattern Recognition 71, 132–143.

Patil, K., Deo, M.C., 2018. Basin-Scale Prediction of Sea Surface Temperature with Artificial Neural Networks, in: 2018 OCEANS - MTS/IEEE Kobe Techno-Oceans (OTO). Presented at the 2018 OCEANS - MTS/IEEE Kobe Techno-Oceans (OTO), pp. 1–5. https://doi.org/10.1109/OCEANSKOBE.2018.8558780

Pearson, R.G., Raxworthy, C.J., 2009. The Evolution of Local Endemism in Madagascar: Watershed Versus Climatic Gradient Hypotheses Evaluated by Null Biogeographic Models. Evolution 63, 959–967. https://doi.org/10.1111/j.1558-5646.2008.00596.x

Pelletier, C., Webb, G.I., Petitjean, F., 2019. Temporal Convolutional Neural Network for the Classification of Satellite Image Time Series. Remote Sensing 11, 523. https://doi.org/10.3390/rs11050523

Pielke, R.A., 2013. Mesoscale Meteorological Modeling. Academic Press.

Pienaar, S.W., Malekian, R., 2019. Human Activity Recognition Using LSTM-RNN Deep Neural Network Architecture. arXiv:1905.00599 [cs, eess, stat].

Powers, J.G., Klemp, J.B., Skamarock, W.C., Davis, C.A., Dudhia, J., Gill, D.O., Coen, J.L., Gochis, D.J., Ahmadov, R., Peckham, S.E., Grell, G.A., Michalakes, J., Trahan, S., Benjamin, S.G., Alexander, C.R., Dimego, G.J., Wang, W., Schwartz, C.S., Romine, G.S., Liu, Z., Snyder, C., Chen, F., Barlage, M.J., Yu, W., Duda, M.G., 2017. The Weather Research and Forecasting Model: Overview, System Efforts, and Future Directions. Bull. Amer. Meteor. Soc. 98, 1717–1737. https://doi.org/10.1175/BAMS-D-15-00308.1

Precision Decisions | Driving Farming Forwards [WWW Document], 2019. URL http://www.precisiondecisions.co.uk/ (accessed 10.9.19).
Purwanto, D., Eswaran, C., Logeswaran, R., 2010. A Comparison of ARIMA, Neural Network and Linear Regression Models for the Prediction of Infant Mortality Rate, in: 2010 Fourth Asia International Conference on Mathematical/Analytical Modelling and Computer Simulation. Presented at the 2010 Fourth Asia International Conference on Mathematical/Analytical Modelling and Computer Simulation, pp. 34–39. https://doi.org/10.1109/AMS.2010.20
Qi, H., Zhang, M., 2001. Rainfall estimation using M-PHONN model, in: IJCNN'01. International Joint Conference on Neural Networks. Proceedings (Cat. No.01CH37222). Presented at the IJCNN'01. International Joint Conference on Neural Networks. Proceedings (Cat. No.01CH37222), pp. 1620–1624 vol.3. https://doi.org/10.1109/IJCNN.2001.938403
Rafiq, M.Y., Bugmann, G., Easterbrook, D.J., 2001. Neural network design for engineering applications. Computers & Structures 79, 1541–1552. https://doi.org/10.1016/S0045-7949(01)00039-6
Ray, S., 2015. 7 Types of Regression Techniques you should know. Analytics Vidhya. URL https://www.analyticsvidhya.com/blog/2015/08/comprehensive-guide-regression/ (accessed 2.22.19).
Reddy, B.S.P., Kumar, K.V., Reddy, B.M., Raja, N., 2012. ANN Approach for Weather Prediction using Back Propagation.
Reddy, P.C., Babu, A.S., 2017. Survey on weather prediction using big data analystics. Presented at the 2017 Second International Conference on Electrical, Computer and Communication Technologies (ICECCT), IEEE, pp. 1–6.
Reimers, N., Gurevych, I., 2017. Optimal Hyperparameters for Deep LSTM-Networks for Sequence Labeling Tasks. arXiv:1707.06799 [cs].
Rémy, P., 2019. philipperemy/keras-tcn.
Rémy, S., Kipling, Z., Flemming, J., Boucher, O., Nabat, P., Michou, M., Bozzo, A., Ades, M., Huijnen, V., Benedetti, A., 2019. Description and evaluation of the tropospheric aerosol scheme in the European Centre for Medium-Range Weather Forecasts (ECMWF) Integrated Forecasting System (IFS-AER, cycle 45R1). Geoscientific Model Development 12, 4627–4659.
Rew, R., Davis, G., 1990. NetCDF: an interface for scientific data access. IEEE Computer Graphics and Applications 10, 76–82. https://doi.org/10.1109/38.56302
Richardson, L.F., Ashford, O.M., Charnock, H., Drazin, P.G., Hunt, J.C.R., 1993. The Collected Papers of Lewis Fry Richardson: CUP Archive.
Rodríguez-Fernández, N.J., Rosnay, P. de, Albergel, C., Aires, F., Prigent, C., Richaume, P., Kerr, Y.H., Drusch, M., 2018. SMOS Neural Network Soil Moisture Data Assimilation, in: IGARSS 2018 - 2018 IEEE International Geoscience and Remote Sensing Symposium. Presented at the IGARSS 2018 - 2018 IEEE International Geoscience and Remote Sensing Symposium, pp. 5548–5551. https://doi.org/10.1109/IGARSS.2018.8519377
Routray, A., Mohanty, U.C., Osuri, K.K., Kar, S.C., Niyogi, D., 2016. Impact of Satellite Radiance Data on Simulations of Bay of Bengal Tropical Cyclones Using the WRF-3DVAR Modeling System. IEEE Transactions on Geoscience and Remote Sensing 54, 2285–2303. https://doi.org/10.1109/TGRS.2015.2498971
Roy, R., 2019. TEMPORAL CONVOLUTIONAL NETWORKS [WWW Document]. Medium. URL https://medium.com/@raushan2807/temporal-convolutional-networks-bfea16e6d7d2 (accessed 10.28.19).

Rumelhart, D.E., McClelland, J.L., 1987. The PDP Perspective, in: Parallel Distributed Processing: Explorations in the Microstructure of Cognition: Foundations. MITP.
Sachidananda, M., Zrnić, D.S., 1987. Rain Rate Estimates from Differential Polarization Measurements. J. Atmos. Oceanic Technol. 4, 588–598. https://doi.org/10.1175/1520-0426(1987)004<0588:RREFDP>2.0.CO;2
Sadoddin, R., Ghorbani, A.A., 2007. A Comparative Study of Unsupervised Machine Learning and Data Mining Techniques for Intrusion Detection, in: Perner, P. (Ed.), Machine Learning and Data Mining in Pattern Recognition, Lecture Notes in Computer Science. Springer, Berlin, Heidelberg, pp. 404–418. https://doi.org/10.1007/978-3-540-73499-4_31
Sahoo, S., 2018. Deciding optimal kernel size for CNN [WWW Document]. Medium. URL https://towardsdatascience.com/deciding-optimal-filter-size-for-cnns-d6f7b56f9363 (accessed 8.1.19).
Salehinejad, H., Sankar, S., Barfett, J., Colak, E., Valaee, S., 2017. Recent Advances in Recurrent Neural Networks. arXiv:1801.01078 [cs].
Salman, A.G., Heryadi, Y., Abdurahman, E., Suparta, W., 2018. Single layer & multi-layer long short-term memory (LSTM) model with intermediate variables for weather forecasting. Procedia Computer Science 135, 89–98.
Salman, A.G., Kanigoro, B., Heryadi, Y., 2015. Weather forecasting using deep learning techniques. Presented at the 2015 international conference on advanced computer science and information systems (ICACSIS), IEEE, pp. 281–285.
Santamaría-Bonfil, G., Reyes-Ballesteros, A., Gershenson, C., 2016. Wind speed forecasting for wind farms: A method based on support vector regression. Renewable Energy 85, 790–809. https://doi.org/10.1016/j.renene.2015.07.004
Sawyer, J.S., 1962. The physics of weather forecasting. Br. J. Appl. Phys. 13, 380–383. https://doi.org/10.1088/0508-3443/13/8/302
Schizas, C.N., Michaelides, S., Pattichis, C.S., Livesay, R.R., 1991. Artificial neural networks in forecasting minimum temperature (weather), in: 1991 Second International Conference on Artificial Neural Networks. Presented at the 1991 Second International Conference on Artificial Neural Networks, pp. 112–114.
Schmidhuber, J., 2015. Deep learning in neural networks: An overview. Neural Networks 61, 85–117. https://doi.org/10.1016/j.neunet.2014.09.003
Schuster, M., Paliwal, K.K., 1997. Bidirectional recurrent neural networks. IEEE Transactions on Signal Processing 45, 2673–2681. https://doi.org/10.1109/78.650093
Schwoegler, B., 2003. Individualized, location specific weather forecasting system. US6590529B2.
Sellers, P.J., Meeson, B.W., Hall, F.G., Asrar, G., Murphy, R.E., Schiffer, R.A., Bretherton, F.P., Dickinson, R.E., Ellingson, R.G., Field, C.B., Huemmrich, K.F., Justice, C.O., Melack, J.M., Roulet, N.T., Schimel, D.S., Try, P.D., 1995. Remote sensing of the land surface for studies of global change: Models — algorithms — experiments. Remote Sensing of Environment, Remote Sensing of Land Surface for Studies of Global Chage 51, 3–26. https://doi.org/10.1016/0034-4257(94)00061-Q
Seo, Y.-D., Kim, Y.-G., Lee, E., Seol, K.-S., Baik, D.-K., 2018. Design of a smart greenhouse system based on MAPE-K and ISO/IEC-11179. Presented at the 2018 IEEE International Conference on Consumer Electronics (ICCE), IEEE, pp. 1–2.
Sermanet, P., Chintala, S., LeCun, Y., 2012. Convolutional neural networks applied to house numbers digit classification. arXiv preprint arXiv:1204.3968.

Sharaff, A., Roy, S.R., 2018. Comparative Analysis of Temperature Prediction Using Regression Methods and Back Propagation Neural Network, in: 2018 2nd International Conference on Trends in Electronics and Informatics (ICOEI). Presented at the 2018 2nd International Conference on Trends in Electronics and Informatics (ICOEI), pp. 739–742. https://doi.org/10.1109/ICOEI.2018.8553803

Shi, W., Dustdar, S., 2016. The promise of edge computing. Computer 49, 78–81.

Shi, X., Chen, Z., Wang, H., Yeung, D.-Y., Wong, W., WOO, W., 2015. Convolutional LSTM Network: A Machine Learning Approach for Precipitation Nowcasting, in: Cortes, C., Lawrence, N.D., Lee, D.D., Sugiyama, M., Garnett, R. (Eds.), Advances in Neural Information Processing Systems 28. Curran Associates, Inc., pp. 802–810.

Shoeb, A.H., Guttag, J.V., 2010. Application of machine learning to epileptic seizure detection. Presented at the Proceedings of the 27th International Conference on Machine Learning (ICML-10), pp. 975–982.

Shrivastava, G., Karmakar, S., Kumar Kowar, M., Guhathakurta, P., 2012. Application of Artificial Neural Networks in Weather Forecasting: A Comprehensive Literature Review. International Journal of Computer Applications 51, 17–29. https://doi.org/10.5120/8142-1867

Simpson, M., 2018. Machine Learning vs Neural Networks: Why It's Not One or the Other [WWW Document]. URL https://www.verypossible.com/blog/machine-learning-vs.-neural-networks (accessed 10.11.19).

Skamarock, C., Klemp, B., Dudhia, J., Gill, O., Barker, D., Duda, G., Huang, X., Wang, W., Powers, G., 2008. A Description of the Advanced Research WRF Version 3. https://doi.org/10.5065/D68S4MVH

Smola, A.J., Schölkopf, B., 2004. A tutorial on support vector regression. Statistics and Computing 14, 199–222. https://doi.org/10.1023/B:STCO.0000035301.49549.88

Society, N.G., 2011. atmospheric pressure [WWW Document]. National Geographic Society. URL http://www.nationalgeographic.org/encyclopedia/atmospheric-pressure/ (accessed 7.23.19).

Stensrud, D.J., 2007. Parameterization schemes: keys to understanding numerical weather prediction models.

Surussavadee, C., Aonchart, P., 2013. Evaluation of WRF physics options for high-resolution weather forecasting in tropics using satellite passive millimeter-wave observations, in: 2013 IEEE International Geoscience and Remote Sensing Symposium - IGARSS. Presented at the 2013 IEEE International Geoscience and Remote Sensing Symposium - IGARSS, pp. 2262–2265. https://doi.org/10.1109/IGARSS.2013.6723268

SwitchDoc Labs, 2016. Tutorial: Part 1 -Building a Solar Powered Raspberry Pi Weather Station - GroveWeatherPi. SwitchDoc Labs. URL https://www.switchdoc.com/2016/12/tutorial-part-1-building-a-solar-powered-raspberry-pi-weather-station-groveweatherpi/ (accessed 5.14.19).

Symcox, J., 2017. Grass is greener for farmers thanks to university link-up [WWW Document]. BusinessCloud.co.uk. URL https://www.businesscloud.co.uk/news/grass-is-greener-for-farmers-thanks-to-university-link-up (accessed 7.26.19).

Szegedy, C., Toshev, A., Erhan, D., 2013. Deep Neural Networks for Object Detection, in: Burges, C.J.C., Bottou, L., Welling, M., Ghahramani, Z., Weinberger, K.Q. (Eds.), Advances in Neural Information Processing Systems 26. Curran Associates, Inc., pp. 2553–2561.

Tai, K.S., Socher, R., Manning, C.D., 2015. Improved Semantic Representations From Tree-Structured Long Short-Term Memory Networks. arXiv:1503.00075 [cs].
Tan, K., Ye, Y., Cao, Q., Du, P., Dong, J., 2014. Estimation of arsenic contamination in reclaimed agricultural soils using reflectance spectroscopy and ANFIS model. IEEE Journal of Selected Topics in Applied Earth Observations and Remote Sensing 7, 2540–2546.
Taylor, J.W., Buizza, R., 2002. Neural network load forecasting with weather ensemble predictions. IEEE Transactions on Power Systems 17, 626–632. https://doi.org/10.1109/TPWRS.2002.800906
Tekinerdogan, B., 2018. Strategies for Technological Innovation in Agriculture 4.0. Reports. Wageningen University, Wageningen, Netherlands.
TensorFlow [WWW Document], 2018. . TensorFlow. URL https://www.tensorflow.org/ (accessed 8.18.19).
Tenzer, R., 2017. Global spectral model of the geoid. Geodesy and Geodynamics 8, 24–33.
Thornton, P.E., Thornton, M.M., Mayer, B.W., Wilhelmi, N., Wei, Y., Devarakonda, R., Cook, R.B., 2014. Daymet: Daily Surface Weather Data on a 1-km Grid for North America, Version 2. Oak Ridge National Lab. (ORNL), Oak Ridge, TN (United States).
Thorp, K.R., DeJonge, K.C., Kaleita, A.L., Batchelor, W.D., Paz, J.O., 2008. Methodology for the use of DSSAT models for precision agriculture decision support. computers and electronics in agriculture 64, 276–285.
Troncoso, A., Salcedo-Sanz, S., Casanova-Mateo, C., Riquelme, J.C., Prieto, L., 2015. Local models-based regression trees for very short-term wind speed prediction. Renewable Energy 81, 589–598. https://doi.org/10.1016/j.renene.2015.03.071
UCAR, 2019. WRF Model Updates [WWW Document]. URL http://www2.mmm.ucar.edu/wrf/users/graphics/WRF-post-processing.htm (accessed 2.1.19).
US Department of Commerce, N., n.d. Model Output Statistics (MOS) [WWW Document]. URL https://www.weather.gov/mdl/mos_home (accessed 7.5.19).
US EPA, O., 2016. Surface and Upper Air Databases | TTN - Support Center for Regulatory Atmospheric Modeling | US EPA [WWW Document]. URL https://www3.epa.gov/scram001/metobsdata_databases.htm (accessed 8.13.19).
Valavanis, K.P., Vachtsevanos, G.J., 2015. Handbook of unmanned aerial vehicles. Springer.
Venäläinen, A., Salo, T., Fortelius, C., 2005. The use of numerical weather forecast model predictions as a source of data for irrigation modelling. Meteorological Applications 12, 307–318. https://doi.org/10.1017/S135048270500188X
Venkatachalam, M., 2019. Recurrent Neural Networks [WWW Document]. Medium. URL https://towardsdatascience.com/recurrent-neural-networks-d4642c9bc7ce (accessed 10.28.19).
Voyant, C., Notton, G., Kalogirou, S., Nivet, M.-L., Paoli, C., Motte, F., Fouilloy, A., 2017. Machine learning methods for solar radiation forecasting: A review. Renewable Energy 105, 569–582. https://doi.org/10.1016/j.renene.2016.12.095
Walczak, S., 2019. Artificial Neural Networks. Advanced Methodologies and Technologies in Artificial Intelligence, Computer Simulation, and Human-Computer Interaction 40–53. https://doi.org/10.4018/978-1-5225-7368-5.ch004
Wang, X., Guo, P., Huang, X., 2011. A Review of Wind Power Forecasting Models. Energy Procedia, The Proceedings of International Conference on Smart Grid and Clean Energy Technologies (ICSGCE 2011 12, 770–778. https://doi.org/10.1016/j.egypro.2011.10.103

Warner, T.T., 2010. Numerical Weather and Climate Prediction. Cambridge University Press.
Willmott, C.J., Matsuura, K., 2005. Advantages of the mean absolute error (MAE) over the root mean square error (RMSE) in assessing average model performance. Climate Research 30, 79–82. https://doi.org/10.3354/cr030079
Wolfert, S., Ge, L., Verdouw, C., Bogaardt, M.-J., 2017. Big data in smart farming–a review. Agricultural Systems 153, 69–80.
Woodcock, F., 1984. Australian Experimental Model Output Statistics Forecasts of Daily Maximum and Minimum Temperature. Mon. Wea. Rev. 112, 2112–2121. https://doi.org/10.1175/1520-0493(1984)112<2112:AEMOSF>2.0.CO;2
Wu, C.-H., Tzeng, G.-H., Lin, R.-H., 2009. A Novel hybrid genetic algorithm for kernel function and parameter optimization in support vector regression. Expert Systems with Applications 36, 4725–4735. https://doi.org/10.1016/j.eswa.2008.06.046
Xin Yao, 1999. Evolving artificial neural networks. Proceedings of the IEEE 87, 1423–1447. https://doi.org/10.1109/5.784219
Xue, M., Wang, D., Gao, J., Brewster, K., Droegemeier, K.K., 2003. The Advanced Regional Prediction System (ARPS), storm-scale numerical weather prediction and data assimilation. Meteorology and Atmospheric Physics 82, 139–170. https://doi.org/10.1007/s00703-001-0595-6
Yáñez-Morroni, G., Gironás, J., Caneo, M., Delgado, R., Garreaud, R., 2018. Using the Weather Research and Forecasting (WRF) Model for Precipitation Forecasting in an Andean Region with Complex Topography. Atmosphere 9, 304. https://doi.org/10.3390/atmos9080304
Yonekura, K., Hattori, H., Suzuki, T., 2018a. Short-term local weather forecast using dense weather station by deep neural network, in: 2018 IEEE International Conference on Big Data (Big Data). Presented at the 2018 IEEE International Conference on Big Data (Big Data), pp. 1683–1690. https://doi.org/10.1109/BigData.2018.8622195
Yonekura, K., Hattori, H., Suzuki, T., 2018b. Short-term local weather forecast using dense weather station by deep neural network, in: 2018 IEEE International Conference on Big Data (Big Data). Presented at the 2018 IEEE International Conference on Big Data (Big Data), pp. 1683–1690. https://doi.org/10.1109/BigData.2018.8622195
Yosinski, J., Clune, J., Bengio, Y., Lipson, H., 2014. How transferable are features in deep neural networks? Presented at the Advances in neural information processing systems, pp. 3320–3328.
Yu, F., Koltun, V., 2015. Multi-Scale Context Aggregation by Dilated Convolutions. arXiv:1511.07122 [cs].
Yulita, I.N., Fanany, M.I., Arymuthy, A.M., 2017. Bi-directional Long Short-Term Memory using Quantized data of Deep Belief Networks for Sleep Stage Classification. Procedia Computer Science 116, 530–538. https://doi.org/10.1016/j.procs.2017.10.042
Zambaldi, V., Raposo, D., Santoro, A., Bapst, V., Li, Y., Babuschkin, I., Tuyls, K., Reichert, D., Lillicrap, T., Lockhart, E., 2018. Relational deep reinforcement learning. arXiv preprint arXiv:1806.01830.
Zander, S., Nguyen, T., Armitage, G., 2005. Automated traffic classification and application identification using machine learning, in: The IEEE Conference on Local Computer Networks 30th Anniversary (LCN'05)l. Presented at the The IEEE Conference on Local Computer Networks 30th Anniversary (LCN'05)l, pp. 250–257. https://doi.org/10.1109/LCN.2005.35

Zeiler, M.D., 2012. ADADELTA: An Adaptive Learning Rate Method. arXiv:1212.5701 [cs].
Zhang, G., Eddy Patuwo, B., Y. Hu, M., 1998. Forecasting with artificial neural networks:: The state of the art. International Journal of Forecasting 14, 35–62. https://doi.org/10.1016/S0169-2070(97)00044-7
Zhang, Shen, Zhang, Shibo, Wang, B., Habetler, T.G., 2019. Machine Learning and Deep Learning Algorithms for Bearing Fault Diagnostics-A Comprehensive Review. arXiv preprint arXiv:1901.08247.
Zhao, R., Yan, R., Chen, Z., Mao, K., Wang, P., Gao, R.X., 2019. Deep learning and its applications to machine health monitoring. Mechanical Systems and Signal Processing 115, 213–237.
Zhao, Z., Chen, W., Wu, X., Chen, P.C., Liu, J., 2017. LSTM network: a deep learning approach for short-term traffic forecast. IET Intelligent Transport Systems 11, 68–75.

8 Appendices

Appendix 1: List of Weathers Parameters

A sample of weather forecasting parameters are given below (i.e. 63 parameters out of 257).

Times
S1 Times(Time, DateStrLen)
Current shape = (1, 19)

XLAT
Float32 XLAT(Time, south_north, west_east)
Description: LATITUDE, SOUTH IS NEGATIVE
Current shape = (1, 69, 74)

XLONG
Float32 XLONG(Time, south_north, west_east)
Description: LONGITUDE, WEST IS NEGATIVE
Current shape = (1, 69, 74)

LU_INDEX
Float32 LU_INDEX(Time, south_north, west_east)
Description: LAND USE CATEGORY
Current shape = (1, 69, 74)

NU
Float32 NU(Time, bottom_top)
Description: eta values on half (mass) levels
Current shape = (1, 34)

NW
Float32 NW(Time, bottom_top_stag)
Description: eta values on full (w) levels
Current shape = (1, 35)

S
Float32 S(Time, soil_layers_stag)
Description: DEPTHS OF CENTERS OF SOIL LAYERS
Units: m
Current shape = (1, 4)

DS
Float32 DS(Time, soil_layers_stag)
Description: THICKNESSES OF SOIL LAYERS
Units: m
Current shape = (1, 4)

VAR_SSO
Float32 VAR_SSO(Time, south_north, west_east)
Description: variance of subgrid-scale orography
Units: m2
Current shape = (1, 69, 74)

U
Float32 U(Time, bottom_top, south_north, west_east_stag)
Description: x-wind component
Units: m s-1
Current shape = (1, 34, 69, 75)

V
Float32 V(Time, bottom_top, south_north_stag, west_east)
Description: y-wind component
Units: m s-1
Current shape = (1, 34, 70, 74)

W
Float32 W(Time, bottom_top_stag, south_north, west_east)
Description: -wind component
Units: m s-1
Current shape = (1, 35, 69, 74)

PH
Float32 PH(Time, bottom_top_stag, south_north, west_east)
Description: perturbation geopotential
Units: m2 s-2
Current shape = (1, 35, 69, 74)

PHB
Float32 PHB(Time, bottom_top_stag, south_north, west_east)

T
Float32 T(Time, bottom_top, south_north, west_east)
Description: perturbation potential temperature (theta-t0)
Units: K
Current shape = (1, 34, 69, 74)

HFX_FORCE
Float32 HFX_FORCE(Time)
Description: SCM ideal surface sensible heat flux
Units: W m-2
Current shape = (1,)

LH_FORCE
Float32 LH_FORCE(Time)
Description: SCM ideal surface latent heat flux
Units: W m-2
Current shape = (1,)

TSK_FORCE
Float32 TSK_FORCE(Time)
Description: SCM ideal surface skin temperature
Units: W m-2
Current shape = (1,)

HFX_FORCE_TEND
Float32 HFX_FORCE_TEND(Time)
Description: SCM ideal surface sensible heat flux tendency
Units: W m-2 s-1
Current shape = (1,)

LH_FORCE_TEND
Float32 LH_FORCE_TEND(Time)
Description: SCM ideal surface latent heat flux tendency
Units: W m-2 s-1
Current shape = (1,)

TSK_FORCE_TEND
Float32 TSK_FORCE_TEND(Time)
Description: SCM ideal surface skin temperature tendency
Units: W m-2 s-1
Current shape = (1,)

MU
Float32 MU(Time, south_north, west_east)
Description: perturbation dry air mass in column
Units: Pa
Current shape = (1, 69, 74)

MUB
Float32 MUB(Time, south_north, west_east)
Description: base state dry air mass in column
Units: Pa
Current shape = (1, 69, 74)

NEST_POS
Float32 NEST_POS(Time, south_north, west_east)
Description: -
Current shape = (1, 69, 74)

P
Float32 P(Time, bottom_top, south_north, west_east)
Description: perturbation pressure
Units: Pa
Current shape = (1, 34, 69, 74)

PB
Float32 PB(Time, bottom_top, south_north, west_east)

Description: BASE STATE PRESSURE
Units: Pa
Current shape = (1, 34, 69, 74)

FNM
Float32 FNM(Time, bottom_top)
Description: upper weight for vertical stretching
Current shape = (1, 34)

FNP
Float32 FNP(Time, bottom_top)
Description: lower weight for vertical stretching
Current shape = (1, 34)

RDNW
Float32 RDNW(Time, bottom_top)
Description: inverse d(eta) values between full (w) levels
Current shape = (1, 34)

RDN
Float32 RDN(Time, bottom_top)
Description: inverse d(eta) values between half (mass) levels
Current shape = (1, 34)

DNW
Float32 DNW(Time, bottom_top)
Description: d(eta) values between full (w) levels
Current shape = (1, 34)

DN
Float32 DN(Time, bottom_top)
Description: d(eta) values between half (mass) levels
Current shape = (1, 34)

CFN
Float32 CFN(Time)
Description: extrapolation constant
Current shape = (1,)

CFN1
Float32 CFN1(Time)
Description: extrapolation constant
Current shape = (1,)

THIS_IS_AN_IDEAL_RUN
int32 THIS_IS_AN_IDEAL_RUN(Time)
Description: T/F flag: this is an ARW ideal simulation
Current shape = (1,)

P_HYD
Float32 P_HYD(Time, bottom_top, south_north, west_east)
Description: hydrostatic pressure
Units: Pa
Current shape = (1, 34, 69, 74)

Q2
Float32 Q2(Time, south_north, west_east)
Description: QV at 2 M
Units: kg kg-1
Current shape = (1, 69, 74)

T2
Float32 T2(Time, south_north, west_east)
Description: TEMP at 2 M
Units: K
Current shape = (1, 69, 74)

TH2
Float32 TH2(Time, south_north, west_east)
Description: POT TEMP at 2 M
Units: K
Current shape = (1, 69, 74)

PSFC
Float32 PSFC(Time, south_north, west_east)
Description: SFC PRESSURE
Units: Pa
Current shape = (1, 69, 74)

U10
Description: U at 10 M
Units: m s-1
Current shape = (1, 69, 74)

V10
Float32 V10(Time, south_north, west_east)
Description: V at 10 M
Units: m s-1
Current shape = (1, 69, 74)

RDX
Float32 RDX(Time)
Description: INVERSE X GRID LENGTH
Current shape = (1,)

CF1
Float32 CF1(Time)
Description: 2nd order extrapolation constant
Current shape = (1,)

CF2
Float32 CF2(Time)
Description: 2nd order extrapolation constant
Current shape = (1,)

CF3
Float32 CF3(Time)
Description: 2nd order extrapolation constant
Current shape = (1,)

ITIMESTEP
int32 ITIMESTEP(Time)
Current shape = (1,)

XTIME
Float32 XTIME(Time)
Description: minutes since 2017-09-12 00:00:00
Units: minutes since 2017-09-12 00:00:00
Current shape = (1,)

QVAPOR
Float32 QVAPOR(Time, bottom_top, south_north, west_east)
Description: Water vapor mixing ratio
Units: kg kg-1
Current shape = (1, 34, 69, 74)

QCLOUD
Float32 QCLOUD(Time, bottom_top, south_north, west_east)
Description: Cloud water mixing ratio
Units: kg kg-1
Current shape = (1, 34, 69, 74)

QRAIN
Float32 QRAIN(Time, bottom_top, south_north, west_east)
Description: Rain water mixing ratio
Units: kg kg-1
Current shape = (1, 34, 69, 74)

QICE
Float32 QICE(Time, bottom_top, south_north, west_east)
Description: Ice mixing ratio
Units: kg kg-1
shape = (1, 34, 69, 74)

QSNOW
Float32 QSNOW(Time, bottom_top, south_north, west_east)
Description: Snow mixing ratio
Units: kg kg-1
Current shape = (1, 34, 69, 74)

QGRAUP
Float32 QGRAUP(Time, bottom_top, south_north, west_east)
Description: Graupel mixing ratio
Units: kg kg-1
Current shape = (1, 34, 69, 74)

QNICE
Float32 QNICE(Time, bottom_top, south_north, west_east)
Description: Ice Number concentration
Units: kg-1
Current shape = (1, 34, 69, 74)

QNRAIN
Float32 QNRAIN(Time, bottom_top, south_north, west_east)
Description: Rain Number concentration
Units: kg(-1)
Current shape = (1, 34, 69, 74)

SHDMAX
Float32 SHDMAX(Time, south_north, west_east)
Description: ANNUAL MAX VEG FRACTION
Current shape = (1, 69, 74)

SHDMIN
Float32 SHDMIN(Time, south_north, west_east)
Description: ANNUAL MIN VEG FRACTION
Current shape = (1, 69, 74)

SNOALB
Float32 SNOALB(Time, south_north, west_east)

Appendix 2: Evaluation Results of MIMO-LSTM variance for Historical Weather Data

The configuration 1 and configuration 6 evaluation results are shown here out of six different configurations.

Configuration 1

```
model = Sequential()
model.add(LSTM(128, return_sequences=True, input_shape=(timesteps, data_dim)))
model.add(LSTM(512, return_sequences=True))  # returns a sequence of vectors of
model.add(LSTM(512, return_sequences=True))
model.add(LSTM(256)) # return a single vector of dimension 32
model.add(Dense(10, activation='tanh'))
```

Optimiser: Adam

Epoch	Loss	Total MSE	Total MAE	Total RMSE	SkinTemp	SufPres	U10	V10	Humidity	Rainc	Rainnc	Snow	SoilTemp	SoilMoist
10	0.007332858	0.007332858	0.048614784	0.08563211	0.010371711	0.000678658	0.007284337	0.004653197	0.01674735	0.003825226	0.01403451	1.03E-07	0.012261818	0.003471669
20	0.006601568	0.006601568	0.043715446	0.08125003	0.007973646	0.000751622	0.006536934	0.004394703	0.0225383	0.006210226	0.004084814	2.33E-08	0.012403292	0.001122066
30	0.007042277	0.007042277	0.046863642	0.08391828	0.0078375	0.001714191	0.008276898	0.006594678	0.025596479	0.003592094	0.003847608	1.41E-07	0.012222861	0.000740319
40	0.0072522	0.0072522	0.047870472	0.08515985	0.007340875	0.001707832	0.012895794	0.006533101	0.024894372	0.003707454	0.002360903	1.34E-07	0.011911398	0.001170145
50	0.008471627	0.008471627	0.051866251	0.09204144	0.008341352	0.001060495	0.009887383	0.010982551	0.0294462	0.003091001	0.003130692	4.24E-08	0.017348982	0.001427575
60	0.007493469	0.007493469	0.048008396	0.08656482	0.006530265	0.00118546	0.0116699	0.008794162	0.028372591	0.002748844	0.001618594	5.05E-09	0.013069782	0.000945087
70	0.0089721	0.0089721	0.053142694	0.09472117	0.007441554	0.001009718	0.014066464	0.011558367	0.033971984	0.003010515	0.002760496	4.38E-09	0.014849813	0.001052088
80	0.007444166	0.007444166	0.048546581	0.08627958	0.006919191	0.000969841	0.011856847	0.00894155	0.025993962	0.003442479	0.001958059	1.74E-09	0.013608329	0.000751398
90	0.00722389	0.00722389	0.046968233	0.08499347	0.006443199	0.001093521	0.008772112	0.007947368	0.026738266	0.003061983	0.002968501	1.57E-08	0.014145585	0.001068347
100	0.007879228	0.007879228	0.050183286	0.08876501	0.00617072	0.001015921	0.009468304	0.015682602	0.027466776	0.003361375	0.002961195	2.08E-09	0.011728673	0.000936711
110	0.007158511	0.007158511	0.047382673	0.08460799	0.006097654	0.000963488	0.008369253	0.013452309	0.024821607	0.003198484	0.002415518	8.50E-09	0.011432038	0.000834755
120	0.008512431	0.008512431	0.051405353	0.092262834	0.006107245	0.00078595	0.009924321	0.018300904	0.029062454	0.003448997	0.004121292	2.60E-08	0.012378479	0.000994646
130	0.007572321	0.007572321	0.048118408	0.087019086	0.006896439	0.000784712	0.010194401	0.011682113	0.02637903	0.003383082	0.003870898	9.81E-09	0.011490157	0.00104237
140	0.009017411	0.009017411	0.052977246	0.09496004	0.008139383	0.000669747	0.009078103	0.01924821	0.030790556	0.003599228	0.003850834	7.25E-08	0.013774752	0.001023217
150	0.008758888	0.008758888	0.051868497	0.09358893	0.007174593	0.000993473	0.008458095	0.018778535	0.030827027	0.003496635	0.005902608	2.00E-08	0.010917694	0.0010402
160	0.008290757	0.008290757	0.050683807	0.09105359	0.006993292	0.000842474	0.010400013	0.011216189	0.032996073	0.003275004	0.004399345	1.56E-08	0.011671004	0.001114156
170	0.00870571	0.00870571	0.052485575	0.0933044	0.006690785	0.001059324	0.011030115	0.015071922	0.029613951	0.004029285	0.005312897	5.20E-08	0.01307984	0.001168931
180	0.009504732	0.009504732	0.054697582	0.09749222	0.007151719	0.000746764	0.010814284	0.017540231	0.033890273	0.003590622	0.004840082	1.07E-07	0.015236142	0.001237101
190	0.008502372	0.008502372	0.051446347	0.0922083	0.005693226	0.00094257	0.010445372	0.012690703	0.032232944	0.003350003	0.004902055	5.18E-08	0.013587017	0.001179778
200	0.008226414	0.008226414	0.049926155	0.090699576	0.006776186	0.001027592	0.01053009	0.010004113	0.030033676	0.00369946	0.004340077	3.28E-08	0.01483124	0.001021668
210	0.008515286	0.008515286	0.051478713	0.09227832	0.005722071	0.000785025	0.008292153	0.014856972	0.031103434	0.003910753	0.005573197	5.22E-07	0.013764947	0.001143788
220	0.008429375	0.008429375	0.051915655	0.09181162	0.006203071	0.000970419	0.009338698	0.014037683	0.029608034	0.003714836	0.005651081	1.03E-07	0.013441819	0.001328005
230	0.00867375	0.00867375	0.052575882	0.093132965	0.006041409	0.001266384	0.010987357	0.010918822	0.03078888	0.003736298	0.006993955	8.24E-08	0.0146744	0.001329914
240	0.008424392	0.008424392	0.050949428	0.091784485	0.006711949	0.001274459	0.008449855	0.011142487	0.031221626	0.003298751	0.006130503	9.14E-08	0.014810914	0.001203288
250	0.008363304	0.008363304	0.050712354	0.09145111	0.006348061	0.000918247	0.010227037	0.010725042	0.0297399	0.003543996	0.006627985	7.82E-08	0.014252353	0.001250345
260	0.008182694	0.008182694	0.050483157	0.09045825	0.006674636	0.000805058	0.009866027	0.011975276	0.029467048	0.003381401	0.004339044	6.69E-08	0.013912845	0.001405538
270	0.00811045	0.00811045	0.049861417	0.09005804	0.006369216	0.000794701	0.010732362	0.010739849	0.031121476	0.003780612	0.003774223	2.44E-07	0.012445986	0.001345831
280	0.008750529	0.008750529	0.052044818	0.09354426	0.006410204	0.000872171	0.011083021	0.012274734	0.033021625	0.003150826	0.004926112	1.21E-07	0.014323738	0.001442745
290	0.008524125	0.008524125	0.051374119	0.092326194	0.006271284	0.000926946	0.009688063	0.012313397	0.032380182	0.003244164	0.005563466	2.67E-07	0.013440331	0.001413151
300	0.007949504	0.007949504	0.049942916	0.08915999	0.005858063	0.0007637	0.009852529	0.012173227	0.029367166	0.003489821	0.004485081	1.23E-07	0.012034901	0.001470429
310	0.007755572	0.007755572	0.048763398	0.088065736	0.006053037	0.000676511	0.009101932	0.009540331	0.031219156	0.003228126	0.0041239	2.58E-08	0.012185729	0.001426979
320	0.008116202	0.008116202	0.050217333	0.09008996	0.005735182	0.000850982	0.010784741	0.01010419	0.03094411	0.003660771	0.006273575	6.51E-08	0.011287782	0.001520619
330	0.008361132	0.008361132	0.0511791	0.09143923	0.006236457	0.001058805	0.010278369	0.010937587	0.03313903	0.003268564	0.005042742	2.05E-08	0.012339517	0.001310227
340	0.007787381	0.007787381	0.04898291	0.08824614	0.005806712	0.000850013	0.009667984	0.008825018	0.030838024	0.003411395	0.004232732	1.19E-07	0.012490736	0.001751078
350	0.008384695	0.008384695	0.050448131	0.09156798	0.005654964	0.000740291	0.009873319	0.011088619	0.034234304	0.003122521	0.006315042	3.10E-08	0.011398595	0.001419271
360	0.007876759	0.007876759	0.049110249	0.08875111	0.005378708	0.000833559	0.010742755	0.010007641	0.031083753	0.00337442	0.003810689	3.01E-07	0.012100036	0.00143573
370	0.007977887	0.007977887	0.049181416	0.08931902	0.005303682	0.000602521	0.011192068	0.009761727	0.032091197	0.003319124	0.004198475	1.14E-07	0.01163695	0.001673015
380	0.007978098	0.007978098	0.049153367	0.0893202	0.005586417	0.000919897	0.0094065	0.010625847	0.03252793	0.003352262	0.004085217	7.62E-08	0.01169837	0.00157846
390	0.008524125	0.008524125	0.05085768	0.092326194	0.006555918	0.000772156	0.010490547	0.010195111	0.037803415	0.003102169	0.002673517	6.34E-08	0.012018439	0.001629915
400	0.008612382	0.008612382	0.051289935	0.09280292	0.005604406	0.0007092	0.009492107	0.014872189	0.035438135	0.003056502	0.004004006	6.06E-08	0.011315399	0.001631817
410	0.007500102	0.007500102	0.047691097	0.08660313	0.005561792	0.000912399	0.00818612	0.010514848	0.031199984	0.003049069	0.004379361	8.58E-09	0.009790685	0.001406752
420	0.007975556	0.007975556	0.048971091	0.08930596	0.005835863	0.000715371	0.008941129	0.010212493	0.034375556	0.003059109	0.004364154	1.76E-08	0.010699609	0.001552252
430	0.008396492	0.008396492	0.050264246	0.09163237	0.00601124	0.000770496	0.009363731	0.012554668	0.034099806	0.003291957	0.003485457	2.23E-08	0.012854167	0.001533373
440	0.008072975	0.008072975	0.049466199	0.08984974	0.005666495	0.000643868	0.009956025	0.010171617	0.034377337	0.003263218	0.00450542	4.24E-08	0.010589303	0.001556428
450	0.008089283	0.008089283	0.049619352	0.08994043	0.005371095	0.000742495	0.01029344	0.013150042	0.031653088	0.003239272	0.003778359	2.75E-08	0.010850218	0.001814794
460	0.008118608	0.008118608	0.048986065	0.09010332	0.005270368	0.000643571	0.010457949	0.008704092	0.034321178	0.003479945	0.004728452	4.61E-08	0.011872632	0.001707851
470	0.008466013	0.008466013	0.05119877	0.09201093	0.006398619	0.000667237	0.010746816	0.011629336	0.034217387	0.003414535	0.004859108	1.42E-07	0.011057256	0.001669695
480	0.008199102	0.008199102	0.049404272	0.0905489	0.005266628	0.000857882	0.00966001	0.009606856	0.036831934	0.00337732	0.003335239	1.07E-07	0.011218764	0.001836281
490	0.008168381	0.008168381	0.049602692	0.0903791	0.005869276	0.000732204	0.009827367	0.010136933	0.03502509	0.00330065	0.003845529	5.10E-08	0.011005907	0.001940795
500	0.008638437	0.008638437	0.050837425	0.0929432	0.005595418	0.000838336	0.010917228	0.010101718	0.03693253	0.003296042	0.005044478	6.02E-08	0.011700599	0.001957957
510	0.008053746	0.008053746	0.049400023	0.08974267	0.00602309	0.000804305	0.009617019	0.010164639	0.033956822	0.003226277	0.003790387	2.31E-08	0.011106661	0.001848236
520	0.008118693	0.008118693	0.049131624	0.09010379	0.005965292	0.000760074	0.008713681	0.010543994	0.034148622	0.003385052	0.003326134	6.12E-08	0.012439463	0.001904553
530	0.008562235	0.008562235	0.050696837	0.092532344	0.006325521	0.000723875	0.010135555	0.010446192	0.037863676	0.003448598	0.002908626	1.01E-07	0.011704979	0.002065233
540	0.008621424	0.008621424	0.050897413	0.092851624	0.005969696	0.000649401	0.010787565	0.011712043	0.035820838	0.003417098	0.003179187	4.82E-08	0.01244536	0.002233009
550	0.00835009	0.00835009	0.049963112	0.09137883	0.005635724	0.000626456	0.011854872	0.009510946	0.034971595	0.003503753	0.003935529	2.95E-07	0.011181403	0.002280328
560	0.00862445	0.00862445	0.051068109	0.092867926	0.00592844	0.000967484	0.010138468	0.010013742	0.03682304	0.003384073	0.004866744	4.96E-08	0.011822766	0.002299699
570	0.008329207	0.008329207	0.049876766	0.09126449	0.005706972	0.000773324	0.008635786	0.01087721	0.0360769	0.003868108	0.004746971	1.00E-07	0.010525278	0.002081428
580	0.008548386	0.008548386	0.050813268	0.09245748	0.006790149	0.000652108	0.009535897	0.011145612	0.03605444	0.0032083 2	0.004671527	3.78E-08	0.011355866	0.0020699
590	0.008467531	0.008467531	0.049993995	0.092019185	0.00605441	0.000685968	0.009226588	0.010643345	0.037235312	0.003541035	0.00357848	6.62E-08	0.011631548	0.002078563
600	0.008996813	0.008996813	0.051834193	0.09485154	0.00666588	0.000737797	0.009050977	0.010503701	0.040425554	0.003313339	0.004532254	1.46E-07	0.012542911	0.002195573
610	0.009213081	0.009213081	0.052699661	0.09598481	0.006381894	0.000720444	0.009804369	0.010494921	0.03963276	0.003576578	0.006261698	4.79E-07	0.012462789	0.002794888
620	0.008669626	0.008669626	0.051275465	0.09311083	0.006406974	0.000926857	0.011047188	0.010131682	0.03674354	0.003406863	0.004095312	4.01E-07	0.011907301	0.002030144
630	0.008556755	0.008556755	0.050946985	0.09250273	0.006570547	0.000899945	0.011389592	0.009089441	0.03631006	0.003523814	0.004027952	8.49E-08	0.011114432	0.002641685
640	0.008548861	0.008548861	0.050502016	0.09246005	0.006524603	0.000849517	0.010604402	0.009087962	0.036696333	0.003597077	0.004191762	1.32E-07	0.011613383	0.002323435

Optimiser: SGD

Epoch	Loss	Total MSE	Total MAE	Total RMSE	SkinTemp	SufPres	U10	V10	Humidity	Rainc	Rainnc	Snow	SoilITemp	SoilMoist
10	0.022919753	0.022919753	0.106350055	0.15139271	0.01480351	0.015914505	0.028357795	0.024992902	0.10610191	0.004629828	0.003904601	0.00139094	0.027846517	0.001255031
20	0.014937797	0.014937797	0.087435061	0.12222029	0.005443028	0.025533063	0.024844587	0.0166966	0.05037601	0.004378898	0.003152672	0.000830909	0.016586741	0.001535464
30	0.010551107	0.010551107	0.072926591	0.10271858	0.003077003	0.017709356	0.019030832	0.01571791	0.026194561	0.004378627	0.003156501	0.000487316	0.014156938	0.001602023
40	0.00862361	0.00862361	0.065632782	0.092863396	0.002699717	0.011446186	0.01398119	0.016664233	0.017644675	0.004575321	0.004030226	0.000416301	0.013237281	0.001540969
50	0.007920666	0.007920666	0.062428687	0.088998124	0.002560776	0.009576065	0.011453209	0.016294748	0.016031148	0.004480101	0.004597088	0.000343886	0.012360503	0.00150914
60	0.007379662	0.007379662	0.059890259	0.08590496	0.002461341	0.008180406	0.009705248	0.01615697	0.015243849	0.004298628	0.004923223	0.000277495	0.011087195	0.001462265
70	0.007103786	0.007103786	0.058358713	0.084283955	0.002322306	0.007778185	0.010350655	0.014163745	0.014901795	0.004116323	0.004963364	0.000216232	0.010549539	0.001675713
80	0.0069163	0.0069163	0.057528169	0.0831643	0.002193065	0.007147738	0.010366159	0.014276747	0.014275963	0.003945937	0.004881175	0.000168344	0.01005477	0.001853106
90	0.006745501	0.006745501	0.056476522	0.082131	0.002120812	0.006674327	0.010667504	0.012230791	0.015500408	0.003807908	0.004753442	0.000125991	0.009544198	0.002029625
100	0.00666694	0.00666694	0.055917032	0.08165134	0.002046993	0.006214765	0.010278772	0.011945753	0.015853604	0.003700857	0.004530883	9.01E-05	0.009629113	0.002378585
110	0.006350168	0.006350168	0.054234504	0.07968794	0.001987501	0.005936605	0.009256597	0.010590026	0.015710885	0.003629532	0.004289136	6.26E-05	0.009248296	0.002790535
120	0.006560595	0.006560595	0.054827544	0.080997504	0.001975221	0.005459938	0.011270083	0.009953881	0.016835209	0.003579039	0.00412251	4.52E-05	0.009159302	0.003205607
130	0.006282107	0.006282107	0.053736388	0.079259746	0.001959008	0.005169312	0.010105088	0.009898826	0.015302379	0.003544565	0.004132845	3.11E-05	0.008800644	0.003877326
140	0.006134519	0.006134519	0.052703322	0.07832316	0.001984542	0.004367852	0.010321767	0.008880086	0.015395306	0.003514439	0.004060493	2.13E-05	0.008466139	0.004333274
150	0.006077367	0.006077367	0.052242808	0.07795746	0.002026109	0.003770829	0.010345699	0.008655005	0.014841182	0.003483831	0.004017103	1.40E-05	0.008368652	0.005251214
160	0.0062916	0.0062916	0.052902417	0.07931961	0.002141304	0.003596676	0.010938664	0.008522637	0.015607752	0.003445743	0.003934173	9.52E-06	0.008351986	0.006367544
170	0.006719578	0.006719578	0.054735812	0.08197304	0.002487799	0.003451406	0.014171671	0.008717527	0.015016284	0.003432927	0.00381345	6.39E-06	0.008448454	0.00764987
180	0.00717559	0.00717559	0.056163327	0.084708855	0.00285086	0.003187068	0.01628897	0.009176318	0.016658857	0.003301879	0.003588668	4.14E-06	0.008869952	0.007829195
190	0.007311285	0.007311285	0.056516144	0.08550605	0.003296586	0.003269936	0.01394545	0.009805308	0.018660069	0.003189979	0.003335487	2.69E-06	0.009508189	0.008099159
200	0.007819698	0.007819698	0.057968552	0.088429056	0.003460589	0.003436551	0.01799567	0.010983198	0.017565327	0.003131808	0.003018874	1.86E-06	0.010251438	0.008351664
210	0.007927769	0.007927769	0.057469565	0.08903802	0.003532832	0.003034635	0.014652479	0.011170417	0.020963533	0.003054603	0.002781731	1.23E-06	0.011119739	0.008966491
220	0.008427976	0.008427976	0.059062414	0.091804005	0.003618717	0.003709272	0.017447075	0.014625301	0.017108396	0.00301229	0.002422532	8.25E-07	0.01230022	0.010035133
230	0.008600433	0.008600433	0.058786951	0.09273851	0.003239252	0.003741958	0.01506228	0.013499735	0.0191369	0.002976835	0.00242122	5.40E-07	0.013356913	0.012568695
240	0.009440906	0.009440906	0.062204672	0.097164325	0.003910444	0.005481989	0.017102046	0.014011731	0.019696115	0.002954204	0.002278865	3.61E-07	0.014819136	0.014154167
250	0.011409243	0.011409243	0.068526141	0.10681405	0.003445185	0.007233956	0.029648772	0.017389359	0.018793458	0.002942688	0.002283952	2.16E-07	0.016185572	0.016169267
260	0.013753862	0.013753862	0.073979572	0.117276855	0.003089883	0.006248908	0.046071388	0.021573665	0.017409533	0.00294063	0.003072269	1.62E-07	0.017490659	0.019641522
270	0.012210927	0.012210927	0.066837845	0.11050306	0.003153417	0.00415937	0.032347582	0.02193688	0.01072695	0.002936329	0.003861729	1.02E-07	0.0184879	0.02449901
280	0.013425812	0.013425812	0.069258523	0.1158698	0.004342475	0.003966115	0.04466783	0.023887256	0.010769516	0.002939166	0.003035338	6.33E-08	0.018904861	0.02174549
290	0.016406083	0.016406083	0.075956303	0.12808624	0.006331148	0.002139897	0.067758046	0.032917827	0.012235257	0.002953079	0.004619264	4.81E-08	0.016622666	0.018483587
300	0.01419564	0.01419564	0.071005678	0.11914545	0.006991603	0.002724565	0.059648097	0.026779672	0.012612414	0.002963038	0.003822438	3.99E-08	0.015413363	0.011001171
310	0.013438285	0.013438285	0.07030409	0.11592361	0.007297562	0.002962584	0.059101153	0.021656869	0.012362898	0.002977379	0.004934575	4.21E-08	0.014570274	0.008519515
320	0.012571518	0.012571518	0.068452824	0.11212278	0.007749897	0.00410448	0.05404773	0.019767571	0.013416841	0.002985512	0.004848961	4.89E-08	0.013120239	0.0056739
330	0.011014046	0.011014046	0.065641613	0.10494783	0.00798521	0.00624928	0.042528424	0.014821881	0.011985074	0.002988927	0.004636699	4.78E-08	0.012656957	0.006287952
340	0.010086764	0.010086764	0.062282841	0.10043288	0.007031716	0.009217441	0.039148692	0.011783412	0.011308089	0.003003005	0.002386331	4.39E-08	0.01172612	0.005262788
350	0.009837128	0.009837128	0.060723291	0.0991823	0.006658524	0.012681477	0.040757984	0.008440831	0.012219885	0.003012044	0.001919304	4.14E-08	0.008417578	0.004263615
360	0.009873449	0.009873449	0.060530624	0.09936523	0.005930703	0.014946444	0.042819615	0.007566238	0.012154198	0.003017082	0.001509268	3.53E-08	0.007175275	0.003615629
370	0.010396699	0.010396699	0.061379555	0.101964206	0.005025899	0.015962444	0.049995024	0.008442455	0.013276552	0.003006447	0.001385789	3.03E-08	0.004596545	0.002275803
380	0.011244675	0.011244675	0.06320732	0.10604091	0.004838011	0.021498505	0.05748226	0.007487961	0.010333328	0.003020957	0.000990944	2.03E-08	0.004007751	0.002787008
390	0.009890947	0.009890947	0.060597495	0.09945324	0.005131297	0.017874278	0.043340154	0.008037055	0.011512732	0.003007749	0.000716017	1.40E-08	0.004269917	0.005020259
400	0.010275134	0.010275134	0.061081858	0.10136633	0.00472651	0.018236943	0.045870993	0.007796826	0.012277189	0.003003416	0.000797068	1.47E-08	0.004183396	0.005858982
410	0.011807925	0.011807925	0.064831467	0.10866427	0.005146365	0.019470718	0.05969434	0.008879089	0.010956855	0.003000044	0.000750733	1.18E-08	0.003697677	0.006483422
420	0.012237319	0.012237319	0.066146021	0.11062242	0.004967975	0.018021384	0.05922626	0.010386347	0.011895888	0.002988816	0.000754256	1.21E-08	0.004105622	0.010026628
430	0.0126717	0.0126717	0.066768149	0.11256865	0.004998065	0.01896578	0.063166395	0.010967399	0.010182713	0.002971316	0.000747457	1.46E-08	0.00390137	0.010816489
440	0.012792585	0.012792585	0.066700774	0.113104306	0.005001736	0.01671078	0.062826835	0.010287279	0.010831521	0.002950346	0.000986866	1.31E-08	0.004126715	0.014203756
450	0.013226266	0.013226266	0.066870408	0.115005516	0.004565417	0.01674015	0.06626923	0.011094343	0.010228618	0.002946888	0.000630258	1.80E-08	0.003577953	0.016209789
460	0.01426345	0.01426345	0.068439145	0.119429685	0.004715283	0.016104937	0.07541132	0.011576436	0.010482498	0.002940322	0.001015353	1.79E-08	0.003171966	0.017216375
470	0.015442147	0.015442147	0.071406572	0.12426643	0.004676826	0.016887568	0.07764603	0.013896223	0.011479707	0.00292903	0.001308052	2.10E-08	0.003159973	0.022438066

Optimiser: Adaptive-Adam

Epoch	Loss	Total MSE	Total MAE	Total RMSE	SkinTemp	SufPres	U10	V10	Humidity	Rainc	Rainnc	Snow	SoilITemp	SoilMoist
10	0.571018543	0.571018543	0.554251921	0.75565773	0.71013933	0.20583192	1.2516543	1.3004148	1.0262195	0.003167429	0.000519068	0	0.3433816	0.8688576
20	0.571018543	0.571018543	0.554251921	0.75565773	0.71013933	0.20583192	1.2516543	1.3004148	1.0262195	0.003167429	0.000519068	0	0.3433816	0.8688576
30	0.571018543	0.571018543	0.554251921	0.75565773	0.71013933	0.20583192	1.2516543	1.3004148	1.0262195	0.003167429	0.000519068	0	0.3433816	0.8688576
40	0.571018543	0.571018543	0.554251921	0.75565773	0.71013933	0.20583192	1.2516543	1.3004148	1.0262195	0.003167429	0.000519068	0	0.3433816	0.8688576
50	0.571018543	0.571018543	0.554251921	0.75565773	0.71013933	0.20583192	1.2516543	1.3004148	1.0262195	0.003167429	0.000519068	0	0.3433816	0.8688576
60	0.571018543	0.571018543	0.554251921	0.75565773	0.71013933	0.20583192	1.2516543	1.3004148	1.0262195	0.003167429	0.000519068	0	0.3433816	0.8688576
70	0.571018543	0.571018543	0.554251921	0.75565773	0.71013933	0.20583192	1.2516543	1.3004148	1.0262195	0.003167429	0.000519068	0	0.3433816	0.8688576
80	0.571018543	0.571018543	0.554251921	0.75565773	0.71013933	0.20583192	1.2516543	1.3004148	1.0262195	0.003167429	0.000519068	0	0.3433816	0.8688576
90	0.571018543	0.571018543	0.554251921	0.75565773	0.71013933	0.20583192	1.2516543	1.3004148	1.0262195	0.003167429	0.000519068	0	0.3433816	0.8688576
100	0.571018543	0.571018543	0.554251921	0.75565773	0.71013933	0.20583192	1.2516543	1.3004148	1.0262195	0.003167429	0.000519068	0	0.3433816	0.8688576
110	0.571018543	0.571018543	0.554251921	0.75565773	0.71013933	0.20583192	1.2516543	1.3004148	1.0262195	0.003167429	0.000519068	0	0.3433816	0.8688576
120	0.571018543	0.571018543	0.554251921	0.75565773	0.71013933	0.20583192	1.2516543	1.3004148	1.0262195	0.003167429	0.000519068	0	0.3433816	0.8688576
130	0.571018543	0.571018543	0.554251921	0.75565773	0.71013933	0.20583192	1.2516543	1.3004148	1.0262195	0.003167429	0.000519068	0	0.3433816	0.8688576
140	0.571018543	0.571018543	0.554251921	0.75565773	0.71013933	0.20583192	1.2516543	1.3004148	1.0262195	0.003167429	0.000519068	0	0.3433816	0.8688576
150	0.571018543	0.571018543	0.554251921	0.75565773	0.71013933	0.20583192	1.2516543	1.3004148	1.0262195	0.003167429	0.000519068	0	0.3433816	0.8688576
160	0.571018543	0.571018543	0.554251921	0.75565773	0.71013933	0.20583192	1.2516543	1.3004148	1.0262195	0.003167429	0.000519068	0	0.3433816	0.8688576
170	0.571018543	0.571018543	0.554251921	0.75565773	0.71013933	0.20583192	1.2516543	1.3004148	1.0262195	0.003167429	0.000519068	0	0.3433816	0.8688576
180	0.571018543	0.571018543	0.554251921	0.75565773	0.71013933	0.20583192	1.2516543	1.3004148	1.0262195	0.003167429	0.000519068	0	0.3433816	0.8688576
190	0.571018543	0.571018543	0.554251921	0.75565773	0.71013933	0.20583192	1.2516543	1.3004148	1.0262195	0.003167429	0.000519068	0	0.3433816	0.8688576
200	0.571018543	0.571018543	0.554251921	0.75565773	0.71013933	0.20583192	1.2516543	1.3004148	1.0262195	0.003167429	0.000519068	0	0.3433816	0.8688576

Optimiser: Adaptive-SGD

Epoch	Loss	Total MSE	Total MAE	Total RMSE	SkinTemp	SufPres	U10	V10	Humidity	Rainc	Rainnc	Snow	SolilTemp	SoilMoist
10	0.006140389	0.006140389	0.053015268	0.07836064	0.002140473	0.006157288	0.00828705	0.011404678	0.014103655	0.003428468	0.00353421	9.77E-05	0.011555845	0.000694502
20	0.004932568	0.004932568	0.04637933	0.07023224	0.002248694	0.002866784	0.008390104	0.012695679	0.010277926	0.003041345	0.0022276	4.58E-06	0.006797443	0.000775526
30	0.006071655	0.006071655	0.049175423	0.077920824	0.002260588	0.002718658	0.01286405	0.011882218	0.017224407	0.002987299	0.001729404	9.27E-07	0.007914529	0.001134476
40	0.009451755	0.009451755	0.05922275	0.09722013	0.002356356	0.002290134	0.033417087	0.010132368	0.029441977	0.002966393	0.002088828	2.43E-07	0.009470561	0.002353604
50	0.009020109	0.009020109	0.059843658	0.09497426	0.002929299	0.00274234	0.025910232	0.009680792	0.027867645	0.00296806	0.004984332	2.19E-07	0.010185719	0.002932453
60	0.009850287	0.009850287	0.059683239	0.0992486	0.002934607	0.001304112	0.022302069	0.009461621	0.025397466	0.002991158	0.01921229	2.68E-07	0.012311907	0.002587377
70	0.010027819	0.010027819	0.059161235	0.100139	0.002667511	0.002154172	0.020179644	0.009062608	0.026415868	0.003021451	0.022194255	2.57E-07	0.012512651	0.002069776
80	0.011831194	0.011831194	0.062675835	0.108771294	0.002931187	0.002375118	0.029360397	0.009259949	0.024021668	0.003040195	0.034002163	2.22E-07	0.011700327	0.00162072
90	0.008919197	0.008919197	0.053441461	0.0944415	0.0027127	0.001914507	0.015465423	0.010029245	0.019388266	0.003056933	0.024411066	1.68E-07	0.010422847	0.001790811
100	0.008936918	0.008936918	0.053274047	0.09453528	0.002844828	0.001818479	0.017893357	0.009767322	0.01842249	0.003064628	0.024230378	1.65E-07	0.009884147	0.001443392
110	0.00910366	0.00910366	0.053196233	0.0954131	0.002929413	0.001717914	0.018215006	0.009784048	0.017445734	0.003065963	0.02716167	1.69E-07	0.009305007	0.001411677
120	0.009253053	0.009253053	0.052858591	0.09619279	0.002913631	0.001811215	0.017809609	0.009311478	0.016569795	0.003066093	0.030909466	1.61E-07	0.008647543	0.001491543
130	0.009220632	0.009220632	0.052804241	0.09602412	0.002916481	0.00174266	0.01874991	0.009110638	0.01598513	0.003066021	0.030673089	1.59E-07	0.008425494	0.001536739
140	0.008868445	0.008868445	0.051939302	0.09417242	0.002912919	0.001794586	0.017162453	0.009190989	0.016436882	0.003069935	0.028232807	1.49E-07	0.008444146	0.001439587
150	0.00928363	0.00928363	0.052829444	0.096351594	0.002962097	0.001845323	0.018356903	0.009152041	0.016124101	0.003068156	0.03169862	1.55E-07	0.008202085	0.001426815
160	0.009373205	0.009373205	0.052604106	0.09681532	0.002977361	0.001822766	0.018113263	0.0089600 6	0.015701216	0.003064402	0.033644684	1.59E-07	0.008065596	0.001382544
170	0.009449833	0.009449833	0.052805777	0.09721025	0.002963057	0.001862865	0.018467963	0.008933318	0.01574943	0.003066327	0.03399245	1.57E-07	0.008025269	0.00143749
180	0.009301283	0.009301283	0.052493819	0.09644316	0.002977329	0.001842273	0.017917981	0.008992844	0.015956042	0.003067264	0.03276245	1.54E-07	0.008096178	0.001400307
190	0.009159879	0.009159879	0.052147382	0.09570725	0.002957153	0.001834597	0.017768199	0.008961176	0.015875231	0.003068113	0.03173608	1.52E-07	0.00798115	0.001416937
200	0.009356844	0.009356844	0.052451955	0.096730776	0.002981261	0.001856978	0.01780262	0.008937399	0.015831843	0.003066699	0.03375046	1.55E-07	0.007933801	0.001407225

Configuration 6

```
model = Sequential()
model.add(LSTM(128, return_sequences=True, input_shape=(timesteps, data_dim)))
model.add(LSTM(512, return_sequences=True))  # returns a sequence of vectors o
model.add(LSTM(256))
model.add(Dense(10, activation='tanh'))
```

Optimiser: Adam

Epoch	Loss	Total MSE	Total MAE	Total RMSE	SkinTemp	SufPres	U10	V10	Humidity	Rainc	Rainnc	Snow	SolilTemp	SoilMoist
10	0.004861248	0.004861248	0.03944366	0.069722645	0.005914994	0.000329398	0.009495722	0.005798255	0.010924905	0.002882386	0.001092145	4.11E-07	0.010381158	0.001793105
20	0.004679357	0.004679357	0.038518958	0.06840583	0.005164234	0.001172217	0.010208915	0.004393526	0.013113426	0.002760861	0.001145572	1.45E-06	0.007642087	0.001191284
30	0.004957572	0.004957572	0.038694018	0.07041003	0.005889151	0.000486901	0.008682326	0.004472998	0.013831741	0.002761903	0.001977452	1.70E-06	0.009430925	0.002040616
40	0.00507524	0.00507524	0.039068443	0.07124072	0.005650543	0.000789923	0.007519924	0.005032941	0.017053653	0.002785851	0.001884586	4.07E-06	0.008590856	0.001440049
50	0.005087072	0.005087072	0.038979462	0.07132371	0.005033014	0.000862831	0.005792975	0.005101474	0.018799176	0.002707252	0.003188049	3.64E-06	0.008206386	0.001175915
60	0.00552473	0.00552473	0.040275603	0.074328534	0.005243165	0.001073437	0.008959366	0.005196353	0.019647105	0.002767109	0.001904001	2.91E-06	0.009282386	0.001171467
70	0.005317096	0.005317096	0.038691032	0.072918415	0.005122894	0.000661152	0.006575864	0.005003905	0.02204747	0.00273307	0.002071277	2.14E-06	0.007775141	0.001178043
80	0.005705704	0.005705704	0.03979722	0.07553611	0.00598003	0.001120292	0.00602005	0.004732224	0.025832651	0.002754844	0.002143773	1.12E-06	0.007844413	0.000627636
90	0.005596329	0.005596329	0.039931477	0.07480862	0.006125335	0.000976473	0.006965253	0.005054285	0.023538865	0.002781224	0.00187794	2.73E-06	0.007875808	0.000765378
100	0.00560969	0.00560969	0.040765302	0.07489786	0.00578459	0.000798913	0.007264938	0.005413828	0.022394286	0.002651491	0.002595422	1.15E-06	0.008085025	0.001107253
110	0.005791074	0.005791074	0.041494155	0.07609911	0.005958491	0.000891161	0.008146378	0.005405059	0.022985687	0.002654804	0.002573715	1.12E-06	0.008157928	0.0011364
120	0.005839428	0.005839428	0.040488072	0.07641615	0.005498123	0.000586752	0.009965678	0.004578863	0.021859875	0.00272078	0.002034539	3.62E-06	0.009041744	0.002104307
130	0.0056141	0.0056141	0.040148722	0.07492729	0.005726966	0.000644516	0.0088342	0.004869473	0.021823477	0.002690072	0.001819911	7.82E-07	0.008376119	0.001355481
140	0.005862871	0.005862871	0.041146528	0.07656938	0.005779817	0.000610084	0.009719716	0.005146749	0.021925665	0.002713303	0.002406256	1.11E-06	0.009213756	0.001112251
150	0.006034437	0.006034437	0.041646471	0.07768164	0.005413776	0.000699619	0.010571566	0.005566212	0.023203012	0.002656599	0.002032548	9.03E-07	0.009100131	0.001100009
160	0.006256695	0.006256695	0.042639437	0.079099275	0.005995432	0.000682049	0.010585511	0.005817674	0.025983535	0.002661423	0.001936571	1.09E-06	0.007898983	0.00100468
170	0.006039092	0.006039092	0.041357248	0.077711605	0.005563336	0.00064529	0.009050801	0.005724294	0.02585202	0.002673706	0.002142167	9.24E-07	0.007668052	0.001070335
180	0.006505292	0.006505292	0.042855272	0.08065539	0.00609435	0.000613023	0.009323246	0.006102398	0.028571125	0.00269548	0.001861212	1.09E-06	0.008636193	0.001154801
190	0.006498361	0.006498361	0.043327375	0.080612406	0.005838181	0.00076622	0.01317541	0.005344067	0.025583401	0.002708602	0.001799617	6.75E-07	0.008456492	0.001310943
200	0.00658723	0.00658723	0.043192499	0.08116175	0.005423089	0.000614523	0.012505858	0.006891101	0.02555141	0.002732478	0.001839258	9.48E-07	0.00910425	0.001209379
210	0.006271544	0.006271544	0.04258063	0.07919308	0.005307211	0.000691933	0.011456299	0.006108502	0.025443042	0.00269528	0.001933951	8.02E-07	0.007895343	0.001183081
220	0.006573652	0.006573652	0.043098692	0.08107806	0.005671613	0.000602746	0.012175292	0.006891576	0.026732253	0.002727112	0.001671284	1.01E-06	0.007899092	0.001364546
230	0.006131167	0.006131167	0.041611716	0.07830178	0.005810751	0.000579029	0.008965684	0.005897127	0.026703868	0.002757207	0.001738031	1.35E-06	0.007426896	0.001431728
240	0.006620094	0.006620094	0.043428923	0.08136396	0.005854594	0.0007562	0.010440787	0.007347617	0.028265389	0.002752474	0.001651034	1.26E-06	0.007588849	0.001542742
250	0.006503075	0.006503075	0.04342466	0.08064165	0.005883333	0.000817173	0.009992057	0.005917899	0.028512111	0.002737743	0.002189918	2.31E-06	0.007520604	0.001457602
260	0.006647514	0.006647514	0.043570892	0.08153229	0.005682848	0.000658339	0.011542152	0.00696189	0.028445698	0.002799702	0.001934944	2.01E-06	0.007051103	0.001396461
270	0.006404637	0.006404637	0.042707364	0.08002897	0.005133099	0.000604966	0.009835185	0.006701052	0.028402895	0.002759583	0.001828324	1.69E-06	0.007214397	0.001565176

Optimiser: SGD

Epoch	Loss	Total MSE	Total MAE	Total RMSE	SkinTemp	SufPres	U10	V10	Humidity	Rainc	Rainnc	Snow	SolilTemp	SoilMoist
10	0.018276248	0.018276248	0.097509523	0.13518967	0.006969704	0.026743824	0.019782048	0.024171676	0.06948714	0.00442288	0.00369892	0.001489522	0.025276568	0.000720207
20	0.010491723	0.010491723	0.07367275	0.10242911	0.003016563	0.017683031	0.016468085	0.014004315	0.026875837	0.003955931	0.002790341	0.000800964	0.018683763	0.000638397
30	0.007523045	0.007523045	0.061365407	0.08673548	0.002516259	0.009656541	0.012383327	0.012098094	0.014679401	0.00391121	0.00303135	0.000535528	0.015856147	0.000562598
40	0.006522759	0.006522759	0.055906084	0.0807636	0.002501436	0.005692685	0.011518328	0.010999072	0.012009272	0.003830122	0.003196626	0.000397381	0.014567475	0.000515194
50	0.005952916	0.005952916	0.052568104	0.07715514	0.002491464	0.004200898	0.010698189	0.010086523	0.010824773	0.003720171	0.003202032	0.000288901	0.013505651	0.000510554
60	0.005502095	0.005502095	0.050302197	0.07417612	0.002493842	0.003399132	0.010006282	0.00934145	0.01026063	0.003608489	0.003223685	0.000217228	0.011954516	0.000515698
70	0.005198917	0.005198917	0.048420096	0.07210351	0.002447826	0.002897133	0.009454106	0.008534861	0.009890192	0.003515361	0.003151641	0.000157288	0.01141835	0.00052241
80	0.004930477	0.004930477	0.047142384	0.070217356	0.002428205	0.002494656	0.009529544	0.008143179	0.009282479	0.00343884	0.003150833	0.000117734	0.010209189	0.000510106
90	0.00474864	0.00474864	0.045854159	0.068910375	0.002404724	0.00229572	0.009298923	0.007470253	0.009175058	0.003374076	0.003054555	8.73E-05	0.0098244	0.000501394
100	0.004560462	0.004560462	0.044633655	0.06753119	0.002431744	0.002158779	0.009102077	0.006859458	0.009048901	0.003310385	0.003057649	6.53E-05	0.009091093	0.000479187
110	0.004453985	0.004453985	0.043926356	0.06673818	0.002420098	0.002146414	0.008998319	0.006655634	0.00881492	0.003272729	0.002980084	4.87E-05	0.008735539	0.00046744
120	0.004355957	0.004355957	0.043357451	0.06599967	0.002534212	0.002182413	0.008570047	0.006454783	0.00912948	0.00323225	0.0030163	3.70E-05	0.007952559	0.000450506
130	0.004116224	0.004116224	0.04188745	0.06415781	0.002478839	0.002191433	0.006959129	0.006509389	0.008898494	0.003178422	0.003018756	2.80E-05	0.007458258	0.000441562
140	0.004153562	0.004153562	0.041957674	0.06444813	0.00259901	0.002093182	0.007394831	0.006686883	0.008982712	0.00314815	0.002951023	2.05E-05	0.007216162	0.000443171
150	0.004177298	0.004177298	0.042055531	0.06463202	0.002789594	0.002019832	0.007554862	0.006774078	0.009240215	0.003113639	0.0030215	1.53E-05	0.006796531	0.00044743
160	0.004201576	0.004201576	0.042109783	0.06481956	0.002856683	0.002138621	0.007472065	0.007279143	0.009165541	0.003059278	0.002941815	1.14E-05	0.006627113	0.000464072
170	0.004133309	0.004133309	0.04139621	0.064290814	0.002775918	0.002202021	0.007054817	0.007569754	0.009055813	0.003012055	0.002859891	8.68E-06	0.006326685	0.000467455
180	0.004200863	0.004200863	0.041605329	0.06481406	0.002906216	0.002147288	0.007198409	0.007529963	0.009703296	0.002991537	0.003012214	6.85E-06	0.006029691	0.000483169
190	0.00416025	0.00416025	0.041214385	0.064500004	0.003182824	0.002058711	0.008289297	0.006892907	0.009314587	0.002962265	0.002879161	5.20E-06	0.005505256	0.000512291
200	0.003944039	0.003944039	0.039649268	0.062801585	0.003082931	0.002042752	0.006270979	0.006971994	0.009410158	0.002934188	0.002997862	4.16E-06	0.005179504	0.000545865
210	0.003935014	0.003935014	0.039518267	0.06272969	0.003195882	0.002144509	0.006549131	0.007374453	0.009164603	0.002912455	0.003100918	3.50E-06	0.004341848	0.00056284
220	0.003844938	0.003844938	0.038622109	0.06200757	0.003307656	0.002010803	0.006408483	0.006311056	0.009872749	0.002897357	0.002992446	2.84E-06	0.004040619	0.000605371
230	0.003699844	0.003699844	0.037537898	0.06082634	0.003271054	0.002112675	0.005394089	0.006311009	0.009881492	0.002878811	0.003070845	2.39E-06	0.003427306	0.000648767
240	0.003880733	0.003880733	0.038505509	0.062295526	0.003460772	0.002177067	0.006689046	0.0053539	0.010723675	0.002871775	0.004023603	2.22E-06	0.00284235	0.000662919
250	0.003972302	0.003972302	0.038337381	0.063026205	0.003516005	0.002096369	0.005313642	0.004716563	0.01118155	0.002896062	0.006496077	2.29E-06	0.002806731	0.000697734
260	0.004139672	0.004139672	0.039369135	0.064340286	0.003877571	0.00225446	0.006052786	0.004741847	0.011367044	0.002885173	0.00643688	1.89E-06	0.002993184	0.000785878
270	0.004190736	0.004190736	0.039129027	0.0647359	0.004579625	0.002133449	0.005444672	0.00423032	0.01055951	0.002900269	0.008351362	1.71E-06	0.002965335	0.000741111

Optimiser: Adaptive-SGD

Epoch	Loss	Total MSE	Total MAE	Total RMSE	SkinTemp	SufPres	U10	V10	Humidity	Rainc	Rainnc	Snow	SolilTemp	SoilMoist
10	0.004721519	0.004721519	0.047033001	0.06871331	0.003446905	0.004146618	0.008477717	0.007225516	0.010672996	0.003305997	0.003200098	1.78E-05	0.006056502	0.000665013
20	0.003832776	0.003832776	0.039561192	0.06190943	0.002772896	0.00117942	0.006019535	0.007741648	0.008845065	0.003020993	0.002573667	2.08E-06	0.005304109	0.000868354
30	0.003736321	0.003736321	0.03836067	0.061125454	0.002899948	0.001514204	0.007505603	0.005178714	0.009777498	0.002924363	0.002142681	7.26E-07	0.004254171	0.001165303
40	0.004015269	0.004015269	0.039578538	0.06336615	0.003516158	0.001237543	0.005074994	0.005322457	0.010736201	0.002868199	0.004398242	3.29E-07	0.005469449	0.001529115
50	0.00495179	0.00495179	0.043568926	0.07036895	0.003494516	0.000757552	0.007231866	0.004702077	0.01039515	0.002895487	0.010139717	2.78E-07	0.007693852	0.002207404
60	0.005919204	0.005919204	0.044593059	0.076936364	0.003094366	0.000681636	0.00666348	0.004229921	0.010230338	0.002862008	0.020337282	1.83E-07	0.009211532	0.001881297
70	0.006086255	0.006086255	0.04457782	0.07801445	0.003255958	0.000693281	0.006377057	0.003788839	0.010456663	0.002852097	0.023954188	1.78E-07	0.00783071	0.001653581
80	0.006207063	0.006207063	0.045426681	0.07878492	0.003328596	0.000726024	0.00650368	0.003854653	0.010383588	0.00285964	0.025049958	1.60E-07	0.00812755	0.001236785
90	0.00645173	0.00645173	0.045264536	0.08032267	0.003370777	0.000769425	0.005717801	0.003847579	0.010174222	0.002862031	0.029252822	1.59E-07	0.007313771	0.001208711
100	0.006160638	0.006160638	0.045465324	0.078489736	0.003350921	0.000797339	0.006462486	0.00392552	0.009869345	0.002854541	0.026009997	1.38E-07	0.007046655	0.001289437
110	0.005758616	0.005758616	0.044171636	0.07588555	0.00322839	0.000826149	0.006446043	0.004000034	0.009771802	0.002849549	0.022472944	1.24E-07	0.00658609	0.001405041
120	0.005224534	0.005224534	0.042149226	0.07228094	0.003097744	0.000831267	0.006266975	0.003825425	0.009591435	0.002832977	0.017944261	1.06E-07	0.006400062	0.001455089
130	0.00582586	0.00582586	0.044216623	0.076327324	0.003192985	0.000823317	0.006675315	0.003819537	0.009579162	0.002835191	0.023588413	1.13E-07	0.00618979	0.00155478
140	0.005090046	0.005090046	0.041909236	0.07134456	0.003041408	0.000838331	0.006771382	0.003861208	0.009513923	0.00283068	0.016503397	1.02E-07	0.005975151	0.001564879
150	0.00512218	0.00512218	0.042025708	0.07156942	0.003023951	0.000823596	0.006955518	0.003839195	0.009487156	0.002830792	0.016728964	1.00E-07	0.005933779	0.001598754
160	0.005368253	0.005368253	0.043068953	0.07326836	0.003030183	0.000830089	0.007159661	0.00389449	0.0941207	0.002833336	0.018976906	1.03E-07	0.00594272	0.001602975
170	0.005234579	0.005234579	0.042567282	0.07235039	0.0030158	0.000840259	0.00725017	0.003856893	0.009395935	0.002832124	0.017632648	1.00E-07	0.005877551	0.001644306
180	0.00523855	0.00523855	0.042581154	0.07237782	0.003009504	0.000832571	0.007229467	0.003867216	0.009366764	0.002831627	0.017769467	9.98E-08	0.005816042	0.001662737
190	0.005212191	0.005212191	0.042646196	0.072195515	0.002996027	0.000842756	0.007429308	0.003879517	0.009338019	0.002831891	0.017316557	9.91E-08	0.005806792	0.001680946
200	0.005086459	0.005086459	0.04208115	0.071319416	0.002976604	0.000841701	0.0072846	0.003864064	0.009331403	0.002830462	0.016256763	9.67E-08	0.005767313	0.001711585
210	0.005217077	0.005217077	0.04263928	0.07222933	0.002995869	0.000839122	0.007417573	0.003878315	0.009336223	0.002831754	0.017383272	9.86E-08	0.005792771	0.001695778
220	0.005073324	0.005073324	0.042040696	0.07122727	0.002973147	0.000841011	0.007333378	0.003857844	0.009328518	0.002830188	0.016108112	9.62E-08	0.005746737	0.001714204
230	0.00510461	0.00510461	0.042171748	0.07144656	0.002977682	0.000840755	0.007347113	0.003859553	0.009325779	0.002830497	0.016401079	9.66E-08	0.005750264	0.001713282
240	0.005125181	0.005125181	0.042266482	0.071590364	0.002979967	0.000841667	0.007387831	0.003861311	0.009324011	0.002830677	0.01656632	9.69E-08	0.005748868	0.001711057
250	0.005105088	0.005105088	0.0421926	0.071449906	0.002977589	0.000841627	0.007368818	0.003859761	0.009317897	0.00283065	0.016388323	9.66E-08	0.005746803	0.001719317
260	0.005111882	0.005111882	0.04220958	0.07149743	0.002977485	0.000841095	0.007372857	0.003860826	0.009319299	0.002830614	0.016458783	9.67E-08	0.005743424	0.001714341
270	0.00510428	0.00510428	0.042173617	0.07144424	0.002976245	0.000841667	0.007359031	0.003859111	0.009317456	0.002830601	0.016402742	9.65E-08	0.005739713	0.001716135

Appendix 3: Evaluation Results of MIMO-TCN variance for Historical Weather Data

The following sample screenshots show the learning process of MIMO-TCN for each configuration and controls. The X-axis represents the number of epochs and the Y-axis represents the MSE for relevant epoch in each graph. Finally, the saved optimal model is evaluated (i.e. the least MSE model out of 200 epochs) and the results are shown in the top of each graph. These evaluation results consist of MSE, MAE, RMSE, and EV respectively.

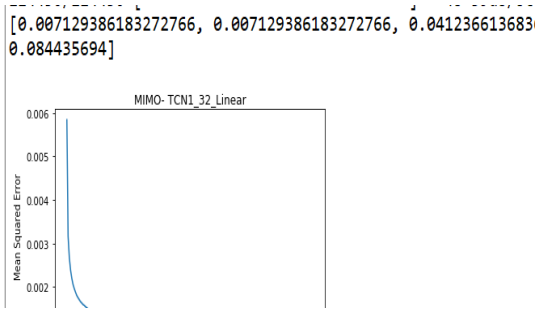

i) Filter 32- TCN 1- Linear activation

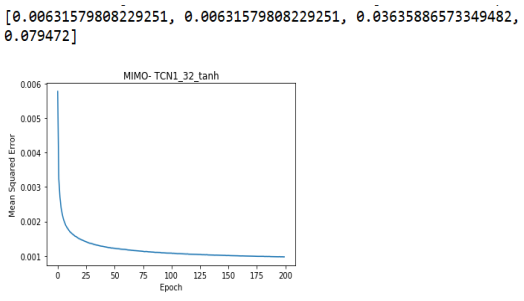

ii) Filter 32- TCN 1- tanh activation

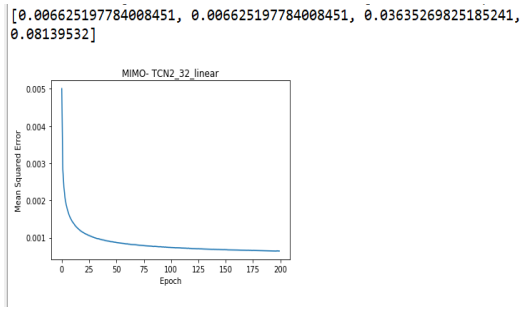

iii) Filter 32- TCN 2- Linear activation

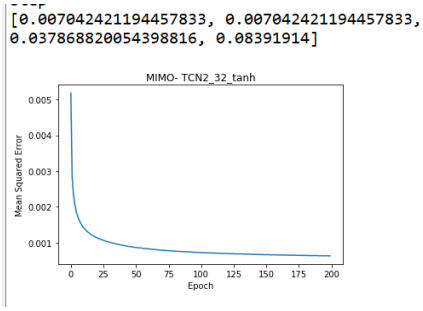

iv) Filter 32- TCN 2- tanh activation

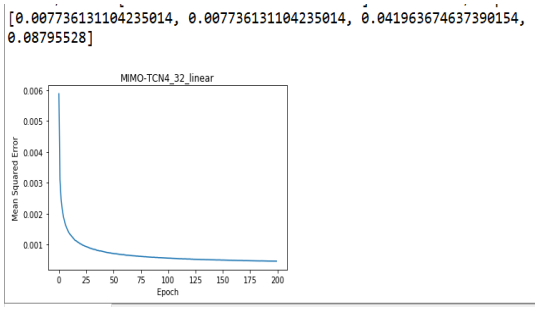

v) Filter 32- TCN 4- Linear activation

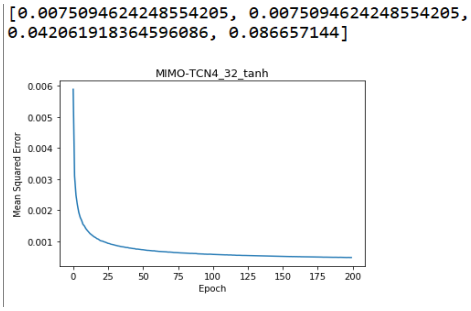

vi) Filter 32- TCN 4- tanh activation

[0.00538064161572498, 0.00538064161572498, 0.03253103352288926, 0.07335285]

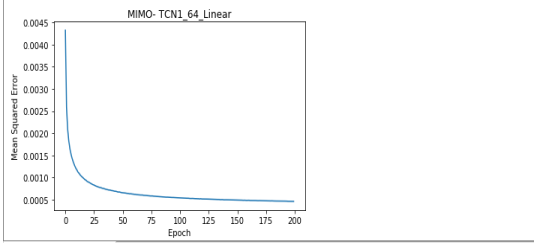

vii) Filter 64- TCN 1- Linear activation

[0.005977791918326916, 0.005977791918326916, 0.033834162966757945, 0.07731618]

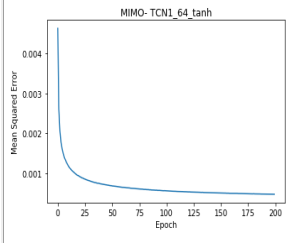

viii) Filter 64- TCN 1- tanh activation

[0.006608715858563737656, 0.006608715858563737656, 0.03635232870683054, 0.08129401]

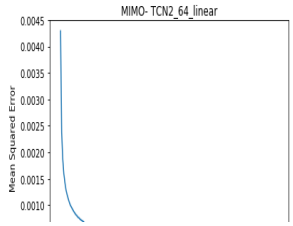

ix) Filter 64- TCN 2- Linear activation

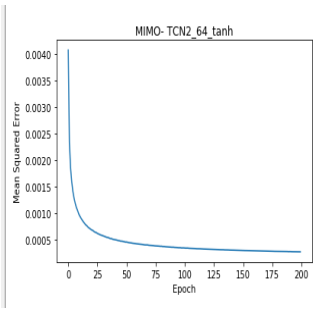

x) Filter 64- TCN 2- tanh activation

[0.009262335269352646, 0.009262335269352646, 0.043837697783044825, 0.096241035]

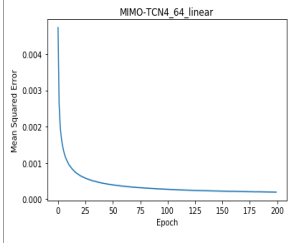

xi) Filter 64- TCN 4- Linear activation

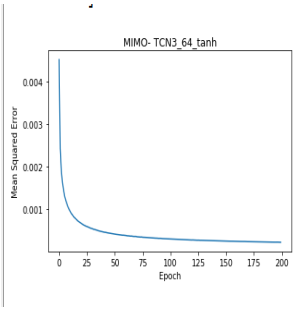

xii) Filter 64- TCN 3- tanh activation

[0.006594511521064712, 0.006594511521064712, 0.03606189111661851, 0.081206605]

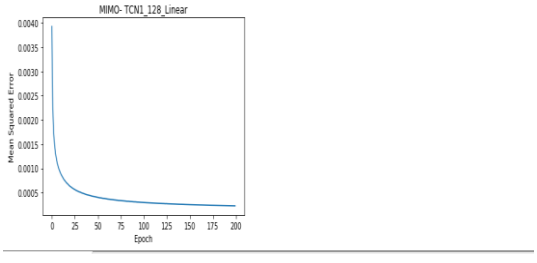

xiii) Filter 128- TCN 1- Linear activation

[0.00575911592100956 5, 0.00575911592100956 5, 0.035995619609828285, 0.075888835]

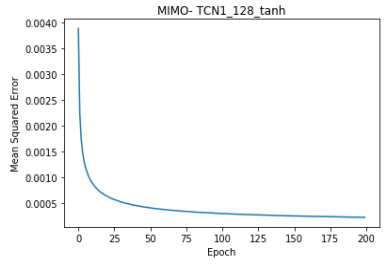

xiv) Filter 128- TCN 1- tanh activation

[0.007439890002745153, 0.007439890002745153, 0.037972729685604445, 0.0862548]

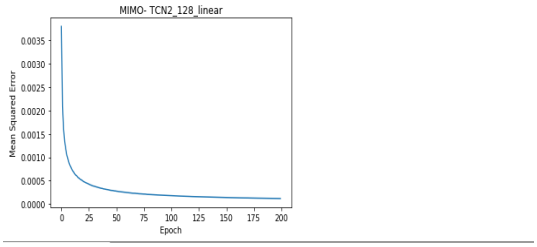

xv) Filter 128- TCN 2- Linear activation

[0.00721856350658153, 0.00721856350658153, 0.03724397914652587, 0.08496214]

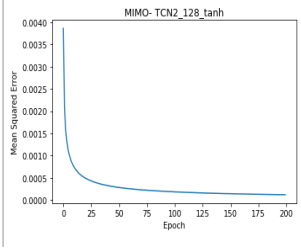

xvi) Filter 128- TCN 2- tanh activation

Explained Variance -0.365826

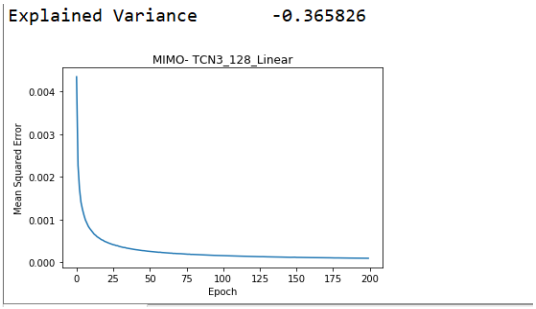

xvii) Filter 128- TCN 3- Linear activation

[0.007603900828592027, 0.007603900828592027, 0.04101575332640456, 0.08720034]

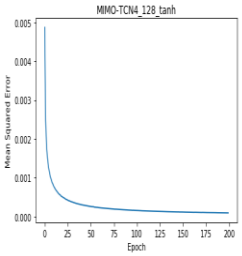

xviii) Filter 128- TCN 4- tanh activation

[0.007088403301956372, 0.007088403301956372, 0.03720950693412867, 0.084192656]

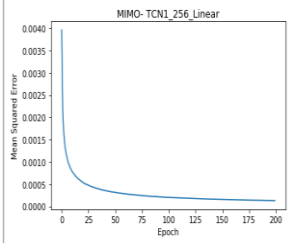

xix) Filter 256- TCN 1- Linear activation

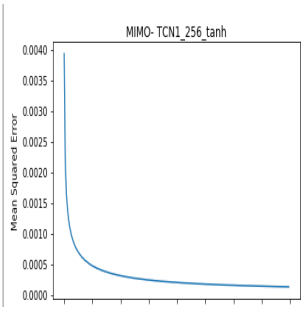

xx) Filter 256- TCN 1- tanh activation

[0.007366489552418335, 0.007366489552418335, 0.038411366446159355, 0.08582826]

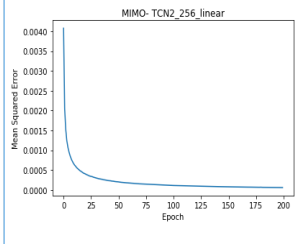

xxi) Filter 256- TCN 2- linear activation

0.08190166]

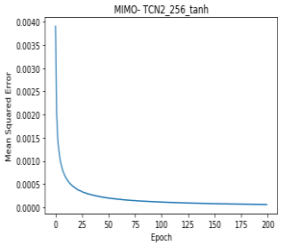

xxii) Filter 256- TCN 2- tanh activation

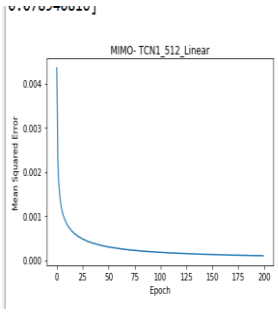

xxiii) Filter 512- TCN 1- Linear activation

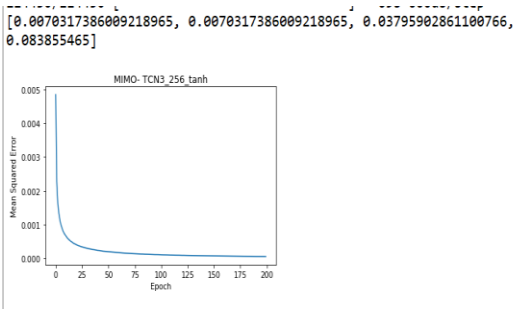

xxiv) Filter 256- TCN 3- tanh activation

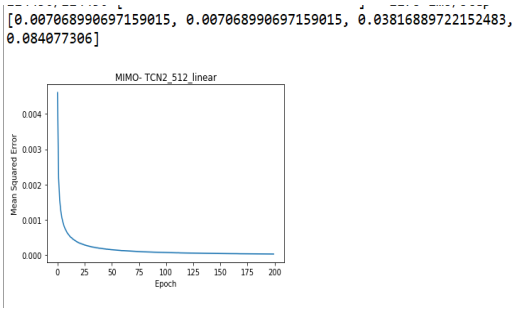

xxv) Filter 512- TCN 2- Linear activation

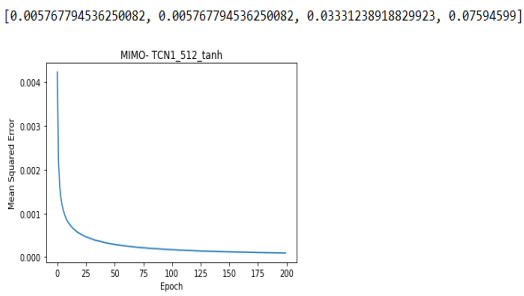

xxvi) Filter 512- TCN 1- tanh activation

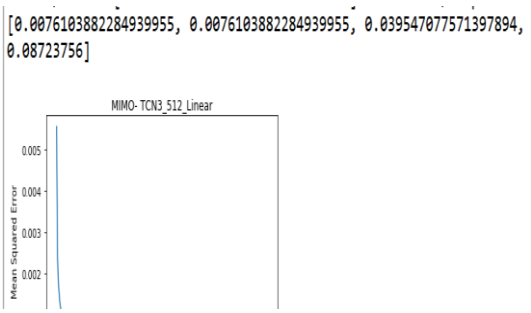

xxvii) Filter 512- TCN 3- Linear activation

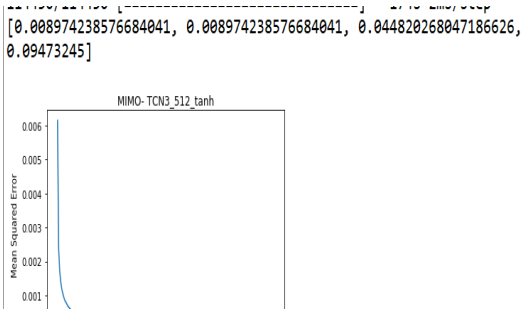

xxviii) Filter 512- TCN 3- tanh activation

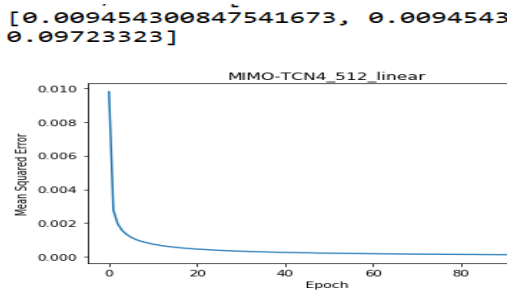

xxix) Filter 512- TCN 4- Linear activation

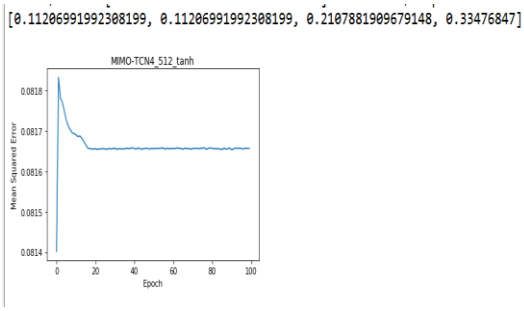

xxx) Filter 512- TCN 4- tanh activation

Appendix 4: Evaluation Results of MISO-LSTM variance for Historical Weather Data

The configuration 1 evaluation results with Adam and SGD is given below out of different configurations and controls.

Configuration 1- Optimiser: Adam

Parameter: Surface Temperature

Epoch	Loss	Total MSE	Total MAE	Total RMSE
10	0.005949996	0.005949996	0.061012667	0.07713621
20	0.006669067	0.006669067	0.062296557	0.08166436
30	0.006621725	0.006621725	0.06267316	0.08137398
40	0.008510581	0.008510581	0.071322167	0.092252806
50	0.007421528	0.007421528	0.068478891	0.086148284
60	0.007615929	0.007615929	0.06793304	0.08726929
70	0.007398951	0.007398951	0.066690263	0.086017154
80	0.010540888	0.010540888	0.082478765	0.10266882
90	0.010759036	0.010759036	0.081671994	0.10372577
100	0.011908467	0.011908467	0.086473292	0.10912592
110	0.012259442	0.012259442	0.086049549	0.110722356
120	0.011782905	0.011782905	0.085788655	0.10854909
130	0.011622726	0.011622726	0.085487085	0.10780875
140	0.012107984	0.012107984	0.087014309	0.110036284
150	0.013629492	0.013629492	0.091756207	0.11674541
160	0.016383952	0.016383952	0.099303437	0.12799981
170	0.013637352	0.013637352	0.093130847	0.116779074
180	0.015278167	0.015278167	0.097568961	0.123604886
190	0.016908894	0.016908894	0.103958764	0.1300342
200	0.016227991	0.016227991	0.102737623	0.12738913
210	0.017363762	0.017363762	0.103800934	0.13177162
220	0.017813487	0.017813487	0.107937534	0.13346718
230	0.020838909	0.020838909	0.115033542	0.14435688
240	0.018435379	0.018435379	0.109100939	0.13577695
250	0.018831725	0.018831725	0.111799259	0.13722873
260	0.018090772	0.018090772	0.1095264	0.13450193
270	0.017412864	0.017412864	0.107563619	0.13195781
280	0.020766861	0.020766861	0.115774665	0.14410712
290	0.019432888	0.019432888	0.112994674	0.1394019
300	0.021243546	0.021243546	0.11703047	0.14575166
310	0.02028816	0.02028816	0.114973774	0.14243652
320	0.022218313	0.022218313	0.12036205	0.14905809
330	0.022435345	0.022435345	0.120221908	0.14978433
340	0.020060253	0.020060253	0.116958266	0.14163423
350	0.02176722	0.02176722	0.121942633	0.14753719
360	0.022346641	0.022346641	0.121822878	0.14948793
370	0.024290147	0.024290147	0.125863877	0.15585296
380	0.023724295	0.023724295	0.126046738	0.15402693
390	0.023380137	0.023380137	0.123726508	0.15290564
400	0.026677834	0.026677834	0.13242576	0.1633335
410	0.027170914	0.027170914	0.133955414	0.16483602
420	0.026066877	0.026066877	0.130570805	0.1614524
430	0.026628509	0.026628509	0.133147706	0.16318244
440	0.027763508	0.027763508	0.135335854	0.16662385
450	0.027977697	0.027977697	0.136037517	0.16726534

Parameter: Surface Pressure

Epoch	Loss	Total MSE	Total MAE	Total RMSE
10	0.000690402	0.000690402	0.02165334	0.026275504
20	0.000333494	0.000333494	0.011648562	0.01826181
30	0.000197254	0.000197254	0.008853848	0.014044732
40	0.000213828	0.000213828	0.009855207	0.01462285
50	0.000233942	0.000233942	0.009884995	0.015295154
60	0.000134118	0.000134118	0.007370031	0.011580916
70	0.000166849	0.000166849	0.008154344	0.012917004
80	0.000141348	0.000141348	0.007790674	0.011888968
90	0.000100625	0.000100625	0.007031562	0.010031208
100	0.000101427	0.000101427	0.007286195	0.010071112
110	9.15E-05	9.15E-05	0.00675089	0.009566846
120	8.40E-05	8.40E-05	0.006534913	0.009164348
130	8.82E-05	8.82E-05	0.006793138	0.009392719
140	0.000104186	0.000104186	0.007303394	0.010207155
150	8.16E-05	8.16E-05	0.006567715	0.009032744
160	8.45E-05	8.45E-05	0.006455654	0.009192157
170	8.37E-05	8.37E-05	0.006488102	0.009148344
180	9.75E-05	9.75E-05	0.006997497	0.009873824
190	9.00E-05	9.00E-05	0.006841374	0.009488388
200	0.00010173	0.00010173	0.007017038	0.010086111
210	0.000103598	0.000103598	0.00722978	0.010178293
220	0.000104705	0.000104705	0.007266599	0.010232571
230	0.000110318	0.000110318	0.007392123	0.010503238
240	0.000120427	0.000120427	0.007695287	0.010973943
250	0.000118382	0.000118382	0.007915517	0.010880365
260	0.000120671	0.000120671	0.008018623	0.010985049
270	0.000128413	0.000128413	0.008162894	0.011331927
280	0.000124954	0.000124954	0.007868015	0.011178284
290	0.00011636	0.00011636	0.008053829	0.010787022
300	0.000125008	0.000125008	0.00806844	0.011180713
310	0.000132903	0.000132903	0.008628623	0.011528343
320	0.000115025	0.000115025	0.007769055	0.010724952
330	0.000121052	0.000121052	0.008230629	0.011002365
340	0.000107613	0.000107613	0.007821992	0.010373653
350	0.000122282	0.000122282	0.00820069	0.011058136
360	0.000130984	0.000130984	0.008607202	0.011444821
370	0.000117248	0.000117248	0.008034547	0.010828122
380	0.000113428	0.000113428	0.007974928	0.010650263
390	0.000121809	0.000121809	0.008290595	0.011036731
400	0.000127404	0.000127404	0.008517991	0.01128732
410	0.000131686	0.000131686	0.008574785	0.011475459
420	0.000132969	0.000132969	0.008709981	0.011531211
430	0.000137408	0.000137408	0.008857521	0.011722121
440	0.000130364	0.000130364	0.008560967	0.011417687
450	0.00013509	0.00013509	0.008661094	0.011622813

Parameter: X-component of Wind

Epoch	Loss	Total MSE	Total MAE	Total RMSE
10	0.003389316	0.003389316	0.045142062	0.058217827
20	0.004270391	0.004270391	0.049317757	0.06534823
30	0.003008846	0.003008846	0.040997274	0.054852948
40	0.003510667	0.003510667	0.043949722	0.059250884
50	0.003446197	0.003446197	0.043948359	0.05870432
60	0.003989131	0.003989131	0.047425653	0.06315956
70	0.003592478	0.003592478	0.044823572	0.059937287
80	0.00356253	0.00356253	0.044705315	0.059686933
90	0.003260346	0.003260346	0.042680823	0.05709944
100	0.003337384	0.003337384	0.044141926	0.057770092
110	0.003527082	0.003527082	0.044727496	0.059389245
120	0.003269211	0.003269211	0.043723805	0.05717701
130	0.003179259	0.003179259	0.042563572	0.05638492
140	0.003470579	0.003470579	0.044634678	0.058911618
150	0.003630232	0.003630232	0.045403515	0.060251407
160	0.003419337	0.003419337	0.044747809	0.058475096
170	0.003395028	0.003395028	0.044181027	0.05826687
180	0.003288102	0.003288102	0.044246518	0.05734197
190	0.003114719	0.003114719	0.042661137	0.055809665
200	0.00325875	0.00325875	0.043508826	0.057085466
210	0.00338112	0.00338112	0.04459773	0.0581474
220	0.003308592	0.003308592	0.044207888	0.05752036
230	0.003308252	0.003308252	0.043897799	0.057517402
240	0.003451407	0.003451407	0.044735708	0.058748674
250	0.003468584	0.003468584	0.04463756	0.058894686
260	0.003758195	0.003758195	0.047920481	0.06130412
270	0.003610205	0.003610205	0.045800371	0.060084976

Parameter: Y-Component of Wind

Epoch	Loss	Total MSE	Total MAE	Total RMSE
10	0.00533791	0.00533791	0.054178461	0.073061004
20	0.005287072	0.005287072	0.055025631	0.07271226
30	0.004969483	0.004969483	0.053334031	0.070494555
40	0.004920537	0.004920537	0.053249888	0.07014654
50	0.004593745	0.004593745	0.050534164	0.067777164
60	0.005163534	0.005163534	0.05502913	0.071857736
70	0.004476656	0.004476656	0.049678988	0.066907816
80	0.004683924	0.004683924	0.051424607	0.06843921
90	0.004784591	0.004784591	0.052208682	0.06917074
100	0.005269012	0.005269012	0.056440138	0.07258796
110	0.004755291	0.004755291	0.052081654	0.06895862
120	0.004780227	0.004780227	0.052339138	0.06913918
130	0.004709613	0.004709613	0.051877658	0.06862662
140	0.004849132	0.004849132	0.052919027	0.06963571
150	0.00473881	0.00473881	0.052223974	0.06883902
160	0.005019185	0.005019185	0.05412081	0.07084621
170	0.004795064	0.004795064	0.052506465	0.0692464
180	0.004810877	0.004810877	0.05256588	0.06936049
190	0.004876858	0.004876858	0.052910741	0.06983451
200	0.00474291	0.00474291	0.052042921	0.068868786
210	0.004806783	0.004806783	0.052460807	0.06933097
220	0.004718274	0.004718274	0.051844828	0.06868969
230	0.004756036	0.004756036	0.052173015	0.06896401
240	0.005095623	0.005095623	0.054312322	0.07138363
250	0.004854841	0.004854841	0.052681366	0.06967669
260	0.004897482	0.004897482	0.052929836	0.069982015
270	0.004966251	0.004966251	0.053435151	0.07047163
280	0.004996868	0.004996868	0.053503513	0.07068853
290	0.004891579	0.004891579	0.052778757	0.06993982
300	0.00484442	0.00484442	0.052655972	0.06960186
310	0.004912006	0.004912006	0.053005224	0.070085704
320	0.004925566	0.004925566	0.053155832	0.07018238
330	0.004837116	0.004837116	0.052536508	0.069549374
340	0.004831143	0.004831143	0.052455318	0.06950642
350	0.004908422	0.004908422	0.052988346	0.070060134
360	0.004987215	0.004987215	0.053511272	0.07062022
370	0.004968903	0.004968903	0.053430709	0.07049044
380	0.004893579	0.004893579	0.052989215	0.06995412
390	0.004863535	0.004863535	0.052718627	0.06973904
400	0.004792861	0.004792861	0.052303982	0.06923049
410	0.004928608	0.004928608	0.053308347	0.07020404
420	0.004793899	0.004793899	0.052457826	0.06923799
430	0.004869406	0.004869406	0.05300661	0.06978113
440	0.004836523	0.004836523	0.052685028	0.06954511
450	0.004808989	0.004808989	0.052580598	0.069346875
460	0.004729356	0.004729356	0.052095129	0.06877031
470	0.004722632	0.004722632	0.052082597	0.068721406
480	0.004803591	0.004803591	0.052622628	0.069307946
490	0.004749246	0.004749246	0.052268339	0.06891477
500	0.004827775	0.004827775	0.052842127	0.069482185

Parameter: Humidity

Epoch	Loss	Total MSE	Total MAE	Total RMSE
10	0.010912588	0.010912588	0.077246315	0.10446333
20	0.012972375	0.012972375	0.083939431	0.11389633
30	0.014264975	0.014264975	0.090206464	0.11943606
40	0.016225185	0.016225185	0.095517711	0.12737812
50	0.015265159	0.015265159	0.093037432	0.12355225
60	0.014885264	0.014885264	0.091121534	0.12200518
70	0.013505588	0.013505588	0.087147024	0.116213545
80	0.015945124	0.015945124	0.09572755	0.126274
90	0.014434802	0.014434802	0.091270487	0.12014492
100	0.015237295	0.015237295	0.092815648	0.12343944
110	0.014341952	0.014341952	0.090448285	0.11975788
120	0.014343267	0.014343267	0.091020315	0.119763374
130	0.015208528	0.015208528	0.093823256	0.12332286
140	0.016464668	0.016464668	0.095682714	0.12831472
150	0.014844768	0.014844768	0.092097699	0.12183911
160	0.014971771	0.014971771	0.09172761	0.12235919
170	0.014655323	0.014655323	0.090432663	0.12105917
180	0.015700283	0.015700283	0.093610147	0.12530077
190	0.016760678	0.016760678	0.097115987	0.12946305
200	0.016865415	0.016865415	0.097984207	0.12986691
210	0.018218465	0.018218465	0.101471112	0.13497579
220	0.018295028	0.018295028	0.100791662	0.1352591
230	0.018236419	0.018236419	0.100417575	0.1350423
240	0.018282912	0.018282912	0.101364188	0.13521431
250	0.018391685	0.018391685	0.101682848	0.13561594
260	0.017498086	0.017498086	0.098680942	0.13228033
270	0.017923545	0.017923545	0.100377425	0.13387884
280	0.017703785	0.017703785	0.099141092	0.13305558
290	0.017728257	0.017728257	0.099308672	0.13314751
300	0.018516302	0.018516302	0.100857319	0.13607462
310	0.01914127	0.01914127	0.103407458	0.13835199
320	0.018395369	0.018395369	0.10048095	0.13562953
330	0.019012017	0.019012017	0.102686827	0.13788407
340	0.01823599	0.01823599	0.100592727	0.1350407
350	0.018791182	0.018791182	0.103062138	0.13708092
360	0.018929163	0.018929163	0.102279001	0.13758329
370	0.017946283	0.017946283	0.100098582	0.13396373
380	0.018068424	0.018068424	0.100936303	0.13441883
390	0.017581685	0.017581685	0.099799731	0.13259594

Parameter: Convective Rain

Epoch	Loss	Total MSE	Total MAE	Total RMSE
10	0.003167429	0.003167429	0.007220125	0.056279916
20	0.003167429	0.003167429	0.007220125	0.056279916
30	0.003167429	0.003167429	0.007220125	0.056279916
40	0.003167429	0.003167429	0.007220125	0.056279916
50	0.003167429	0.003167429	0.007220125	0.056279916
60	0.003167429	0.003167429	0.007220125	0.056279916
70	0.003167429	0.003167429	0.007220125	0.056279916
80	0.003167429	0.003167429	0.007220125	0.056279916
90	0.003167429	0.003167429	0.007220125	0.056279916
100	0.003167429	0.003167429	0.007220125	0.056279916
110	0.003167429	0.003167429	0.007220125	0.056279916
120	0.003167429	0.003167429	0.007220125	0.056279916
130	0.003167429	0.003167429	0.007220125	0.056279916
140	0.003167429	0.003167429	0.007220125	0.056279916
150	0.003167429	0.003167429	0.007220125	0.056279916
160	0.003167429	0.003167429	0.007220125	0.056279916
170	0.003167429	0.003167429	0.007220125	0.056279916
180	0.003167429	0.003167429	0.007220125	0.056279916
190	0.003167429	0.003167429	0.007220125	0.056279916
200	0.003167429	0.003167429	0.007220125	0.056279916
210	0.003167429	0.003167429	0.007220125	0.056279916
220	0.003167429	0.003167429	0.007220125	0.056279916
230	0.003167429	0.003167429	0.007220125	0.056279916
240	0.003167429	0.003167429	0.007220125	0.056279916
250	0.003167429	0.003167429	0.007220125	0.056279916
260	0.003167429	0.003167429	0.007220125	0.056279916
270	0.003167429	0.003167429	0.007220125	0.056279916
280	0.003167429	0.003167429	0.007220125	0.056279916
290	0.003167429	0.003167429	0.007220125	0.056279916
300	0.003167429	0.003167429	0.007220125	0.056279916
310	0.003167429	0.003167429	0.007220125	0.056279916
320	0.003167429	0.003167429	0.007220125	0.056279916
330	0.003167429	0.003167429	0.007220125	0.056279916
340	0.003167429	0.003167429	0.007220125	0.056279916
350	0.003167429	0.003167429	0.007220125	0.056279916
360	0.003167429	0.003167429	0.007220125	0.056279916
370	0.003167429	0.003167429	0.007220125	0.056279916
380	0.003167429	0.003167429	0.007220125	0.056279916
390	0.003167429	0.003167429	0.007220125	0.056279916
400	0.003167429	0.003167429	0.007220125	0.056279916
410	0.003167429	0.003167429	0.007220125	0.056279916
420	0.003167429	0.003167429	0.007220125	0.056279916
430	0.003167429	0.003167429	0.007220125	0.056279916
440	0.003167429	0.003167429	0.007220125	0.056279916
450	0.003167429	0.003167429	0.007220125	0.056279916
460	0.003167429	0.003167429	0.007220125	0.056279916
470	0.003167429	0.003167429	0.007220125	0.056279916

Parameter: Non-convective Rain

Epoch	Loss	Total MSE	Total MAE	Total RMSE
10	0.000519068	0.000519068	0.004258942	0.022783063
20	0.000519068	0.000519068	0.004258942	0.022783063
30	0.000519068	0.000519068	0.004258942	0.022783063
40	0.000519068	0.000519068	0.004258942	0.022783063
50	0.000519068	0.000519068	0.004258942	0.022783063
60	0.000519068	0.000519068	0.004258942	0.022783063
70	0.000519068	0.000519068	0.004258942	0.022783063
80	0.000519068	0.000519068	0.004258942	0.022783063
90	0.000519068	0.000519068	0.004258942	0.022783063
100	0.000519068	0.000519068	0.004258942	0.022783063
110	0.000519068	0.000519068	0.004258942	0.022783063
120	0.000519068	0.000519068	0.004258942	0.022783063
130	0.000519068	0.000519068	0.004258942	0.022783063
140	0.000519068	0.000519068	0.004258942	0.022783063
150	0.000519068	0.000519068	0.004258942	0.022783063
160	0.000519068	0.000519068	0.004258942	0.022783063
170	0.000519068	0.000519068	0.004258942	0.022783063
180	0.000519068	0.000519068	0.004258942	0.022783063
190	0.000519068	0.000519068	0.004258942	0.022783063
200	0.000519068	0.000519068	0.004258942	0.022783063
210	0.000519068	0.000519068	0.004258942	0.022783063
220	0.000519068	0.000519068	0.004258942	0.022783063
230	0.000519068	0.000519068	0.004258942	0.022783063
240	0.000519068	0.000519068	0.004258942	0.022783063
250	0.000519068	0.000519068	0.004258942	0.022783063
260	0.000519068	0.000519068	0.004258942	0.022783063
270	0.000519068	0.000519068	0.004258942	0.022783063
280	0.000519068	0.000519068	0.004258942	0.022783063
290	0.000519068	0.000519068	0.004258942	0.022783063
300	0.000519068	0.000519068	0.004258942	0.022783063
310	0.000519068	0.000519068	0.004258942	0.022783063
320	0.000519068	0.000519068	0.004258942	0.022783063
330	0.000519068	0.000519068	0.004258942	0.022783063
340	0.000519068	0.000519068	0.004258942	0.022783063
350	0.000519068	0.000519068	0.004258942	0.022783063
360	0.000519068	0.000519068	0.004258942	0.022783063
370	0.000519068	0.000519068	0.004258942	0.022783063
380	0.000519068	0.000519068	0.004258942	0.022783063
390	0.000519068	0.000519068	0.004258942	0.022783063
400	0.000519068	0.000519068	0.004258942	0.022783063
410	0.000519068	0.000519068	0.004258942	0.022783063
420	0.000519068	0.000519068	0.004258942	0.022783063
430	0.000519068	0.000519068	0.004258942	0.022783063
440	0.000519068	0.000519068	0.004258942	0.022783063
450	0.000519068	0.000519068	0.004258942	0.022783063
460	0.000519068	0.000519068	0.004258942	0.022783063
470	0.000519068	0.000519068	0.004258942	0.022783063
480	0.000519068	0.000519068	0.004258942	0.022783063
490	0.000519068	0.000519068	0.004258942	0.022783063
500	0.000519068	0.000519068	0.004258942	0.022783063

Parameter: Snow

Epoch	Loss	Total MSE	Total MAE	Total RMSE
10	0	0	0	0
20	0	0	0	0
30	0	0	0	0
40	0	0	0	0
50	0	0	0	0
60	0	0	0	0
70	0	0	0	0
80	0	0	0	0
90	0	0	0	0
100	0	0	0	0
110	0	0	0	0
120	0	0	0	0
130	0	0	0	0
140	0	0	0	0
150	0	0	0	0
160	0	0	0	0
170	0	0	0	0
180	0	0	0	0
190	0	0	0	0
200	0	0	0	0
210	0	0	0	0
220	0	0	0	0
230	0	0	0	0
240	0	0	0	0
250	0	0	0	0
260	0	0	0	0
270	0	0	0	0
280	0	0	0	0
290	0	0	0	0
300	0	0	0	0
310	0	0	0	0
320	0	0	0	0
330	0	0	0	0
340	0	0	0	0
350	0	0	0	0
360	0	0	0	0
370	0	0	0	0

Parameter: Soil Temperature

Epoch	Loss	Total MSE	Total MAE	Total RMSE
10	0.004325722	0.004325722	0.03244979	0.06577022
20	0.005962332	0.005962332	0.035708922	0.07721613
30	0.007555746	0.007555746	0.042686129	0.0869238
40	0.010001173	0.010001173	0.049882613	0.100005865
50	0.014629738	0.014629738	0.062389513	0.120953456
60	0.013272205	0.013272205	0.058943588	0.11520506
70	0.01382341	0.01382341	0.05989389	0.117573
80	0.015730582	0.015730582	0.064035932	0.12542161
90	0.014482706	0.014482706	0.061311557	0.12034411
100	0.015374269	0.015374269	0.063061433	0.123993024
110	0.014873757	0.014873757	0.062228781	0.12195801
120	0.015024387	0.015024387	0.06239988	0.12257401
130	0.014782799	0.014782799	0.062123049	0.121584535
140	0.014277657	0.014277657	0.06069513	0.11948915
150	0.014358289	0.014358289	0.06127317	0.11982608
160	0.013906519	0.013906519	0.060346016	0.117925905
170	0.014566163	0.014566163	0.06179604	0.12069036
180	0.014224615	0.014224615	0.061239155	0.11926699
190	0.014569046	0.014569046	0.061653188	0.120702304
200	0.014610975	0.014610975	0.06177741	0.12087587
210	0.014864409	0.014864409	0.062689539	0.121919684
220	0.015094801	0.015094801	0.063214129	0.1228609
230	0.014691196	0.014691196	0.061957876	0.121207245
240	0.015136985	0.015136985	0.062810426	0.12303246
250	0.014746004	0.014746004	0.061890271	0.121433124
260	0.014862495	0.014862495	0.063038071	0.12191183
270	0.014510261	0.014510261	0.061509129	0.12045854
280	0.014483398	0.014483398	0.061466523	0.12034699
290	0.01503762	0.01503762	0.062557838	0.12262797
300	0.013848975	0.013848975	0.059960045	0.11768167
310	0.014199242	0.014199242	0.060703218	0.11916057
320	0.014331307	0.014331307	0.061180286	0.11971344
330	0.013972634	0.013972634	0.060315273	0.1182059
340	0.014185912	0.014185912	0.060668353	0.119104624
350	0.014328071	0.014328071	0.06114898	0.11969992
360	0.014303627	0.014303627	0.060952251	0.11959777
370	0.014574041	0.014574041	0.061882019	0.120722994
380	0.014524249	0.014524249	0.061479188	0.12051659
390	0.014795361	0.014795361	0.061979305	0.121636175
400	0.014597343	0.014597343	0.061517855	0.120819464

Parameter: Soil Moisture

Epoch	Loss	Total MSE	Total MAE	Total RMSE
10	0.000871767	0.000871767	0.013673123	0.029525695
20	0.000975133	0.000975133	0.013090764	0.031227121
30	0.000906907	0.000906907	0.012503516	0.03011489
40	0.000919722	0.000919722	0.012971612	0.030326916
50	0.000914846	0.000914846	0.012860503	0.030246418
60	0.001078131	0.001078131	0.01419247	0.0328349
70	0.001381693	0.001381693	0.014472424	0.037171133
80	0.001257002	0.001257002	0.014952845	0.035454225
90	0.002276821	0.002276821	0.01554296	0.047716044
100	0.001223589	0.001223589	0.015404479	0.034979835
110	0.002386915	0.002386915	0.02305516	0.04885606
120	0.00141311	0.00141311	0.016683725	0.03759136
130	0.001208888	0.001208888	0.014838992	0.034769073
140	0.002033074	0.002033074	0.015350088	0.045089617
150	0.001509242	0.001509242	0.014238895	0.03884897
160	0.001049787	0.001049787	0.013145691	0.03240042
170	0.001239827	0.001239827	0.014882491	0.03521118
180	0.001150222	0.001150222	0.014761602	0.03391492
190	0.001422894	0.001422894	0.014533121	0.03772127
200	0.001092286	0.001092286	0.014607342	0.033049755
210	0.001325332	0.001325332	0.016233248	0.03640511
220	0.001462754	0.001462754	0.017296437	0.03824596
230	0.001374508	0.001374508	0.01385759	0.037074357
240	0.001800791	0.001800791	0.018578506	0.042435724
250	0.001207902	0.001207902	0.015625934	0.03475489
260	0.001389616	0.001389616	0.01696321	0.03727755
270	0.001504685	0.001504685	0.017581184	0.038790274
280	0.001197258	0.001197258	0.01537139	0.034601413
290	0.001043726	0.001043726	0.01411267	0.03230675
300	0.001148366	0.001148366	0.014873643	0.033887543
310	0.001185463	0.001185463	0.015133841	0.034430552
320	0.001032207	0.001032207	0.014178688	0.03212798
330	0.001283915	0.001283915	0.016131399	0.03583176
340	0.001433679	0.001433679	0.016780438	0.03786396
350	0.001151899	0.001151899	0.015148334	0.033939634
360	0.001161933	0.001161933	0.015165073	0.03408714

Configuration 1- Optimiser: SGD

Parameter: Surface Temperature

Epoch	Loss	Total MSE	Total MAE	Total RMSE
10	0.004315138	0.004315138	0.040485377	0.065689705
20	0.002539409	0.002539409	0.033373678	0.050392553
30	0.002104029	0.002104029	0.030370576	0.045869693
40	0.002066529	0.002066529	0.029531769	0.045459095
50	0.002305738	0.002305738	0.030539084	0.0480181
60	0.002600313	0.002600313	0.031683459	0.05099326
70	0.00264985	0.00264985	0.031731029	0.051476695
80	0.002815923	0.002815923	0.032558988	0.053065278
90	0.002733463	0.002733463	0.03189345	0.05228253
100	0.002456428	0.002456428	0.030872571	0.04956236
110	0.002590396	0.002590396	0.03132886	0.050895933
120	0.002488608	0.002488608	0.030997502	0.04988595
130	0.002727123	0.002727123	0.031990594	0.05222187
140	0.002602675	0.002602675	0.031568294	0.05101642
150	0.002605658	0.002605658	0.031650928	0.051045645
160	0.002840472	0.002840472	0.032894644	0.05329608
170	0.002840692	0.002840692	0.033198184	0.053298146
180	0.003133885	0.003133885	0.034567499	0.055981115
190	0.00306771	0.00306771	0.034218803	0.05538691
200	0.003049551	0.003049551	0.034189149	0.055222735
210	0.003222539	0.003222539	0.035670724	0.05676741
220	0.0030003	0.0030003	0.033953329	0.054774996
230	0.003052424	0.003052424	0.035111932	0.055248745
240	0.003107104	0.003107104	0.035114689	0.0557414
250	0.003184718	0.003184718	0.036034041	0.056433305
260	0.003217325	0.003217325	0.036968399	0.056721468
270	0.003132088	0.003132088	0.036006978	0.05596506
280	0.003096268	0.003096268	0.035831025	0.055644125
290	0.003090005	0.003090005	0.035019572	0.05558781
300	0.003177595	0.003177595	0.037027532	0.05637016
310	0.003311395	0.003311395	0.036998136	0.05754472
320	0.003334187	0.003334187	0.037454405	0.057742424
330	0.003390932	0.003390932	0.037689651	0.05823171
340	0.003678902	0.003678902	0.038511957	0.06065395
350	0.003997269	0.003997269	0.040050354	0.06322396
360	0.004277605	0.004277605	0.040681755	0.0654034

Parameter: Surface Pressure

Epoch	Loss	Total MSE	Total MAE	Total RMSE
10	0.00464657	0.00464657	0.056597094	0.06816575
20	0.002617814	0.002617814	0.043623016	0.051164575
30	0.002367853	0.002367853	0.042662164	0.048660595
40	0.001770709	0.001770709	0.036690742	0.04207979
50	0.001103444	0.001103444	0.028218266	0.033218134
60	0.000708817	0.000708817	0.021925542	0.02662362
70	0.000650205	0.000650205	0.021032854	0.025499115
80	0.000545777	0.000545777	0.019092521	0.023361873
90	0.000641337	0.000641337	0.02118701	0.025324635
100	0.000606843	0.000606843	0.020443	0.024634192
110	0.000606163	0.000606163	0.020512109	0.02462037
120	0.000575123	0.000575123	0.019829025	0.023981715
130	0.000540651	0.000540651	0.019065556	0.023251904
140	0.000579408	0.000579408	0.019796484	0.024070902
150	0.00078924	0.00078924	0.023710856	0.028093418
160	0.000606194	0.000606194	0.020242241	0.024621015
170	0.000667094	0.000667094	0.021301468	0.025828162
180	0.000698992	0.000698992	0.021877108	0.026438462
190	0.00050335	0.00050335	0.017980447	0.022435464
200	0.000691882	0.000691882	0.021783214	0.026303641
210	0.000518916	0.000518916	0.018239181	0.022779727
220	0.000587497	0.000587497	0.019703488	0.02423833
230	0.000482895	0.000482895	0.017398341	0.021974863
240	0.000439629	0.000439629	0.016254349	0.020967336
250	0.000455231	0.000455231	0.01673404	0.021336151
260	0.000469173	0.000469173	0.017092199	0.021660408
270	0.000462487	0.000462487	0.016676566	0.021505522
280	0.000469641	0.000469641	0.016938849	0.021671213
290	0.000480707	0.000480707	0.017176524	0.021925025
300	0.000486272	0.000486272	0.017477128	0.02205157
310	0.000474736	0.000474736	0.016861806	0.021788433

Parameter: X-component of Wind

Epoch	Loss	Total MSE	Total MAE	Total RMSE
10	0.00661923	0.00661923	0.064233028	0.08135866
20	0.006298636	0.006298636	0.061840736	0.07936394
30	0.006154231	0.006154231	0.060847856	0.078448914
40	0.005226318	0.005226318	0.054693734	0.072293274
50	0.005158919	0.005158919	0.05391246	0.071825616
60	0.0049421	0.0049421	0.052540797	0.07030007
70	0.005046507	0.005046507	0.053220474	0.07103877
80	0.00507771	0.00507771	0.053990803	0.07125805
90	0.005180307	0.005180307	0.05587889	0.07197435
100	0.004478428	0.004478428	0.0507512	0.06692106
110	0.004362287	0.004362287	0.051463877	0.06604761
120	0.003843528	0.003843528	0.04781587	0.061996188
130	0.003481969	0.003481969	0.043983731	0.05900821
140	0.00327017	0.00327017	0.042551359	0.0571854
150	0.00352218	0.00352218	0.046255553	0.059347957
160	0.003222834	0.003222834	0.043130612	0.056770008
170	0.003452525	0.003452525	0.046196792	0.058758184
180	0.003532083	0.003532083	0.044678175	0.059431326
190	0.003090299	0.003090299	0.041616402	0.05559046
200	0.003217705	0.003217705	0.0423378	0.056724824
210	0.003170918	0.003170918	0.042972775	0.056310907
220	0.003225273	0.003225273	0.042888279	0.056791488
230	0.003200221	0.003200221	0.043069226	0.056570496
240	0.00327754	0.00327754	0.043504032	0.057249807
250	0.003366076	0.003366076	0.04480317	0.05801789
260	0.003340131	0.003340131	0.04476016	0.057793863
270	0.003377431	0.003377431	0.044633665	0.058115672
280	0.003616478	0.003616478	0.047199397	0.06013716
290	0.003696532	0.003696532	0.047384827	0.06079911
300	0.003672661	0.003672661	0.047418997	0.060602482
310	0.004117548	0.004117548	0.051018256	0.064168125

Parameter: Y-Component of Wind

Epoch	Loss	Total MSE	Total MAE	Total RMSE
10	0.011322848	0.011322848	0.082019111	0.10640887
20	0.007827131	0.007827131	0.065916713	0.08847108
30	0.006378119	0.006378119	0.058661536	0.07986312
40	0.005419766	0.005419766	0.05190506	0.07361906
50	0.004707667	0.004707667	0.049795712	0.068612434
60	0.006119629	0.006119629	0.06236851	0.07822806
70	0.007129335	0.007129335	0.069429404	0.08443539
80	0.005287818	0.005287818	0.057234873	0.07271738
90	0.004897259	0.004897259	0.054372708	0.06998042
100	0.005795687	0.005795687	0.060788626	0.07612941
110	0.004998208	0.004998208	0.055166647	0.070698
120	0.005531033	0.005531033	0.05913983	0.07437092
130	0.005226806	0.005226806	0.056981094	0.07229666
140	0.004757407	0.004757407	0.053395641	0.06897396
150	0.004566476	0.004566476	0.051776032	0.06757571
160	0.004066796	0.004066796	0.04725139	0.063771434
170	0.004521732	0.004521732	0.051093552	0.06724383
180	0.004120883	0.004120883	0.047569187	0.064194106
190	0.004638179	0.004638179	0.051702921	0.06810418
200	0.003934127	0.003934127	0.045550609	0.062722616
210	0.003790195	0.003790195	0.044285917	0.061564557
220	0.003803394	0.003803394	0.044441027	0.061671663
230	0.00410347	0.00410347	0.047307545	0.06405833
240	0.004397789	0.004397789	0.049827479	0.06631583
250	0.004045963	0.004045963	0.046893387	0.06360789
260	0.003732091	0.003732091	0.044288916	0.061090846
270	0.004896285	0.004896285	0.053921917	0.06997346
280	0.004394042	0.004394042	0.049886431	0.06628757
290	0.00608137	0.00608137	0.06211155	0.07798314
300	0.004780159	0.004780159	0.052229112	0.0691387
310	0.004923526	0.004923526	0.053221376	0.07016785

Parameter: Humidity

Epoch	Loss	Total MSE	Total MAE	Total RMSE
10	0.011995386	0.011995386	0.088553865	0.10952345
20	0.010641815	0.010641815	0.083558399	0.10315917
30	0.009105792	0.009105792	0.075388974	0.09542427
40	0.009789752	0.009789752	0.073925953	0.098943174
50	0.010595163	0.010595163	0.074725362	0.1029328
60	0.011813101	0.011813101	0.077140978	0.108688086
70	0.01275712	0.01275712	0.078984997	0.11294743
80	0.013672509	0.013672509	0.080916442	0.11692951
90	0.014255342	0.014255342	0.08217787	0.11939574
100	0.015966474	0.015966474	0.086001702	0.12635852
110	0.015626589	0.015626589	0.085025025	0.12500635
120	0.015870135	0.015870135	0.087041119	0.12597673
130	0.016248088	0.016248088	0.08604891	0.12746798
140	0.015635962	0.015635962	0.087514664	0.12504384
150	0.015090529	0.015090529	0.083513127	0.12284351
160	0.013864973	0.013864973	0.083839003	0.117749624
170	0.014558335	0.014558335	0.080950509	0.12065793
180	0.015771016	0.015771016	0.085565691	0.1255827
190	0.013319924	0.013319924	0.077685626	0.115411974
200	0.012033987	0.012033987	0.074109537	0.109699525
210	0.011219843	0.011219843	0.073068696	0.10592376
220	0.011202527	0.011202527	0.071406737	0.105841994
230	0.009904239	0.009904239	0.069439683	0.09952004
240	0.010437482	0.010437482	0.068784629	0.10216399
250	0.010144349	0.010144349	0.067780549	0.100719154
260	0.009019323	0.009019323	0.064146394	0.09497012
270	0.008658992	0.008658992	0.062825581	0.093053706
280	0.008221732	0.008221732	0.061195732	0.09067377
290	0.00779305	0.00779305	0.060196431	0.08827825
300	0.007412029	0.007412029	0.05970253	0.08609314
310	0.008555043	0.008555043	0.063033296	0.092493474

Parameter: Convective Rain

Epoch	Loss	Total MSE	Total MAE	Total RMSE
10	0.003435665	0.003435665	0.031770317	0.05861454
20	0.003153297	0.003153297	0.024802122	0.05615423
30	0.003030591	0.003030591	0.021334248	0.0550508
40	0.002975198	0.002975198	0.020205744	0.05454538
50	0.002940716	0.002940716	0.017805794	0.05422837
60	0.002931897	0.002931897	0.015654017	0.054146994
70	0.002925053	0.002925053	0.015374983	0.054083757
80	0.002923223	0.002923223	0.014796105	0.054066833
90	0.002912509	0.002912509	0.014791884	0.05396767
100	0.002905913	0.002905913	0.013722177	0.05390652
110	0.00289047	0.00289047	0.013636058	0.05376309
120	0.002855341	0.002855341	0.014823554	0.053435393
130	0.002848399	0.002848399	0.014038999	0.05337039
140	0.002833072	0.002833072	0.013942229	0.05322661
150	0.00283352	0.00283352	0.013673553	0.05323082
160	0.002863454	0.002863454	0.012235921	0.053511247
170	0.002831799	0.002831799	0.012622883	0.05321465
180	0.002860067	0.002860067	0.011591997	0.053479597
190	0.002826046	0.002826046	0.013037381	0.05316057
200	0.002834763	0.002834763	0.012386168	0.053242486
210	0.002856114	0.002856114	0.012005765	0.05344262
220	0.002907488	0.002907488	0.010609718	0.05392113
230	0.002925584	0.002925584	0.010155271	0.05408867
240	0.002885166	0.002885166	0.010337973	0.05371374
250	0.002919455	0.002919455	0.009638143	0.054031983
260	0.002889656	0.002889656	0.009994591	0.053755518
270	0.002907378	0.002907378	0.009779388	0.05392011
280	0.002885704	0.002885704	0.010595431	0.053718753
290	0.002878443	0.002878443	0.011527904	0.053651124
300	0.002889001	0.002889001	0.011208236	0.053749423
310	0.002923131	0.002923131	0.011271158	0.05406599

Parameter: Non-convective Rain

Epoch	Loss	Total MSE	Total MAE	Total RMSE
10	0.002740355	0.002740355	0.048156025	0.0523484
20	0.002342371	0.002342371	0.044418242	0.048398048
30	0.002405055	0.002405055	0.045047432	0.049041364
40	0.002325328	0.002325328	0.044243323	0.04822166
50	0.002409259	0.002409259	0.045051375	0.0490842
60	0.002342398	0.002342398	0.044474999	0.048398323
70	0.00232866	0.00232866	0.043692481	0.048256185
80	0.00294707	0.00294707	0.049265916	0.054286923
90	0.003773301	0.003773301	0.05268452	0.061427202
100	0.001496186	0.001496186	0.02915689	0.038680557
110	0.00109045	0.00109045	0.019150896	0.033021968
120	0.000502061	0.000502061	0.005585323	0.02240671
130	0.000509582	0.000509582	0.005043287	0.022573913
140	0.000507184	0.000507184	0.004924883	0.022520743
150	0.000506757	0.000506757	0.00498746	0.022511274
160	0.000503243	0.000503243	0.005157225	0.022433082
170	0.000509482	0.000509482	0.004730643	0.0225717
180	0.000511628	0.000511628	0.004849307	0.02261919
190	0.000512188	0.000512188	0.004731989	0.022631565
200	0.00051245	0.00051245	0.004558236	0.022637365
210	0.000511961	0.000511961	0.004516261	0.022626555
220	0.000509308	0.000509308	0.004689447	0.022567848
230	0.0005091	0.0005091	0.00478917	0.022563253
240	0.000507346	0.000507346	0.005009527	0.022524336
250	0.000508035	0.000508035	0.005296135	0.022539642
260	0.000509121	0.000509121	0.005408367	0.022563716
270	0.000511053	0.000511053	0.005709776	0.022606486
280	0.000509488	0.000509488	0.00562895	0.02257185
290	0.000510852	0.000510852	0.005650038	0.02260204
300	0.0005099	0.0005099	0.005418034	0.022580959
310	0.000512125	0.000512125	0.005591334	0.022630172

Parameter: Snow

Epoch	Loss	Total MSE	Total MAE	Total RMSE
10	3.81E-05	3.81E-05	0.003800577	0.00617167
20	6.69E-06	6.69E-06	0.001608997	0.002586512
30	1.86E-06	1.86E-06	0.000884373	0.001362557
40	7.11E-07	7.11E-07	0.000583378	0.000843096
50	4.69E-07	4.69E-07	0.000499326	0.00068452
60	4.45E-07	4.45E-07	0.000506359	0.000667426
70	5.19E-07	5.19E-07	0.000556741	0.000720345
80	5.78E-07	5.78E-07	0.000592561	0.000760195
90	6.05E-07	6.05E-07	0.000613568	0.000777813
100	6.86E-07	6.86E-07	0.000658449	0.000828044
110	7.02E-07	7.02E-07	0.000669845	0.000837571
120	7.25E-07	7.25E-07	0.000683252	0.000851195
130	7.31E-07	7.31E-07	0.000690196	0.000854897
140	7.52E-07	7.52E-07	0.000699249	0.000867114
150	7.64E-07	7.64E-07	0.000701616	0.000874205
160	7.65E-07	7.65E-07	0.000700599	0.00087463
170	7.29E-07	7.29E-07	0.000681773	0.000853721
180	7.20E-07	7.20E-07	0.000672406	0.000848503
190	7.51E-07	7.51E-07	0.000681152	0.00086653
200	7.40E-07	7.40E-07	0.000669931	0.000860169
210	7.56E-07	7.56E-07	0.000668859	0.000869494
220	7.32E-07	7.32E-07	0.000651355	0.000855731
230	7.48E-07	7.48E-07	0.00064814	0.000865094
240	7.80E-07	7.80E-07	0.000652942	0.000883029
250	8.30E-07	8.30E-07	0.000662273	0.000910804
260	8.98E-07	8.98E-07	0.000676355	0.000947557
270	8.75E-07	8.75E-07	0.000658102	0.000935623
280	8.89E-07	8.89E-07	0.000655189	0.00094304
290	9.40E-07	9.40E-07	0.000663371	0.000969517
300	1.02E-06	1.02E-06	0.000679561	0.001011125
310	1.01E-06	1.01E-06	0.000668745	0.001004325

Parameter: Soil Temperature

Epoch	Loss	Total MSE	Total MAE	Total RMSE
10	0.00435162	0.00435162	0.054064852	0.06596681
20	0.001380475	0.001380475	0.027854023	0.037154753
30	0.000960173	0.000960173	0.018611912	0.030986652
40	0.000909574	0.000909574	0.015859125	0.030159138
50	0.000918757	0.000918757	0.015791806	0.030311013
60	0.001015686	0.001015686	0.016753705	0.03186983
70	0.001067173	0.001067173	0.017338268	0.03266762
80	0.001092124	0.001092124	0.017597275	0.033047296
90	0.001071769	0.001071769	0.017513137	0.032737873
100	0.00129776	0.00129776	0.019370907	0.036024433
110	0.001518767	0.001518767	0.021179839	0.03897137
120	0.001404195	0.001404195	0.020068381	0.037472587
130	0.001869718	0.001869718	0.023127635	0.043240238
140	0.002350691	0.002350691	0.025931427	0.04848393
150	0.002838167	0.002838167	0.028238764	0.053274453
160	0.00336581	0.00336581	0.030594392	0.058015596
170	0.003329442	0.003329442	0.029709695	0.057701316
180	0.003522614	0.003522614	0.030341069	0.059351616
190	0.004046964	0.004046964	0.032490161	0.063615754
200	0.004133778	0.004133778	0.032661923	0.06429446
210	0.003967145	0.003967145	0.032129398	0.06298528
220	0.004289886	0.004289886	0.033195632	0.06549722
230	0.004009039	0.004009039	0.031880295	0.06331698
240	0.003843906	0.003843906	0.031115863	0.06199924
250	0.004145807	0.004145807	0.032568536	0.06438794
260	0.003981705	0.003981705	0.031691601	0.063100755
270	0.003560804	0.003560804	0.029756541	0.05967248
280	0.003947956	0.003947956	0.031766975	0.06283276
290	0.003909838	0.003909838	0.031430775	0.06252871
300	0.003736707	0.003736707	0.030669629	0.061128605
310	0.003562748	0.003562748	0.029999979	0.05968876

Parameter: Soil Moisture

Epoch	Loss	Total MSE	Total MAE	Total RMSE
10	0.000645901	0.000645901	0.015930841	0.025414592
20	0.000748406	0.000748406	0.015617871	0.027357014
30	0.000818298	0.000818298	0.015569233	0.028605904
40	0.000853318	0.000853318	0.015508733	0.029211616
50	0.00085819	0.00085819	0.015316221	0.029294875
60	0.000955741	0.000955741	0.016059867	0.030915061
70	0.000964856	0.000964856	0.016013952	0.031062126
80	0.001020306	0.001020306	0.016422532	0.031942233
90	0.000951668	0.000951668	0.015698387	0.030849108
100	0.001053601	0.001053601	0.016518158	0.03245922
110	0.001030748	0.001030748	0.016263691	0.032105267
120	0.000989998	0.000989998	0.015833622	0.03146423
130	0.001038893	0.001038893	0.016212813	0.032231867
140	0.001035117	0.001035117	0.016143966	0.03217323
150	0.624376297	0.624376297	0.677614765	0.79017484
160	0.618267654	0.618267654	0.702045409	0.7863
170	0.618780889	0.618780889	0.698205917	0.7866263
180	0.623948803	0.623948803	0.678734529	0.7899043
190	0.620148537	0.620148537	0.691192617	0.7874951
200	0.618163596	0.618163596	0.703023055	0.7862338
210	0.618877838	0.618877838	0.697595538	0.7866879
220	0.618003276	0.618003276	0.704785318	0.7861318
230	0.618292006	0.618292006	0.701830334	0.7863155
240	0.620873491	0.620873491	0.688303927	0.7879553
250	0.618729825	0.618729825	0.698538706	0.7865938
260	0.619320358	0.619320358	0.695087628	0.7869691
270	0.620350183	0.620350183	0.690350316	0.7876231
280	0.618493724	0.618493724	0.700198625	0.7864437
290	0.618734982	0.618734982	0.698504735	0.78659713
300	0.619473112	0.619473112	0.694304393	0.78706616
310	0.618902853	0.618902853	0.697442187	0.78670377
320	0.619228413	0.619228413	0.69557703	0.78691065

Appendix 5: Evaluation Results of MISO-TCN model variance for Historical Weather Data

As described in Section 5.1.1.2.4, the 'saved the best model' approach is utilised within MISO-TCN with different configurations and controls. Different models are trained and tested for TCN controls of filter size 32 and activation 'linear' as shown in the following first table. The fields with the least MSE is highlighted in the yellow. Then, further experiments are carried out with different configurations and controls to find the optimal model with least MSE for MISO-TCN for the chosen locations from the first table. The optimal models with Least MSE for overall experiments are highlighted in orange colour.

Experiments with TCN Filter 32 and linear activation

No. of. Layers	TSK	PSFC	U10	V10	Q2	Rainc	Rainnc	Snow	TSLB	SMOIS
TCN 1	0.002453652	0.000117024	0.007725683	0.009650737	0.584595084	0.004469885	0.025263477	1.08796E-05	0.000553659	0.000121713
TCN 2	0.002995189	0.000111919	0.007443365	0.009031167	0.006752483	0.003882241	0.023368442	1.81E-06	0.000740585	0.000138616
TCN 3	0.003422687	0.000138637	0.00564751	0.008417731	0.02141227	0.00449783	0.020072713	1.34E-07	0.000874251	0.000147898
TCN 4	0.003791149	0.000943237	0.006979346	0.008473003	0.02186048	0.0040008	0.025671681	2.05E-06	0.00075906	0.000185795

Experiments with TCN Filter 32 and tanh activation

No. of. Layers	TSK	PSFC	U10	V10	Q2	Rainc	Rainnc	Snow	TSLB	SMOIS
TCN 1	0.00214117	0.000104854							0.000522798	0.000134437
TCN 2					0.019250417	0.003870775				
TCN 3			0.006918387	0.009074003			0.022560284	3.93E-06		
TCN 4										

Experiments with TCN Filter 64 and linear activation

TCN 64 Linear										
No. of. Layers	TSK	PSFC	U10	V10	Q2	Rainc	Rainnc	Snow	TSLB	SMOIS
TCN 1	0.001756939	0.000109458							0.000394593	0.000108187
TCN 2					0.015559356	0.003984757				
TCN 3			0.006219904	0.009182908			0.001895714	8.55E-06		
TCN 4										

Experiments with TCN Filter 64 and tanh activation

No. of. Layers	TSK	PSFC	U10	V10	Q2	Rainc	Rainnc	Snow	TSLB	SMOIS
TCN 1	0.002120781	8.74041E-05							0.000376134	9.98907E-05
TCN 2					0.01665926	0.004118798				
TCN 3			0.006656023	0.008955006			0.020810314	1.09E-06		
TCN 4										

Experiments with TCN Filter 128 and linear activation

No. of. Layers	TSK	PSFC	U10	V10	Q2	Rainc	Rainnc	Snow	TSLB	SMOIS
TCN 1	0.001730864	0.000118985							0.000396664	0.00013462
TCN 2					0.018242057	0.003804835				
TCN 3			0.005518949	0.008325078			0.023688085	6.28E-06		
TCN 4										

Experiments with TCN Filter 128 and tanh activation

No. of. Layers	TSK	PSFC	U10	V10	Q2	Rainc	Rainnc	Snow	TSLB	SMOIS
TCN 1	0.00193089	0.000114233							0.000525219	0.000113312
TCN 2					0.016153175	0.003260107				
TCN 3			0.005567687	0.007609961			0.021609113	4.99E-07		
TCN 4										

Experiments with TCN Filter 256 and linear activation

No. of. Layers	TSK	PSFC	U10	V10	Q2	Rainc	Rainnc	Snow	TSLB	SMOIS
TCN 1	0.001795899	0.000136203							0.000529617	0.000103382
TCN 2					0.019025626	0.003937547				
TCN 3			0.004384032	0.007517624			0.024127014	1.84E-07		
TCN 4										

Experiments with TCN Filter 256 and tanh activation

No. of. Layers	TSK	PSFC	U10	V10	Q2	Rainc	Rainnc	Snow	TSLB	SMOIS
TCN 1	0.001738656	0.000124911							0.000407729	0.00012975
TCN 2					0.019054703	0.003953935				
TCN 3			0.006049865	0.007427616			0.027586088	4.30E-07		
TCN 4										

Experiments with TCN Filter 512 and linear activation

No. of. Layers	TSK	PSFC	U10	V10	Q2	Rainc	Rainnc	Snow	TSLB	SMOIS
TCN 1	0.002031068	0.000107959							0.002718029	0.000119393
TCN 2					0.017963067	0.004049633				
TCN 3			0.006172244	0.007435963			0.022650335	5.36E-06		
TCN 4										

Experiments with TCN Filter 512 and tanh activation

No. of. Layers	TSK	PSFC	U10	V10	Q2	Rainc	Rainnc	Snow	TSLB	SMOIS
TCN 1	0.002411199	0.00011554							0.000651595	0.000132483
TCN 2					0.017074438	0.003978814				
TCN 3			0.005801443	0.007577378			0.025088904	5.34E-07		
TCN 4										

Appendix 6: Evaluation Results of LSTM-LW, LSTM-WL, and Bi-LSTM model variances for Historical Weather Data

Bi-directional MIMO-LSTM models are evaluated for weather forecasting using historical weather data. All Bi-LSTM models are trained for 500 epochs and models' weights are saved in every 5 epochs. The WRF testing dataset is used to evaluate these saved models. A sample of 3 hours and 6 hours evaluation results are given below. The optimal model with least MSE is highlighted in each timeslot.

Bidirectional 3 hour

Epoch	Loss	Total MSE	Total MAE	Total RMSE	SkinTemp	SufPres	U10	V10	Humidity	Rainc	Rainnc	Snow	SolilTemp	SoilMoist
5	0.016445302	0.016445302	0.080928917	0.12823921	0.006236865	0.009799781	0.018420912	0.031202529	0.04156172	0.004744033	0.040650014	0.001076678	0.009769526	0.000990968
10	0.0124013	0.0124013	0.066172013	0.11136113	0.003801145	0.005094086	0.013610125	0.022651682	0.02272952	0.004585788	0.040341944	0.000751421	0.009614749	0.000832548
15	0.010958407	0.010958407	0.059753369	0.1046824	0.003461215	0.003893965	0.011448377	0.019295642	0.017364487	0.004489971	0.039991427	0.000582728	0.008207924	0.000848333
20	0.010118114	0.010118114	0.055690031	0.10058883	0.003335752	0.003425037	0.010814544	0.017536374	0.014372881	0.004421863	0.03969179	0.000456714	0.006229922	0.000896255
25	0.009470471	0.009470471	0.052238863	0.09731635	0.003324253	0.003102392	0.010091835	0.015872214	0.012739426	0.004378971	0.039505094	0.00033275	0.004408621	0.000949162
30	0.009053576	0.009053576	0.049643884	0.0951503	0.003348792	0.002856958	0.00945571	0.01495505	0.011964563	0.004359669	0.039411504	0.000218041	0.002992453	0.000973022
35	0.008758462	0.008758462	0.047577913	0.09358667	0.003260285	0.002635311	0.009106035	0.014192452	0.011479748	0.004357071	0.039360017	0.000139531	0.002089206	0.000964961
40	0.008550024	0.008550024	0.046237729	0.092466325	0.003200667	0.00247109	0.008748713	0.013596987	0.011157977	0.004371846	0.03932483	9.25E-05	0.001561262	0.000974392
45	0.008406311	0.008406311	0.045442473	0.091685936	0.003148886	0.002347683	0.008806826	0.012902564	0.010881829	0.004378691	0.03927295	6.22E-05	0.001300297	0.000961137
50	0.008317885	0.008317885	0.044800566	0.09120245	0.003002914	0.00225462	0.008808282	0.012727348	0.010627669	0.0043781	0.039196875	4.26E-05	0.001157953	0.000982541
55	0.008204353	0.008204353	0.044089649	0.090577886	0.002848225	0.002151547	0.008565777	0.012626899	0.010308671	0.004368059	0.039076366	2.88E-05	0.001098239	0.000970939
60	0.008084349	0.008084349	0.043435739	0.08991301	0.002713899	0.002123344	0.008306676	0.012229469	0.01016789	0.004331122	0.038899872	1.97E-05	0.001093327	0.00095823
65	0.007972146	0.007972146	0.042901069	0.08928687	0.00258207	0.002016048	0.008247562	0.01189272	0.00992585	0.004302433	0.03866904	1.35E-05	0.001099824	0.000972417
70	0.007897416	0.007897416	0.042474016	0.08886742	0.002552034	0.001960596	0.008109999	0.011854332	0.009795896	0.004270409	0.038380403	1.00E-05	0.001097665	0.000942829
75	0.007816144	0.007816144	0.04208295	0.08840896	0.002519193	0.001879814	0.008264385	0.011552198	0.009598595	0.004245164	0.03804851	7.54E-06	0.001138017	0.000908036
80	0.007743512	0.007743512	0.041772661	0.08799723	0.002505297	0.00179395	0.00833907	0.011360248	0.009541232	0.004220296	0.03765038	6.11E-06	0.001144082	0.00087446
85	0.007608912	0.007608912	0.041149496	0.087229066	0.002497719	0.001657346	0.007986369	0.011090861	0.009525859	0.004203678	0.03714358	5.01E-06	0.001151732	0.000826965
90	0.007499049	0.007499049	0.040768892	0.086597055	0.002488624	0.001537482	0.008263931	0.010679039	0.009363569	0.00418842	0.036521506	4.44E-06	0.001145688	0.000797784
95	0.007368336	0.007368336	0.039985059	0.08583901	0.002547223	0.001457883	0.007795495	0.01045306	0.0094642	0.004184844	0.035857096	4.06E-06	0.001150601	0.000768903
100	0.007292161	0.007292161	0.039699081	0.085394144	0.002525257	0.001409718	0.007942164	0.010521431	0.009395157	0.00418781	0.035028625	3.79E-06	0.001159684	0.00074797
105	0.007201266	0.007201266	0.039340775	0.08486027	0.002509945	0.001405521	0.007904421	0.010384054	0.009302947	0.004193177	0.03444184	3.61E-06	0.001128274	0.000738876
110	0.007070725	0.007070725	0.038956018	0.08408761	0.002553138	0.001396897	0.007630064	0.010273772	0.009204168	0.004205052	0.033630766	3.42E-06	0.00108733	0.000722643
115	0.007044578	0.007044578	0.038789474	0.083931975	0.00256238	0.001413533	0.007707248	0.010263166	0.009098054	0.004211185	0.03338915	3.16E-06	0.001073901	0.000723996
120	0.00702517	0.00702517	0.0386841	0.08381628	0.002583695	0.001439641	0.007788286	0.010299048	0.00913472	0.004219944	0.03302175	2.91E-06	0.00105537	0.000706332
125	0.006993816	0.006993816	0.038683636	0.083629034	0.002646274	0.001461208	0.007950658	0.010190069	0.009048133	0.004221677	0.03266293	2.67E-06	0.001041256	0.000713284
130	0.006918564	0.006918564	0.038610004	0.083177894	0.00263252	0.001483994	0.007866357	0.010249249	0.008958215	0.004234938	0.032041367	2.52E-06	0.001024018	0.000692465
135	0.006894274	0.006894274	0.038592091	0.08303176	0.002718298	0.001507298	0.007927412	0.010194406	0.008886682	0.004238013	0.03174142	2.43E-06	0.001023651	0.000703125
140	0.006846762	0.006846762	0.038377756	0.082745165	0.002673347	0.00151876	0.007944684	0.01010805	0.008822181	0.004242504	0.03146585	2.35E-06	0.000995397	0.000694496
145	0.00683234	0.00683234	0.038547428	0.08265798	0.0027574	0.001549707	0.008059253	0.010074364	0.008794909	0.00424493	0.031132039	2.28E-06	0.001012699	0.00069582
150	0.006808814	0.006808814	0.038575018	0.082515545	0.002705523	0.00154449	0.008072388	0.01021398	0.00867912	0.004239629	0.030947648	2.29E-06	0.000995731	0.000687344

155	0.00679995	0.00679995	0.038373274	0.08246182	0.002764161	0.001546399	0.008011828	0.009929869	0.008802431	0.004240147	0.030966619	2.15E-06	0.00101717	0.00071872
160	0.006735267	0.006735267	0.038299435	0.082068674	0.002700437	0.001506535	0.00804267	0.009943075	0.008630637	0.00423801	0.030586613	2.15E-06	0.001000175	0.000702369
165	0.006669199	0.006669199	0.038204928	0.081665166	0.002741322	0.001482134	0.00804189	0.009719342	0.008642025	0.004238706	0.030125825	2.03E-06	0.001006396	0.000692319
170	0.006660732	0.006660732	0.038128232	0.0816133	0.002705589	0.001411054	0.008043063	0.009800504	0.008652559	0.004238972	0.030029064	1.89E-06	0.001032758	0.000691869
175	0.00657269	0.00657269	0.038375689	0.08107214	0.002671971	0.001369162	0.0081391	0.009791267	0.008696506	0.004257556	0.029091999	1.89E-06	0.001018472	0.000688978
180	0.0064941	0.0064941	0.038362536	0.08058598	0.002688136	0.001298536	0.008111534	0.009903667	0.008667781	0.004263512	0.028309561	1.80E-06	0.001014273	0.000682197
185	0.006477509	0.006477509	0.038091424	0.080482975	0.002642845	0.001255456	0.008116997	0.009861741	0.008563045	0.004256928	0.028344776	1.61E-06	0.001044221	0.000687464
190	0.0064461	0.0064461	0.038188557	0.08028761	0.002641527	0.001230966	0.008148461	0.009943428	0.008687088	0.004253775	0.027826814	1.52E-06	0.001043313	0.000684113
195	0.006423156	0.006423156	0.038177205	0.0801446	0.002615459	0.001161338	0.008140408	0.010142223	0.008736646	0.004258383	0.027447406	1.47E-06	0.001058966	0.000669263
200	0.006401316	0.006401316	0.038248848	0.08000821	0.002556249	0.001121079	0.008308182	0.010342464	0.008695617	0.00424909	0.027008807	1.36E-06	0.001050946	0.000679364
205	0.006367084	0.006367084	0.038248646	0.079794005	0.002589333	0.001090066	0.008294596	0.01042477	0.008863028	0.004240986	0.026423102	1.29E-06	0.001069735	0.000673931
210	0.00633951	0.00633951	0.038231296	0.07962104	0.002565551	0.001073501	0.008376442	0.010426684	0.008719056	0.004228722	0.026262049	1.23E-06	0.001061164	0.000680703
215	0.006344767	0.006344767	0.038144904	0.079654045	0.002464469	0.00104369	0.008489009	0.010558456	0.00890159	0.004223409	0.02603187	1.18E-06	0.00107428	0.000659715
220	0.006376559	0.006376559	0.037970562	0.07985336	0.002444732	0.001030115	0.008551283	0.01065255	0.008952754	0.004217016	0.02616432	1.12E-06	0.001077469	0.00067423
225	0.006360372	0.006360372	0.037916908	0.079751946	0.002415541	0.001015549	0.008613585	0.01076027	0.008904081	0.004207726	0.025936209	1.07E-06	0.001076155	0.000673532
230	0.006371485	0.006371485	0.037986219	0.07982158	0.002341469	0.001050446	0.008673452	0.010816983	0.009036575	0.004205024	0.02586532	1.06E-06	0.001059734	0.000664787
235	0.006318646	0.006318646	0.037894649	0.07948991	0.002371392	0.001007641	0.008889356	0.010825	0.00885295	0.004197211	0.025307791	1.06E-06	0.001056143	0.000677912
240	0.006330022	0.006330022	0.038110549	0.07956143	0.002361904	0.001023148	0.009108759	0.011049334	0.008740839	0.004192899	0.025129488	1.07E-06	0.001024141	0.000668635
245	0.006347493	0.006347493	0.038030704	0.07967116	0.002202028	0.001014039	0.009313337	0.011070498	0.008529188	0.004190407	0.025452327	1.04E-06	0.001012279	0.000689793
250	0.006362314	0.006362314	0.038052452	0.079764105	0.002257361	0.001002048	0.009468563	0.011205513	0.00861588	0.004189546	0.025214665	1.00E-06	0.000991685	0.00067688
255	0.00633653	0.00633653	0.038214358	0.07960232	0.002230126	0.001120323	0.009604586	0.011291327	0.00839535	0.004187773	0.024879036	1.00E-06	0.000983054	0.000672716
260	0.006408694	0.006408694	0.037977374	0.080054305	0.00229308	0.001032223	0.009603768	0.011319961	0.008664027	0.004191939	0.025290255	9.48E-07	0.000982717	0.000708017
265	0.006414784	0.006414784	0.037786883	0.08009235	0.002195714	0.001051422	0.009395271	0.011448873	0.008538793	0.004192875	0.025659543	8.91E-07	0.000980647	0.000683813
270	0.006414508	0.006414508	0.037691064	0.08009063	0.002192848	0.001062804	0.009476461	0.011394355	0.008416551	0.004189114	0.025761252	8.71E-07	0.000959727	0.0006911
275	0.006435176	0.006435176	0.037862215	0.08021956	0.002159243	0.001063393	0.009641403	0.011675084	0.008502783	0.004196451	0.025477532	8.72E-07	0.00093482	0.000700172
280	0.006464495	0.006464495	0.037834826	0.08040209	0.002192951	0.00107843	0.009655051	0.011561434	0.008463739	0.00419373	0.025851997	8.29E-07	0.00094194	0.000704859
285	0.006386603	0.006386603	0.038049752	0.079916224	0.002110913	0.001117691	0.009799247	0.011841283	0.00832605	0.004199767	0.024860753	8.75E-07	0.000915072	0.000694381
290	0.006508793	0.006508793	0.038155146	0.0806771	0.002229936	0.001091535	0.009731266	0.011917324	0.008644247	0.004202148	0.025640085	8.18E-07	0.000917602	0.000712978
295	0.006532633	0.006532633	0.038055412	0.08082472	0.002150481	0.001119811	0.009813735	0.011753199	0.008556028	0.004205721	0.026123669	8.07E-07	0.00090517	0.000697712
300	0.006544968	0.006544968	0.038201666	0.080900975	0.002147547	0.00112438	0.009877068	0.012046634	0.008572523	0.004211517	0.025874283	7.87E-07	0.000907265	0.000687677
305	0.006545873	0.006545873	0.038134876	0.08090658	0.002129968	0.001158999	0.009633999	0.012008149	0.008603855	0.004220495	0.026119644	7.90E-07	0.000899248	0.000683584
310	0.006498025	0.006498025	0.038084236	0.080610335	0.00211325	0.001187782	0.009640751	0.011967447	0.008281314	0.004233311	0.025998525	7.78E-07	0.000888432	0.000668656
315	0.006588315	0.006588315	0.038005059	0.081168436	0.002150905	0.001189534	0.009637262	0.01193245	0.008438534	0.004229766	0.02669948	7.35E-07	0.000899736	0.000704753
320	0.006639465	0.006639465	0.038301708	0.081482925	0.002218248	0.001192767	0.009592346	0.011979859	0.008789574	0.004241488	0.026780315	7.44E-07	0.000904826	0.000694486
325	0.006586862	0.006586862	0.038222966	0.08115948	0.002143107	0.001190522	0.009602706	0.012088588	0.008669494	0.004244936	0.026337547	7.26E-07	0.000894537	0.000696463
330	0.006565967	0.006565967	0.038187285	0.08103067	0.002117003	0.001239078	0.009555668	0.012224485	0.008363132	0.004260827	0.026306883	7.71E-07	0.000897594	0.000694227
335	0.006654926	0.006654926	0.038334784	0.08157772	0.002201073	0.001217078	0.009671475	0.01223436	0.008749118	0.004264351	0.026618022	7.38E-07	0.000906177	0.000686868
340	0.006650413	0.006650413	0.038118754	0.08155007	0.002146165	0.001251538	0.009521758	0.012027998	0.008614974	0.004280486	0.027085034	7.29E-07	0.000904162	0.000671284
345	0.006686161	0.006686161	0.038308563	0.081768945	0.002126064	0.001262379	0.009517982	0.012247583	0.008634399	0.004285225	0.027195066	7.39E-07	0.00089958	0.000692594
350	0.006759407	0.006759407	0.038578903	0.082215615	0.002165763	0.001281023	0.00981886	0.012502446	0.008648248	0.00428513	0.027278736	7.24E-07	0.00092272	0.000690417
355	0.00667828	0.00667828	0.038474347	0.08172075	0.002088128	0.00126873	0.00956089	0.01247528	0.008590381	0.004296115	0.026895117	7.31E-07	0.000911971	0.000695461
360	0.006757825	0.006757825	0.038809982	0.082205996	0.002162911	0.001286024	0.010103396	0.012748176	0.008671259	0.004322066	0.026685901	7.36E-07	0.000908841	0.000688945
365	0.006779125	0.006779125	0.038578979	0.08233545	0.00215017	0.001293933	0.009963889	0.012627298	0.008577262	0.004324905	0.02723699	7.22E-07	0.000933297	0.000682788
370	0.006781732	0.006781732	0.038673275	0.08235128	0.002175964	0.001278446	0.010232765	0.012566784	0.008664761	0.004325814	0.026938155	7.18E-07	0.000927091	0.000706822
375	0.006847061	0.006847061	0.038812278	0.08274697	0.002175099	0.001274134	0.01008557	0.012680098	0.008961346	0.004327543	0.027346212	7.15E-07	0.000939836	0.000680053
380	0.006754007	0.006754007	0.039539871	0.082182765	0.002153712	0.001263258	0.010798708	0.013388261	0.008755135	0.00433649	0.025240675	7.68E-07	0.000920081	0.000682979

385	0.006815506	0.006815506	0.039819975	0.08255607	0.002168721	0.001324461	0.010603995	0.013306186	0.008739974	0.004347387	0.02598031	7.82E-07	0.000950086	0.000733154
390	0.00682865	0.00682865	0.039386793	0.08263565	0.002101719	0.001271082	0.010477533	0.013320379	0.008832695	0.004361479	0.026297595	7.21E-07	0.000931052	0.000692251
395	0.007022977	0.007022977	0.039432051	0.08380321	0.00225365	0.001292662	0.010629069	0.013261264	0.009268437	0.004367062	0.027493203	6.68E-07	0.00096139	0.000702367
400	0.00692101	0.00692101	0.039909778	0.0831926	0.00219992	0.001265546	0.0118586	0.013528472	0.008858914	0.004353684	0.02551339	7.06E-07	0.000930083	0.000700786
405	0.006935808	0.006935808	0.039419579	0.0832815	0.002178039	0.001248488	0.011066793	0.013433409	0.008746143	0.00436166	0.026684528	6.78E-07	0.000935841	0.000702507
410	0.007038864	0.007038864	0.039903683	0.08389793	0.002169383	0.001259656	0.011238954	0.013768141	0.009045407	0.004373294	0.026888164	6.66E-07	0.000932584	0.000712388
415	0.007062808	0.007062808	0.040207558	0.084040515	0.002270954	0.001240934	0.01128928	0.014297093	0.009141305	0.004381101	0.026362563	6.76E-07	0.000957277	0.000686895
420	0.007059144	0.007059144	0.040020932	0.08401871	0.002238527	0.001235389	0.011357156	0.014077	0.009219006	0.00437246	0.02641718	6.65E-07	0.000962997	0.000711056
425	0.00697869	0.00697869	0.039753658	0.083538555	0.002235777	0.001182704	0.011072928	0.014196089	0.008988183	0.004364622	0.026105734	6.60E-07	0.000951708	0.000688496
430	0.007079464	0.007079464	0.040206725	0.08413955	0.002213086	0.001228011	0.0110453	0.014638323	0.008903974	0.004376478	0.026722865	6.54E-07	0.000965075	0.000700878
435	0.007209226	0.007209226	0.040491747	0.08490716	0.002266296	0.001226861	0.01097983	0.014594492	0.009183284	0.004394659	0.02776175	6.66E-07	0.000964018	0.000720403
440	0.00731192	0.00731192	0.040918953	0.08550977	0.002292326	0.001215146	0.011763393	0.014769401	0.009540241	0.004387509	0.027431088	6.39E-07	0.000983054	0.000736409
445	0.007248156	0.007248156	0.040652389	0.0851361	0.002327919	0.001200621	0.01122485	0.014882266	0.009423583	0.004379135	0.027335798	6.22E-07	0.000990409	0.000716362
450	0.007385839	0.007385839	0.040879269	0.085940905	0.002329739	0.001200262	0.011409188	0.015468983	0.009100204	0.004368063	0.028289836	6.21E-07	0.000989921	0.000701575
455	0.007371617	0.007371617	0.040627137	0.08585812	0.002298096	0.001191561	0.01112972	0.014794677	0.009489088	0.004374233	0.028720876	6.03E-07	0.000984054	0.000733266
460	0.007576906	0.007576906	0.040858852	0.08704543	0.002357822	0.001195377	0.011764705	0.014862885	0.00953272	0.004369885	0.029999558	5.69E-07	0.000976273	0.000709274
465	0.007577001	0.007577001	0.041153706	0.08704598	0.002336633	0.001181485	0.011446679	0.015584734	0.009325815	0.00439122	0.029790195	5.63E-07	0.001008077	0.000704613
470	0.007427984	0.007427984	0.041263756	0.08618575	0.002392231	0.001227455	0.011259315	0.0152819	0.009635469	0.004378241	0.028411357	5.87E-07	0.00098362	0.000709666
475	0.007472597	0.007472597	0.040930664	0.086444184	0.002392147	0.001198279	0.011001897	0.01531837	0.009749885	0.00437113	0.028972188	5.38E-07	0.001036612	0.000684926
480	0.007587413	0.007587413	0.041463044	0.08710576	0.002401936	0.001204232	0.011617867	0.01590358	0.009674365	0.004351886	0.029028116	5.46E-07	0.001008456	0.000683151
485	0.007535771	0.007535771	0.041193628	0.08680882	0.002418264	0.001191056	0.011024548	0.015395408	0.010157772	0.004417356	0.028980354	5.35E-07	0.001074571	0.000697846
490	0.0076955	0.0076955	0.040938873	0.08772401	0.002558803	0.00116751	0.010835593	0.015286124	0.010332707	0.004363186	0.030643703	4.80E-07	0.001086982	0.000679908
495	0.007464616	0.007464616	0.041114863	0.08639802	0.002425724	0.001217336	0.011050604	0.015435395	0.009833541	0.004388895	0.028553851	5.20E-07	0.001000315	0.000739979
500	0.00776562	0.00776562	0.041747418	0.08812277	0.00253126	0.001209956	0.012079123	0.015815781	0.010250852	0.004452042	0.029569484	4.77E-07	0.001031585	0.000715643

Bidirectional 6 hour

Epoch	Loss	Total MSE	Total MAE	Total RMSE	SkinTemp	SufPres	U10	V10	Humidity	Rainc	Rainnc	Snow	SolilTemp	SoilMoist
5	0.020283072	0.020283072	0.08550117	0.14241864	0.005795796	0.01101351	0.017472088	0.035705972	0.04769646	0.006664174	0.0691611	0.000946195	0.007473511	0.000901915
10	0.016304699	0.016304699	0.072829031	0.12768985	0.003950915	0.006806063	0.013731088	0.027888922	0.025361607	0.006514285	0.06835814	0.000673206	0.008999419	0.000763348
15	0.014937036	0.014937036	0.066975049	0.122217186	0.003627025	0.005003789	0.012683022	0.024721967	0.019523941	0.006399477	0.067676	0.000553999	0.00842259	0.000758536
20	0.014120572	0.014120572	0.06298625	0.11883001	0.003484757	0.004396359	0.012108778	0.022871446	0.01697401	0.006227641	0.06720232	0.000467664	0.006687542	0.000785199
25	0.013598564	0.013598564	0.060136888	0.11661289	0.00345316	0.00400513	0.011760637	0.021710323	0.015817352	0.00610077	0.06696543	0.000378652	0.004973213	0.000820966
30	0.013222089	0.013222089	0.05783162	0.114987336	0.003374769	0.003716589	0.011627837	0.021042172	0.014997928	0.006005043	0.06682305	0.000287089	0.003492809	0.000853596
35	0.012957543	0.012957543	0.055901305	0.11383121	0.003292591	0.003458738	0.011236075	0.020737113	0.014576168	0.005911264	0.06668727	0.000200652	0.002582992	0.000892572
40	0.012796804	0.012796804	0.054745504	0.11312296	0.003281787	0.003222171	0.011163119	0.020297425	0.014616779	0.005848166	0.066524185	0.000139766	0.001948235	0.00092641
45	0.012696867	0.012696867	0.053568169	0.11268039	0.003167469	0.00300921	0.011310569	0.020315442	0.014475971	0.005810058	0.06620501	9.49E-05	0.001627688	0.000952375
50	0.012452825	0.012452825	0.052376148	0.11159224	0.003098761	0.002805869	0.010849002	0.01984612	0.013941238	0.005770544	0.065755256	6.70E-05	0.001452266	0.000942214
55	0.012361774	0.012361774	0.051843807	0.1111835	0.003070673	0.00261517	0.011114323	0.019844558	0.013811697	0.00576038	0.06503771	4.71E-05	0.001358218	0.000957949
60	0.012199179	0.012199179	0.050853963	0.11044989	0.003003252	0.002392553	0.010882387	0.019947331	0.01371657	0.005735168	0.06400384	3.29E-05	0.001312655	0.000965182
65	0.012084775	0.012084775	0.049970729	0.10993077	0.002985973	0.002172404	0.01105359	0.020245448	0.013554119	0.005750069	0.062786676	2.48E-05	0.001311101	0.000963527
70	0.011867584	0.011867584	0.049326088	0.10893846	0.003020788	0.001986391	0.010998727	0.020246783	0.01339177	0.005756556	0.06101513	2.11E-05	0.001303269	0.000935371
75	0.011861364	0.011861364	0.048622406	0.10890988	0.003075831	0.0019075	0.011108541	0.020499552	0.013480105	0.005763695	0.060538273	1.54E-05	0.001319543	0.000905157

80	0.011743397	0.011743397	0.048138827	0.10836696	0.003035904	0.00181004	0.011249364	0.020352963	0.013073959	0.005789002	0.059997	1.21E-05	0.001271595	0.000842031
85	0.011693995	0.011693995	0.048204493	0.10813878	0.003188309	0.001765188	0.011121104	0.020542521	0.013029117	0.005804947	0.059457872	9.55E-06	0.001216633	0.000804715
90	0.011962067	0.011962067	0.048602177	0.10937122	0.003476371	0.001818217	0.011736421	0.020343564	0.013173824	0.005797565	0.061136123	7.23E-06	0.001298685	0.000832661
95	0.012057689	0.012057689	0.049293634	0.10980752	0.003620019	0.001814618	0.012660196	0.0206001	0.013242989	0.005756593	0.060678802	5.96E-06	0.001329101	0.000868507
100	0.012138938	0.012138938	0.049726903	0.110176854	0.003933187	0.001845992	0.013054737	0.020215057	0.013264145	0.005716674	0.06122468	4.78E-06	0.001270694	0.000859434
105	0.012138503	0.012138503	0.049333219	0.11017488	0.00385986	0.001935845	0.01303928	0.019542377	0.013367185	0.005699763	0.061686806	3.66E-06	0.001301563	0.000948696
110	0.0120815	0.0120815	0.050123985	0.10991586	0.004141289	0.002081788	0.012987152	0.02021746	0.01321769	0.005683695	0.060258348	3.11E-06	0.001306903	0.00091757
115	0.01209875	0.01209875	0.050054357	0.10999432	0.004070074	0.002006019	0.013795078	0.020556135	0.01270554	0.005658245	0.059939936	2.87E-06	0.00135132	0.000902283
120	0.012247756	0.012247756	0.050508955	0.11066959	0.004523458	0.001996578	0.014217135	0.021201527	0.012832319	0.005639379	0.05961708	2.37E-06	0.00159163	0.000856069
125	0.012374806	0.012374806	0.050083175	0.111242115	0.004376336	0.002071425	0.014305913	0.021425864	0.012596155	0.005618615	0.06085536	2.15E-06	0.001650573	0.000845671
130	0.012153958	0.012153958	0.049749073	0.11024498	0.003931904	0.002017197	0.015004235	0.021206332	0.011919542	0.005605533	0.05939762	2.18E-06	0.001665936	0.0007891
135	0.012122378	0.012122378	0.049932274	0.11010167	0.003806406	0.00196554	0.015297734	0.021971853	0.01180574	0.005582314	0.058369383	2.26E-06	0.001652162	0.000770384
140	0.01215045	0.01215045	0.049792756	0.11022909	0.003803087	0.001955674	0.015194052	0.02194704	0.011917475	0.0055789	0.058673512	2.32E-06	0.001689266	0.000743173
145	0.011979202	0.011979202	0.048688586	0.10944954	0.003633966	0.001886074	0.01476237	0.021149952	0.011638853	0.005555829	0.05865814	2.23E-06	0.001747556	0.000757046
150	0.011969389	0.011969389	0.049172537	0.10940469	0.003547166	0.002079243	0.014582463	0.022196328	0.011564954	0.005556054	0.05775659	2.43E-06	0.001653557	0.000755107
155	0.012020088	0.012020088	0.04834729	0.10963618	0.003645465	0.001973949	0.0145608	0.02156889	0.011606275	0.005540908	0.058786727	2.10E-06	0.00175756	0.000758196
160	0.012193034	0.012193034	0.048856148	0.11042207	0.003629277	0.002133293	0.014565049	0.023227314	0.011530462	0.005539145	0.05882422	2.00E-06	0.001729131	0.000750458
165	0.011905682	0.011905682	0.049351129	0.10911318	0.003223231	0.002303293	0.014749652	0.024299614	0.011277486	0.00553703	0.055380993	2.24E-06	0.001519732	0.000763555
170	0.011882161	0.011882161	0.049647516	0.10900533	0.003379542	0.002275101	0.015145252	0.023759324	0.011181873	0.005530448	0.055307783	2.25E-06	0.001454207	0.000785827
175	0.011677248	0.011677248	0.048575993	0.108061306	0.003375287	0.002242924	0.014492277	0.021943057	0.011232816	0.005537389	0.05560357	2.29E-06	0.001502663	0.000840205
180	0.011837538	0.011837538	0.050841545	0.10880044	0.003248716	0.002639578	0.015428361	0.024473848	0.011161918	0.005529457	0.05369677	2.37E-06	0.001369356	0.000825005
185	0.011968568	0.011968568	0.049255404	0.109400935	0.003498985	0.002270429	0.015052092	0.02331555	0.011578996	0.005533012	0.05604362	1.96E-06	0.001544665	0.000846372
190	0.011887666	0.011887666	0.049692967	0.10903058	0.003421328	0.002321946	0.015470515	0.023419635	0.011606169	0.005529278	0.05465453	1.79E-06	0.00156719	0.000884271
195	0.012015055	0.012015055	0.051992716	0.10961319	0.003129713	0.002549543	0.015681542	0.027026106	0.011323893	0.005532746	0.05273266	2.09E-06	0.001447221	0.000725035
200	0.012189446	0.012189446	0.050660448	0.11040582	0.003662334	0.0023487	0.015062252	0.02495477	0.012226945	0.005536044	0.055395562	1.69E-06	0.001809375	0.000896789
205	0.011878647	0.011878647	0.050504374	0.10898921	0.003298584	0.002282769	0.015260537	0.025060238	0.011746533	0.005537535	0.053079803	1.83E-06	0.0016745	0.000844143
210	0.011975367	0.011975367	0.051120447	0.109432004	0.003308591	0.002401027	0.015284161	0.025440618	0.011943692	0.005537356	0.05322503	1.73E-06	0.001754405	0.000857051
215	0.012125042	0.012125042	0.05156825	0.11011377	0.003108511	0.002623453	0.015606795	0.026758773	0.011975015	0.00554358	0.05309695	1.68E-06	0.00174688	0.000788783
220	0.012314088	0.012314088	0.053132603	0.110968865	0.003028995	0.002909158	0.016160449	0.02953229	0.011948812	0.005546686	0.051570017	1.72E-06	0.001702366	0.000740378
225	0.012246625	0.012246625	0.05141172	0.11066449	0.003205124	0.002468878	0.015403035	0.02629581	0.012720717	0.005542301	0.054190487	1.74E-06	0.001811457	0.000826705
230	0.012360165	0.012360165	0.05187031	0.11117629	0.003249622	0.00260344	0.01570764	0.027247718	0.012812477	0.005540331	0.053726822	1.65E-06	0.001872347	0.000839603
235	0.012349058	0.012349058	0.052040621	0.1111263	0.003203389	0.002671018	0.015764432	0.028022004	0.012544308	0.005543291	0.05303271	1.60E-06	0.00185798	0.00084984
240	0.012297012	0.012297012	0.052342656	0.110891886	0.003115809	0.002697242	0.015695889	0.028556332	0.012506455	0.005533298	0.05238839	1.61E-06	0.001760382	0.000714718
245	0.012591197	0.012591197	0.053399754	0.11221048	0.003180271	0.002805562	0.016184926	0.029141948	0.013601908	0.005544181	0.052747793	1.59E-06	0.001924853	0.000778945
250	0.01282933	0.01282933	0.055152352	0.113266654	0.002998343	0.002937463	0.017082902	0.033360627	0.012568306	0.005537204	0.05132485	1.60E-06	0.001785458	0.00069655
255	0.012557032	0.012557032	0.05247708	0.11205816	0.003145988	0.00278096	0.01613221	0.029119633	0.012955025	0.005542781	0.05325668	1.54E-06	0.001885107	0.000750402
260	0.012850909	0.012850909	0.054232123	0.11336184	0.003104773	0.002858397	0.016853996	0.031330515	0.013785317	0.005553518	0.05237899	1.42E-06	0.001863803	0.000778372
265	0.012842666	0.012842666	0.053506862	0.11332548	0.003289551	0.002781246	0.016699564	0.030226912	0.013870067	0.005559135	0.053365484	1.35E-06	0.001895965	0.000737386
270	0.012887508	0.012887508	0.054427195	0.11352319	0.003091768	0.002889065	0.01744891	0.031388525	0.013408399	0.005560507	0.05258538	1.39E-06	0.00182072	0.000680425
275	0.012982596	0.012982596	0.05336613	0.1139412	0.003379294	0.002685039	0.016882846	0.03023205	0.014624385	0.005568688	0.053774454	1.32E-06	0.001953334	0.000724546
280	0.013054973	0.013054973	0.053914821	0.11425834	0.003218212	0.002817228	0.017491035	0.031351257	0.013992707	0.005570963	0.053478792	1.24E-06	0.001910229	0.000718058
285	0.013015018	0.013015018	0.054176334	0.11408339	0.003206475	0.002863653	0.01740574	0.03204093	0.014168329	0.005587089	0.052332852	1.21E-06	0.001828509	0.000715394
290	0.013138344	0.013138344	0.053548442	0.114622615	0.003369723	0.002744987	0.017317666	0.031693146	0.014245844	0.005577299	0.053794276	1.21E-06	0.001911897	0.000727385
295	0.013217019	0.013217019	0.054461158	0.1149653	0.00335466	0.002912196	0.017228257	0.03216232	0.014761167	0.005598533	0.053439245	1.19E-06	0.002037148	0.000675467
300	0.013596723	0.013596723	0.055021713	0.11660499	0.003326168	0.002868471	0.017404366	0.034490112	0.014390147	0.00559786	0.055396836	1.10E-06	0.00182939	0.000662781
305	0.013655821	0.013655821	0.054732068	0.11685812	0.003371921	0.002897946	0.017668158	0.03374588	0.0143982	0.005592728	0.056276727	1.05E-06	0.001981746	0.000623845

310	0.013525199	0.013525199	0.054280788	0.11629787	0.003333917	0.002971553	0.017097956	0.03329033	0.014735045	0.005629267	0.05558564	1.02E-06	0.00196285	0.000644413
315	0.013679245	0.013679245	0.054958076	0.116958305	0.003428404	0.003257917	0.017512677	0.034487385	0.014436325	0.005615789	0.055306934	9.63E-07	0.002093523	0.000652537
320	0.013919373	0.013919373	0.055821436	0.1179804	0.003456901	0.00305129	0.018184757	0.036568847	0.014724218	0.005607686	0.054895796	9.61E-07	0.002106672	0.000596599
325	0.013591864	0.013591864	0.053954697	0.11658417	0.003479815	0.002875309	0.016997635	0.033092536	0.01511288	0.005629846	0.055912394	9.25E-07	0.002173084	0.000644209
330	0.013645133	0.013645133	0.054361123	0.11681239	0.003421082	0.003027465	0.017246382	0.0343903	0.013912953	0.005590863	0.056269776	8.90E-07	0.001988069	0.000603558
335	0.013645179	0.013645179	0.054753805	0.11681257	0.003390091	0.003072125	0.017634345	0.03544157	0.01380104	0.005624923	0.0547711	8.77E-07	0.002076468	0.000639254
340	0.013747623	0.013747623	0.054787182	0.11725026	0.003440397	0.003221488	0.017404838	0.035808563	0.013815288	0.005591279	0.055395063	8.46E-07	0.002135939	0.000662531
345	0.013404222	0.013404222	0.052814826	0.11577659	0.003500754	0.002842676	0.01660208	0.031557072	0.014233407	0.005600788	0.056811787	8.83E-07	0.002223858	0.000668913
350	0.013805563	0.013805563	0.055152165	0.11749708	0.003419449	0.003355136	0.017171312	0.036249395	0.013521639	0.00561384	0.05599203	8.36E-07	0.002074201	0.000657798
355	0.013594757	0.013594757	0.055461644	0.11659656	0.003492537	0.003247673	0.01679604	0.03574461	0.013659252	0.005632649	0.054622248	8.47E-07	0.002098095	0.000653626
360	0.013504926	0.013504926	0.054827842	0.11621069	0.003478961	0.003206903	0.017212719	0.034456693	0.013270222	0.005651351	0.05504093	8.66E-07	0.00206961	0.00066101
365	0.01359639	0.01359639	0.054702218	0.11660357	0.003390926	0.003158831	0.017087717	0.03515411	0.013206264	0.005638037	0.055736538	8.30E-07	0.002003762	0.000586885
370	0.013692585	0.013692585	0.054645754	0.117015325	0.003440414	0.003119457	0.017594103	0.03576592	0.012991038	0.005602516	0.055862077	7.62E-07	0.001901074	0.000648486
375	0.013454794	0.013454794	0.054636067	0.11599478	0.003741279	0.003106131	0.016993122	0.033284456	0.013669538	0.005648947	0.055311654	7.93E-07	0.002118508	0.000673512
380	0.013450399	0.013450399	0.053906397	0.11597586	0.003425759	0.003049702	0.017005092	0.033252954	0.013216514	0.005619001	0.05629567	7.66E-07	0.002000923	0.0006376
385	0.013830193	0.013830193	0.055341305	0.11760184	0.00375245	0.003231753	0.017694408	0.035081953	0.013466531	0.005674058	0.056594625	8.25E-07	0.002113541	0.000691796
390	0.013583637	0.013583637	0.054619155	0.116548866	0.003572627	0.0030355	0.017344283	0.034006935	0.013610338	0.005589531	0.055902053	7.64E-07	0.00207573	0.000698617
395	0.013595666	0.013595666	0.054805203	0.11660046	0.003590111	0.003173621	0.017221453	0.034734957	0.013882463	0.005672555	0.055000562	7.75E-07	0.001991954	0.000688211
400	0.0136242	0.0136242	0.054627656	0.116722755	0.003680607	0.003116615	0.01727205	0.033979908	0.013777962	0.005619649	0.05602342	7.14E-07	0.002090825	0.000680259
405	0.013673297	0.013673297	0.055186604	0.116932884	0.00364887	0.003158472	0.017343637	0.03440958	0.013669376	0.005761501	0.055970766	7.20E-07	0.002029116	0.000740931
410	0.013851557	0.013851557	0.055851909	0.11769264	0.003641144	0.003233641	0.01864124	0.03454432	0.013580881	0.00568407	0.0564521	7.14E-07	0.002011192	0.000726271
415	0.013814764	0.013814764	0.055816762	0.117536224	0.003387633	0.00322353	0.017716281	0.03559084	0.013193762	0.005886374	0.056505125	7.10E-07	0.001906126	0.000737255
420	0.013842125	0.013842125	0.055325031	0.117652565	0.003868009	0.003135761	0.017771631	0.035496827	0.014083816	0.005767115	0.05552738	7.80E-07	0.002054296	0.000715627
425	0.013654262	0.013654262	0.055361481	0.11685144	0.00362289	0.003116819	0.017722517	0.034568086	0.013518014	0.005782932	0.05537769	7.84E-07	0.002076131	0.000756764
430	0.013941099	0.013941099	0.056542415	0.11807241	0.003596877	0.003259164	0.017975096	0.036052227	0.01388706	0.005979746	0.05578662	7.77E-07	0.002100423	0.000772998
435	0.01415842	0.01415842	0.056382637	0.118989155	0.003708975	0.003294151	0.018221568	0.036138	0.014348128	0.005910064	0.057093743	7.22E-07	0.002068955	0.000799882
440	0.013916735	0.013916735	0.05638154	0.117969215	0.003569376	0.003311609	0.018557075	0.034427498	0.013672147	0.00609314	0.05656631	7.76E-07	0.0020614	0.000908025
445	0.014148633	0.014148633	0.057029936	0.118948035	0.003651463	0.003206556	0.018968739	0.0373469	0.014176694	0.006045259	0.0552622	7.48E-07	0.002019025	0.000808746
450	0.014221391	0.014221391	0.056772773	0.119253464	0.003651092	0.003263195	0.019836722	0.036042746	0.014076098	0.006025933	0.056407597	7.50E-07	0.002140369	0.000769414
455	0.014187959	0.014187959	0.057380721	0.119113214	0.003788904	0.003224662	0.018849349	0.0364935	0.014498167	0.006168399	0.055926044	7.41E-07	0.00209379	0.000836026
460	0.014506064	0.014506064	0.057986434	0.12044113	0.003860436	0.003278041	0.019481817	0.037749305	0.014881026	0.006538113	0.056271233	7.37E-07	0.002199759	0.000800166
465	0.014342621	0.014342621	0.057345051	0.11976067	0.003593174	0.003160513	0.019670118	0.03641202	0.01418529	0.0064529	0.057071153	7.65E-07	0.002034632	0.000845646
470	0.014848559	0.014848559	0.06022873	0.121854655	0.003882028	0.003261672	0.02074007	0.037861444	0.014501902	0.008232368	0.056959353	8.43E-07	0.002074829	0.000971087
475	0.014649212	0.014649212	0.057486397	0.12103393	0.003866037	0.003094883	0.021062186	0.036374126	0.015291512	0.006331804	0.0573956	7.04E-07	0.002273189	0.000802086
480	0.014579237	0.014579237	0.057663165	0.120744504	0.004030357	0.002972014	0.020111684	0.037135962	0.014477626	0.006465117	0.057598773	7.27E-07	0.002174665	0.000825445
485	0.01467065	0.01467065	0.058435399	0.12112244	0.004160498	0.003139168	0.01906554	0.03726748	0.015432001	0.006809668	0.057646845	7.07E-07	0.002213482	0.000971118
490	0.014839136	0.014839136	0.05844327	0.12181599	0.003905288	0.003073841	0.019865338	0.037794463	0.015296328	0.006954568	0.05818463	7.15E-07	0.002365275	0.000950923
495	0.015006523	0.015006523	0.05857997	0.12250113	0.003912072	0.003094061	0.021138001	0.03857933	0.015577091	0.007202501	0.057410173	7.37E-07	0.002276697	0.000874558
500	0.01497635	0.01497635	0.058135613	0.12237791	0.003907653	0.003008775	0.021061677	0.037248157	0.016557535	0.006968557	0.057788365	7.17E-07	0.002382882	0.000839185

LSTM-WL evaluation for long-term forecasting

Similar to Bi-LSTM, the MIMO LSTM-WL models are evaluated for long-term weather forecasting for different timeslots. All LSTM-WL models are trained for 300 epochs and model weights are saved in every 5 epochs. A sample of 6 hours and 9 hours evaluation results are given below. The optimal model with least MSE is highlighted in each timeslot.

LSTM-WL 6 hour

Epoch	Loss	Total MSE	Total MAE	Total RMSE	SkinTemp	SufPres	U10	V10	Humidity	Rainc	Rainnc	Snow	SolilTemp	SoilMoist
5	0.022414174	0.022414174	0.0939502	0.14971367	0.010031259	0.011534203	0.026124865	0.03680424	0.050837882	0.007338984	0.07027322	0.000930371	0.00888613	0.001380575
10	0.017764555	0.017764555	0.078556138	0.13328375	0.005448476	0.007926699	0.01882312	0.030983457	0.028650776	0.006941002	0.068814896	0.000664598	0.008113109	0.001279417
15	0.016543629	0.016543629	0.073106631	0.12862204	0.005126626	0.006885565	0.017086811	0.028881341	0.023834452	0.006589848	0.06785878	0.00051417	0.007247873	0.001410818
20	0.015928381	0.015928381	0.069497977	0.1262077	0.005119907	0.006401513	0.01653182	0.027925547	0.021921724	0.006280204	0.06744451	0.00035627	0.005916965	0.001385348
25	0.01556949	0.01556949	0.067073478	0.12477776	0.004934089	0.00628149	0.016463816	0.02827817	0.020017596	0.006123868	0.06736065	0.000236374	0.004693503	0.001305341
30	0.015218683	0.015218683	0.065042863	0.123364046	0.004958522	0.006093643	0.015530288	0.027653027	0.019452712	0.006081073	0.06737587	0.000171943	0.003680299	0.001189467
35	0.014890849	0.014890849	0.063018621	0.12202806	0.004784875	0.005936836	0.015081909	0.026686836	0.018763043	0.006031819	0.06739823	0.000125545	0.002949962	0.001149432
40	0.01464314	0.01464314	0.061136856	0.121008836	0.004503369	0.005862603	0.014901317	0.025897853	0.018304592	0.00595291	0.067393176	8.95E-05	0.002464172	0.001061873
45	0.014501445	0.014501445	0.060067559	0.12042194	0.004308695	0.005947388	0.014748776	0.025679912	0.017746862	0.00592637	0.06738201	6.39E-05	0.002160112	0.001050407
50	0.014333282	0.014333282	0.058737149	0.11972168	0.004105279	0.005540686	0.014688206	0.025033828	0.017667126	0.00586743	0.06737671	4.59E-05	0.001974501	0.001033139
55	0.014168474	0.014168474	0.057566161	0.11903141	0.003949024	0.005318294	0.014299074	0.024437783	0.017531766	0.005819714	0.06736401	3.35E-05	0.001886781	0.001044756
60	0.014018452	0.014018452	0.05680187	0.11839954	0.003848595	0.005062948	0.013860821	0.024295058	0.017118838	0.005805542	0.067337625	2.57E-05	0.001785447	0.001043923
65	0.013952059	0.013952059	0.056447311	0.118118845	0.003739563	0.005073377	0.013713046	0.0243612	0.016786892	0.005773227	0.06730428	1.94E-05	0.001755756	0.000993832
70	0.013791142	0.013791142	0.055635661	0.11743569	0.00361989	0.004675886	0.013439506	0.023918277	0.016526781	0.005765527	0.067250796	1.61E-05	0.001704338	0.000994357
75	0.013718391	0.013718391	0.055307278	0.11712553	0.003569532	0.004585134	0.012831308	0.024346732	0.016213113	0.005743641	0.067178234	1.27E-05	0.001711499	0.000991982
80	0.013665511	0.013665511	0.054882348	0.11689958	0.003554245	0.004346681	0.013029473	0.023878168	0.016245391	0.005727679	0.06712464	1.08E-05	0.001768117	0.000969945
85	0.013620111	0.013620111	0.054640387	0.11670523	0.003517286	0.004142646	0.013241126	0.023481863	0.016259545	0.005721421	0.06703354	9.42E-06	0.001798884	0.000995377
90	0.013548221	0.013548221	0.05447198	0.116396815	0.003464681	0.004016172	0.013299936	0.023517817	0.015773738	0.00573087	0.06692151	8.57E-06	0.001769964	0.000978954
95	0.013532088	0.013532088	0.054565691	0.116327494	0.003537399	0.004062178	0.012953406	0.02397378	0.015505341	0.005720303	0.06681938	7.97E-06	0.001832973	0.000908155
100	0.013401961	0.013401961	0.053868142	0.11576684	0.003515252	0.004067625	0.012702137	0.023481393	0.015084154	0.00570772	0.06673341	7.10E-06	0.00183284	0.000887977
105	0.01342739	0.01342739	0.054330809	0.11587663	0.003558016	0.003920403	0.012778109	0.02391559	0.015144708	0.005742667	0.06655884	7.10E-06	0.001822541	0.000825932
110	0.013391375	0.013391375	0.054094055	0.115721114	0.003765801	0.004009213	0.012740324	0.02308084	0.015330496	0.005732904	0.0664906	6.29E-06	0.001940942	0.000816336
115	0.013396986	0.013396986	0.053979356	0.115745336	0.003767194	0.003864035	0.013132761	0.022981502	0.015216896	0.005750901	0.066406675	5.73E-06	0.001983097	0.000861071
120	0.013408722	0.013408722	0.05390889	0.115796044	0.003873608	0.003740326	0.013787211	0.022718053	0.014923036	0.005757792	0.06622404	4.78E-06	0.002133034	0.000925347
125	0.013330405	0.013330405	0.054064127	0.11545738	0.004022846	0.003901173	0.013042938	0.02287912	0.014646684	0.00579911	0.06614605	4.84E-06	0.002024139	0.000837146
130	0.013450973	0.013450973	0.053999839	0.11597832	0.004281018	0.003809495	0.014188983	0.022063643	0.01493468	0.00577568	0.066178694	3.52E-06	0.002329693	0.000944331
135	0.013318015	0.013318015	0.053663225	0.1154037	0.004639609	0.003858151	0.012810514	0.022046281	0.01462115	0.005784144	0.066059604	3.09E-06	0.002381156	0.000976452
140	0.013393904	0.013393904	0.053864587	0.11573203	0.004823206	0.003721913	0.013456618	0.021855615	0.014829316	0.005827054	0.0658913	2.44E-06	0.002500529	0.00103105
145	0.013263946	0.013263946	0.053636546	0.1151692	0.004730743	0.004029587	0.013253746	0.021873929	0.013993448	0.005831303	0.06560797	2.18E-06	0.002344848	0.000971699
150	0.013501682	0.013501682	0.054140638	0.11619674	0.005223346	0.004213012	0.013554422	0.02175627	0.014723933	0.005833417	0.06589901	1.56E-06	0.00268207	0.00112979
155	0.013577226	0.013577226	0.05393603	0.116521366	0.005482897	0.003982358	0.013483964	0.02143989	0.015108997	0.005850582	0.06590138	1.05E-06	0.003328134	0.001193012
160	0.0136207	0.0136207	0.053583005	0.11670775	0.00509115	0.003750135	0.013938145	0.021637851	0.015425773	0.005875147	0.06601915	9.21E-07	0.003285737	0.001183

165	0.013665296	0.013665296	0.053121848	0.116898656	0.004547733	0.003672225	0.013846602	0.022007918	0.015535436	0.005927933	0.06642256	8.56E-07	0.00338378	0.001307913
170	0.013934235	0.013934235	0.053464004	0.118043356	0.004665324	0.003268354	0.015430715	0.022545233	0.016243972	0.006049516	0.06661181	1.01E-06	0.003308608	0.001217809
175	0.014010166	0.014010166	0.053711154	0.11836454	0.005097196	0.003250742	0.015433976	0.02314886	0.01558116	0.006085265	0.06694055	9.49E-07	0.003414884	0.001148077
180	0.014420222	0.014420222	0.055050784	0.12008421	0.005311596	0.003232	0.018386537	0.02401742	0.015845506	0.006120498	0.066997685	9.47E-07	0.003177639	0.001112394
185	0.014775267	0.014775267	0.05653622	0.121553555	0.005711442	0.003410973	0.019536544	0.024743022	0.01645855	0.006048538	0.06753946	6.39E-07	0.003153228	0.001150277
190	0.014577239	0.014577239	0.055934658	0.12073624	0.00514692	0.003484109	0.01827535	0.023872845	0.016788404	0.00625096	0.06753077	5.33E-07	0.003154038	0.001268452
195	0.014406827	0.014406827	0.055441691	0.12002845	0.005114146	0.003765975	0.017276697	0.022904793	0.016592007	0.006209747	0.06782698	4.44E-07	0.00296904	0.00140843
200	0.014331757	0.014331757	0.055267891	0.11971531	0.004550984	0.003938125	0.016849296	0.024165722	0.016030053	0.006225417	0.067433864	4.20E-07	0.00266482	0.001458883
205	0.014716593	0.014716593	0.056384701	0.12131196	0.005006013	0.004088576	0.019179974	0.022896774	0.017629296	0.006232991	0.06797939	3.54E-07	0.002540496	0.00161206
210	0.014636744	0.014636744	0.055956307	0.120982416	0.004558456	0.004171998	0.017439805	0.02597418	0.01654936	0.006365384	0.067366466	3.50E-07	0.002403612	0.001537834
215	0.014946183	0.014946183	0.056921612	0.122254565	0.00522397	0.00422072	0.020022396	0.023313908	0.01832035	0.006207848	0.068222165	2.87E-07	0.002286863	0.001643324
220	0.014580893	0.014580893	0.05555159	0.12075137	0.004693559	0.004251367	0.0189747	0.024894396	0.01608941	0.006198917	0.06743006	3.26E-07	0.001900649	0.001375559
225	0.014988317	0.014988317	0.056646842	0.122426786	0.005223664	0.004129902	0.021557795	0.023748046	0.017469458	0.006052447	0.068226345	2.29E-07	0.002037242	0.001438052
230	0.015033121	0.015033121	0.056755435	0.122609615	0.005393547	0.004043862	0.019898795	0.02479343	0.018745039	0.006166741	0.068040304	2.63E-07	0.001986947	0.00126228
235	0.014868241	0.014868241	0.055938067	0.121935405	0.005126333	0.004153604	0.020759022	0.023604028	0.017297652	0.006010277	0.06824702	2.69E-07	0.002162058	0.001322136
240	0.015407248	0.015407248	0.057767097	0.12412594	0.004959579	0.004366703	0.025672365	0.024410645	0.017835988	0.006081911	0.06773312	2.75E-07	0.001875328	0.001136574
245	0.015486434	0.015486434	0.058059063	0.12444452	0.005034522	0.004639091	0.02594825	0.025861671	0.01647501	0.00631437	0.067909405	3.18E-07	0.001690307	0.000991393
250	0.015686362	0.015686362	0.058094538	0.1252452	0.005351822	0.004347616	0.027559718	0.024339082	0.017743519	0.006254975	0.06820412	2.77E-07	0.002074024	0.000988458
255	0.016584908	0.016584908	0.060230616	0.12878242	0.004666843	0.004411259	0.036489293	0.025277456	0.017326852	0.006375922	0.06864609	3.07E-07	0.001724786	0.000930266
260	0.016759438	0.016759438	0.060190089	0.12945823	0.00473273	0.00428595	0.038487475	0.025006067	0.018365284	0.006247992	0.06759724	2.73E-07	0.001873241	0.000998126
265	0.017356419	0.017356419	0.06173181	0.13174374	0.004364005	0.00418029	0.04338253	0.027419578	0.017047832	0.00628826	0.06818693	3.01E-07	0.001799595	0.000894865
270	0.017183477	0.017183477	0.061175131	0.13108578	0.004503644	0.004042882	0.042328432	0.027004575	0.017755935	0.006259415	0.06692675	3.19E-07	0.002052663	0.000960145
275	0.017786079	0.017786079	0.062475436	0.13336447	0.004078054	0.00405325	0.04813856	0.027838198	0.017807113	0.006272558	0.06658179	3.38E-07	0.002094215	0.000996717
280	0.017794729	0.017794729	0.062419768	0.13339688	0.004129331	0.003905453	0.048243646	0.027460428	0.018317422	0.006252917	0.066432506	3.56E-07	0.002114279	0.001090958
285	0.018776455	0.018776455	0.064086232	0.13702722	0.004086437	0.003621116	0.053066585	0.030437866	0.020324033	0.006339358	0.06644203	3.17E-07	0.002254828	0.001191988
290	0.018080846	0.018080846	0.063087268	0.13446501	0.00411146	0.003838797	0.04971124	0.029782584	0.017992424	0.006091405	0.066195086	3.54E-07	0.002128396	0.00095672
295	0.018317879	0.018317879	0.064747051	0.13534355	0.004598451	0.003867979	0.050494518	0.030142432	0.01839249	0.006138175	0.06611344	3.18E-07	0.002454073	0.000976909
300	0.019483095	0.019483095	0.065828427	0.13958184	0.004388827	0.003982899	0.058141455	0.030979631	0.021059142	0.005971437	0.06673305	2.47E-07	0.0025314	0.001042851

LSTM-WL 9 hour

Epoch	Loss	Total MSE	Total MAE	Total RMSE	SkinTemp	SufPres	U10	V10	Humidity	Rainc	Rainnc	Snow	SolilTemp	SoilMoist
5	0.026275521	0.026275521	0.101761362	0.16209728	0.013174409	0.011629769	0.022632407	0.041043743	0.058566898	0.009642377	0.09327717	0.001128815	0.010221067	0.001438553
10	0.021407644	0.021407644	0.085084076	0.14631353	0.007406938	0.008504082	0.020242997	0.036150087	0.03229127	0.008403188	0.089277156	0.00062207	0.010040337	0.001138306
15	0.019901981	0.019901981	0.078185017	0.14107437	0.006241981	0.007236892	0.019551422	0.032554295	0.026911238	0.007680261	0.08798393	0.000375009	0.009311087	0.001173685
20	0.019184853	0.019184853	0.074631175	0.13850941	0.005766419	0.007031727	0.019357577	0.031510834	0.02361178	0.007366702	0.08775671	0.00023386	0.008048513	0.001164407
25	0.018722763	0.018722763	0.072153713	0.13683113	0.005374539	0.006841946	0.019154776	0.03135262	0.021942195	0.007271178	0.08772898	0.000156304	0.006243635	0.001161474
30	0.01846531	0.01846531	0.070855127	0.13588712	0.005069285	0.006831492	0.01915723	0.031442802	0.020925367	0.007291769	0.08776427	0.000114852	0.004939552	0.00111646
35	0.01838234	0.01838234	0.069542231	0.1355815	0.004900442	0.006686455	0.019035341	0.033148192	0.019833775	0.007255781	0.0877553	7.67E-05	0.004013221	0.001118242
40	0.018098963	0.018098963	0.067831101	0.13453238	0.004368685	0.006567199	0.019177698	0.03200961	0.0193943	0.0072393	0.08778276	5.69E-05	0.003301797	0.001091352
45	0.01807716	0.01807716	0.066964513	0.13445131	0.004450665	0.006424032	0.01867395	0.033144794	0.01894425	0.007226858	0.08777138	4.10E-05	0.003003016	0.001091635
50	0.017977385	0.017977385	0.065909431	0.13407975	0.004189851	0.00627675	0.017964058	0.03399596	0.018524725	0.007196101	0.0877683	3.05E-05	0.002731896	0.001095686
55	0.017896984	0.017896984	0.06569254	0.1337796	0.004059058	0.006251269	0.01801654	0.033725362	0.018384306	0.007221302	0.087753095	2.62E-05	0.002475557	0.001057111
60	0.017719513	0.017719513	0.064943969	0.13311465	0.004104341	0.006103051	0.017727807	0.032815482	0.018009545	0.007197962	0.08773593	2.13E-05	0.002375133	0.001104605
65	0.017623323	0.017623323	0.064527148	0.13275285	0.003916253	0.005903432	0.017435784	0.033081055	0.017469669	0.007240002	0.08782583	1.95E-05	0.002264369	0.001077371
70	0.017623463	0.017623463	0.064150447	0.13275339	0.004030704	0.005613887	0.017603258	0.033335596	0.017421225	0.007161198	0.08763264	1.52E-05	0.002259516	0.001161364

75	0.017570399	0.017570399	0.064104309	0.13255338	0.003785324	0.005435103	0.01789222	0.032980144	0.017330563	0.007261488	0.087723635	1.39E-05	0.002125454	0.001156121
80	0.017759231	0.017759231	0.064603945	0.13326375	0.003915984	0.005202694	0.019374834	0.03287042	0.017797193	0.007262243	0.08778462	1.19E-05	0.002102287	0.001270098
85	0.017737703	0.017737703	0.064387969	0.13318297	0.003605413	0.005147065	0.020027319	0.032431446	0.017551718	0.007409593	0.08803263	1.05E-05	0.00194199	0.001219319
90	0.018037181	0.018037181	0.0646765	0.13430256	0.003845482	0.005063482	0.021927735	0.03245828	0.018216103	0.007372594	0.08795897	6.94E-06	0.002013054	0.001509169
95	0.018196616	0.018196616	0.065023264	0.13489483	0.004154565	0.004850584	0.021989118	0.032273322	0.019659521	0.007435813	0.08779946	4.69E-06	0.002184178	0.001614896
100	0.018166132	0.018166132	0.06475562	0.1347818	0.004233669	0.005041287	0.021303525	0.03242171	0.019246435	0.007487273	0.08850328	3.59E-06	0.001985068	0.001435489
105	0.018456643	0.018456643	0.064877757	0.13585524	0.00466254	0.005082296	0.022525378	0.03216174	0.020049073	0.007509431	0.08840842	1.87E-06	0.002429272	0.001736415
110	0.018544228	0.018544228	0.064428491	0.13617717	0.004733233	0.005168534	0.02196873	0.031791255	0.020708399	0.007450937	0.0887746	1.11E-06	0.002944004	0.001901482
115	0.018657551	0.018657551	0.064951354	0.13659266	0.005057793	0.005844035	0.020375092	0.03217637	0.022164509	0.007642551	0.08885965	9.43E-07	0.003020125	0.001434448
120	0.018634566	0.018634566	0.064426622	0.1365085	0.005171152	0.006336034	0.018444398	0.031894263	0.021818472	0.007624168	0.08983677	5.64E-07	0.003687673	0.001532168
125	0.018815735	0.018815735	0.065277751	0.13717046	0.005258968	0.007481029	0.018518887	0.03281355	0.021383077	0.007418594	0.09014923	4.87E-07	0.003688528	0.001445
130	0.018927665	0.018927665	0.066517556	0.13757786	0.0053357	0.008250065	0.019256553	0.033420097	0.020541636	0.007481385	0.08996735	4.48E-07	0.003454088	0.001569332
135	0.019681574	0.019681574	0.069689528	0.14029102	0.006026587	0.009436766	0.022533102	0.033734083	0.021607112	0.007195051	0.09040496	2.72E-07	0.003875535	0.002002279
140	0.020120138	0.020120138	0.071065718	0.14184548	0.005295146	0.010176069	0.02778382	0.033286158	0.02061904	0.007066625	0.08969243	2.10E-07	0.004623326	0.002658555
145	0.021055573	0.021055573	0.073563635	0.14510536	0.005363931	0.010016319	0.035667967	0.033229876	0.02092173	0.006988117	0.089711756	1.78E-07	0.005625201	0.003030641
150	0.021037861	0.021037861	0.072436314	0.14504436	0.004981833	0.009081511	0.036600746	0.033966325	0.021078406	0.006995814	0.09017637	1.96E-07	0.004956763	0.002540646
155	0.020950628	0.020950628	0.070046832	0.14474334	0.003823496	0.007302241	0.039900437	0.033787888	0.020587858	0.007107885	0.09086849	1.98E-07	0.00387324	0.002254545
160	0.021077197	0.021077197	0.070608101	0.1451799	0.004234404	0.006914011	0.039934997	0.034289178	0.021835456	0.007060802	0.090543605	2.27E-07	0.003666643	0.002292638
165	0.02048257	0.02048257	0.069262746	0.14311732	0.004102228	0.006289692	0.035845306	0.03445634	0.02169116	0.007121289	0.08972221	2.78E-07	0.003461089	0.002136113
170	0.02012672	0.02012672	0.069059672	0.14186868	0.003732007	0.006145316	0.032608498	0.03553623	0.021019282	0.007148744	0.08995004	3.24E-07	0.00318217	0.00194459
175	0.020295917	0.020295917	0.070570681	0.14246373	0.004724188	0.005863053	0.030224757	0.036228687	0.021303715	0.007048319	0.092555575	3.46E-07	0.003042962	0.001967561
180	0.020665298	0.020665298	0.070388875	0.1437543	0.004638486	0.005668575	0.031259794	0.035693564	0.024027783	0.007027842	0.09365876	3.52E-07	0.002764163	0.001913653
185	0.021428162	0.021428162	0.071173268	0.1463836	0.004628113	0.005559258	0.029682102	0.03673707	0.02297968	0.00708443	0.10340069	3.81E-07	0.002600482	0.001609425
190	0.021031039	0.021031039	0.069704643	0.14502083	0.003725145	0.005842929	0.029785715	0.037890896	0.022835257	0.007052975	0.0984438	3.41E-07	0.002837829	0.001895507
195	0.024521026	0.024521026	0.075673534	0.1565919	0.004951991	0.005811547	0.0268534	0.04005555	0.022324435	0.006945954	0.1339322	4.13E-07	0.002591013	0.001743762
200	0.022560364	0.022560364	0.072370302	0.15020108	0.004412673	0.006034426	0.02924547	0.041945253	0.02361499	0.006971865	0.10876384	3.81E-07	0.002981989	0.001632744
205	0.023215886	0.023215886	0.072955479	0.15236759	0.004165188	0.006104286	0.030297788	0.044136852	0.022941208	0.006965982	0.11285683	4.65E-07	0.003065187	0.001625072
210	0.022184211	0.022184211	0.071171069	0.14894366	0.004208001	0.006406521	0.03192459	0.044922747	0.022219494	0.006934915	0.100244135	4.17E-07	0.003430264	0.001551017
215	0.023176762	0.023176762	0.072991119	0.15223916	0.004520199	0.006288634	0.032815035	0.045736175	0.021763945	0.006905764	0.108771145	4.83E-07	0.0034992	0.00146705
220	0.023802774	0.023802774	0.074021354	0.1542815	0.004319681	0.006362602	0.037907124	0.048157096	0.020278415	0.00690402	0.10918618	4.87E-07	0.003499082	0.001413057
225	0.023675155	0.023675155	0.0740605	0.1538673	0.004399443	0.006573606	0.04055143	0.049955033	0.021022242	0.006906653	0.10204375	4.87E-07	0.003900105	0.0013988
230	0.025199936	0.025199936	0.076297552	0.15874489	0.00465372	0.006333379	0.038374703	0.04978445	0.021169107	0.006875772	0.12000209	5.22E-07	0.003420144	0.001385463
235	0.02542081	0.02542081	0.077143896	0.15943906	0.004392353	0.006392765	0.043201275	0.050784286	0.021771498	0.006893645	0.11545781	4.86E-07	0.003787598	0.001526365
240	0.025194379	0.025194379	0.077277088	0.15872735	0.004416023	0.006595906	0.043406595	0.052676804	0.022848746	0.006879174	0.110119395	5.22E-07	0.003623997	0.001376623
245	0.025665687	0.025665687	0.077790293	0.16020516	0.004461962	0.006518664	0.04261739	0.05458412	0.021702558	0.006872979	0.11495795	5.63E-07	0.003520796	0.001419885
250	0.025713864	0.025713864	0.078707288	0.16035543	0.004103075	0.006673066	0.04418755	0.05502684	0.023130093	0.006878718	0.11225963	5.84E-07	0.003461687	0.001417425
255	0.024951605	0.024951605	0.077653737	0.15796077	0.00418938	0.006430139	0.04034193	0.051226735	0.022446994	0.006868654	0.11306329	6.04E-07	0.003402635	0.001545694
260	0.026092007	0.026092007	0.080365659	0.1615302	0.004729026	0.006359334	0.043436054	0.052569143	0.023253713	0.006845983	0.11835017	5.88E-07	0.003706941	0.00166912
265	0.025028355	0.025028355	0.078354251	0.15820351	0.004311704	0.006241739	0.041254755	0.050937146	0.024167178	0.0069095	0.11108785	5.90E-07	0.003810503	0.001562581
270	0.02478968	0.02478968	0.078273831	0.1574474	0.003670111	0.006543657	0.042346634	0.05549914	0.023357155	0.00688186	0.104307376	5.00E-07	0.003712597	0.001577768
275	0.025452541	0.025452541	0.078594047	0.15953851	0.003633024	0.005907488	0.038150016	0.051935017	0.02300392	0.006895899	0.11972114	5.43E-07	0.003700077	0.001578297
280	0.024821104	0.024821104	0.077332118	0.15754715	0.004035065	0.006086757	0.03949553	0.054329686	0.022337625	0.006875606	0.10976225	4.99E-07	0.003807572	0.001480436
285	0.026223551	0.026223551	0.079322344	0.1619369	0.003893481	0.006055305	0.03718238	0.054733925	0.024720265	0.006933306	0.12361965	5.34E-07	0.0035913	0.001505357
290	0.025797573	0.025797573	0.07924305	0.16061625	0.004103503	0.005680767	0.036171846	0.05436686	0.023839863	0.006897199	0.12142194	5.44E-07	0.003967876	0.00152533
295	0.025530395	0.025530395	0.077953213	0.15978234	0.003908843	0.00578132	0.035028648	0.054469768	0.02353533	0.006930125	0.12070233	5.42E-07	0.003611514	0.001335535
300	0.024644043	0.024644043	0.076778826	0.15698422	0.004212673	0.005902861	0.03405233	0.054389387	0.024067752	0.006999387	0.11186775	5.95E-07	0.003582568	0.001365119

LSTM-LW evaluation for long-term forecasting

Similar to LSTM-WL, the MIMO LSTM-LW models are evaluated for long-term weather forecasting for different timeslots. All LSTM-LW models are trained for 200 epochs and model weights are saved in every 10 epochs. A sample of 6 hours and 9 hours evaluation results are given below. The optimal model with least MSE is highlighted in each timeslot.

LSTM-LW 6 hour

Epoch	Loss	Total MSE	Total MAE	Total RMSE	SkinTemp	SufPres	U10	V10	Humidity	Rainc	Rainnc	Snow	SolilTemp	SoilMoist
10	0.011880832	0.011880832	0.047026494	0.108999215	0.00373121	0.002185203	0.012854352	0.013167098	0.014048727	0.006119361	0.063629046	2.48E-06	0.002096815	0.000974029
20	0.011889752	0.011889752	0.051545577	0.109040126	0.005614922	0.002947571	0.011071177	0.013335191	0.01677148	0.007184937	0.059253287	2.00E-06	0.00180137	0.000915595
30	0.011946544	0.011946544	0.046494962	0.10930026	0.003721001	0.0022465	0.012735943	0.01419268	0.013358736	0.006295456	0.064201206	7.44E-07	0.001755331	0.000957846
40	0.012283988	0.012283988	0.048452309	0.11083315	0.003946102	0.002666186	0.015601515	0.013403405	0.013299466	0.005994819	0.065014794	3.90E-07	0.002092412	0.000820788
50	0.011968353	0.011968353	0.047357106	0.109399974	0.003802319	0.002693907	0.012771716	0.014566889	0.013339048	0.006059668	0.06385493	3.64E-07	0.001811673	0.000783019
60	0.01184735	0.01184735	0.047151309	0.108845524	0.003671956	0.002680889	0.013538075	0.013685755	0.013493523	0.005832097	0.06298571	2.26E-07	0.001729121	0.000856148
70	0.011799956	0.011799956	0.046568167	0.10862758	0.003252286	0.002202216	0.011237701	0.01622022	0.015044644	0.005824219	0.06160926	1.83E-07	0.00192054	0.000688296
80	0.011741312	0.011741312	0.045655386	0.108357325	0.003105633	0.001950991	0.013234701	0.013633886	0.012803255	0.005710668	0.06383751	1.21E-07	0.002277339	0.000859006
90	0.012112958	0.012112958	0.04740905	0.11005889	0.003269029	0.001732615	0.013996867	0.01698269	0.013135998	0.005770418	0.06306092	1.51E-07	0.002452568	0.000728323
100	0.012187444	0.012187444	0.048374469	0.11039675	0.003405049	0.001708889	0.013968434	0.018579261	0.013793162	0.005720335	0.061504878	1.70E-07	0.00249288	0.000701383
110	0.012657643	0.012657643	0.05070106	0.11250619	0.004262536	0.002003955	0.015268126	0.02327254	0.012695582	0.005686414	0.06064813	1.63E-07	0.001822816	0.000916166
120	0.012829151	0.012829151	0.049755243	0.113265835	0.003915706	0.002255355	0.01458518	0.02340477	0.012871401	0.00566747	0.062535815	1.67E-07	0.00239053	0.000665109
130	0.013627052	0.013627052	0.053838368	0.11673497	0.004222805	0.002664993	0.016297309	0.03063119	0.013408243	0.00567446	0.060534995	1.34E-07	0.001795727	0.001040662
140	0.013653389	0.013653389	0.053063726	0.116847716	0.004031833	0.002775423	0.014514714	0.02910935	0.014565311	0.005629259	0.06255872	1.13E-07	0.002342	0.001007178
150	0.013472496	0.013472496	0.051782125	0.116071075	0.003526571	0.002482961	0.013233547	0.030468164	0.013498244	0.005674074	0.06269933	1.27E-07	0.002138502	0.001003449
160	0.013516137	0.013516137	0.052800921	0.116258934	0.003454343	0.002500062	0.016590854	0.028890422	0.013912486	0.005647554	0.061493102	9.34E-08	0.001607068	0.001065381
170	0.013407045	0.013407045	0.05258392	0.11578879	0.003472978	0.00250838	0.014671385	0.028681722	0.014318332	0.005668049	0.06124811	7.22E-08	0.002071	0.001430414
180	0.013301829	0.013301829	0.051897612	0.11533356	0.003659899	0.002420059	0.012969964	0.027121764	0.015814813	0.005646311	0.061921947	7.29E-08	0.002188269	0.001275198
190	0.013242478	0.013242478	0.052232255	0.11507596	0.003871053	0.002349507	0.013302174	0.026180876	0.015240627	0.005633408	0.06210364	5.09E-08	0.002199922	0.001543519
200	0.013652145	0.013652145	0.052859727	0.116842404	0.003343507	0.002428929	0.012679976	0.03132901	0.015193537	0.00563848	0.062400546	3.83E-08	0.002390753	0.001116677

LSTM-LW 9 hour

Epoch	Loss	Total MSE	Total MAE	Total RMSE	SkinTemp	SufPres	U10	V10	Humidity	Rainc	Rainnc	Snow	SolilTemp	SoilMoist
10	0.015757935	0.015757935	0.055693333	0.12553059	0.004679656	0.00337704	0.016287696	0.022693845	0.016228491	0.007961646	0.08320849	2.14E-06	0.002113115	0.001027248
20	0.016377352	0.016377352	0.05758737	0.12797405	0.004780752	0.004161583	0.015768358	0.024669867	0.017805502	0.007928615	0.08485703	3.95E-07	0.002780593	0.001020818
30	0.016225789	0.016225789	0.056997567	0.12738049	0.004396642	0.00394337	0.016345497	0.024135446	0.018725771	0.007424103	0.08399795	1.34E-07	0.002588698	0.000700276
40	0.016889573	0.016889573	0.058274614	0.12995991	0.004091627	0.003541212	0.023068156	0.025812227	0.017774226	0.007382475	0.08432323	5.62E-08	0.00227121	0.000631322
50	0.015881893	0.015881893	0.055916136	0.12602338	0.003115935	0.003512865	0.017332496	0.025864141	0.017602265	0.007014104	0.081535935	7.06E-08	0.00186925	0.000971862
60	0.016796989	0.016796989	0.058133409	0.12960319	0.003795971	0.003075606	0.021199834	0.026161082	0.021123258	0.006922953	0.08180809	8.14E-08	0.002633235	0.001249783
70	0.017635695	0.017635695	0.06026591	0.13279945	0.003228196	0.003066612	0.023100615	0.027171036	0.025604945	0.006963012	0.08208669	7.75E-08	0.003423439	0.001712335
80	0.017547182	0.017547182	0.060411342	0.13246578	0.002949332	0.003273398	0.022983102	0.029731503	0.02371691	0.006989821	0.080700785	9.12E-08	0.0037328	0.001394077
90	0.017949101	0.017949101	0.060925115	0.13397425	0.002661645	0.003416948	0.02212525	0.032491915	0.025065918	0.006881265	0.08195113	9.08E-08	0.003301371	0.001595485
100	0.018190717	0.018190717	0.062394377	0.13487296	0.002803703	0.003402452	0.024458399	0.034984346	0.026161322	0.006845449	0.07862746	1.12E-07	0.003748103	0.000875838
110	0.017026861	0.017026861	0.060662873	0.13048702	0.002764516	0.00336351	0.024438854	0.030594964	0.022807699	0.006948222	0.074446276	1.25E-07	0.003371792	0.00153265
120	0.01747755	0.01747755	0.06080798	0.13220268	0.002764753	0.003259942	0.023535227	0.031763922	0.024674775	0.007017958	0.07808133	1.94E-07	0.002698125	0.000979277
130	0.017094668	0.017094668	0.060410833	0.13074657	0.002576924	0.003335403	0.023330005	0.030339586	0.025773872	0.00703206	0.074659914	1.97E-07	0.002670562	0.001228146
140	0.018113356	0.018113356	0.064531514	0.13458587	0.00334275	0.003557617	0.024213657	0.031598367	0.024424609	0.007457991	0.082915045	3.71E-07	0.002859531	0.000763623
150	0.018422959	0.018422959	0.06482559	0.1357312	0.002699622	0.003552596	0.02457906	0.031169334	0.024581714	0.007370967	0.0866783	3.61E-07	0.002456277	0.001141363
160	0.017858673	0.017858673	0.063119786	0.13363636	0.002892328	0.003501765	0.020936118	0.032180637	0.025767589	0.007646391	0.08192321	5.47E-07	0.002749522	0.000988633
170	0.017876867	0.017876867	0.062951145	0.13370441	0.003300311	0.003563964	0.020314913	0.032290924	0.027064811	0.007804983	0.08029603	5.55E-07	0.002957341	0.001174839
180	0.017933326	0.017933326	0.062476464	0.13391536	0.003237417	0.003455933	0.021472199	0.032769695	0.025042387	0.007832415	0.08121826	6.22E-07	0.003055916	0.001248424
190	0.017714157	0.017714157	0.061627537	0.13309455	0.003638247	0.003581857	0.019355508	0.032510065	0.023253022	0.007725931	0.08291529	5.32E-07	0.00310764	0.001053481
200	0.018595811	0.018595811	0.063346221	0.13636644	0.004599463	0.003611667	0.02131773	0.033541203	0.02467186	0.007319229	0.08648799	5.27E-07	0.003480847	0.000927581

Appendix 7: Comparing WRF and Model Predictions against Ground Truth for Long-term Forecasting for Historical Weather Data

The proposed forecasting model predictions (i.e. MIMO-LSTM) are compared with the ground truth and calculated the error (i.e. MSE, MAE, RMSE, and EV) values for each timeslot (i.e. 3-hour, 6-hour, 9-hour, 12-hour, 18-hour, 24-hour, and 48-hour). Similarly, the WRF model predictions are taken for the same dataset and results are compared with the ground truth. The evaluations results are shown in the following tables.

3-Hour

WRF predicted vs Ground truth

Parameter	Mean Squared Error	Mean Absolute Error	Root Mean Squared Error	Explained Variance
TSK	4.0209727	1.3728781	2.0052364	0.598463266
PSFC	227869.02	292.8511	477.35626	0.952012899
U10	10.540705	2.1308465	3.2466452	0.273865967
V10	12.0824	2.3409169	3.4759748	0.070946071
Q2	1.11E-06	0.00075617	0.001054385	0.435844499
Rainc	15.942339	1.0590441	3.992786	-83586.53548
Rainnc	18.627722	2.0209315	4.3159842	-34551.06168
Snow	0	0	0	1
TSLB	8.140333	1.1551077	2.853127	0.898683916
SMOIS	8.52E-05	0.003237576	0.009232116	0.999333581

Proposed deep learning model prediction vs Ground truth

Parameter	Mean Squared Error	Mean Absolute Error	Root Mean Squared Error	Explained Variance
TSK	2.7882845	1.1496421	1.6698158	0.703170069
PSFC	123881.22	270.10614	351.96765	0.920364491
U10	5.327054	1.6960033	2.308041	0.526840189
V10	4.6248293	1.6266266	2.1505415	0.587397454
Q2	7.72E-07	0.000680343	0.000878442	0.606375528
Rainc	0.11341145	0.12714593	0.33676615	-22.36565644
Rainnc	0.83847433	0.29947627	0.91568244	-68.36666132
Snow	0.016857434	0.051807187	0.12983619	0
TSLB	2.6088953	0.8744249	1.6152076	0.944945478
SMOIS	0.000242468	0.007548864	0.015571397	0.9983361

6-Hour

WRF predicted vs Ground truth

Parameter	Mean Squared Error	Mean Absolute Error	Root Mean Squared Error	Explained Variance
TSK	3.8616908	1.3092792	1.9651185	0.679486661
PSFC	199244.28	255.92368	446.3679	0.964351791
U10	8.100931	1.892945	2.8462136	0.454539605
V10	9.456813	2.0524755	3.0751932	0.162074942
Q2	1.05E-06	0.000719599	0.001025496	0.526853802
Rainc	14.03519	0.9750483	3.746357	-4717.644658
Rainnc	15.6952505	1.8532413	3.961723	-78029.06774
Snow	0	0	0	1
TSLB	1.8618562	0.59466535	1.3644985	0.941514505
SMOIS	6.81E-05	0.00281954	0.008251033	0.999460899

Proposed deep learning model prediction vs Ground truth

Parameter	Mean Squared Error	Mean Absolute Error	Root Mean Squared Error	Explained Variance
TSK	3.0542436	1.2428628	1.7476394	0.684033881
PSFC	99677.38	246.17464	315.71725	0.947786787
U10	8.569923	2.2902873	2.9274433	0.325438266
V10	7.3790517	2.0471332	2.716441	0.392834985
Q2	7.24E-07	0.000651605	0.000850862	0.584265945
Rainc	0.1278994	0.09724788	0.35763025	-1.469248733
Rainnc	1.4281658	0.24116634	1.195059	-29.30952399
Snow	0.000284262	0.008008379	0.01686006	0
TSLB	1.0853431	0.65626615	1.041798	0.969951174
SMOIS	1.67E-04	0.005793437	0.012913092	0.998837461

9-Hour

WRF predicted vs Ground truth

Parameter	Mean Squared Error	Mean Absolute Error	Root Mean Squared Error	Explained Variance
TSK	4.8804314	2.1699972	2.209169844	0.443244587
PSFC	211367.33	263.46463	459.74704	0.963658898
U10	8.089221	1.9187737	2.8441556	0.479886788
V10	8.927932	2.0298445	2.9879644	0.077082639
Q2	1.03E-06	0.000711496	0.001016092	0.352471958
Rainc	14.073741	0.9864279	3.7514985	-3754.817955
Rainnc	16.408337	1.9012688	4.0507207	-23480.4512
Snow	0	0	0	1
TSLB	1.4240651	0.50377595	1.193342	0.95203226
SMOIS	6.39E-05	0.002740025	0.007996412	0.999494317

Proposed deep learning model prediction vs Ground truth

Parameter	Mean Squared Error	Mean Absolute Error	Root Mean Squared Error	Explained Variance
TSK	4.7985396	1.4987899	2.190557	0.020309352
PSFC	169287.05	330.76126	411.44507	0.936599115
U10	11.142194	2.5796661	3.3379924	0.131567981
V10	12.19173	2.6290748	3.4916658	0.029548321
Q2	8.99E-07	0.000737917	0.000948218	0.364967766
Rainc	0.17841245	0.15835106	0.42238897	-9.885370822
Rainnc	1.861943	0.34450766	1.3645303	-25.17475432
Snow	0.004922504	0.02689071	0.07016056	0
TSLB	1.0127658	0.59626704	1.0063627	0.969353857
SMOIS	2.28E-04	0.007184558	0.015089214	0.998454706

12-Hour

WRF predicted vs Ground truth

Parameter	Mean Squared Error	Mean Absolute Error	Root Mean Squared Error	Explained Variance
TSK	5.9721785	1.4909863	2.443804	0.709277451
PSFC	212751.3	265.8883	461.24973	0.964588445
U10	8.127483	1.9504818	2.8508742	0.455252368
V10	8.473837	1.9777623	2.9109855	0.084304162
Q2	1.12E-06	0.000736931	0.001058385	0.306559231
Rainc	14.091678	0.9991061	3.7538884	-3678.906364
Rainnc	16.816736	1.9331105	4.1008215	-10991.37736
Snow	0	0	0	1
TSLB	1.1918795	0.43876836	1.0917324	0.971078668
SMOIS	6.16E-05	0.002682853	0.007847165	0.999514562

Proposed deep learning model prediction vs Ground truth

Parameter	Mean Squared Error	Mean Absolute Error	Root Mean Squared Error	Explained Variance
TSK	5.14835	1.5206286	2.2689974	0.730837682
PSFC	278060.44	441.90314	527.3144	0.918347118
U10	11.737519	2.6507785	3.4260063	0.12629787
V10	14.429697	2.893559	3.798644	-0.179446057
Q2	1.18E-06	0.000860272	0.001085298	0.305365308
Rainc	0.2467392	0.20587602	0.49672848	-17.15295028
Rainnc	2.0544894	0.44475895	1.433349	-50.73551842
Snow	0.004690081	0.027695747	0.068484165	0
TSLB	0.88332826	0.58412516	0.93985546	0.978172188
SMOIS	1.41E-04	0.005464147	0.011879317	0.998996234

24-Hour

WRF predicted vs Ground truth

Parameter	Mean Squared Error	Mean Absolute Error	Root Mean Squared Error	Explained Variance
TSK	3.0667834	1.1959156	1.7512234	0.509475117
PSFC	196150.56	282.5408	442.8889	0.953624725
U10	10.561917	2.1142447	3.2499104	0.262932891
V10	10.861656	2.258384	3.2957027	0.055455091
Q2	1.03E-06	0.000725441	0.001017325	0.324697756
Rainc	15.557926	1.1486559	3.9443538	-191853.956
Rainnc	18.624685	2.0981896	4.315633	-4037.288909
Snow	0	0	0	1
TSLB	1.400409	0.42546007	1.1833888	0.979126194
SMOIS	7.48E-05	0.00292553	0.008646647	0.999411738

Proposed deep learning model prediction vs Ground truth

Parameter	Mean Squared Error	Mean Absolute Error	Root Mean Squared Error	Explained Variance
TSK	3.5168703	1.3444608	1.875332	0.281050306
PSFC	623330.6	652.0653	789.5129	0.825341279
U10	18.152727	3.4335885	4.2606015	0.089148203
V10	19.64028	3.2381313	4.4317355	0.012588636
Q2	1.41E-06	0.000940488	0.001188894	0.318042193
Rainc	1.890364	0.5094838	1.3749051	-84.91942292
Rainnc	3.5724075	0.6843118	1.8900813	-22.60096013
Snow	0.001066969	0.011419334	0.032664493	0
TSLB	1.9721501	0.8552	1.4043326	0.976954069
SMOIS	3.24E-04	0.008576588	0.017998956	0.997834794

48-Hour

WRF predicted vs Ground truth

Parameter	Mean Squared Error	Mean Absolute Error	Root Mean Squared Error	Explained Variance
TSK	3.163105	1.2206486	1.778512	0.496017955
PSFC	205029.55	294.31467	452.80188	0.951546336
U10	11.014908	2.1830323	3.3188715	0.23495815
V10	11.322241	2.331488	3.3648539	0.018787902
Q2	1.07E-06	0.000745183	0.001036694	0.300172118
Rainc	16.184252	1.1870828	4.0229654	-200574.6255
Rainnc	19.419767	2.187251	4.4067864	-4220.760187
Snow	0	0	0	1
TSLB	1.4589597	0.4386343	1.2078741	0.97825771
SMOIS	7.71E-05	0.00300141	0.008778173	0.999394688

Proposed deep learning model prediction vs Ground truth

Parameter	Mean Squared Error	Mean Absolute Error	Root Mean Squared Error	Explained Variance
TSK	4.493951	1.4288149	2.119894	0.274816304
PSFC	959890.44	828.9889	979.74	0.721577327
U10	31.083189	4.3905144	5.57523	-0.612951888
V10	24.162054	3.9043639	4.915491	-0.284100966
Q2	2.76E-06	0.001347067	0.001660245	0.172068878
Rainc	1.4888092	0.6026417	1.2201678	-665.7803979
Rainnc	3.7990644	0.8607666	1.9491189	-3.817349848
Snow	0.008917561	0.040089395	0.09443284	0
TSLB	3.4580653	1.1488392	1.8595874	0.954103668
SMOIS	3.00E-04	0.008149375	0.017334767	0.998027008

The comparison results (i.e. proposed model predictions and WRF model predictions) are shown in the following graphs for each timeslot with respect to the ground truth for each parameter. The overall comparison graph is shown at the bottom of each timeslot. MSE is selected as the evaluation matrix for each graph.

Graphs to compare proposed model prediction vs WRF model prediction for each parameter for 6-Hour

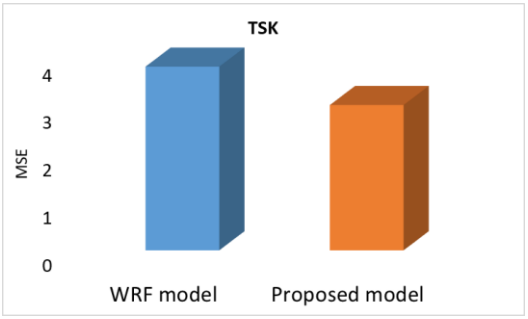

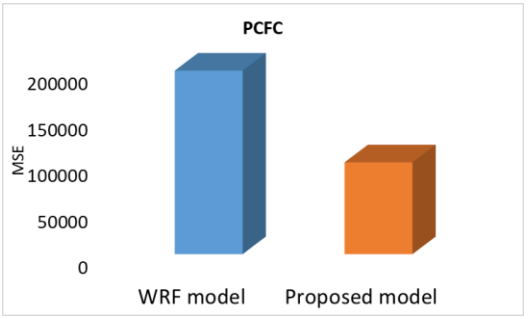

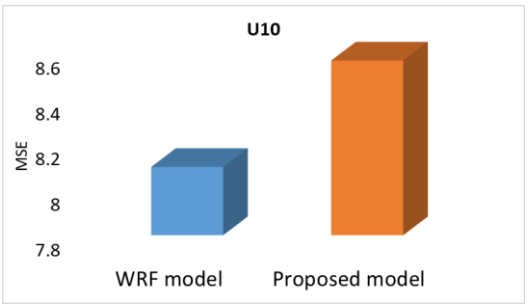

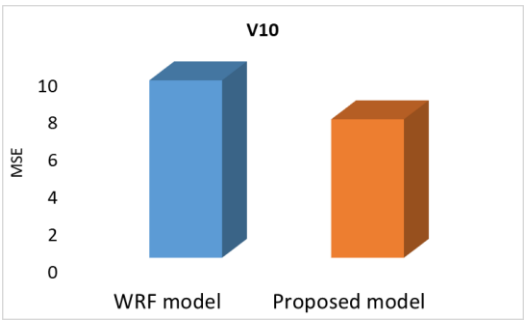

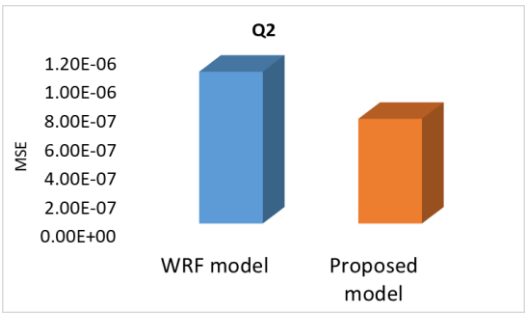

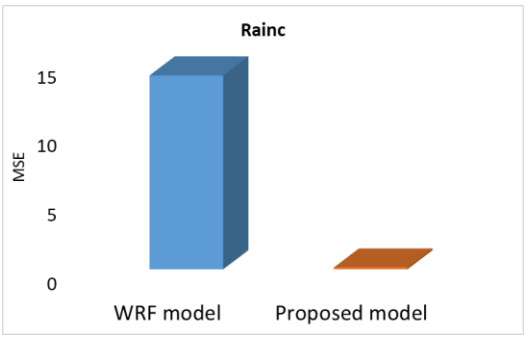

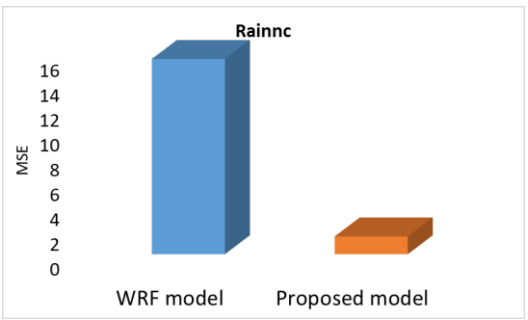

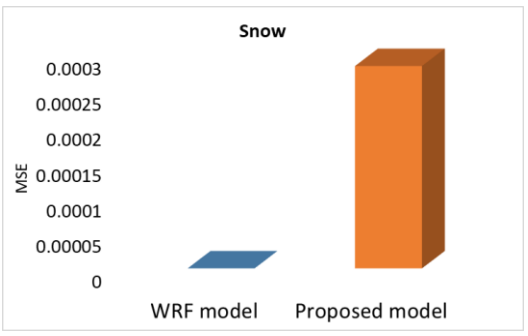

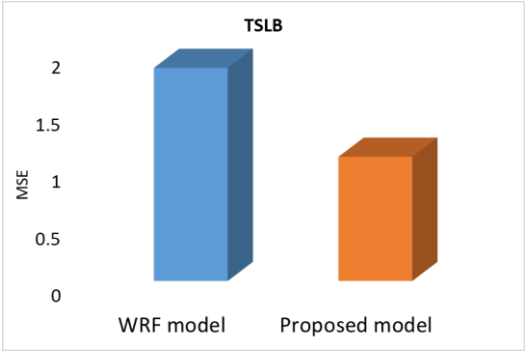

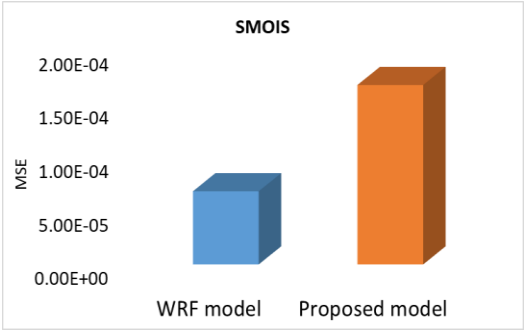

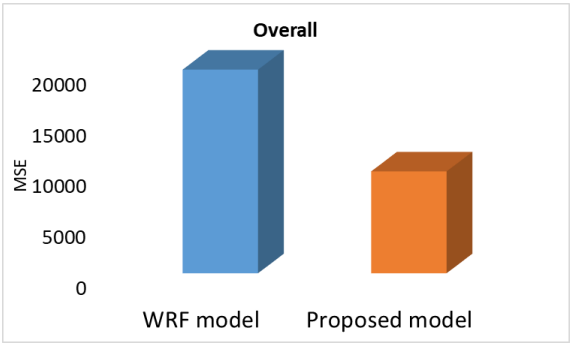

Graphs to compare proposed model prediction vs WRF model prediction for each parameter for 9-Hour

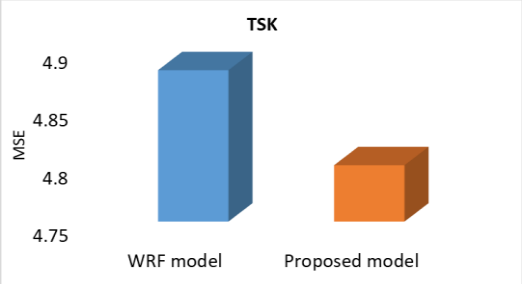

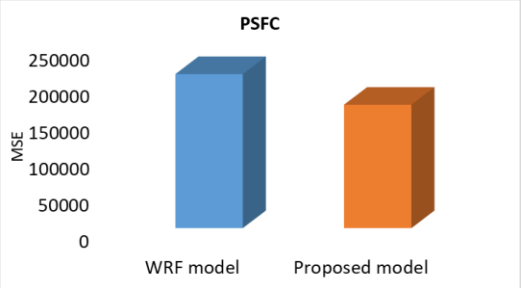

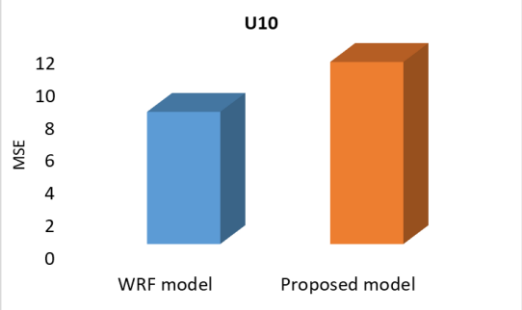

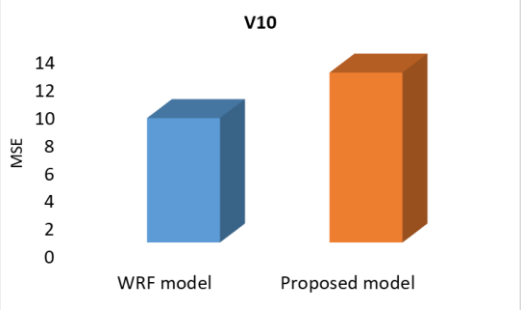

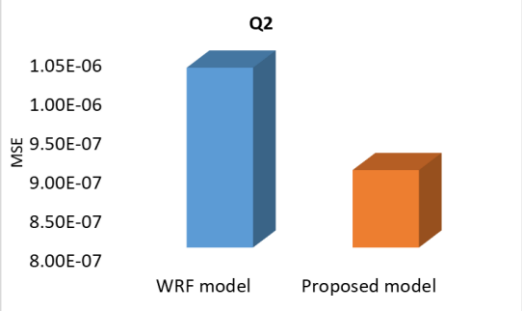

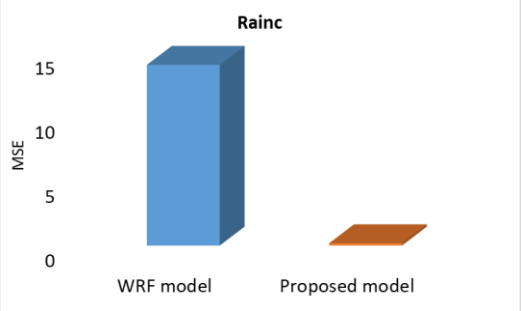

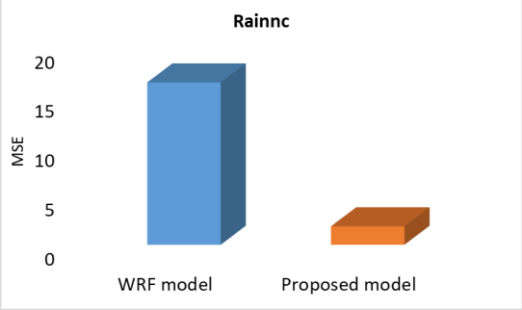

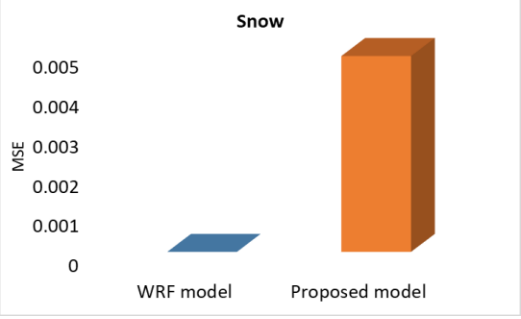

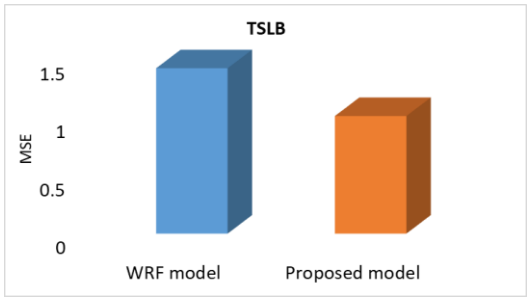

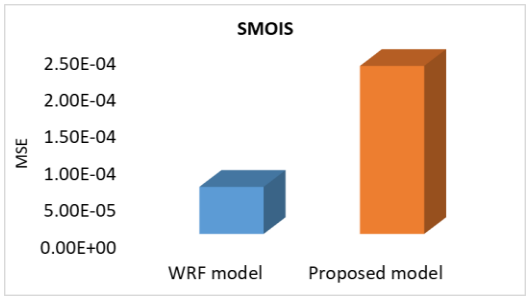

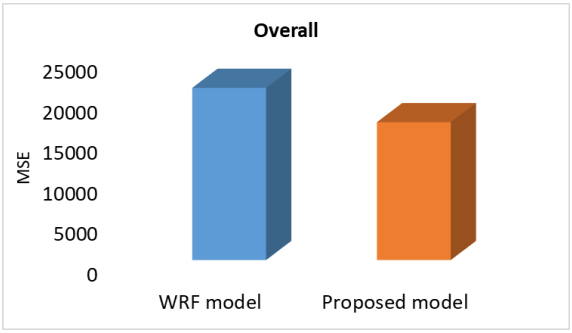

Graphs to compare proposed model prediction vs WRF model prediction for each parameter for 12-Hour

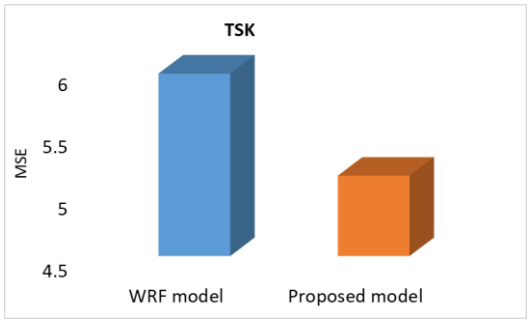

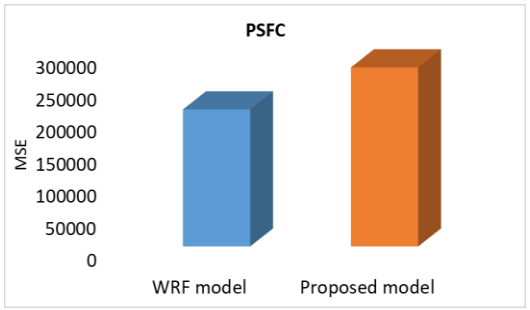

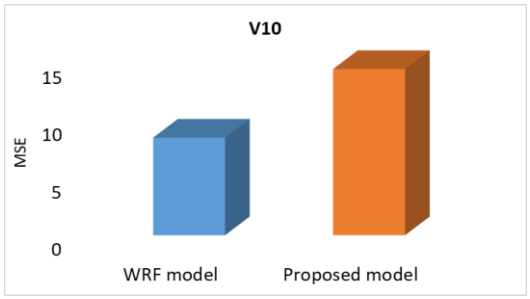

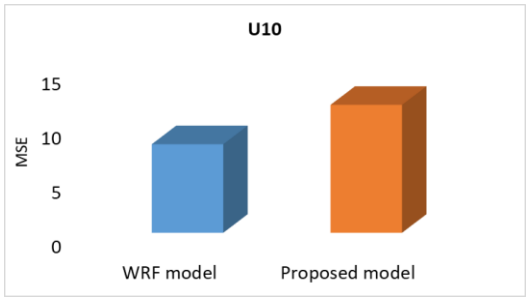

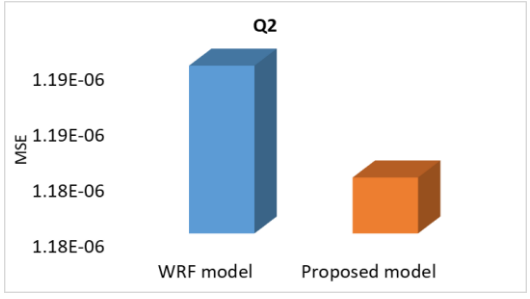

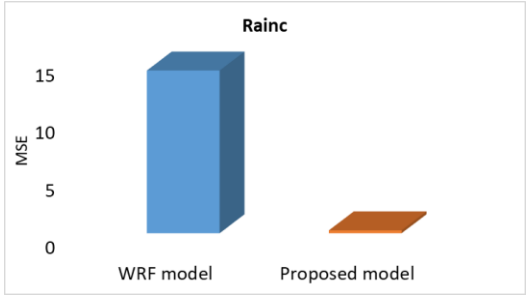

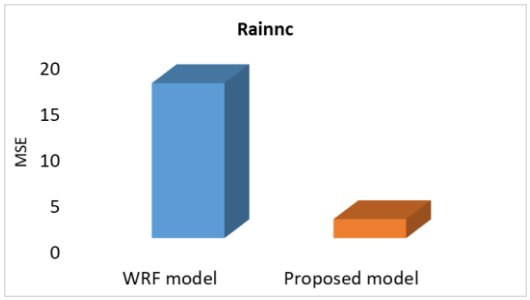

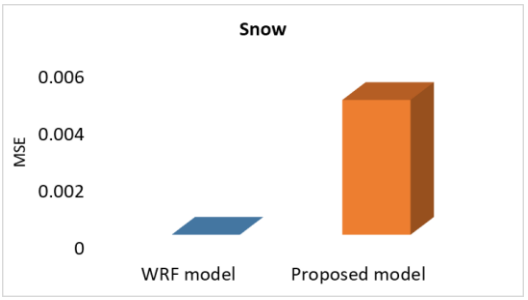

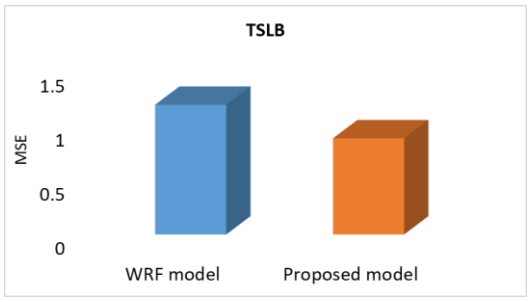

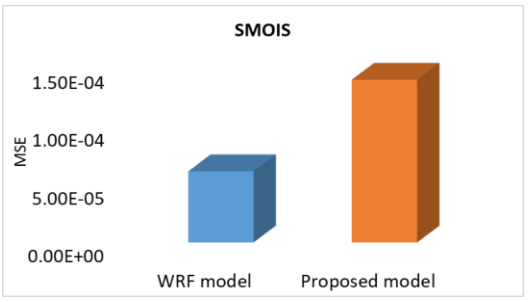

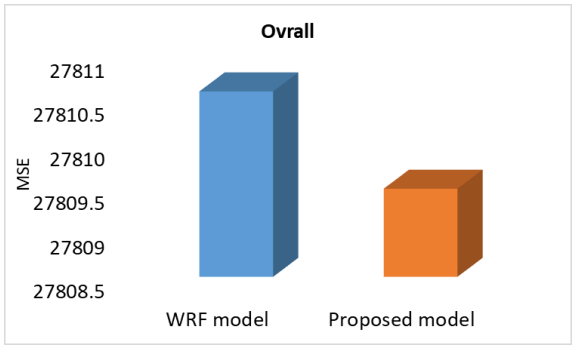

Graphs to compare proposed model prediction vs WRF model prediction for each parameter for 24-Hour

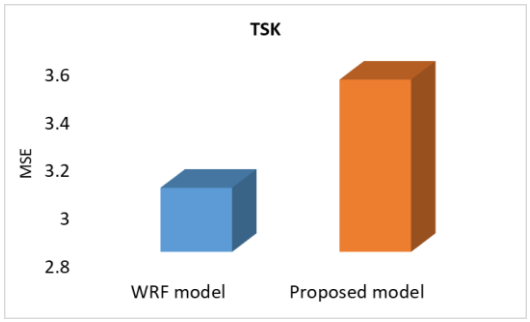

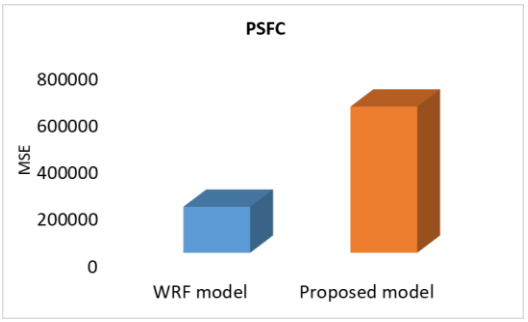

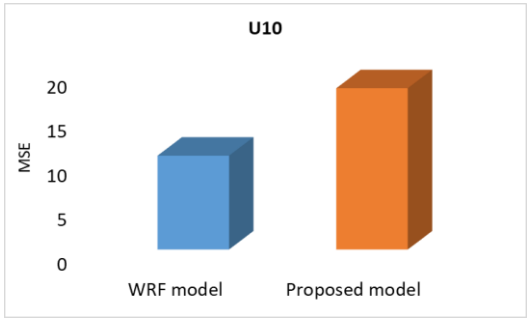

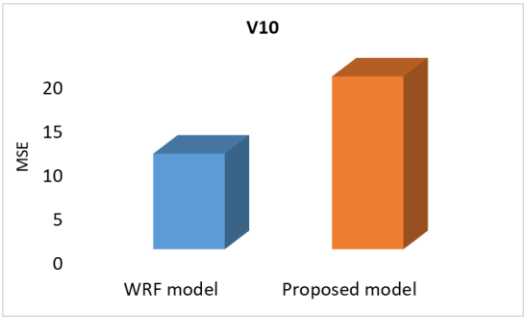

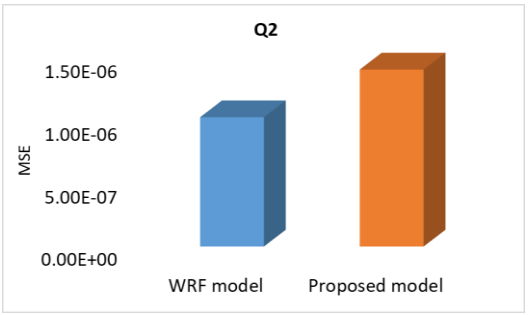
Q2
1.50E-06
1.00E-06
5.00E-07
0.00E+00
MSE
WRF model
Proposed model

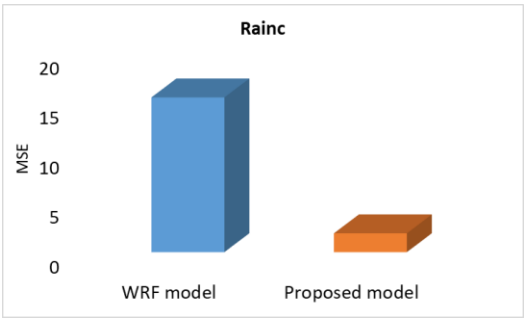
Rainc
20
15
10
5
0
MSE
WRF model
Proposed model

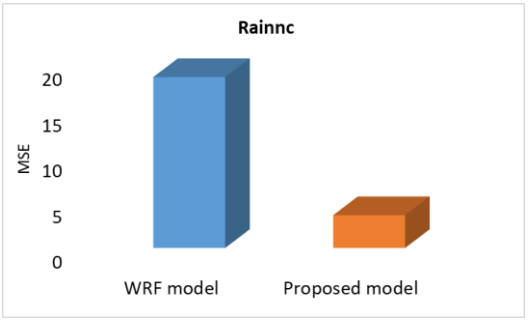
Rainnc
20
15
10
5
0
MSE
WRF model
Proposed model

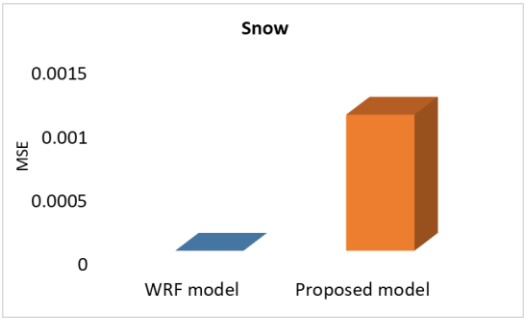
Snow
0.0015
0.001
0.0005
0
MSE
WRF model
Proposed model

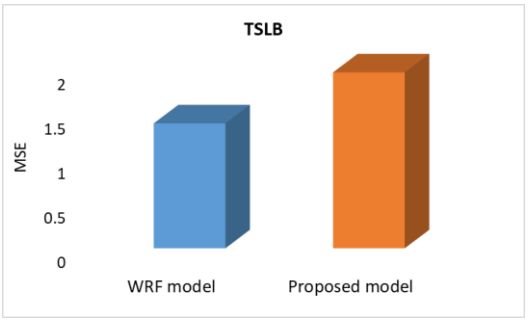
TSLB
2
1.5
1
0.5
0
MSE
WRF model
Proposed model

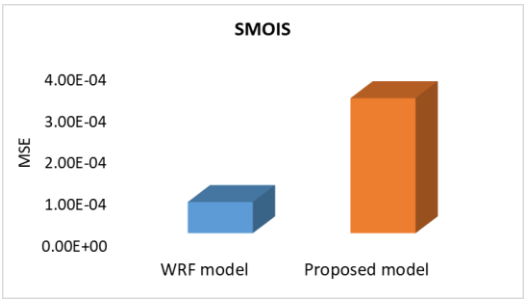
SMOIS
4.00E-04
3.00E-04
2.00E-04
1.00E-04
0.00E+00
MSE
WRF model
Proposed model

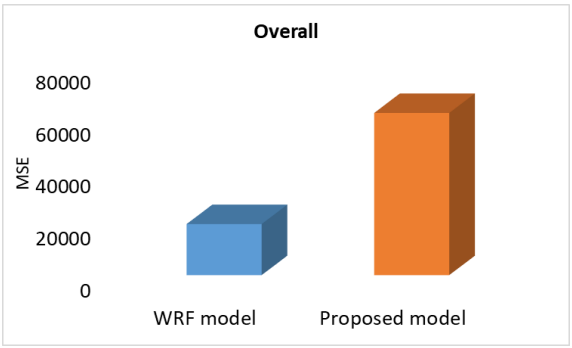
Overall
80000
60000
40000
20000
0
MSE
WRF model
Proposed model

Graphs to compare proposed model prediction vs WRF model prediction for each parameter for 48-Hour

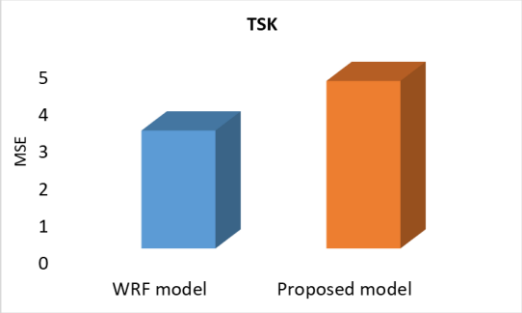

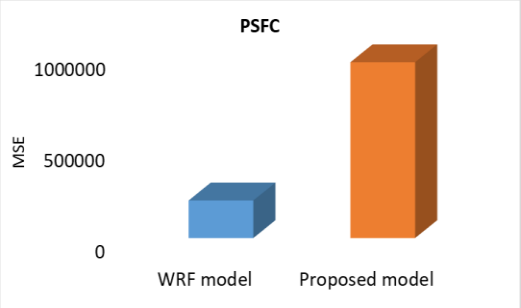

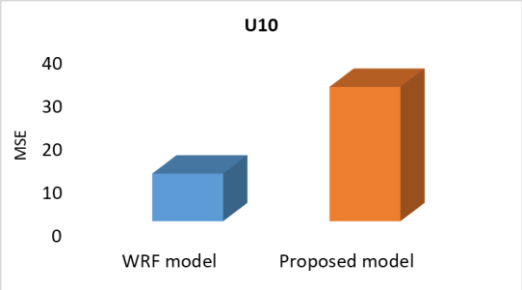

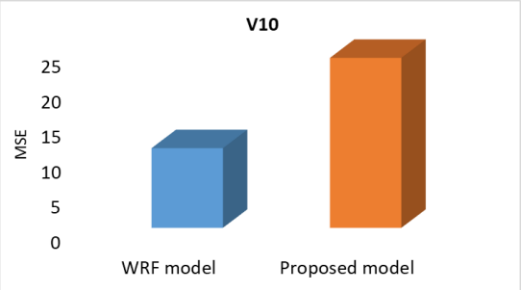

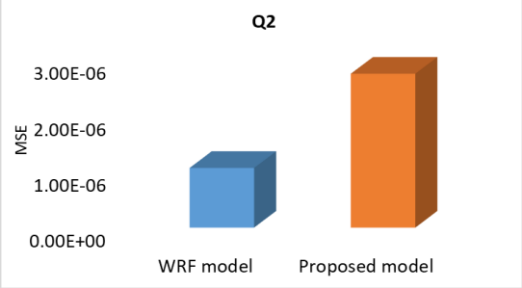

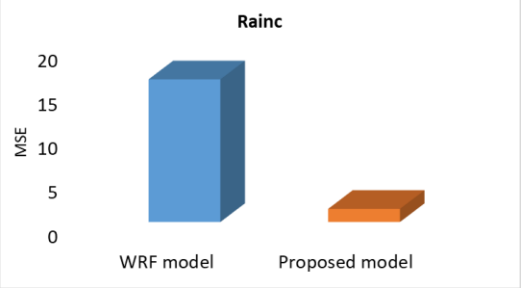

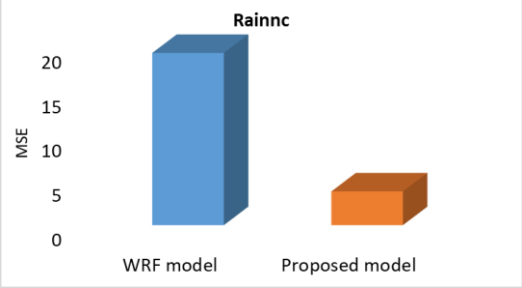

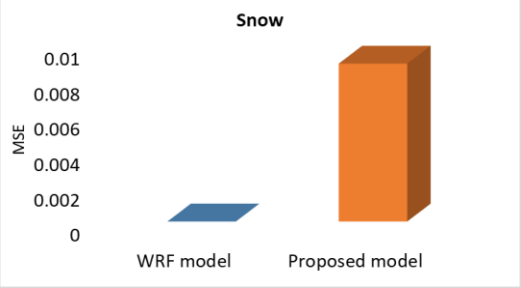

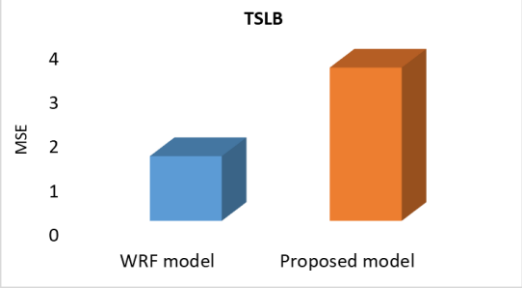

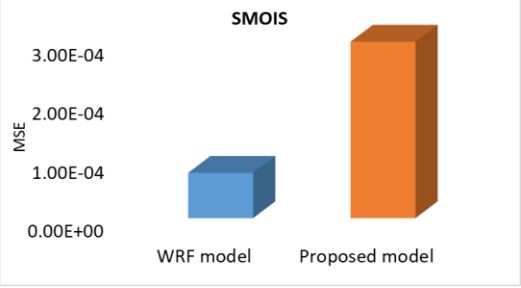

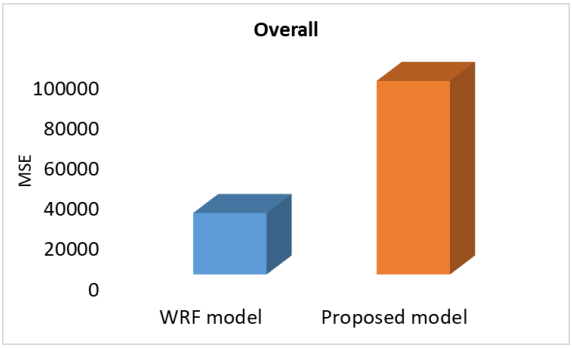
Overall
100000
80000
60000
40000
20000
0
MSE
WRF model
Proposed model

Appendix 8: Comparison of 100 Random Samples for Historical Weather Data

Comparative results of 100 data samples are shown in the following graphs. Each graph compares the proposed model prediction, WRF prediction, and the ground truth.

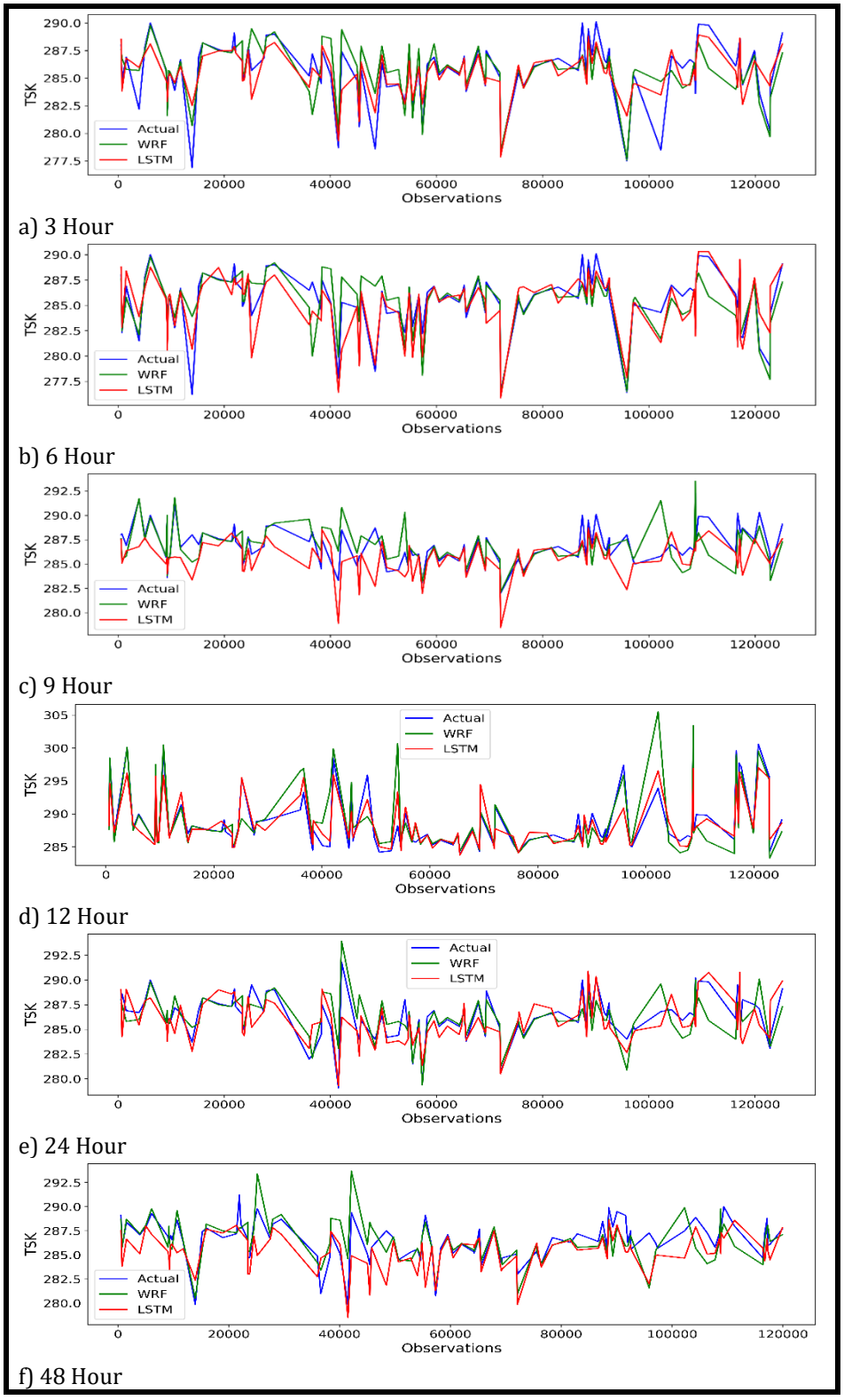

a) 3 Hour

b) 6 Hour

c) 9 Hour

d) 12 Hour

e) 24 Hour

f) 48 Hour

i) TSK

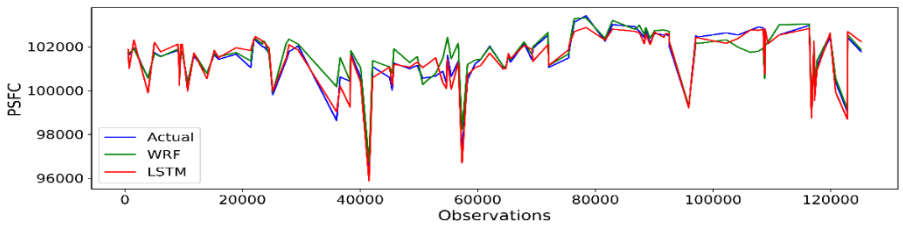

a) 3 Hour

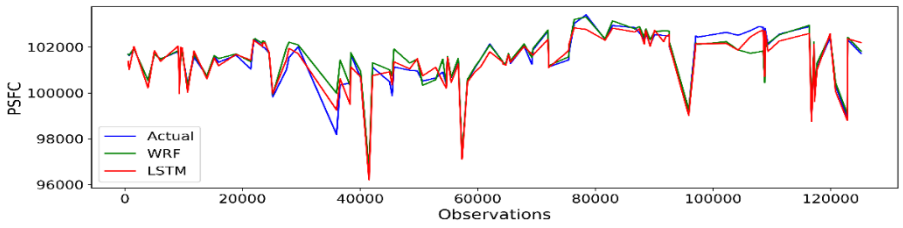

b) 6 Hour

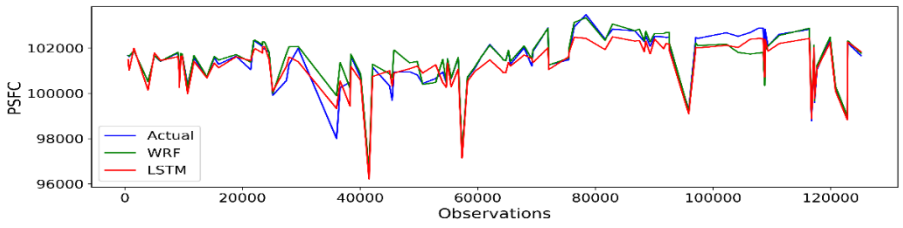

c) 9 Hour

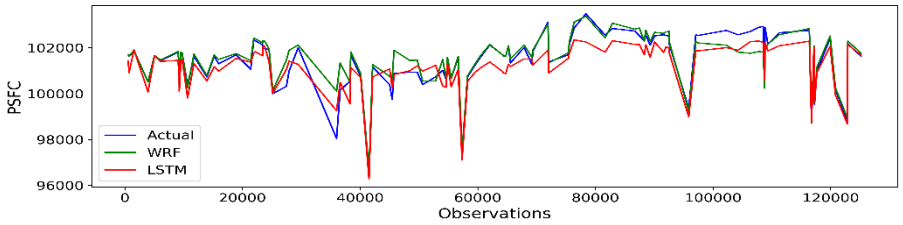

d) 12 Hour

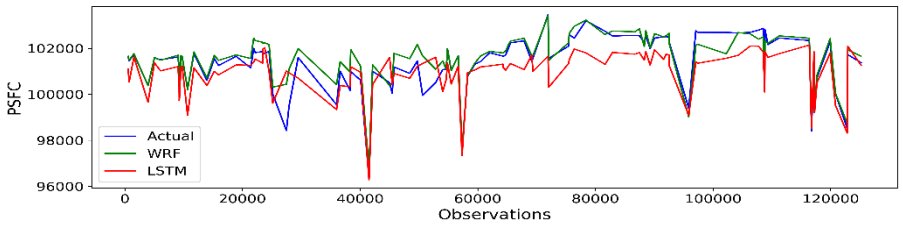

e) 24 Hour

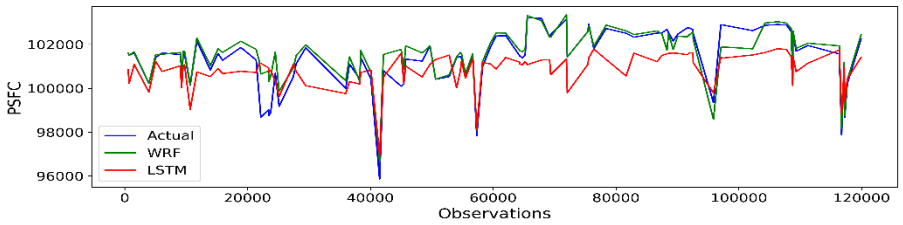

f) 48 Hour

ii) PSFC

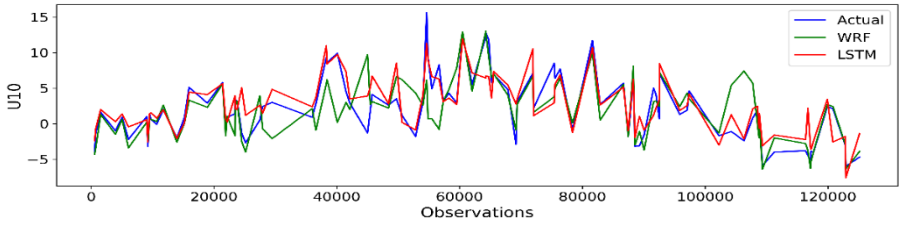

a) 3 Hour

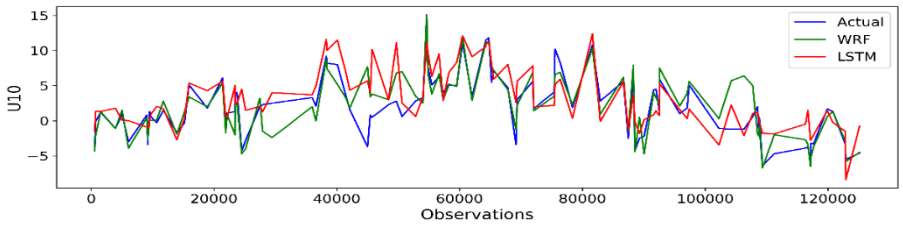

b) 6 Hour

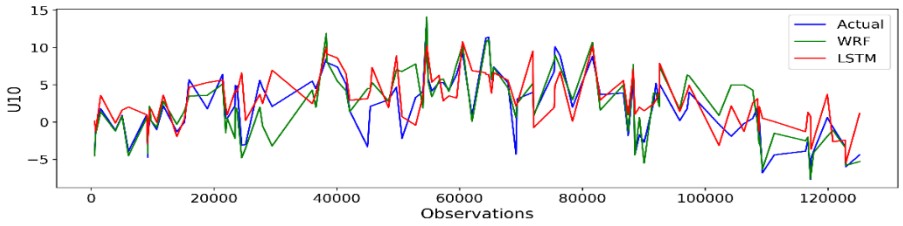

c) 9 Hour

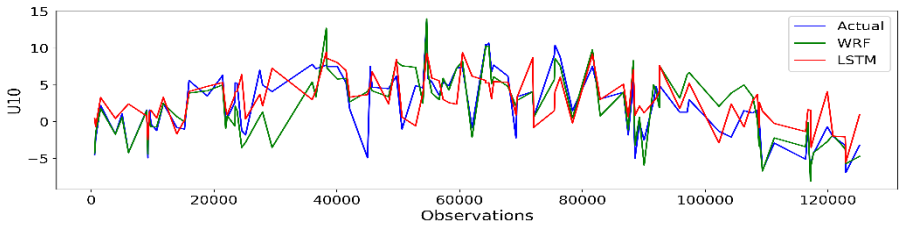

d) 12 Hour

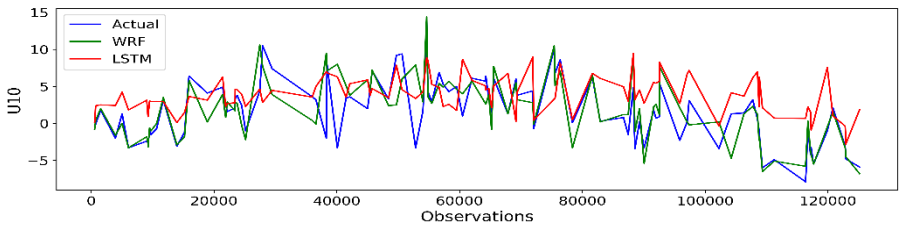

e) 24 Hour

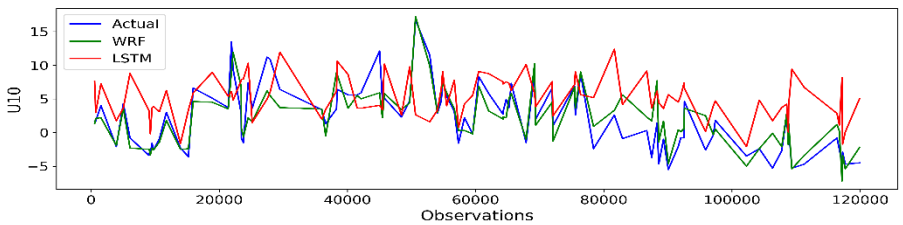

f) 48 Hour

iii) U10

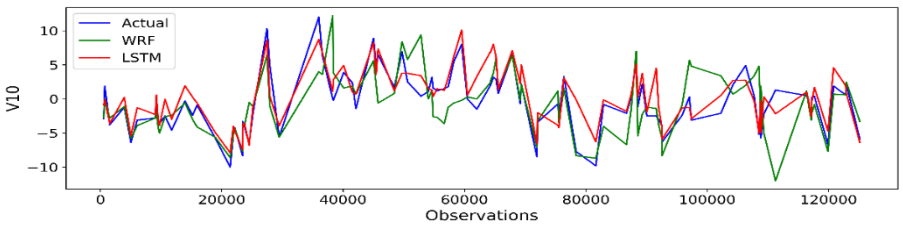

a) 3 Hour

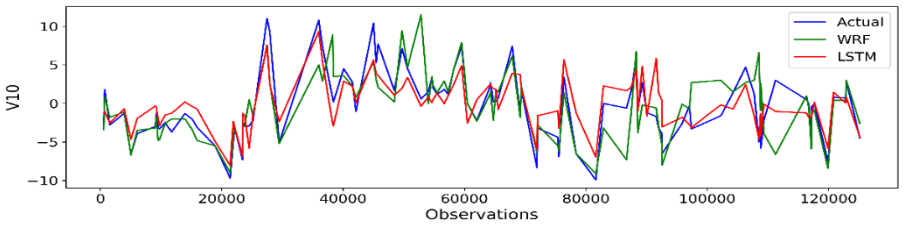

b) 6 Hour

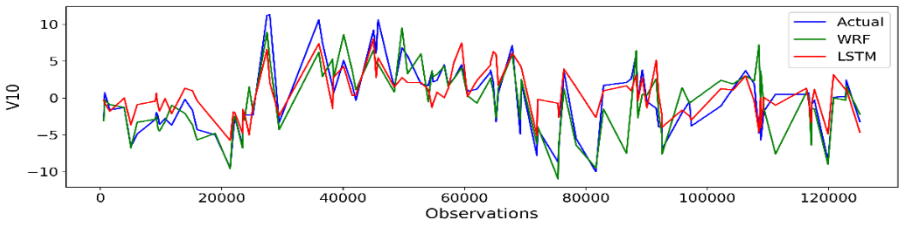

c) 9 Hour

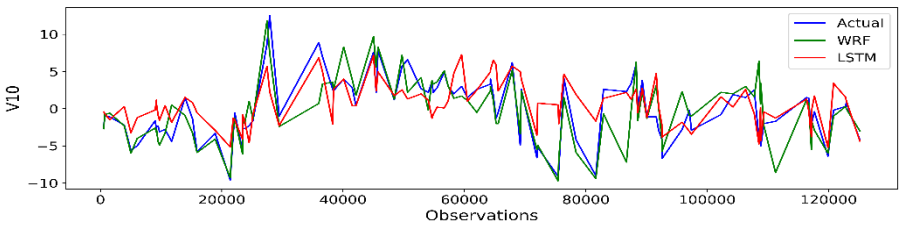

d) 12 Hour

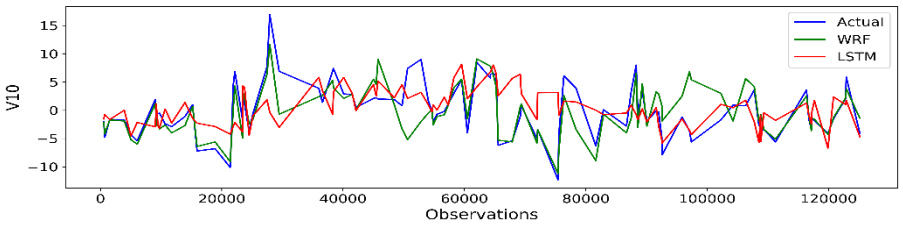

e) 24 Hour

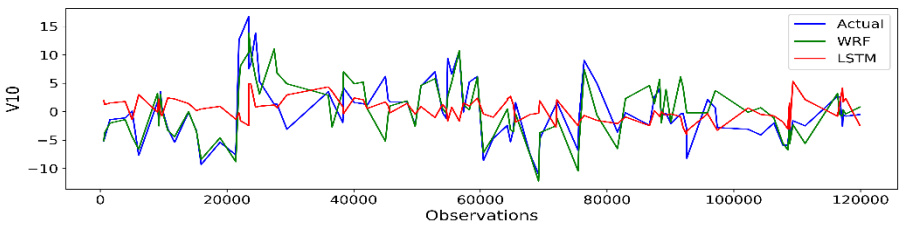

f) 48 Hour

iv) V10

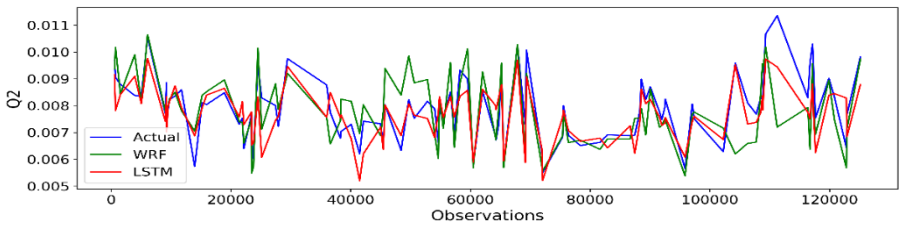

a) 3 Hour

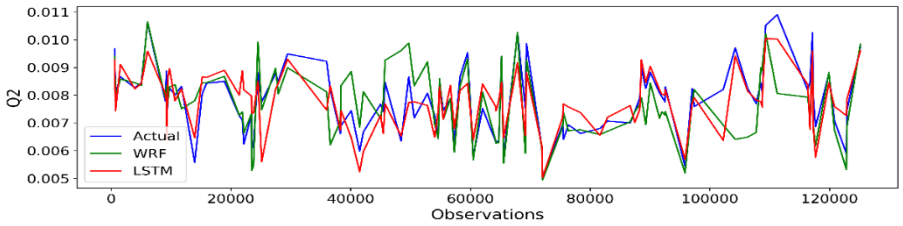

b) 6 Hour

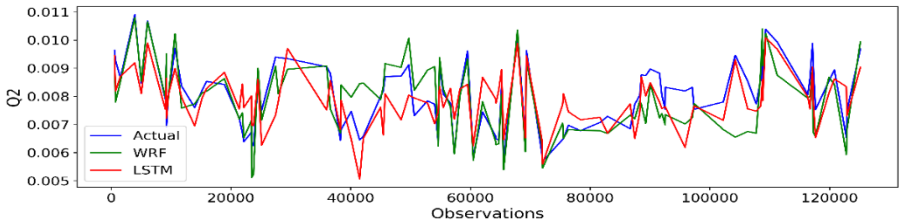

c) 9 Hour

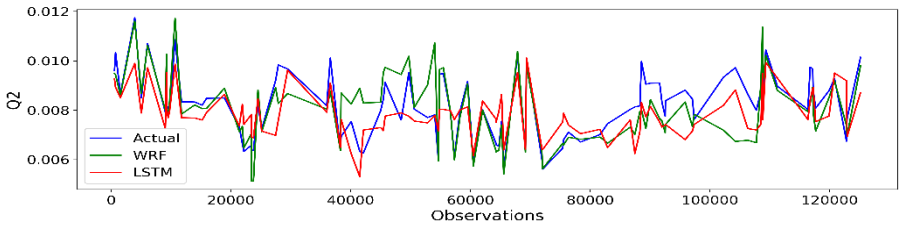

d) 12 Hour

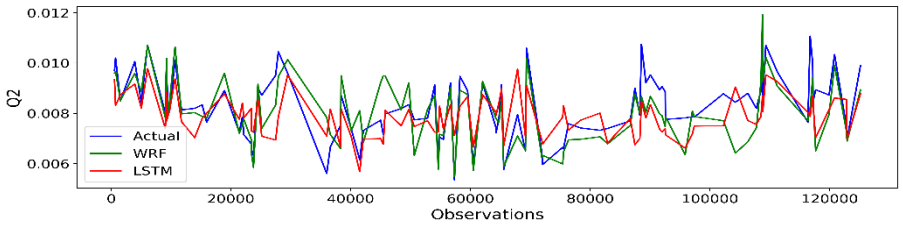

e) 24 Hour

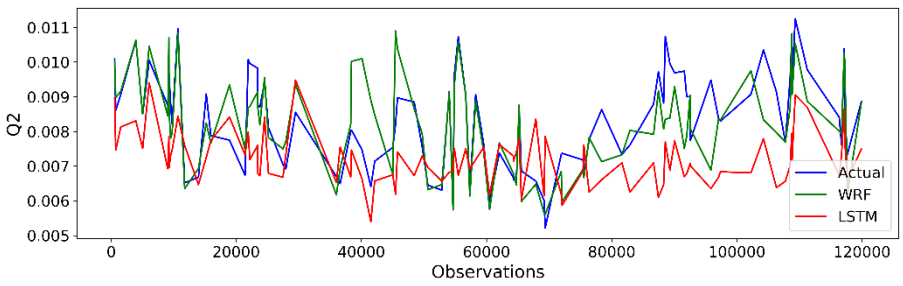

f) 48 Hour

v) Q2

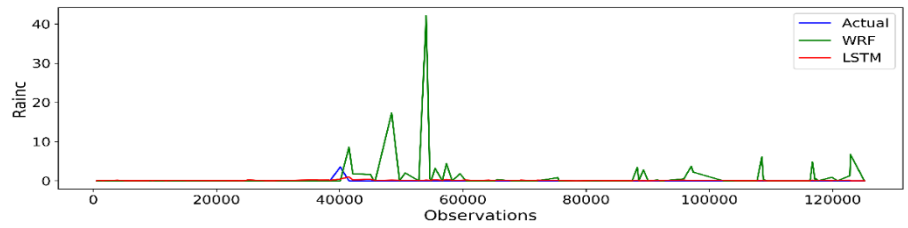

a) 3 Hour

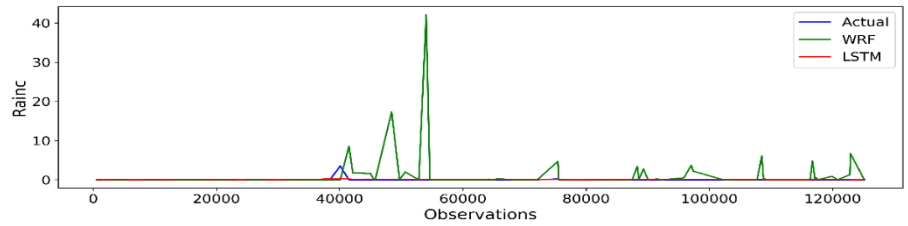

b) 6 Hour

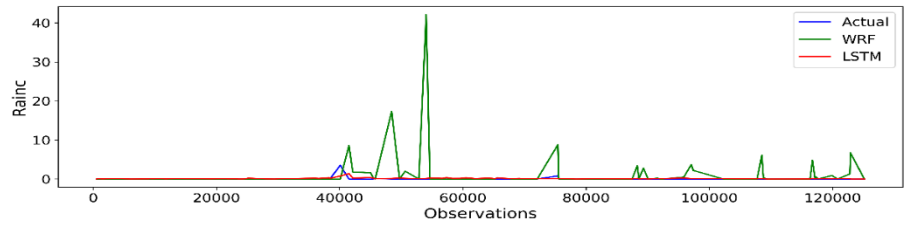

c) 9 Hour

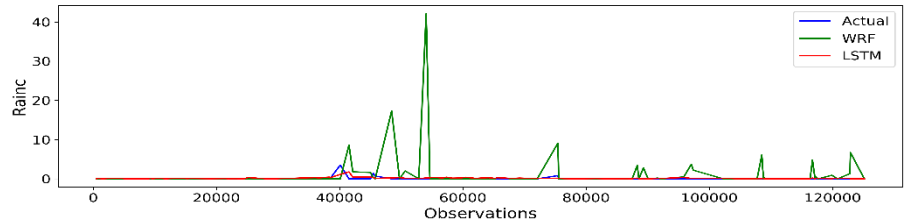

d) 12 Hour

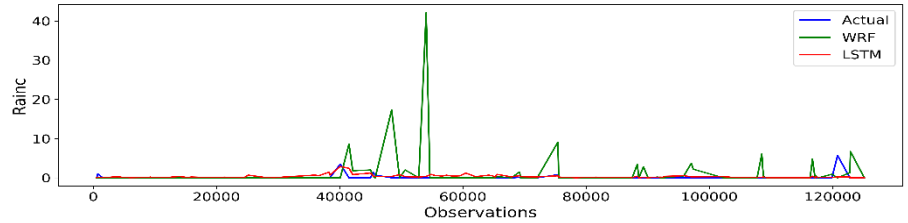

e) 24 Hour

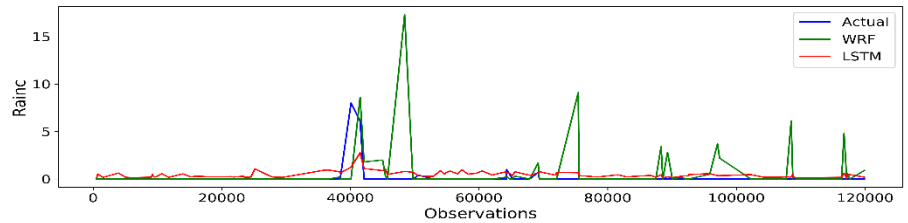

f) 48 Hour

vi) Rainc

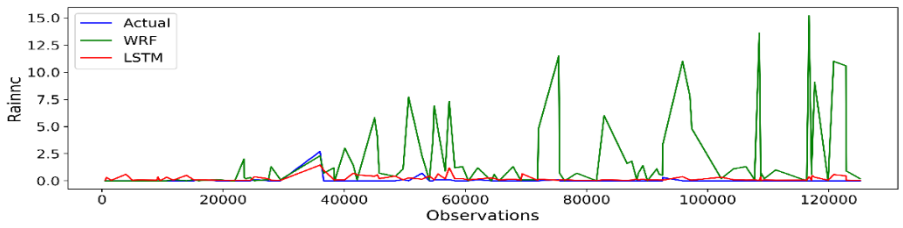

a) 3 Hour

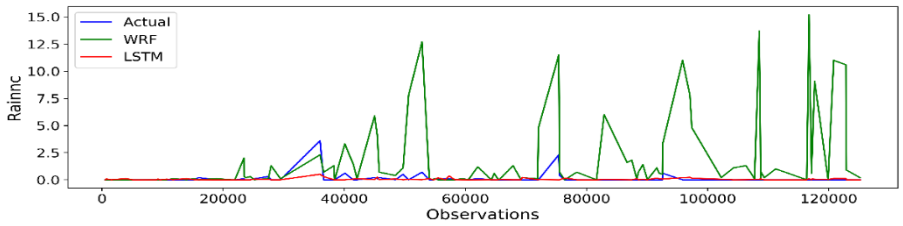

b) 6 Hour

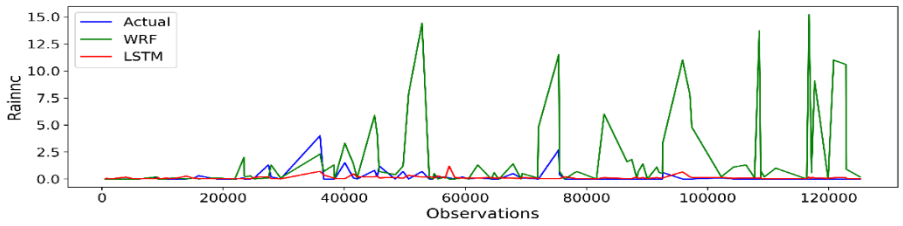

c) 9 Hour

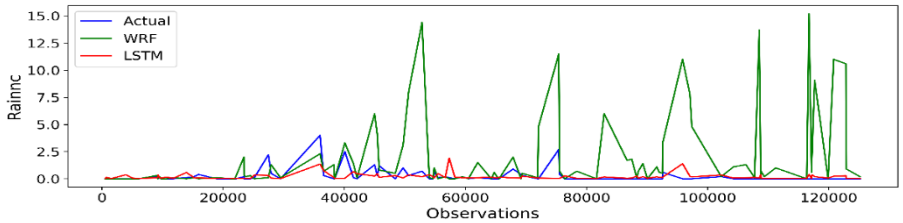

d) 12 Hour

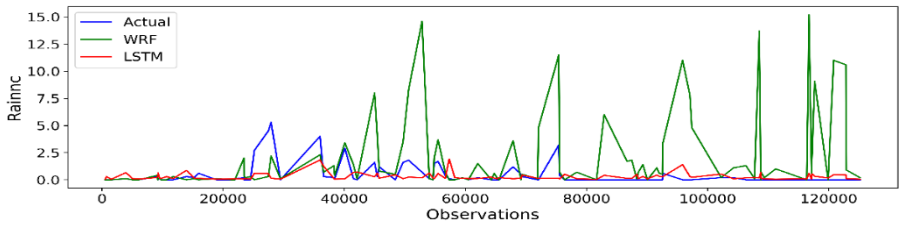

e) 24 Hour

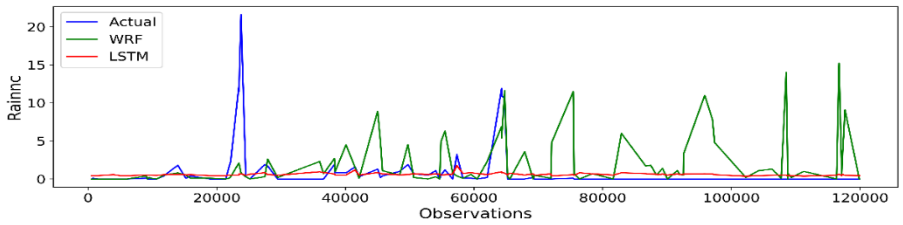

f) 48 Hour

vii) Rainnc

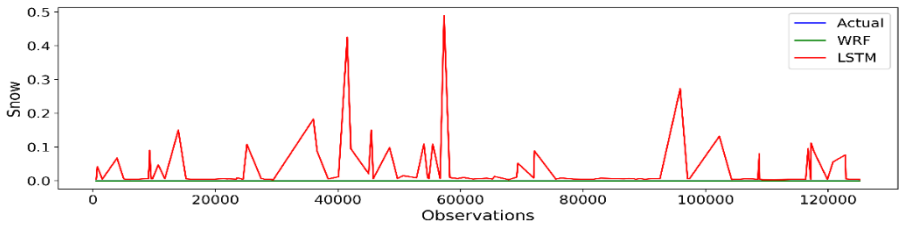

a) 3 Hour

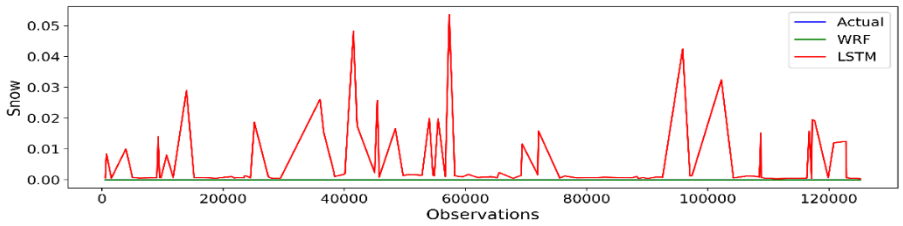

b) 6 Hour

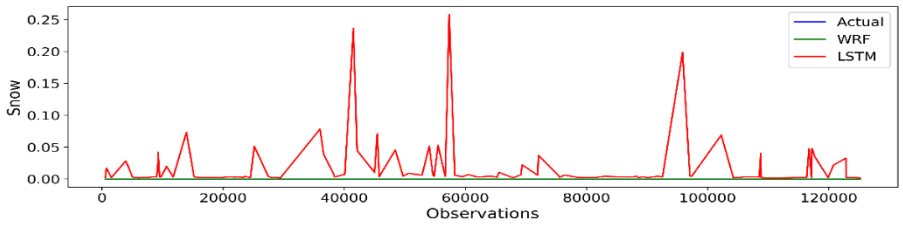

c) 9 Hour

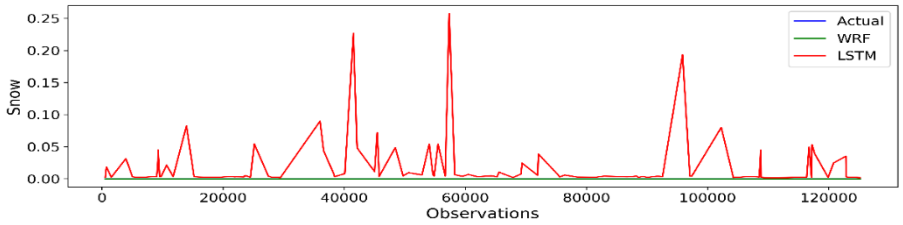

d) 12 Hour

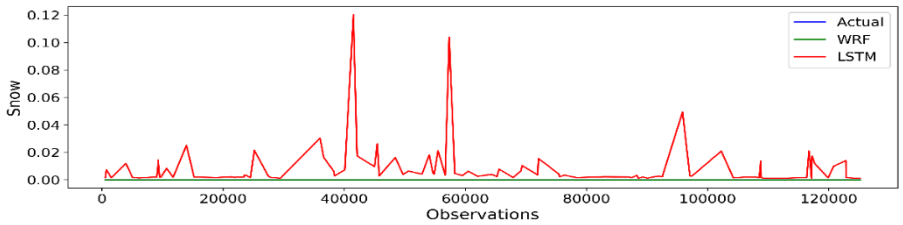

e) 24 Hour

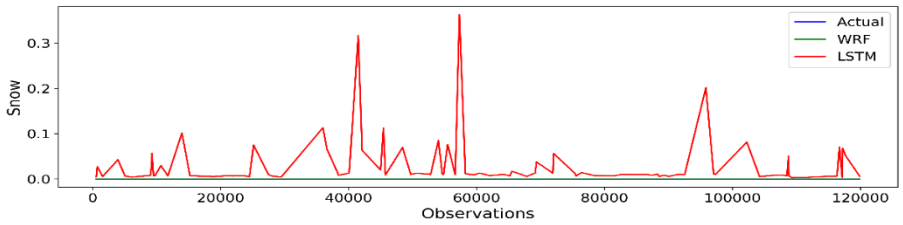

f) 48 Hour

viii) Snow

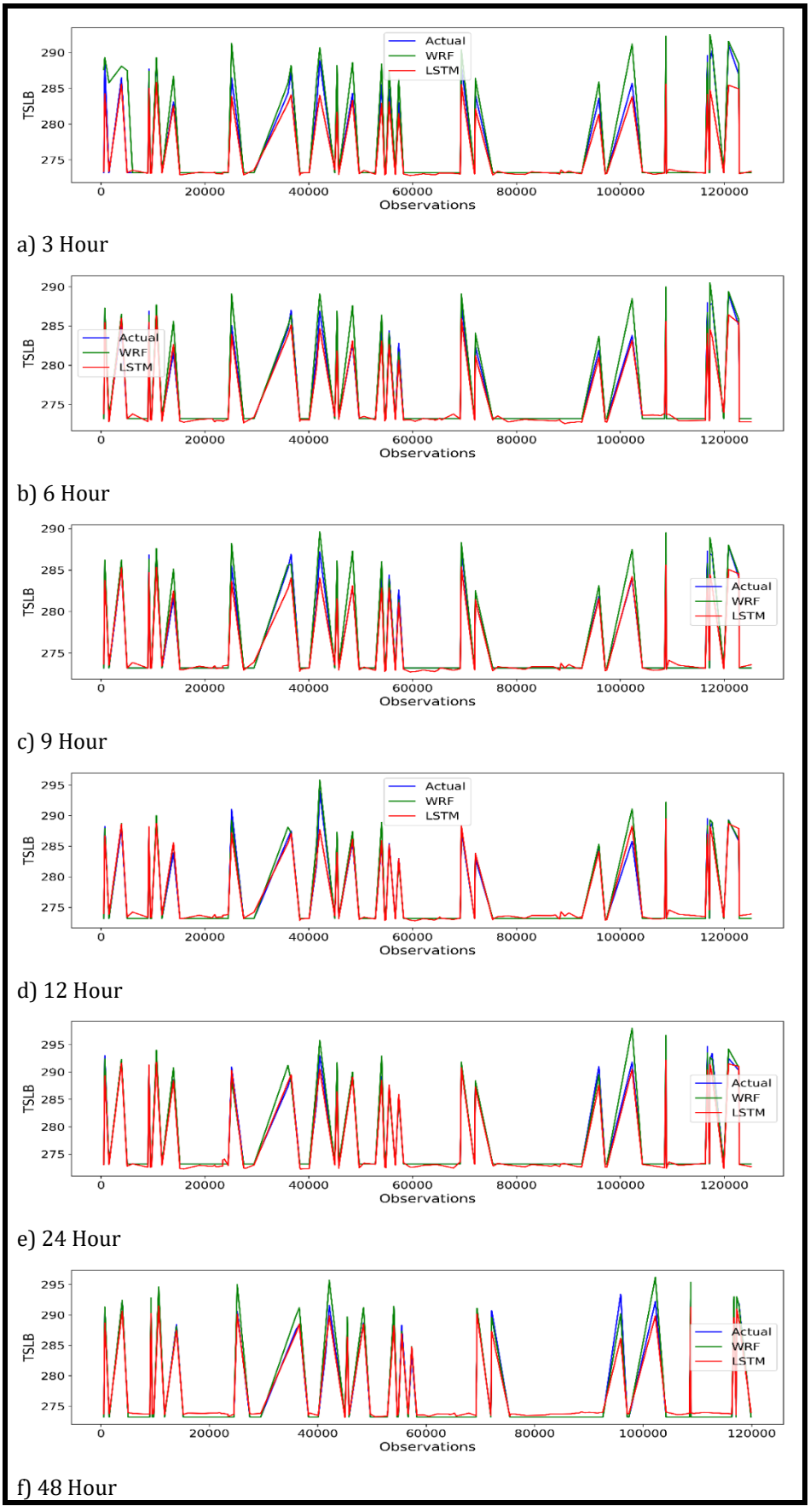

a) 3 Hour

b) 6 Hour

c) 9 Hour

d) 12 Hour

e) 24 Hour

f) 48 Hour

ix) TSLB

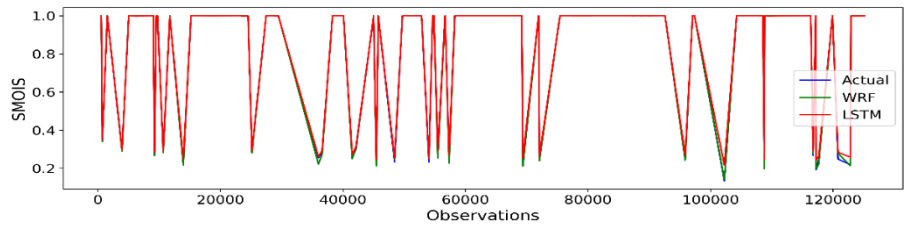

a) 3 Hour

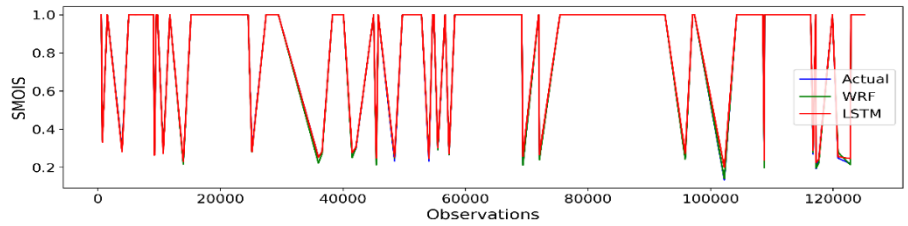

b) 6 Hour

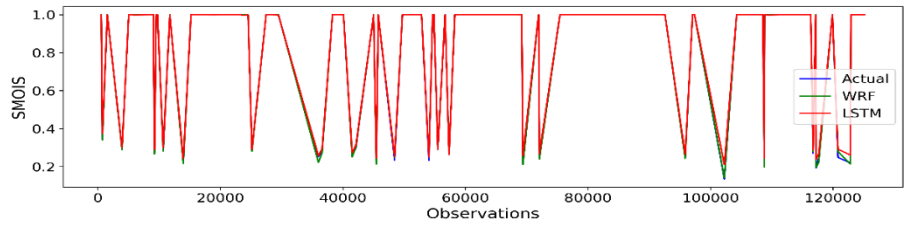

c) 9 Hour

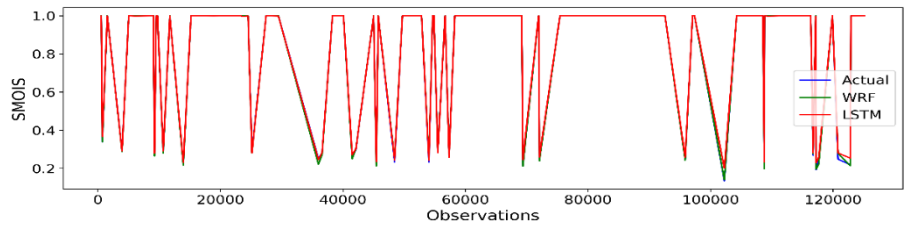

d) 12 Hour

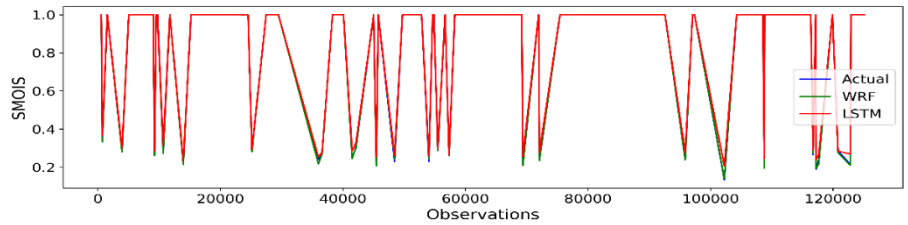

e) 24 Hour

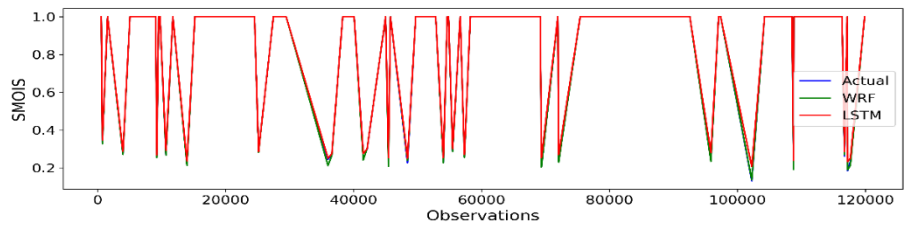

f) 48 Hour

x) SMOIS

Appendix 9: Evaluation Results of MIMO-LSTM variance for Weather Station Data

The configuration 1 evaluation results are shown below out of 6 different configurations.

Configuration 1:

```
model = Sequential()
model.add(LSTM(128, return_sequences=True, input_shape=(timesteps, data_dim)))
model.add(LSTM(512, return_sequences=True))  # returns a sequence of vectors of
model.add(LSTM(512, return_sequences=True))
model.add(LSTM(256)) # return a single vector of dimension 32
model.add(Dense(10, activation='tanh'))
```

Optimiser: Adam

Epoch	Loss	Total MSE	Total MAE	Total RMSE	Barometer	Pressure	Temp	Humid	Wspeed	Wdirec	Rrate	Rain	Dpoint	Hindex
10	0.033973697	0.033973697	0.109229047	0.18431956	0.19935271	0.19068268	0.13388583	0.13408744	0.23954566	0.35139233	0.07110414	0.06985047	0.1332392	0.138508
20	0.031351413	0.031351413	0.102048307	0.17706329	0.1881076	0.18650822	0.1316465	0.1394781	0.23181346	0.33234456	0.07151128	0.071784556	0.12476157	0.12859501
30	0.030383936	0.030383936	0.094841591	0.17430988	0.17301606	0.16689388	0.122136444	0.11631523	0.24498312	0.34294155	0.07196153	0.069767684	0.11783447	0.12668106
40	0.031714372	0.031714372	0.098796238	0.17808528	0.17465979	0.17339343	0.13782687	0.13841584	0.22533564	0.35303956	0.072076544	0.07076933	0.12345987	0.13250828
50	0.035631876	0.035631876	0.106916994	0.18876408	0.18234168	0.17459275	0.13134018	0.15158327	0.23465534	0.39212167	0.072479546	0.06968785	0.12497234	0.13345261
60	0.04001413	0.04001413	0.113715047	0.20003533	0.18390049	0.17892748	0.13392022	0.15116824	0.27386487	0.41517988	0.07311381	0.07012754	0.13456902	0.13331102
70	0.03737174	0.03737174	0.107502311	0.19331773	0.17733333	0.17025025	0.12864931	0.16290541	0.2327824	0.40932617	0.074229114	0.07209963	0.13978948	0.13494948
80	0.042316057	0.042316057	0.115823316	0.20570868	0.18514057	0.18252963	0.14302336	0.1605604	0.25121793	0.4436757	0.07336235	0.07190082	0.13738479	0.14123124
90	0.042731606	0.042731606	0.117935339	0.20671624	0.18960142	0.1857296	0.14690706	0.16819876	0.2767979	0.42670414	0.07325582	0.07248164	0.12843996	0.14556453
100	0.043046275	0.043046275	0.117282535	0.20747596	0.19866663	0.19799446	0.14468192	0.1655598	0.2698677	0.4301357	0.07199504	0.06944853	0.12917323	0.13752174
110	0.044279437	0.044279437	0.122280985	0.21042679	0.20365636	0.203061	0.14679298	0.17198837	0.2720525	0.43021742	0.071403496	0.06865177	0.13765024	0.14525093
120	0.043797126	0.043797126	0.119743602	0.20927763	0.19944057	0.19882227	0.14748427	0.17340863	0.27542245	0.42689073	0.07216136	0.06916592	0.13135277	0.14664349
130	0.044151975	0.044151975	0.118435755	0.21012372	0.20362255	0.20090525	0.14479856	0.1761154	0.27169427	0.42872554	0.07190697	0.06915091	0.13484754	0.14816122
140	0.04444433	0.04444433	0.121474599	0.21081823	0.20159288	0.19934393	0.15476726	0.17624977	0.28005788	0.42212614	0.07167983	0.070508756	0.13521603	0.15502565
150	0.043959641	0.043959641	0.120280885	0.20966554	0.20455015	0.20041436	0.14957969	0.17498395	0.2809659	0.4180703	0.07069986	0.07369417	0.1330447	0.15080275
160	0.044858061	0.044858061	0.121681253	0.21179721	0.20568785	0.20285262	0.14844412	0.17414917	0.280358	0.42665836	0.07045555	0.07035303	0.13866997	0.15158994
170	0.043864506	0.043864506	0.118911164	0.20943855	0.20534386	0.20314553	0.14828858	0.16801032	0.27949208	0.41821155	0.07130752	0.07041336	0.13771866	0.1515517
180	0.044460784	0.044460784	0.119536761	0.21085726	0.20494293	0.20277888	0.14821291	0.16499072	0.2815107	0.425801	0.07169269	0.070245616	0.13743556	0.1509316
190	0.044015249	0.044015249	0.11862213	0.20979811	0.20942618	0.20501947	0.1503266	0.16227978	0.28119904	0.41821796	0.0715199	0.07062551	0.1354591	0.15131421
200	0.044253712	0.044253712	0.119978016	0.21036567	0.20832114	0.20470951	0.1506241	0.16618754	0.277891	0.4205559	0.07213942	0.07546453	0.13652574	0.1526387

Optimiser: SGD

Epoch	Loss	Total MSE	Total MAE	Total RMSE	Barometer	Pressure	Temp	Humid	Wspeed	Wdirec	Rrate	Rain	Dpoint	Hindex
10	0.168503508	0.168503508	0.31751663	0.4104918	0.6555278	0.643936	0.31784332	0.29650363	0.33986676	0.517674	0.20076431	0.25384402	0.23288654	0.33053142
20	0.156072022	0.156072022	0.294295892	0.39505953	0.64187527	0.6294111	0.3169108	0.28774437	0.34133923	0.5131227	0.12372554	0.14792967	0.22968623	0.31555402
30	0.150592638	0.150592638	0.285703954	0.3880627	0.62781435	0.61355734	0.31602895	0.28658718	0.34268224	0.5098584	0.10424273	0.11914835	0.23106858	0.3122084
40	0.144655018	0.144655018	0.278920822	0.3803354	0.61112267	0.5948973	0.3124302	0.28169078	0.34135595	0.5067136	0.09550523	0.10609205	0.23297867	0.3070437
50	0.138265197	0.138265197	0.272275496	0.37184027	0.59133273	0.57285964	0.30908653	0.2759198	0.33883235	0.5035077	0.09120988	0.09940715	0.23516181	0.30218178
60	0.130937872	0.130937872	0.264987346	0.36185336	0.5668498	0.5457667	0.30601367	0.26804397	0.33608416	0.50010973	0.08905517	0.09571498	0.23736759	0.29699975
70	0.122503878	0.122503878	0.256869062	0.35000554	0.5355435	0.5116021	0.3042387	0.2586129	0.3333963	0.4968076	0.0880612	0.093537755	0.23935565	0.2920399
80	0.11314883	0.11314883	0.247317957	0.336376	0.49612316	0.4698489	0.30584127	0.24747437	0.33067587	0.49261114	0.08788103	0.09231873	0.24089618	0.28899938
90	0.1036663	0.1036663	0.236768854	0.32197252	0.44823852	0.42137018	0.3121789	0.23853429	0.32725006	0.48778808	0.08841022	0.09179334	0.24179086	0.29000542
100	0.095168807	0.095168807	0.226632615	0.30849442	0.39649194	0.37173805	0.32006675	0.23310629	0.32372582	0.48326412	0.08918157	0.09142414	0.24182339	0.2939028
110	0.088718998	0.088718998	0.218475551	0.29785734	0.3487776	0.3280015	0.32892793	0.23352207	0.31960255	0.47689417	0.090388715	0.09160938	0.24109483	0.30161253
120	0.083889841	0.083889841	0.211871898	0.28963742	0.31221476	0.2959448	0.33254927	0.23332515	0.31620908	0.47011158	0.09104366	0.09137426	0.2391799	0.3065437
130	0.08052611	0.08052611	0.207104636	0.28377122	0.28664234	0.27402186	0.3347493	0.23455562	0.31328413	0.46212372	0.09105167	0.09079916	0.23610933	0.3113648
140	0.077653606	0.077653606	0.203154925	0.27866396	0.27043676	0.26055673	0.3327062	0.23396358	0.31119642	0.4534156	0.0903503	0.08980182	0.2323234	0.31216532
150	0.075457358	0.075457358	0.200143629	0.27469504	0.25939718	0.25143245	0.33076975	0.2347287	0.30960292	0.44490343	0.08925742	0.0886308	0.22809528	0.3129208
160	0.073500964	0.073500964	0.197452172	0.2711106	0.25288397	0.24623284	0.32702196	0.23430674	0.3083849	0.4369739	0.08796571	0.08737635	0.22397026	0.31145304
170	0.071610654	0.071610654	0.194828618	0.26760167	0.24823156	0.24249955	0.32241118	0.23238224	0.30752245	0.42980814	0.08651469	0.086061954	0.21998021	0.3084531
180	0.069962622	0.069962622	0.192290556	0.2645045	0.2445685	0.23956333	0.317478	0.23032577	0.30701068	0.42445883	0.085019924	0.08473946	0.21628869	0.3049079
190	0.068706049	0.068706049	0.190141355	0.2621184	0.24256293	0.23805319	0.313612	0.22857872	0.3065415	0.4199944	0.08375557	0.083657764	0.21295077	0.30204147
200	0.067523283	0.067523283	0.188062888	0.25985244	0.24025765	0.23619013	0.30931953	0.22747354	0.30612013	0.41689247	0.082526006	0.08258796	0.20971672	0.298629

Optimiser: Adaptive- Adam

Epoch	Loss	Total MSE	Total MAE	Total RMSE	Barometer	Pressure	Temp	Humid	Wspeed	Wdirec	Rrate	Rain	Dpoint	Hindex
10	0.518730355	0.518730355	0.530312657	0.7202294	1.0885997	1.0870552	0.7635553	0.5865449	0.5196623	0.94020414	0.07427683	0.070526935	0.38192514	0.7636248
20	0.518730355	0.518730355	0.530312657	0.7202294	1.0885997	1.0870552	0.7635553	0.5865449	0.5196623	0.94020414	0.07427683	0.070526935	0.38192514	0.7636248
30	0.518730355	0.518730355	0.530312657	0.7202294	1.0885997	1.0870552	0.7635553	0.5865449	0.5196623	0.94020414	0.07427683	0.070526935	0.38192514	0.7636248
40	0.518730355	0.518730355	0.530312657	0.7202294	1.0885997	1.0870552	0.7635553	0.5865449	0.5196623	0.94020414	0.07427683	0.070526935	0.38192514	0.7636248
50	0.518730355	0.518730355	0.530312657	0.7202294	1.0885997	1.0870552	0.7635553	0.5865449	0.5196623	0.94020414	0.07427683	0.070526935	0.38192514	0.7636248
60	0.518730355	0.518730355	0.530312657	0.7202294	1.0885997	1.0870552	0.7635553	0.5865449	0.5196623	0.94020414	0.07427683	0.070526935	0.38192514	0.7636248
70	0.518730355	0.518730355	0.530312657	0.7202294	1.0885997	1.0870552	0.7635553	0.5865449	0.5196623	0.94020414	0.07427683	0.070526935	0.38192514	0.7636248
80	0.518730355	0.518730355	0.530312657	0.7202294	1.0885997	1.0870552	0.7635553	0.5865449	0.5196623	0.94020414	0.07427683	0.070526935	0.38192514	0.7636248
90	0.518730355	0.518730355	0.530312657	0.7202294	1.0885997	1.0870552	0.7635553	0.5865449	0.5196623	0.94020414	0.07427683	0.070526935	0.38192514	0.7636248
100	0.518730355	0.518730355	0.530312657	0.7202294	1.0885997	1.0870552	0.7635553	0.5865449	0.5196623	0.94020414	0.07427683	0.070526935	0.38192514	0.7636248
110	0.518730355	0.518730355	0.530312657	0.7202294	1.0885997	1.0870552	0.7635553	0.5865449	0.5196623	0.94020414	0.07427683	0.070526935	0.38192514	0.7636248
120	0.518730355	0.518730355	0.530312657	0.7202294	1.0885997	1.0870552	0.7635553	0.5865449	0.5196623	0.94020414	0.07427683	0.070526935	0.38192514	0.7636248
130	0.518730355	0.518730355	0.530312657	0.7202294	1.0885997	1.0870552	0.7635553	0.5865449	0.5196623	0.94020414	0.07427683	0.070526935	0.38192514	0.7636248
140	0.518730355	0.518730355	0.530312657	0.7202294	1.0885997	1.0870552	0.7635553	0.5865449	0.5196623	0.94020414	0.07427683	0.070526935	0.38192514	0.7636248
150	0.518730355	0.518730355	0.530312657	0.7202294	1.0885997	1.0870552	0.7635553	0.5865449	0.5196623	0.94020414	0.07427683	0.070526935	0.38192514	0.7636248
160	0.518730355	0.518730355	0.530312657	0.7202294	1.0885997	1.0870552	0.7635553	0.5865449	0.5196623	0.94020414	0.07427683	0.070526935	0.38192514	0.7636248
170	0.518730355	0.518730355	0.530312657	0.7202294	1.0885997	1.0870552	0.7635553	0.5865449	0.5196623	0.94020414	0.07427683	0.070526935	0.38192514	0.7636248
180	0.518730355	0.518730355	0.530312657	0.7202294	1.0885997	1.0870552	0.7635553	0.5865449	0.5196623	0.94020414	0.07427683	0.070526935	0.38192514	0.7636248
190	0.518730355	0.518730355	0.530312657	0.7202294	1.0885997	1.0870552	0.7635553	0.5865449	0.5196623	0.94020414	0.07427683	0.070526935	0.38192514	0.7636248
200	0.518730355	0.518730355	0.530312657	0.7202294	1.0885997	1.0870552	0.7635553	0.5865449	0.5196623	0.94020414	0.07427683	0.070526935	0.38192514	0.7636248

Optimiser: Adaptive- SGD

Epoch	Loss	Total MSE	Total MAE	Total RMSE	Barometer	Pressure	Temp	Humid	Wspeed	Wdirec	Rrate	Rain	Dpoint	Hindex
10	0.103525094	0.103525094	0.238541103	0.32175314	0.3518625	0.35975903	0.402552	0.2551514	0.35194117	0.47850865	0.08178038	0.08289638	0.23410618	0.3656066
20	0.072148569	0.072148569	0.194705359	0.26860484	0.24119562	0.23775117	0.3267512	0.23267108	0.315799	0.42732298	0.07699366	0.075891234	0.22913103	0.31521434
30	0.067988091	0.067988091	0.185931892	0.26074526	0.23511833	0.23137376	0.30916741	0.22855467	0.3113166	0.4236302	0.074760795	0.07387621	0.21463756	0.29957968
40	0.064642987	0.064642987	0.179549087	0.25424984	0.23075995	0.22688787	0.29286045	0.21713312	0.3098953	0.42328978	0.07346989	0.07258144	0.20531054	0.28418288
50	0.063299359	0.063299359	0.177026446	0.25159365	0.22884463	0.2250733	0.28553683	0.21505885	0.30836576	0.42282575	0.07308724	0.07221439	0.20219378	0.27726182
60	0.061934387	0.061934387	0.174632354	0.2488662	0.22771749	0.22394998	0.27712658	0.21212916	0.30762297	0.4219562	0.07275858	0.07188666	0.19984183	0.26918373
70	0.061348057	0.061348057	0.173627113	0.2476854	0.22704946	0.22330527	0.27402073	0.21142729	0.30648732	0.42145857	0.07264034	0.07178624	0.1988176	0.2659979
80	0.060832334	0.060832334	0.172780865	0.24664213	0.22648655	0.22284466	0.27095422	0.21041724	0.30569425	0.42147174	0.07255266	0.07170667	0.197753	0.262824
90	0.060526411	0.060526411	0.172144095	0.24602117	0.22604673	0.22245891	0.26921687	0.20910433	0.30554754	0.421547	0.072505645	0.07165302	0.19719596	0.26103267
100	0.06029115	0.06029115	0.171699061	0.24554256	0.22573727	0.22217993	0.26774007	0.20883486	0.30535054	0.4214982	0.0724542	0.07161057	0.19666179	0.25950003
110	0.060126788	0.060126788	0.171378711	0.24520764	0.22567631	0.22211777	0.26670074	0.20805202	0.30522227	0.42155766	0.07242811	0.071582906	0.19635774	0.25843576
120	0.060005014	0.060005014	0.171129985	0.2449592	0.22547455	0.22194235	0.26600423	0.20793621	0.30506223	0.42148426	0.07240355	0.0715639	0.19613497	0.25770658
130	0.059934633	0.059934633	0.171004705	0.24481551	0.22540045	0.22187163	0.26558548	0.20781264	0.30493605	0.4214702	0.072393246	0.07155562	0.19601196	0.2572692
140	0.059866059	0.059866059	0.170876288	0.2446754	0.22534874	0.22182392	0.26518303	0.20760056	0.30482045	0.42146793	0.07238176	0.071545824	0.19588886	0.25684926
150	0.059825285	0.059825285	0.170809771	0.24459209	0.22530395	0.22178459	0.2649473	0.20747261	0.30478206	0.4214424	0.07237673	0.071540676	0.19583459	0.2566071
160	0.059795879	0.059795879	0.170753785	0.24453196	0.22527476	0.22176109	0.26478136	0.20744446	0.30472896	0.42140582	0.07237174	0.071536824	0.19578885	0.2564345
170	0.059773587	0.059773587	0.1707174	0.24448638	0.22526133	0.22174919	0.26463774	0.20734352	0.30473006	0.42139283	0.07236889	0.071533285	0.19576158	0.25629446
180	0.059753768	0.059753768	0.170678212	0.24444585	0.2252372	0.22172594	0.26452118	0.20726155	0.30472445	0.4213896	0.0723657	0.071530096	0.19572806	0.2561751
190	0.059745758	0.059745758	0.170661113	0.24442945	0.22522525	0.22171548	0.2644717	0.20724417	0.30471218	0.42139617	0.07236424	0.07152894	0.19570917	0.25612235
200	0.059738597	0.059738597	0.170645716	0.24441479	0.22521654	0.22170846	0.26443067	0.20722225	0.3047037	0.42139614	0.072362974	0.07152792	0.19569373	0.25607896

Appendix 10: Evaluation Results of MIMO-TCN variance for Weather Station Data

Similar to Appendix 3, sample screenshots are given below to show the learning process of MIMO-TCN for weather station data. The X-axis represents the number of epochs, and the Y-axis represents the MSE for relevant epoch in each graph. Finally, the saved optimal model is evaluated (i.e. the least MSE model out of 200/300/400 epochs) and the results are shown in above each graph. These evaluation results consist of MSE, MAE, RMSE, and EV respectively.

[0.0368734165819871, 0.0368734165819871, 0.10844986787819945, 0.19202453]

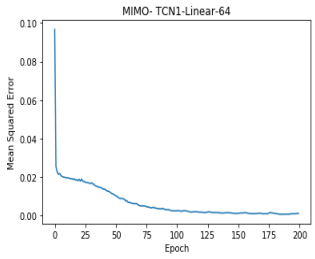

i) TCN1-Linear-64 filters

[0.0290381749286268, 0.0290381749286268, 0.09419349116953186, 0.17040591]

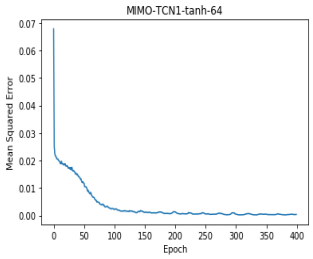

ii) TCN1-tanh-64 filters

[0.03589790931235754, 0.03589790931235754, 0.10823919920566585, 0.18946745]

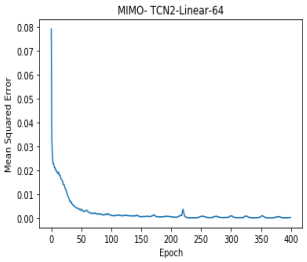

iii) TCN2-Linear-64 filters

[0.0376782325518585, 0.0376782325518585, 0.11397365596673893, 0.19410881]

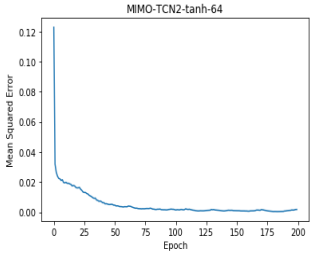

vi)TCN2-tanh-64 filters

[0.03832707091340969, 0.03832707091340969, 0.11670155797450188, 0.195773]

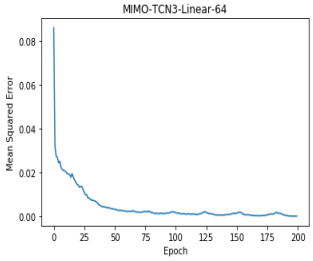

v) TCN3-Linear-64 filters

[0.04765299078605579, 0.04765299078605579, 0.13189281703691583, 0.21829565]

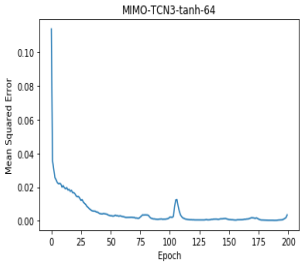

vi) TCN3-tanh-64 filters

[0.04484420047370414, 0.04484420047370414, 0.12593982154729044, 0.21176448]

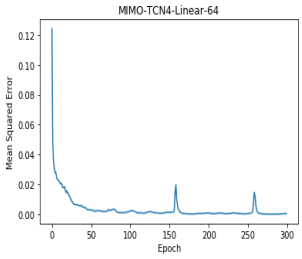

vii) TCN4-Linear-64 filters

[0.045162811424183595, 0.045162811424183595, 0.13031213083481707, 0.21251544]

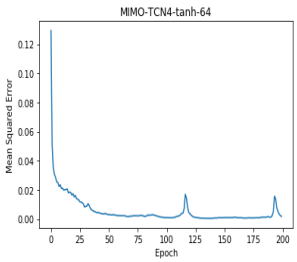

viii)TCN4-tanh-64 filters

[0.02795428058912391, 0.02795428058912391, 0.09234011719796072, 0.16719534

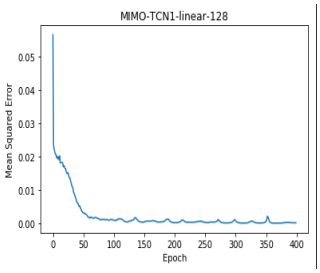

xi) TCN1-Linear-128 fileters

[0.026724572973422525, 0.026724572973422525, 0.08873544896350187, 0.16347653]

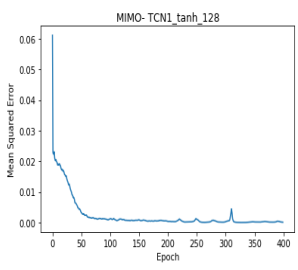

x) TCN1-tanh-128 filters

[0.03723601434882537, 0.03723601434882537, 0.11000724350807989, 0.19296636]

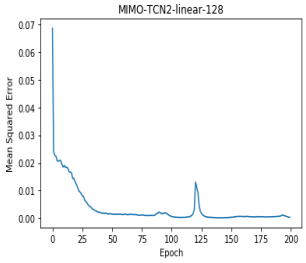

xi) TCN2-Linear-128 filters

[0.03780691097506602, 0.03780691097506602, 0.11086913432835707, 0.19443999]

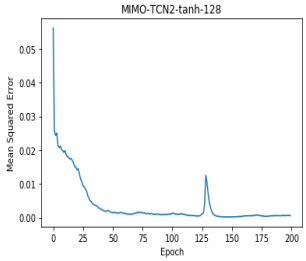

xii) TCN2-tanh-128 filters

[0.04326013862364845, 0.04326013862364845, 0.12230405051609224, 0.20799072]

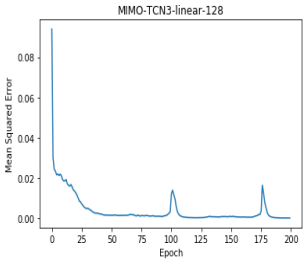

xiii) TCN3-Linear-128 filters

[0.04068349314705311, 0.04068349314705311, 0.11642710122063911, 0.2017015]

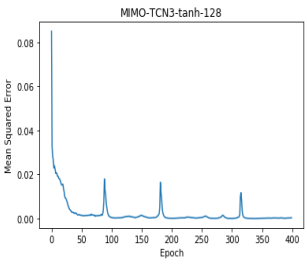

xiv) TCN3-tanh-128 filters

[0.029045782789948904, 0.029045782789948904, 0.09283831462934355, 0.17042823]

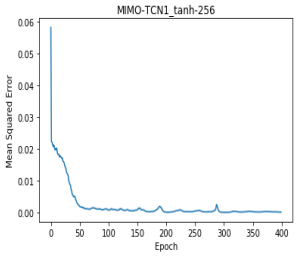

xv) TCN1-tanh-256 filters

[0.02726874936848982, 0.02726874936848982, 0.08719942778039556, 0.16513252]

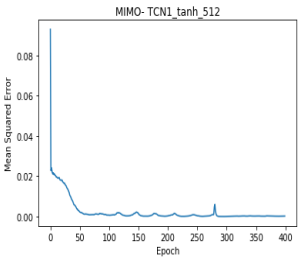

xvi) TCN1-tanh- 512 filters

[0.03058784836613183, 0.03058784836613183, 0.09746832751175936, 0.17489383]

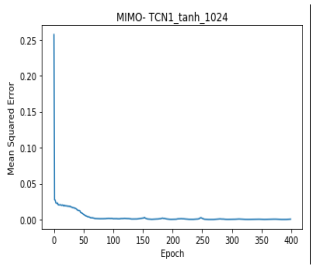

xvii) TCN1-tanh-1024 filters

Appendix 11: Evaluation Results of MISO-LSTM variance for Weather Station Data

The configuration 1 evaluation results are shown here with Adam and SGD optimisers out of several configurations and controls.

Configuration 1- Optimiser Adam

Parameter: Barometer

Epoch	Loss	Total MSE	Total MAE	Total RMSE
10	0.018819744	0.018819744	0.085053361	0.13718507
20	0.016433489	0.016433489	0.075720529	0.12819317
30	0.015437085	0.015437085	0.071722687	0.12424606
40	0.016149865	0.016149865	0.074797286	0.12708212
50	0.014757629	0.014757629	0.068995964	0.12148098
60	0.014861924	0.014861924	0.068050569	0.12190949
70	0.014348842	0.014348842	0.066464941	0.11978665
80	0.014376222	0.014376222	0.067324554	0.11990089
90	0.015031401	0.015031401	0.06968993	0.12260261
100	0.014065959	0.014065959	0.065008268	0.1186
110	0.015471866	0.015471866	0.074585842	0.12438596
120	0.015484543	0.015484543	0.073156299	0.1244369
130	0.015309297	0.015309297	0.071124439	0.12373074
140	0.014673642	0.014673642	0.066477736	0.12113481
150	0.014856243	0.014856243	0.067914507	0.121886194
160	0.015040168	0.015040168	0.068229508	0.12263837
170	0.015903618	0.015903618	0.071864872	0.12610954
180	0.014889238	0.014889238	0.067028055	0.12202146
190	0.015367861	0.015367861	0.07040529	0.12396717
200	0.014944634	0.014944634	0.067828176	0.12224825

Parameter: Temperature

Epoch	Loss	Total MSE	Total MAE	Total RMSE
10	0.014804283	0.014804283	0.067665604	0.12167285
20	0.012211481	0.012211481	0.060255334	0.11050557
30	0.011345458	0.011345458	0.048464764	0.10651505
40	0.011860069	0.011860069	0.048499261	0.108903944
50	0.013556476	0.013556476	0.056891195	0.11643228
60	0.012364725	0.012364725	0.050406869	0.111196786
70	0.012216545	0.012216545	0.057358572	0.110528484
80	0.012066463	0.012066463	0.051737159	0.10984745
90	0.011725435	0.011725435	0.052091945	0.10828405
100	0.012232595	0.012232595	0.06102942	0.11060106
110	0.012413247	0.012413247	0.057107019	0.11141475
120	0.014299767	0.014299767	0.067855311	0.119581625
130	0.013205861	0.013205861	0.065199481	0.11491675
140	0.013520089	0.013520089	0.064222595	0.116275914
150	0.015301147	0.015301147	0.070151756	0.12369781
160	0.014507446	0.014507446	0.070187899	0.12044687
170	0.014287739	0.014287739	0.070086587	0.11953133
180	0.012496289	0.012496289	0.064492023	0.1117868
190	0.012962833	0.012962833	0.067690819	0.11385444
200	0.013517586	0.013517586	0.067530177	0.116265155

Parameter: Pressure

Epoch	Loss	Total MSE	Total MAE	RMSE
10	0.018635879	0.018635879	0.089953669	0.1365133
20	0.016249882	0.016249882	0.077670365	0.12747502
30	0.015125187	0.015125187	0.072253802	0.1229845
40	0.014283792	0.014283792	0.068894416	0.11951482
50	0.014213993	0.014213993	0.068559119	0.11922245
60	0.014469907	0.014469907	0.069671433	0.12029093
70	0.014179327	0.014179327	0.067520561	0.11907698
80	0.013591958	0.013591958	0.063738266	0.11658455
90	0.014208694	0.014208694	0.068164098	0.11920023
100	0.01359247	0.01359247	0.063469422	0.11658675
110	0.014234469	0.014234469	0.066503899	0.11930829
120	0.013790644	0.013790644	0.064443507	0.11743358
130	0.013762422	0.013762422	0.062999449	0.11731335
140	0.014650361	0.014650361	0.067239293	0.12103867
150	0.014363983	0.014363983	0.06737027	0.11984984
160	0.014335643	0.014335643	0.06561675	0.119731545
170	0.014480797	0.014480797	0.066963814	0.12033619
180	0.01408206	0.01408206	0.064398431	0.118667856
190	0.014000452	0.014000452	0.064349398	0.118323505
200	0.014322732	0.014322732	0.066648064	0.11967762

Parameter: Humidity

Epoch	Loss	Total MSE	Total MAE	Total RMSE
10	0.014964063	0.014964063	0.082681524	0.122327685
20	0.01033968	0.01033968	0.062362071	0.10168422
30	0.009414103	0.009414103	0.059814217	0.097026296
40	0.014101172	0.014101172	0.074730865	0.11874836
50	0.017145395	0.017145395	0.078471378	0.13094042
60	0.015716316	0.015716316	0.078474102	0.12536472
70	0.014333407	0.014333407	0.072925968	0.119722195
80	0.018088883	0.018088883	0.084713576	0.13449492
90	0.016205244	0.016205244	0.078092961	0.12729982
100	0.017653115	0.017653115	0.086573092	0.13286503
110	0.018172152	0.018172152	0.092026106	0.13480413
120	0.017036436	0.017036436	0.08452483	0.1305237
130	0.022782945	0.022782945	0.101320847	0.1509402
140	0.017375851	0.017375851	0.086982053	0.13181749
150	0.017169518	0.017169518	0.086249468	0.1310325
160	0.0174926	0.0174926	0.088164659	0.13225959
170	0.018556982	0.018556982	0.089664673	0.136224
180	0.017385017	0.017385017	0.085276476	0.13185225
190	0.01841868	0.01841868	0.0888396	0.13571544
200	0.01873292	0.01873292	0.090195463	0.13686827

Parameter: Wind Speed

Epoch	Loss	Total MSE	Total MAE	Total RMSE
10	0.27004831	0.27004831	0.378120669	0.5196617
20	0.270037892	0.270037892	0.378113212	0.5196517
30	2.757562018	2.757562018	1.621878169	1.6605909
40	0.134729372	0.134729372	0.283255827	0.36705503
50	0.133421305	0.133421305	0.282889321	0.3652688
60	0.131365465	0.131365465	0.282461206	0.36244375
70	0.131837771	0.131837771	0.282554895	0.36309472
80	0.131978347	0.131978347	0.282586363	0.36328825
90	0.132613404	0.132613404	0.282723252	0.36416122
100	0.134219447	0.134219447	0.283074328	0.36635974
110	0.131871096	0.131871096	0.282562374	0.3631406
120	0.132779543	0.132779543	0.282757749	0.36438927
130	0.131666422	0.131666422	0.282515881	0.36285868
140	0.132271014	0.132271014	0.282650487	0.36369082
150	0.131904136	0.131904136	0.282569802	0.36318606
160	0.133388173	0.133388173	0.282881379	0.36522344
170	0.137750778	0.137750778	0.284326429	0.3711479
180	0.133556969	0.133556969	0.282921541	0.36545447
190	0.129971616	0.129971616	0.282251944	0.36051577
200	0.132744358	0.132744358	0.282750479	0.364341

Parameter: Wind Direction

Epoch	Loss	Total MSE	Total MAE	Total RMSE
10	0.118686167	0.118686167	0.233147962	0.3445086
20	0.133908525	0.133908525	0.247376153	0.36593515
30	0.117587778	0.117587778	0.22313131	0.34291074
40	0.122671984	0.122671984	0.237771822	0.35024562
50	0.130006033	0.130006033	0.246381153	0.36056352
60	0.164691161	0.164691161	0.263808946	0.40582162
70	0.129360791	0.129360791	0.252654094	0.35966763
80	0.124444087	0.124444087	0.248638382	0.35276634
90	0.152446247	0.152446247	0.267247823	0.39044365
100	0.155081816	0.155081816	0.276644519	0.39380428
110	0.135612716	0.135612716	0.249453833	0.36825633
120	0.146414063	0.146414063	0.25504098	0.38264093
130	0.16063205	0.16063205	0.273886619	0.4007893
140	0.146592511	0.146592511	0.264111569	0.382874
150	0.196865122	0.196865122	0.312011037	0.44369486
160	0.187305473	0.187305473	0.298900706	0.432788
170	0.194224812	0.194224812	0.302722305	0.44070944
180	0.221235271	0.221235271	0.321973539	0.47035655
190	0.220863562	0.220863562	0.31886314	0.46996123
200	0.230380637	0.230380637	0.328284253	0.4799798

Parameter: Rain Rate

Epoch	Loss	Total MSE	Total MAE	Total RMSE
10	0.005517046	0.005517046	0.017729989	0.07427683
20	0.005517046	0.005517046	0.017729989	0.07427683
30	0.005517046	0.005517046	0.017729989	0.07427683
40	0.005517046	0.005517046	0.017729989	0.07427683
50	0.005517046	0.005517046	0.017729989	0.07427683
60	0.005517046	0.005517046	0.017729989	0.07427683
70	0.005517046	0.005517046	0.017729989	0.07427683
80	0.005517046	0.005517046	0.017729989	0.07427683
90	0.005517046	0.005517046	0.017729989	0.07427683
100	0.005517046	0.005517046	0.017729989	0.07427683
110	0.005517046	0.005517046	0.017729989	0.07427683
120	0.005517046	0.005517046	0.017729989	0.07427683
130	0.005517046	0.005517046	0.017729989	0.07427683
140	0.005517046	0.005517046	0.017729989	0.07427683
150	0.005517046	0.005517046	0.017729989	0.07427683
160	0.005517046	0.005517046	0.017729989	0.07427683
170	0.005517046	0.005517046	0.017729989	0.07427683
180	0.005517046	0.005517046	0.017729989	0.07427683
190	0.005517046	0.005517046	0.017729989	0.07427683
200	0.005517046	0.005517046	0.017729989	0.07427683

Parameter: Rain

Epoch	Loss	Total MSE	Total MAE	Total RMSE
10	0.004974048	0.004974048	0.012975779	0.070526935
20	0.004974048	0.004974048	0.012975779	0.070526935
30	0.004974048	0.004974048	0.012975779	0.070526935
40	0.004974048	0.004974048	0.012975779	0.070526935
50	0.004974048	0.004974048	0.012975779	0.070526935
60	0.004974048	0.004974048	0.012975779	0.070526935
70	0.004974048	0.004974048	0.012975779	0.070526935
80	0.004974048	0.004974048	0.012975779	0.070526935
90	0.004974048	0.004974048	0.012975779	0.070526935
100	0.004974048	0.004974048	0.012975779	0.070526935
110	0.004974048	0.004974048	0.012975779	0.070526935
120	0.004974048	0.004974048	0.012975779	0.070526935
130	0.004974048	0.004974048	0.012975779	0.070526935
140	0.004974048	0.004974048	0.012975779	0.070526935
150	0.004974048	0.004974048	0.012975779	0.070526935
160	0.004974048	0.004974048	0.012975779	0.070526935
170	0.004974048	0.004974048	0.012975779	0.070526935
180	0.004974048	0.004974048	0.012975779	0.070526935
190	0.004974048	0.004974048	0.012975779	0.070526935
200	0.004974048	0.004974048	0.012975779	0.070526935

Parameter: Dew Point

Epoch	Loss	Total MSE	Total MAE	Total RMSE
10	0.01316156	0.01316156	0.054098692	0.11472385
20	0.012308633	0.012308633	0.037332247	0.11094427
30	0.012143813	0.012143813	0.034301712	0.11019897
40	0.01275111	0.01275111	0.03684418	0.112920806
50	0.013612931	0.013612931	0.034061623	0.11667447
60	0.012952085	0.012952085	0.041346817	0.113807224
70	0.012478923	0.012478923	0.035503921	0.111709096
80	0.011752147	0.011752147	0.038568745	0.10840732
90	0.012030619	0.012030619	0.042008007	0.10968418
100	0.011947219	0.011947219	0.039448787	0.10930333
110	0.011979941	0.011979941	0.03834703	0.10945291
120	0.011839829	0.011839829	0.039716828	0.108810976
130	0.011590301	0.011590301	0.035954659	0.10765825
140	0.013266549	0.013266549	0.049398321	0.11518051
150	0.012319759	0.012319759	0.043151327	0.110994406
160	0.011814053	0.011814053	0.041290528	0.10869248
170	0.011471883	0.011471883	0.038331006	0.10710688
180	0.011999584	0.011999584	0.043037531	0.109542616
190	0.012607652	0.012607652	0.04685286	0.112283796
200	0.011537577	0.011537577	0.04032074	0.10741312

Parameter: Heat Index

Epoch	Loss	Total MSE	Total MAE	Total RMSE
10	0.014668656	0.014668656	0.063557267	0.12111423
20	0.01176377	0.01176377	0.050919995	0.10846092
30	0.011136857	0.011136857	0.04855798	0.105531305
40	0.011079868	0.011079868	0.048381461	0.10526096
50	0.012034796	0.012034796	0.050417939	0.10970321
60	0.013058267	0.013058267	0.059896486	0.11427278
70	0.011291652	0.011291652	0.049021982	0.106262185
80	0.015980941	0.015980941	0.069288989	0.12641574
90	0.014303416	0.014303416	0.059644434	0.11959688
100	0.01327996	0.01327996	0.057361152	0.115238704
110	0.012211812	0.012211812	0.058949437	0.11050707
120	0.013811182	0.013811182	0.065732224	0.11752098
130	0.01448827	0.01448827	0.068625232	0.12036723
140	0.013949398	0.013949398	0.065048382	0.11810757
150	0.014815486	0.014815486	0.069909425	0.12171888
160	0.014561707	0.014561707	0.068783521	0.1206719
170	0.014576847	0.014576847	0.068324918	0.12073462
180	0.013295184	0.013295184	0.064716045	0.115304746
190	0.013808108	0.013808108	0.067146395	0.117507905
200	0.014125281	0.014125281	0.067466376	0.11884983

Configuration 1- Optimiser: SGD

Parameter: Barometer

Epoch	Loss	Total MSE	Total MAE	RMSE
10	0.195428716	0.195428716	0.351947867	0.4420732
20	0.057740241	0.057740241	0.177974075	0.24029198
30	0.050953492	0.050953492	0.167580189	0.22572881
40	0.049312287	0.049312287	0.16443421	0.2220637
50	0.048582633	0.048582633	0.163544463	0.22041468
60	0.047216438	0.047216438	0.160116704	0.21729343
70	0.046526902	0.046526902	0.158961568	0.21570095
80	0.046267174	0.046267174	0.158623183	0.21509805
90	0.045788669	0.045788669	0.157470794	0.21398288
100	0.045491433	0.045491433	0.156831207	0.2132872
110	0.045140866	0.045140866	0.156242607	0.2124638
120	0.044826442	0.044826442	0.155389876	0.21172257
130	0.044500254	0.044500254	0.154676799	0.21095082
140	0.044395329	0.044395329	0.154645052	0.21070199
150	0.044153473	0.044153473	0.154066013	0.2101273
160	0.043512595	0.043512595	0.15223819	0.20859672
170	0.043703448	0.043703448	0.153074287	0.2090537
180	0.043212039	0.043212039	0.151660897	0.20787506
190	0.043157293	0.043157293	0.151727874	0.20774333
200	0.043033303	0.043033303	0.151417779	0.2074447
210	0.042878009	0.042878009	0.151012237	0.20707005
220	0.042680188	0.042680188	0.150496431	0.20659184
230	0.042713595	0.042713595	0.150778032	0.2066727
240	0.04251258	0.04251258	0.150362183	0.20618579
250	0.042318679	0.042318679	0.149735217	0.20571505
260	0.042035639	0.042035639	0.149145862	0.20502594
270	0.041865312	0.041865312	0.148527587	0.20461014
280	0.041688725	0.041688725	0.148157075	0.20417817
290	0.041530706	0.041530706	0.147715802	0.20379084
300	0.041495232	0.041495232	0.147732465	0.20370379
310	0.041431725	0.041431725	0.147726857	0.20354785
320	0.041215525	0.041215525	0.146956629	0.20301607
330	0.041134933	0.041134933	0.146989235	0.20281748
340	0.040793121	0.040793121	0.145778256	0.20197307
350	0.04063787	0.04063787	0.145496728	0.20158836
360	0.040681902	0.040681902	0.145727801	0.20169756
370	0.040653666	0.040653666	0.145704551	0.20162754
380	0.040348281	0.040348281	0.14471084	0.20086883
390	0.040350816	0.040350816	0.144966621	0.20087512
400	0.040128638	0.040128638	0.144254611	0.20032133
410	0.039928942	0.039928942	0.143556252	0.19982228
420	0.039827181	0.039827181	0.143450605	0.1995675
430	0.039816015	0.039816015	0.143427756	0.19953951
440	0.03983716	0.03983716	0.143658997	0.19959249
450	0.039589017	0.039589017	0.142931743	0.1989699
460	0.039517582	0.039517582	0.142798294	0.19879031
470	0.039264141	0.039264141	0.142013795	0.19815181
480	0.039280435	0.039280435	0.142086969	0.19819291
490	0.039312306	0.039312306	0.142224397	0.19827332
500	0.039034844	0.039034844	0.141354925	0.19757238
500	0.039034844	0.039034844	0.141354925	0.19757238
510	0.038905948	0.038905948	0.140970376	0.19724591
520	0.038725003	0.038725003	0.140478432	0.19678669
530	0.039070229	0.039070229	0.141696024	0.19766189
540	0.038894119	0.038894119	0.141253987	0.19721591
550	0.038754687	0.038754687	0.14077446	0.19686212
560	0.038596556	0.038596556	0.140312798	0.19646004
570	0.038244792	0.038244792	0.139121108	0.19556275
580	0.038345046	0.038345046	0.139706556	0.1958189
590	0.038210714	0.038210714	0.139194949	0.19547561
600	0.038328759	0.038328759	0.139784605	0.19577733
610	0.038135049	0.038135049	0.138985229	0.19528197
620	0.038128751	0.038128751	0.138992475	0.19526584
630	0.038001543	0.038001543	0.138638471	0.19493984
640	0.037761333	0.037761333	0.138087176	0.19432276
650	0.03779199	0.03779199	0.138036805	0.19440162
660	0.03771576	0.03771576	0.137953574	0.19420546
670	0.037772744	0.037772744	0.13818372	0.1943521
680	0.037617979	0.037617979	0.13765259	0.19395354
690	0.03753376	0.03753376	0.137497853	0.1937363
700	0.037386494	0.037386494	0.137056743	0.19335587
710	0.037395825	0.037395825	0.137012638	0.19338001
720	0.037135555	0.037135555	0.136226497	0.19270588
730	0.037130439	0.037130439	0.136241783	0.1926926
740	0.037043555	0.037043555	0.135985408	0.19246702
750	0.036916417	0.036916417	0.135573832	0.19213647
760	0.036919329	0.036919329	0.135713464	0.19214402
770	0.036724609	0.036724609	0.135039355	0.19163665
780	0.036920352	0.036920352	0.135681007	0.19214669
790	0.036809331	0.036809331	0.135351569	0.19185758
800	0.036633526	0.036633526	0.134753313	0.19139887
810	0.036667807	0.036667807	0.134897043	0.1914884
820	0.036445309	0.036445309	0.134278337	0.19090654
830	0.036503091	0.036503091	0.134456454	0.19105782
840	0.036392708	0.036392708	0.134223358	0.19076873
850	0.036246162	0.036246162	0.13360064	0.19038425
860	0.036293811	0.036293811	0.13378229	0.19050933
870	0.036123928	0.036123928	0.1332934	0.19006296
880	0.036184049	0.036184049	0.133494948	0.19022104
890	0.036003166	0.036003166	0.132831709	0.189745
900	0.036004232	0.036004232	0.132972612	0.18974781
910	0.035796031	0.035796031	0.132337175	0.18919839
920	0.035884548	0.035884548	0.132609638	0.18943219
930	0.03564528	0.03564528	0.131885563	0.18879957
940	0.035782963	0.035782963	0.13233962	0.18916385
950	0.035495698	0.035495698	0.131349983	0.18840303
960	0.035565152	0.035565152	0.131600885	0.18858726
970	0.035506631	0.035506631	0.131323547	0.18843204
980	0.035578956	0.035578956	0.131615871	0.18862385
990	0.035398591	0.035398591	0.131136784	0.18814513
1000	0.03524592	0.03524592	0.130638924	0.18773897

Parameter: Pressure

Epoch	Loss	Total MSE	Total MAE	RMSE
10	0.150605568	0.150605568	0.304157301	0.38807935
20	0.050104333	0.050104333	0.163805934	0.22383997
30	0.047336963	0.047336963	0.160332422	0.21757059
40	0.046666489	0.046666489	0.159116073	0.21602428
50	0.045959963	0.045959963	0.157527684	0.21438274
60	0.045687053	0.045687053	0.157012164	0.2137453
70	0.045198786	0.045198786	0.155841553	0.21260005
80	0.044746807	0.044746807	0.154976485	0.21153441
90	0.04478296	0.04478296	0.155283749	0.21161984
100	0.044259035	0.044259035	0.153816324	0.21037832
110	0.043927129	0.043927129	0.152930546	0.20958799
120	0.043788542	0.043788542	0.152753892	0.20925713
130	0.043718016	0.043718016	0.152770227	0.20908853
140	0.043427897	0.043427897	0.151893642	0.2083936
150	0.043122801	0.043122801	0.151096509	0.2076603
160	0.042817765	0.042817765	0.150261578	0.20692454
170	0.043035144	0.043035144	0.151147979	0.20744914
180	0.042839014	0.042839014	0.150651301	0.20697588
190	0.042439688	0.042439688	0.149670414	0.20600896
200	0.042424276	0.042424276	0.149668241	0.20597154
210	0.042010038	0.042010038	0.148529385	0.2049635
220	0.041867978	0.041867978	0.148007629	0.20461665
230	0.041676729	0.041676729	0.147729576	0.20414877
240	0.041535281	0.041535281	0.147366184	0.20380205
250	0.041717041	0.041717041	0.148158453	0.2042475
260	0.041257507	0.041257507	0.146786231	0.20311944
270	0.04110558	0.04110558	0.146465544	0.2027451
280	0.041164068	0.041164068	0.146652354	0.2028893
290	0.040802394	0.040802394	0.14555896	0.20199603
300	0.040904356	0.040904356	0.146060293	0.20224825
310	0.040846869	0.040846869	0.145858559	0.20210609
320	0.040657317	0.040657317	0.145361422	0.2016366
330	0.040448045	0.040448045	0.144751325	0.201117
340	0.040184139	0.040184139	0.14393346	0.20045982
350	0.040105219	0.040105219	0.143827292	0.20026287
360	0.040108359	0.040108359	0.143898232	0.20027071
370	0.039963994	0.039963994	0.143507936	0.19990997
380	0.039889505	0.039889505	0.143198625	0.19972357
390	0.039802526	0.039802526	0.142974573	0.1995057
400	0.039699056	0.039699056	0.142982547	0.19924621
410	0.039533796	0.039533796	0.142328997	0.19883108
420	0.039501308	0.039501308	0.142443608	0.19874935
430	0.039523949	0.039523949	0.142626867	0.1988063
440	0.039082928	0.039082928	0.141133554	0.19769402
450	0.039068165	0.039068165	0.141219012	0.19765668
460	0.039093646	0.039093646	0.141453866	0.19772114
470	0.038809644	0.038809644	0.140526636	0.19700164
480	0.03866874	0.03866874	0.140128282	0.1966437
490	0.038642468	0.038642468	0.140083131	0.19657686
500	0.038553719	0.038553719	0.139884486	0.196351

500	0.038553719	0.038553719	0.139884486	0.196351
510	0.038515761	0.038515761	0.139842351	0.19625433
520	0.038395407	0.038395407	0.139487055	0.19594747
530	0.038128373	0.038128373	0.138679964	0.19526489
540	0.038101537	0.038101537	0.138619264	0.19519615
550	0.038047627	0.038047627	0.138501413	0.19505802
560	0.038035469	0.038035469	0.138664768	0.19502684
570	0.038037933	0.038037933	0.138688667	0.19503315
580	0.037717222	0.037717222	0.137595405	0.19420923
590	0.037758307	0.037758307	0.137850231	0.19431497
600	0.037600781	0.037600781	0.137542622	0.1939092
610	0.037703286	0.037703286	0.137828209	0.19417334
620	0.037343185	0.037343185	0.136581795	0.19324385
630	0.037501524	0.037501524	0.137163663	0.19365309
640	0.037287876	0.037287876	0.136475989	0.19310069
650	0.0372525	0.0372525	0.136424002	0.19300906
660	0.037134147	0.037134147	0.136014347	0.19270223
670	0.03697719	0.03697719	0.135542387	0.19229454
680	0.037152353	0.037152353	0.136240235	0.19274946
690	0.036947749	0.036947749	0.135423389	0.19221799
700	0.036852984	0.036852984	0.135300932	0.1919713
710	0.036859608	0.036859608	0.135400821	0.19198857
720	0.036607064	0.036607064	0.134632442	0.19132973
730	0.036641689	0.036641689	0.134645679	0.19142017
740	0.036509264	0.036509264	0.134288198	0.19107397
750	0.036521135	0.036521135	0.134434595	0.19110504
760	0.036418375	0.036418375	0.134167864	0.190836
770	0.036357402	0.036357402	0.133945154	0.19067617
780	0.036260938	0.036260938	0.133765507	0.19042304
790	0.036290495	0.036290495	0.133871333	0.19050065
800	0.036101202	0.036101202	0.133233439	0.19000316
810	0.036191998	0.036191998	0.133537962	0.19024193
820	0.035822813	0.035822813	0.132313594	0.18926914
830	0.03598196	0.03598196	0.132820245	0.18968911
840	0.035798363	0.035798363	0.132229671	0.18920456
850	0.035734988	0.035734988	0.132081946	0.18903701
860	0.035509623	0.035509623	0.131387362	0.18843998
870	0.035383178	0.035383178	0.131093866	0.18810417
880	0.035612778	0.035612778	0.131803355	0.18871346
890	0.035414547	0.035414547	0.131211507	0.18818752
900	0.035408634	0.035408634	0.131147351	0.18817183
910	0.035347409	0.035347409	0.130974726	0.18800907
920	0.03521287	0.03521287	0.130522415	0.18765093
930	0.034965945	0.034965945	0.129784747	0.18699183
940	0.035083882	0.035083882	0.130213644	0.18730693
950	0.034867518	0.034867518	0.129542204	0.18672846
960	0.034804741	0.034804741	0.129304904	0.18656029
970	0.034656039	0.034656039	0.128877581	0.18616132
980	0.034600932	0.034600932	0.128707592	0.18601327
990	0.034448337	0.034448337	0.128201727	0.18560262
1000	0.034433334	0.034433334	0.128165202	0.18556221

Parameter: Temperature

Epoch	Loss	Total MSE	Total MAE	RMSE
10	0.119111219	0.119111219	0.303285045	0.34512493
20	0.312812045	0.312812045	0.461592744	0.559296
30	0.28387282	0.28387282	0.429352134	0.53279716
40	0.161014433	0.161014433	0.254786451	0.40126604
50	0.173887674	0.173887674	0.277837345	0.41699842
60	0.231415039	0.231415039	0.364218307	0.48105615
70	0.219910171	0.219910171	0.348452068	0.4689458
80	0.15923633	0.15923633	0.252885952	0.39904428
90	0.121102207	0.121102207	0.305632962	0.34799743
100	0.108930465	0.108930465	0.289911783	0.33004615
110	0.101188748	0.101188748	0.275282445	0.3181018
120	0.111520652	0.111520652	0.293604617	0.3339471
130	0.099935112	0.099935112	0.270454749	0.31612515
140	0.132317342	0.132317342	0.253524692	0.3637545
150	0.282918435	0.282918435	0.428254044	0.53190076
160	0.309827111	0.309827111	0.458348059	0.55662113
170	0.124823139	0.124823139	0.309972423	0.3533032
180	0.206913131	0.206913131	0.404721497	0.45487708
190	0.288886181	0.288886181	0.435074254	0.53748137
200	0.182279446	0.182279446	0.291796018	0.426942
210	0.188833909	0.188833909	0.302291025	0.43455023
220	0.172525864	0.172525864	0.275498986	0.41536233
230	0.268288299	0.268288299	0.411048136	0.5179655
240	0.208570952	0.208570952	0.332191104	0.45669568
250	0.100323494	0.100323494	0.264534483	0.31673884
260	0.102212287	0.102212287	0.277898423	0.31970656
270	0.124125494	0.124125494	0.3091493	0.35231447
280	0.108057601	0.108057601	0.288600171	0.32872117
290	0.130224596	0.130224596	0.253708244	0.36086643
300	0.100858958	0.100858958	0.274323028	0.317583
310	0.170815829	0.170815829	0.272531453	0.41329873
320	0.224931006	0.224931006	0.423283104	0.47426894
330	0.102591886	0.102591886	0.278755036	0.32029969
340	0.231199827	0.231199827	0.429487183	0.48083246
350	0.202632299	0.202632299	0.400127765	0.45014694
360	0.118433894	0.118433894	0.302477316	0.34414226
370	0.207465276	0.207465276	0.405307255	0.45548356
380	0.111670628	0.111670628	0.25705912	0.33417156
390	0.254988155	0.254988155	0.394745802	0.5049635
400	0.17814818	0.17814818	0.285017591	0.42207605
410	0.114126881	0.114126881	0.297071832	0.3378267
420	0.221641611	0.221641611	0.35087166	0.4707883
430	0.167790237	0.167790237	0.267192168	0.40962207
440	0.226422157	0.226422157	0.357464271	0.4758383
450	0.106087595	0.106087595	0.285474633	0.3257109
460	0.117275955	0.117275955	0.301062941	0.34245577
470	0.099755438	0.099755438	0.267308495	0.31584084
480	0.196170447	0.196170447	0.313688476	0.44291136
490	0.101982503	0.101982503	0.277349179	0.319347
500	0.118275869	0.118275869	0.302286926	0.34391257
500	0.118275869	0.118275869	0.302286926	0.34391257
510	0.23203114	0.23203114	0.365042774	0.48169607
520	0.174428316	0.174428316	0.278759713	0.41764617
530	0.112747344	0.112747344	0.295253951	0.33577868
540	0.228863637	0.228863637	0.36078329	0.47839695
550	0.172252086	0.172252086	0.275026236	0.41503263
560	0.171437757	0.171437757	0.273614822	0.41405043
570	0.262282176	0.262282176	0.40376907	0.5121349
580	0.123316232	0.123316232	0.25456079	0.35116413
590	0.126728179	0.126728179	0.254087345	0.355989
600	0.173676301	0.173676301	0.36805694	0.4167449
610	0.274984096	0.274984096	0.41901181	0.5243892
620	0.109776166	0.109776166	0.291150957	0.33132485
630	0.160796116	0.160796116	0.352984404	0.40099388
640	0.146208427	0.146208427	0.335739122	0.3823721
650	0.110506884	0.110506884	0.292199923	0.33242577
660	0.140670319	0.140670319	0.329168941	0.37506044
670	0.111287935	0.111287935	0.293287686	0.33359846
680	0.134427953	0.134427953	0.321615603	0.3666442
690	0.120727286	0.120727286	0.305194811	0.34745833
700	0.18567073	0.18567073	0.381432497	0.43089524
710	0.110156599	0.110156599	0.291699265	0.33189848
720	0.100100069	0.100100069	0.27145017	0.31638592
730	0.334826927	0.334826927	0.484853334	0.57864225
740	0.289796052	0.289796052	0.436104606	0.5383271
750	0.170942355	0.170942355	0.272752262	0.41345176
760	0.112817707	0.112817707	0.25672178	0.33588347
770	0.107406806	0.107406806	0.258640903	0.32772976
780	0.099773909	0.099773909	0.268867273	0.31587008
790	0.110819622	0.110819622	0.257320009	0.33289582
800	0.208127878	0.208127878	0.331542126	0.45621032
810	0.137601849	0.137601849	0.253088902	0.37094724
820	0.099999055	0.099999055	0.265527034	0.31622627
830	0.218940508	0.218940508	0.347089424	0.4679108
840	0.289241093	0.289241093	0.435476479	0.5378114
850	0.159842877	0.159842877	0.252898822	0.39980355
860	0.218721325	0.218721325	0.346780586	0.4676765
870	0.268718182	0.268718182	0.411564129	0.51838034
880	0.300873451	0.300873451	0.448515752	0.5485193
890	0.220575193	0.220575193	0.349383427	0.46965435
900	0.297359709	0.297359709	0.444608314	0.545307
910	0.172520747	0.172520747	0.366720879	0.4153562
920	0.121912737	0.121912737	0.306574061	0.34916005
930	0.151019584	0.151019584	0.252747486	0.3886124
940	0.226456611	0.226456611	0.424804682	0.4758746
950	0.103575632	0.103575632	0.280844765	0.32183167
960	0.136411087	0.136411087	0.253181941	0.36933872
970	0.099812315	0.099812315	0.26938843	0.31593087
980	0.177793282	0.177793282	0.372734184	0.4216554
990	0.100386475	0.100386475	0.272727925	0.31683826
1000	0.231449696	0.231449696	0.364264747	0.48109218

Parameter: Humidity

Epoch	Loss	Total MSE	Total MAE	RMSE
10	0.061859458	0.061859458	0.201196614	0.24871562
20	0.04605645	0.04605645	0.157858817	0.21460767
30	0.044244115	0.044244115	0.156180534	0.21034285
40	0.042050289	0.042050289	0.152251349	0.20506167
50	0.038860718	0.038860718	0.144886009	0.19713122
60	0.037247626	0.037247626	0.140476041	0.19299644
70	0.035496653	0.035496653	0.137041438	0.18840556
80	0.034011071	0.034011071	0.143677131	0.18442091
90	0.036408407	0.036408407	0.144146484	0.19080986
100	0.03477279	0.03477279	0.141837804	0.18647465
110	0.032582713	0.032582713	0.141920661	0.18050683
120	0.033803635	0.033803635	0.137982455	0.18385766
130	0.032961775	0.032961775	0.136030951	0.18155378
140	0.032429258	0.032429258	0.133732805	0.18008125
150	0.030794362	0.030794362	0.133705779	0.17548323
160	0.031057907	0.031057907	0.131858424	0.17623253
170	0.030302665	0.030302665	0.132083762	0.17407662
180	0.029592626	0.029592626	0.131307727	0.17202507
190	0.031571163	0.031571163	0.129196155	0.17768276
200	0.030049937	0.030049937	0.128900488	0.17334919
210	0.029618987	0.029618987	0.12763273	0.17210168
220	0.028319054	0.028319054	0.127445282	0.16828266
230	0.030036475	0.030036475	0.125573868	0.17331034
240	0.028538754	0.028538754	0.125786544	0.16893417
250	0.028866401	0.028866401	0.124380312	0.16990115
260	0.029142997	0.029142997	0.123755087	0.1707132
270	0.027742816	0.027742816	0.12275014	0.16656175
280	0.027115036	0.027115036	0.126471625	0.16466644
290	0.027348829	0.027348829	0.122899753	0.16537482
300	0.026866089	0.026866089	0.121763733	0.16390878
310	0.027250422	0.027250422	0.12096576	0.16507702
320	0.027020307	0.027020307	0.121135093	0.16437854
330	0.02734342	0.02734342	0.120862607	0.16535847
340	0.027002719	0.027002719	0.120954035	0.16432504
350	0.026814874	0.026814874	0.119754707	0.16375247
360	0.026685336	0.026685336	0.119785849	0.16335647
370	0.026292951	0.026292951	0.119458525	0.16215101
380	0.026652538	0.026652538	0.117236857	0.16325605
390	0.027094625	0.027094625	0.117181399	0.16460444
400	0.026854181	0.026854181	0.116130081	0.16387245
410	0.026773223	0.026773223	0.115811323	0.16362526
420	0.026005473	0.026005473	0.116808218	0.16126212
430	0.026620408	0.026620408	0.116500702	0.16315761
440	0.027884469	0.027884469	0.115260374	0.16698644
450	0.025440459	0.025440459	0.115977248	0.15950066
460	0.02597423	0.02597423	0.114157705	0.16116522
470	0.025834978	0.025834978	0.113919493	0.16073263
480	0.02524725	0.02524725	0.115369494	0.15889384
490	0.025800624	0.025800624	0.112924996	0.16062573
500	0.0259208	0.0259208	0.113291367	0.16099937
500	0.0259208	0.0259208	0.113291367	0.16099937
510	0.026881694	0.026881694	0.113215442	0.16395639
520	0.026011376	0.026011376	0.113018769	0.16128042
530	0.026833457	0.026833457	0.112372868	0.16380921
540	0.026403363	0.026403363	0.113487802	0.16249111
550	0.025276097	0.025276097	0.113977616	0.15898457
560	0.02528289	0.02528289	0.112861598	0.15900594
570	0.025069034	0.025069034	0.113711048	0.15833203
580	0.025516026	0.025516026	0.11289385	0.15973736
590	0.025593254	0.025593254	0.112197999	0.15997893
600	0.025520947	0.025520947	0.112056452	0.15975277
610	0.02645122	0.02645122	0.112259781	0.1626383
620	0.024948704	0.024948704	0.113180883	0.1579516
630	0.026528885	0.026528885	0.112779416	0.1628769
640	0.025859717	0.025859717	0.112208631	0.16080956
650	0.024734497	0.024734497	0.112249172	0.15727204
660	0.024671105	0.024671105	0.11175083	0.15707037
670	0.02449408	0.02449408	0.112002153	0.15650585
680	0.023966309	0.023966309	0.111843718	0.15481056
690	0.024200637	0.024200637	0.113076376	0.15556553
700	0.024755504	0.024755504	0.111203983	0.15733881
710	0.024369593	0.024369593	0.111958596	0.15610763
720	0.024966177	0.024966177	0.112011	0.15800688
730	0.024891154	0.024891154	0.111433353	0.15776931
740	0.024940242	0.024940242	0.110751209	0.1579248
750	0.025163457	0.025163457	0.111464888	0.15862994
760	0.026582856	0.026582856	0.112468827	0.1630425
770	0.025138567	0.025138567	0.111348439	0.15855147
780	0.024559981	0.024559981	0.110886724	0.15671624
790	0.02512559	0.02512559	0.110691639	0.15851055
800	0.024039196	0.024039196	0.110700058	0.15504579
810	0.023807513	0.023807513	0.110333507	0.15429683
820	0.023283831	0.023283831	0.111860219	0.1525904
830	0.0241462	0.0241462	0.1109583	0.15539047
840	0.023864067	0.023864067	0.110776379	0.15447998
850	0.025655379	0.025655379	0.111911925	0.16017297
860	0.024603861	0.024603861	0.111421893	0.15685616
870	0.023846541	0.023846541	0.111857599	0.15442325
880	0.023581225	0.023581225	0.11128966	0.1535618
890	0.024334805	0.024334805	0.111009637	0.15599617
900	0.023688245	0.023688245	0.110153284	0.15390986
910	0.023866803	0.023866803	0.10999984	0.15448885
920	0.023502714	0.023502714	0.110177811	0.15330596
930	0.023362261	0.023362261	0.110800528	0.15284719
940	0.023529632	0.023529632	0.110846496	0.15339372
950	0.024236285	0.024236285	0.110365073	0.15568008
960	0.022887007	0.022887007	0.111359291	0.15128452
970	0.023135045	0.023135045	0.10988597	0.1521021
980	0.02368224	0.02368224	0.109386628	0.15389034
990	0.022972099	0.022972099	0.110055614	0.15156549
1000	0.022676789	0.022676789	0.111310961	0.15058814

Parameter: Wind Speed

Epoch	Loss	Total MSE	Total MAE	RMSE
10	0.119271419	0.119271419	0.267809666	0.34535694
20	0.112282052	0.112282052	0.260287308	0.33508515
30	0.104294743	0.104294743	0.251612573	0.32294697
40	0.096897129	0.096897129	0.242722926	0.31128305
50	0.089101049	0.089101049	0.233265988	0.29849797
60	0.083080846	0.083080846	0.225247303	0.28823748
70	0.078300938	0.078300938	0.219115283	0.27982304
80	0.074781645	0.074781645	0.214365667	0.27346233
90	0.07224223	0.07224223	0.210262682	0.26877916
100	0.070543512	0.070543512	0.206953549	0.2656003
110	0.069022549	0.069022549	0.204329377	0.26272142
120	0.067843612	0.067843612	0.20313271	0.26046807
130	0.067440781	0.067440781	0.20104135	0.25969365
140	0.067020027	0.067020027	0.19942017	0.25888228
150	0.066072135	0.066072135	0.198842929	0.257045
160	0.065872962	0.065872962	0.197451722	0.25665727
170	0.065397465	0.065397465	0.197000766	0.2557293
180	0.065161113	0.065161113	0.19594495	0.25526676
190	0.06536088	0.06536088	0.194256621	0.25565773
200	0.064133954	0.064133954	0.194458457	0.25324684
210	0.063816168	0.063816168	0.193873516	0.25261864
220	0.063835943	0.063835943	0.192251145	0.25265777
230	0.063617983	0.063617983	0.191748485	0.25222605
240	0.063715362	0.063715362	0.191260581	0.252419
250	0.062396546	0.062396546	0.192655933	0.24979301
260	0.063328828	0.063328828	0.190294994	0.25165218
270	0.0628931	0.0628931	0.190493066	0.25078496
280	0.062134732	0.062134732	0.190796695	0.2492684
290	0.062216502	0.062216502	0.1906859	0.24943237
300	0.061753323	0.061753323	0.191397796	0.24850215
310	0.061396359	0.061396359	0.194280862	0.24778287
320	0.062092574	0.062092574	0.189646096	0.24918382
330	0.06307871	0.06307871	0.187934761	0.25115475
340	0.062240399	0.062240399	0.188423797	0.24948026
350	0.061844464	0.061844464	0.188954558	0.24868546
360	0.061405761	0.061405761	0.189640527	0.24780184
370	0.061250776	0.061250776	0.190047969	0.24748893
380	0.062878643	0.062878643	0.187093484	0.25075614
390	0.062158626	0.062158626	0.187281099	0.24931632
400	0.061137299	0.061137299	0.189377458	0.24725959
410	0.061683529	0.061683529	0.187796382	0.24836169
420	0.061584997	0.061584997	0.187753871	0.24816324
430	0.061462045	0.061462045	0.187632236	0.2479154
440	0.061242024	0.061242024	0.188143755	0.24747126
450	0.061641099	0.061641099	0.187264611	0.24827626
460	0.060672318	0.060672318	0.190309136	0.2463175
470	0.061047199	0.061047199	0.188278528	0.2470773
480	0.061063681	0.061063681	0.187802747	0.24711068
490	0.061634077	0.061634077	0.186838878	0.24826212
500	0.061050986	0.061050986	0.187820782	0.24708496
500	0.061050986	0.061050986	0.187820782	0.24708496
510	0.060919078	0.060919078	0.187967599	0.2468179
520	0.06114557	0.06114557	0.187156998	0.24727632
530	0.060877637	0.060877637	0.187283727	0.24673393
540	0.061048967	0.061048967	0.1868227	0.24708088
550	0.060643749	0.060643749	0.188138081	0.24625951
560	0.060974413	0.060974413	0.186356471	0.24692997
570	0.060880977	0.060880977	0.186494874	0.24674071
580	0.06089864	0.06089864	0.186344793	0.24677648
590	0.060440509	0.060440509	0.18747905	0.24584651
600	0.060428357	0.060428357	0.186919313	0.24582179
610	0.06031946	0.06031946	0.186952962	0.24560021
620	0.060395657	0.060395657	0.186778589	0.24575529
630	0.060891269	0.060891269	0.185137853	0.24676156
640	0.060927306	0.060927306	0.184804237	0.24683458
650	0.060352027	0.060352027	0.185760261	0.24566649
660	0.060670255	0.060670255	0.184965229	0.24631332
670	0.06026429	0.06026429	0.185360267	0.24548785
680	0.060170595	0.060170595	0.185306397	0.24529694
690	0.059956717	0.059956717	0.185858563	0.2448606
700	0.059944746	0.059944746	0.185739269	0.24483617
710	0.060066001	0.060066001	0.184495999	0.24508366
720	0.059752388	0.059752388	0.18595452	0.24444301
730	0.060302398	0.060302398	0.183583196	0.24556547
740	0.060581896	0.060581896	0.183055317	0.24613391
750	0.05963587	0.05963587	0.185440084	0.24420457
760	0.059814671	0.059814671	0.183918092	0.24457037
770	0.059644686	0.059644686	0.184118894	0.24422261
780	0.059570861	0.059570861	0.184809077	0.24407144
790	0.059641024	0.059641024	0.183427523	0.24421512
800	0.059842413	0.059842413	0.182804918	0.24462709
810	0.059472356	0.059472356	0.183640167	0.24386956
820	0.059317943	0.059317943	0.184320035	0.24355274
830	0.059248082	0.059248082	0.184968688	0.24340929
840	0.05930772	0.05930772	0.1837322	0.24353176
850	0.059327778	0.059327778	0.182994272	0.24357294
860	0.059185118	0.059185118	0.183458418	0.24327992
870	0.059362165	0.059362165	0.182108406	0.24364352
880	0.059085892	0.059085892	0.183385142	0.24307589
890	0.059148186	0.059148186	0.182227376	0.243204
900	0.059461971	0.059461971	0.181332231	0.24384825
910	0.05891043	0.05891043	0.183444433	0.2427147
920	0.059314537	0.059314537	0.181326288	0.24354576
930	0.059701349	0.059701349	0.18059475	0.24433859
940	0.058868816	0.058868816	0.181933558	0.24262898
950	0.059077916	0.059077916	0.181012927	0.2430595
960	0.058784632	0.058784632	0.182145272	0.24245542
970	0.05894202	0.05894202	0.180845056	0.24277979
980	0.058718044	0.058718044	0.181829478	0.24231806
990	0.058777603	0.058777603	0.181148457	0.24244094

Parameter: Wind Direction

Epoch	Loss	Total MSE	Total MAE	RMSE
10	0.207067887	0.207067887	0.41123502	0.45504713
20	0.173859779	0.173859779	0.330255492	0.41696495
30	0.167909317	0.167909317	0.318290513	0.4097674
40	0.164623283	0.164623283	0.313507657	0.40573797
50	0.160950656	0.160950656	0.308143226	0.40118656
60	0.157745203	0.157745203	0.304585525	0.3971715
70	0.155142798	0.155142798	0.301630219	0.3938817
80	0.152764936	0.152764936	0.297983268	0.39085156
90	0.149316445	0.149316445	0.293179823	0.38641486
100	0.146490619	0.146490619	0.289646492	0.38274094
110	0.143655723	0.143655723	0.284943818	0.3790194
120	0.141408349	0.141408349	0.28161962	0.37604302
130	0.139470221	0.139470221	0.278888768	0.37345713
140	0.138172642	0.138172642	0.276289175	0.3717158
150	0.136391296	0.136391296	0.273957829	0.36931193
160	0.13456867	0.13456867	0.271121688	0.36683604
170	0.134625474	0.134625474	0.270556251	0.36691344
180	0.132579972	0.132579972	0.267507827	0.36411533
190	0.131409924	0.131409924	0.266346958	0.36250505
200	0.130569717	0.130569717	0.264408795	0.36134434
210	0.130634234	0.130634234	0.263141469	0.3614336
220	0.129725347	0.129725347	0.262382802	0.36017403
230	0.129307785	0.129307785	0.261310025	0.3595939
240	0.128683618	0.128683618	0.260498907	0.358725
250	0.128373072	0.128373072	0.259913874	0.35829186
260	0.127886204	0.127886204	0.260252554	0.3576118
270	0.127553135	0.127553135	0.258614369	0.35714582
280	0.127296373	0.127296373	0.25788303	0.35678616
290	0.126818853	0.126818853	0.256719625	0.35611635
300	0.126366093	0.126366093	0.256543349	0.3554801
310	0.126814744	0.126814744	0.256804813	0.35611057
320	0.126451517	0.126451517	0.255952589	0.3556002
330	0.125664343	0.125664343	0.255810838	0.35449165
340	0.125682223	0.125682223	0.255809623	0.3545169
350	0.126125741	0.126125741	0.255669618	0.35514185
360	0.125008699	0.125008699	0.2543374	0.3535657
370	0.12469784	0.12469784	0.25437394	0.35312578
380	0.124544593	0.124544593	0.253819447	0.35290876
390	0.124594938	0.124594938	0.25364461	0.35298008
400	0.124471038	0.124471038	0.253051933	0.35280454
410	0.124640179	0.124640179	0.253406052	0.35304415
420	0.124422259	0.124422259	0.253549589	0.3527354
430	0.124449562	0.124449562	0.253181077	0.35277408
440	0.123362563	0.123362563	0.25169887	0.35123006
450	0.124031507	0.124031507	0.252787672	0.35218105
460	0.123159658	0.123159658	0.252220403	0.3509411
470	0.123122112	0.123122112	0.251865744	0.3508876
480	0.122770747	0.122770747	0.250796498	0.35038656
490	0.122946288	0.122946288	0.251334689	0.350637
500	0.123400479	0.123400479	0.251640267	0.35128406

500	0.123400479	0.123400479	0.251640267	0.35128406
510	0.123489373	0.123489373	0.25189219	0.35141057
520	0.122636328	0.122636328	0.250533297	0.35019472
530	0.122314586	0.122314586	0.249897382	0.34973502
540	0.122334424	0.122334424	0.249636016	0.34976336
550	0.122052047	0.122052047	0.249479798	0.34935948
560	0.122293463	0.122293463	0.249772904	0.3497048
570	0.122611672	0.122611672	0.250306801	0.3501595
580	0.122832697	0.122832697	0.250866726	0.35047495
590	0.121941564	0.121941564	0.249351142	0.34920132
600	0.121696465	0.121696465	0.248904698	0.34885022
610	0.121710468	0.121710468	0.248871233	0.34887028
620	0.122169434	0.122169434	0.248969709	0.34952745
630	0.121827302	0.121827302	0.248599399	0.34903768
640	0.12209745	0.12209745	0.249415545	0.34942445
650	0.122536705	0.122536705	0.249509267	0.35005245
660	0.122020268	0.122020268	0.249044743	0.34931397
670	0.121415298	0.121415298	0.24855124	0.34844697
680	0.121574134	0.121574134	0.248489881	0.3486748
690	0.121873896	0.121873896	0.249317399	0.34910443
700	0.121524301	0.121524301	0.248194954	0.34860337
710	0.121733577	0.121733577	0.247980003	0.3489034
720	0.12117067	0.12117067	0.248160153	0.34809577
730	0.121334923	0.121334923	0.248094332	0.34833163
740	0.121765683	0.121765683	0.24869431	0.3489494
750	0.121239445	0.121239445	0.24817952	0.34819454
760	0.12148158	0.12148158	0.248162055	0.3485421
770	0.121239296	0.121239296	0.248064228	0.34819433
780	0.121258464	0.121258464	0.247572132	0.34822187
790	0.12130795	0.12130795	0.247778121	0.3482929
800	0.122739139	0.122739139	0.248818097	0.35034147
810	0.121028685	0.121028685	0.247044463	0.34789175
820	0.121215638	0.121215638	0.246831571	0.34816036
830	0.121020191	0.121020191	0.247331641	0.34787956
840	0.121512572	0.121512572	0.248268193	0.34858653
850	0.121658192	0.121658192	0.248046093	0.34879535
860	0.121689678	0.121689678	0.248589266	0.34884048
870	0.121062337	0.121062337	0.2474207	0.34794015
880	0.120866384	0.120866384	0.247341223	0.34765843
890	0.121373158	0.121373158	0.246950665	0.34838653
900	0.122341066	0.122341066	0.247878385	0.3497729
910	0.120838371	0.120838371	0.246829836	0.34761813
920	0.120723445	0.120723445	0.246633452	0.3474528
930	0.123365994	0.123365994	0.248942739	0.35123497
940	0.121198038	0.121198038	0.247003263	0.34813508
950	0.122355723	0.122355723	0.248312642	0.34979382
960	0.120842834	0.120842834	0.246966381	0.34762457
970	0.120790271	0.120790271	0.24671568	0.34754893
980	0.121064011	0.121064011	0.246524743	0.34794253
990	0.120334177	0.120334177	0.245897413	0.34689218
1000	0.121535721	0.121535721	0.247070591	0.34861973

Parameter: Rain Rate

Epoch	Loss	Total MSE	Total MAE	RMSE
10	0.006216895	0.006216895	0.059369456	0.07884729
20	0.005266106	0.005266106	0.044266398	0.07256795
30	0.005101624	0.005101624	0.038521854	0.071425654
40	0.005059547	0.005059547	0.035364015	0.071130484
50	0.005050923	0.005050923	0.03334664	0.071069844
60	0.005053512	0.005053512	0.031921542	0.07108805
70	0.005060175	0.005060175	0.030857952	0.07113491
80	0.005068281	0.005068281	0.030020662	0.07119186
90	0.005076721	0.005076721	0.029341763	0.07125111
100	0.00508488	0.00508488	0.028785269	0.07130835
110	0.005092657	0.005092657	0.028314435	0.07136285
120	0.005099902	0.005099902	0.027914058	0.07141359
130	0.005106584	0.005106584	0.027569506	0.07146037
140	0.005112847	0.005112847	0.027265372	0.071504176
150	0.005118677	0.005118677	0.026995562	0.07154493
160	0.005124103	0.005124103	0.026754794	0.07158285
170	0.005129118	0.005129118	0.026540103	0.071617864
180	0.005133612	0.005133612	0.026352316	0.07164923
190	0.005137799	0.005137799	0.02618175	0.07167844
200	0.00514169	0.00514169	0.02602645	0.07170558

Parameter: Rain

Epoch	Loss	Total MSE	Total MAE	RMSE
10	0.006857423	0.006857423	0.066763532	0.08280956
20	0.005370492	0.005370492	0.047471631	0.073283635
30	0.005039894	0.005039894	0.040153982	0.07099221
40	0.004913976	0.004913976	0.036158152	0.070099756
50	0.004853175	0.004853175	0.033573542	0.06966473
60	0.004820253	0.004820253	0.031762625	0.06942804
70	0.004800736	0.004800736	0.030398772	0.06928734
80	0.004788671	0.004788671	0.029336822	0.069200225
90	0.004780915	0.004780915	0.028476347	0.06914416
100	0.004775926	0.004775926	0.027778563	0.06910808
110	0.004772683	0.004772683	0.027203804	0.06908461
120	0.004770524	0.004770524	0.026704284	0.06906898
130	0.00476914	0.00476914	0.026272483	0.06905896
140	0.004768289	0.004768289	0.025894375	0.0690528
150	0.004767819	0.004767819	0.025556938	0.069049396
160	0.004767614	0.004767614	0.025263982	0.069047906
170	0.004767587	0.004767587	0.025007012	0.06904771
180	0.004767701	0.004767701	0.02477377	0.06904854
190	0.004767904	0.004767904	0.024561749	0.069050014
200	0.00476817	0.00476817	0.024371153	0.069051936

Parameter: Dew Point

Epoch	Loss	Total MSE	Total MAE	RMSE
10	0.817569852	0.817569852	0.891280751	0.90419567
20	0.891930536	0.891930536	0.932382169	0.94442075
30	0.908230911	0.908230911	0.941756436	0.9530116
40	0.911375107	0.911375107	0.944522906	0.95465964
50	0.914518842	0.914518842	0.947301591	0.9563048
60	0.894202716	0.894202716	0.937188848	0.9456229
70	0.899295741	0.899295741	0.940026017	0.9483121
80	0.91851676	0.91851676	0.949957696	0.95839286
90	0.909231566	0.909231566	0.944365458	0.95353633
100	0.895808683	0.895808683	0.936394482	0.94647175
110	0.928830867	0.928830867	0.953378572	0.96375877
120	0.922652864	0.922652864	0.949787225	0.9605482
130	0.924466016	0.924466016	0.950545877	0.9614915
140	0.910343427	0.910343427	0.942939746	0.95411915
150	0.920198919	0.920198919	0.94822447	0.95927
160	0.92198045	0.92198045	0.94913458	0.9601981
170	0.913664436	0.913664436	0.944686003	0.95585793
180	0.916224955	0.916224955	0.946037366	0.95719635
190	0.896861475	0.896861475	0.935635361	0.9470277
200	0.90948613	0.90948613	0.942513674	0.9536698
210	0.90149362	0.90149362	0.938207904	0.9494702
220	0.907759684	0.907759684	0.941606564	0.9527643
230	0.90000914	0.90000914	0.93748592	0.9486881
240	0.930614004	0.930614004	0.953783427	0.96468335
250	0.917262891	0.917262891	0.946729572	0.95773846
260	0.895944237	0.895944237	0.935393882	0.9465434
270	0.915261011	0.915261011	0.945721721	0.95669276
280	0.920008185	0.920008185	0.94821189	0.9591705
290	0.929333914	0.929333914	0.953151326	0.96401966
300	0.911346951	0.911346951	0.943667502	0.9546449
310	0.889518762	0.889518762	0.931896446	0.94314295
320	0.932272705	0.932272705	0.954777894	0.96554273
330	0.911181339	0.911181339	0.943564229	0.9545582
340	0.925861639	0.925861639	0.951424164	0.96221703
350	0.911703298	0.911703298	0.943895329	0.95483154
360	0.916972094	0.916972094	0.946655391	0.9575866
370	0.931233827	0.931233827	0.954236184	0.96500456
380	0.914451257	0.914451257	0.945369644	0.95626944
390	0.909133963	0.909133963	0.942458842	0.9534852
400	0.912255307	0.912255307	0.944207276	0.95512056
410	0.91673845	0.91673845	0.94658986	0.9574646
420	0.915632712	0.915632712	0.945978882	0.956887
430	0.896910357	0.896910357	0.936015914	0.9470535
440	0.918285187	0.918285187	0.947371125	0.95827204
450	0.912107479	0.912107479	0.944086077	0.9550432
460	0.910371464	0.910371464	0.943179345	0.95413387
470	0.916899131	0.916899131	0.946612842	0.9575485
480	0.91547997	0.91547997	0.945872569	0.9568072
490	0.916034063	0.916034063	0.946193169	0.95709664
500	0.922229353	0.922229353	0.949507464	0.96032774
500	0.922229353	0.922229353	0.949507464	0.96032774
510	0.917831814	0.917831814	0.947136013	0.95803535
520	0.927153554	0.927153554	0.952070428	0.9628881
530	0.90384834	0.90384834	0.939656151	0.95070934
540	0.935473435	0.935473435	0.9564833	0.9671987
550	0.89590262	0.89590262	0.935359924	0.9465214
560	0.923562314	0.923562314	0.950171139	0.9610215
570	0.928037264	0.928037264	0.952595507	0.96334696
580	0.918513074	0.918513074	0.94749097	0.9583909
590	0.928540751	0.928540751	0.952801769	0.96360815
600	0.923064608	0.923064608	0.949885566	0.96076256
610	0.912502229	0.912502229	0.94425547	0.9552498
620	0.928167865	0.928167865	0.952576371	0.96341467
630	0.917721263	0.917721263	0.947071888	0.95797765
640	0.931183209	0.931183209	0.954165993	0.96497834
650	0.917714535	0.917714535	0.947017778	0.95797414
660	0.92481838	0.92481838	0.950757645	0.9616748
670	0.924264137	0.924264137	0.950487859	0.96138656
680	0.895482451	0.895482451	0.935046092	0.9462994
690	0.905413543	0.905413543	0.940360672	0.95153224
700	0.90535547	0.90535547	0.940342607	0.9515017
710	0.916297913	0.916297913	0.94616545	0.95723456
720	0.918863378	0.918863378	0.947554041	0.9585736
730	0.914272252	0.914272252	0.945116101	0.95617586
740	0.922144569	0.922144569	0.949269856	0.9602836
750	0.922072047	0.922072047	0.949235204	0.96024585
760	0.932525661	0.932525661	0.954755229	0.96567374
770	0.91289622	0.91289622	0.944380982	0.9554561
780	0.919817191	0.919817191	0.947993839	0.95907104
790	0.913159259	0.913159259	0.944464391	0.9555937
800	0.921453156	0.921453156	0.948868182	0.9599235
810	0.928730327	0.928730327	0.952667608	0.96370655
820	0.91809957	0.91809957	0.947062935	0.9581751
830	0.904623466	0.904623466	0.939855442	0.951117
840	0.919637132	0.919637132	0.94786932	0.95897716
850	0.893168808	0.893168808	0.933623569	0.94507605
860	0.900347221	0.900347221	0.937533216	0.9488663
870	0.921991102	0.921991102	0.949091555	0.9602037
880	0.91266753	0.91266753	0.944054803	0.9553364
890	0.90946778	0.90946778	0.942373638	0.9536602
900	0.904211002	0.904211002	0.939601446	0.9509001
910	0.908836965	0.908836965	0.942030779	0.9533294
920	0.910771051	0.910771051	0.94309452	0.95434326
930	0.917786088	0.917786088	0.946765303	0.9580115
940	0.928725318	0.928725318	0.952574405	0.96370393
950	0.910628702	0.910628702	0.94294994	0.95426863
960	0.905708911	0.905708911	0.94025038	0.9516874
970	0.937014223	0.937014223	0.956954544	0.967995
980	0.926655694	0.926655694	0.951427851	0.96262956
990	0.913900322	0.913900322	0.944669078	0.9559814
1000	0.913041883	0.913041883	0.944250829	0.9555322

Parameter: Heat Index

Epoch	Loss	Total MSE	Total MAE	RMSE
10	0.103120094	0.103120094	0.248814477	0.32112315
20	0.084978191	0.084978191	0.229556653	0.2915102
30	0.06943764	0.06943764	0.203584384	0.26351023
40	0.057763034	0.057763034	0.183960326	0.2403394
50	0.050580059	0.050580059	0.164022599	0.2249001
60	0.044708983	0.044708983	0.149433493	0.21144499
70	0.040005201	0.040005201	0.139304906	0.200013
80	0.036778816	0.036778816	0.132098731	0.19177805
90	0.035177766	0.035177766	0.127156225	0.18755737
100	0.033222886	0.033222886	0.122322589	0.18227145
110	0.032257734	0.032257734	0.120307005	0.17960438
120	0.033654003	0.033654003	0.122363799	0.18345028
130	0.032714614	0.032714614	0.121188353	0.18087181
140	0.031709725	0.031709725	0.121694576	0.17807224
150	0.032517842	0.032517842	0.121917993	0.18032706
160	0.032176061	0.032176061	0.121360193	0.17937687
170	0.03223775	0.03223775	0.121054956	0.17954876
180	0.031979279	0.031979279	0.120596212	0.17882752
190	0.032470174	0.032470174	0.120317779	0.18019482
200	0.031911328	0.031911328	0.119536988	0.17863742
210	0.031502352	0.031502352	0.118683135	0.17748901
220	0.031237932	0.031237932	0.117969356	0.17674255
230	0.031151062	0.031151062	0.117619102	0.17649664
240	0.030483695	0.030483695	0.116098704	0.1745958
250	0.0304543	0.0304543	0.115828767	0.1745116
260	0.029684551	0.029684551	0.115138455	0.17229205
270	0.02985188	0.02985188	0.114715361	0.17277697
280	0.030088447	0.030088447	0.1139999	0.17346022
290	0.028921247	0.028921247	0.11312225	0.17006248
300	0.028836136	0.028836136	0.112406919	0.16981205
310	0.028762825	0.028762825	0.11180058	0.16959608
320	0.028566373	0.028566373	0.111061737	0.16901591
330	0.028719243	0.028719243	0.110369047	0.16946754
340	0.028469881	0.028469881	0.110006616	0.16873018
350	0.028597838	0.028597838	0.109637436	0.16910896
360	0.028211299	0.028211299	0.108937973	0.1679622
370	0.027739428	0.027739428	0.108080316	0.16655159
380	0.028063962	0.028063962	0.107752577	0.16752303
390	0.027353151	0.027353151	0.106959323	0.16538787
400	0.027384716	0.027384716	0.106438282	0.16548328
410	0.027563575	0.027563575	0.106565167	0.1660228
420	0.026931913	0.026931913	0.105432423	0.16410945
430	0.027111646	0.027111646	0.105569628	0.16465615
440	0.027266617	0.027266617	0.104972747	0.16512607
450	0.026601021	0.026601021	0.104248157	0.16309819
460	0.026697475	0.026697475	0.103780249	0.16339362
470	0.027107845	0.027107845	0.103847782	0.1646446
480	0.025954129	0.025954129	0.102531885	0.16110285
490	0.026308165	0.026308165	0.102309161	0.16219792
500	0.026774279	0.026774279	0.102759331	0.16362847
500	0.026774279	0.026774279	0.102759331	0.16362847
510	0.026040624	0.026040624	0.101577422	0.16137108
520	0.025725716	0.025725716	0.101099408	0.16039237
530	0.02607291	0.02607291	0.100860084	0.16147108
540	0.025842859	0.025842859	0.100449676	0.16075715
550	0.026117947	0.026117947	0.100722436	0.16161048
560	0.026093517	0.026093517	0.100474004	0.16153488
570	0.025907436	0.025907436	0.099775235	0.16095787
580	0.025314632	0.025314632	0.099024996	0.15910573
590	0.025058975	0.025058975	0.098702129	0.15830027
600	0.025159265	0.025159265	0.098561835	0.15861672
610	0.025673563	0.025673563	0.098589013	0.16022971
620	0.025739342	0.025739342	0.098466394	0.16043484
630	0.025102304	0.025102304	0.097131202	0.15843707
640	0.02514133	0.02514133	0.097579152	0.15856017
650	0.025705223	0.025705223	0.097783438	0.16032848
660	0.024754913	0.024754913	0.096145103	0.15733694
670	0.024552924	0.024552924	0.09614579	0.15669374
680	0.025143863	0.025143863	0.096775861	0.15856816
690	0.024273925	0.024273925	0.095058322	0.15580091
700	0.025128947	0.025128947	0.096028928	0.15852112
710	0.026129118	0.026129118	0.098061271	0.16164503
720	0.024222566	0.024222566	0.094568793	0.155636
730	0.02442989	0.02442989	0.094323231	0.15630063
740	0.024839206	0.024839206	0.094772097	0.15760459
750	0.024141264	0.024141264	0.09371029	0.1553746
760	0.024330862	0.024330862	0.093916215	0.15598354
770	0.024228368	0.024228368	0.093498575	0.15565464
780	0.023946319	0.023946319	0.093096373	0.15474598
790	0.023663253	0.023663253	0.092987138	0.15382865
800	0.023972314	0.023972314	0.092640815	0.15482995
810	0.02384801	0.02384801	0.09215768	0.154428
820	0.023471078	0.023471078	0.092484278	0.15320274
830	0.02355403	0.02355403	0.09180348	0.15347321
840	0.023264223	0.023264223	0.091440998	0.15252614
850	0.023818818	0.023818818	0.091568102	0.15433347
860	0.023597735	0.023597735	0.091288384	0.15361553
870	0.023699791	0.023699791	0.091033609	0.15394737
880	0.023531111	0.023531111	0.090594208	0.15339854
890	0.023440173	0.023440173	0.090421533	0.15310183
900	0.023765574	0.023765574	0.09059552	0.15416086
910	0.023148367	0.023148367	0.090608986	0.15214586
920	0.023286586	0.023286586	0.089877738	0.15259944
930	0.02338884	0.02338884	0.090202476	0.1529341
940	0.022928559	0.022928559	0.090326823	0.15142179
950	0.022701502	0.022701502	0.089909476	0.15067019
960	0.023042564	0.023042564	0.089105496	0.15179777
970	0.023535562	0.023535562	0.089530988	0.15341304
980	0.022700371	0.022700371	0.089300952	0.15066643
990	0.023105978	0.023105978	0.088634982	0.1520065
1000	0.02256223	0.02256223	0.089110706	0.1502073

Appendix 12: Evaluation Results of SISO-LSTM variance for Weather Station Data

The same MISO-LSTM optimal model configurations and controls are utilised within this LSTM-SISO analysis, such as; barometer: config1-Adam, temperature: config5-Adam, wind direction: config5-SGD, etc. Evaluation results of these models for each parameter are given in the following tables.

Parameter: Barometer

Epoch	Loss	Total MSE	Total MAE	Total RMSE
10	0.189322228	0.189322228	0.253653132	0.435111742
20	0.185883395	0.185883395	0.243289064	0.431141966
30	0.185217349	0.185217349	0.242114273	0.430368852
40	0.184870602	0.184870602	0.240164884	0.429965815
50	0.183852257	0.183852257	0.234834608	0.428779963
60	0.183751104	0.183751104	0.234317912	0.428661993
70	0.183539215	0.183539215	0.232944652	0.42841477
80	0.183160323	0.183160323	0.229442155	0.427972339
90	0.184773325	0.184773325	0.241613974	0.429852678
100	0.183811043	0.183811043	0.233760983	0.428731901
110	0.183484323	0.183484323	0.233438502	0.428350701
120	0.182893887	0.182893887	0.229050855	0.427660949
130	0.183328021	0.183328021	0.232242415	0.428168216
140	0.183533241	0.183533241	0.232537974	0.428407798
150	0.183190769	0.183190769	0.232937403	0.428007907
160	0.183076434	0.183076434	0.230328572	0.42787432
170	0.183691284	0.183691284	0.230740969	0.428592212
180	0.183475744	0.183475744	0.230247213	0.428340687
190	0.185519138	0.185519138	0.241297305	0.430719326
200	0.182832389	0.182832389	0.229418313	0.427589042
210	0.183160545	0.183160545	0.22908875	0.427972599
220	0.183056504	0.183056504	0.228955959	0.42785103
230	0.183157784	0.183157784	0.231752581	0.427969373
240	0.182857603	0.182857603	0.231447204	0.427618525
250	0.182672697	0.182672697	0.229121545	0.427402266
260	0.18283724	0.18283724	0.228700585	0.427594715
270	0.182574441	0.182574441	0.227886634	0.427287305
280	0.182685827	0.182685827	0.227136334	0.427417626
290	0.182388832	0.182388832	0.225255307	0.427070055
300	0.182479781	0.182479781	0.225977934	0.427176522

Parameter: Pressure

Epoch	Loss	Total MSE	Total MAE	Total RMSE
10	0.188956253	0.188956253	0.252938722	0.434690986
20	0.187460164	0.187460164	0.249002369	0.432966701
30	0.185977771	0.185977771	0.2448351	0.431251401
40	0.184505918	0.184505918	0.238437585	0.429541521
50	0.184739505	0.184739505	0.239204526	0.429813338
60	0.184307536	0.184307536	0.237582325	0.429310536
70	0.184283835	0.184283835	0.23624328	0.429282931
80	0.184205946	0.184205946	0.237204246	0.429192202
90	0.182964698	0.182964698	0.230713725	0.42774373
100	0.183413957	0.183413957	0.233436787	0.428268557
110	0.182971494	0.182971494	0.228834084	0.427751673

120	0.183780585	0.183780585	0.235213868	0.428696379
130	0.182771762	0.182771762	0.230337789	0.427518142
140	0.183374939	0.183374939	0.236263018	0.428223002
150	0.182394047	0.182394047	0.227592558	0.427076161
160	0.182364318	0.182364318	0.22622939	0.427041354
170	0.182352824	0.182352824	0.226544234	0.427027896
180	0.182329364	0.182329364	0.227140549	0.427000426
190	0.183077093	0.183077093	0.234413926	0.427875091
200	0.182587428	0.182587428	0.228488392	0.427302502
210	0.182383907	0.182383907	0.227612735	0.427064289
220	0.182350946	0.182350946	0.227595174	0.427025697
230	0.182470144	0.182470144	0.229046262	0.427165242
240	0.182485037	0.182485037	0.228429863	0.427182674
250	0.182533881	0.182533881	0.22959962	0.42723984
260	0.182363238	0.182363238	0.228240483	0.42704009
270	0.182223182	0.182223182	0.225588988	0.426876073
280	0.182318112	0.182318112	0.226319119	0.42698725
290	0.18259163	0.18259163	0.228478851	0.427307419
300	0.18246659	0.18246659	0.227873268	0.427161082

Parameter: Temperature

Epoch	Loss	Total MSE	Total MAE	Total RMSE
10	0.237543993	0.237543993	0.297102902	0.487384851
20	0.233982241	0.233982241	0.279799471	0.483717109
30	0.232254164	0.232254164	0.26952706	0.481927551
40	0.231829274	0.231829274	0.265610543	0.481486525
50	0.231204352	0.231204352	0.262441127	0.480837137
60	0.23141607	0.23141607	0.266022293	0.481057241
70	0.231083682	0.231083682	0.269661163	0.480711641
80	0.231465935	0.231465935	0.264082528	0.481109067
90	0.232015803	0.232015803	0.27562689	0.481680188
100	0.232597793	0.232597793	0.268871612	0.482283934
110	0.236240997	0.236240997	0.277762431	0.486046291
120	0.2319925	0.2319925	0.270721664	0.481655998
130	0.231766064	0.231766064	0.268548056	0.481420881
140	0.232337369	0.232337369	0.271173117	0.482013868
150	0.231897922	0.231897922	0.271925395	0.481557808
160	0.232387875	0.232387875	0.265302171	0.482066256
170	0.233132351	0.233132351	0.270276376	0.48283781
180	0.232434086	0.232434086	0.266059912	0.482114183
190	0.232120706	0.232120706	0.267250644	0.481789068
200	0.232145789	0.232145789	0.26769992	0.481815098
210	0.232453186	0.232453186	0.269836836	0.482133992
220	0.232718833	0.232718833	0.269681152	0.482409404
230	0.233451513	0.233451513	0.26891516	0.483168204
240	0.233199505	0.233199505	0.269338483	0.482907346
250	0.232293384	0.232293384	0.268105176	0.481968239
260	0.234480451	0.234480451	0.275967871	0.484231816
270	0.234717998	0.234717998	0.27809094	0.484477035
280	0.23506069	0.23506069	0.281968211	0.484830579
290	0.23476916	0.23476916	0.284297417	0.484529834
300	0.234697276	0.234697276	0.280603231	0.484455649

Parameter: Humidity

Epoch	Loss	Total MSE	Total MAE	Total RMSE
10	0.230880143	0.230880143	0.279789021	0.480499889
20	0.229677666	0.229677666	0.280944075	0.479246978
30	0.227605674	0.227605674	0.26584615	0.477080365
40	0.227312026	0.227312026	0.263423089	0.47677251

50	0.228557727	0.228557727	0.274792609	0.478077114
60	0.227434835	0.227434835	0.266483594	0.476901284
70	0.228331184	0.228331184	0.274623099	0.477840124
80	0.227977168	0.227977168	0.267241956	0.477469547
90	0.228428217	0.228428217	0.272196087	0.477941646
100	0.229628682	0.229628682	0.280709399	0.47919587
110	0.230989785	0.230989785	0.28960577	0.480613967
120	0.2315282	0.2315282	0.292721621	0.481173773
130	0.230148127	0.230148127	0.28156073	0.47973756
140	0.228678785	0.228678785	0.279704983	0.478203706
150	0.231442974	0.231442974	0.287491769	0.481085205
160	0.232783083	0.232783083	0.297004119	0.482475992
170	0.234031726	0.234031726	0.307085871	0.483768257
180	0.238877518	0.238877518	0.325233657	0.488750978
190	0.232814257	0.232814257	0.306415171	0.482508298
200	0.244486668	0.244486668	0.333217212	0.494455931
210	0.250205165	0.250205165	0.358262011	0.500205122
220	0.260835514	0.260835514	0.379819742	0.510720583
230	0.267548016	0.267548016	0.392265111	0.517250438
240	0.260554823	0.260554823	0.37989251	0.51044571
250	0.266261958	0.266261958	0.391330651	0.516005774
260	0.262357931	0.262357931	0.384352969	0.512208875
270	0.258841379	0.258841379	0.36899195	0.508764561
280	0.274239429	0.274239429	0.403607105	0.523678746
290	0.26391597	0.26391597	0.385588603	0.513727525
300	0.263275084	0.263275084	0.383773148	0.513103385

Parameter: Wind Speed

Epoch	Loss	Total MSE	Total MAE	Total RMSE
10	0.249683342	0.249683342	0.351123389	0.49968324
20	0.239742867	0.239742867	0.346742487	0.48963544
30	0.239745032	0.239745032	0.336405312	0.48963765
40	0.237223203	0.237223203	0.334010982	0.48705565
50	0.237174219	0.237174219	0.338607592	0.48700536
60	0.23809194	0.23809194	0.340929092	0.48794666
70	0.241903746	0.241903746	0.34245275	0.49183711
80	0.243690842	0.243690842	0.341261153	0.49365053
90	0.243911919	0.243911919	0.349228904	0.4938744
100	0.254751127	0.254751127	0.358186027	0.50472877
110	0.247474098	0.247474098	0.348617777	0.49746769
120	0.245561897	0.245561897	0.345305089	0.49554202
130	0.246685981	0.246685981	0.350514213	0.49667492
140	0.248486536	0.248486536	0.354104737	0.49848424
150	0.249573365	0.249573365	0.353328271	0.49957318
160	0.247490865	0.247490865	0.349925552	0.49748454
170	0.259402071	0.259402071	0.371654301	0.5093153
180	0.253432347	0.253432347	0.365140489	0.50342065
190	0.250507952	0.250507952	0.36114169	0.50050769
200	0.255403648	0.255403648	0.37231914	0.50537476
210	0.261536919	0.261536919	0.37639449	0.5114068
220	0.253953746	0.253953746	0.362579166	0.50393824
230	0.259741299	0.259741299	0.374077933	0.50964821
240	0.257121523	0.257121523	0.371407604	0.50707152
250	0.25507509	0.25507509	0.367052882	0.50504959
260	0.256580133	0.256580133	0.369993631	0.5065374
270	0.254362898	0.254362898	0.369603236	0.50434403
280	0.253406057	0.253406057	0.363907575	0.50339453
290	0.252883354	0.252883354	0.361820106	0.50287509
300	0.253739243	0.253739243	0.362813945	0.50372537

Parameter: Wind direction

Epoch	Loss	Total MSE	Total MAE	Total RMSE
10	0.444765006	0.444765006	0.639559642	0.666907045
20	0.423490531	0.423490531	0.576535459	0.650761501
30	0.41857029	0.41857029	0.568904266	0.646970084
40	0.414498465	0.414498465	0.563035747	0.643815552
50	0.410401789	0.410401789	0.557374823	0.640626092
60	0.406926491	0.406926491	0.552218893	0.637907901
70	0.404015067	0.404015067	0.54750508	0.635621795
80	0.400711201	0.400711201	0.543681475	0.633017536
90	0.398002308	0.398002308	0.539919025	0.630874241
100	0.395789375	0.395789375	0.535769884	0.629117934
110	0.39314028	0.39314028	0.53234666	0.627008995
120	0.391045812	0.391045812	0.52835845	0.625336559
130	0.389192609	0.389192609	0.525542258	0.623853034
140	0.387803548	0.387803548	0.523515737	0.622738748
150	0.385833931	0.385833931	0.519808066	0.62115532
160	0.3849833	0.3849833	0.517189604	0.620470225
170	0.38364197	0.38364197	0.515149704	0.619388384
180	0.382464825	0.382464825	0.512117726	0.618437406
190	0.381666102	0.381666102	0.510376522	0.61779131
200	0.381503962	0.381503962	0.510299755	0.61766007
210	0.380373095	0.380373095	0.507747033	0.616743946
220	0.379759047	0.379759047	0.507122108	0.61624593
230	0.379760393	0.379760393	0.505678654	0.616247023
240	0.379075019	0.379075019	0.504655162	0.615690684
250	0.378578976	0.378578976	0.503419235	0.615287718
260	0.378249288	0.378249288	0.502651044	0.615019746
270	0.377947245	0.377947245	0.501655604	0.614774141
280	0.377765906	0.377765906	0.501267421	0.61462664
290	0.377628138	0.377628138	0.501057392	0.614514555
300	0.377385136	0.377385136	0.500781559	0.614316804
310	0.376991167	0.376991167	0.49945704	0.613996064
320	0.376874787	0.376874787	0.498525364	0.613901284
330	0.376660104	0.376660104	0.498248137	0.613726408
340	0.376657989	0.376657989	0.497615069	0.613724685
350	0.37637178	0.37637178	0.497672751	0.613491467
360	0.376275147	0.376275147	0.497348119	0.613412705
370	0.375996316	0.375996316	0.496672289	0.613185385
380	0.376195352	0.376195352	0.497258452	0.61334766
390	0.375676137	0.375676137	0.495271322	0.612924251
400	0.375505662	0.375505662	0.495418503	0.612785168
410	0.375364496	0.375364496	0.494996171	0.612669973
420	0.375234162	0.375234162	0.495139316	0.612563599
430	0.375105784	0.375105784	0.494632461	0.612458802
440	0.374979394	0.374979394	0.495053633	0.612355611
450	0.375040635	0.375040635	0.494651297	0.612405613
460	0.374778939	0.374778939	0.4945909	0.612191914
470	0.374873097	0.374873097	0.495126031	0.612268811
480	0.374658537	0.374658537	0.493544666	0.612093569
490	0.374518704	0.374518704	0.494013599	0.611979333
500	0.374393404	0.374393404	0.49350035	0.611876951
510	0.374433918	0.374433918	0.493718907	0.611910057
520	0.374362557	0.374362557	0.492419679	0.611851745
530	0.374202358	0.374202358	0.493574829	0.611720817
540	0.374276056	0.374276056	0.493041417	0.611781052
550	0.373994377	0.373994377	0.492685321	0.611550796
560	0.373935178	0.373935178	0.492009094	0.611502395
570	0.374045516	0.374045516	0.492519645	0.611592606
580	0.373862374	0.373862374	0.492198032	0.611442863
590	0.373828411	0.373828411	0.492040911	0.611415089
600	0.373903687	0.373903687	0.492341699	0.611476645
610	0.374099713	0.374099713	0.491989393	0.611636913
620	0.373698977	0.373698977	0.491896965	0.611309232
630	0.373672304	0.373672304	0.491296871	0.611287415
640	0.373882171	0.373882171	0.491842138	0.611459051
650	0.373465931	0.373465931	0.491471708	0.61111859
660	0.373498228	0.373498228	0.491725199	0.611145014
670	0.373360114	0.373360114	0.491201757	0.611032008
680	0.373306332	0.373306332	0.491320234	0.610987997
690	0.373371523	0.373371523	0.491097823	0.611041343
700	0.37327896	0.37327896	0.490245378	0.610965596
710	0.373112505	0.373112505	0.490292337	0.610829359
720	0.373081598	0.373081598	0.490595996	0.610804059
730	0.373353521	0.373353521	0.491129491	0.611026613
740	0.373151588	0.373151588	0.489998997	0.610861349
750	0.373033695	0.373033695	0.489968997	0.610764845
760	0.37295891	0.37295891	0.489717038	0.610703619
770	0.372806977	0.372806977	0.489785942	0.610579215
780	0.372777774	0.372777774	0.489963475	0.6105553
790	0.372859688	0.372859688	0.489457731	0.610622378
800	0.372739823	0.372739823	0.48921286	0.61052422
810	0.372613254	0.372613254	0.489502526	0.610420555
820	0.372561943	0.372561943	0.48904269	0.610378525
830	0.372525325	0.372525325	0.489503426	0.610348527
840	0.372478413	0.372478413	0.488886582	0.610310096
850	0.372619586	0.372619586	0.489421727	0.610425742
860	0.372547069	0.372547069	0.489243619	0.61036634
870	0.372418891	0.372418891	0.488847934	0.61026133
880	0.372508933	0.372508933	0.488822725	0.610335099
890	0.37232009	0.37232009	0.488878856	0.610180375
900	0.372207615	0.372207615	0.489221348	0.610088202
910	0.372349564	0.372349564	0.488500239	0.610204526
920	0.372013669	0.372013669	0.488359087	0.609929233
930	0.37194135	0.37194135	0.488200781	0.609869945
940	0.371881631	0.371881631	0.488221608	0.609820983
950	0.371890306	0.371890306	0.488323096	0.609828096
960	0.371861612	0.371861612	0.488677879	0.609804569
970	0.371935451	0.371935451	0.488073108	0.609865109
980	0.371774892	0.371774892	0.487613982	0.60973346
990	0.371728207	0.371728207	0.48823378	0.609695175
1000	0.371560259	0.371560259	0.487503175	0.609557429

Parameter: Rain rate

Epoch	Loss	Total MSE	Total MAE	Total RMSE
10	0.097492988	0.097492988	0.161976796	0.312238671
20	0.095716642	0.095716642	0.141606634	0.309381063
30	0.095364807	0.095364807	0.133973208	0.308811929
40	0.095247597	0.095247597	0.129815278	0.308622094
50	0.095199992	0.095199992	0.127137617	0.308544959
60	0.095179598	0.095179598	0.125250952	0.308511908
70	0.095171462	0.095171462	0.123839308	0.308498723
80	0.095169354	0.095169354	0.122731833	0.308495307
90	0.095170384	0.095170384	0.121843758	0.308496976
100	0.095173078	0.095173078	0.121107177	0.308501342
110	0.095176639	0.095176639	0.120487247	0.308507114
120	0.095180661	0.095180661	0.119952722	0.308513631
130	0.09518483	0.09518483	0.119492314	0.308520388
140	0.095189025	0.095189025	0.119088559	0.308527187
150	0.095193157	0.095193157	0.118731343	0.308533883
160	0.095197162	0.095197162	0.118413721	0.308540374
170	0.095201003	0.095201003	0.11813001	0.308546598
180	0.095204736	0.095204736	0.117870475	0.308552647
190	0.095208317	0.095208317	0.117633996	0.30855845
200	0.095211746	0.095211746	0.117417668	0.308564007
210	0.095214936	0.095214936	0.117224253	0.308569176
220	0.095218089	0.095218089	0.117039576	0.308574284
230	0.095221057	0.095221057	0.116871061	0.308579094
240	0.095223875	0.095223875	0.116715655	0.308583659
250	0.095226497	0.095226497	0.116574601	0.308587908
260	0.095229032	0.095229032	0.11644119	0.308592015
270	0.095231479	0.095231479	0.116315184	0.30859598
280	0.095233822	0.095233822	0.116196792	0.308599777
290	0.095236041	0.095236041	0.116086617	0.308603372
300	0.095238216	0.095238216	0.115980559	0.308606895
310	0.095240217	0.095240217	0.11588433	0.308610138
320	0.095242171	0.095242171	0.115791674	0.308613304
330	0.095243996	0.095243996	0.115706294	0.30861626
340	0.095245796	0.095245796	0.115623092	0.308619177
350	0.095247462	0.095247462	0.115546984	0.308621876
360	0.095249112	0.095249112	0.11547235	0.308624549
370	0.095250666	0.095250666	0.115402827	0.308627066
380	0.095252216	0.095252216	0.115334127	0.308629577
390	0.095253579	0.095253579	0.115274264	0.308631785
400	0.095254961	0.095254961	0.115213993	0.308634024

Parameter: Rain

Epoch	Loss	Total MSE	Total MAE	Total RMSE
10	0.097914038	0.097914038	0.166611726	0.312912188
20	0.095754588	0.095754588	0.143671765	0.309442382
30	0.09525621	0.09525621	0.134903178	0.308636048
40	0.095058482	0.095058482	0.1300577	0.308315556
50	0.094959708	0.094959708	0.126911072	0.308155331
60	0.094903763	0.094903763	0.124677574	0.308064543
70	0.094869539	0.094869539	0.123003233	0.308008991
80	0.094847239	0.094847239	0.121684452	0.30797279
90	0.094832339	0.094832339	0.120628214	0.307948598
100	0.094822003	0.094822003	0.119754415	0.307931816
110	0.094814681	0.094814681	0.11901691	0.307919926

120	0.094809346	0.094809346	0.118373848	0.307911263
130	0.094805567	0.094805567	0.117825408	0.307905127
140	0.094802852	0.094802852	0.117347155	0.307900718
150	0.094800845	0.094800845	0.11691042	0.307897459
160	0.09479947	0.09479947	0.116532156	0.307895226
170	0.094798499	0.094798499	0.116181879	0.307893649
180	0.094797886	0.094797886	0.115874158	0.307892653
190	0.094797508	0.094797508	0.115579984	0.30789204
200	0.094797344	0.094797344	0.115317102	0.307891773
210	0.094797334	0.094797334	0.115086304	0.307891758
220	0.094797443	0.094797443	0.114864745	0.307891933
230	0.094797646	0.094797646	0.11466144	0.307892263
240	0.094797921	0.094797921	0.114472825	0.307892711
250	0.094798251	0.094798251	0.114297963	0.307893246
260	0.094798624	0.094798624	0.114134923	0.307893851
270	0.094799033	0.094799033	0.113981332	0.307894517
280	0.094799456	0.094799456	0.113840944	0.307895204
290	0.094799903	0.094799903	0.113706818	0.307895928
300	0.094800367	0.094800367	0.113579385	0.307896682
310	0.094800792	0.094800792	0.113471209	0.307897372
320	0.094801274	0.094801274	0.113356211	0.307898155
330	0.094801752	0.094801752	0.113248592	0.307898932
340	0.094802231	0.094802231	0.113146713	0.307899709
350	0.094802709	0.094802709	0.113049795	0.307900485
360	0.094803165	0.094803165	0.112961238	0.307901227
370	0.094803645	0.094803645	0.112871767	0.307902005
380	0.094804094	0.094804094	0.112790911	0.307902735
390	0.094804522	0.094804522	0.112716519	0.307903429
400	0.094804959	0.094804959	0.112642702	0.307904139

Parameter: Dew Point

Epoch	Loss	Total MSE	Total MAE	Total RMSE
10	0.152605714	0.152605714	0.19013514	0.390647813
20	0.152107771	0.152107771	0.176269643	0.390009963
30	0.152693005	0.152693005	0.183754074	0.390759524
40	0.152618194	0.152618194	0.173572083	0.390663786
50	0.15501389	0.15501389	0.168195478	0.393718033
60	0.155182282	0.155182282	0.165660158	0.393931824
70	0.153150239	0.153150239	0.16443302	0.391344144
80	0.151483955	0.151483955	0.170464348	0.389209398
90	0.151123974	0.151123974	0.16237598	0.388746671
100	0.150823129	0.150823129	0.163016644	0.388359536
110	0.150715861	0.150715861	0.171364284	0.388221407
120	0.150981259	0.150981259	0.16400496	0.388563069
130	0.150991594	0.150991594	0.167321734	0.388576368
140	0.150715849	0.150715849	0.164376835	0.388221391
150	0.151384125	0.151384125	0.163549166	0.389081129
160	0.150921206	0.150921206	0.168527095	0.388485786
170	0.151465912	0.151465912	0.165454018	0.389186218
180	0.151492741	0.151492741	0.167909241	0.389220684
190	0.150858301	0.150858301	0.164509429	0.388404816
200	0.15201214	0.15201214	0.180161488	0.389887343
210	0.151042516	0.151042516	0.163236282	0.388641887
220	0.1512299	0.1512299	0.16467396	0.388882887
230	0.151826775	0.151826775	0.164088787	0.389649554
240	0.153729293	0.153729293	0.164999117	0.392083273
250	0.151626586	0.151626586	0.17425603	0.389392587
260	0.152557052	0.152557052	0.165212068	0.390585524
270	0.154135467	0.154135467	0.176122622	0.3926009
280	0.15272009	0.15272009	0.168874653	0.390794179
290	0.154079252	0.154079252	0.16761233	0.3925293
300	0.152535796	0.152535796	0.166526148	0.390558314

Parameter: Heat index

Epoch	Loss	Total MSE	Total MAE	Total RMSE
10	0.255212246	0.255212246	0.255212246	0.505185358
20	0.253026069	0.253026069	0.253026069	0.503016967
30	0.25192248	0.25192248	0.25192248	0.501918798
40	0.251057567	0.251057567	0.251057567	0.501056451
50	0.253393284	0.253393284	0.253393284	0.503381847
60	0.251413024	0.251413024	0.251413024	0.501411033
70	0.251592785	0.251592785	0.251592785	0.501590256
80	0.251081782	0.251081782	0.251081782	0.501080614
90	0.251389701	0.251389701	0.251389701	0.501387775
100	0.252221254	0.252221254	0.252221254	0.502216342
110	0.251712719	0.251712719	0.251712719	0.501709796
120	0.252418106	0.252418106	0.252418106	0.502412287
130	0.252084571	0.252084571	0.252084571	0.502080243
140	0.252157217	0.252157217	0.252157217	0.502152584
150	0.253340411	0.253340411	0.253340411	0.503329326
160	0.253314555	0.253314555	0.253314555	0.503303641
170	0.253363568	0.253363568	0.253363568	0.50335233
180	0.253448478	0.253448478	0.253448478	0.503436667
190	0.252383381	0.252383381	0.252383381	0.502377727
200	0.253053765	0.253053765	0.253053765	0.503044496
210	0.253080448	0.253080448	0.253080448	0.503071017
220	0.252444994	0.252444994	0.252444994	0.502439045
230	0.253562062	0.253562062	0.253562062	0.503549463
240	0.252704077	0.252704077	0.252704077	0.502696804
250	0.252805422	0.252805422	0.252805422	0.502797595
260	0.252623228	0.252623228	0.252623228	0.502616383
270	0.252603619	0.252603619	0.252603619	0.502596876
280	0.252148351	0.252148351	0.252148351	0.502143755
290	0.251654976	0.251654976	0.251654976	0.501652246
300	0.2538985	0.2538985	0.2538985	0.503883419

Appendix 13: Evaluation Results of MISO-TCN variance for Weather Station Data

Similar to Appendix 5, the 'saved the best model' approach is utilised within MISO-TCN with different configurations and controls. TCN filter size 64 and activation function linear is selected to train and test different models, as shown in the following first table. The fields with the least MSE is highlighted in yellow and green colour. Then, further experiments are carried out with different configurations and controls to find the optimal model with least MSE for MISO-TCN for the chosen locations from the first table. The optimal models with Least MSE for overall experiments are highlighted in pink colour. TCN 32 linear, TCN 32 tanh, and TCN 512 tanh models have not experimented in this section here as they have shown weaker results in the MISO-TCN for weather station data as shown in Appendix 5.

Experiments with TCN Filter 64 and linear activation

No of Layers	Barometer	Pressure	Temperature	Humidity	Wind speed	Wind direction	Rain rate	Rain	Dew point	Heat Index
TCN1	0.00354015	0.005494023	0.012791453	0.011405239	0.04709761	0.126322064	0.005239517	0.006210215	0.01126207	0.011278534
TCN2	0.042442685	0.021834819	0.014268266	0.01006111	0.046393493	0.133475001	0.005197365	0.006290908	0.013388504	0.013983016
TCN3	0.04475502	0.041353253	0.015470253	0.012951975	0.04759925	0.140976274	0.005485423	0.006672506	0.012442742	0.015708846
TCN4	0.055579474	0.045103316	0.01622633	0.013287516	0.051208662	0.143728186	0.005125052	0.005979988	0.0124494	0.016473801

Experiments with TCN Filter 64 and tanh activation

No of Layers	Barometer	Pressure	Temperature	Humidity	Wind speed	Wind direction	Rain rate	Rain	Dew point	Heat Index
TCN1	0.00436578	0.005838542	0.011898229			0.1286487			0.011949166	0.011625779
TCN2				0.013091234	0.045204762					
TCN3										
TCN4							0.005447469	0.005024305		

Experiments with TCN Filter 128 and linear activation

No of Layers	Barometer	Pressure	Temperature	Humidity	Wind speed	Wind direction	Rain rate	Rain	Dew point	Heat Index
TCN1	0.002812565	0.00343222	0.011698888			0.132569564			0.011865982	0.011445478
TCN2				0.012385414	0.047236323					
TCN3										
TCN4							0.005325655	0.005436025		

Experiments with TCN Filter 128 and tanh activation

No of Layers	Barometer	Pressure	Temperature	Humidity	Wind speed	Wind direction	Rain rate	Rain	Dew point	Heat Index
TCN1	0.001802133	0.002717845	0.010855555			0.119125454			0.011665458	0.010245455
TCN2				0.013488451	0.043865656					
TCN3										
TCN4							0.005517472	0.004965657		

Experiments with TCN Filter 256 and linear activation

No of Layers	Barometer	Pressure	Temperature	Humidity	Wind speed	Wind direction	Rain rate	Rain	Dew point	Heat Index
TCN1	0.001757744	**0.002024501**	**0.009870145**			0.133209657			0.012988021	0.011924613
TCN2				0.012512791	0.055012686					
TCN3							[128]	[128]		
TCN4							0.005668297	0.005287431		

Experiments with TCN Filter 256 and tanh activation

No of Layers	Barometer	Pressure	Temperature	Humidity	Wind speed	Wind direction	Rain rate	Rain	Dew point	Heat Index
TCN1	**0.001521964**	0.003601076	0.01136774			0.115209464			0.011570406	0.010076128
TCN2				0.011837113	0.044360427					
TCN3										
TCN4							0.00594513	0.004834251		

Experiments with TCN Filter 512 and tanh activation

No of Layers	Barometer	Pressure	Temperature	Humidity	Wind speed	Wind direction	Rain rate	Rain	Dew point	Heat Index
TCN1	0.001640099	0.015594856	0.012496985	512	512	0.124141844			0.013018639	0.012358227
TCN2				0.013249137	0.04536406					
TCN3										
TCN4							0.005773957	0.004893288		

Appendix 14: Evaluation of MISO-TCN variance for Long Term Forecasting for Weather Station Data

Evaluation of MISO-TCN long-term weather forecasting is carried out in two different methods, namely TCN-WL (without loading optimal weights) and TCN-LW (load with optimal weights). The optimal weights are taken from in the MISO-TCN short-term weather forecasting. The 'save the best model' concept is utilised in each method in each timeslot for each parameter. The weather predictions for each timeslot using long-term optimal models is taken to a single file and are compared with the ground truth. The evaluation results are shown in the following tables. The overall results are shown in the last column of each table in each timeslot.

TCN-WL (Without loading optimal weights)

1 Hour

	Barometer	Pressure	Temperature	Humidity	Wind Speed	Wind Direction	Rain Rate	Rain	Dew Point	Heat Index	Overall
MSE	0.000423817	0.000558613	2.048237085	19.33102036	1.866814494	3732.787109	0.001163059	1.08E-05	18.02802277	6.774312019	378.0837708
MAE	0.014543533	0.016262714	0.699143231	2.73633194	0.952295125	40.0724411	0.009628055	0.001413302	1.478936911	1.219032526	4.720003605
RMAE	0.020586805	0.023634989	1.431166291	4.396705627	1.366314173	61.09653854	0.034103647	0.003284824	4.245942116	2.602750778	19.44437599
Explained Variance	0.996797621	0.996156454	0.901093423	0.833309591	0.65909785	0.573306084	0.058757544	3.17E-05	0.735624433	0.899322689	0.665350038

2 Hour

	Barometer	Pressure	Temperature	Humidity	Wind Speed	Wind Direction	Rain Rate	Rain	Dew Point	Heat Index	Overall
MSE	0.004428064	0.003049337	5.074848652	51.99474716	3.16159606	5616.935547	0.000916466	1.05E-05	11.7768774	15.77750301	570.4730225
MAE	0.048941761	0.0383556	1.670940518	5.834616184	1.286972165	52.77642059	0.010241257	0.000723583	2.647352457	2.870783329	6.718537331
RMAE	0.066543698	0.055220805	2.252742529	7.210738182	1.778087735	74.9462204	0.030273186	0.003241309	3.431745529	3.972090483	23.8845768
Explained Variance	0.968791664	0.977398753	0.749786973	0.549916983	0.408701122	0.355494857	0.030602753	-0.031198859	0.7962448	0.760903001	0.556663436

3 Hour

	Barometer	Pressure	Temperature	Humidity	Wind Speed	Wind Direction	Rain Rate	Rain	Dew Point	Heat Index	Overall
MSE	0.006707133	0.003592565	9.38936615	80.26189423	3.906514406	7070.062988	0.001175222	9.86E-06	15.40388584	30.21232224	720.9248047
MAE	0.058829006	0.045041122	2.484406471	7.123254776	1.393435836	63.46803284	0.010748263	0.000937563	2.94009304	4.127209663	8.165198326
RMAE	0.081897087	0.05993801	3.064207315	8.958900452	1.976490378	84.08366394	0.034281507	0.003140707	3.924778461	5.496573448	26.85004234
Explained Variance	0.951001287	0.972094655	0.537258863	0.309991241	0.261973023	0.192350745	-0.209867835	0	0.74384129	0.539179325	0.429781795

6 Hour

	Barometer	Pressure	Temperature	Humidity	Wind Speed	Wind Direction	Rain Rate	Rain	Dew Point	Heat Index	Overall
MSE	0.014785552	0.013024277	18.29678345	149.9286804	5.580564022	9046.199219	0.001100039	1.64E-05	36.80418396	52.7662468	930.9603271
MAE	0.09304437	0.086297601	3.569617271	9.93812561	1.762805462	74.72014618	0.009388261	0.001289073	4.521187782	5.935126305	10.06370163
RMAE	0.12159586	0.114123955	4.277473927	12.2445364	2.362321854	95.11151123	0.033166829	0.004052536	6.066645145	7.264038086	30.51164246
Explained Variance	0.892837226	0.902861476	0.088444233	-0.332543015	-0.050191164	-0.02477479	-0.149203062	-0.660833716	0.428342581	0.198798299	0.129373771

9 Hour

	Barometer	Pressure	Temperature	Humidity	Wind Speed	Wind Direction	Rain Rate	Rain	Dew Point	Heat Index	Overall
MSE	0.020567911	0.027455119	20.67517853	198.0704803	5.294323921	9658.273438	0.000998435	9.97E-06	45.68065643	66.65924072	999.4702148
MAE	0.110589333	0.12786366	3.70506072	11.33890247	1.712778687	80.68969727	0.009006926	0.000774964	5.435975075	6.74786377	10.987854
RMAE	0.143415168	0.165695861	4.546996593	14.07375145	2.300939798	98.27651215	0.031598028	0.003158045	6.758746624	8.164510727	31.61439896
Explained Variance	0.84443903	0.794400513	-0.035512209	-0.676677704	-0.012471676	-0.095321059	-0.056598306	-0.055481553	0.294357419	-0.02293551	0.097820479

12 Hour

	Barometer	Pressure	Temperature	Humidity	Wind Speed	Wind Direction	Rain Rate	Rain	Dew Point	Heat Index	Overall
MSE	0.03480228	0.033350196	20.7863903	227.8525848	6.301308155	10146.48242	0.000972028	1.05E-05	54.68219757	69.88866425	1052.606689
MAE	0.145681247	0.140758812	3.800368547	12.21276569	1.852321982	80.26992035	0.006797587	0.000937238	5.933532238	6.908661842	11.12717056
RMAE	0.186553687	0.182620361	4.559209347	15.09478664	2.510240555	100.7297516	0.031177357	0.003245656	7.394741058	8.359944344	32.44390106
Explained Variance	0.733329117	0.741795897	-0.033310652	-0.790013075	-0.033422351	-0.149166465	0.001620233	-0.047274351	0.168684065	-0.079478502	0.051276779

18 Hour

	Barometer	Pressure	Temperature	Humidity	Wind Speed	Wind Direction	Rain Rate	Rain	Dew Point	Heat Index	Overall
MSE	0.053502895	0.058717392	17.27202415	188.8525085	5.891963005	14777.14551	0.001070688	9.98E-06	64.50003815	53.21825027	1510.699463
MAE	0.175811559	0.185160041	3.131498098	11.53988647	1.833759189	95.67175293	0.008400062	0.00055452	6.382219315	5.681056023	12.46101093
RMAE	0.231306925	0.242316723	4.155962467	13.74236202	2.427336693	121.5612793	0.032721367	0.003159191	8.031191826	7.295084	38.86771774
Explained Variance	0.594287992	0.545465291	0.140019894	-0.5529387	-0.038070798	-0.532718062	-0.113400102	-0.041538596	-0.013898253	0.18016237	0.016737658

24 Hour

	Barometer	Pressure	Temperature	Humidity	Wind Speed	Wind Direction	Rain Rate	Rain	Dew Point	Heat Index	Overall
MSE	0.083154261	0.074229404	20.68071556	207.6312103	5.849805355	12633.76172	0.000951781	9.75E-06	69.67667389	57.99225998	1299.575684
MAE	0.222368494	0.205878139	3.581858158	11.18483162	1.861962318	88.39208221	0.010143428	0.000581386	6.947082996	5.474588871	11.78814125
RMAE	0.288364798	0.272450745	4.547605515	14.40941429	2.418637037	112.4000092	0.030850943	0.003122737	8.347255707	7.615264893	36.04962921
Explained Variance	0.372691631	0.433764696	0.029447734	-0.61262238	-0.075997949	-0.377081037	0.003142655	7.75E-07	-0.125004888	0.154587924	-0.019706488

TCN-LW (Load with optimal weights)

2 Hour

	Barometer	Pressure	Temperature	Humidity	Wind Speed	Wind Direction	Rain Rate	Rain	Dew Point	Heat Index	Overall
MSE	0.001473487	0.001575661	3.350741386	46.62782669	2.746556759	5557.623047	0.001346818	1.05E-05	8.254271507	11.43598938	563.0042725
MAE	0.028378153	0.029728372	1.30325222	5.276236057	1.18815279	53.3603363	0.012054191	0.000690347	2.115549326	2.443633795	6.575800896
RMAE	0.038386028	0.039694592	1.830502987	6.828457355	1.657273889	74.54946899	0.036699016	0.003242519	2.873024702	3.381713867	23.72771072
Explained Variance	0.988654017	0.987857401	0.83422792	0.577722192	0.471100032	0.374403596	-0.426896811	-0.052457571	0.862511396	0.825594783	0.544270718

3 Hour

	Barometer	Pressure	Temperature	Humidity	Wind Speed	Wind Direction	Rain Rate	Rain	Dew Point	Heat Index	Overall
MSE	0.003160522	0.003232682	6.38130188	69.38207245	3.737125158	6593.77832	0.001393367	1.08E-05	11.93449306	18.48752022	670.3707886
MAE	0.042463139	0.043459188	1.952229977	6.843741894	1.393076301	61.80714035	0.011515509	0.00168227	2.513658285	3.380310297	7.798926353
RMAE	0.05621852	0.056856684	2.526124001	8.329589844	1.933164597	81.20207977	0.037327833	0.003282822	3.454633474	4.299711704	25.89151955
Explained Variance	0.975972176	0.974835157	0.684772551	0.380838037	0.307893574	0.261131465	-0.470527768	-0.041828513	0.799235702	0.71827352	0.459058648

6 Hour

	Barometer	Pressure	Temperature	Humidity	Wind Speed	Wind Direction	Rain Rate	Rain	Dew Point	Heat Index	Overall
MSE	0.011437681	0.010000351	11.51352119	97.35475922	4.874496937	9313.105469	0.001483254	9.94E-06	18.27707291	27.93671036	929.4086914
MAE	0.083170295	0.076510377	2.698511362	8.470344543	1.625154853	74.73007202	0.012762412	0.001103769	3.236363983	4.1916852	9.102567673
RMAE	0.106947094	0.100001752	3.393157959	9.866214638	2.207826376	96.50443268	0.038513038	0.003152338	4.274631691	5.285514228	30.81247711
Explained Variance	0.913546622	0.921841443	0.429406464	0.037787199	0.116843462	-0.043914914	-0.573617935	-0.007850409	0.620260954	0.482316494	0.289662039

9 Hour

	Barometer	Pressure	Temperature	Humidity	Wind Speed	Wind Direction	Rain Rate	Rain	Dew Point	Heat Index	Overall
MSE	0.020350289	0.020227928	15.25052738	184.377655	5.858074188	9165.623047	0.001075203	9.80E-06	37.45243454	43.52372742	945.2125854
MAE	0.110765718	0.108781226	3.29406476	11.13470268	1.781769156	77.7646637	0.008765711	0.00061887	4.740557194	5.560070038	10.45047379
RMAE	0.142654434	0.142224923	3.905192375	13.57857323	2.420345783	95.73725891	0.032790281	0.003129931	6.119839191	6.597251415	30.74431038
Explained Variance	0.843980014	0.843306541	0.245642424	-0.671938658	0.02044785	-0.029209495	-0.085913301	1.13E-06	0.400117815	0.340500593	0.190693945

12 Hour

	Barometer	Pressure	Temperature	Humidity	Wind Speed	Wind Direction	Rain Rate	Rain	Dew Point	Heat Index	Overall
MSE	0.030770708	0.027298748	17.37869263	160.9000397	5.383164406	10287.25293	0.001823783	9.79E-06	49.7885437	57.20755768	1052.396973
MAE	0.134413332	0.126017511	3.584066391	10.14227905	1.70492661	79.62091064	0.012173633	0.00085175	5.495501995	6.344595432	10.57657604
RMAE	0.175415814	0.16522333	4.168776035	12.6846398	2.32016468	101.4260941	0.042705774	0.003128565	7.056099892	7.563567638	32.44001239
Explained Variance	0.763346732	0.788089037	0.176549435	-0.467151523	-0.004339457	-0.164786577	-0.944095016	-0.038489223	0.216169	0.135778248	0.046108007

18 Hour

	Barometer	Pressure	Temperature	Humidity	Wind Speed	Wind Direction	Rain Rate	Rain	Dew Point	Heat Index	Overall
MSE	0.053041022	0.04886033	15.79842567	180.3284302	6.409871101	10183.73145	0.001177394	1.11E-05	54.38592148	51.77476501	1049.252563
MAE	0.172588706	0.162596032	3.151162863	11.19069195	1.877619386	82.50418091	0.010427825	0.000911588	6.100488186	5.939394951	11.11100578
RMAE	0.230306372	0.221043736	3.974723339	13.42864227	2.531772375	100.9144745	0.034313172	0.003337807	7.374680996	7.195468426	32.39216995
Explained Variance	0.594231665	0.621362448	0.216314077	-0.483261466	-0.00839293	-0.14476943	-0.237253785	-0.169569254	0.204315007	0.210426867	0.080341053

24 Hour

	Barometer	Pressure	Temperature	Humidity	Wind Speed	Wind Direction	Rain Rate	Rain	Dew Point	Heat Index	Overall
MSE	0.068163186	0.068715617	16.55856705	184.592453	6.430088043	11776.50195	0.001089382	9.86E-06	63.59426498	64.31478119	1211.212646
MAE	0.191958398	0.189573511	2.923578501	10.54314804	1.918166637	87.47290039	0.008857095	0.001064806	6.832616806	6.207621098	11.62895012
RMAE	0.261080801	0.262136638	4.069221973	13.58648014	2.535761833	108.5195923	0.033005789	0.003139627	7.974601269	8.019649506	34.80247879
Explained Variance	0.484831154	0.473291993	0.196980357	-0.455725908	-0.145457029	-0.294278979	-0.148429275	-0.045829892	0.048507631	0.020472884	0.013436878

Appendix 15: Comparison of 100 Random Samples for Weather Station Data

Comparative results of 100 data samples are shown in the following graphs for weather station data. Each graph compares the proposed model prediction, WRF prediction, and the ground truth.

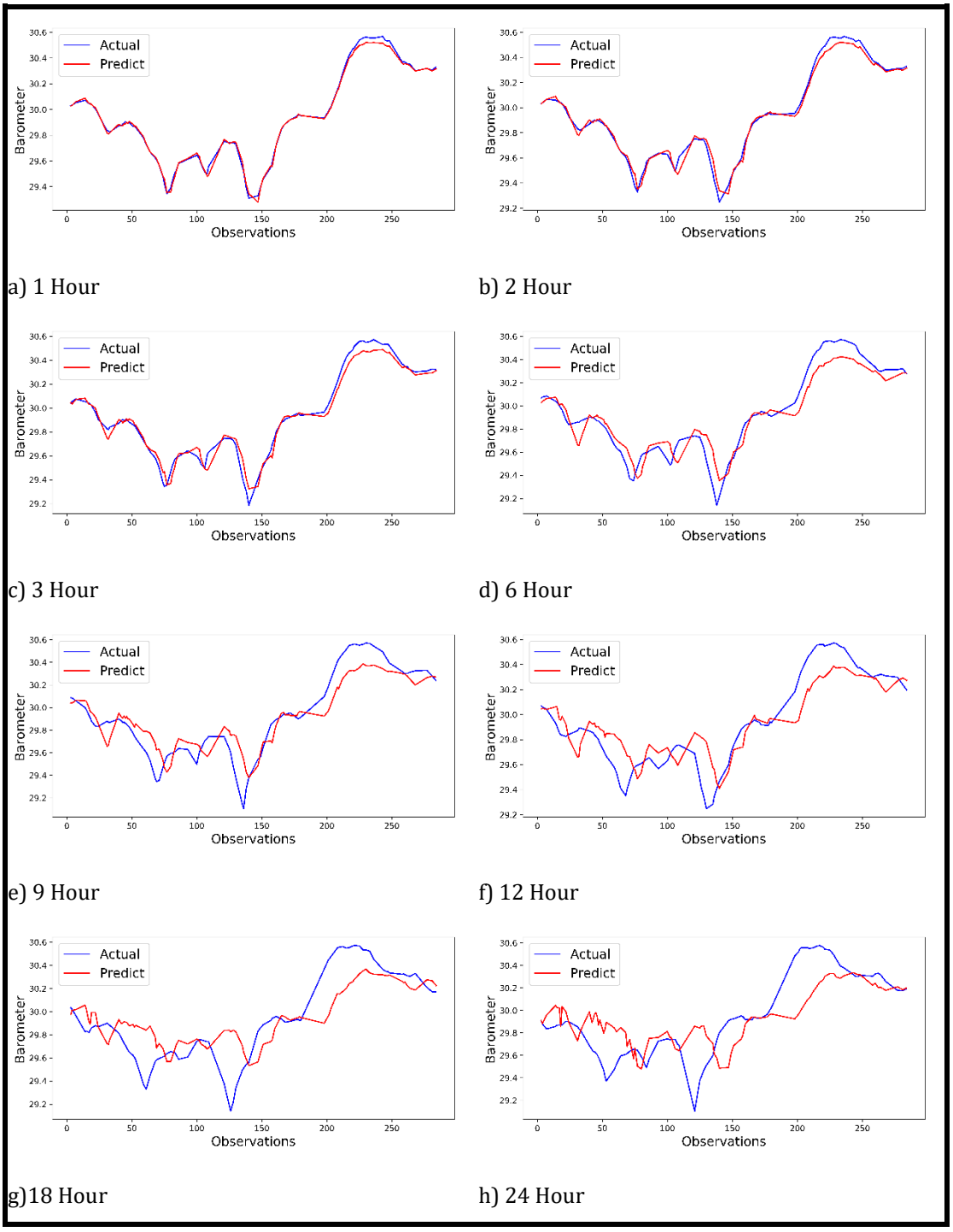

a) 1 Hour

b) 2 Hour

c) 3 Hour

d) 6 Hour

e) 9 Hour

f) 12 Hour

g)18 Hour

h) 24 Hour

i) Barometer

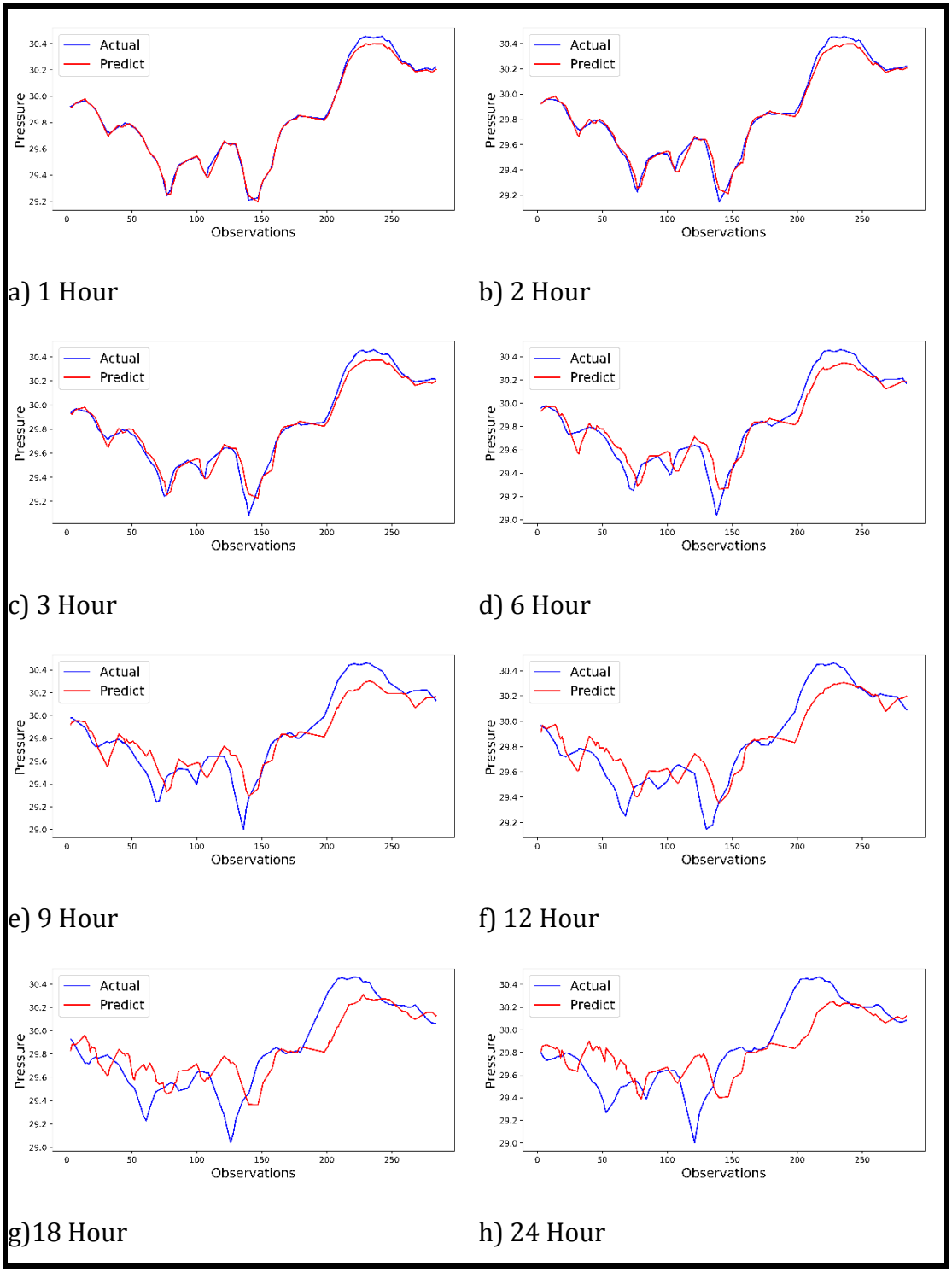

a) 1 Hour

b) 2 Hour

c) 3 Hour

d) 6 Hour

e) 9 Hour

f) 12 Hour

g)18 Hour

h) 24 Hour

ii) Pressure

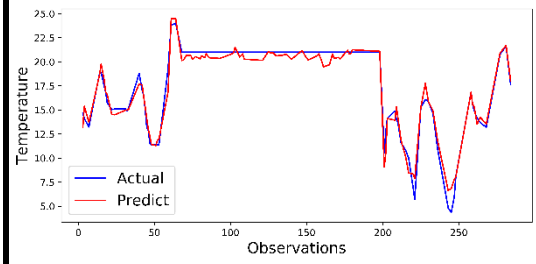

a) 1 Hour

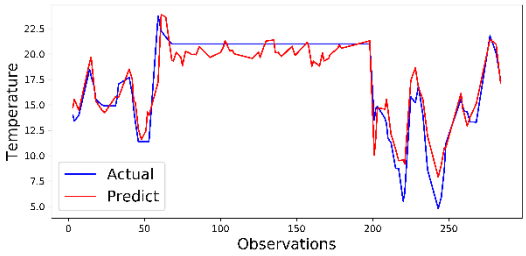

b) 2 Hour

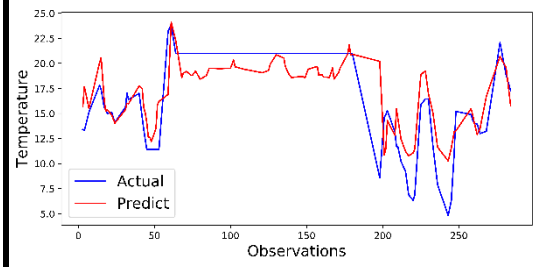

c) 3 Hour

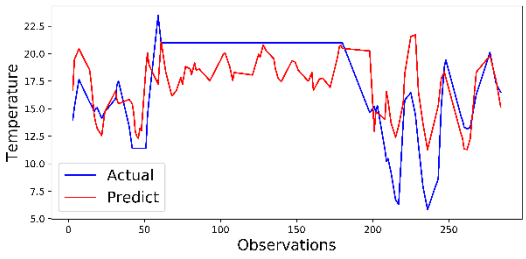

d) 6 Hour

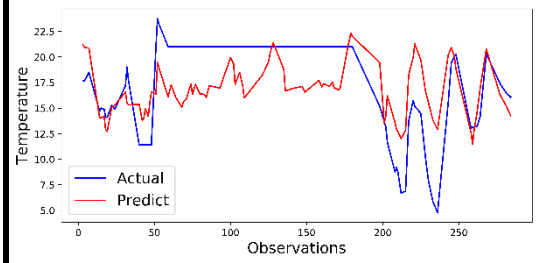

e) 9 Hour

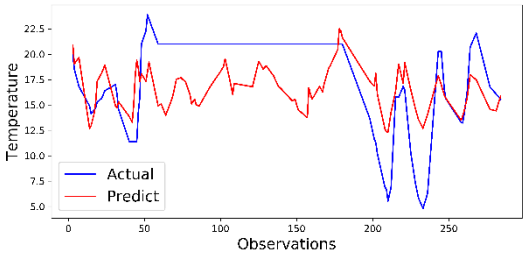

f) 12 Hour

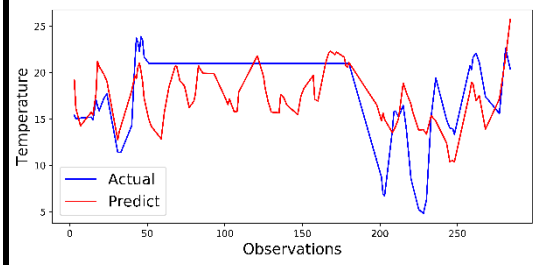

g)18 Hour

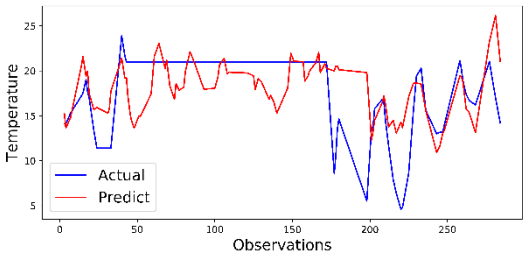

h) 24 Hour

iii) Temperature

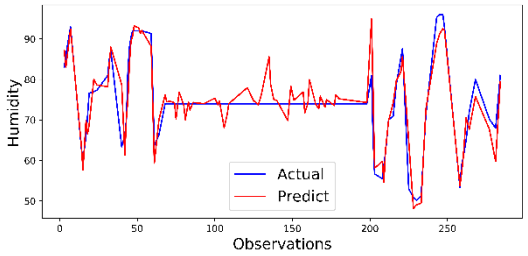

a) 1 Hour

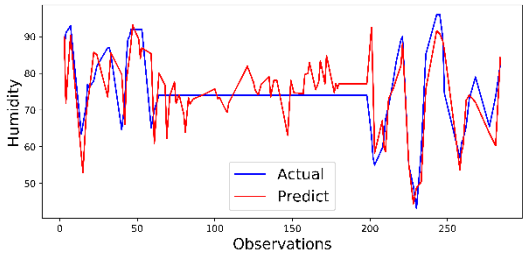

b) 2 Hour

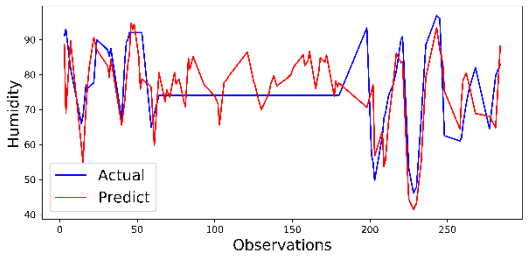

c) 3 Hour

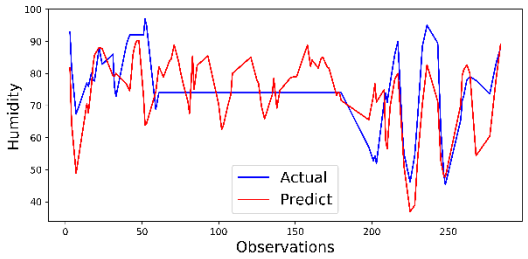

d) 6 Hour

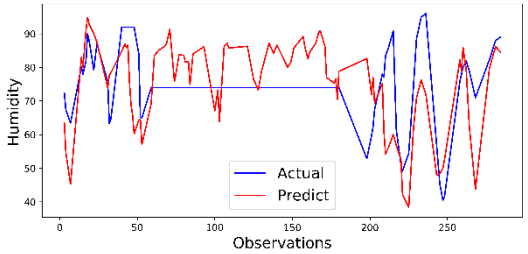

e) 9 Hour

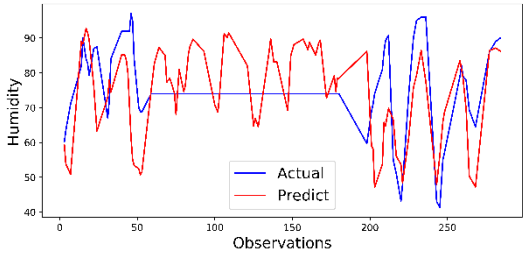

f) 12 Hour

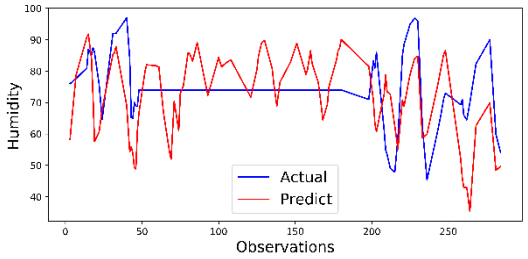

g)18 Hour

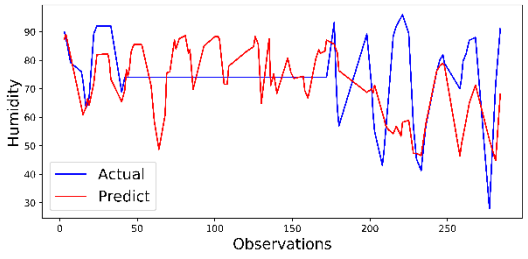

h) 24 Hour

iv) Humidity

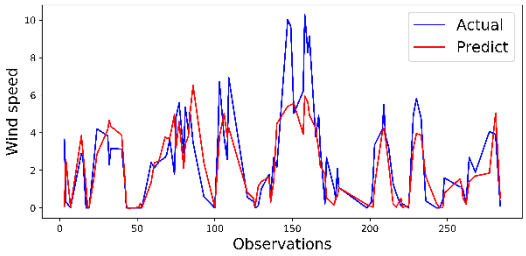

a) 1 Hour

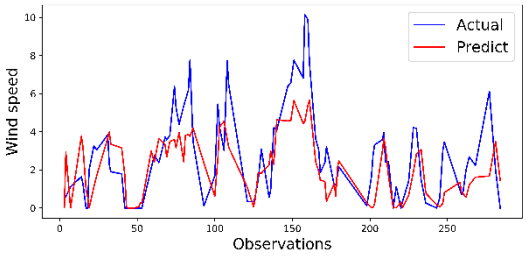

b) 2 Hour

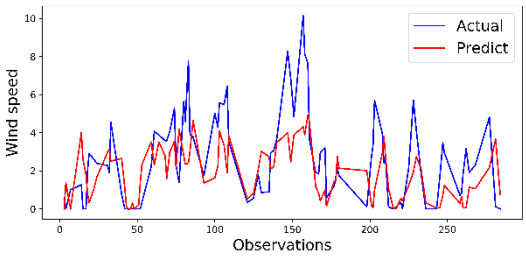

c) 3 Hour

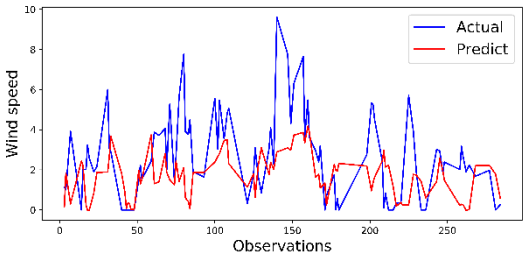

d) 6 Hour

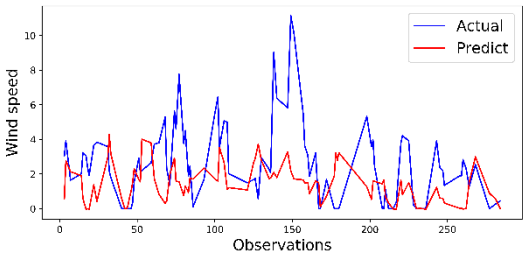

e) 9 Hour

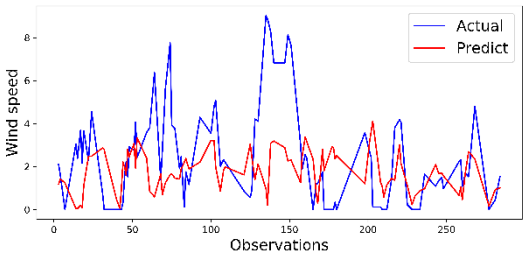

f) 12 Hour

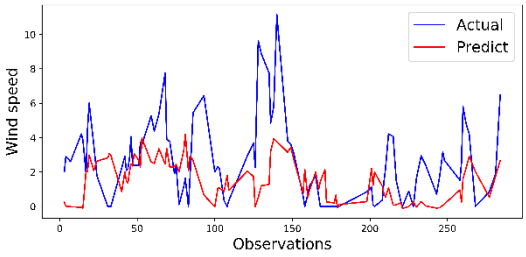

g)18 Hour

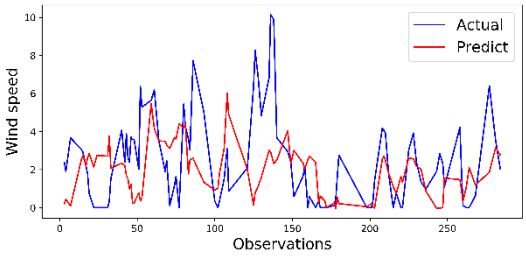

h) 24 Hour

v)Wind speed

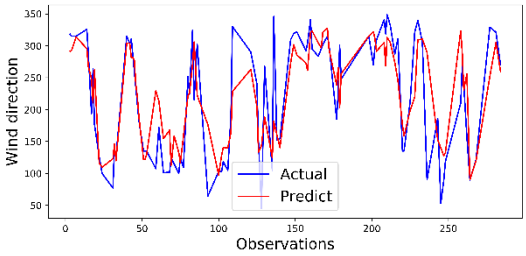

a) 1 Hour

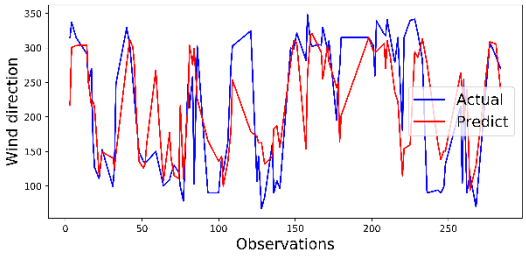

b) 2 Hour

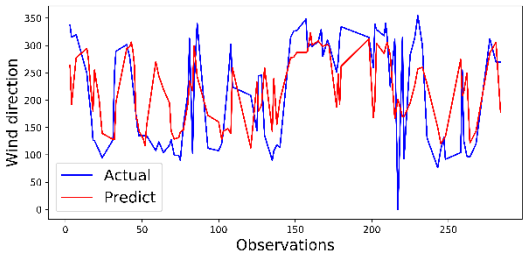

c) 3 Hour

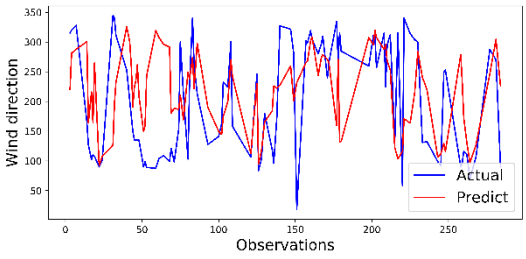

d) 6 Hour

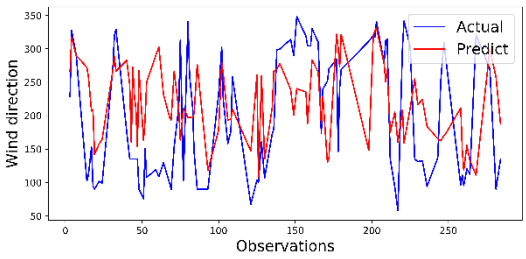

e) 9 Hour

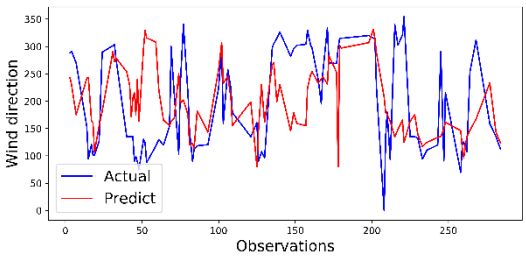

f) 12 Hour

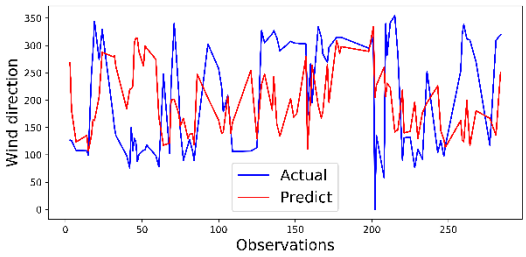

g)18 Hour

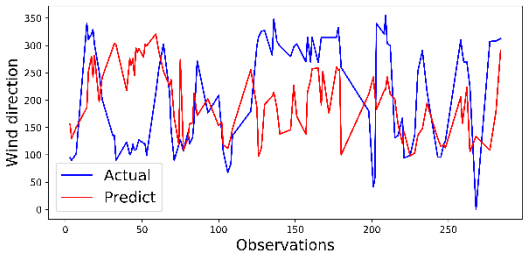

h) 24 Hour

vi) Wind direction

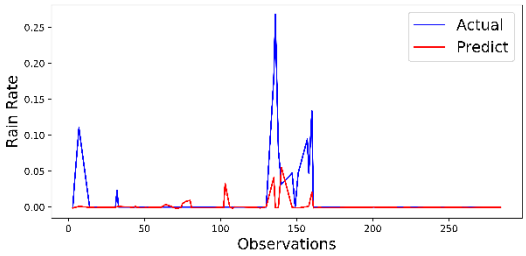

a) 1 Hour

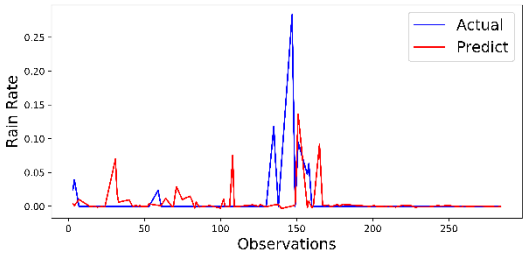

b) 2 Hour

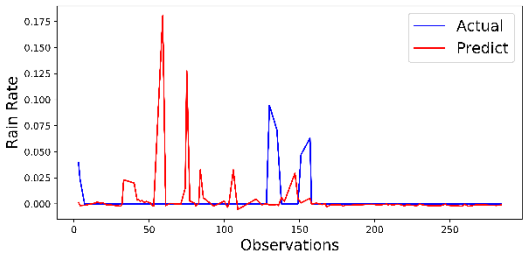

c) 3 Hour

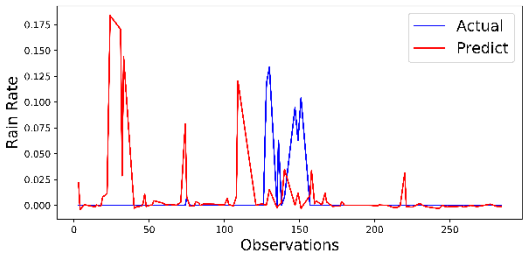

d) 6 Hour

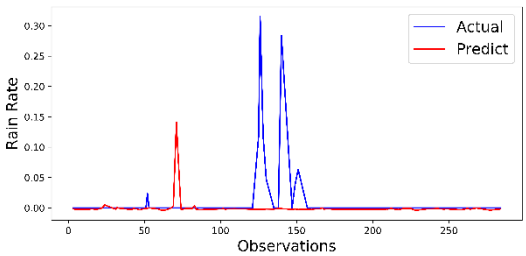

e) 9 Hour

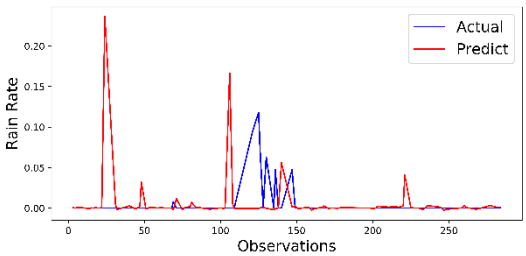

f) 12 Hour

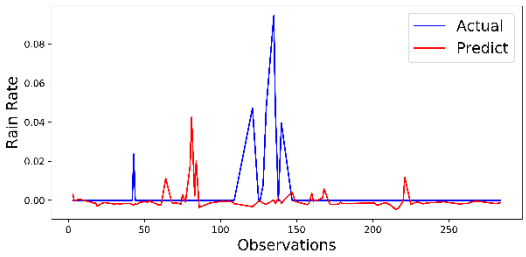

g)18 Hour

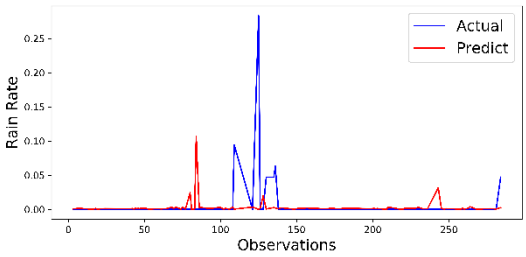

h) 24 Hour

vii) Rain rate

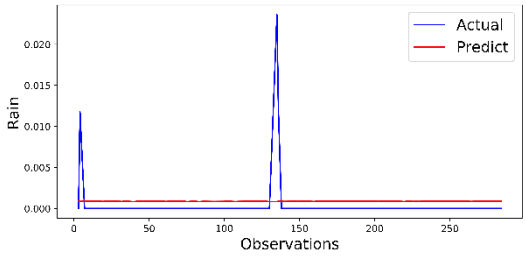

a) 1 Hour

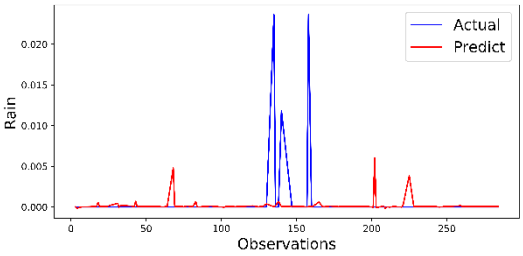

b) 2 Hour

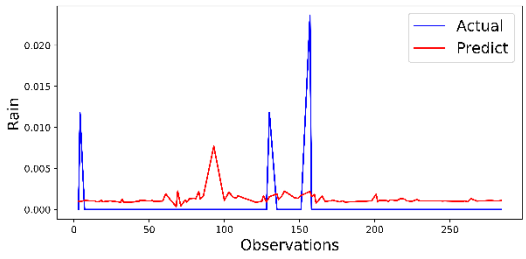

c) 3 Hour

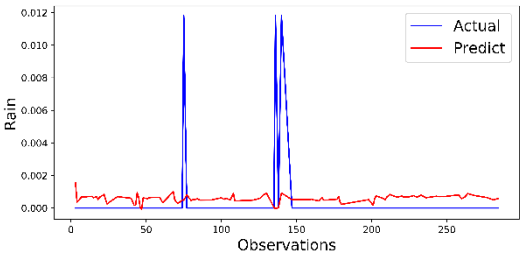

d) 6 Hour

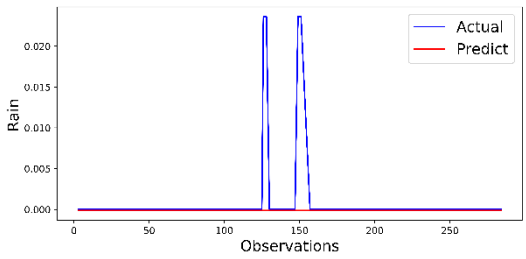

e) 9 Hour

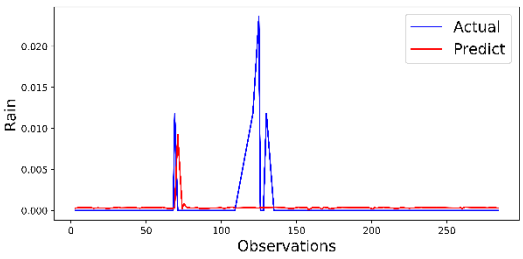

f) 12 Hour

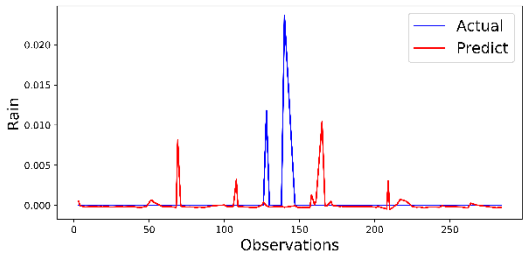

g)18 Hour

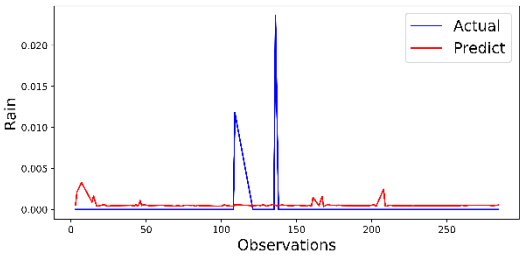

h) 24 Hour

viii) Rain

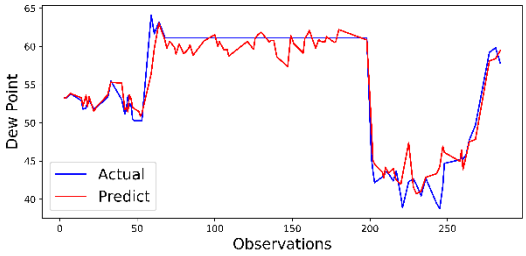

a) 1 Hour

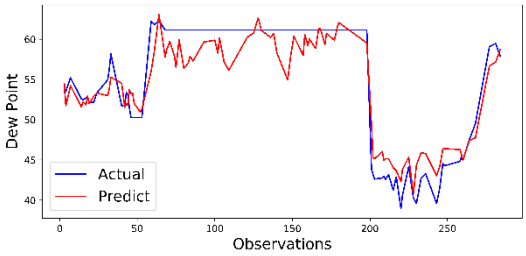

b) 2 Hour

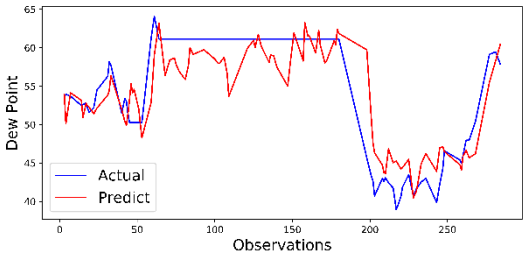

c) 3 Hour

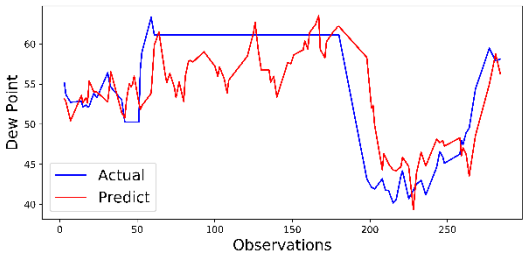

d) 6 Hour

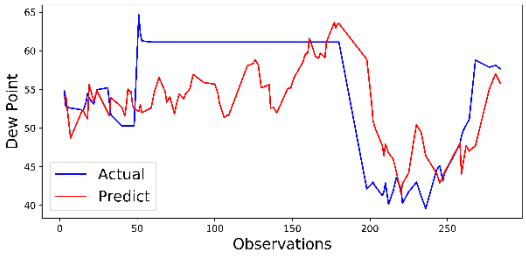

e) 9 Hour

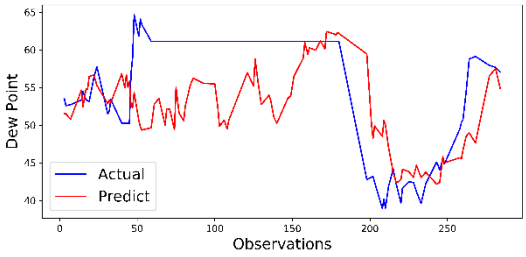

f) 12 Hour

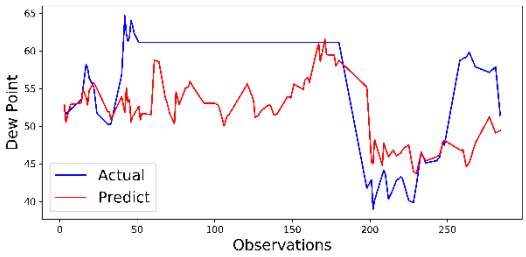

g)18 Hour

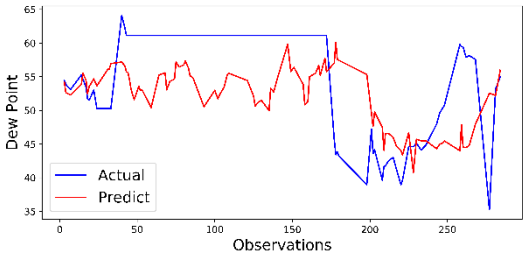

h) 24 Hour

ix) Dew point

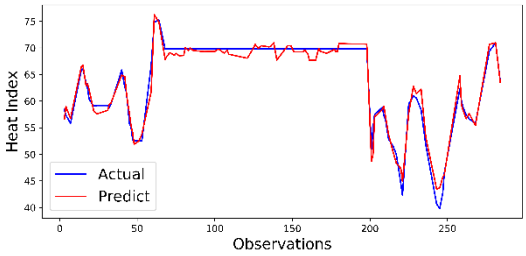

a) 1 Hour

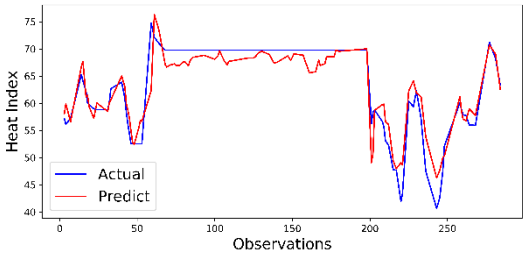

b) 2 Hour

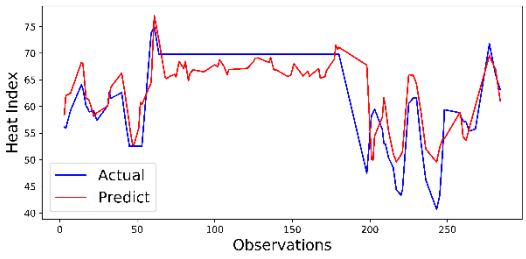

c) 3 Hour

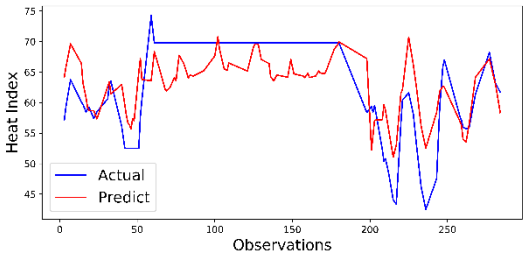

d) 6 Hour

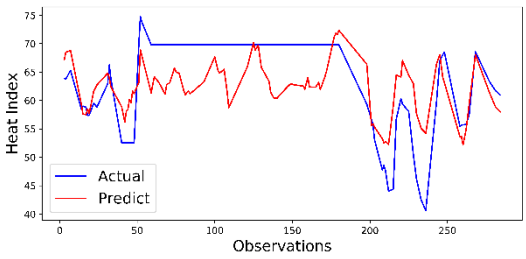

e) 9 Hour

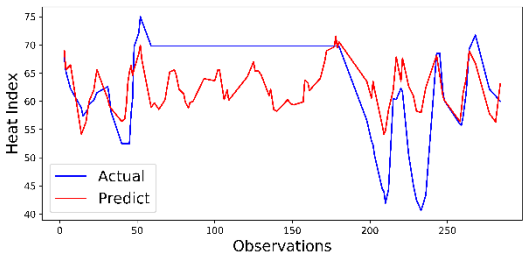

f) 12 Hour

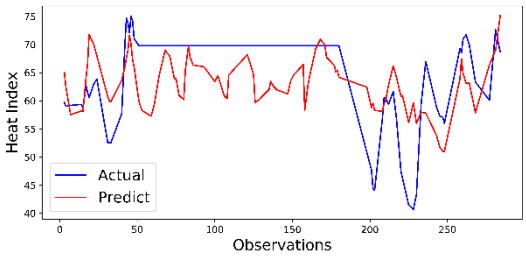

g)18 Hour

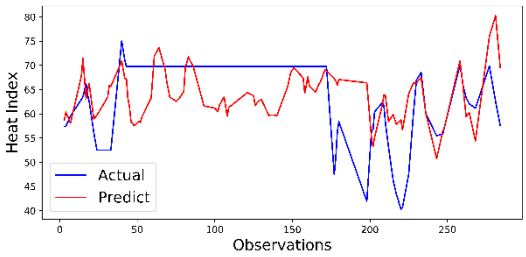

h) 24 Hour

x) Heat index